Health assessment of marine environments: Parasites of the evileye blaasop, *Amblyrhynchote honckenii* (Bloch), as bioindicators

L de Klerk

orcid.org/ 0000-0003-4492-6588

Thesis accepted in fulfilment of the requirements for the degree *Doctor of Philosophy in Science with Environmental Sciences* at the North-West University

Promoter: Prof NJ Smit
Co-promoter: Prof V Wepener
Co-promoter: Prof KA Malherbe

Graduation: November 2025

Disclaimer

This PhD is disclaimed for purposes of Zoological nomenclature following the International Code of Zoological Nomenclature, Fourth Edition, Articles 8.2 and 8.3 (ICZN 1999). No new names or nomenclatural changes are available from statements in this PhD thesis.

All rights reserved. No part of the publication may be reproduced in any form by print, photoprint, microfilm, electronic, or any other means without written permission from the publisher.

Preface

"Individually, one small drop, but together an entire ocean"
Ryunosuke Satoro

The ocean is made up of countless smaller components, many of which go unnoticed. Each organism, no matter how small, plays an essential role in the broader marine ecosystem. Among the most overlooked components are parasites, tiny, often hidden creatures that are integral to the health of their hosts and the environment. Though frequently overlooked, parasites can provide valuable insight into the condition of marine systems, acting as early indicators of ecological change.

This thesis explores the health of marine systems through the lens of fish parasites, using *Amblyrhynchote honckenii* and its parasitic fauna as bioindicators. By examining the diversity, distribution, and ecological roles of these parasites, this study highlights how they can reflect the broader health of marine ecosystems, offering a unique tool for monitoring and conserving marine biodiversity.

Conservation is the preservation of life on Earth, and at its heart lies the preservation of marine ecosystems. Understanding the role of parasites as bioindicators is an essential step toward safeguarding these delicate systems. In this interconnected world, every small piece matters, and together, they form the foundation for a healthy ocean and a healthy planet.

This thesis is dedicated to my loving mother, Jeanine van der Spuy
Your strength, sacrifices, and unwavering support have been the foundation of every achievement in my life. This thesis is dedicated with deepest love and gratitude to you, for your endless encouragement, your belief in me when I doubted myself, and for always being my greatest inspiration and champion.

Acknowledgements

I would like to express my deepest gratitude to everyone who has supported, motivated, and encouraged me throughout my PhD journey. This project has been a fascinating and enriching experience that has significantly broadened my understanding of marine and environmental parasitology, a field to which I have developed a deep passion. My lifelong affinity for biological sciences, especially marine life, has made this study far more meaningful than just an academic pursuit.

First and foremost, I am profoundly thankful to my supervisors, Prof. Nico J. Smit, Prof. Victor Wepener, Prof. Kerry A. Malherbe, and Prof. Bjoern C. Schaeffner. Your expert guidance, unwavering support, and insightful mentorship have been instrumental in shaping me as a researcher. Thank you for sharing your knowledge and enthusiasm, for your constructive feedback, and for constantly encouraging me to push beyond my limits. The opportunities you afforded me and the passion you brought to this project made my PhD journey both enjoyable and inspiring. I consider myself truly privileged to have completed this doctorate under your expert mentorship and remain forever grateful for your confidence in my potential.

I am also deeply grateful to Hokkaido University for hosting me during a two-month training period, where I gained invaluable experience and conducted critical data analyses that greatly enriched this research. Special thanks go to Prof. Mayumi Ishizuka and Prof. Yoshinori Ikenaka for their outstanding leadership of the Africa–Japan Collaborative Research (AJ-CORE) Programme, jointly funded by the Japan Science and Technology Agency (JST), whose generous support made this work possible. I wish to acknowledge the countless hours of assistance from Dr. Yared B. Yohannes and Dr. Collins Nimako, whose dedication and hard work greatly facilitated the progress of this study.

I further extend sincere thanks to the co-authors of the manuscripts included in this thesis: Prof. Bernd Sures, Dr. Milen Nachev, Dr. Hannes J. Erasmus, Dr. Yared B. Yohannes, Prof. Yoshinori Ikenaka, Dr. Collins Nimako, Dr. Shouta M.M. Nakayama, Prof. Mayumi Ishizuka, and Mr. Rodrigo B. Narciso, for their invaluable intellectual contributions, critical insights, and continuous collaboration throughout this research.

I am thankful to the Unit for Environmental Sciences and Management at North-West University for providing access to essential field equipment and laboratory facilities, which were critical to the success of this study. Furthermore, I wish to thank my friends and colleagues for their unwavering moral support, encouragement, and wise advice both in the laboratory and in

the field. I am grateful to Mrs. Anine Jordaan, Mrs. Coret van Wyk, Dr. Marliese Truter, Prof. Francois Retief, Prof. Reese Alberts, Dr. Anja Erasmus, Dr. Anja Vermaak, Dr. Hannes Erasmus, Ms. Chandra le Roux, and Ms. Angela Minnie, all of whom generously shared their time and expertise and were vital to sample collection and numerous research activities.

Last but certainly not least, I owe my deepest and most heartfelt thanks to my family. To my mother, Jeanine J. van der Spuy, thank you for your unwavering love, sacrifices, and for single-handedly supporting and shaping me into the person I am today. Your belief in me, even in moments of doubt, was the foundation of my strength and perseverance. This achievement is as much yours as it is mine, and no words can fully express my gratitude. It is a privilege to share this accomplishment with you. I would also like to extend my sincerest gratitude to my husband, Stern W.S.P. de Klerk. Your patience, steadfast support, and wise guidance throughout this entire journey have been truly amazing. In moments of challenge and triumph alike, your encouragement has been my anchor, helping me stay focused and motivated. Beyond your unwavering emotional support, your insightful advice and thoughtful perspective have enriched both my personal and academic growth. I am profoundly grateful for your belief in my dreams and for standing beside me every step of the way.

This study was made possible through financial support from the Africa–Japan Collaborative Research (AJ-CORE) Programme, co-funded by the Japan Science and Technology Agency (JST; Grant Number: PJ36210002, Principal Investigator: Prof. Mayumi Ishizuka) as well as the National Research Foundation (NRF) of South Africa (Grant Number: 132805, Principal Investigator: Prof. Victor Wepener). Additional support was also received from the NRF Competitive Programme for Rated Researchers (Grant Number: CPRR240430216732, Principal Investigator: Prof. NJ Smit). I also gratefully acknowledge the NRF for personal funding support (Grant Number: 132805). The opinions, findings, conclusions, and recommendations expressed herein are those of the authors and do not necessarily reflect the views of the NRF or North-West University (NWU), both of which disclaim any liability. The funders had no role in the study design, data collection and analysis, decision to publish, or preparation of this thesis.

Table of contents

Disclaimer i
Preface ii
Acknowledgements iii
Summary 1
1. General introduction 4
1.1 General introduction 4
1.2 Hypotheses 7
1.3 Study aim 8
1.4 Objectives 8
1.5 Thesis layout 9
1.6 Thesis outputs 10
1.6.1 Publications 10
1.6.2 Conference outputs 11
1.6.3 Awards 12
References 13
2. Sampling localities and host selection 16
2.1 Study area/ Sampling localities 16
2.2 Host selection 18
2.3 Host collection 19
References 22
3. Metazoan parasite diversity of *Amblyrhynchote honckenii* (Bloch), along the South African coastline 24
3.1 Introduction 24
3.2 Materials and methods 26
3.2.1 Parasite collection 26
2.2.2 Parasite identification 28
3.2.3 Statistical analyses 32
3.3 Results 33
3.3.1 General results 33
3.3.2 Morphological and molecular characterisation of metazoan parasites 37
3.3.2.1 Phylum Acanthocephala 37
3.3.2.2 Phylum Arthropoda 42
3.3.2.3 Phylum Nematoda 52
3.3.2.4 Phylum Platyhelminthes 63
3.4 Discussion 89
3.5 Conclusion 92

References 93
4. The use of fish parasitic isopods as element accumulation indicators in marine pollution monitoring 104
4.1 Introduction 104
4.2 Materials and methods 105
4.2.1 Sampling and locality selection 105
4.2.2 Sample preparation 106
4.2.3 Analyses 106
4.2.5 Statistical analyses 108
4.3 Results 108
4.4 Discussion 112
4.5 Conclusion 113
References: 115
5. Persistent organic pollutants in South African coastal ecosystems: analysing the evileye blaasop *Amblyrhynchote honckenii* (Bloch) for PCB and OCP accumulation 118
5.1 Introduction 118
5.2 Materials and methods 120
5.2.1 Sampling and locality selection 120
5.2.2 Sample preparation 121
5.2.3 Analyses 122
5.2.4 Quality control 123
5.2.5 Statistical analyses 124
5.3 Results 124
5.4 Discussion 129
5.5 Conclusion 133
References 134
6. Metazoan parasite diversity of the evileye blaasop *Amblyrhynchote honckenii* (Bloch): factors influencing parasite community composition. 139
6.1 Introduction 139
6.2 Materials and methods 141
6.2.1 Sampling 141
6.2.2 Statistical analyses 142
6.3 Results 143
6.3.1 Parasite diversity 143
6.3.2 Infra-community composition 143
6.3.3 Component community composition 146
6.3.4 Factors contributing to community composition 149
6.3.5 Estimated parasite diversity 151

6.4 Discussion 152
6.5 Conclusion 155
References: 157
7. Evaluating the combined effect of *Cinusa tetrodontis* Schioedte & Meinert, 1884, infestation and copper exposure on the accumulation and metallothionein expression in the evileye blaasop, *Amblyrhynchote honckenii* (Bloch) 161
7.1 Introduction 161
7.2 Materials and Methods 164
7.2.1 Fish source, husbandry and acclimation 164
7.2.2 Exposure design and experimental procedures 166
7.2.3 Analytical procedures 168
7.2.4 Statistical analysis 169
7.3 Results 170
7.4 Discussion 176
7.5. Conclusion 180
References 182
8. General discussion and conclusions 187
8.1 General discussion 187
8.1.1 Rich parasite diversity 187
8.1.2 *Cinusa tetrodontis* as bioindicators 188
8.1.3 *Amblyrhynchote honckenii* as bioindicator 190
8.1.5 Experimental insight into host-parasite-pollutant interactions 192
8.2 Knowledge gaps and future recommendations 194
8.3 Conclusions 196
References: 199
Supplementary material: 202
Appendix A: 231
Appendix B: 237
Appendix C: 256
Appendix D: 265

Summary

Marine parasitology in South Africa remains a largely neglected field, with few comprehensive studies available to inform understanding of parasite diversity, host-parasite interactions, and the influence of anthropogenic stressors on these relationships. Notably, parasites are increasingly recognised as sensitive bioindicators of environmental change, reflecting pollution levels and habitat disturbances with great fidelity. Integrating parasites into environmental monitoring can thus provide early-warning signs of ecosystem degradation that traditional measures might overlook. This research adopted an environmental parasitology framework, integrating parasitology with ecotoxicology, to investigate the parasite communities of the evileye blaasop, *Amblyrhynchote honckenii* (Bloch), along the coast of South Africa. The project aimed to fill critical knowledge gaps in the taxonomy, ecology, and environmental sensitivity of marine parasites in the region.

Field sampling was conducted at five localities located inside, near, and outside marine protected areas (MPAs) to assess spatial variation in parasite diversity and community composition. A total of 10–15 *A. honckenii* specimens were collected per locality and subjected to thorough parasitological screening, targeting all major parasitic taxa, including ecto- and endoparasites. Parasites were identified and documented, with notes on prevalence, intensity, and site specificity. This provided baseline data on parasite biodiversity, host associations, and life cycle characteristics within this poorly studied host species. Furthermore, host tissues (muscle and liver) were sampled for contaminant analysis to quantify concentrations of element contaminants (e.g., As, Cd, Cu, Mn, Ni, Pb, Se, and Zn) and persistent organic pollutants (including organochlorine pesticides, OCPs, and polychlorinated biphenyls, PCBs). Chemical analyses were conducted using standard, well-established protocols to ensure reliable quantification and comparison across localities. These data allowed for the assessment of pollution loads in fish hosts and their potential correlation with parasite community structure, richness, and infection patterns. Moreover, this study also explored the potential role of MPAs in conserving parasite biodiversity and mitigating contaminant-related impacts on fish health. In addition to field-based assessments, a short-term laboratory exposure experiment was conducted to evaluate copper (Cu) accumulation in both the hosts and their ectoparasites, *Cinusa tetrodontis* Schjödte & Meinert, 1884. Twenty *A. honckenii* individuals were exposed to Cu concentrations for 24 hours. The accumulation of Cu was measured in various tissues of all fish, as well as in *Cin. tetrodontis* (when present). Comparisons were made between parasitised and non-parasitised fish to assess differences in metal accumulation potentially linked to parasite presence. Furthermore, biomarker analyses were conducted on liver and muscle tissue to quantify metallothionein (MT) levels as indicators of metal exposure and physiological stress. By

integrating parasitological, toxicological, and biomarker data, this study provides novel insights into how anthropogenic pollution influences host-parasite interactions in coastal marine systems.

Across five coastal localities, a remarkably diverse assemblage of metazoan parasites was recorded, including several taxa that represent new host and geographic records. These findings provide the first comprehensive baseline of parasite biodiversity in this species, highlighting its role as a reservoir for both specialist and generalist parasites. Parasite assemblages varied strongly with environmental conditions. In and near MPAs, parasite communities were species-rich and included complex multi-host taxa, whereas communities from more degraded, urbanised localities were simplified and dominated by tolerant, direct-cycle species. This clear pattern demonstrates the sensitivity of parasite biodiversity to habitat quality and the broader conservation value of MPAs. Element analyses revealed that the isopod parasite, *Cin. tetrodontis*, accumulated elements at concentrations far higher than those found in the host, establishing this species as an effective biological accumulator for local metal pollution. Analyses of host tissues showed that persistent organic pollutants such as OCPs and PCBs were highest in non-protected urban localities and lowest in protected or lightly impacted areas, directly linking contaminant burdens to land use and management regimes. The controlled Cu exposure experiment confirmed that *Cin. tetrodontis* alters the host-pollutant relationship by sequestering the metal, thereby reducing metal loads and lessening the need for detoxification responses in its host. The parasite exhibited strong metal accumulation and metallothionein induction, with female isopods showing particularly high metal uptake. These findings reveal a dual role for this abundant parasite: it acts as a sensitive sentinel of local contamination and alleviates the physiological burden of pollution on its host. Comparisons between localities revealed the potential role of MPAs not only in conserving fish populations but also in maintaining parasite diversity, which is often overlooked despite its ecological importance. This study highlights the value of using parasites as bioindicators of environmental change and anthropogenic stress and demonstrates the need to include parasitic taxa in marine conservation and monitoring frameworks.

This work provides essential new data on parasite diversity, distributions and their interactions with pollution along the South African coast. By linking field surveys with experimental evidence, the study offers a comprehensive understanding of how parasite communities respond to and modulate environmental stressors. These insights are not only academically significant, filling key knowledge gaps, but also offer applied value for ecosystem management. In a broader context, this thesis underscores that the “hidden” biodiversity of parasites holds valuable information about ecosystem integrity. Incorporating parasites into routine marine monitoring and pollution assessment can thus enhance our ability to detect ecological change, inform

conservation strategies, and ultimately better safeguard the health of coastal marine environments.

Keywords: Taxonomy; Environmental Toxicology; South Africa; Environmental Parasitology

1 General introduction

1.1 General introduction

Parasites constitute a vital yet often overlooked component of marine biodiversity and ecosystem functioning. It is estimated that parasitic species globally outnumber free-living species, with each free-living host providing habitat for a variety of specialised parasites (Rohde, 2002; Weston *et al*., 2021; Smit and Sures, 2025). Parasites play crucial ecological roles by regulating host populations, altering community dynamics, modifying food web interactions, and contributing to energy flow within ecosystems (Rohde, 2002; Weston *et al*., 2021; Smit and Sures, 2025). By affecting host behaviour, reproduction, and survival, parasites shape ecosystem structure in ways that extend well beyond their roles as mere pathogens (Weston *et al*., 2021; Smit and Sures, 2025).

Establishing comprehensive baseline data on marine parasite communities is crucial for conserving marine biodiversity and ecosystem health. Knowing which parasites are present in a given ecosystem reveals the full scope of host-parasite interactions, including cryptic and undescribed species that remain hidden without detailed inventories (Smit and Hadfield, 2015; Marcogliese, 2023; Truter *et al*., 2025). These baseline datasets enable the detection of changes in parasite diversity and community composition over time, serving as sensitive indicators of environmental disturbances, pollution, habitat degradation, and shifts in host populations (Lafferty and Kuris, 2005; Wood and Johnson, 2015; Truter *et al*., 2025). Without such reference points, it is difficult to distinguish natural ecological variability from anthropogenic impacts or to anticipate emerging threats to ecosystem stability (Lafferty and Kuris, 2005; Truter *et al*., 2025). Moreover, parasites mediate key ecological and evolutionary processes and contribute to ecosystem resilience; thus, their loss can destabilise food webs and affect host species conservation (Dobson *et al*., 2008; Lafferty and Kuris, 1999; Carlson *et al*., 2020; Truter *et al*., 2025). Rich

parasite assemblages typically indicate intact, stable ecosystems, whereas degraded habitats often show impoverished parasite diversity dominated by a few tolerant species (Lafferty and Kuris, 1999). Understanding and protecting parasite biodiversity is therefore integral to marine conservation strategies. Yet, parasites are among the most extinction-prone groups, often disappearing before they are even documented, which underscores the urgent need to incorporate parasites into conservation planning and monitoring efforts (Dunne *et al*., 2013; Lees and Pimm, 2015; Carlson *et al*., 2020; Truter *et al*., 2025). In regions of high biodiversity and escalating anthropogenic pressure, such as southern Africa's marine environments, robust baseline data on parasite communities are indispensable for effective spatial planning and the evaluation of marine protected areas, ultimately helping to safeguard these hidden yet essential components of marine ecosystems (Truter *et al*., 2025).

This not only advances our understanding of parasite ecology but also highlights the crucial role parasites play as sensitive bioindicators, offering valuable insights for ecosystem management and conservation of environmental change (Nachev and Sures, 2016; Sures *et al*., 2017; Sures *et al*., 2025). This shift gave rise to the interdisciplinary field of environmental parasitology, which integrates parasitology, ecology and ecotoxicology to understand how parasites interact with their environments and how these interactions can be utilised for environmental monitoring (Sures *et al*., 2017; Sures *et al*., 2025; Smit and Sures, 2025). Environmental parasitology emphasises the sensitivity of parasites to pollution and habitat disturbance, revealing their utility as highly responsive bioindicators of ecosystem condition (Nachev and Sures, 2016). Many endoparasites, including acanthocephalans and cestodes, bioaccumulate metals and persistent organic pollutants (POPs) at concentrations exceeding those in their hosts, effectively functioning as living accumulators that reveal the bioavailability of pollutants (Sures, 2004; Vidal-Martínez *et al*., 2010; Nachev and Sures, 2016; Sures *et al*., 2017). Beyond revealing pollution, some parasites act as biological sinks, sequestering toxicants and thus mitigating pollutant burdens on their hosts (Sures *et al*., 2025). Parasite infections can modulate host physiology, including immune responses and detoxification processes, altering host sensitivity and responses to pollution (Sures *et al*., 2025). Failure to account for these interactions can confound standard ecotoxicological assessments, whereas incorporating parasite-associated dynamics can substantially improve biomonitoring accuracy (Sures *et al*., 2025). Over recent decades, research has increasingly supported the role of parasites as sensitive bioindicators, and advanced understanding of parasite-pollution interactions (Nachev and Sures, 2016; Sures *et al*., 2017; Sures *et al*., 2025).

Marine environments face mounting anthropogenic pressures, including chemical pollution and habitat degradation, which threaten biodiversity and ecosystem integrity worldwide

(Pinsino *et al*., 2008; Webb and Mindel, 2015; Mahmoud *et al*., 2019). Traditional pollution monitoring commonly relies on free-living sentinel species such as bivalves, which are sampled to assess temporal and spatial pollution patterns (Farrington *et al*., 2016; Wepener and Degger, 2020). However, there is growing recognition that host-parasite systems offer complementary advantages in pollution bioindication due to their sensitivity and integrative nature (Sures *et al*., 2017; Chine *et al*., 2021; Sures *et al*., 2023). Previous work has primarily focused on freshwater environments and endoparasitic helminths (e.g., acanthocephalans and cestodes) (Sures, 2004; Nachev and Sures, 2016), with fewer studies addressing marine ectoparasites, particularly crustacean parasites (Vidal-Martínez *et al*., 2010; Pérez del Olmo *et al*., 2019).

Furthermore, parasite communities reflect broader ecosystem integrity and environmental quality. Intact and unpolluted habitats support diverse parasite assemblages, including specialised multi-host taxa, whereas degraded or polluted ecosystems often show reduced parasite richness dominated by resilient, monoxenous species (Lafferty and Kuris, 1999; Smit and Hadfield, 2015; Erasmus *et al*., 2022). Marine protected areas (MPAs) preserve food web complexity and water quality, often harbouring richer and more balanced parasite communities compared to adjacent agricultural or polluted zones, reinforcing the value of habitat protection for maintaining parasite biodiversity and ecosystem resilience (Wood *et al*., 2018; Marcogliese, 2023). Heteroxenous parasites with complex, multi-host life cycles are especially vulnerable to disruption from environmental stressors, making their presence effective indicators of ecosystem health and restoration (Nachev and Sures, 2016). Therefore, integrating parasitological data alongside traditional biotic and abiotic metrics enriches environmental assessments and supports robust conservation planning (Sures *et al*., 2017).

Despite these advances, substantial knowledge gaps remain, especially in biodiverse yet understudied regions such as southern Africa. Although the marine biodiversity is exceptionally rich, the diversity of marine parasites remains poorly documented (Smit and Hadfield, 2015). Existing research efforts often focused on commercially important species, leaving niche and cryptic parasite taxa understudied. Increasingly, surveys reveal many undescribed parasite species, emphasising the need for expanded baseline data (Smit and Hadfield, 2015). Filling such gaps is critical for accurate biodiversity inventories and understanding ecological dynamics in these complex ecosystems. Hence, to fill this gap, this study focuses on parasites of the evileye blaasop, *Amblyrhynchote honckenii* (Bloch), an endemic reef-associated fish distributed widely along the South African coast. Its non-commercial status and broad parasite fauna, including the ectoparasitic isopod, *Cinusa tetrodontis* Schioedte & Meinert, 1884, make it an excellent sentinel for environmental parasitology and marine biodiversity monitoring (Smith and Heemstra, 2012; Froese and Pauly, 2025). Through a combination of integrative field surveys and laboratory

experiments, research on the *A. honckenii*-parasite system advances environmental parasitology in several ways. It expands baseline records of marine parasite biodiversity and helps to uncover cryptic species. This research also demonstrates how parasites can bioaccumulate pollutants and act as indicators of local pollution. In addition, it shows how parasite communities reflect habitat quality and management regimes. Finally, these studies clarify the mechanisms by which parasites influence host pollutant uptake and physiological responses. Together, these contributions provide a powerful framework to enhance marine environmental health assessments, informing biodiversity conservation and pollution mitigation strategies in a rapidly changing world.

1.2 Hypotheses

The following hypotheses were formulated and tested in the individual chapters of the study. The relevant chapter(s) where the hypothesis is tested are indicated in parentheses:

1. *Amblyrhynchote honckenii* hosts a greater diversity of metazoan parasites than currently documented, including undescribed or regionally rare taxa, reflecting potentially host-specific associations (Chapter 3).
2. External crustacean parasites, particularly *Cin. tetrodontis* of *A. honckenii* accumulate significantly higher levels of elements than their host (Chapter 4).
3. Levels of POPs in *A. honckenii* are significantly lower in MPAs than in non-protected localities (Chapter 5).
4. Parasite diversity displays spatial trends, with richness and complexity expected to peak in subtropical regions, particularly the Natal ecoregion, and decline toward temperate and colder zones like the Agulhas Bank (Chapter 6).
5. Elevated organic pollutants in hosts correlate with reduced parasite richness and dominance of directly transmitted or opportunistic taxa, while pristine and ecologically intact localities, especially within or near-MPAs, are expected to support rich, complex parasite communities (Chapter 6).
6. Infestation by the ectoparasite *Cin. tetrodontis* reduces copper (Cu) accumulation in host tissues by acting as a biological sink (Chapter 7).
7. The presence of *Cin. tetrodontis* alters host detoxification, particularly metallothionein (MT) expression, reducing biomarker activation needs (Chapter 7).
8. *Cinusa tetrodontis* itself actively responds to Cu exposure, exhibiting sex-specific MT induction patterns linked to physiological differences (Chapter 7).
9. Short-term laboratory exposures can reproduce Cu accumulation and biomarker trends observed in environmental conditions, validating controlled experiments for host-parasite-pollutant interaction studies (Chapter 7).

1.3 Study aim

To test these hypotheses, the main aim of the study is to advance the understanding of marine parasites as ecological indicators of environmental health by using *A. honckenii* and its parasite fauna as a model system. Specifically, it seeks to characterise the biodiversity, spatial patterns, and pollutant interactions of *A. honckenii's* parasites, evaluating their capacity to serve as integrative bioindicators of marine ecosystem condition across varying pollution gradients and management regimes.

1.4 Objectives

To achieve this aim, the study was designed to address the following specific objectives:

1. **Document the metazoan parasite diversity of *A. honckenii:*** Conduct comprehensive parasitological surveys across multiple marine regions (Agulhas Bank and the Natal ecoregion), spanning protected and unprotected localities along the South African coast. Identify and describe metazoan parasites, including previously undescribed or regionally rare taxa, thereby expanding baseline taxonomic and biodiversity knowledge.

2. **Quantify metal pollutant bioaccumulation in host and parasites:** Measure concentrations of selected elements in tissues of *A. honckenii* and their external parasites. Determine if parasites accumulate elements at significantly higher levels than their hosts, supporting their use as sensitive bioindicators.

3. **Evaluate organic pollutant burdens in *A. honckenii* across localities:** Analyse POP concentrations, specifically organochlorine pesticides (OCPs) and polychlorinated biphenyls (PCBs), in fish tissues from multiple locations to assess contaminant levels. Determine differences between MPA, near-MPA and non-MPA localities.

4. **Assess spatial variation in parasite community structure:** Analyse differences in parasite diversity, richness, and community composition related to biogeographic gradients (e.g., Agulhas Bank versus the Natal ecoregion) and conservation status (MPA, near-MPA, and non-MPA localities). Evaluate whether parasite assemblages at protected localities are richer and more complex compared to those at impacted localities.

5. **Examine correlations between parasite community metrics and contaminant exposure:** Integrate contaminant concentration data with parasite diversity and community composition to investigate whether higher contaminant concentrations

correlate with reduced parasite richness, increased dominance of contaminant-tolerant taxa, or shifts in parasite communities, indicating environmental filtering effects.

6. **Conduct controlled laboratory exposures to elucidate host-parasite-pollutant interactions:** Experimentally expose both infested and uninfested *A. honckenii* to Cu under controlled short-term conditions. Specifically:
    - Measure concentrations of Cu in tissues of *A. honckenii* and their external parasites.
    - Determine whether infestation by *Cin. tetrodontis* reduces Cu accumulation in host tissues by acting as a biological sink.
    - Assess whether the presence of *Cin. tetrodontis* alters host detoxification responses, particularly MT expression.
    - Characterise the physiological responses of *Cin. tetrodontis* itself to Cu exposure, including potential sex-specific patterns of MT induction.

This structured approach systematically addresses both fundamental biodiversity questions and applied ecotoxicological topics, positioning the *A. honckenii*-parasite system as a suitable, holistic tool for marine ecosystem assessment.

1.5 Thesis layout

The structure of the thesis reflects this integrative approach, as outlined below:

Chapter 1 – General introduction: This chapter establishes the study's context, reviewing marine environmental parasitology and the ecological importance of parasites as bioindicators. It highlights knowledge gaps, especially in southern Africa, and introduces *A. honckenii* as the focal host, outlining the study's hypotheses, aims, and objectives.

Chapter 2 – Sampling localities and host selection: This chapter details the study design, describing sampling localities along the South African coast across MPAs and non-MPA zones. Further, it describes the host selection and host collection.

Chapter 3 – Metazoan parasite diversity of *A. honckenii*: This chapter documents a rich parasite fauna in *A. honckenii*, including numerous metazoan taxa with new species and host association records.

Chapter 4 – The use of *C. tetrodontis* as element accumulation indicators: This chapter investigates element accumulation in *A. honckenii* and its ectoparasite *Cin. tetrodontis*. It provides evidence that parasites act as biological sinks, mitigating host element burden and serving as sensitive indicators of local element pollution.

Chapter 5 – Persistent organic pollutants in *A. honckenii*: POP pollution (OCPs and PCBs) are quantified in *A. honckenii* tissues across localities with varying human impact. The chapter reveals higher contaminant loads at non-protected urban localities and lower burdens in MPAs, confirming the fish's suitability as an organic contaminant bioindicator and emphasising the role of MPAs in reducing pollutant exposure.

Chapter 6 – Factors influencing parasite community composition: Analysing parasite community variation, this chapter demonstrates latitudinal gradients in diversity and complexity. It highlights the influence of contaminants and protection status, showing polluted localities have impoverished parasite fauna dominated by opportunistic taxa, while MPAs maintain higher diversity and trophic complexity.

Chapter 7 – Experimental host-parasite-pollutant interactions: Controlled Cu exposure experiments reveal that *Cin. tetrodontis* infestation reduces host Cu accumulation and modifies detoxification biomarker responses, including MT induction. The parasite itself exhibits sex-specific physiological responses to Cu exposure, and these laboratory findings reproduce environmental patterns, validating parasite effects on host pollutant dynamics.

Chapter 8 – Discussion and conclusions: This final chapter summarises all findings, confirming whether hypotheses related to parasite biodiversity, pollutant bioaccumulation, and community responses to environmental gradients are supported or not.

1.6 Thesis outputs

1.6.1 Publications

Papers already published or online:

Van Der Spuy, L., Erasmus, J.H., Nachev, M., Schaeffner, B.C., Sures, B., Wepener, V. & Smit, N.J., 2023. The use of fish parasitic isopods as element accumulation indicators in marine pollution monitoring. *Marine Pollution Bulletin*, 194: 115385 (Chapter 4, full) (see Appendix A)

Van Der Spuy, L., Narciso, R.B., Hadfield, K.A., Wepener, V. & Smit, N.J., 2025. Exploring South Africa's hidden marine parasite diversity: Two new marine *Ergasilus* species (Copepoda: Cyclopoida: Ergasilidae) from the evileye blaasop, *Amblyrhynchotes honckenii* (Bloch). *Parasitology*, 152(1): 30–50 (Chapter 3, in part) (see Appendix B).

de Klerk, L., Smit, N.J., Yohannes, Y.B., Ikenaka, Y., Nimako, C., Nakayama, S.M.M., Ishizuka, M. & Wepener, V., 2025. Persistent organic pollutants in South African coastal ecosystems: analysing the evileye blaasop *Amblyrhynchote honckenii* (Bloch, 1785) for PCB and OCP accumulation. *Regional Studies in Marine Science*, 89: 104368 (Chapter 5, full) (see Appendix C).

Papers submitted:

de Klerk, L., Yong, R.Q-Y, Hadfield, K.A. & Smit, N.J. Taxonomic reassessment of the opistholebetine opecoelid *Pseudoheterolebes cotylophorus* (Ozaki, 1935) Yamaguti, 1959, in South Africa (Chapter 3, in part) (see Appendix D).

1.6.2 Conference outputs

Van Der Spuy, L., Hadfield, K., Smit, N.J., 2022. Unique diversity of parasites of the evileye pufferfish, *Amblyrhynchote honckenii* (Bloch, 1785) of South Africa. The 15th International Congress of Parasitology (ICOPA). Denmark, Copenhagen.

Van Der Spuy, L., Erasmus, J.H., Nachev, M., Schaeffner, B.C., Sures, B., Wepener, V. & Smit, N.J., 2023. Element accumulation in the evileye blaasop, *Amblyrhynchote honckenii* (Bloch), and its parasitic isopod, *Cinusa tetrodontis* Schjödte & Meinert, 1884, in South Africa. SETAC Europe 33rd Annual Meeting: Data-Driven Environmental Decision-Making. Ireland, Dublin.

Van Der Spuy, L., Yong, R.Q-Y, Hadfield, K.A. & Smit, N.J., 2024. Unpuzzling marine mysteries: unlocking taxonomic riddles in opistholebetine trematodes of South Africa. 52nd Annual Conference of the Parasitological Society of Southern Africa (PARSA). Hartbeespoort, South Africa.

Van Der Spuy, L., Yong, R.Q-Y, Hadfield, K.A. & Smit, N.J., 2024. Marine mysteries: unlocking taxonomic riddles in opistholebetine trematodes of South Africa. Trematodes. Brisbane, Australia.

Van Der Spuy, L., Smit, N.J., Yohannes, Y.B., Ikenaka, Y., Nimako, C., Nakayama, S.M.M., Ishizuka, M. & Wepener, V., 2024. Exploring pesticide presence: the evileye blaasop's journey along South Africa's coastline. Southern African Society of Aquatic Scientists (SASAqS) Joint Society of Environmental Toxicology and Chemistry (SETAC) Southern African Regional Conference. Gold Reef City, Johannesburg, South Africa.

Van Der Spuy, L., Yohannes, Y.B., Ikenaka, Y., Ishizuka, M., Wepener, V. & Smit, N.J. 2025. Pollution's ripple effect: unravelling pesticide influence on fish parasite diversity in South Africa's coastal ecosystems. XI International Symposium on Fish Parasites, Fish Health, Parasites and Biodiversity Conservation (ISFP XI). Mérida, Mexico.

Van Der Spuy, L., Schaeffner, B.C., Hadfield, K.A., Wepener, V. & Smit, N.J., 2025. Larval cestodes and poisonous intermediate hosts: rethinking transmission pathways and ecological interactions. XI International Symposium on Fish Parasites, Fish Health, Parasites and Biodiversity Conservation (ISFP XI). Mérida, Mexico.

Van Der Spuy, L., Erasmus, J.H., Nachev, M., Schaeffner, B.C., Sures, B., Wepener, V. & Smit, N.J., 2025. Beyond bivalves: The role of the fish parasitic isopod *Cinusa tetrodontis* Schjödte & Meinert, 1884, in tracking marine pollution. XI International Symposium on Fish Parasites, Fish Health, Parasites and Biodiversity Conservation (ISFP XI). Mérida, Mexico.

1.6.3 Awards

2024: First place for best PhD poster presentation. Unpuzzling marine mysteries: unlocking taxonomic riddles in opistholebetine trematodes of South Africa.52nd Annual Conference of the Parasitological Society of Southern Africa (PARSA). Hartbeespoort, South Africa.

2024: Second place for best PhD oral presentation. Exploring pesticide presence: the evileye blaasop's journey along South Africa's coastline. Southern African Society of Aquatic Scientists (SASAqS) Joint Society of Environmental Toxicology and Chemistry (SETAC) Southern African Regional Conference. Gold Reef City, Johannesburg, South Africa.

References

Carlson, C.J., Hopkins, S., Bell, K.C., Doña, J., Godfrey, S.S., Kwak, M.L., Lafferty, K.D., Moir, M.L., Speer, K.A., Strona, G., Torchin, M., & Wood, C.L., 2020. A global parasite conservation plan. *Biological Conservation*, 250: 108596.

Chine, J.H., Nachev, M., Sures, B. & Gargouri, L., 2021. Trace element assessment in *Neoechinorhynchus agilis* (Rudolphi, 1918) (Acanthocephala: Neoechinorhynchidae) and its fish hosts, *Mugil cephalus* (Linnaeus, 1758) and *Chelon ramada* (Risso, 1827) from Ichkeul Lagoon, Tunisia. *Journal of Helminthology*, 95(e61): 1–7.

Dobson, A., Lafferty, K.D., Kuris, A.M., Hechinger, R.F. & Jetz, W., 2008. Homage to Linnaeus: How many parasites? How many hosts? *Proceedings of the National Academy of Sciences of the United States of America*, 105: 11482–11489.

Dunne, J.A., Lafferty, K.D., Dobson, A.P., Hechinger, R.F., Kuris, A.M., Martinez, N.D., McLaughlin, J.P., Mouritsen, K.N., Poulin, R., Reise, K., Stouffer, D.B., Thieltges, D.W., Williams, R.J. & Zander, C.D., 2013. Parasites affect food web structure primarily through increased diversity and complexity. *PLoS Biology*, 11(6): e1001579.

Erasmus, A., Wepener, V., Hadfield, K.A., Sures, B. & Smit, N.J., 2022. Metazoan parasite diversity of the endemic South African intertidal klipfish, *Clinus superciliosus*: factors influencing parasite community composition. *Parasitology International*, 90: 102611.

Farrington, J.W., Tripp, B.W., Tanabe, S., Subramanian, A., Sericano, J.L., Wade, T.L., Knap, A.H., 2016. Edward D. Goldberg's proposal of "the Mussel Watch": reflections after 40 years. *Marine Pollution Bulletin*, 110: 501–510.

Froese, R. & Pauly, D., 2025. FishBase. Available at: www.fishbase.org/search.php. (Date of access: 8 May 2025).

Lafferty, K.D. & Kuris, A.M., 1999. How environmental stress affects the impacts of parasites. *Limnology and Oceanography*, 44(3 part 2): 925–931.

Lafferty, K.D. & Kuris, A.M., 2005. Parasitism and environmental disturbances. In *Parasitism and Ecosystems*, pp.113–123.

Lees AC, Pimm SL (2015) Species, extinct before we know them? Curr Biol 25(5):177–180

Mahmoud, N.E., Fahmy, M.M., Abuowarda, M.M., Zaki, M.M., Ismael, E., Ismail, E.M., 2019. Influence of water quality parameters on the prevalence of *Livoneca redmanii* (Isopoda: Cymothoidae) infestation of Mediterranean Sea fishes, Egypt. *International Journal of Veterinary Science*, 8(3): 174–181.

Marcogliese, D.J., 2023. Major drivers of biodiversity loss and their impacts on helminth parasite populations and communities. *Journal of Helminthology*, 97:e34.

Nachev, M. & Sures, B., 2016. Environmental parasitology: parasites as accumulation bioindicators in the marine environment. *Journal of Sea Research*, 113: 45–50.

Pinsino, A., Della Torre, C., Sammarini, V., Bonaventura, R., Amato, E. & Matranga, V., 2008. Sea urchin coelomocytes as a novel cellular biosensor of environmental stress: a field study in the Tremiti Island Marine Protected Area, Southern Adriatic Sea, Italy. *Cell Biology and Toxicology*, 24: 541–552.

Rohde, K., 2002. Ecology and biogeography of marine parasites. *Advances in Marine Biology*, 43: 1–83.

Smit, N.J. & Hadfield, K.A., 2015. Marine fish parasitology in South Africa: History of discovery and future direction. *African Zoology*, 50(2): 79–92.

Smit, N.J. & Sures, B. eds., 2025. *Aquatic Parasitology: Ecological and Environmental Concepts and Implications of Marine and Freshwater Parasites*. Cham: Springer.

Smith, M.M. & Heemstra, P.C., 2012. *Smith's Sea Fishes*. Heidelberg, Germany: Springer Science & Business Media, pp. 1191.

Sures, B., 2004. Environmental parasitology: relevancy of parasites in monitoring environmental pollution. *Trends in Parasitology*, 20: 170–177.

Sures, B., Nachev, M., Grabner, D., Wepener, V. & Zimmermann, S., 2025. Environmental Parasitology: Interactions Between Parasites and Pollutants. In: N.J. Smit & B. Sures, eds. *Aquatic Parasitology: Ecological and Environmental Concepts and Implications of Marine and Freshwater Parasites.* Cham: Springer, pp.509–534.

Sures, B., Nachev, M., Schwelm, J., Grabner, D. & Selbach, C., 2023. Environmental parasitology: stressor effects on aquatic parasites. *Trends in Parasitology*, 39: 461–474.

Sures, B., Nachev, M., Selbach, C. & Marcogliese, D.J., 2017. Parasite responses to pollution: what we know and where we go 'Environmental parasitology'. *Parasites and Vectors*, 10: 65.

Truter, M., Schaeffner, B.C. & Smit, N.J., 2025. Aquatic Parasite Conservation. In: N.J. Smit & B. Sures, eds. *Aquatic Parasitology: Ecological and Environmental Concepts and Implications of Marine and Freshwater Parasites.* Cham: Springer, pp. 325–360.

Vidal-Martínez, V.M., Pech, D., Sures, B., Purucker, S.T. & Poulin, R., 2010. Can parasites really reveal environmental impact? *Trends in Parasitology*, 26: 44–51.

Webb, T.J. & Mindel, B.L., 2015. Global patterns of extinction risk in marine and non-marine systems. *Current Biology*, 25: 506–511.

Wepener, V. & Degger, N., 2020. Monitoring of metals in South African harbours using resident brown mussels (*Perna perna)* as indicator organisms. *African Zoology*, 55(4): 267–277.

Weston, M., Nunkoo, I., Reed, C. & van der Lingen, C.D., 2021. Ectoparasites infecting the heads and gills of commercially valuable marine fishes in South Africa. *African Zoology*, 56(4): 303–311.

Wood, C.L. & Johnson, P.T., 2015. A world without parasites: exploring the hidden ecology of infection. *Frontiers in Ecology and the Environment*, 13(8): 425–434.

Wood, C.L., Zgliczynski, B.J., Haupt, A.J., Guerra, A.S., Micheli, F. & Sandin, S.A., 2018. Human impacts decouple a fundamental ecological relationship. The positive association between host diversity and parasite diversity. *Global Change Biology*, 24(8): 3666–3679.

2 Sampling localities and host selection

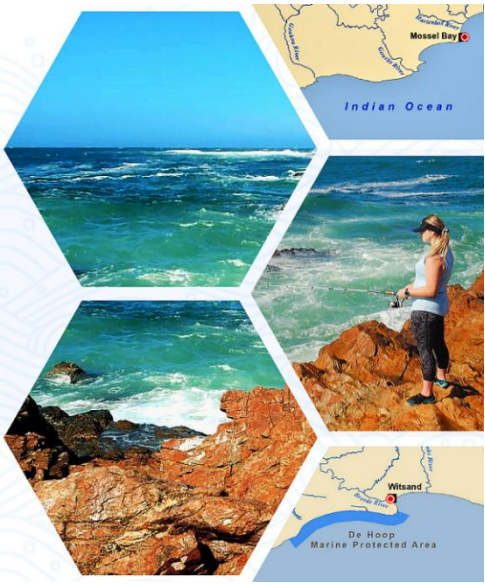

2.1 Study area/ Sampling localities

MPAs are defined as clearly demarcated marine spaces managed through legal or other effective means to achieve long-term conservation of nature, ecosystem services, and cultural values (Day *et al*., 2012). These are instrumental in reducing human pressures, supporting fisheries, and preserving marine biodiversity (Spalding *et al*., 2016). For this study, five sampling localities were selected along the southern and eastern coastlines of South Africa, representing a range of environmental conditions, anthropogenic pressures and protection statuses. The sampling design aimed to assess parasite diversity along with ecological and contaminant dynamics across a gradient of management regimes, from long-established MPAs to non-protected areas.

Sampling localities were categorised into three groups: those located within an MPA (MPA localities), those within 15 km of a qualifying MPA (near-MPA localities), and those situated beyond the influence of any qualifying MPA (non-MPA localities). This spatial arrangement was chosen to allow sufficient time for ecological responses such as pollutant attenuation, species protection, and habitat recovery, while avoiding the confounding transitional dynamics associated with recently declared MPAs (Kaplan *et al*., 2019). To ensure measurable conservation effects, only MPAs with a minimum of 10 years (Kaplan *et al*., 2019) of enforcement at the time of sampling were included under MPA localities. Following this classification, the sampling localities consisted of one locality within an established MPA (Sodwana Bay), two localities near (<10 km) established MPAs (Witsand and Chintsa East) and two outside (>15 km) established MPA boundaries (Uvongo Beach and Mossel Bay) (Figure 2.1).

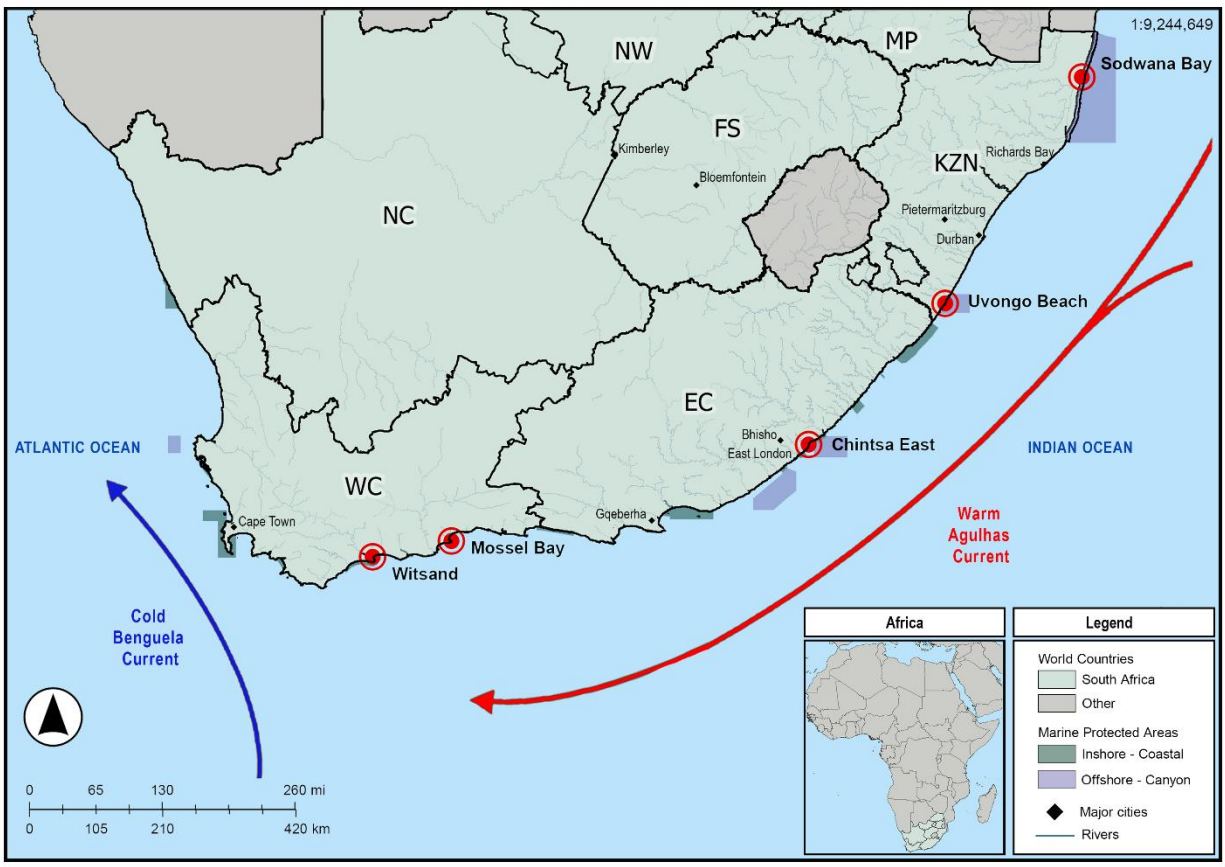

Figure 2.1: Map indicating the sampling localities (red circles) of specimens of *Amblyrhynchote honckenii* (Bloch), along the South African Coastline. Map generated by Linda de Klerk on ArcGIS Online.

Sodwana Bay (SB) (-27.539760, 32.680600), situated within the iSimangaliso Wetland Park, has been a well-established and ecologically significant MPA since 1979. As part of a UNESCO World Heritage Site, it represents one of South Africa's most iconic and well-managed marine conservation areas (UNESCO, 1999). Witsand (WS) (-34.397323, 20.837474), located at the mouth of the Breede River Estuary, is not formally within an MPA but lies approximately 7 km from the De Hoop MPA, which has been an active MPA since 1985. Witsand is considered a near-pristine locality and serves as a near-MPA reference locality due to its low levels of industrial activity (Breede River Estuarine Management Plan, 2016). Similarly, Chintsa East (CE) (-32.836538, 28.116997), located just less than 10 km from the Amathole MPA, declared in 2011, qualifies as a near-MPA site due to its proximity and relatively undisturbed condition; however, it may experience contamination from agricultural runoff and tourism (Binning and Baird, 2001). In contrast, Uvongo Beach (UB) (-30.836667, 30.395556) is considered a non-MPA locality despite its proximity to two MPAs (i.e., Protea Banks and Trafalgar), because the former was only declared in 2019 and the latter lies more than 15 km away and is positioned down current relative to UB. This locality is heavily urbanised, experiences high seasonal tourism, and is exposed to runoff

and stormwater discharges (Firth *et al*., 2023). Mossel Bay (MB) (-34.179656, 22.152093), also designated as a non-MPA locality, is situated over 75 km from any qualifying MPA and is characterised by substantial industrial activity, including proximity to a commercial harbour and known sources of pollution, such as vessel operations, fuel discharge, and urban runoff (Wepener and Degger, 2020).

Biogeographically, all localities fall within the Temperate Southern Africa marine realm as defined by the Marine Ecoregions of the World (MEOW) framework (Spalding *et al*., 2007) (Figure 2.1). More specifically, the localities span two marine provinces (Spalding *et al*., 2007): the Agulhas Province, which includes WS and MB, and the Natal Province encompassing CE, UB and SB. These ecoregions are shaped by the dynamic convergence of the cold Benguela and warm Agulhas currents (Bustamante and Branch, 1996; Turpie *et al*., 2000), resulting in a rich biodiversity. The Agulhas Bank biogeographic ecoregion is characterised by a broad, shallow continental shelf, which further supports these diverse ecosystems (Lombard *et al*., 2004; Griffiths *et al*., 2010), making them valuable for understanding regional-scale patterns in biodiversity, pollution loads, and conservation outcomes.

2.2 Host selection

A good bioindicator species should meet several key criteria: it should be sensitive to environmental changes, meaning that its health, behaviour, or parasite community composition responds to alterations in environmental conditions; it should be abundant and widespread, facilitating sampling across diverse environments and ensuring that findings are broadly applicable; and it should be easily monitored with minimal disruption to the ecosystem (Rainbow, 1995). The evileye blaasop, *A. honckenii*, meets all these criteria, with its widespread distribution across both protected and unprotected coastal regions of South Africa, its ease of identification, and its underexplored yet diverse parasite community.

Amblyrhynchote honckenii (Figure 2.2), is a common demersal pufferfish found across a variety of marine habitats, including estuarine systems, shallow reefs, and intertidal zones (Smith and Heemstra, 2012), from the southern coast of South Africa to other regions across the Indo-West Pacific, including China and the Marshall Islands (Smith and Heemstra, 2012; Froese and Pauly, 2025). Its wide geographic range and adaptability to different coastal habitats make it an ideal subject for studying ecological gradients and the effects of environmental stressors such as pollution. Additionally, *A. honckenii* can be easily identified and distinguished from other species, an essential feature for any bioindicator (Rainbow, 1995). This tetraodontid fish typically reaches lengths of 12–30 cm and is characterised by its distinctive flattened body with large, red eyes (Smith and Heemstra, 2012; Froese and Pauly, 2025) (Figure 2.2). The ability to reliably identify

the host species ensures that parasite data are consistently linked to the correct species, minimising identification errors and ensuring accurate, reproducible data collection across different localities (Rainbow, 1995). Moreover, its size and demersal lifestyle make it accessible to researchers for sampling in both shallow and deeper marine environments. This is particularly important in environmental monitoring, where accurate species identification is key to tracking ecological health over time.

Despite its abundance, *A. honckenii* remains largely understudied, particularly in terms of its ecological and parasitological roles. Its widespread occurrence across diverse environmental conditions and management regimes makes it an ideal candidate for studying spatial variation in parasite diversity and contaminant exposure. Furthermore, its scavenger feeding habits and benthic lifestyle (Smith and Heemstra, 2012) possibly enhance its exposure to benthic prey-associated parasites and sediment-bound pollutants, offering a more dynamic representation of trophic interactions and pollutant pathways than is afforded by sessile indicators.

Figure 2.2: Photograph of the fish host, *Amblyrhynchote honckenii* (Bloch), scale bar 5 cm. Photograph by Prof. Nico J. Smit.

2.3 Host collection

Using rod, reel and baited hooks, a total of 55 specimens of *A. honckenii* were collected from the five coastal localities mentioned above. Photographs of the sampling localities are shown in Figure 2.3. Fifteen individuals (13 males and two females) were sampled from WS in November 2021, while 10 individuals (eight males and two juveniles) were collected from MB during February and March 2022. Another 10 specimens (one male, eight females, and one juvenile) were obtained from the rocky shore at CE in July 2022. Ten specimens (one male and nine females) were sampled from UB in December 2022, and the remaining 10 (two males and eight females) from SB in September 2022. All fish were identified using Smith's Sea Fishes (Smith and

Heemstra, 2012), with taxonomic nomenclature following FishBase (Froese and Pauly, 2025) and Eschmeyer's Catalogue of Fishes (Fricke *et al*., 2024).

Following capture, fish were transported in aerated containers to a nearby field station for dissection. Each specimen was identified, photographed, weighed, measured, and humanely killed by percussive stunning followed by spinal severance and pithing, according to the standard operating procedure approved by the North-West University Animal Ethics Committee (NWU-00267-17-A5). Internal organs were carefully removed from each specimen for parasitological and contaminant analyses. For parasitological analysis, the organs were examined, and parasites were recovered and fixed, as detailed in Chapter 3. Material collected for contaminant analysis, including liver and muscle tissues, was processed and analysed for elements as described in Chapter 4. The methods for the processing of samples for OCP and PCB analyses are outlined in Chapter 5. Chapter 6 provides a detailed explanation of the statistics involved to analyse the factors influencing parasite community composition. The laboratory procedures for assessing Cu accumulation and MT response in infested versus uninfested *A. honckenii* are described in Chapter 7.

Ethical approval for this project was received from the AnimCare Research Ethics Committee of the North-West University (NWU-00565-19-A5). Permits for the collection of *A. honckenii* for research were issued by the South African Department of Agriculture, Forestry and Fisheries (permit nos: RES2020-29; RES2022-44; RES2022-86; and RES2025-16) and Cape Nature (permit no: CN44-87-18289).

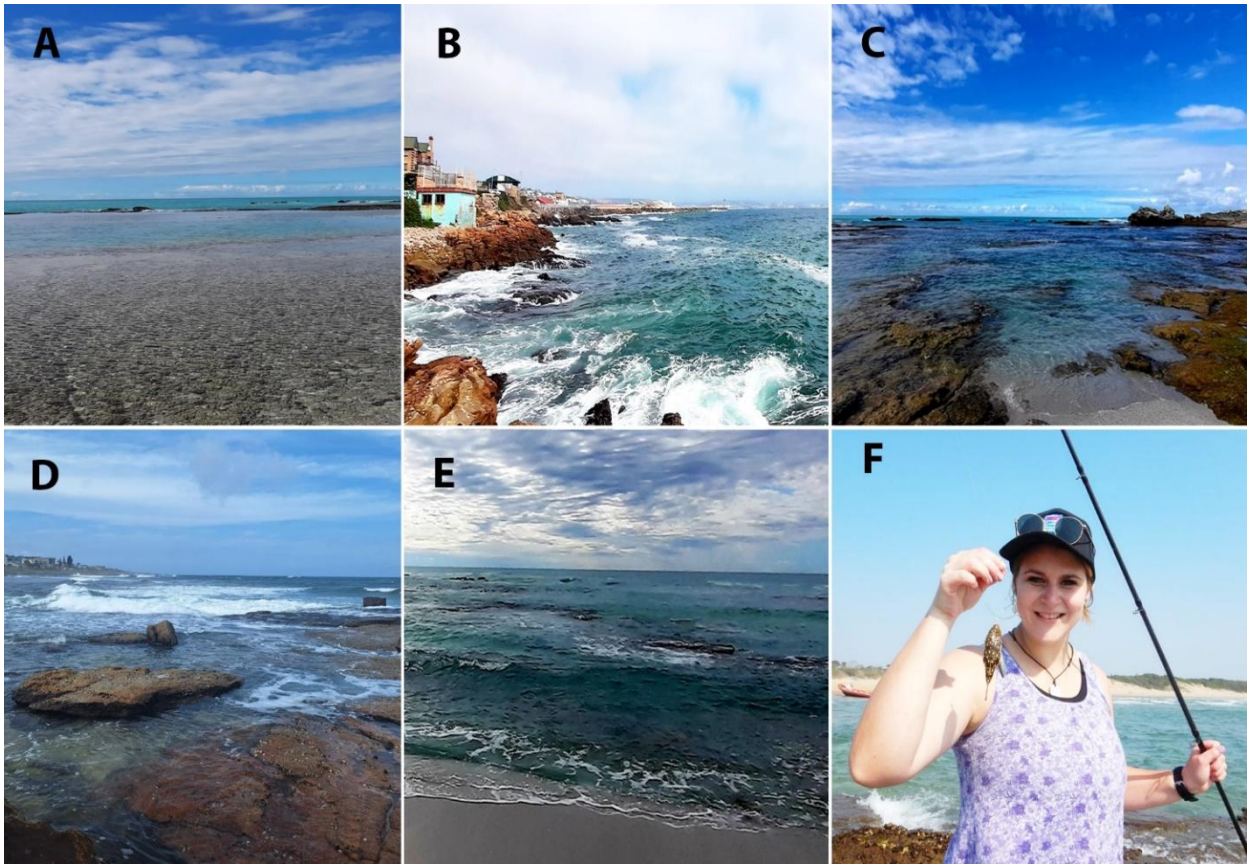

Figure 2.3: Photographs of the sampling localities. **A** – Witsand (-34.397323, 20.837474); **B** – Mossel Bay (-34.179656, 22.152093); **C** – Chintsa East (-32.836538, 28.116997); **D** – Uvongo Beach (-30.836667, 30.395556); **E** – Sodwana Bay; **F** – *Amblyrhynchote honckenii* (Bloch) specimen caught at Sodwana Bay (-27.539760, 32.680600). Photographs **A–E** by Linda de Klerk, **F** by Dr. Marliese Truter.

References

Binning, K. & Baird, D., 2001. Survey of heavy metals in the sediments of the Swartkops River Estuary, Port Elizabeth, South Africa. *Water SA*, 27(4): 461–466.

Breede River Estuarine Management Plan, 2016. Western Cape Estuary Management Framework and Implementation Strategy. SSI Environmental, 1st edition. Royal Haskoning D.H.V. (revised 2011, 2nd Edition, 2016).

Bustamante, R.H. & Branch, G.M., 1996. Large scale patterns and trophic structure of Southern African rocky shores: The roles of geographic variation and wave exposure. *Journal of Biogeography*, 23: 339–351.

Day, J., Dudley, N., Hockings, M., Holmes, G., Laffoley, D.D.A., Stolton, S. & Wells, S.M., 2012. Guidelines for applying the IUCN protected area management categories to marine protected areas. IUCN.

Firth, D.C., Auerswald, L., Strydom, P.E. & Hoffman, L.C., 2023. The status of marine mussel pollution research in South Africa (2012–2022). *Foods*, 12(21): 3983.

Fricke, R., Eschmeyer, W.N. & Van Der Laan, R. (eds), 2024. Eschmeyer's catalog of fishes: genera, species, references. Available at: http://researcharchive.calacademy.org/research/ichthyology/catalog/fishcatmain.asp. (Date of access: 8 May 2025).

Froese, R. & Pauly, D., 2025. FishBase. Available at: www.fishbase.org/search.php. (Date of access: 8 May 2025).

Griffiths, C.L., Robinson, T.B., Lange, L. & Mead, A., 2010. Marine biodiversity in South Africa: An evaluation of current states of knowledge. *PLOS ONE*, 5(8): e12008.

Kaplan, K.A., Yamane, L., Botsford, L.W., Baskett, M.L., Hastings, A., Worden, S. & White, J.W., 2019. Setting expected timelines of fished population recovery for the adaptive management of a marine protected area network. *Ecological Applications*, 29(6): e01949.

Lombard, A.T., Strauss, T., Harris, J., Sink, K., Attwood, C. & Hutchings, L., 2004. South African National Spatial Biodiversity Assessment 2004: Technical Report, Marine component. Volume 4. South African National Biodiversity Institute, Pretoria.

Rainbow, P.S., 1995. Biomonitoring of heavy metal availability in the marine environment. *Marine Pollution Bulletin*, 31(4-12): 183–192.

Smith, M.M. & Heemstra, P.C., 2012. Smith's Sea Fishes. Heidelburg, Germany: Springer Science & Business Media, pp. 1191.

Spalding, M.D, Meliane, I., Bennett, J.N., Dearden, P., Patil, G.P. & Brumbaugh, D.R., 2016. Building towards the marine conservation end-game: Consolidating the role of MPAs in a future ocean. *Aquatic Conservation: Marine and Freshwater Ecosystems*, 26: 185–199.

Spalding, M.D., Fox, H.E., Allen, G.R., Davidson, N., Ferdaña, Z.A., Finlayson, M., Halpern, B.S., Jorge, M.A., Lombana, A., Lourie, S.A., Martin, K.D., McManus, E., Molnar, J., Recchia, C.A. & Robertson, J., 2007. Marine ecoregions of the world: A bioregionalization of coastal and shelf areas. *BioScience*, 57(7): 573–583.

Turpie, J.K., Beckley, L.E. & Katua, S.M., 2000. Biogeography and the selection of priority areas for conservation of South African coastal fishes. *Biological Conservation*, 92: 59–72.

UNESCO, 1999. UNESCO. World Communication and Information 1999–2000 Report Published by United Nations Educational, Scientific and Cultural Organization.

Wepener, V.W. & Degger, N.D., 2020. Monitoring metals in South African harbours between 2008 and 2009, using resident mussels as indicator organisms. *African Zoology*, 55(4): 267–277.

3 Metazoan parasite diversity of *Amblyrhynchote honckenii* (Bloch), along the South African coastline

3.1 Introduction

Metazoan parasites represent ecologically significant, yet often overlooked, components of marine biodiversity. As regulators of host populations and indicators of ecosystem health, they contribute to key ecological processes including food web dynamics and energy transfer (Hudson *et al*., 2006; Adlard *et al*., 2015; Smit and Sures, 2025). Despite their importance, our understanding of marine parasite diversity, particularly in biogeographically complex regions like South Africa, remains limited due to insufficient baseline data (Smit and Hadfield, 2015).

South Africa's marine environment, where the cold Benguela Current and warm Agulhas Current converge, forms a dynamic marine ecotone, characterised by high species richness and endemism, supporting one of the richest marine biodiversity zones globally (Griffiths *et al*., 2010; Sell *et al*., 2024). While over 1,960 marine fish species are known from off South Africa (Froese and Pauly, 2025), parasitological studies in this region have been largely opportunistic and taxonomically narrow, focusing primarily on conspicuous crustacean ectoparasites, such as isopods and copepods (Smit and Hadfield, 2015). Other important groups, such as monopisthocotyleans, polyopisthocotyleans, cestodes, and acanthocephalans, remain comparatively under-described (Smit and Hadfield, 2015; Schaeffner and Smit, 2019). As a result, our current understanding of the broader metazoan parasite diversity in many native fish hosts is incomplete, leaving major gaps in our knowledge of parasite-host interactions.

This study aims to enhance our knowledge of the parasite fauna associated with the evileye blaasop, *A. honckenii*, a native tetraodontid fish distributed along the southern African

coastline. Although this species is not of commercial importance, *A. honckenii* has been documented to host a diverse, and in some cases, highly specialised parasite fauna, including the cymothoid isopod *Cinusa tetrodontis* (Hadfield *et al*., 2010), the caligid copepod *Caligus tetrodontis* Barnard, 1948 (Hayes *et al*., 2021), the ergasilid copepods, *Ergasilus arenalbus* van der Spuy, Narciso, Hadfield, Wepener & Smit, 2024 and *E. chintensis* van der Spuy, Narciso, Hadfield, Wepener & Smit, 2024 (Van Der Spuy *et al*., 2025), the haemogregarine *Haemogregarina koppiensis* Smit & Davies, 2001 (Smit and Davies, 2001), the acanthocephalan *Rhadinorhynchus gerberi* Lisitsyna, Kudlai, Cribb & Smit, 2019 (Lisitsyna *et al*., 2019), the polyopisthocotylean, *Heterobothrium victorwepeneri* Acosta & Smit, 2021 (Acosta and Smit, 2021), and the digenean *Pseudoheterolebes cotylophorus* (Ozaki, 1935) Yamaguti, 1959 (Bray, 1986).

In contrast to the limited work on South African tetraodontids, pufferfish in Japan, particularly species in the genus *Takifugu* Abe, are among the most thoroughly studied fish hosts for metazoan parasites worldwide (see Ogawa and Inouye, 1997; Park and Park, 2006; Ogawa *et al*., 2007; Ogawa and Itoh, 2022). Notably, the commercially significant tiger pufferfish, *Takifugu rubripes* (Temminck & Schlegel), has been reported to host at least 18 described metazoan parasite species, based on comprehensive aquaculture and parasitological surveys (Ogawa and Inouye, 1997; Ogawa *et al*., 2007; Ogawa and Itoh, 2022). These include several well-documented monopisthocotyleans such as *Udonella caligorum* (Yamaguti, 1958) and *Neobenedenia girellae* (Hargis, 1955), and polyopisthocotylean species of *Heterobothrium* Cerfontaine, 1895 such as *Heterobothrium gotoi* Ogawa & Itoh, 2022, *H. tabetai* Ogawa & Itoh, 2022, *H. aljufailiae* Ogawa & Itoh, 2022, *H. iwatai* Ogawa & Itoh, 2022, and *H. matsubarai* Ogawa & Itoh, 2022, as well as parasitic copepods such as *Pseudocaligus fugu* Yamaguti, 1936 and *Caligus fugu* (Yamaguti, 1936), acanthocephalans like *Pomphorhynchus pagrosomi* (Yamaguti, 1935), Zhao, Chen, Wayland, Yang, Gu & Li, 2025, along with blood flukes represented by species of *Paradeontacylix* McIntosh, 1934 (Ogawa and Inouye, 1997; Park and Park, 2006; Ogawa *et al*., 2007; Ogawa and Itoh, 2022). Ongoing research continues to reveal new parasite species from Japanese puffers. For example, the five new species of *Heterobothrium* were described from *Takifugu* hosts as recently as 2022 (Ogawa and Itoh, 2022). These parasites are well-characterised in terms of their life cycles, pathogenicity, and aquaculture relevance. This extensive literature has not only advanced aquaculture health management but also provided a model for studying host-parasite ecology and evolution (Ogawa and Inouye, 1997). By contrast, *A. honckenii* remains vastly underexplored, underscoring the need for systematic surveys of non-commercial but ecologically valuable species in Africa. Although a few recent studies have described parasites from this species in South Africa (e.g. Acosta & Smit, 2021; Smit & Hadfield, 2022; Van Der Spuy *et al.*, 2025), comparable parasitological work on other African pufferfish is

virtually absent, and the parasite fauna of most species across the continent remains undescribed.

Establishing baseline data on the parasite diversity of *A. honckenii* is critical for multiple reasons. Documenting host-specific or endemic parasite species can reveal evolutionary histories and co-adaptation, offering insight into host-parasite coevolution (Hoberg *et al*., 1997; Lymbery and Smit, 2023). Additionally, parasites can serve as indicators of host ecology, behaviour, and environmental conditions, and understanding their presence and diversity is essential for ecosystem-level assessments (Timi and Poulin, 2020). Baseline data, therefore, allow us to detect changes over time, due to climate change, fishing pressure, or MPA implementation, and provide foundational knowledge necessary for conservation planning (Wood *et al*., 2010; 2013). These foundational datasets are increasingly important for supporting emerging technologies such as environmental DNA (eDNA) monitoring. As noted by Hupalo *et al*. (2025), without prior knowledge of the metazoan parasite community, eDNA signals cannot be accurately interpreted or validated, reducing their effectiveness for biodiversity assessment and early detection of ecological change.

Due to the limited historical sampling and taxonomic effort directed at non-commercial fish species in South Africa, it is hypothesised that *A. honckenii* hosts a greater diversity of metazoan parasites than currently documented, including undescribed or regionally rare taxa, reflecting potentially host-specific associations (Hypothesis 1, Chapter 1). Furthermore, this diversity may reflect host-specific associations not yet recorded elsewhere. By establishing a baseline inventory of *A. honckenii*'s parasite community, this chapter contributes critical data to the broader understanding of marine parasite diversity in South Africa. These findings support future research into ecological, evolutionary, and conservation dynamics and lay the groundwork for integrating parasitological knowledge into broader marine biodiversity frameworks.

3.2 Materials and methods

3.2.1 Parasite collection

Fish hosts were collected and humanely killed following the ethical and procedural protocols detailed in Chapter 2. All external and internal organs, including the gills, eyes, fins, liver, gonads, intestines, spleen, gallbladder, heart, and brain, were removed using dissection tools. Each internal organ was individually transferred into a petri dish containing a saline solution to maintain osmotic balance and reduce stress on any live parasites present, while external organs, such as the gills, were kept in water from the collection locality (Panikkar and Sproston, 1941; Scholz *et al*., 2018). This approach was chosen to closely simulate the natural microhabitats that various parasites occupy within or on the host. As noted by Scholz *et al*. (2018), recreating such environmental conditions during initial screening enhances the likelihood of detecting viable,

motile parasites and allows for more accurate observations of their morphology and behaviour. Careful handling at this stage was critical to preserving parasite integrity for subsequent identification and classification.

Detailed parasitological screening was carried out using a Zeiss Stemi 305 stereomicroscope (Zeiss, Oberkochen, Germany). Each organ was screened, and parasites were categorised into morphotypes primarily based on movement, shape, and site of infection. Parasites observed were removed using precision tools such as fine-tipped brushes or needles to minimise structural damage. Following the taxon-specific protocols outlined by Scholz *et al.* (2018), each specimen was processed and preserved in individually labelled 2–5 mL Eppendorf tubes. The preservation medium, method of relaxation, and storage conditions varied according to parasite group to optimise their morphological and molecular integrity for later analyses.

From the buccal cavity, cymothoid isopods of the genus *Cinusa* Schioedte & Meinert, 1884, were extracted and promptly frozen at −20°C for element analyses. Ectoparasites from the fins and external body surfaces, including copepods of the genus *Caligus* Müller O.F., 1785, were preserved in 80% ethanol for morphological studies and 96% for DNA extraction and molecular analyses. Gill-associated parasites were treated with taxon-specific handling procedures. Copepods of the genus *Ergasilus* von Nordmann, 1832, were fixed in 80% and 96% ethanol, while monopisthocotyleans and polyopisthocotyleans were first relaxed in near-boiling saline to allow full extension of body structures, then fixed in 80% ethanol. Trematode metacercariae (family Bucephalidae), isolated from the eyes and heart, were manually excysted using fine needles and preserved in 96% ethanol to ensure DNA viability for molecular analyses. Other trematodes and cestodes from the intestinal tract were also relaxed in heated saline to fully extend their bodies before fixation in 80% ethanol, aiding in subsequent morphological and molecular examination. Nematodes removed from the liver and intestinal tract followed a similar relaxation and preservation procedure, ensuring accurate visualisation of cuticular features and internal anatomy. Acanthocephalans, primarily located in the intestinal tract and occasionally the spleen, were carefully detached from host tissue using fine needles. To facilitate full eversion of the proboscis, specimens were placed in tap water within a refrigerator overnight. Once fully everted and relaxed, they were fixed in 80% ethanol for further analysis. This carefully standardised multi-step approach across all organ systems and parasite taxa ensured that all specimens were preserved in a state suitable for both morphological identification and molecular characterisation.

2.2.2 Parasite identification

Morphological analyses

All parasites were morphologically examined using standard taxon-specific procedures to preserve diagnostic features for accurate identification. Specimens were either temporarily mounted or permanently mounted on microscope slides, depending on their structure and analytical needs. All parasite imaging was conducted using Nikon ECLIPSE Ni and 80i light microscopes equipped with a Nikon Y-TV55 camera (Nikon Instruments, Tokyo, Japan). Scanning electron microscopy (SEM) was done with the aid of a FEI Nova NanoSEM 450. All measurements obtained were carried out using Image-Pro Express software (Nikon), and all drawings were made using a drawing tube attached to a Nikon ECLIPSE Ni microscope (Nikon). Final photo plates and illustrations were digitised in Adobe Photoshop v23.0.1.

Cymothoid isopods (*Cinusa* sp.) from the buccal cavity were morphologically examined and identified under a stereomicroscope before freezing at −20°C. No staining or mounting was required, and identification was based on external morphology, as described by Hadfield *et al*. (2010). Copepods (*Caligus* sp.) collected from the fins and external body surfaces were rehydrated in distilled water, cleared in lactophenol, and temporarily mounted onto slides (wet mounts) for microscopic observation. Copepods (*Ergasilus* spp.) collected from the gills were processed following Van Der Spuy *et al*. (2025). Specimens were cleared in lactic acid, dissected, and temporarily mounted in glycerine. Morphometric measurements and photomicrographs were obtained with the above-mentioned microscopes and software packages. Terminology followed Boxshall and Montú (1997), with measurements summarised in tabular form. Additional specimens were used for SEM. Following surface cleaning, specimens were dehydrated, treated with hexamethyldisilazane (HMDS), mounted on carbon tape, and sputter-coated with carbon and gold/palladium (Van Der Spuy *et al*., 2025). Key morphological features were photographed for comparative analysis (Van Der Spuy *et al*., 2025). Monopisthocotyleans and polyopisthocotyleans were processed according to their genus. *Heterobothrium* specimens were rehydrated, stained with Delafield's Haematoxylin, destained in 1% hydrochloric acid, dehydrated to 70% ethanol, cleared in clove oil, and permanently mounted on microscope slides in Canada balsam (Van Der Spuy *et al*., 2020). For *Udonella* sp., the method by Freeman and Ogawa (2010) was followed with minor adaptations. Specimens were stained with aceto-carmine, cleared in methyl salicylate, and permanently mounted. Trematode metacercariae (family Bucephalidae) from the eyes and heart were rehydrated and mounted onto microscope slides for temporary observations. Trematodes from the intestinal tract were stained with Mayer's Haematoxylin. Specimens were destained with 1% hydrochloric acid, neutralised in ammonia, dehydrated through a graded ethanol series, cleared in methyl salicylate, and permanently mounted in Canada balsam. Morphological identification followed Martin *et al*. (2018), with measurements summarised in

tabular form. Cestodes from the intestinal tract were processed following Van Der Spuy *et al*. (2020). After rehydration and staining with Delafield's Haematoxylin, specimens were destained, dehydrated to 70% ethanol, cleared in clove oil, and permanently mounted in Canada balsam. Morphological structures were documented microscopically and digitally recorded. Nematodes recovered from the intestinal tract and liver were processed according to Svitin *et al*. (2019). Specimens were placed in distilled water for 20 min, cleared in lactophenol and temporarily mounted for observation. Internal and external features were recorded and photographed. Acanthocephalans from the intestinal tract and spleen were rehydrated and observed as wet mounts. All voucher specimens and associated images are archived in the parasite reference collection of the Water Research Group, North-West University, Potchefstroom, South Africa.

Genetic analyses

For molecular characterisation of parasite species, DNA was extracted from selected specimens representing each taxonomic group. For copepods (*Caligus* sp. and *Ergasilus* sp.), genomic DNA was extracted specifically from egg strings, following the method described by Van Der Spuy *et al.* (2025). This protocol employed the Macherey-Nagel NucleoSpin® Tissue Kit (Macherey-Nagel GmbH & Co. KG, Sandton, South Africa), with two modifications: a 4-hour pre-lysis incubation step and the addition of 50% more buffer BE, as recommended in Van Der Spuy *et al.* (2025). For all other parasite taxa, DNA was extracted using the PCR-Biosystems Rapid DNA Extraction Kit, following the manufacturer's instructions with minor adjustments. Each extraction used 10 µL of lysis buffer and 5 µL of a proteinase K-containing buffer, and the resulting DNA solution was diluted to a final volume of 300 µL to ensure a sufficient yield for multiple applications.

Gene amplification targeted both nuclear and mitochondrial markers. Specifically, internal transcribed spacer 2 (ITS2), partial 18S, and 28S regions of ribosomal DNA (rDNA), as well as the cytochrome c oxidase subunit I (COI) and NADH dehydrogenase subunit 1 (nad1) regions of mitochondrial DNA (mtDNA), were amplified using taxon-specific primers. Details of the primer sets and their thermocycling conditions are provided in Table 3.1. Amplification success was verified through electrophoresis on 1% agarose gels stained with a SafeView™ Classic. Verified PCR products were submitted to Inqaba Biotechnical Industries (Pty) Ltd. (Pretoria, South Africa) for purification and sequencing. Raw sequence data were assembled, quality-checked, and edited in Geneious Prime v2024.0.7 (Biomatters, Auckland, New Zealand). Sequences were aligned using the MAFFT v7.490 plugin (Katoh *et al*., 2002; Katoh and Stanley, 2013) under default settings in the Geneious platform. Alignments were further trimmed and edited for phylogenetic analyses.

Table 3.1: List of primers used, and the protocols followed for the amplification of the genomic DNA of metazoan parasites collected from *Amblyrhynchote honckenii* (Bloch).

Locus	Taxon	Primer	Sequence	Reference	Protocol
ITS2	Trematoda	3S	5'-GGTACCGGTGGATCACGTGGCTAGTG-3'	Morgan and Blair (1995)	Yong *et al*. (2016)
		ITS2.2	5'-CCTGGTTAGTTTCTTTTCCTCCGC-3'	Cribb *et al*. (1998)	
18S	Acanthocephala	18SU467F	5'-ATCCAAGGAAGGCAGCAGGC-3'	Suzuki *et al*. (2006)	Lisitsyna, *et al*. (2019)
		18SL1310R	5'-CTCCACCAACTAAGAACGGC-3'	Suzuki *et al*. (2006)	
	Copepoda	18SF	5'-AAGGTGTGMCCTATCAACT-3'	Song *et al*., (2008)	Van Der Spuy *et al*. (2025)
		18SR	5'-TTACTTCCTCTAAACGCTC-3'	Song *et al*., (2008)	
	Nematoda	18SU467F	5'-ATCCAAGGAAGGCAGCAGGC-3'	Suzuki *et al*. (2006)	Svitin *et al*. (2019)
		18SL1310R	5'-CTCCACCAACTAAGAACGGC-3'	Suzuki *et al*. (2006)	
	Monopisthocotyla	18S F-INT	5'-CTATTGGAGGGCAAGTCTGG-3'	Prikrylová *et al*. (2013)	Prikrylová *et al*. (2013)
		18S R-INT	5'-CCGAACATCTAAGGCATCA-3'	Prikrylová *et al*. (2013)	
		SSUF	5'-GATCCTTCTGCAGGTTCACCTAC-3'	Cunningham *et al*. (1995)	
		SSUR	5'-AAGCTGGTTGATCCTGCCAGT-3'	Cunningham *et al*. (1995)	
28S	Acanthocephala	LSU5	5'-TAGGTCGACCCGCTGAAYTTAAGCA-3'	Littlewood, (1994)	Lisitsyna, *et al*. (2019)
		1200R	5'-GCTATCCTGAGGGAAACTTCG-3'	Lockyer *et al*. (2003)	
	Copepoda	28SF	5'-ACAACTGTGATGCCCTTAG-3'	Song *et al*. (2008)	Van Der Spuy *et al*. (2025)
		28SR	5'-TGGTCCGTGTTTCAAGACG-3'	Song *et al*. (2008)	
	Nematoda	CTEf	5'-AGTGAATGGGGAAAAGCCCA-3'	Svitin *et al*. (2019)	Svitin *et al*. (2019)
		CTEr	5'-GGACCTCCACCAGAGTTTCC-3'	Svitin *et al*. (2019)	
	Cestoda	LSU5	5'-TAGGTCGACCCGCTGAAYTTAAGCA-3'	Littlewood (1994)	Tkach *et al*. (2003)
		1200R	5'-GCTATCCTGAGGGAAACTTCG-3'	Lockyer *et al*. (2003)	

Table 3.1: Continued.

Locus	Taxon	Primer	Sequence	Reference	Protocol
28S	Monopisthocotyla	L1200R	5'-GCATAGTTCACCATCTTTCGG-3'	Littlewood *et al*. (2000)	Acosta and Smit (2021)
		U178	5'-GCACCCGCTGAAYTTAAG-3'	Lockyer *et al*. (2003)	
		L1642	5'-CCAGCGCCATCCATTTTCA-3'	Lockyer *et al*. (2003)	
	Polyopisthocotyla	L1200R	5'-GCATAGTTCACCATCTTTCGG-3'	Littlewood *et al*. (2000)	Acosta and Smit (2021)
		U178	5'-GCACCCGCTGAAYTTAAG-3'	Lockyer *et al*. (2003)	
		L1642	5'-CCAGCGCCATCCATTTTCA-3'	Lockyer *et al*. (2003)	
	Trematoda	LSU5	5'-TAGGTCGACCCGCTGAAYTTAAGCA-3'	Littlewood (1994)	Yong *et al*. (2016)
		300F	5'-CAAGTACCGTGAGGGAAAGTTG-3'	Littlewood *et al*. (1999)	
		ECD2	5'-CCTTGGTCCGTGTTTCAAGACGGG-3'	Littlewood *et al*. (1997)	
		1500R	5'-GCTATCCTGAGGGAAACTTCG-3'	Snyder and Tkach (2001)	
COI	Acanthocephala	LCO1490	5'-GGTCAACAAATCATAAAGATATTGG-3'	Folmer *et al*. (1994)	Van Der Spuy *et al*. (2025)
		HCO2198	5'-TAAACTTCAGGGTGACCAAAAAATCA-3'	Folmer *et al*. (1994)	
	Copepoda	LCO1490	5'-GGTCAACAAATCATAAAGATATTGG-3'	Folmer *et al*. (1994)	Van Der Spuy *et al*. (2025)
		HCO2198	5'-TAAACTTCAGGGTGACCAAAAAATCA-3'	Folmer *et al*. (1994)	
	Polyopisthocotyla	LCO1490	5'-GGTCAACAAATCATAAAGATATTGG-3'	Folmer *et al*. (1994)	Van Der Spuy *et al*. (2025)
		HCO2198	5'-TAAACTTCAGGGTGACCAAAAAATCA-3'	Folmer *et al*. (1994)	
	Trematoda	Digcox1Fa	5'-ATGATWTTYTTYTTYYTDATGCC-3'	Wee *et al*. (2017)	Vermaak *et al*. (2023)
		Digcox1R	5'-TCNGGRTGHCCRAARAAYCAAAA-3'	Wee *et al*. (2017)	
		DICE1F	5'-ATTAACCCTCACTAAATTWCNTTRGATCATAAG-3'	Moszczynska *et al*. (2009)	Wee *et al*. (2017)
		DICE14R	5'-TAATACGACTCACTATACCHACMRTAAACATATGATG-3'	Van Steenkiste *et al*. (2015)	

Table 3.1: Continued.

Locus	Taxon	Primer	Sequence	Reference	Protocol
NAD1	Trematoda	NDJ11	5'-AGATTCGTAAGGGGCCTAATA-3'	Kostadinova *et al*. (2003)	Kostadinova *et al*. (2003)
		NDJ2a	5'-CTTCAGCCTCAGCATAAT-3'	Kostadinova *et al*. (2003)	

To confirm species-level identification and guide outgroup selection, the Basic Local Alignment Search Tool (BLAST) was used to compare each sequence against reference sequences available in the NCBI GenBank database (see Supplementary Table S3.1). Genetic divergence between sequences was calculated within Geneious Prime, with results presented as percentage similarity and base-pair differences. The best-fitting nucleotide substitution model for each dataset was determined using the Akaike Information Criterion (AIC) implemented in jModelTest v2.1.4 (Posada, 2008; Darriba *et al*., 2012). These models informed both Maximum Likelihood (ML) and Bayesian Inference (BI) phylogenetic analyses. Bayesian analyses were conducted via the CIPRES Science Gateway v3.3 (Miller *et al*., 2010) using MrBayes v3.2.7a (Ronquist *et al*., 2012). Two independent runs of four Markov Chain Monte Carlo (MCMC) chains were performed for 10 million generations, with sampling every 1,000 generations and a burn-in of the first 25,000 generations. ML analyses were performed in PhyML v3.0 (Guindon *et al*., 2010) on the ATGC bioinformatics platform, with model parameters estimated from the dataset and 1,000 bootstrap replicates used to assess nodal support. Resulting phylogenetic trees were visualised and annotated using TreeViewer v2.2.0 (Bianchini and Sánchez-Baracaldo, 2024). Final trees were evaluated for congruence between ML and BI topologies and used to support species-level identification and assess interspecific relationships.

3.2.3 Statistical analyses

Parasitic infection patterns in *A. honckenii* were analysed using descriptive statistics to quantify parasite burdens along the South African coastline. The primary metrics calculated were prevalence of infection (P), abundance (A), and mean intensity of infection (MI), following Bush *et al*. (1997). Prevalence represents the proportion of hosts infected by at least one parasite species, providing a general indication of infection occurrence within the host population (Bush *et al*., 1997). Mean abundance reflects the average number of parasites per host, including uninfected individuals, while mean intensity describes the average number of parasites among only the infected hosts (Bush *et al*., 1997).

3.3 Results

3.3.1 General results

A total of 55 *A. honckenii* specimens were collected at five localities along the coast of South Africa. Twenty-two distinct metazoan parasite species were collected from five subsets of 10–15 specimens of *A. honckenii* measuring 85–185 mm in total length, 40–155 mm in standard length and 11–140 g in weight (Table 3.2).

A total of 22 metazoan parasite taxa, representing four phyla and eight classes, were identified. These included two acanthocephalans (*Pomphorhynchus* sp. and *R. gerberi*), five crustaceans, including the cymothoid isopod *Cin. tetrodontis* and three copepods (*Cal. tetrodontis*, *E. arenalbus*, *E. chintensis*), five nematodes (*Anisakis simplex* (Rudolphi, 1809) Dujardin, 1845, *Dichelyne (Cucullanellus) szidati* Timi & Sardella, 2002*, Dichelyne (Cucullanellus)* sp., Physalopteridae gen. sp., *Raphidascaris* sp.), four cestodes [*Acanthobothrium* sp., *Scyphophyllidium* sp., *Kotorella pronosoma* (Stossich, 1901) Euzet & Radujkovic, 1989, and *Nybelinia* sp. Poche, 1926], one monopisthocotylean (*Udonella australis* Carvajal & Sepulveda, 2002) and one polyopisthocotylean (*H. victorwepeneri*), and five trematodes (including *Rhipidocotyle* sp. Diesing, 1858, Bucephalidae gen. sp., *Helicometrina* sp., *Opistholebes amplicoelus* Nicoll, 1915, and Zoogonidae gen. sp.). Of these, 14 were classified as heteroxenous taxa, involving two or more hosts in their life cycles, while the remaining eight displayed monoxenous (direct) life cycles. Several taxa represent new geographic or host records, with some likely representing undescribed species. In total, 3,894 individual parasites were recovered (Table 3.3).

Table 3.2: Summary of the total length, standard length, and body weight of *Amblyrhynchote honckenii* (Bloch), as well as the number of metazoan parasite individuals and species recorded at each sampling locality along the South African coastline. Abbreviations: **WS** – Witsand, **MB** – Mossel Bay; **CE** – Chintsa East; **UB** – Uvongo Beach; **SB** – Sodwana Bay. Measurements are presented as the mean, followed by the standard deviation.

Locality	Host information				Parasite information	
	Total length (mm)	Standard length (mm)	Weight (g)	Male/ female	No. of individuals	No. of species
WS	154 ± 13	127 ± 12	80 ± 24	13/ 2	16 ± 8	4 ± 2
MB	109 ± 7	89 ± 6	28 ± 8	8/ 2	199 ± 146	3 ± 1
CE	114 ± 18	92 ± 14	29 ± 14	2/ 9	12 ± 7	4 ± 1
UB	131 ± 9	97 ± 21	52 ± 16	1/ 9	97 ± 70	2 ± 1
SB	119 ± 16	97 ± 16	53 ± 18	2/ 8	57 ± 56	3 ± 1

Table 3.3: List of the metazoan parasites infecting *Amblyrhynchote honckenii* (Bloch) along the coast of South Africa. The life stage and abundance of specimens collected are indicated for each locality. Abbreviations: **WS** – Witsand, **MB** – Mossel Bay; **CE** – Chintsa East; **UB** – Uvongo Beach; **SB** – Sodwana Bay; **HA** – heteroxenous life cycle, adult specimen; **MA** – monoxenous life cycle, adult specimen; **HL** – heteroxenous life cycle, larval specimen.

	Species identification	Life stage	Abundance				
			WS	MB	CE	UB	SB
Phylum Rotifera, Clade Acanthocephala							
Class Palaeacanthocephala							
1	*Order:* Echinorhynchida *Family:* Pomphorhynchidae *Genus: Pomphorhynchus* Monticelli, 1905 ***Pomphorhynchus* sp.**	HA	-	-	14	-	-
2	*Order:* Echinorhynchida *Family:* Rhadinorhynchidae *Genus: Rhadinorhynchus* Lühe, 1911 ***Rhadinorhynchus gerberi*** Lisitsyna, Kudlai, Cribb & Smit, 2019	HA	-	-	-	-	53
Phylum Arthropoda							
Class Malacostraca							
3	*Order:* Isopoda *Family:* Cymothoidae *Genus: Cinusa* Schioedte & Meinert, 1884 ***Cinusa tetrodontis*** Schioedte & Meinert, 1884	MA	16	18	-	-	-
Class Copepoda							
4	*Order:* Siphonostomatoida *Family:* Caligidae *Genus: Caligus* Müller O.F., 1785 ***Caligus tetrodontis*** Barnard, 1948	MA	27	36	3	-	-
5	*Order:* Cyclopoida *Family:* Ergasilidae *Genus: Ergasilus* von Nordmann, 1832 ***Ergasilus arenalbus*** van der Spuy, Narciso, Hadfield, Wepener & Smit, 2024	MA	151	-	-	-	-
6	*Order:* Cyclopoida *Family:* Ergasilidae *Genus: Ergasilus* von Nordmann, 1832 ***Ergasilus chintensis*** van der Spuy, Narciso, Hadfield, Wepener & Smit, 2024	MA	-	-	3	1	-
Phylum Nematoda							
Class Chromadorea							
7	*Order:* Rhabditida *Family:* Anisakidae *Genus: Anisakis* Dujardin, 1845 ***Anisakis simplex*** (Rudolphi, 1809) Dujardin, 1845	HL	6	-	-	-	-
8	*Order:* Rhabditida *Family:* Cucullanidae *Genus: Dichelyne* Jägerskiöld, 1902 ***Dichelyne (Cucullanellus) szidati*** Timi & Sardella, 2002	HA	-	1	1	-	-

Table 3.3: Continued.

Species identification		Life stage	Abundance				
			WS	MB	CE	UB	SB
9	*Order:* Rhabditida *Family:* Cucullanidae *Genus: Dichelyne* Jägerskiöld, 1902 ***Dichelyne (Cucullanellus)* sp.**	HA	-	-	-	2	-
10	*Order:* Rhabditida *Family:* Physalopteridae **Physalopteridae gen. sp.**	HL	-	-	-	-	3
11	*Order:* Rhabditida *Family:* Raphidascarididae *Genus: Raphidascaris* Railliet & Henry, 1915 ***Raphidascaris* sp.**	HL	2	-	-	-	-
Phylum Platyhelminthes							
Class Cestoda							
12	*Order:* Onchoproteocephalidea *Family:* Onchobothriidae *Genus: Acanthobothrium* Blanchard, 1848 ***Acanthobothrium* sp.**	HL	-	-	-	3	-
13	*Order:* Phyllobothriidea *Family:* Phyllobothriidae *Genus: Scyphophyllidium* Woodland, 1927 ***Scyphophyllidium* sp.**	HL	10	-	4	-	310
14	*Order:* Trypanorhyncha *Family:* Tentaculariidae *Genus: Kotorella* Euzet & Radujkovic, 1989 ***Kotorella pronosoma*** (Stossich, 1901) Euzet & Radujkovic, 1989	HL	-	-	1	6	5
15	*Order:* Trypanorhyncha *Family:* Tentaculariidae *Genus: Nybelinia* Poche, 1926 ***Nybelinia* sp.**	HL	10	-	-	-	-
Class Monopisthocotyla							
16	*Order:* Gyrodactylidea *Family:* Udonellidae *Genus: Udonella* Johnston, 1835 ***Udonella australis*** Carvajal & Sepulveda, 2002	MA	-	12	-	-	-
Class Polyopisthocotyla							
17	*Order:* Mazocraeidea *Family:* Diclidophoridae *Genus: Heterobothrium* Cerfontaine, 1895 ***Heterobothrium victorwepeneri*** Acosta & Smit, 2021	MA	3	-	6	14	-
Class Trematoda							
18	*Order:* Plagiorchiida *Family:* Bucephalidae *Genus: Rhipidocotyle* Diesing, 1858 ***Rhipidocotyle* sp.**	HL	17	-	13	947	-
19	*Order:* Plagiorchiida *Family:* Bucephalidae **Bucephalidae gen. sp.**	HL	-	1919	1	-	30

Table 3.3: Continued.

	Species identification	Life stage	Abundance				
			WS	MB	CE	UB	SB
20	*Order:* Plagiorchiida *Family:* Opecoelidae *Genus: Helicometrina* Linton, 1910 ***Helicometrina* sp.**	HL	-	-	-	-	1
21	*Order:* Plagiorchiida *Family:* Opecoelidae *Genus: Opistholebes* Nicoll, 1915 ***Opistholebes amplicoelus*** Nicoll, 1915	HA	5	-	13	-	-
22	*Order:* Plagiorchiida *Family: Zoogonidae* **Zoogonidae gen. sp.**	HL	-	1	61	-	167

3.3.2 Morphological and molecular characterisation of metazoan parasites

3.3.2.1 Phylum Rotifera, Clade Acanthocephala

Acanthocephala comprises obligate thorny-headed endoparasitic worms that typically inhabit the gastrointestinal tract of aquatic vertebrates, especially teleost fishes (Amin, 2013; Sures *et al*., 2025). In South African marine ecosystems, acanthocephalans remain understudied, with only a few species formally described (Lisitsyna *et al*., 2019). Historically, records of marine acanthocephalans in South Africa have been limited to three articles. The first was by Dollfus and Golvan (1963), who described *Pomphorhynchus chabanaudi* (Dollfus & Golvan, 1963), Zhao, Chen, Wayland, Yang, Gu & Li, 2025, from marine fish hosts, and the second was by Bray (1974), who added *Rhadinorhynchus capensis* Bray, 1974, to the known regional fauna. More recently, Lisitsyna *et al*. (2019) expanded this knowledge with the formal description of *R. gerberi*, parasitising *A. honckenii* in SB. To date, *R. gerberi* remains the only acanthocephalan species confirmed from *A. honckenii*. The current study adds to this baseline by reporting two acanthocephalan taxa: *Pomphorhynchus* sp., recovered from CE, and *R. gerberi*, reconfirmed from SB. The occurrence of *Pomphorhynchus* in a marine tetraodontid host is especially significant, as no species of this genus has been previously reported from marine pufferfish. These findings therefore expand both the known host associations and geographic range of marine acanthocephalans along the South African coastline, highlighting the need for continued parasitological surveys in underexplored habitats.

***Pomphorhynchus* sp.**

A total of 14 specimens were identified as *Pomphorhynchus* sp. Identification was limited to the genus level, as this represents the first known record of *Pomphorhynchus* in this host species. The precise species affiliation remains uncertain; however, preliminary morphological and genetic analyses suggest that the specimens may represent a previously undescribed species. As the associated manuscript is still in preparation and has not yet been published, this

chapter will refer to the taxon as *Pomphorhynchus* sp., with the full taxonomic classification and summary as follows:

Class: Palaeacanthocephala
Order: Echinorhynchida
Family: Pomphorhynchidae
Genus: *Pomphorhynchus* Monticelli, 1905
Species: Unknown
Present host: *Amblyrhynchote honckenii (Bloch)*
Present locality: Chintsa East, South Africa
Site of infection: Intestine and Spleen
Prevalence (P): 40%
Mean intensity (MI): 3.5
Life stage: Adult
Representative DNA sequences: One sequence for 18S rDNA, two sequences for 28S rDNA, and two sequences for COI mtDNA
Voucher material: Four specimens fixed on slides (Figure 3.1A) and 10 specimens fixed in ethanol (Figure 3.1B) are kept in the collection of the Water Research Group (WRG) at the North-West University (NWU), Potchefstroom, South Africa

The family Pomphorhynchidae comprises three genera, including *Paralongicollum* Amin, Bauer & Sidorov, 1991, *Pomphorhynchus* Monticelli, 1905, and *Tenuiproboscis* Yamaguti, 1935 (WoRMS, 2025). Species of the family Pomphorhynchidae are morphologically diverse, particularly in neck and proboscis structure, which has historically guided taxonomic placement. However, recent molecular studies challenge the validity of many of these characters (Li *et al*., 2019; Zhao *et al*., 2025). The study by Zhao *et al.* (2025) demonstrated, through comparative mitogenomic analysis and multilocus phylogenetics, that *Longicollum pagrosomi* Yamaguti, 1935 and *Pomphorhynchus zhoushanensis* Li, Chen, Amin & Yang, 2017 represent the same species, despite striking morphological differences in neck structure. Historically, the genus *Longicollum* Yamaguti, 1935, was distinguished from *Pomphorhynchus* Monticelli, 1905, by the absence of a true neck bulb, whereas *Pomphorhynchus* possessed a symmetrical or asymmetrical neck bulb (Amin *et al*., 2003). This is also seen in the present study (Fig. 3.1A–B). Hence, morphologically, the South African species more closely resembles that of *L. pagrosomi*. However, Zhao *et al*. (2025) found that this distinction reflects phenotypic plasticity rather than discrete species boundaries. Consequently, *Longicollum* was formally relegated to a junior synonym of *Pomphorhynchus*, and several species, including *L. pagrosomi*, were reclassified as *P. pagrosomi*.

Figure 3.1: Light microscopy images of Acanthocephala spp. parasitising *Amblyrhynchote honckenii* (Bloch) off the coast of South Africa. **A** – Stained specimen of *Pomphorhynchus* sp. Monticelli, 1905, scale bar 500 µm; **B** – Voucher specimen of *Pomphorhynchus* sp., scale bar 500 µm; **C** – Stained specimen of *Rhadinorhynchus gerberi* Lisitsyna, Kudlai, Cribb & Smit, 2019, scale bar 1000 µm. Photographs **A–C** by Linda de Klerk.

In contrast, based on 18S rDNA phylogenetic analysis, the new specimens from *A. honckenii* grouped most closely with *P. kashmirensis* Kaw, 1941 (Figure 3.2), differing by only 3 bp (0.4%). In comparison, these specimens differ from *P. pagrosomi* by 11 base pairs (1.4%). Given their distinct morphology, genetic divergence, and unique host and geographic origin, we tentatively propose that these specimens may represent a new species.

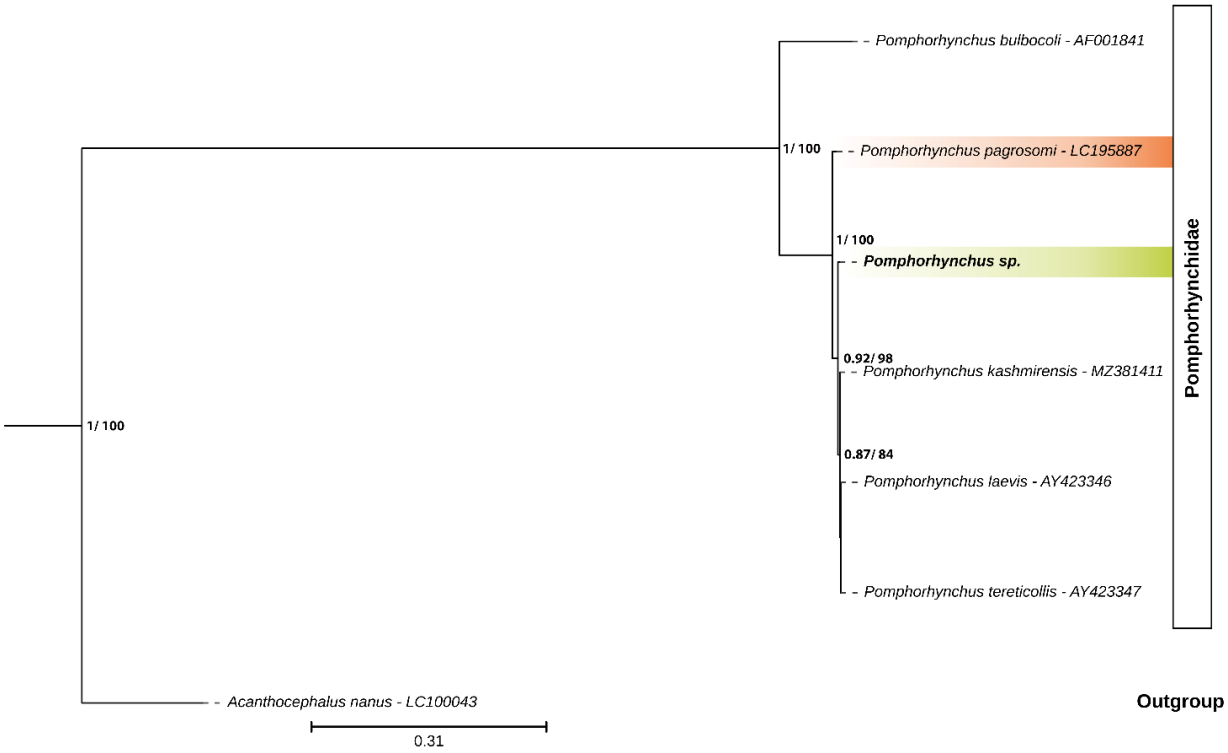

Figure 3.2: Bayesian inference (BI) phylogenetic tree of the family Pomphorhynchidae, based on 18S rDNA sequences. Nodal support values are indicated as BI/ Maximum Likelihood (ML); only values ≥0.7 (BI) and ≥70 (ML) are displayed. Newly sequenced isolates generated in this study are highlighted in green with bold text. The orange-highlighted sequence indicates the closest genetic match. *Acanthocephalus nanus* Van Cleave, 1925, was selected as the outgroup.

Rhadinorhynchus gerberi

A total of 53 specimens were identified as *R. gerberi*. These specimens were recovered from the type locality originally reported for this species, confirming their identification. The complete taxonomic classification and summary are as follows:

Class: Palaeacanthocephala
Order: Echinorhynchida
Family: Rhadinorhynchidae
Genus: *Rhadinorhynchus* Lühe, 1911
Species: *Rhadinorhynchus gerberi* Lisitsyna, Kudlai, Cribb & Smit, 2019
Type host: *Trachinotus botla (*Shaw)
Type locality: Sodwana Bay, South Africa
Present host: *Amblyrhynchote honckenii* (Bloch)
Present locality: Sodwana Bay, South Africa
Site of infection: Intestine
Prevalence (P): 40%

Mean intensity (MI): 13.25

Life stage: Adult

Representative DNA sequences: Two sequences for 18S rDNA, two sequences for 28S rDNA, and one sequence for COI mtDNA

Voucher material: Four specimens fixed on slides (Figure 3.1C) and 10 specimens fixed in ethanol are kept in the collection of the Water Research Group (WRG) at the North-West University (NWU), Potchefstroom, South Africa. The other remaining specimens were frozen for future element analyses.

Specimens were identified based on a combination of distinctive morphological traits and molecular evidence. Morphologically, the specimens exhibit an elongate, cylindrical trunk with an uninterrupted anterior field of tegumental spines, a long proboscis armed with 10 longitudinal rows of 28–32 hooks, a cephalic ganglion located mid-way within the proboscis receptacle, and four cement glands arranged in pairs. The species is morphologically similar to *R. gerberi* with measurements all within the range described by Lisitsyna *et al*. (2019).

Furthermore, molecular analysis of the mitochondrial COI gene revealed 100% sequence similarity with published sequences of *R. gerberi* from the same host and locality (Lisitsyna *et al*., 2019). Phylogenetic analyses using both Bayesian Inference and Maximum Likelihood methods placed the specimens within a monophyletic *R. gerberi* clade with 100% nodal support, confirming their conspecificity (Figure 3.3).

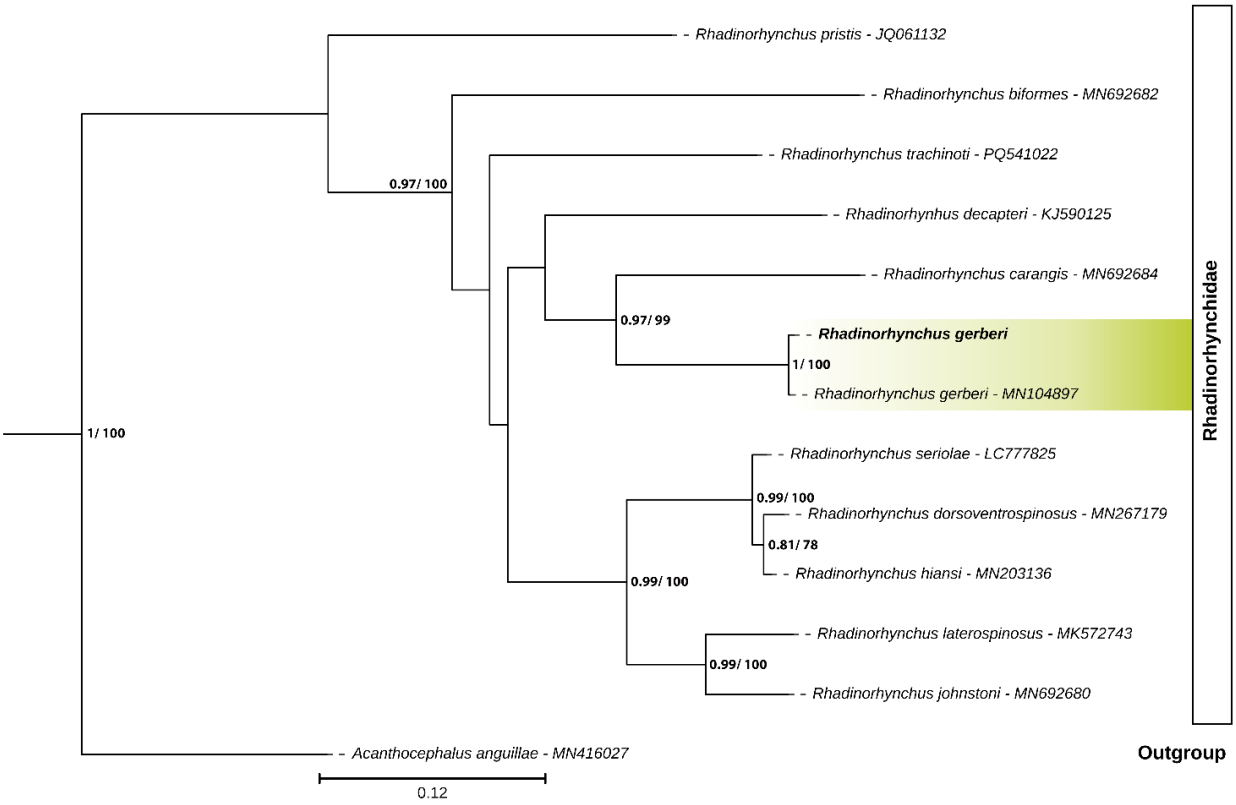

Figure 3.3: Bayesian inference (BI) phylogenetic tree of the family Rhadinorhynchidae, based on COI mtDNA sequences. Nodal support values are indicated as BI/ Maximum Likelihood (ML); only values ≥0.7 (BI) and ≥70 (ML) are displayed. Newly sequenced isolates generated in this study are highlighted in green with bold text. *Acanthocephalus anguillae* (Müller, 1780) Lühe, 1911, was selected as the outgroup.

3.3.2.2 Phylum Arthropoda

The phylum Arthropoda includes organisms with segmented bodies, jointed appendages, and a chitinous exoskeleton (Hadfield *et al*., 2025). The phylum includes a highly diverse assemblage of organisms, with parasitic representatives playing significant ecological roles in both marine and freshwater environments (Hadfield *et al*., 2025). In South Africa, parasitic arthropods, particularly crustaceans, are among the most frequently encountered ectoparasites of marine fishes, with copepods and isopods comprising the majority of described species (Smit *et al*., 2014). Among the parasitic copepods, species of the families Caligidae, Lernaeopodidae, and Pennellidae have been reported from various host taxa, frequently attaching to the skin, fins, and gills of marine teleosts (Hadfield *et al*., 2025). Notably, *Cal. tetrodontis* remains the only formally described parasitic copepod from the tetraodontid fish, *A. honckenii*, in South Africa (Hayes *et al*., 2021; Hadfield *et al*., 2025). In terms of parasitic isopods, South African marine systems host numerous species from the family Cymothoidae, known for occupying the branchial or buccal cavities of teleost fishes (Smit *et al*., 2014). *Cinusa tetrodontis*, a buccal cymothoid, was also described from *A. honckenii* and remains one of the few formally identified isopods from

tetraodontid hosts in the region (Hadfield *et al*., 2025). Despite these few host-specific records, the overall diversity of parasitic arthropods associated with tetraodontiform fishes in South Africa remains poorly explored.

The current study contributes to the baseline knowledge of marine parasitic arthropods in South Africa by reporting one known isopod species, *Cin. tetrodontis*, and three copepod taxa, including the known *Cal. tetrodontis* and two newly described species of *Ergasilus* von Nordmann, 1832: *E. arenalbus* and *E. chintensis*. These findings underscore the rich biodiversity of the region's marine ecosystems and highlight the value of continued exploration in under-studied habitats. Importantly, the two newly described *Ergasilus* species offer the first insights into the phylogenetic relationships of marine *Ergasilus* in the South Atlantic and Indian Ocean regions (Van Der Spuy, L., Narciso, R.B., Hadfield, K.A., Wepener, V. & Smit, N.J., 2025. Exploring South Africa's hidden marine parasite diversity: Two new marine Ergasilus species (Copepoda: Cyclopoida: Ergasilidae) from the evileye blaasop, *Amblyrhynchotes honckenii* (Bloch). Parasitology, 152(1): 30–50).

Cinusa tetrodontis

A total of 34 specimens were identified as *Cin. tetrodontis*. These specimens were recovered from the type host originally reported for this species. The complete taxonomic classification and summary are as follows:

Class: Malacostraca
Order: Isopoda
Family**:** Cymothoidae
Genus: *Cinusa* Schioedte & Meinert, 1884
Species: *Cinusa tetrodontis* Schioedte & Meinert, 1884
Type host: *Amblyrhynchote honckenii* (Bloch)
Type locality: Simons Bay, South Africa
Present host: *Amblyrhynchote honckenii* (Bloch)
Present locality: Breede River estuary, Witsand; and Mossel Bay, South Africa
Site of infection: Buccal cavity
Prevalence (P): 68%
Mean intensity (MI): 2
Life stage: Adult

Specimens were identified based on morphological comparison with the detailed redescription provided by Hadfield *et al*. (2010) (Figure 3.4). This identification was supported by

key diagnostic features, including the oval and asymmetrical body widest at pereonites 3–4, a small cephalon deeply immersed in pereonite 1, acute lateral margins of the pleonites, and nearly contiguous bases of the antennae. The specimens were consistently located within the buccal cavity of their host, which corresponds with the known site specificity of *Cin. tetrodontis* (Hadfield *et al*., 2010). Although no molecular data were available, the complete morphological consistency with Hadfield *et al*.'s (2010) figures and descriptions support the identification.

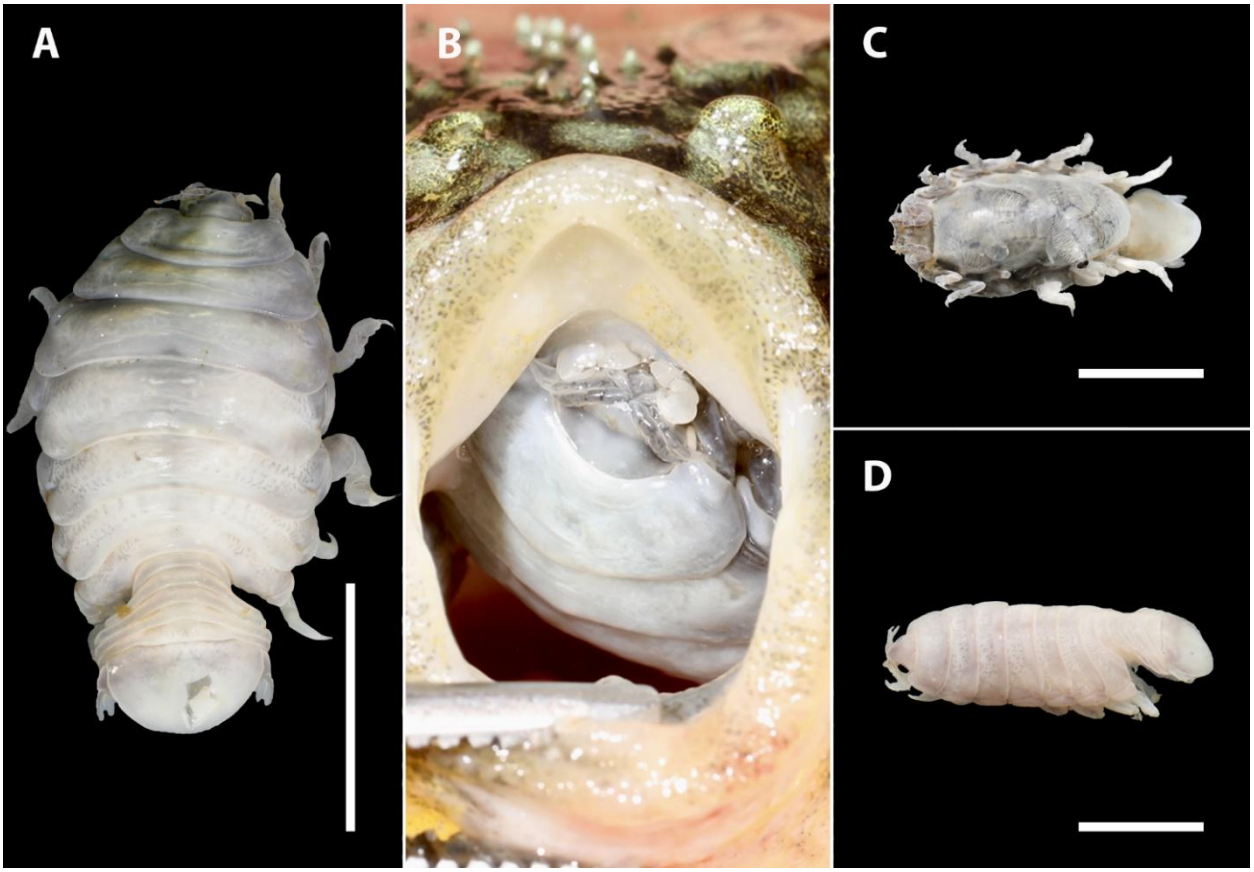

Figure 3.4: Photos of *Cinusa tetrodontis* Schioedte & Meinert, 1884, parasitising *Amblyrhynchote honckenii* (Bloch) off the coast of South Africa. **A** – Female specimen, scale bar 12 mm; **B** – Female specimen in the buccal cavity; **C** – Ovigerous female specimen, scale bar 12 mm; **D** – Male specimen, scale bar 8 mm. Photographs **A–D** by Prof. Nico J. Smit.

Caligus tetrodontis

A total of 66 specimens were identified as *Cal. tetrodontis*. While *A. honckenii* is not the type host for this species, its association with *Cal. tetrodontis* has been previously documented by Hayes *et al*. (2021). The complete taxonomic classification and summary are as follows:

Class: Copepoda
Order: Siphonostomatoida
Family: Caligidae
Genus: *Caligus* Müller O.F., 1785
Species: *Caligus tetrodontis* Barnard, 1948
Type host: *Torquigener hypselogeneion* (Bleeker)
***Type locality*:** Gqeberha, South Africa
Present host: *Amblyrhynchote honckenii* (Bloch)
Present locality: Breede River estuary, Witsand; Mossel Bay; and Chintsa East, South Africa
Site of infection: External skin and fins
Prevalence (P): 69%
Mean intensity (MI): 2.73
Life stage: Adult
Representative DNA sequences: three sequences for 28S rDNA, and four sequences for COI mtDNA
Voucher material: Ten specimens fixed in ethanol (Figure 3.5) are kept in the collection of the Water Research Group (WRG) at the North-West University (NWU), Potchefstroom, South Africa. Any remaining specimens were frozen for future element analyses.

Specimens were identified based on a combination of morphological traits and strong molecular evidence. Morphological examination revealed that the adult females possessed a subcircular dorsal cephalothoracic shield, a genital complex with rounded posterolateral corners that was slightly longer than wide, a single-segmented abdomen, and the fourth leg was distinctive, bearing three distal spines that decreased in length from inner to outer. These features are consistent with the supplementary description of *Cal. tetrodontis* from *A. honckenii*, as provided by Hayes *et al*. (2021).

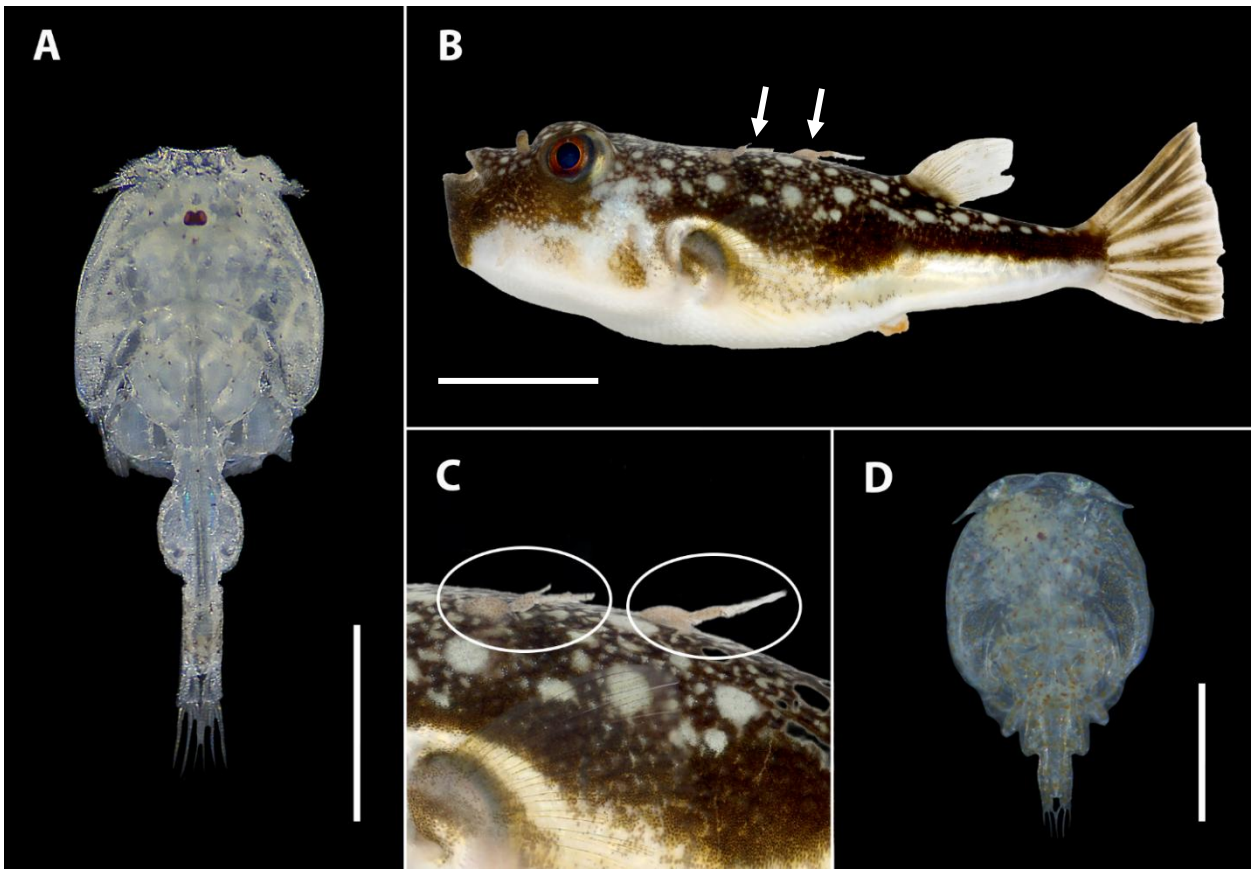

Figure 3.5: Photos of *Caligus tetrodontis* Barnard, 1948, parasitising *Amblyrhynchote honckenii* (Bloch) off the coast of South Africa. **A** – Female specimen, scale bar 2 mm; **B** – Specimens on *A. honckenii,* scale bar 2 cm; **C** – Specimens on *A. honckenii;* **D** – Male specimen, scale bar 2 mm. Photographs **A–C** by Prof. Nico J. Smit, **D** by Linda de Klerk.

Molecular analyses further supported the morphological identification. Molecular analysis of the mitochondrial COI gene revealed 100% sequence identity with published sequences of *Cal. tetrodontis* (Hayes *et al*., 2021). Furthermore, the phylogenetic analysis confirmed that the South African *Cal. tetrodontis* specimens clustered within a distinct subclade (Figure 3.6).

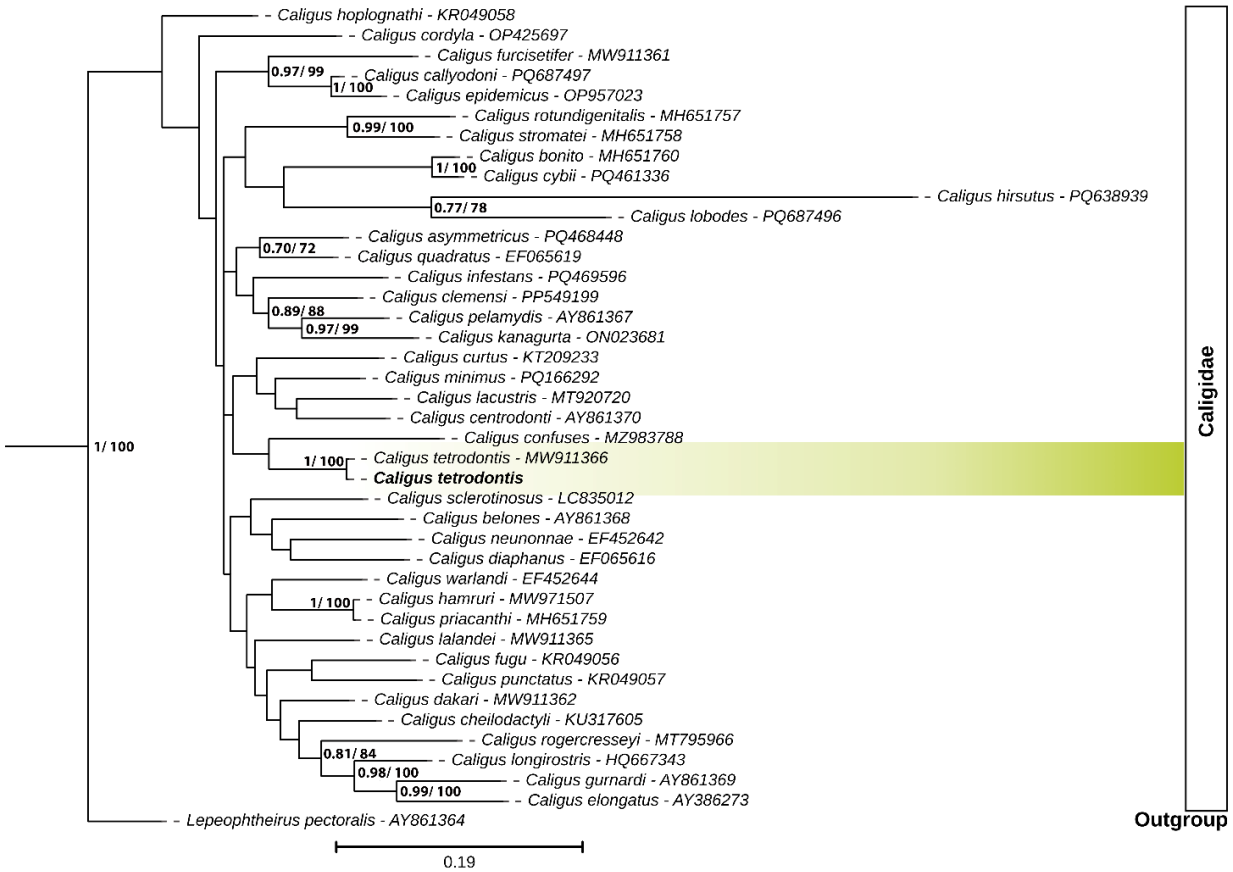

Figure 3.6: Bayesian Inference (BI) phylogenetic tree of the family Caligidae, based on COI mtDNA sequences. Nodal support values are indicated as BI/ Maximum Likelihood (ML); only values ≥0.7 (BI) and ≥70 (ML) are displayed. Newly sequenced isolates generated in this study are highlighted in green with bold text. *Lepeophtheirus pectoralis* (Müller O.F., 1776) was selected as the outgroup.

***Ergasilus* spp.**

Two new, distinct, gill-associated ergasilid species infecting *A. honckenii*, were described as part of this study (Van Der Spuy *et al*. 2025). The full manuscript, including their descriptions, is already published (see Appendix B).

Species were morphologically and molecularly differentiated. Both morphotypes were classified as *Ergasilus* von Nordmann, 1832, based on genus-specific characteristics following descriptions by Boxshall and Montú (1997) and Boxshall and Halsey (2004). This includes a body typically cyclopiform with clear segmentation, biramous legs IV with 2-segmented exopods and 3-segmented endopods, 6-segmented antennules, antennas featuring a single claw and the absence of maxillipeds in females. The full classification and taxonomic summary for the first specimen, *E. arenalbus*, are as follows:

Class: Copepoda

Order: Cyclopoida

Family: Ergasilidae

Genus: *Ergasilus* von Nordmann, 1832

Species: *Ergasilus arenalbus* van der Spuy, Narciso, Hadfield, Wepener & Smit, 2024

Type host: *Amblyrhynchote honckenii* (Bloch)

Type locality: Breede River estuary, Witsand, South Africa

Site of infection: Gill filaments

Prevalence (P): 67%

Mean intensity (MI): 11.62

Life stage: Adult

Representative DNA sequences: GenBank accession numbers and numbers of bases (bp) are given as follows: 18S: 1333 and 1344 bp long sequences of 2 specimens, accession numbers: PQ451954 and PQ451956; 28S: 668 and 664 bp long sequences of 2 specimens, accession numbers: PQ451957 and PQ451958; and COI: 701 bp long sequence of 1 specimen, accession number: PQ439339

Type material: 151 *Ergasilus* specimens (adult females) were collected. Only adult females were examined: 6 were used for SEM, 2 for dissection, 12 for morphology, and 2 egg strings were used for DNA extraction. The hologenophores (NMB P 1044–NMB P 1045), holotype (NMB P 1042) and 11 paratypes (NMB P 1043) were deposited in the parasitological collections of the National Museum, Bloemfontein (NMB), South Africa; the remaining specimens are in the possession of the Water Research Group, North-West University, Potchefstroom, South Africa

Specimens of *E. arenalbus* (Figures 3.7A–B) were recovered from the gill filaments of *A. honckenii* collected at WS, Western Cape, South Africa. The body has a length averaging 1182 µm and features a five-segmented prosome composed of the cephalosome and four free pedigerous somites. The antennae bear a single prominent spine on the anterior margin of the second endopodal segment, a key diagnostic trait. Notably, *E. arenalbus* also displays unique spine-like projections on the basis of leg I, absent in other regional congeners. Compared to 17 other known marine *Ergasilus* species from the southern Atlantic and Indian Ocean regions, *E. arenalbus* is set apart by its larger size, segmentation of the prosome (free vs. fused), and appendage ornamentation. It differs morphologically from *E. lizae* Krøyer, 1863, which shares some similarities, in having a distinct antennal armature and spine ornamentation on leg I. The antennule is 6-segmented, unlike the 5-segmented structure seen in species such as *E. ilani* Oldewage & van As, 1988, and *E. uniseriatus*. Furthermore, the absence of a spine on the second

exopod segment of leg I helps to distinguish it from several other species, including *E. atafonensis* Amado & Rocha, 1996, and *E. xenomelanirisi* Carvalho, 1955.

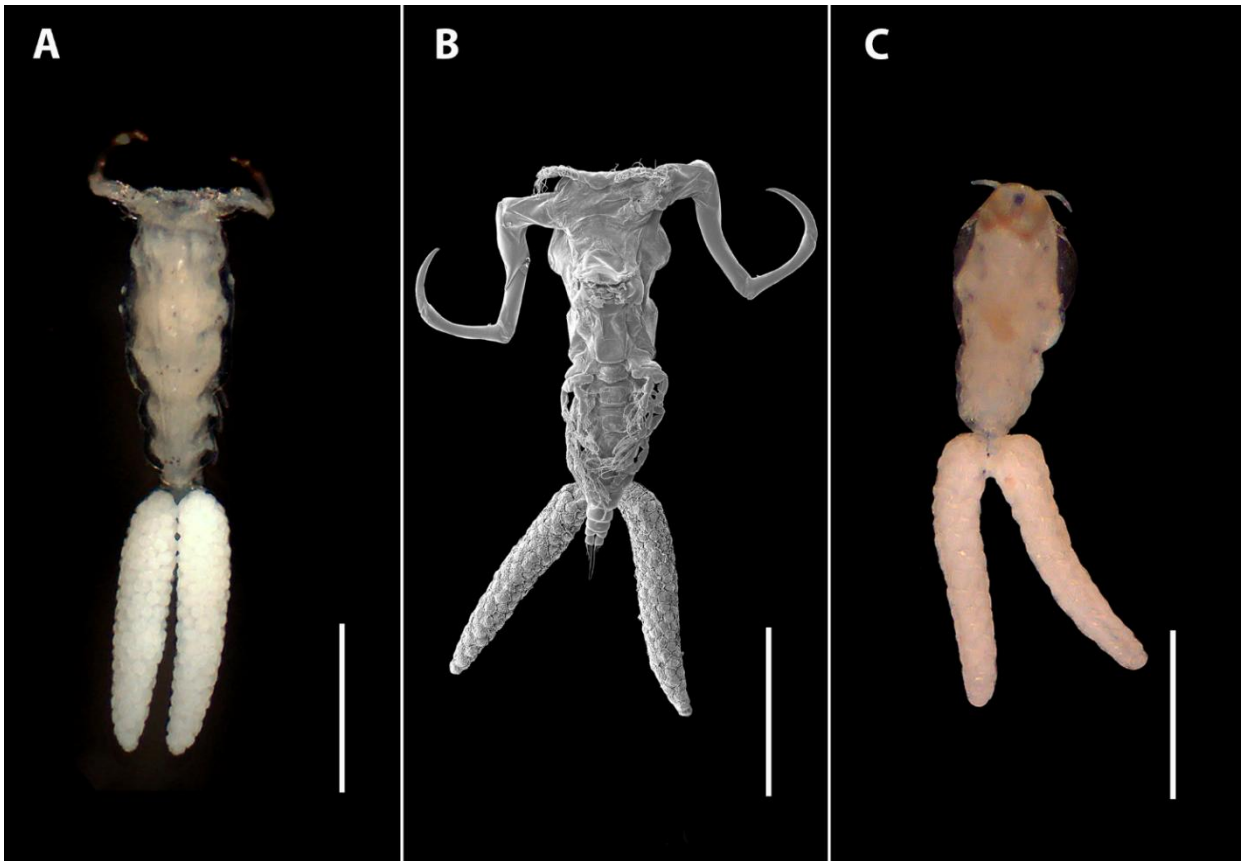

Figure 3.7: Light microscopy and scanning electron microscope (SEM) photomicrographs of adult female *Ergasilus* spp. von Nordmann, 1832, parasitising *Amblyrhynchote honckenii* (Bloch). **A** – Light microscopy of entire specimen of *E. arenalbus* van der Spuy, Narciso, Hadfield, Wepener & Smit, 2024, scale bar 500 µm; **B** – SEM of entire specimen of *E. arenalbus,* scale bar 500 µm; **C** – Light microscopy of entire specimen of *E. chintensis* van der Spuy, Narciso, Hadfield, Wepener & Smit, 2024, scale bar 500 µm. Photographs **A–C** by Linda de Klerk.

Molecular analyses further confirmed the distinctiveness of *E. arenalbus* based on both 28S rDNA and COI gene sequences. These genetic differences validate its status as a separate species and position it within a proposed sixth clade (Clade F) of African marine *Ergasilus* species (Figure 3.8). Additionally, the analysis revealed that other *Ergasilus* taxa were genetically distant from the newly described species, underscoring the utility of 28S rDNA in resolving phylogenetic relationships within the family Ergasilidae.

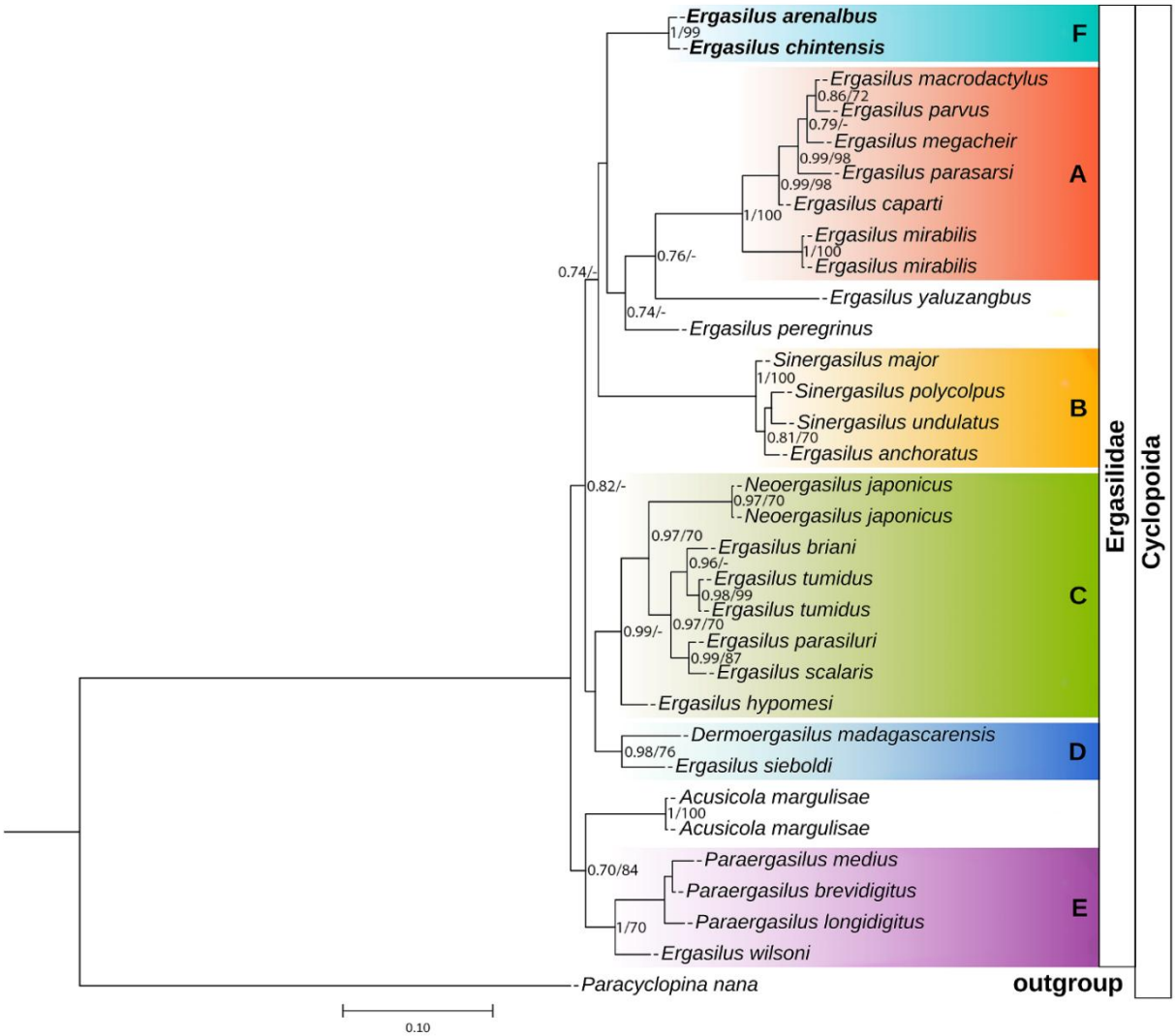

Figure 3.8: Bayesian Inference (BI) phylogenetic tree of the family Ergasilidae, based on 28S rDNA sequences. Nodal support values are indicated as BI/ Maximum Likelihood (ML); only values ≥0.7 (BI) and ≥70 (ML) are displayed. Dashes indicate values below 0.7 and 70%, respectively. Newly sequenced isolates generated in this study are highlighted in teal with bold text. *Paracyclopina nana* Smirnov, 1935, was used as the outgroup.

The classification and taxonomic summary for the second specimen, *E. chintensis,* are as follows:

Class: Copepoda
Order: Cyclopoida
Family: Ergasilidae
Genus: *Ergasilus* von Nordmann, 1832
Species: *Ergasilus chintensis* van der Spuy, Narciso, Hadfield, Wepener & Smit, 2024
Type host: *Amblyrhynchote honckenii* (Bloch)
Type locality: Chintsa East; and Uvongo Beach, South Africa
Site of infection: Gill filaments
Prevalence (P): 20%
Mean intensity (MI): 1
Life stage: Adult
Representative DNA sequences: GenBank accession numbers and numbers of bases (bp) are given as follows: 18S: 1353 bp long sequence of 1 specimen, accession number: PQ451955; 28S: 668 bp long sequence of 1 specimen, accession number: PQ451959; and COI: 692 bp long sequence of 1 specimen, accession number: PQ439340.
Type material: 2 ergasilids (adult females) were collected. Only adult females were examined: 2 were used for morphology, and 1 egg string was used for DNA extraction. The hologenophore (NMB P 1047) and holotype (NMB P 1046) were deposited in the parasitological collections of the National Museum, Bloemfontein (NMB), South Africa.

Ergasilus chintensis was described from *A. honckenii* collected at CE, Eastern Cape, South Africa (Figure 3.7C). Both adult females collected were examined, one of which was used for molecular analysis. The body length averages 1035 µm, and the species is immediately distinguishable by its fused 2-segmented prosome, a rare condition among marine *Ergasilus* species. The antennae are more robust than in *E. arenalbus*, and the second endopodal segment has two developed spines rather than one. The antennules are 6-segmented and differ in setal formula from other southern African marine congeners. In addition to size and segmentation, *E. chintensis* differs in ornamentation, such as the more intricate structure of its intercoxal sclerites and interpodal plates, and the configuration of leg V. These morphological features, in combination, clearly distinguish *E. chintensis* from all other described *Ergasilus* species from the southern hemisphere, including the closely related *E. arenalbus*.

Genetic analysis further supports this differentiation. *Ergasilus chintensis* differs from *E. arenalbus* by 43 bp in COI, 6 bp in 28S, and 14 bp in 18S rDNA sequences. Phylogenetic trees constructed using both Maximum Likelihood and Bayesian Inference confirmed the placement of

E. chintensis and *E. arenalbus* in a unique African marine clade, separate from freshwater and brackish *Ergasilus* species (Figure 3.8). These findings underscore both the cryptic diversity of marine ergasilids and the host-specific endemism associated with *A. honckenii*.

3.3.2.3 Phylum Nematoda

The phylum Nematoda includes a diverse group of roundworms, many of which are parasitic in aquatic vertebrates, particularly marine fishes (Anderson, 1996; 2000). In South Africa, nematodes are frequently encountered in marine teleosts and form a key part of their helminth communities. However, their diversity and taxonomy remain poorly documented compared to other parasitic groups (Smit and Hadfield, 2015). This knowledge gap is largely due to a shortage of taxonomic expertise and limited comprehensive surveys targeting parasitic nematodes in marine systems (Smit and Hadfield, 2015; Schaeffner and Smit, 2019). Furthermore, some host groups, such as tetraodontiform fishes, have also received minimal attention. To date, no nematodes have been formally described from *A. honckenii* or related tetraodontids in South African waters. Still, some progress has been made, particularly with *Anisakis* spp., several of which have been identified in the region, including *A. berlandi* Mattiucci, Cipriani, Webb, Paoletti, Marcer, Bellisario, Gibson & Nascetti, 2014, *A. pegreffii* Campana-Rouget & Biocca, 1955, and *A. simplex* (González *et al*., 2006; Le Roux, 2013; Nunkoo *et al*., 2016; Mackintosh *et al*., 2018). Additional nematode species reported from South African marine fishes include *Camallanus sodwanaensis* Svitin, Truter, Kudlai, Smit & Du Preez, 2019, *Cucullanus* sp., *Pseudoterranova* sp. Mozgovoi, 1951, and *Proleptus obtusus* Dujardin, 1845 (Moravec *et al*., 2002; Yeld, 2009; Morris *et al*., 2016; Svitin *et al*., 2019).

The current study expands the baseline knowledge of marine parasitic helminths in South African waters by reporting five nematode taxa: *A. simplex*; *D. szidati*; *Dichelyne* sp.; Physalopteridae gen. sp.; and *Raphidascaris* sp. As the majority of specimens were in the larval stage, formal species-level identification remains unresolved, since many key morphological diagnostic features are only expressed in adult nematodes. In particular, the *Physalopteridae* gen. sp. specimens could not be reliably assigned to a known genus or species and are therefore referred to at family level. The lack of adult material prevents accurate morphological comparisons and highlights the challenges of identifying larval nematodes, especially in ecologically complex marine systems.

Anisakis simplex

A total of six nematode specimens were identified as *A. simplex*. This represents the first known record of *Anisakis* Dujardin, 1845, in this host species. The full taxonomic classification and summary are as follows:

Class: Chromadorea
Order: Rhabditida
Family: Anisakidae
Genus: *Anisakis* Dujardin, 1845
Species: *Anisakis simplex* (Rudolphi, 1809) Dujardin, 1845
Type host: *Merluccius merluccius* (Linnaeus)
Type locality: Hurghada City, Egypt
Present host: *Amblyrhynchote honckenii* (Bloch)
Present locality: Breede River estuary, Witsand, South Africa
Site of infection: Intestine and body cavity
Prevalence (P): 27%
Mean intensity (MI): 1.5
Life stage: Larvae
Representative DNA sequences: three sequences for 18S and 28S rDNA, and one sequence for COI mtDNA
Voucher material: Six specimens fixed in lactophenol and ethanol (Figure 3.9) are kept in the collection of the Water Research Group (WRG) at North-West University (NWU), Potchefstroom, South Africa

Morphological identification was limited due to the specimen being in the third larval stage (L3), where many adult diagnostic features are either absent or underdeveloped. The larva exhibited typical characteristics of the *Anisakis simplex* complex, including a cylindrical body tapering at both ends, a rounded anterior end with a prominent apical tooth, a ventral excretory pore posterior to the tooth, and a smooth cuticle (Umehara *et al*., 2006; Mattiucci *et al*., 1997). However, these traits are insufficient to distinguish between sibling species such as *A. pegreffii*, and *A. simplex* C, which are morphologically indistinguishable at this stage (Umehara *et al*., 2006).

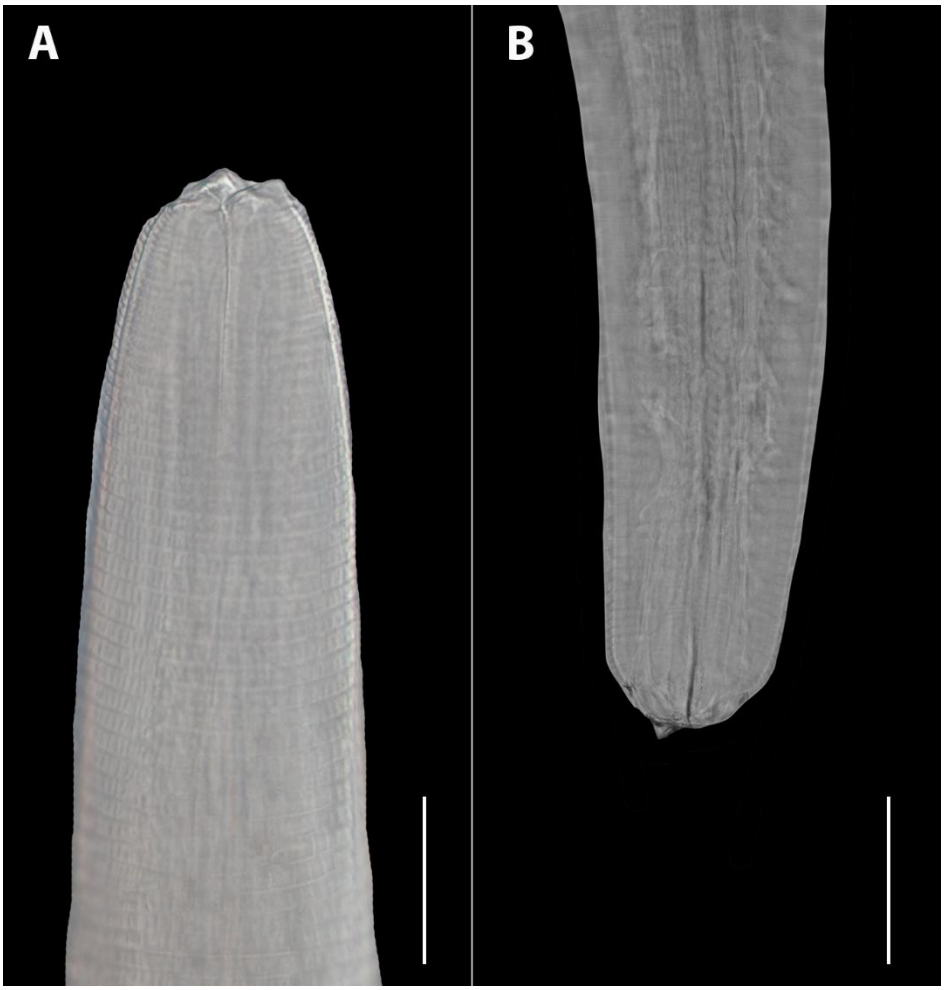

Figure 3.9: Light microscopy images of *Anisakis simplex* (Rudolphi, 1809) Dujardin, 1845, parasitising *Amblyrhynchote honckenii* (Bloch) off the coast of South Africa. **A** – Cephalic end, scale bar 200 µm; **B** – Caudal end, scale bar 200 µm. Photographs **A–B** by Dr. Marliese Truter.

To resolve the species identity, molecular analyses were conducted using partial sequences of the 18S rRNA, 28S rRNA, and mitochondrial COI genes. All three markers produced sequences with 100% identity to *A. simplex* C reference sequences. Phylogenetic analyses confirmed this result, with the specimen clustering within the *A. simplex* complex and forming a distinct clade with *A. simplex* C, clearly separated from *A. pegreffii* (Figure 3.10).

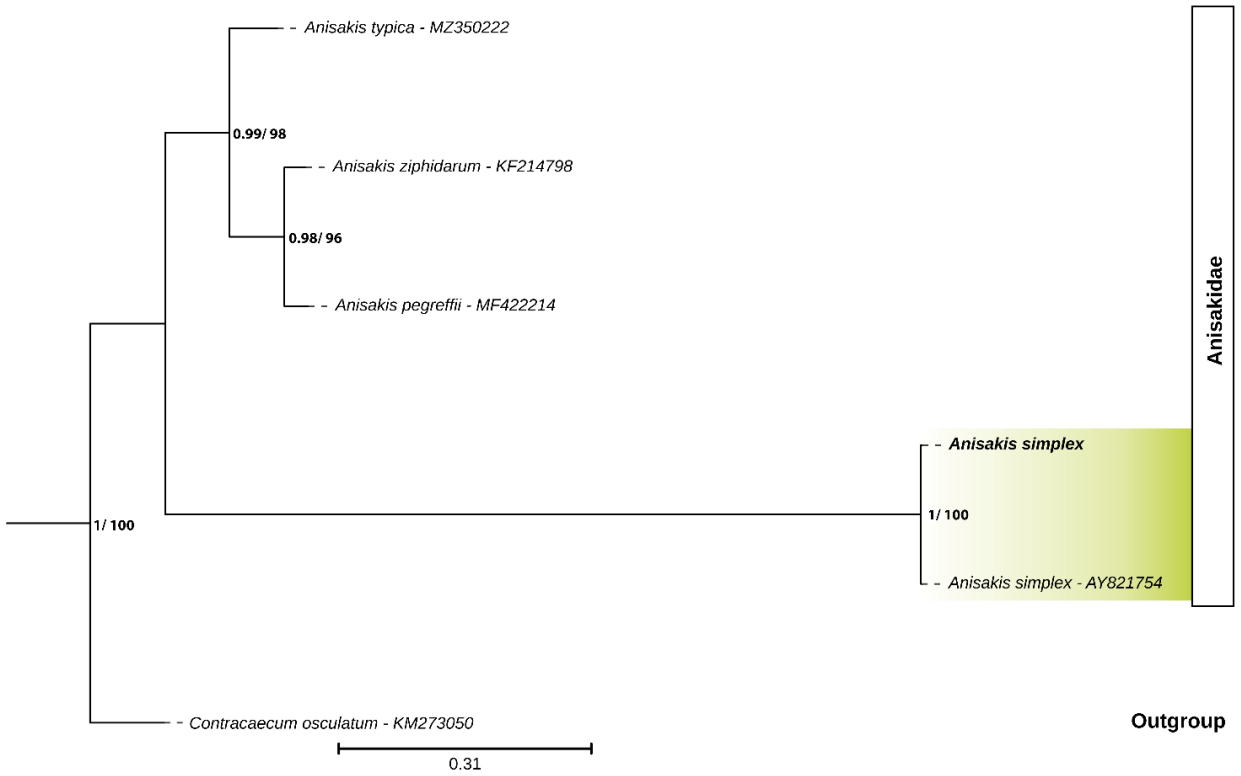

Figure 3.10: Bayesian Inference (BI) phylogenetic tree of the family Anisakidae, based on 28S rDNA sequences. Nodal support values are indicated as BI/Maximum Likelihood (ML); only values ≥0.7 (BI) and ≥70 (ML) are displayed. Newly sequenced isolates generated in this study are highlighted in green with bold text. *Contracaecum osculatum* (Rudolphi, 1802) Baylis, 1920 was selected as the outgroup.

***Dichelyne* spp.**

A total of four specimens were identified as two different species in the genus *Dichelyne* Jägerskiöld, 1902. The first species was identified as *D. szidati*; however, due to divergence in molecular sequences, the second species could only be identified to genus level. Further collection and examination will be necessary to confirm its taxonomic status. This represents the first known record of *Dichelyne* in this host species. For *D. szidati*, the full taxonomic classification and summary are as follows:

Class: Chromadorea
Order: Rhabditida
Family: Cucullanidae
Genus: *Dichelyne* Jägerskiöld, 1902
Species: *Dichelyne (Cucullanellus) szidati* Timi & Sardella, 2002
Type host: *Acanthisthius brasilianus* (Valenciennes)
Type locality: Mar del Plata, Argentina

Present host: *Amblyrhynchote honckenii* (Bloch)
Present locality: Mossel Bay; and Uvongo Beach, South Africa
Site of infection: Intestine, liver and body cavity
Prevalence (P): 10%
Mean intensity (MI): 1
Life stage: Larvae
Representative DNA sequences: two sequences for 18S and 28S rDNA
Voucher material: Two specimens fixed in lactophenol and ethanol (Figure 3.11) are kept in the collection of the Water Research Group (WRG) at the North-West University (NWU), Potchefstroom, South Africa

Morphological and molecular evidence support the identification of the present nematode specimens as *D. szidati*. Key diagnostic features observed include the posterior position of the excretory pore relative to the oesophagus, the location of the derrids near the posterior end of the oesophagus, and the presence of a ventrally positioned intestinal cecum, features consistent with the original species description.

Although the specimens were in the larval stage, additional support comes from molecular analysis of the 28S rDNA gene region, which showed 99.85% similarity to reference sequences of *D. szidati*, differing by only a single base pair (Figure 3.12). This high level of genetic concordance, in conjunction with congruent morphological traits, strongly indicates that these larvae belong to *D. szidati*.

Figure 3.11: Light microscopy images of *Dichelyne (Cucullanellus) szidati* Timi & Sardella, 2002, parasitising *Amblyrhynchote honckenii* (Bloch) off the coast of South Africa. **A** – Cephalic end, scale bar 100 µm; **B** – Caudal end, scale bar 100 µm. Photographs **A–B** by Dr. Marliese Truter.

Dichelyne sp. represents the second known record of *Dichelyne* in this host species. The full taxonomic classification and summary are as follows:

Class: Chromadorea
Order: Rhabditida
Family: Cucullanidae
Genus: *Dichelyne* Jägerskiöld, 1902
Species: Unknown
Present host: *Amblyrhynchote honckenii* (Bloch)
Present locality: Chintsa East, South Africa
Site of infection: Intestine, liver and body cavity
Prevalence (P): 20%
Mean intensity (MI): 1

Life stage: Larvae

Representative DNA sequences: two sequences for 18S and 28S rDNA

Voucher material: Two specimens fixed in lactophenol and ethanol (Figure 3.13) are kept in the collection of the Water Research Group (WRG) at the North-West University (NWU), Potchefstroom, South Africa

Figure 3.13: Light microscopy images of *Dichelyne* sp. Jägerskiöld, 1902, parasitising *Amblyrhynchote honckenii* (Bloch) off the coast of South Africa. **A** – Cephalic end, scale bar 200 µm; **B** – Caudal end, scale bar 200 µm. Photographs **A–B** by Dr. Marliese Truter.

The second specimen displayed notable morphological differences from *D. szidati*, including variation in body form and the position of key anatomical features, with several characters inconsistent with the original species description. Molecular analysis of the 28S rDNA gene revealed a 76 bp (9.5%) sequence divergence from *D. szidati*, which exceeds expected intraspecific variation within the species. Phylogenetically, these larvae clustered within the same major clade as *D. szidati* but formed a separate and well-supported subclade, further reinforcing their genetic distinctiveness (Figure 3.12).

Accordingly, we refer to these nematodes as *Dichelyne* sp. pending the collection of more material and more detailed morphological and molecular analyses.

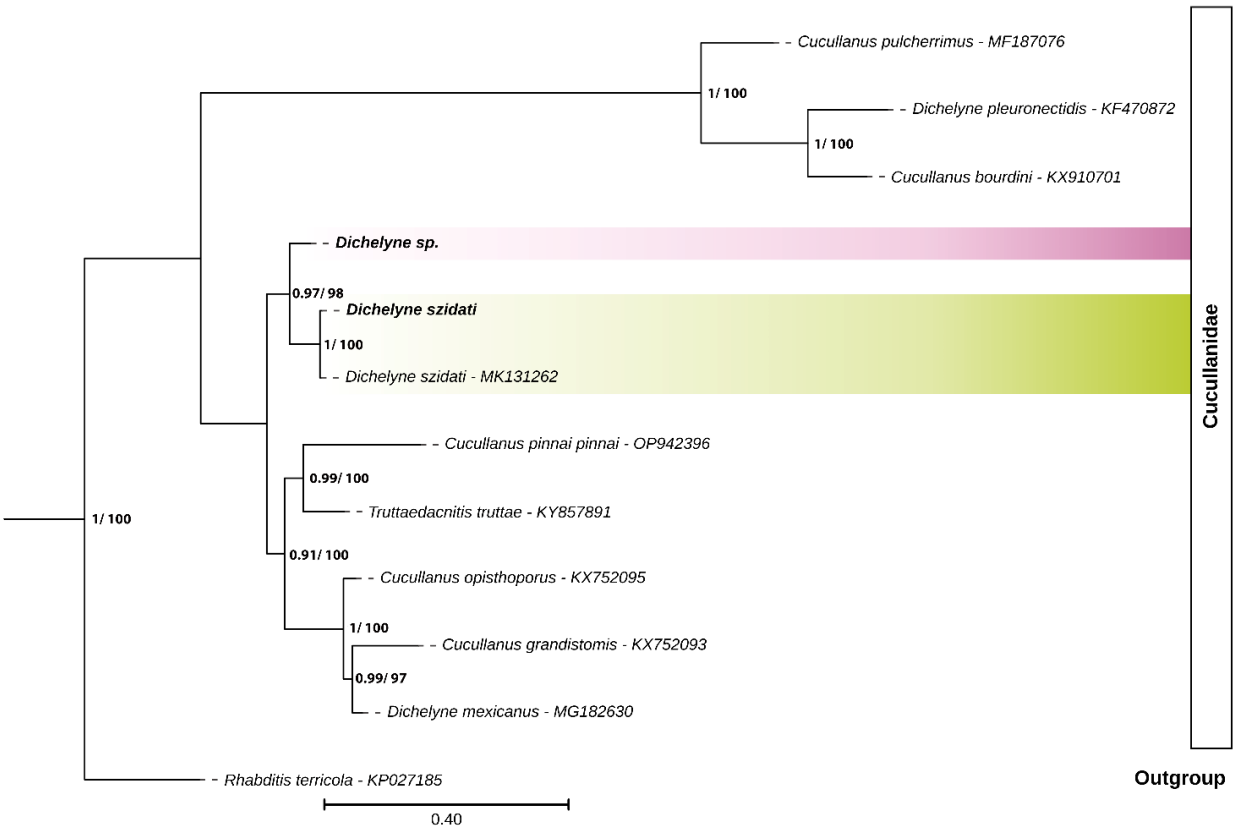

Figure 3.12: Bayesian Inference (BI) phylogenetic tree of the family Cucullanidae, based on 28S rDNA sequences. Nodal support values are indicated as BI/Maximum Likelihood (ML); only values ≥0.7 (BI) and ≥70 (ML) are displayed. Newly sequenced isolates generated in this study are highlighted in green and pink, with bold text. *Rhabditis terricola* Dujardin, 1844, was selected as the outgroup.

Physalopteridae gen. sp.

A total of three specimens were identified as belonging to the family Physalopteridae. Further collection and examination of adult specimens will be necessary to confirm their taxonomic status. This represents the first known record of Physalopteridae in this host species. The full taxonomic classification and summary are as follows:

Class: Chromadorea
Order: Rhabditida
Family: Physalopteridae
Genus: Unknown
Species: Unknown
Present host: *Amblyrhynchote honckenii* (Bloch)

Present locality: Sodwana Bay, South Africa
Site of infection: Intestine and liver
Prevalence (P): 30%
Mean intensity (MI): 1
Life stage: Larvae
Representative DNA sequences: one sequence for each 18S and 28S rDNA
Voucher material: Three specimens fixed in lactophenol and ethanol (Figure 3.14) are kept in the collection of the Water Research Group (WRG) at the North-West University (NWU), Potchefstroom, South Africa.

Morphologically, the anterior region of these larvae closely resembles that of *Paraleptus* species, characterised by a reduced pseudolabial region and cuticular thickening typical of physalopterid nematodes. Molecular analysis was conducted using partial sequences of the 18S and 28S rDNA genes. BLAST comparisons yielded inconsistent results: the 18S sequence matched most closely with *Proleptus* spp., while the 28S sequence aligned more closely with *Paraleptus* spp. This suggests that the larvae may represent a previously undescribed species or a taxon for which no comparative data yet exists in public databases. Additional sampling and the recovery of adult specimens will be required to clarify their identity.

Figure 3.14: Light microscopy images of *Physalopteridae* gen. sp., parasitising *Amblyrhynchote honckenii* (Bloch) off the coast of South Africa. **A** – Cephalic end, scale bar 50 µm; **B** – Caudal end, scale bar 50 µm. Photographs **A–B** by Dr. Marliese Truter.

***Raphidascaris* sp.**

A total of two specimens were identified as *Raphidascaris* sp. Further collection and examination of adult specimens will be necessary to confirm their taxonomic status. This represents the first known record of *Raphidascaris* in this host species. The full taxonomic classification and summary are as follows:

Class: Chromadorea
Order: Rhabditida
Family: Raphidascarididae
Genus: *Raphidascaris* Railliet & Henry, 1915
Species: Unknown
Present host: *Amblyrhynchote honckenii* (Bloch)
Present locality: Breede River estuary, Witsand, South Africa

Site of infection: Intestine

Prevalence (P): 13%

Mean intensity (MI): 2

Life stage: Larvae

Representative DNA sequences: one sequence for each 18S and 28S rDNA

Voucher material: two specimens fixed in lactophenol and ethanol are kept in the collection of the Water Research Group (WRG) at the North-West University (NWU), Potchefstroom, South Africa

Molecular analysis based on partial sequences of the 18S and 28S rDNA genes supports the placement of the specimens within the genus *Raphidascaris*. Phylogenetic reconstruction using 28S rDNA positioned the larvae within the *Raphidascaris* clade, clustering closely with *R. acus* (Bloch, 1779) Railliet & Henry, 1915, the type species of the genus (Figure 3.15). Although the sequences fell within the same clade, a genetic divergence of 32 base pairs (3.63%) from *R. acus* indicates that the specimens may represent a distinct species. Given the limited availability of comparative reference sequences and the larval nature of the material, the specimens are not currently identified to species level.

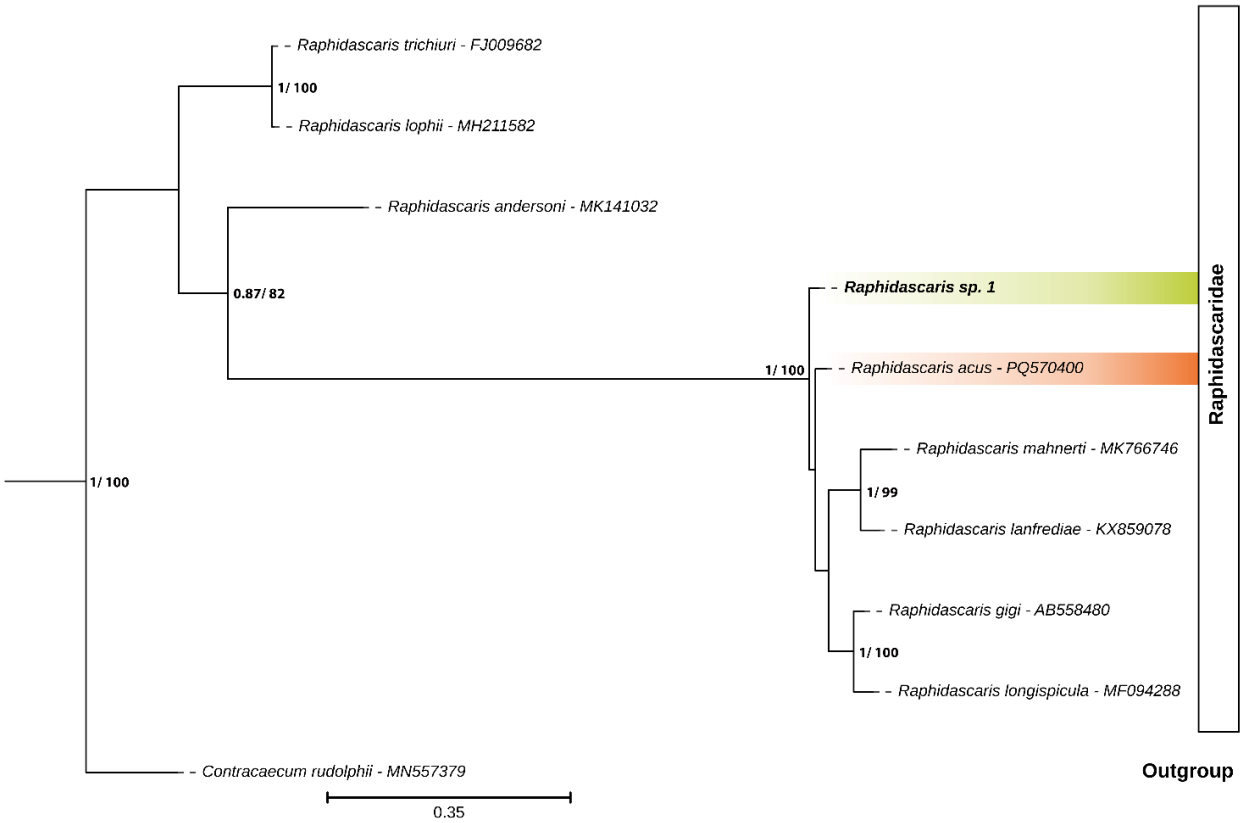

Figure 3.15: Bayesian Inference (BI) phylogenetic tree of the family Raphidascaridae, based on 28S rDNA sequences. Nodal support values are indicated as BI/Maximum Likelihood (ML); only values ≥0.7 (BI) and ≥70 (ML) are displayed. Newly sequenced isolates generated in this study are highlighted in green with bold text. The orange highlighted sequence indicates the closest genetic match. *Contracaecum rudolphii* Hartwich, 1964, was selected as the outgroup.

3.3.2.4 Phylum Platyhelminthes

The phylum Platyhelminthes comprises a wide diversity of flatworm taxa, with four major parasitic classes, Cestoda, Monopisthocotyla, Polyopisthocotyla and Trematoda (Littlewood *et al*., 2004; WORMS, 2025).

Class Cestoda

Cestodes are diverse endoparasites in marine ecosystems, primarily inhabiting the gastrointestinal tracts of elasmobranchs (sharks, skates, and rays) and other teleost fishes (Caira *et al*., 2017). In South Africa, the diversity of cestodes parasitising marine teleosts remains largely underexplored, with most documented species described from elasmobranch hosts (Smit and Hadfield, 2015; Schaeffner and Smit, 2019). However, increased parasitological efforts in recent years have significantly expanded the known fauna. To date, 11 species have been described from local waters, including *Acanthobothrium* crassum Van Der Spuy, Smit & Schaeffner, 2020, *A. dolichocollum* Van Der Spuy, Smit & Schaeffner, 2020, *A. microhabentes* crassum Van Der

Spuy, Smit & Schaeffner, 2020, and *A. microtenuis* crassum Van Der Spuy, Smit & Schaeffner, 2020 (Van der Spuy *et al*., 2020), *A. umbungus* Van Der Spuy, Smit & Schaeffner, 2022, *A. usengozinius* Van Der Spuy, Smit & Schaeffner, 2022, and *A. ulondolozus* Van Der Spuy, Smit & Schaeffner, 2022 (Van der Spuy *et al*., 2022), as well as *Phoreiobothrium martini* Van Der Spuy, Smit, Naidoo & Schaeffner, 2022 (Van der Spuy *et al*., 2023). Additional records include *Poecilancistrium caryophyllum* (Diesing, 1850) Dollfus, 1929 (Linton, 1924), *Grillotia sasciae* Oosthuizen, Acosta, Smit & Schaeffner, 2021 (Oosthuizen *et al*., 2021), and *Eniochobothrium acostae* Oosthuizen, Smit & Schaeffner (Oosthuizen *et al*., 2022), though all were described from elasmobranchs. While adult cestodes are rarely reported from South African marine teleosts, larval stages such as plerocercoids and merocercoids are more frequently recovered from intermediate or paratenic fish hosts (Scholz *et al*., 2021). These larval forms often exhibit reduced morphological complexity, making species-level identification difficult without molecular data (Cutmore *et al*., 2024).

In this study, four larval cestode types were recovered from the intestinal tracts of *A. honckenii*, including representatives of the genera *Acanthobothrium* (*Acanthobothrium* sp.), *Scyphophyllidium* (*Scyphophyllidium* sp.), *Kotorella* (*K. pronosoma*), and *Nybelinia* (*Nybelinia* sp.). These represent the first records of cestodes infecting *A. honckenii* in South Africa, providing novel insights into cestode transmission pathways within this ecosystem. Despite its toxicity, *A. honckenii* appears to play a key ecological role as an intermediate or paratenic host in the life cycles of elasmobranch cestodes. The identification of larval cestodes from exclusively elasmobranch-associated genera supports the hypothesis that certain sharks and rays may possess physiological adaptations allowing them to consume toxic prey, thereby facilitating cestode transmission. While pufferfishes (Family Tetraodontidae) are infamous for their potent tetrodotoxin (TTX), which deters most predators, certain elasmobranchs are known to prey on these otherwise poisonous fish. For example, tiger sharks, *Galeocerdo cuvier* (Péron & Lesueur, 1822) routinely include pufferfish in their diet (Dicken *et al*., 2017; Ulman *et al*., 2021). A long-term study of tiger shark stomach contents in South African waters found that porcupinefish (Diodontidae), pufferfish (Tetraodontidae), and boxfish (Ostraciidae) were among the most common prey items across all shark size classes, indicating tiger sharks regularly consume these toxic (Dicken *et al*., 2017; Ulman *et al*., 2021). These observations confirm that at least some sharks can safely eat puffers despite their lethal toxin load. While bony fish and seabirds generally avoid pufferfish, tiger sharks and a few other high-level predators appear to have evolved a tolerance. This ability to exploit a toxic prey source gives such elasmobranchs a unique ecological advantage in accessing prey that most predators cannot.

Alternatively, *A. honckenii* may serve as a reservoir host, contributing to the persistence and circulation of larval stages within marine food webs. This finding highlights the importance of non-commercial or understudied hosts in maintaining parasite biodiversity and sustaining complex life cycles in marine systems.

***Acanthobothrium* sp.**

A total of three specimens were identified as *Acanthobothrium* sp. This represents the first record of representatives of this genus in *A. honckenii*. The full taxonomic classification and summary are as follows:

Class: Cestoda
Order: Onchoproteocephalidea
Family: Onchobothriidae
Genus: *Acanthobothrium* Blanchard, 1848
Species: Unknown
Present host: *Amblyrhynchote honckenii* (Bloch)
Present locality: Uvongo Beach, South Africa
Site of infection: Intestine
Prevalence (P): 30%
Mean intensity (MI): 1
Life stage: Larvae
Representative DNA sequences: One sequence for 28S rDNA
Voucher material: One specimen fixed on a slide (Figure 3.16A) and one specimen fixed in ethanol are kept in the collection of the Water Research Group (WRG) at the North-West University (NWU), Potchefstroom, South Africa

Specimens were identified based on a combination of morphological characters typical of larval onchobothriids and molecular sequence data from the 28S rDNA gene. Although adult features were absent, the larval scolex had four bothridia, which is characteristic of the genus *Acanthobothrium* (Caira and Jensen, 2001).

Molecularly, the partial 28S rDNA sequences showed a high degree of similarity to *A. hypermekkolpos* Fyler & Caira, 2010, differing by only 14 bp (1.26%), and clustered phylogenetically within a clade of other *Acanthobothrium* species known to parasitise elasmobranch hosts (Figure 3.17). The ecology of *Acanthobothrium* also supports this identification. The genus is highly host-specific in its adult stage, typically infecting elasmobranchs, such as rays and guitarfishes (Caira and Jensen, 2014). The larval stage

recovered here likely represents a plerocercoid, using *A. honckenii* as an intermediate or paratenic host. While *A. honckenii* is toxic and thus seldom predated upon, the presence of such cestodes suggests that some elasmobranchs may consume it.

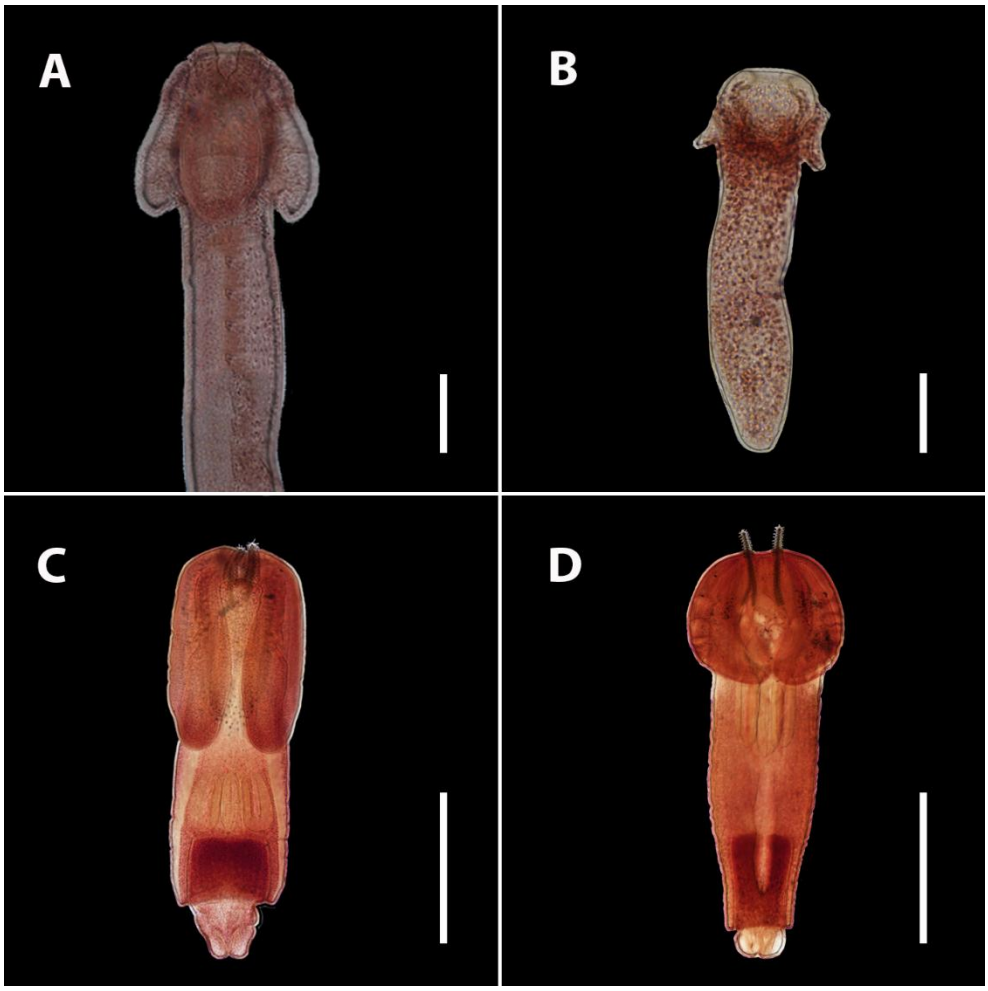

Figure 3.16: Light microscopy images of cestodes, parasitising *Amblyrhynchote honckenii* (Bloch) off the coast of South Africa. **A** – *Acanthobothrium* sp. Blanchard, 1848, scale bar 100 µm; **B** – *Scyphophyllidium* sp. Woodland, 1927, scale bar 100 µm; **C** – *Kotorella pronosoma* Euzet & Radujkovic, 1989, scale bar 50 µm; **D** – *Nybelinia* sp. Poche, 1926, scale bar 50 µm. Photographs **A–D** by Linda de Klerk.

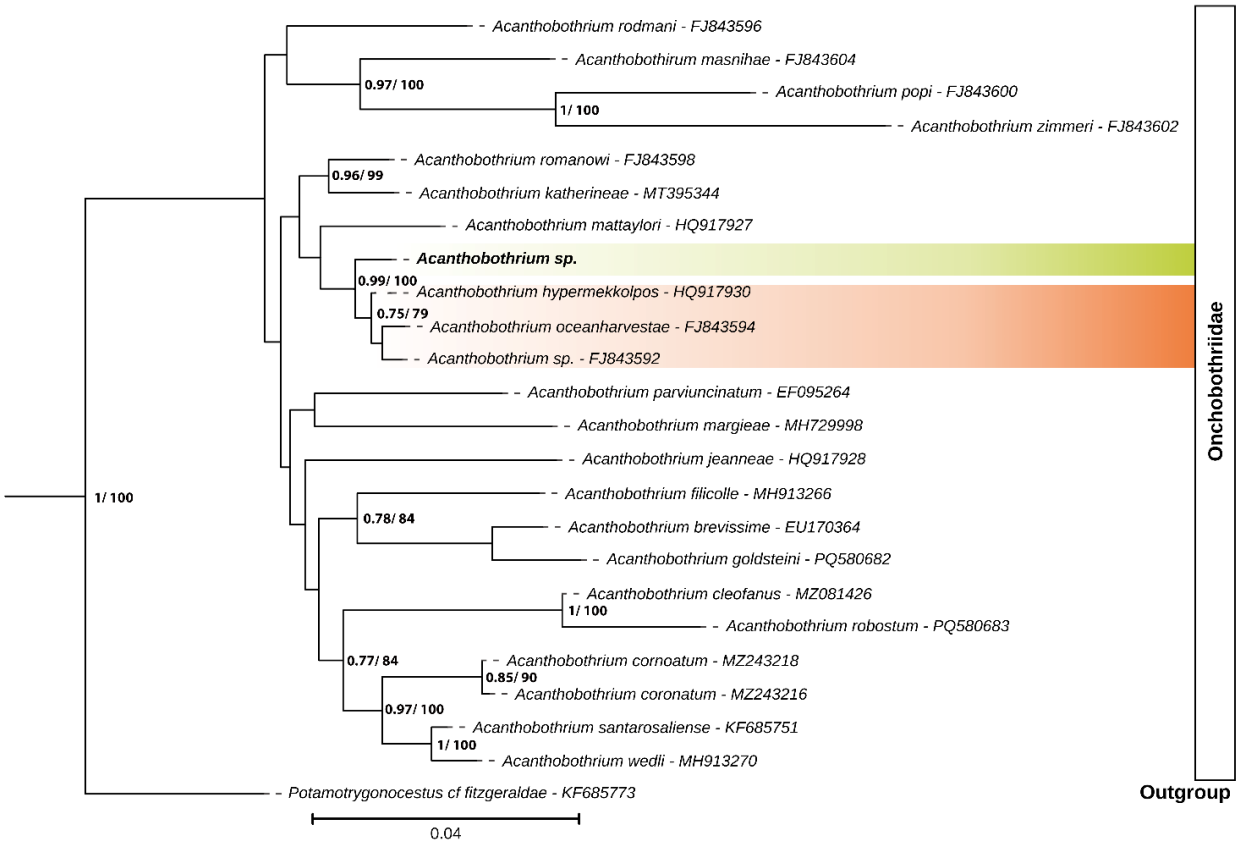

Figure 3.17: Bayesian Inference (BI) phylogenetic tree of the family Onchobothriidae, based on 28S rDNA sequences. Nodal support values are indicated as BI/Maximum Likelihood (ML); only values ≥0.7 (BI) and ≥70 (ML) are displayed. Newly sequenced isolates generated in this study are highlighted in green with bold text. The orange highlighted sequence indicates the closest genetic match. *Potamotrygonocestus fitzgeraldae* Marques, Brooks & Araujo, 2003, was selected as the outgroup.

***Scyphophyllidium* sp.**

A total of 324 specimens were identified as *Scyphophyllidium sp*. This represents the first record of members of this genus in *A. honckenii*. The full taxonomic classification and summary are as follows:

Class: Cestoda
Order: Phyllobothriidea
Family: Phyllobothriidae
Genus: *Scyphophyllidium* Woodland, 1927
Species: Unknown
Present host: *Amblyrhynchote honckenii* (Bloch)
Present locality: Breede River estuary, Witsand; Chintsa East; and Sodwana Bay, South Africa

Site of infection: Intestine
Prevalence (P): 38%
Mean intensity (MI): 27
Life stage: Larvae
Representative DNA sequences: Three sequences for 28S rDNA
Voucher material: Ten specimens fixed on slides (Figure 3.16B) and 310 specimens fixed in ethanol are kept in the collection of the Water Research Group (WRG) at the North-West University (NWU), Potchefstroom, South Africa

Specimens were identified based on distinctive morphological and genetic data. Morphologically, the specimens had a scolex with four bothridia and a developing strobila consistent with a developmental form of larval phyllobothriids (Caira *et al*., 2017).

Molecular analysis targeting the 28S rDNA gene showed close affinity to *Scyphophyllidium sinclairtaylori* (Cutmore, Bennett, Miller & Cribb, 2017) Caira, Jensen & Ruhnke in Caira, Jensen, Hayes & Ruhnke, 2020, with 14 bp differences (1.5%). Phylogenetic analyses placed the sequences in a well-supported clade comprising exclusively *Scyphophyllidium* species parasitising batoid fishes (Figure 3.18). The presence of larvae in *A. honckenii* suggests that this host serves as a trophic intermediate or paratenic host. Given that *Scyphophyllidium* spp. typically mature in rays and skates, the infection may occur through ingestion of fish already infected with earlier larval stages.

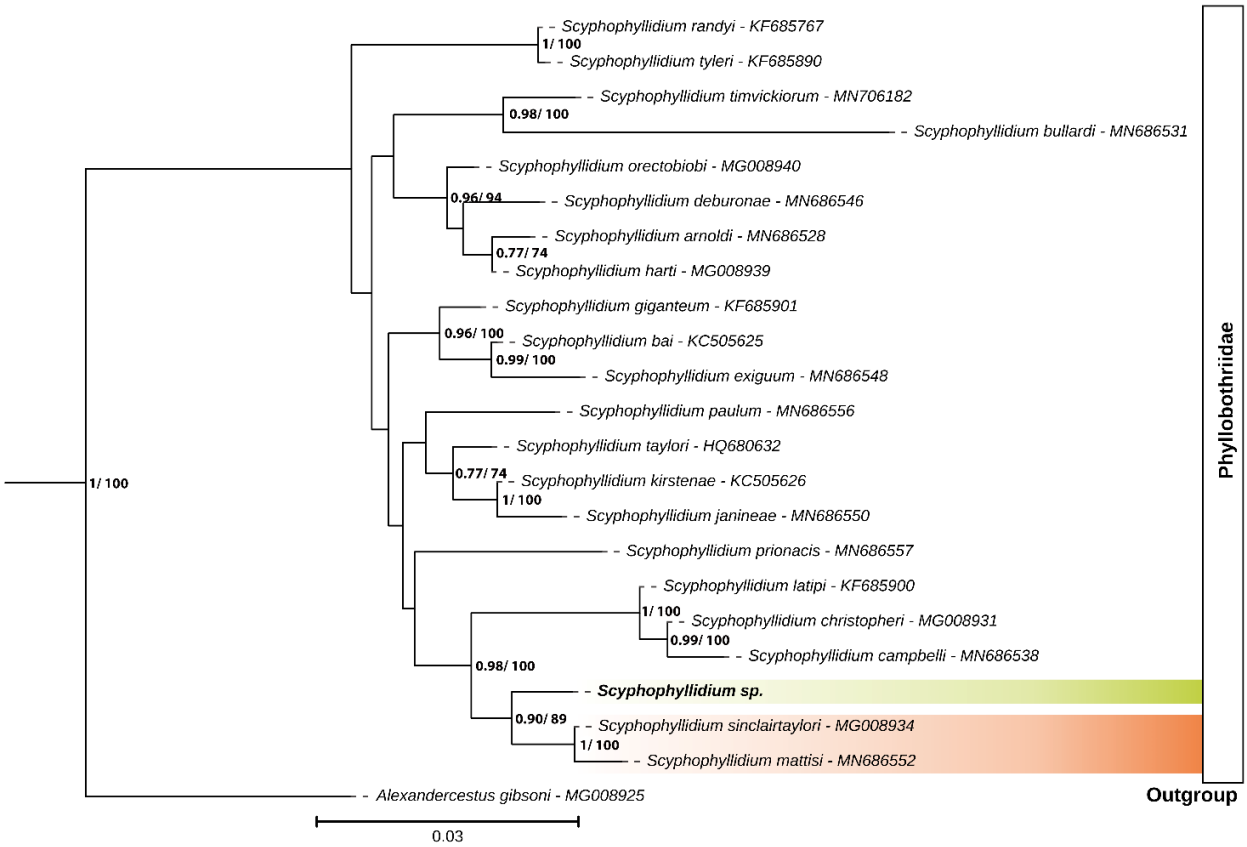

Figure 3.18: Bayesian Inference (BI) phylogenetic tree of the family Phyllobothriidae, based on 28S rDNA sequences. Nodal support values are indicated as BI/Maximum Likelihood (ML); only values ≥0.7 (BI) and ≥70 (ML) are displayed. Newly sequenced isolates generated in this study are highlighted in green with bold text. The orange highlighted sequence indicates the closest genetic match. *Alexandercestus gibsoni* Ruhnke & Workman, 2013, was selected as the outgroup.

Kotorella pronosoma

A total of 12 specimens were identified as *K. pronosoma*. This represents the first record of representatives of this genus in *A. honckenii*. The full taxonomic classification and summary are as follows:

Class: Cestoda
Order: Trypanorhyncha
Family: Tentaculariidae
Genus: *Kotorella* Euzet & Radujkovic, 1989
Species: *Kotorella pronosoma* (Stossich, 1901) Euzet & Radujkovic, 1989
Type host: *Syacium papillosum* (Linnaeus, 1758) (Paralichthyidae)
Type locality: Yucatan shelf, Gulf of México
Present host: *Amblyrhynchote honckenii* (Bloch)

Present locality: Chintsa East; Uvongo Beach; and Sodwana Bay, South Africa
Site of infection: Intestine
Prevalence (P): 40
Mean intensity (MI): 1
Life stage: Larvae
Representative DNA sequences: 3 sequences for 28S rDNA
Voucher material: Three specimens fixed on slides (Figure 3.16C) and 6 specimens fixed in ethanol are kept in the collection of the Water Research Group (WRG) at the North-West University (NWU), Potchefstroom, South Africa

Specimens were identified based on both morphology and 28S rDNA sequences. The tentacular armature, glandular bulbs, and scolex morphology match existing descriptions of larval tentaculariids (Palm, 2004). Genetic analysis revealed a 100% sequence match with *K. pronosoma*, and phylogenetic placement was fully congruent with this identification (Figure 3.19).

Kotorella pronosoma has been described in adult form from elasmobranch hosts, and its larval stages are known to use marine teleosts as paratenic hosts (Palm and Overstreet, 2000). The presence of this species in *A. honckenii* aligns with this pattern and represents the first report from this host species and from multiple localities along the South African coast. It also highlights the pufferfish's potential role in facilitating the life cycle of trypanorhynchs.

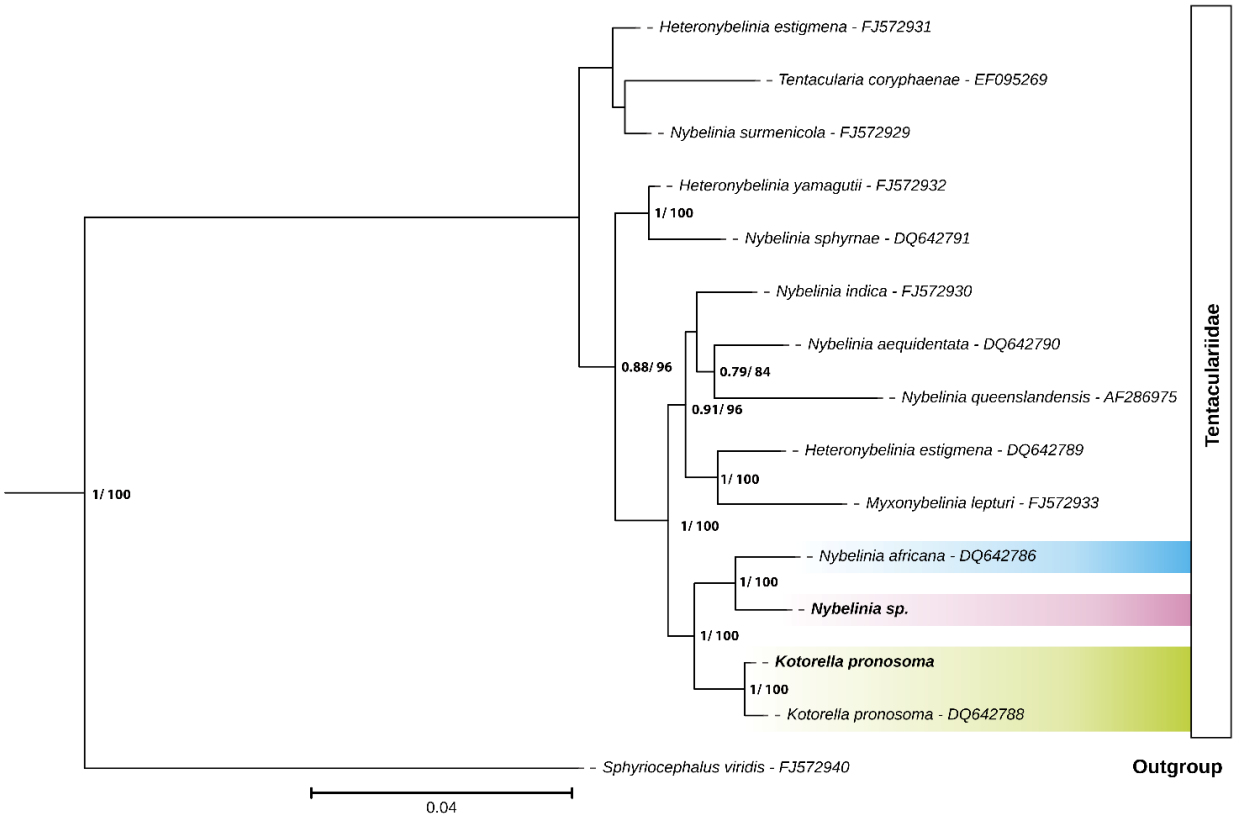

Figure 3.19: Bayesian Inference (BI) phylogenetic tree of the family Tentaculariidae, based on 28S rDNA sequences. Nodal support values are indicated as BI/Maximum Likelihood (ML); only values ≥0.7 (BI) and ≥70 (ML) are displayed. Newly sequenced isolates generated in this study are highlighted in green and pink, with bold text. The blue highlighted sequence indicates the closest genetic match. *Sphyriocephalus viridis* (Wagener, 1854) Pintner, 1913 was selected as the outgroup.

***Nybelinia* sp.**

A total of 10 specimens were identified as *Nybelinia* sp. This represents the first record of this genus in *A. honckenii*. The full taxonomic classification and summary are as follows:

Class: Cestoda
Order: Trypanorhyncha
Family: Tentaculariidae
Genus: *Nybelinia* Poche, 1926
Species: Unknown
Present host: *Amblyrhynchote honckenii* (Bloch)
Present locality: Breede River estuary, Witsand, South Africa
Site of infection: Intestine
Prevalence (P): 67%
Mean intensity (MI): 0.7

Life stage: Larvae

Representative DNA sequences: 3 sequences for 28S rDNA

Voucher material: Three specimens fixed on slides (Figure 3.16D) and three specimens fixed in ethanol are kept in the collection of the Water Research Group (WRG) at the North-West University (NWU), Potchefstroom, South Africa.

Specimens were identified based on typical trypanorhynch larval traits, four tentacles; hook rows, and tentacular bulbs (Palm, 2004). The 28S rDNA sequences aligned closely with *Nybelinia africana* Dollfus, 1960, differing by 22 bp (1.8%), placing them in a *Nybelinia* clade in the phylogenetic analysis (Figure 3.19). *Nybelinia* spp. are well-documented in marine environments, with complex life cycles involving crustaceans, teleosts, and elasmobranchs (Palm and Overstreet, 2000). Larval stages often infect pelagic fish species that are subsequently consumed by sharks or rays, the definitive hosts. Although definitive species identification cannot be confirmed without adult material, the genetic divergence and morphological consistency provide strong support for genus-level identification. Given the phylogenetic proximity to *N. africana*, it is likely that the definitive host is an elasmobranch species occurring in the same region. Further sampling of adult cestodes from elasmobranchs will be necessary to confirm this link.

Class Monopisthocotylea and Polyopisthocotylea

Monopisthocotyleans and polyopisthocotyleans are a diverse group of ectoparasitic flatworms that typically inhabit the gills, skin, and fins of both marine and freshwater fishes (Buchmann and Bresciani, 2006). They possess a monoxenous life cycle, wherein a free-swimming oncomiracidium larva hatches from the egg and directly infects a new host (Kearn, 2011). In South Africa, although the marine monopisthocotylean and polyopisthocotylean fauna remains only partially documented, considerable progress has been made in recent years, particularly on elasmobranch and sparid hosts (Vaughan *et al*., 2010; Smit and Hadfield, 2015; Nunkoo, 2019). Early contributions to this field include the descriptions of *Callorhynchocotyle callorhynchi* (Manter, 1955) Boeger, Kritsky & Pereira, 1989 and *Callorhynchicola multitesticulatus* Manter, 1955 (Manter, 1955), followed by *Udonella myliobati* (Guberlet, 1936) (Olivier et al., 2000), *Udonella caligorum* Johnston, 1835 (Grobler *et al*., 2003), *Branchotenthes robinoverstreeti* Bullard & Dippenaar, 2003 (Bullard and Dippenaar, 2003) and *Dermophthirius carcharhini* MacCallum, 1926 (Bullard *et al*., 2004). Subsequent studies led to the identification of several additional species, including *Dendromonocotyle* spp. Hargis, 1955 (Vaughan *et al*., 2008; Vaughan and Chisholm, 2009), *Heterocotyle tokoloshei* Vaughan & Chisholm, 2010 (Vaughan and Chisholm, 2010a), *Neoheterocotyle robii* Vaughan & Chisholm, 2010 (Vaughan and Chisholm, 2010b), *Myxinidocotyle eptatreti* Vaughan & Christison, 2010 (Vaughan and Christison,

2010), *Gyrodactylus eyipayipi* Vaughan, Christison, Hansen & Shinn, 2010 (Vaughan *et al*., 2010), and *Pseudoleptobothrium christisoni* Vaughan & Chisholm, 2011 (Vaughan and Chisholm, 2011). Most recently, *H. victorwepeneri* was described by Acosta and Smit (2021), marking a significant addition to the known diversity of monopisthocotyleans and polyopisthocotyleans in South African marine systems. Despite these advancements, several host groups, particularly tetraodontiform fishes, remain underexplored. At present, *H. victorwepeneri* is the only polyopisthocotylean species formally described from *A. honckenii* in South African marine systems. Given the cryptic morphology and high host specificity of many monopisthocotyleans and polyopisthocotyleans, it is highly probable that additional, yet undiscovered species are present on tetraodontid hosts in the region.

In this study, *H. victorwepeneri* was recovered from its type host, at the type locality in South Africa, confirming its presence in this region. In addition, *U. australis*, was observed as an epibiont attached to the parasitic copepod *Cal. tetrodontis*, (identification described earlier), representing a notable ecological association. These findings contribute to the limited but growing knowledge of monopisthocotylean and polyopisthocotylean diversity and their interactions within tetraodontiform hosts in South African marine environments.

Udonella australis

A total of 12 specimens were identified as *U. australis*. The occurrence of *Udonella* on parasitic copepods also highlights its unique hyperparasitic lifestyle, one of the few known examples in marine platyhelminths (Freeman and Ogawa, 2010). This represents the first record of this genus on *Cal. tetrodontis* and *A. honckenii*. The full taxonomic classification and summary are as follows:

Class: Monopisthocotylea
Order: Gyrodactylidea
Family: Udonellidae
Genus: *Udonella* Johnston, 1835
Species: *Udonella australis Carvajal & Sepulveda, 2002*
Type host: *Lepeophtheirus mugiloidis* Villalba & Duran, 1986 ex. *Pinguipes chilensis* Valenciennes
Type locality: Concepción, Chile
Present host: *Caligus tetrodontis* Barnard, 1948 ex. *Amblyrhynchote honckenii* (Bloch)
Present locality: Mossel Bay, South Africa
Site of infection: External body surface of *Cal. tetrodontis* ex *A. honckenii*
Prevalence (P): 10% in fish hosts, 8% in copepod host

Mean intensity (MI): 12

Life stage: Adult

Representative DNA sequences: Three sequences for 18S rDNA and two sequences for 28S

Voucher material: Eight specimens fixed on slides (Figure 3.20) and four specimens fixed in ethanol are kept in the collection of the Water Research Group (WRG) at the North-West University (NWU), Potchefstroom, South Africa

Specimens were identified using both morphological characteristics and molecular analyses. All morphometric data for the newly collected specimens fell within the range previously described for *U. australis* by Carvajal and Sepúlveda (2002), with some measurements slightly extending known limits. Molecular analysis of the 18S rDNA gene region revealed a 99.70% sequence similarity to *U. australis*, and phylogenetic analyses placed the specimens within a strongly supported clade alongside this species (Figure 3.21). To date, only two other udonellid species have been reported from South Africa, *U. myliobati* and *U. caligorum*. However, genetic comparisons of 18S rDNA, clearly distinguish the current specimens from these species, with sequence differences of 67 base pairs (6.90%) and 36 base pairs (3.72%), respectively. This is the first known record of *U. australis* from the South African coastline. Although *U. australis* was originally described from Chile (Carvajal and Sepúlveda, 2002), this finding represents a significant geographic range extension to the South African coast.

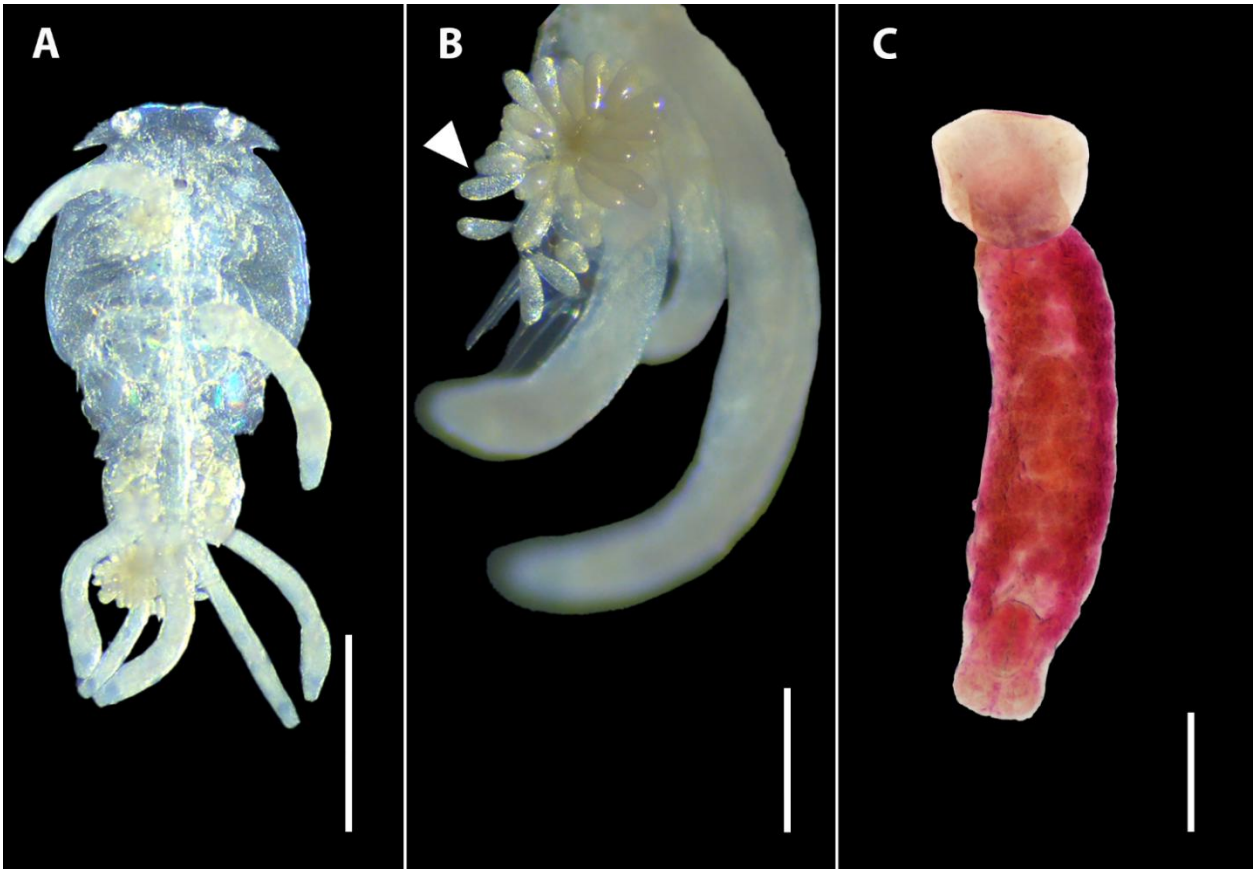

Figure 3.20: Light microscopy images of *Udonella australis* Carvajal & Sepulveda, 2002 ex *Caligus tetrodontis* Barnard, 1948, parasitising *Amblyrhynchote honckenii* (Bloch) off the coast of South Africa. **A** – *Udonella australis* ex *Cal. tetrodontis*, scale bar 2 mm; **B** – Specimens with eggs (arrow indicates eggs), scale bar 500 µm; **C** – Stained whole specimen, scale bar 200 µm. Photographs **A–C** by Linda de Klerk.

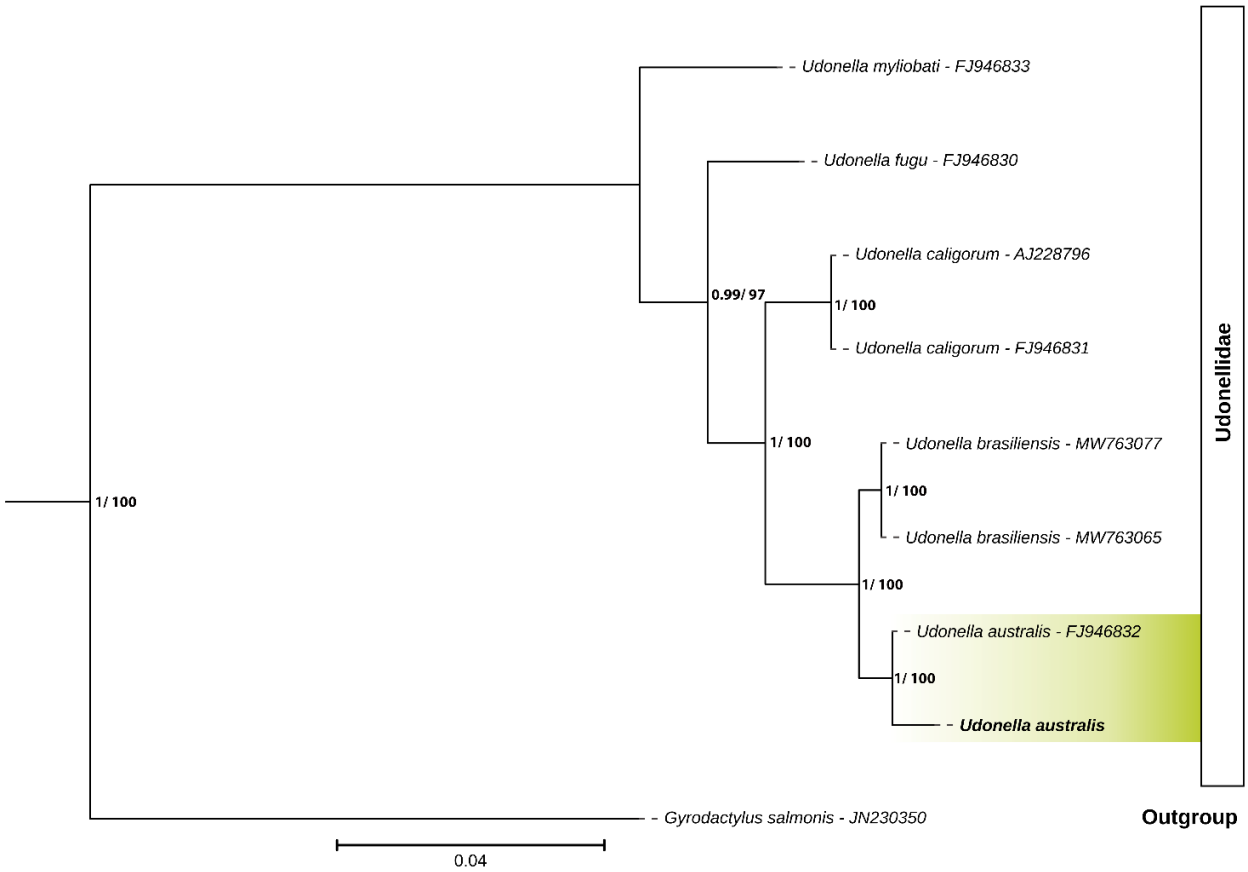

Figure 3.21: Bayesian Inference (BI) phylogenetic tree of the family Udonellidae, based on 18S rDNA sequences. Nodal support values are indicated as BI/Maximum Likelihood (ML); only values ≥0.7 (BI) and ≥70 (ML) are displayed. Newly sequenced isolates generated in this study are highlighted in green with bold text. *Gyrodactylus salmonis* Yin & Sproston, 1948 was selected as the outgroup.

Heterobothrium victorwepeneri

A total of 23 specimens were identified as *H. victorwepeneri*. These specimens were collected from the type host species and type locality for the species, as originally described by Acosta and Smit (2019). The full taxonomic classification and summary are as follows:

Class: Polyopisthocotylea
Order: Mazocraeidea
Family: Diclidophoridae
Genus: *Heterobothrium* Cerfontaine, 1895
Species: *Heterobothrium victorwepeneri* Acosta & Smit, 2021
Type host: *Amblyrhynchote honckenii* (Bloch)
Type locality: Chintsa East, South Africa
Present host: *Amblyrhynchote honckenii* (Bloch)

Present locality: Breede River estuary, Witsand; Chintsa East; and Uvongo Beach, South Africa

Site of infection: Gills

Prevalence (P): 66%

Mean intensity (MI): 1

Life stage: Adult

Representative DNA sequences: Three sequences for 28S rDNA and two sequences for COI mtDNA

Voucher material: Six specimens fixed on slides (Figure 3.22) and 17 specimens fixed in ethanol are kept in the collection of the Water Research Group (WRG) at the North-West University (NWU), Potchefstroom, South Africa

Specimens were identified through a combination of morphological and molecular analyses and were consistent with the original description of *H. victorwepeneri* by Acosta and Smit (2021). This study confirms the continued presence of *H. victorwepeneri* in *A. honckenii* across multiple sites along the South African coastline. Morphologically, the specimens displayed all key diagnostic features of the species, including characteristic body shape, haptoral structures, and reproductive anatomy. Molecular analysis of the COI mtDNA gene further supported this identification, with sequences showing a 100% match to previously published *H. victorwepeneri* data and clustering within the same well-supported phylogenetic clade (Figure 3.23). These findings reinforce the species' identity and its persistence within its type host and geographical range.

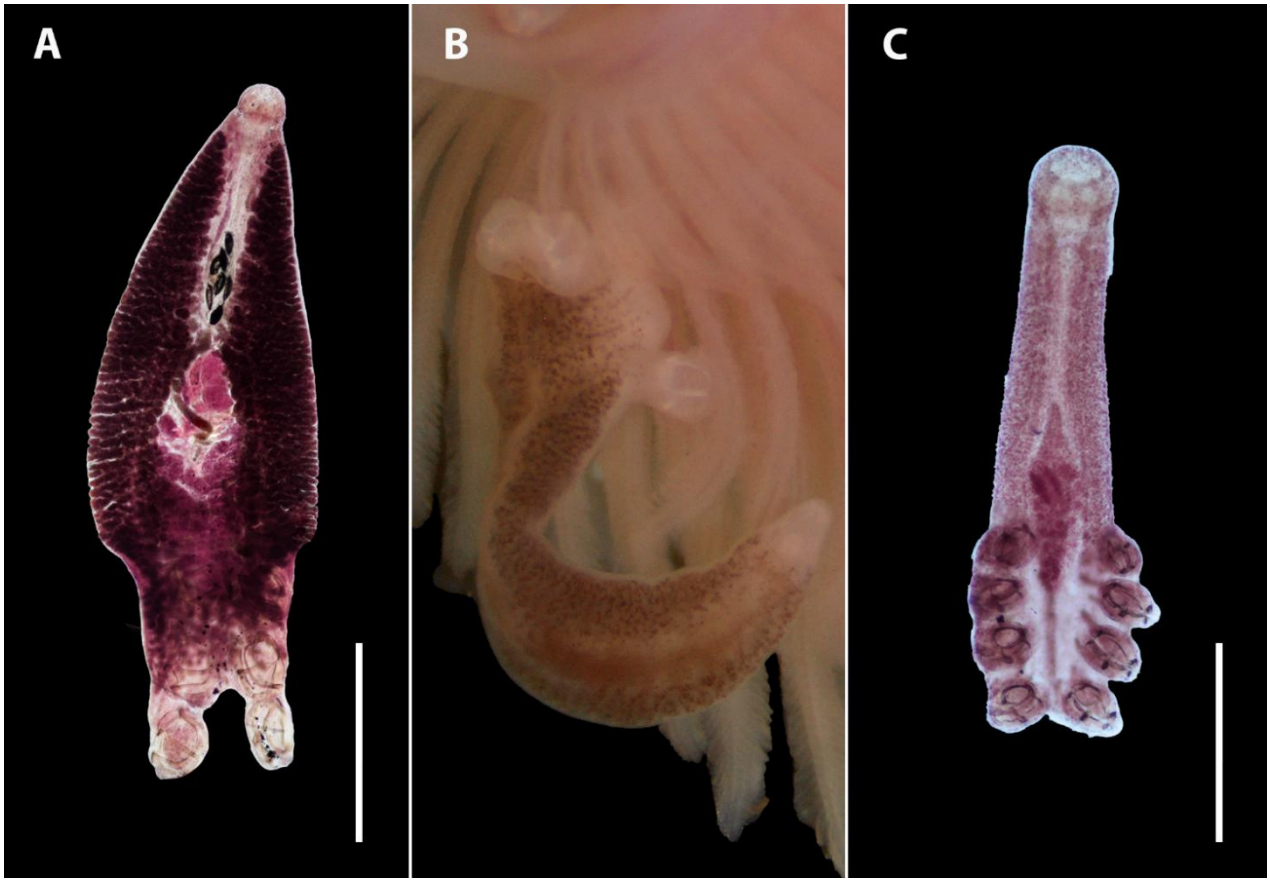

Figure 3.22: Light microscopy images of *Heterobothrium victorwepeneri* Acosta & Smit, 2021, parasitising *Amblyrhynchote honckenii* (Bloch) off the coast of South Africa. **A** – Stained adult specimen, scale bar 500 µm; **B** – Specimen on gills; **C** – Stained larval specimen, scale bar 500 µm.Photographs **A–C** by Linda de Klerk.

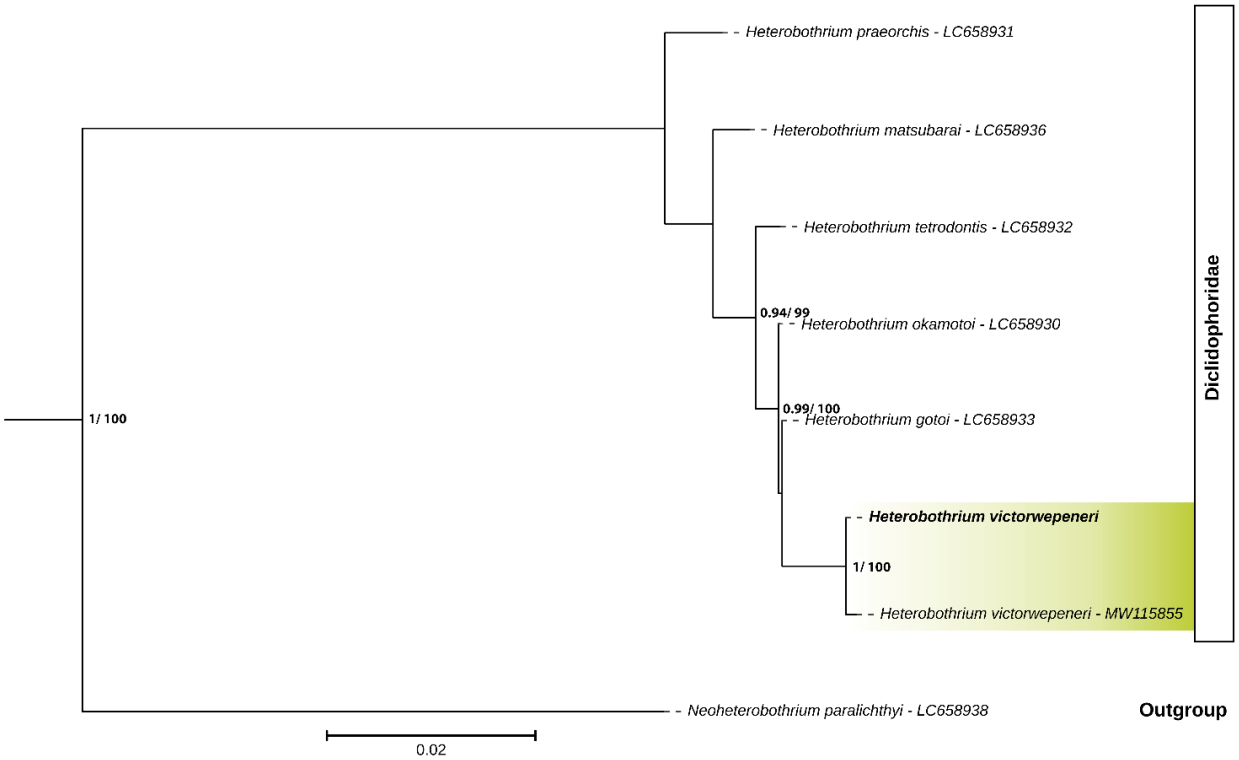

Figure 3.23: Bayesian Inference (BI) phylogenetic tree of the family Diclidophoridae, based on COI mtDNA sequences. Nodal support values are indicated as BI/Maximum Likelihood (ML); only values ≥0.7 (BI) and ≥70 (ML) are displayed. Newly sequenced isolates generated in this study are highlighted in green with bold text. *Neoheterobothrium paralichthyi* Suriano & Labriola, 1999, was selected as the outgroup.

Class Trematoda

Trematodes are obligate endoparasitic flatworms characterised by complex, heteroxenous life cycles involving at least two hosts, typically an aquatic mollusc as the first intermediate host and a vertebrate, such as a fish, bird, or mammal, as the definitive host (Cribb *et al*., 2001). These life cycles often include free-living larval stages (such as miracidia and cercariae) and occasionally involve additional intermediate or paratenic hosts (Cribb *et al*., 2001).

Research on the trematode parasites of South African marine fishes has historically been limited, with only a small number of detailed studies conducted over the years (Yong *et al*., 2023). Although contributions by several international and local researchers significantly advanced knowledge of the region's digenean fauna, comprehensive surveys have remained scarce (Yong *et al*., 2023). In 2022, approximately only 70 trematode species had been formally recorded from South African marine fishes, a figure significantly lower than the 190 species recorded from southern Australia or the 529 species reported from subtropical eastern China (Bray *et al*., 2016; Cribb *et al*., 2016, Yong *et al*., 2023). Most recent work in South Africa has focused on freshwater

trematodes, particularly on larval stages in intermediate hosts (Malatji and Mukaratirwa, 2019; Hoogendoorn *et al*., 2020; Rakgole *et al*., 2019; Dos Santos *et al*., 2021; Truter *et al*., 2025), while relatively few studies have investigated marine systems (Vermaak *et al*., 2023a; b). The limited number of new species described in recent years reflects both the lack of systematic sampling and the undiscovered hidden diversity of trematodes in South African coastal ecosystems (Yong *et al*., 2023). The evileye blaasop, *A. honckenii*, exemplifies the extent of this knowledge gap. To date, only a single digenean species, *Pseudoheterolebes cotylophorus* (Yamaguti, 1934) Bray, 1986 (Bray, 1986; Martin *et al*., 2018), has been recorded from this host, originally described from the gastrointestinal tract.

In this study, five digenean taxa were recovered from *A. honckenii* at various sites along the South African coast: *Rhipidocotyle* sp. (metacercariae), *Bucephalidea* gen. sp. (metacercariae), *Helicometrina* sp. (larvae), *O. cotylophorus* (adult) as *O. amplicoelus* Nicoll 1915 (adult), and *Zoogonidae* gen. sp. (larvae). Of these, only *O. amplicoelus* was represented by adult specimens; the others were found as larval stages, particularly bucephalid metacercariae, suggesting that *A. honckenii* likely serves as a second-intermediate or accidental host. These findings reflect both the under-sampling of this host species and the broader underestimation of trematode diversity in South African marine ecosystems. Comprehensive surveys incorporating molecular tools are urgently needed to improve understanding of digenean biodiversity and host associations in the region.

***Rhipidocotyle* sp.**

A total of 977 specimens were identified as a new species of *Rhipidocotyle* sp. This represents the first record of this genus and species in *A. honckenii*. As part of a larger project on the Bucephalidae, a manuscript (Louvard *et al*. 2025) describing the larval (including those from the present study) and adult stages of this new species has already been accepted for publication. The full taxonomic classification and summary are as follows:

Class: Trematoda
Order: Plagiorchiida
Family: Bucephalidae
Genus: *Rhipidocotyle* Diesing, 1858
Species: Unknown
Present host: *Amblyrhynchote honckenii* (Bloch)
Present locality: Breede River estuary, Witsand; Chintsa East; and Uvongo Beach, South Africa
Site of infection: Heart and eyes

Prevalence of infection: 62%
Intensity of infection: 44.4
Life stage: Larvae (Metacercaria)
Representative DNA sequences: 14 sequences for 28S
Voucher material: 963 specimens fixed in ethanol are kept in the collection of the Water Research Group (WRG) at the North-West University (NWU), Potchefstroom, South Africa

Specimens were identified based on distinct morphological features consistent with the genus *Rhipidocotyle* and confirmed using partial 28S rDNA sequences (Figure 3.24), which matched identically to adult specimens collected from *Lichia amia* (Linnaeus, 1758) and sporocysts from *Perna perna* (Linnaeus, 1758) (see Louvard et al. 2025). This work contributes to our understanding of parasite diversity in *A. honckenii,* and highlights its role as a second intermediate host in the complex life cycle of *Rhipidocotyle* sp.

Bucephalidae gen. sp.

A total of 1,950 larval specimens were identified as members of the family Bucephalidae. These were all recovered as metacercarial cysts, and due to the absence of corresponding adult stages and lack of clear morphological diagnostic features, the genus and species remain unidentified. This represents the second record of a bucephalid metacercaria in *A. honckenii*. The full taxonomic classification and summary are as follows:

Class: Trematoda
Order: Plagiorchiida
Family: Bucephalidae
Genus: Unknown
Species: Unknown
Present host: *Amblyrhynchote honckenii* (Bloch)
Present locality: Mossel Bay; Chintsa East; and Sodwana Bay, South Africa
Site of infection: Intestine, heart and eyes
Prevalence (P): 51%
Mean intensity (MI): 102.6
Life stage: Larvae
Representative DNA sequences: Three sequences for 28S
Voucher material: 1,947 specimens fixed in ethanol are kept in the collection of the Water Research Group (WRG) at the North-West University (NWU), Potchefstroom, South Africa

The Bucephalidae is a large, cosmopolitan family of trematodes infecting marine, brackish, and freshwater fishes, with fish typically serving as second intermediate hosts (Overstreet and Curran in Jones *et al*., 2005). The specimens recovered in this study differ genetically from *Rhipidocotyle meridionalis* by 108 bp (9.72%) based on 28S rDNA sequence analysis. Although precise identification is not yet possible without adult forms, phylogenetic analysis places these metacercariae in a clade with *Prosorhynchoides* Dollfus, 1929, species (Figure 3.24). The closest match is *P. moretonensis* Hammond, Cribb & Bott, 2018, differing by only 30 base pairs (2.45%). This is also seen in the Bayesian inference (BI) phylogenetic tree (Figure 3.24), where the isolate forms a well-supported subclade alongside *Prosorhynchoides* sequences.

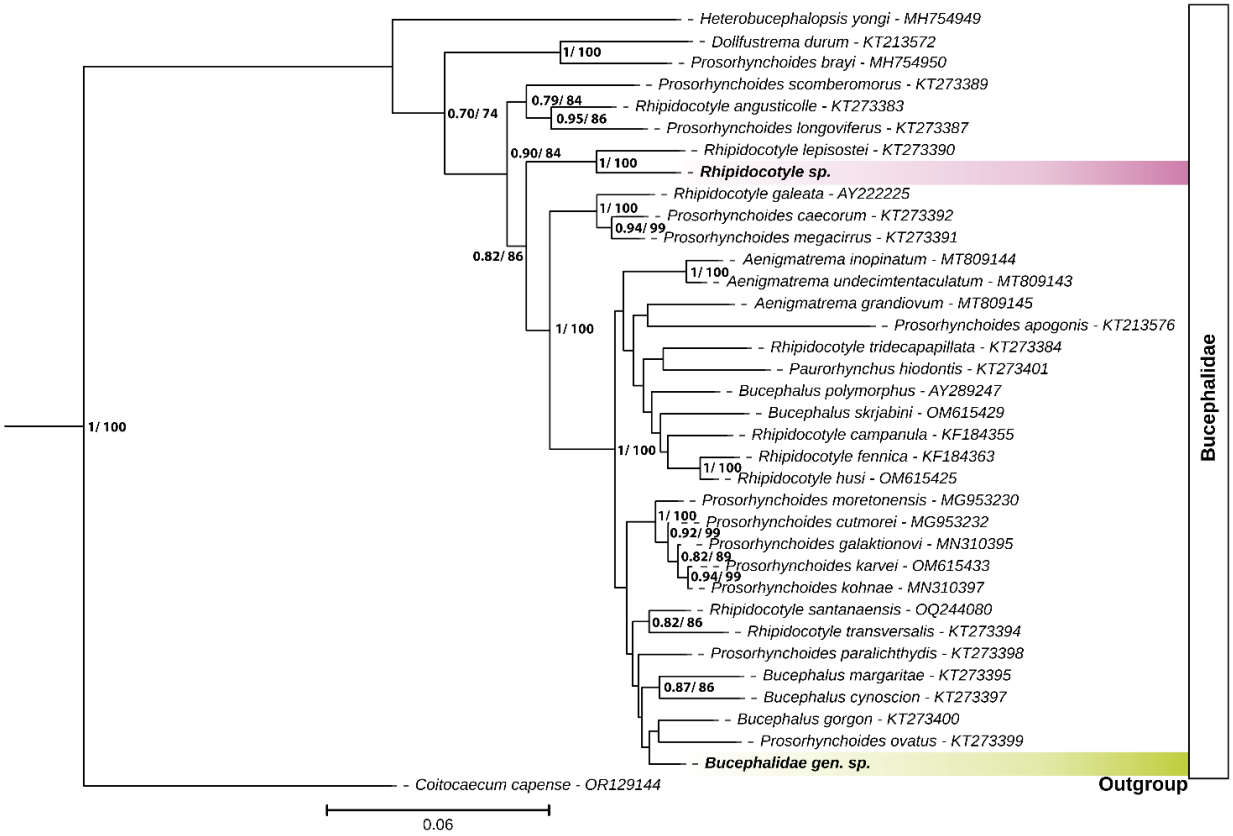

Figure 3.24: Bayesian Inference (BI) phylogenetic tree of the family Bucephalidae, based on 28S rDNA sequences. Nodal support values are indicated as BI/Maximum Likelihood (ML); only values ≥0.7 (BI) and ≥70 (ML) are displayed. Newly sequenced isolates generated in this study are highlighted in green and pink, with bold text. *Coitocaecum capense* Bray, 1987 was selected as the outgroup.

***Helicometrina* sp.**

A single specimen was identified as *Helicometrina* sp. This is the first record of a species of *Helicometrina* in *A. honckenii*. The full classification and summary are as follows:

Class: Trematoda

Order: Plagiorchiida

Family: Opecoelidae

Genus: *Helicometrina* Linton, 1910

Species: Unknown

Present host: *Amblyrhynchote honckenii* (Bloch)

Present locality: Sodwana Bay, South Africa

Site of infection: Intestine

Prevalence (P): *10*%

Mean intensity (MI): 1

Life stage: Larvae

Representative DNA sequences: One sequence for ITS2 and one sequence for 28S rDNA

Voucher material: One hologenophore fixed in ethanol (Figure 3.25A) is kept in the collection of the Water Research Group (WRG) at the North-West University (NWU), Potchefstroom, South Africa

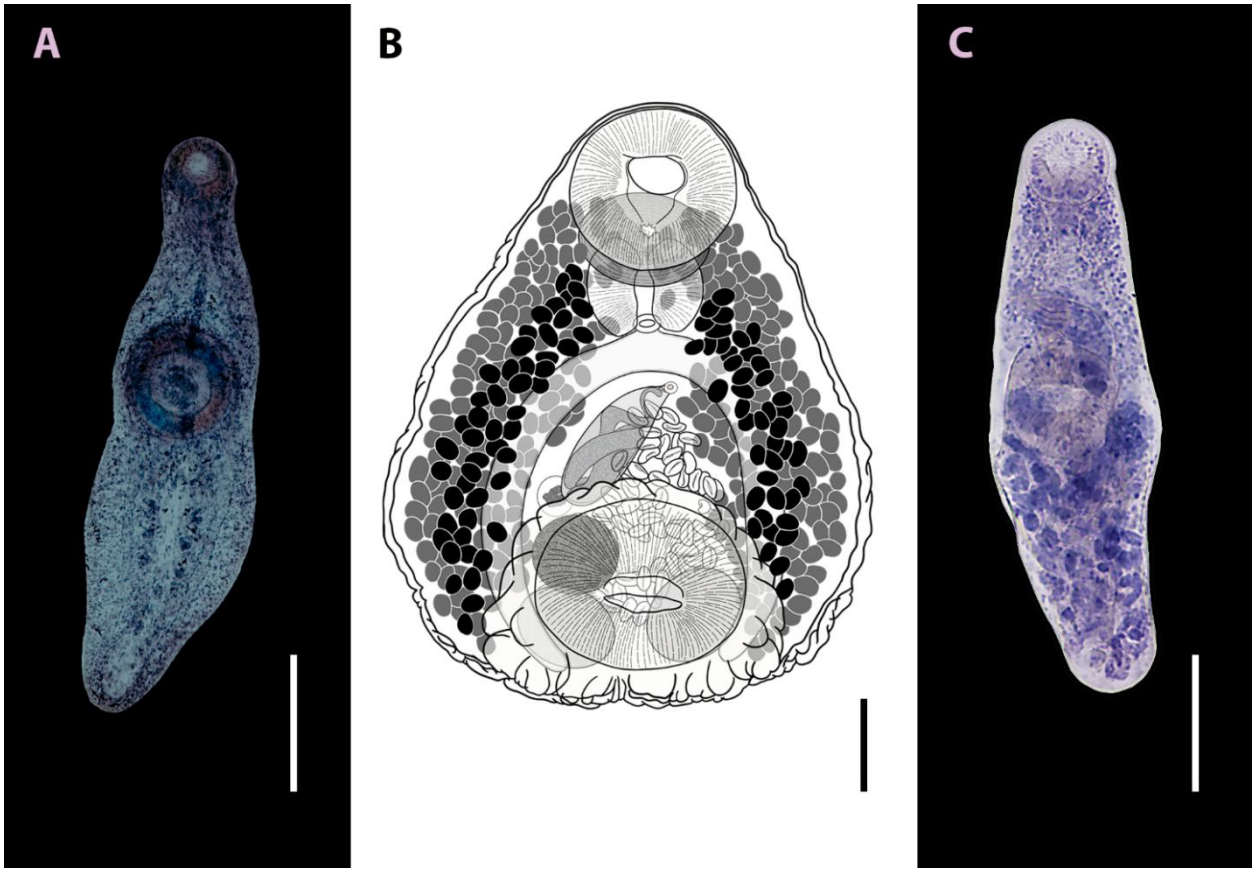

Figure 3.25: Light microscopy photos and line drawing of trematode specimens parasitising *Amblyrhynchote honckenii* (Bloch) along the South African coastline. **A** – *Helicometrina* sp. Linton, 1910, scale bar 200µm; **B** – Line drawing of *Opistholebes amplicoelus* Nicoll, 1915, scale bar 500µm; **C** – Zoogonidae gen. sp., scale bar 100µm. Photographs **A, C** by Dr. Russel Q-Y. Yong, **B** by Linda de Klerk.

The Opecoelidae is one of the most diverse families of digeneans, yet only a single *Helicometrina* species, *H. nimia* Linton, 1910, has previously been reported from South Africa (Bray, 1987). Although immature, the specimen collected in this study shows morphological features consistent with *Helicometrina*, including a helical uterus, filamented eggs, and caeca terminating blindly in the hindbody (Cribb in Jones *et al*., 2005). Molecular data from the 28S rDNA gene place this isolate in proximity to *Helicometrina* species originally described from South Africa; however, it forms a distinct lineage, differing from *H. nimia* by 97 base pairs (7.68%) (Figure 3.26). Due to the limited availability of reference sequences for *Helicometrina*, the isolate rather forms a clade with *Helicometra* species in the phylogenetic analysis. Interestingly, the isolate is genetically more similar to *Helicometra fasciata (Rudolphi, 1819) Odhner, 1902*, differing by only 58 base pairs (4.60%). This apparent affinity with *Helicometra* is likely an artefact of incomplete taxon sampling, as the genus *Helicometrina* was established to accommodate species morphologically similar to *Helicometra* but with more than two testes. While morphological observations strongly support placement within *Helicometrina*, additional material and more

comprehensive molecular datasets will be required to confirm the taxonomic identity of this isolate.

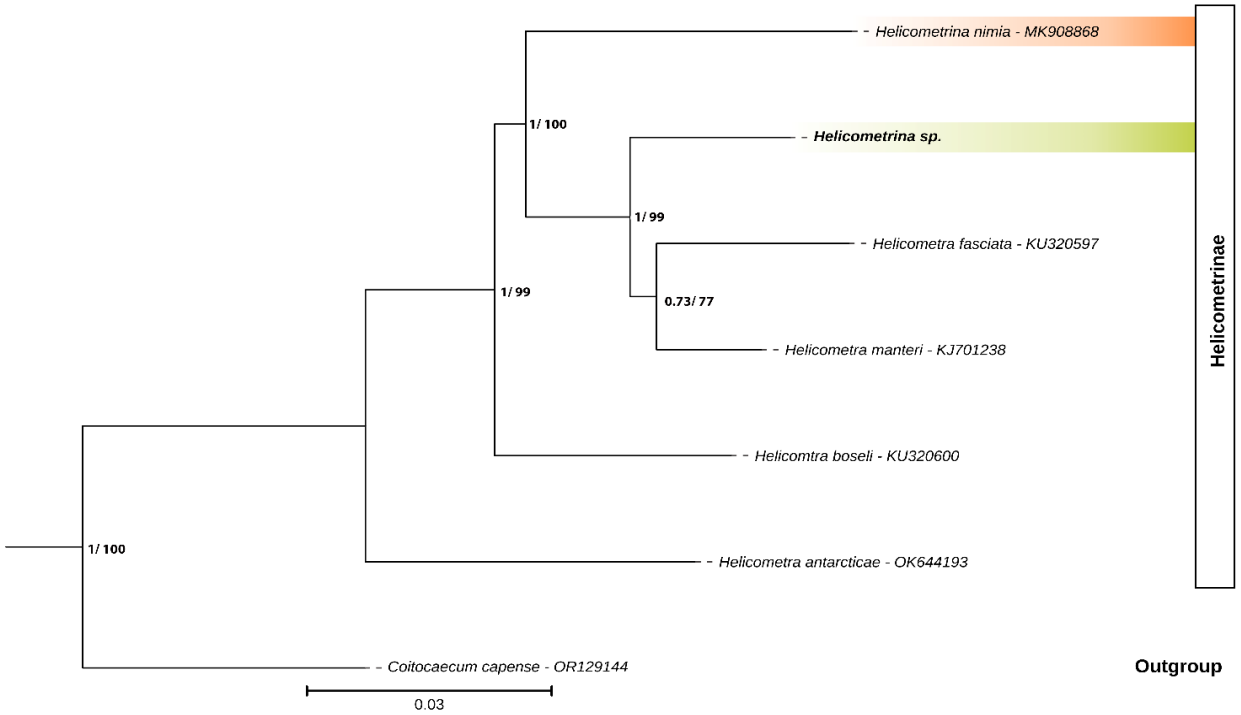

Figure 3.26: Bayesian Inference (BI) phylogenetic tree of the family Helicometrinae, based on 28S rDNA sequences. Nodal support values are indicated as BI/Maximum Likelihood (ML); only values ≥0.7 (BI) and ≥70 (ML) are displayed. Newly sequenced isolates generated in this study are highlighted in green with bold text. The orange highlighted sequence indicates the closest genetic match. *Coitocaecum capense* Bray, 1987 was selected as the outgroup.

Opistholebes amplicoelus

A total of 18 specimens were identified as *O. amplicoelus*. This species was previously reported in *A. honckenii* as *O. cotylophorus*, which was then reassigned to *P. cotylophorus* based on morphological characters. During this study, genetic analyses were employed, and the species is now reassigned to *O. amplicoelus*. The full manuscript for the description of this species is prepared to be submitted. The full taxonomic classification and summary are as follows:

Class: Trematoda
Order: Plagiorchiida
Family: Opecoelidae
Genus: *Opistholebes* Nicoll, 1915
Species: *Opistholebes amplicoelus* Nicoll, 1915
Type host: *Lagocephalus lunaris* (Bloch & Schneider)
Type locality: Cleveland Bay, Australia.
Present host: *Amblyrhynchote honckenii* (Bloch)
Present locality: Breede River estuary, Witsand; and Chintsa East, South Africa
Site of infection: Intestine
Prevalence (P): 56%
Mean intensity (MI): 1.3
Life stage: Adult
Representative DNA sequences: Five sequences for ITS2 rDNA, three sequences for 28S rDNA, 11 sequences for COI mtDNA, and 10 sequences for nad1
Voucher material: 15 specimens fixed on slides (Figure 3.25B) and five specimens fixed in ethanol are kept in the collection of the Water Research Group (WRG) at the North-West University (NWU), Potchefstroom, South Africa

Adult trematodes were initially identified as *P. cotylophorus* (Yamaguti, 1934) Bray, 1986, based on previous records from this host and general morphological similarity. However, detailed morphological assessment revealed that key features, specifically the position and size of the ventral sucker, the arrangement of the reproductive organs, and the extent of the caeca, are more consistent with the diagnostic characters of *O. amplicoelus* as outlined by Martin *et al*. (2018). We propose the reassignment of these specimens to *O. amplicoelus*. This conclusion is substantiated by molecular evidence: the partial 28S rDNA sequence obtained from our specimen clustered within a strongly supported *Opistholebes* clade in the phylogenetic analysis, showing a 100% match with existing sequences and full nodal support. The 28S phylogenetic tree (Figure 3.27) clearly illustrates this placement. A comprehensive justification for this taxonomic reassignment,

including comparative morphometrics and molecular analyses, is presented in the submitted manuscript (see Appendix D; de Klerk *et al*., 2025, to be submitted).

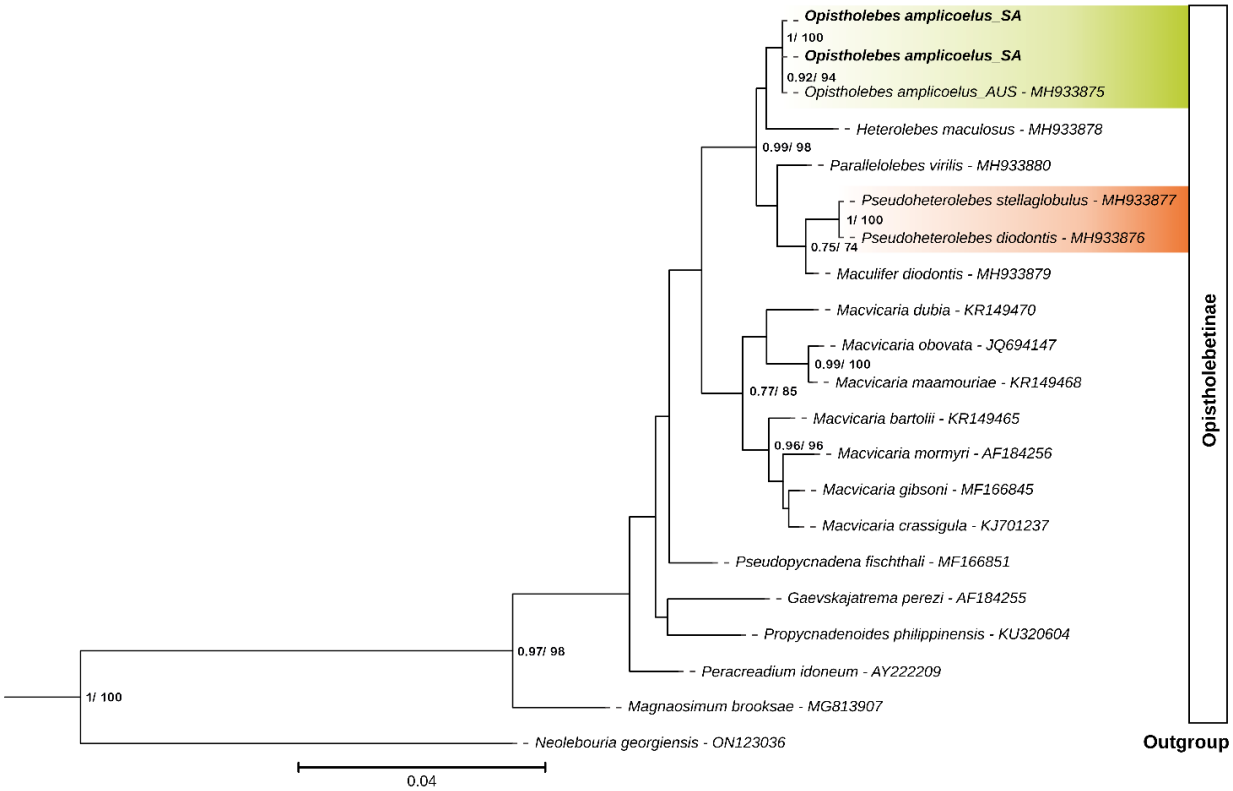

Figure 3.27: Bayesian Inference (BI) phylogenetic tree of the family Opistholebetinae, based on 28S rDNA sequences. Nodal support values are indicated as BI/Maximum Likelihood (ML); only values ≥0.7 (BI) and ≥70 (ML) are displayed. Newly sequenced isolates generated in this study are highlighted in green with bold text. The orange highlighted sequence indicates specimens from the genus Psudohetrolebes. *Neolebouria georgiensis* Gibson, 1976, was selected as the outgroup.

Zoogonidae gen. sp.

A total of 229 specimens were identified as belonging to the family Zoogonidae gen. sp. This is the first record of Zoogonidae larvae in *A. honckenii*. The full classification and summary are as follows:

Class: Trematoda
Order: Plagiorchiida
Family: Zoogonidae
Genus: *Unknown*
Species: Unknown
Present host: *Amblyrhynchote honckenii* (Bloch)
Present locality: Mossel Bay; Chintsa East; and Sodwana Bay, South Africa

Site of infection: Intestine

Prevalence (P): 40%

Mean intensity (MI): 16.4

Life stage: Larvae

Representative DNA sequences: Three sequences for ITS2 rDNA, three sequences for 28S rDNA, and three sequences for COI mtDNA

Voucher material: 229 specimens fixed in ethanol (Figure 3.25C) are kept in the collection of the Water Research Group (WRG) at the North-West University (NWU), Potchefstroom, South Africa

Zoogonids are small-bodied digeneans that typically inhabit the gastrointestinal tract of marine teleosts (Bray in Jones *et al*., 2005). To date, five species of Zoogonidae have been reported from South African marine fishes: *Cephaloporus bakeri* Bray, 1985; *Lecithostaphylus retroflexus* (Molin, 1859); *Overstreetia sodwanaensis* Bray, 1985; *Steganoderma* sp. Stafford, 1904; and *Steganodermatoides allocytti* (Tkachuk, 1979) (Fantham, 1938; Bray, 1985, 1987; Parukhin, 1989). Morphologically, the larval specimens collected in this study most closely resemble members of the genus *Zoogonoides*, based on features such as body shape, sucker and organ distribution. Specimens yielded partial 28S rDNA sequences with 96 bp difference (7.60%) from *Zoogonoides viviparus* (Olsson, 1868) Odhner, 1902 (Figure 3.28). This phylogenetic affinity supports the tentative assignment of these larvae to *Zoogonoides* gen. sp. However, due to the limitations of larval morphology and the moderate divergence from known species, additional specimens and more variable genetic markers will be needed to confirm this identification at the species level.

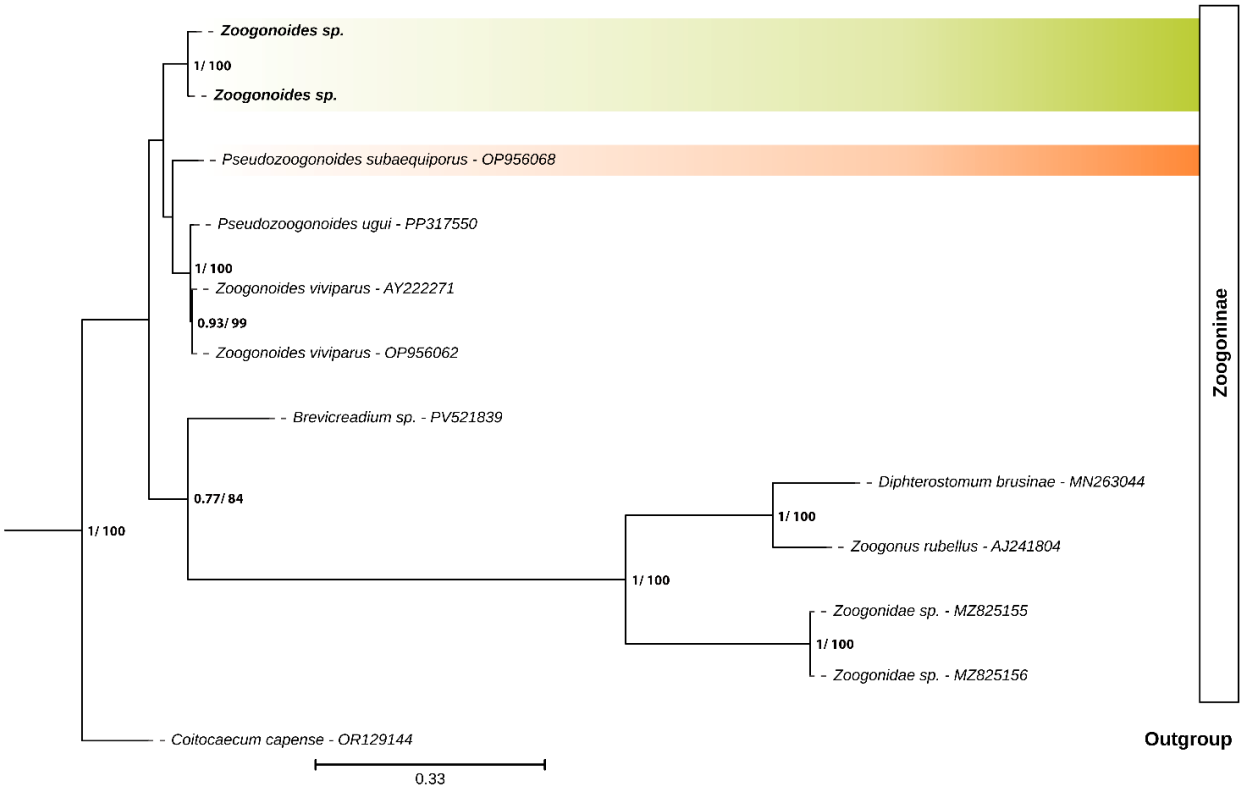

Figure 3.28: Bayesian Inference (BI) phylogenetic tree of the family Zoogoninae, based on 28S rDNA sequences. Nodal support values are indicated as BI/Maximum Likelihood (ML); only values ≥0.7 (BI) and ≥70 (ML) are displayed. Newly sequenced isolates generated in this study are highlighted in green with bold text. The orange highlighted sequence indicates the closest genetic match. *Coitocaecum capense* Bray, 1987, was selected as the outgroup.

3.4 Discussion

The diversity and composition of the metazoan parasite communities recovered from *A. honckenii* across multiple ecoregions illustrate the remarkable but historically underestimated complexity of South African marine parasite faunas (Smit and Hadfield, 2015). This study documented 22 parasite taxa, spanning several phyla and life history strategies, including significant representation from acanthocephalans, cestodes, crustaceans, digeneans, monopisthocotyleans, nematodes, and polyopisthocotyleans. Notably, while crustacean ectoparasites such as *Cin. tetrodontis* and *Cal. tetrodontis* dominated prior reports of parasites from this host (Hadfield *et al*., 2010; Hayes *et al*., 2021), the current baseline assessment revealed both high prevalence and diversity of helminth endoparasites, particularly larval cestodes and trematodes, highlighting the ecological centrality of *A. honckenii* as an intermediate and paratenic host within regional trophic webs.

The parasite assemblage of *A. honckenii* reveals a mix of highly host-specific taxa and more cosmopolitan species. Several metazoan parasites appear unique or largely restricted to

this pufferfish, reflecting specialised host-parasite associations. For instance, the buccal cymothoid isopod *Cin. tetrodontis* was originally described from *A. honckenii* and remains one of the few isopods documented from any tetraodontid in South Africa (Hadfield *et al*., 2010). Likewise, the gill associated polyopisthocotylean *Heterobothrium victorwepeneri* was recently described as a new species from *A. honckenii*, and it is currently the only polyopisthocotylean formally recorded directly on this fish host (Acosta and Smit, 2021). Two novel copepod parasites, *E. arenalbus* and *E. chintensis*, were discovered on *A. honckenii* as well, representing the second and third ergasilid species ever reported from any pufferfish worldwide (Van Der Spuy *et al*., 2025). *Amblyrhynchote honckenii* is also the type host for the acanthocephalan *R. gerberi*, described in 2019 (Lisitsyna *et al*., 2019), underscoring that several components of its parasite fauna are endemic to this host. At the same time, *A. honckenii* harbours parasites that it shares with other tetraodontid fishes, hinting at broader host ranges within the Tetraodontidae family. Notably, the caligid copepod *Cal. tetrodontis*, while prevalent on *A. honckenii*, was originally described from a different pufferfish, *T. hypselogeneion* (Hayes *et al*., 2021), indicating this ectoparasite infects multiple tetraodontid hosts in the region. Similarly, the digenean *O. amplicoelus,* the only trematode historically reported from *A. honckenii*, was first described in Australian waters, suggesting that at least some helminths of *A. honckenii* are shared with tetraodontids beyond Africa (Martin *et al*., 2018). Such findings highlight that *A. honckenii* supports both a set of host-specific parasites and others that are common to pufferfishes more generally, paralleling patterns seen in better-studied relatives. For example, polyopisthocotyleans in the genus *Heterobothrium* are recurrent parasites of pufferfish globally, and the occurrence of *H. victorwepeneri* on *A. honckenii* aligns with this trend even as it represents a unique species confined to African waters. This blend of specialised and shared parasites in *A. honckenii* reflects a complex host-parasite history, with certain lineages possibly co-diverging with the evileye puffer while others colonise it opportunistically from related hosts.

Equally important is the subset of *A. honckenii*'s parasites that are widely distributed among unrelated fish hosts, emphasising this puffer's role in regional food webs. The present survey revealed a high diversity and prevalence of trophically-transmitted endoparasites in *A. honckenii*, particularly larval stages of helminths, which had been underrepresented in earlier reports focused on conspicuous ectoparasites. Many of these larval parasites are not specific to pufferfish but rather exploit *A. honckenii* as an accidental, intermediate or paratenic host. The prominence of such generalist or heteroxenous parasites in *A. honckenii* mirrors findings in other coastal fish and underscores that, despite its potent defences, this pufferfish is embedded in the broader parasite ecology of the ecosystem. When comparing *A. honckenii*'s parasite fauna to that of well-studied Asian puffers, notable similarities and differences emerge. *Takifugu rubripes* hosts at least 18 metazoan parasite species, including numerous monopisthocotyleans (including *U.*

caligorum and *N. girellae*) and polyopisthocotyleans (including *Heterobothrium* spp.), specialist copepods (*P. fugu*, *C. fugu*), acanthocephalans (*P. pagrosomi*), and even blood flukes (*Paradeontacylix* spp.) (Ogawa and Inouye, 1997; Park and Park, 2006, Ogawa *et al*., 2007; Ogawa and Itoh, 2022). *Amblyrhynchote honckenii* also harbours *Heterobothrium, Udonella, Caligus,* as well as *Pomphorhynchus* species. Although the parasite fauna of *A. honckenii* is unique, with its own host-specific parasites, such as *Cin. tetrodontis*, it also hosts some broadly shared genera. This comparison underlines how regional host ecology and research effort influence our perception of parasite diversity, reaffirming the importance of new surveys on previously overlooked hosts to fully elucidate the diversity and host-specificity of fish parasites worldwide.

The prominence of larval cestodes, exclusively linked to adults in elasmobranch hosts, attests to the complexity of transmission routes and the pivotal function of this pufferfish as a conduit for parasite life cycles involving multiple hosts. The regular recovery of *O. amplicoelus* (de Klerk *et al*., 2025), previously reported as *O. cotylophorus* (Bray, 1986) from this system, corroborates earlier, isolated findings and highlights both persistent host associations and the need for continued systematic integrative surveys. Additionally, new and cryptic digenean taxa, including a new *Rhipidocotyle* species, were revealed by the integrative use of morphological and molecular diagnostics (Louvard *et al*., 2025), demonstrating the value of combined approaches for resolving tropical parasite diversity and unravelling hidden host-specific lineages (Smit and Sures, 2025).

Marked spatial variation in parasite assemblages across sampling localities suggests significant influences of environmental gradients, host population structure, and site-specific ecological processes on community composition (Griffiths *et al*., 2010; Sell *et al*., 2024). Such findings echo broader patterns reported from the region (Smit and Hadfield, 2015; Timi and Poulin, 2020), and they support the view that host and parasite diversity in South African marine systems remain substantially underestimated and inadequately surveyed, particularly for non-commercial hosts and those lacking aquaculture relevance (Smit and Hadfield, 2015). Furthermore, the recovery of two new *Ergasilus* species with site-specificity and unique morphological traits further exemplifies the latent cryptic diversity awaiting discovery (Van der Spuy *et al*., 2025).

This work helps fill a major knowledge gap in the documentation of marine parasites from South African tetraodontids, in sharp contrast to the extensive parasite records for Asian pufferfishes, particularly those in aquaculture (Ogawa and Inouye, 1997; Ogawa *et al*., 2007; Park and Park, 2006). The absence of comparable baseline datasets in Africa constrains both ecological interpretation and the application of emerging biomonitoring tools, such as

environmental DNA (eDNA), which rely on well-resolved reference databases (Hupalo *et al*., 2025). By providing the first integrative inventory of *A. honckenii* parasites, including both adults and larvae, this study advances our capacity to use parasites as indicators of ecosystem integrity, changing environmental conditions, and anthropogenic impact (Adlard *et al*., 2015; Hudson *et al*., 2006; Smit and Sures, 2025). It also reinforces the importance of non-commercial hosts as reservoirs of parasite diversity, reflecting both natural patterns and responses to environmental change (Timi and Poulin, 2020; Wood *et al*., 2013).

3.5 Conclusion

The identification of four distinct parasite phyla, spanning isopods, copepods, monopisthocotyleans, polyopisthocotyleans, digeneans, acanthocephalans and cestodes, reveals a more complex and diverse parasite fauna than previously reported, thereby supporting the initial hypothesis (Hypothesis 1, Chapter 1) that parasite diversity in this host is underestimated. This chapter establishes a critical baseline for understanding the metazoan parasite diversity of *A. honckenii*, revealing a host that supports rich and underappreciated parasite assemblages in South African coastal waters. The synergy of morphological and molecular approaches was essential for resolving cryptic and larval taxa, highlighting considerable undiscovered diversity and restrictive gaps in current taxonomic knowledge. These findings call for urgent, systematic, and regionally coordinated surveys across host taxa and habitats, employing integrative methods to inform both scientific understanding and conservation policy. Importantly, the ubiquitous presence and abundance of the cymothoid isopod *Cin. tetrodontis* in surveyed populations suggests that it may serve as a practical and sensitive bioindicator. The next chapter of this thesis will explore the potential of *Cinusa* as an indicator for environmental pollution and element accumulation within *A. honckenii*, thus linking host-parasite ecology to pressing questions in environmental health assessment and management.

References

Acosta, A.A. & Smit, N.J., 2021. A first for Southern Africa: Description of a new *Heterobothrium* (Monogenea: Diclidophoridae) parasitizing the evileye pufferfish *Amblyrhynchotes honckenii* (Tetraodontiformes: Tetraodontidae). *Parasitology Research*, 120(3): 819–830.

Adlard, R.D., Miller, T.L. & Smit, N.J., 2015. The butterfly effect: Parasite diversity, environment, and emerging disease in aquatic wildlife. *Trends in Parasitology*, 31(4): 160–166.

Amin, O.M., 2013. Classification of the Acanthocephala. *Folia Parasitologica*, 60: 273–305.

Amin, O.M., Abdullah, S.M. & Mhaisen, F.T., 2003. Description of *Pomphorhynchus spindletruncatus* n. sp. (Acanthocephala: Pomphorhynchidae) from freshwater fishes in northern Iraq, with the erection of a new pomphorhynchid genus, *Pyriproboscis* n. g., and keys to genera of the Pomphorhynchidae and the species of *Pomphorhynchus* Monticelli, 1905. *Systematic Parasitology*, 54(3): 229–235.

Anderson, R.C., 1996. Why do fish have so few roundworm (nematode) parasites? *Environmental Biology of Fishes*, 46(1): 1–5.

Anderson, R.C., 2000. Nematode parasites of vertebrates: Their development and transmission. Wallingford: CABI. Bianchini, G. & Sánchez Baracaldo, P., 2024. Treeviewer: flexible, modular software to visualise and manipulate phylogenetic trees. *Ecology and Evolution*, 14, e10873.

Bianchini, G. & Sánchez Baracaldo, P., 2024. Treeviewer: Flexible, modular software to visualise and manipulate phylogenetic trees. *Ecology and Evolution*, 14: e10873.

Boxshall, G.A. & Halsey, S.H., 2004. An Introduction to Copepod Diversity. London: The Ray Society.

Boxshall, G.A. & Montú, M.A., 1997. Copepods parasitic on Brazilian coastal fishes: A handbook. *Nauplius*, 5: 1–225.

Bray, R.A., 1974. Acanthocephala in the flatfish *Solea bleekeri* (Soleidae) from Cape province, South Africa. *Journal of Helminthology*, 48: 179–185.

Bray, R.A., 1985. Macvicaria taksengi n. sp. (Digenea: Opecoelidae) in marine teleosts from Pinang, Malaysia. *Systematic Parasitology*, 7: 75–80.

Bray, R.A., 1986. Some helminth parasites of marine fishes of South Africa: Families Enenteridae, Opistholebetidae and Pleorchiidae (Digenea). Journal of Natural History, 20(2): 471–488.

Bray, R.A., 1987. Some helminth parasites of marine fishes of South Africa: Family Opecoelidae (Digenea). *Journal of Natural History*, 21: 1049–1075.

Bray, R.A., 2005. Family Acanthocoplidae. In: Jones, A., Bray, R.A. & Gibson, D.I. (eds.), Keys to the Trematoda, Volume 1. Wallingford: CAB International and The Natural History Museum.

Bray, R.A., Diaz, P.E. & Cribb, T.H., 2016. Knowledge of marine fish trematodes of Atlantic and Eastern Pacific oceans. *Systematic Parasitology*, 93: 223–235.

Buchmann, K. & Bresciani, J., 2006. Monogenea (phylum Platyhelminthes). In: Woo, P.T.K. (ed.), Fish diseases and disorders, Vol. 1: Protozoan and metazoan infections. Wallingford: CABI, pp. 297–344.Bullard SA, Dippenaar SM, Hoffmayer ER, Benz GW. 2004. New locality records for *Dermophthirius carcharhini* (Monogenea: Microbothriidae) and *Dermophthirius maccallumi* and a list of hosts and localities for species of *Dermophthirius*. *Comparative Parasitology*, 71: 78–80.

Bullard, S.A. & Dippenaar, S.M., 2003. *Branchotenthes robinoverstreeti* n. gen. and n. sp. (Monogenea: Hexabothriidae) from gill filaments of the Bowmouth guitarfish, *Rhina ancylostoma* (Rhynchobatidae), in the Indian Ocean. *Journal of Parasitology*, 89: 595–601.

Bullard, S.A., Dippenaar, S.M. & Hoffmayer, E.R., Benz, G.W., 2004. New locality records for *Dermophthirius carcharhini* (Monogenea: Microbothriidae) and *Dermophthirius maccallumi* and a list of hosts and localities for species of *Dermophthirius*. *Comparative Parasitology*, 71: 78–80.

Bush, A.O., Lafferty, K.D., Lotz, J.M. & Shostak, A.W., 1997. Parasitology meets ecology on its own terms: Margolis et al. revisited. *Journal of Parasitology*, 83: 575–583.

Caira, J.N. & Jensen, K., 2001. An investigation of the co-evolutionary relationships between onchobothriid tapeworms and their elasmobranch hosts. *International Journal for Parasitology*, 31(9): 960–975.

Caira, J.N. & Jensen, K., 2014. A digest of elasmobranch tapeworms. *Journal of Parasitology*, 100(4): 373–391.

Caira, J.N., Jensen, K., Georgiev, B.B., Kuchta, R.O., Littlewood, T., Mariaux, J., Scholz, T., Tkach, V.V. & Waeschenbach, A., 2017. An overview of the tapeworms of vertebrate bowels of the earth.

Carvajal, J. & Sepúlveda, F., 2002. *Udonella australis* n. sp. (Monogenea), an epibiont on sea-lice from native fish off southern Chile. *Systematic Parasitology*, 52(1): 67–74.

Cribb, T.H, 2005. Family Opecoelidae Ozaki, 1925. In: Jones, A., Bray, R.A. & Gibson, D.I. (eds.), Keys to the Trematoda, Volume 2. Wallingford: CAB International and The Natural History Museum.

Cribb, T.H., Adlard, R.D. & Bray, R.A., 1998. A DNA based demonstration of a three host life cycle for the Bivesiculidae (Platyhelminthes: Digenea). *International Journal for Parasitology*, 28(11): 1791–1795.

Cribb, T.H., Bray, R.A. & Littlewood, D.T.J., 2001. The nature and evolution of the association among digeneans, molluscs and fishes. *International Journal for Parasitology*, 31(9): 997–1011.

Cribb, T.H., Bray, R.A., Diaz, P.E., Huston, D.C., Kudlai, O., Martin, S.B., Yong, R.Q.-Y. & Cutmore, S.C., 2016. Trematodes of fishes of the Indo-West Pacific: told and untold richness. *Systematic Parasitology*, 93: 237–247.

Cunningham, C.O., McGillivray, D.M., MacKenzie, K. & Melvin, W.T., 1995. Identification of *Gyrodactylus* (Monogenea) species parasitizing salmonid fish using DNA probes. *Journal of Fish Diseases*, 18(6): 539–544.

Cutmore, S.C., Bennett, M.B. & Cribb, T.H., 2024. Morphological and molecular identification of metacestodes infecting teleost fishes of Moreton Bay, Australia. *Systematic Parasitology*, 101(5): 57.

Darriba, D., Taboada, G.L., Doallo, R. & Posada, D., 2012. jModelTest 2: more models, new heuristics and parallel computing. *Nature Methods*, 9: 772.

Dicken, M.L., Hussey, N.E., Christiansen, H.M., Smale, M.J., Nkabi, N., Cliff, G. & Wintner, S.P., 2017. Diet and trophic ecology of the tiger shark (*Galeocerdo cuvier*) from South African waters.*PloS One*, 2(6): e0177897.

Dollfus, R.P. & Golvan, Y.J., 1963. Extension à l'Afrique du sud de la distribution géographique du genre *Longicollum* S. Yamaguti 1935; *L. chabanaudi* n. sp. (Palaeacanthocephala, Pomphorhynchidae) parasite d'un *Barnardichthys* (Soleidae). *Bulletin de la Société Zoologique de France*, 88: 65–70.

Dos Santos, Q.M., Gilbert, B.M., Avenant-Oldewage, A. & Dumbo, J.C., 2021. Morphological and molecular description of *Allocreadium apokryf* sp. n. (Digenea: Allocreadiidae) from native *Labeobarbus aeneus* (Cyprinidae) in South Africa, including notes on its biology, evolutionary history and an updated key of African *Allocreadium*. *Folia Parasitologica*, 68: e013.

Fantham, H.B., 1938. *Lecithostaphylus spondyliosomae* n. s. p., a trematode parasite of the Hottentot fish, *Spondyliosoma blochii*, found in South African waters. *Transactions of the Royal Society of South Africa*, 26(4): 387–393.

Folmer, O., Black, M., Hoeh, W., Lutz, R. & Vrijenhoek, R., 1994. DNA primers for amplification of mitochondrial cytochrome c oxidase subunit I from diverse metazoan invertebrates. *Molecular Marine Biology and Biotechnology*, 3: 294–299.

Freeman, M.A. & Ogawa, K., 2010. Variation in the small subunit ribosomal DNA confirms that *Udonella* (Monogenea: Udonellidae) is a species-rich group. *International Journal for Parasitology*, 40(2): 255–264.

Froese, R. & Pauly, D., 2025. FishBase. Available at: www.fishbase.org/search.php. (date of access: 08 May 2025).

González, M.T., Barrientos, C. & Moreno, C.A., 2006. Biogeographical patterns in endoparasite communities of a marine fish (*Sebastes capensis* Gmelin) with extended range in the Southern Hemisphere. *Journal of Biogeography*, 33: 1086–1095.

Griffiths, C.L., Robinson, T.B., Lange, L. & Mead, A., 2010. Marine biodiversity in South Africa: An evaluation of current states of knowledge. *PLOS ONE*, 5(8): e12008.

Grobler, N.J., Christison, K.W., Olivier, P.A.S. & Van As, J.G., 2003. Observations on the development of *Udonella caligorum* Johnston, 1835 (Monogenea: Polyonchoinea) on a parasitic copepod species of *Caligus* (Copepoda: Caligidae), collected from Lake St Lucia, South Africa. *African Zoology*, 38(2): 393–396.

Guindon, S., Dufayard, J.F., Lefort, V., Anisimova, M., Hordijk, W. & Gascuel, O., 2010. New algorithms and methods to estimate maximum likelihood phylogenies: Assessing the performance of PhyML 3.0. *Systematic Biology*, 59: 307–321.

Hadfield, K.A., Bruce, N.L. & Smit, N.J., 2010. Redescription of the monotypic genus *Cinusa* Schioedte & Meinert, 1884 (Isopoda, Cymothoidae), a buccal-cavity isopod from South Africa. *Zootaxa*, 2437(1): 51–68.

Hadfield, K.A., Erasmus, A., Bruce, N.L. & Smit, N.J., 2025. Biology and life cycles of parasitic Arthropoda infesting aquatic hosts. In: Smit, N.J. & Sures, B. (eds.), Aquatic Parasitology: Ecological and Environmental Concepts and Implications of Marine and Freshwater Parasites. Cham: Springer, pp. 125–164.

Hayes, P.M., Christison, K.W., Vaughan, D.B., Smit, N.J. & Boxshall, G.A., 2021. Sea lice (Copepoda: Caligidae) from South Africa, with descriptions of two new species of *Caligus*. *Systematic Parasitology*, 98(4): 369–397.

Hoberg, E.P., Brooks, D.R. & Siegel-Causey, D., 1997. Host–parasite co-speciation: History, principles, and prospects. In: Clayton, D.H. & Moore, J. (eds.), Host–parasite evolution: General principles and avian models. Oxford: Oxford University Press, pp. 212–235.

Hoogendoorn, C., Smit, N.J. & Kudlai, O., 2020. Resolution of the identity of three species of *Diplostomum* (Digenea: Diplostomidae) parasitising freshwater fishes in South Africa, combining molecular and morphological evidence. *International Journal for Parasitology: Parasites and Wildlife*, 11: 50–61.

Hudson, P.J., Dobson, A.P. & Lafferty, K.D., 2006. Is a healthy ecosystem one that is rich in parasites? *Trends in Ecology & Evolution*, 21(7): 381–385.

Hupało, K., Blasco-Costa, I., Trujillo-González, A. & Leese, F., 2025. Detecting and assessing aquatic parasite diversity using environmental DNA. In: Smit, N.J. & Sures, B. (eds.), Aquatic Parasitology: Ecological and Environmental Concepts and Implications of Marine and Freshwater Parasites. Cham: Springer, pp. 361–382.

Katoh, K. & Standley, D.M., 2013. MAFFT multiple sequence alignment software version 7: Improvements in performance and usability. *Molecular Biology and Evolution*, 30: 772–780.

Katoh, K., Misawa, K., Kuma, K.I. & Miyata, T., 2002. MAFFT: A novel method for rapid multiple sequence alignment based on fast Fourier transform. *Nucleic Acids Research*, 30: 3059–3066.

Kearn, G.C., 2011. Monogeneans – the ultimate fish parasites. *Monogenea*, 58(2): 28–32.

Kostadinova, A., Herniou, E.A., Barrett, J. & Littlewood, D.T.J., 2003. Phylogenetic relationships of *Echinostoma* Rudolphi, 1809 (Digenea: Echinostomatidae) and related genera reassessed via DNA and morphological analyses. *Systematic Parasitology*, 54: 159–176.

Le Roux, J., 2013. Parasite assemblages of Cape horse mackerel (*Trachurus capensis* Castelnau, 1861) from the northern and southern Benguela. (MSc dissertation) University of Cape Town.

Linton, E., 1924. *Gyrocotyle plana* sp. nov. with notes on South African cestodes of fishes. *Fisheries and Marine Biological Survey Report*, 3.

Lisitsyna, O.I., Kudlai, O., Cribb, T.H. & Smit, N.J., 2019. Three new species of acanthocephalans (Palaeacanthocephala) from marine fishes collected off the East coast of South Africa. *Folia Parasitologica*, 66: 1–20.

Littlewood, D.T.J., 1994. Molecular phylogenetics of cupped oysters based on partial 28S rRNA gene sequences. *Molecular Phylogenetics and Evolution*, 3(3): 221–229.

Littlewood, D.T.J., Curini-Galletti, M. & Herniou, E.A., 2000. The interrelationships of *Proseriata* (Platyhelminthes: Seriata) tested with molecules and morphology. *Molecular Phylogenetics and Evolution*, 16: 449–466.

Littlewood, D.T.J., Rohde, K. & Bray, R.A., 1997. Parasite speciation within or between host species? Phylogenetic evidence from site-specific polystome monogeneans. *International Journal for Parasitology*, 27(11): 1289–1297.

Littlewood, D.T.J., Rohde, K., Bray, R.A. & Herniou, E.A., 1999. Phylogeny of the Platyhelminthes and the evolution of parasitism. *Biological Journal of the Linnean Society*, 68(1–2): 257–287.

Littlewood, D.T.J., Telford, M.J. & Bray, R.A., 2004. Protostomes and Platyhelminthes. In: Cracraft, J. & Donoghue, M.J., (eds.), Assembling the Tree of Life. Oxford: Oxford University Press, pp. 209–234.

Lockyer, A.E., Olson, P.D. & Littlewood, D.T.J., 2003. Utility of complete large and small subunit rRNA genes in resolving the phylogeny of the Neodermata (Platyhelminthes): implications and a review of the cercomer theory. *Biological Journal of the Linnean Society*, 78: 155–171.

Lymbery, A.J. & Smit, N.J., 2023. Conservation of parasites: A primer. *International Journal for Parasitology: Parasites and Wildlife*, 21: 255–263.

Mackintosh, A.L., Reed, C.C., Nunkoo, M.A.I., King, P.H. & van der Lingen, C.D., 2018. Macroparasites of angelfish *Brama brama* (Bonnaterre, 1788) in the southern Benguela Current ecosystem. *African Journal of Marine Science*, 40: 245–252.

Malatji, M.P. & Mukaratirwa, S., 2019. Molecular detection of natural infection of *Lymnaea* (Pseudosuccinea) *columella* (Gastropoda: Lymnaeidae) with *Fasciola gigantica* (Digenea: Fasciolidae) from two provinces of South Africa. *Journal of Helminthology*, 94: e38.

Manter, H.W., 1955. Two new monogenetic trematodes from elephant fishes (Callorhynchus) from South Africa and New Zealand. In: Essays in the Natural Sciences in Honor of Captain Allan Hancock, University of Southern California Press, pp. 211–220.

Martin, S.B., Ribu, D., Cutmore, S.C. & Cribb, T.H., 2018. Opistholobetines (Digenea: Opecoelidae) in Australian tetraodontiform fishes. *Systematic Parasitology*, 95(8): 743–781.

Mattiucci, S., Nascetti, G., Cianchi, R., Paggi, L., Arduino, P., Margolis, L., Brattey, J., Webb, S., D'Amelio, S., Orecchia, P. & Bullini, L., 1997. Genetic and ecological data on *the Anisakis simplex* complex, with evidence for a new species (Nematoda, Ascaridoidea, Anisakidae). *Journal of Parasitology*, 83(3): 401–416.

Miller, M., Pfeiffer, W.T. & Schwartz, T., 2010. Creating the CIPRES science gateway for inference of large phylogenetic trees. *Proceedings of the Gateway Computing Environments Workshop*, 14: 1–8.

Moravec, F., van As, J.G. & Dyková, I., 2002. *Proleptus obtusus* Dujardin, 1845 (Nematoda: Physalopteridae) from the puffadder shyshark *Haploblepharus edwardsii* (Scyliorhinidae) from off South Africa. *Systematic Parasitology*, 53: 169–173.

Morgan, J.A.T. & Blair, D., 1995. Nuclear rDNA ITS sequence variation in the trematode genus *Echinostoma*: An aid to establishing relationships within the 37 collar spine group. *Parasitology*, 111(5): 609–615.

Morris, T., Avenant-Oldewage, A., Lamberth, S. & Reed, C., 2016. Shark parasites as bio-indicators of metals in two South African embayments. *Marine Pollution Bulletin*, 104: 221–228.

Moszczynska, A., Locke, S.A., McLaughlin, J.D., Marcogliese, D.J. & Crease, T.J., 2009. Development of primers for the mitochondrial cytochrome c oxidase I gene in digenetic trematodes (Platyhelminthes) illustrates the challenge of barcoding parasitic helminths. *Molecular Ecology Resources*, 9: 75–82.

Nunkoo, M.A.I., 2019. Studies on the diversity and distribution of marine ichthyoparasites in Southern Africa. (PhD thesis), University of Cape Town.

Nunkoo, M.A.I., Reed, C.C. & Kerwath, S.E., 2016. Community ecology of the metazoan parasites of snoek *Thyrsites atun* (Euphrasen, 1791) (Perciformes: Gempylidae) off South Africa. *African Journal of Marine Science*, 38: 363–371.

Ogawa, K. & Inouye, K., 1997. *Heterobothrium* infection of cultured tiger puffer, *Takifugu rubripes* (Teleostei: Tetraodontidae)—a field study. *Fish Pathology*, 32: 15–20.

Ogawa, K. & Itoh, N., 2022. Five new and two known species of *Heterobothrium* (Monogenea: Diclidophoridae) infecting puffers of the genus *Takifugu* from Japanese waters. *Systematic Parasitology*, 99(3): 317–340.

Ogawa, K., Nagano, T., Akai, N., Sugita, A. & Hall, K.A., 2007. Blood fluke infection of cultured tiger puffer *Takifugu rubripes* imported from China to Japan. *Fish Pathology*, 42(2): 91–99.

Olivier, P.A.S., Dippenaar, S.M., Khalil, L.F. & Mokgalong, N.M., 2000. Observations on a lesser-known monogenean, *Udonella myliobati*, from a copepod parasite, *Lepeophtheirus natalensis*, parasitizing the spotted ragged-tooth shark, *Carcharias taurus*, from South African waters. *Onderstepoort Journal of Veterinary Research*, 67(2): 135–140.

Oosthuizen, G., Acosta, A.A., Smit, N.J. & Schaeffner, B.C., 2021. A new species of *Grillotia* Guiart, 1927 (Cestoda: Trypanorhyncha) from the spotted skate, *Raja straeleni* Poll, in South Africa. *Parasitology International*, 82: 102307.

Oosthuizen, G., Naidoo, K., Smit, N.J. & Schaeffner, B.C., 2022. Adding one more to the list: A new species of *Eniochobothrium* (Cestoda: Lecanicephalidea) from the Oman cownose ray in South Africa. *International Journal for Parasitology: Parasites and Wildlife*, 19: 138–147.

Overstreet, R.M. & Curran, S.S., 2005. Family Bucephalidae. In: Jones, A., Bray, R.A. & Gibson, D.I. (eds.), Keys to the Trematoda, Volume 1. Wallingford: CAB International and The Natural History Museum.

Palm, H.W. & Overstreet, R.M., 2000. New records of trypanorhynch cestodes from the Gulf of Mexico, including *Kotorella pronosoma* (Stossich, 1901) and *Heteonybelinia palliata* (Linton, 1924) comb. nov. *Folia Parasitologica*, 47: 293–302.

Palm, H.W., 2004. The Trypanorhyncha Diesing, 1863. Bogor: PKSPL-IPB Press, x + 710 pp.

Panikkar, N.K. & Sproston, N.G., 1941. Osmotic relations of some metazoan parasites. *Parasitology*, 33(2): 214–223.

Park, S.W. & Park, G.C., 2006. Heterobothrium infection of tiger puffer, *Takifugu rubripes* cultured in ponds on land. *Journal of Fish Pathology*, 19(2): 99–108.

Parukhin, A.M., 1989. Parasitic worms of bottom fishes of the southern seas. Kiev: Naukova Dumka, p. 155.

Posada, D., 2008. jModelTest: Phylogenetic model averaging. *Molecular Biology and Evolution*, 25(7): 1253–1256.

Přikrylová, I., Vanhove, M.P., Janssens, S.B., Billeter, P.A. & Huyse, T., 2013. Tiny worms from a mighty continent: High diversity and new phylogenetic lineages of African monogeneans. *Molecular Phylogenetics and Evolution*, 67(1): 43–52.

Rakgole, J., Moema, E.B. & King, P.H., 2019. Phylogenetic studies of larval digenean trematodes from freshwater snails and fish species in the proximity of Tshwane metropolitan, South Africa. *Onderstepoort Journal of Veterinary Research*, 86: 1–7.

Ronquist, F., Teslenko, M., van der Mark, P., Ayres, D.L., Darling, A., Höhna, S., Larget, B., Liu, L., Suchard, M.A. & Huelsenbeck, J.P., 2012. MrBayes 3.2: Efficient Bayesian phylogenetic inference and model choice across a large model space. *Systematic Biology*, 61: 539–542.

Schaeffner, B.C. & Smit, N.J., 2019. Parasites of cartilaginous fishes (Chondrichthyes) in South Africa – a neglected field of marine science. *Folia Parasitologica*, 66: 002.

Scholz, T., Vanhove, M.P., Smit, N., Jayasundera, Z. & Gelnar, M. (eds.), 2018. A guide to the parasites of African freshwater fishes. Brussels: Royal Belgian Institute of Natural Sciences, Vol. 18, pp. 9–13.

Sell, A.F., von Maltitz, G.P., Auel, H., Biastoch, A., Bode-Dalby, M., Brandt, P., Duncan, S.E., Ekau, W., Fock, H.O., Hagen, W. & Huggett, J.A., 2024. Unique southern African terrestrial and oceanic biomes and their relation to steep environmental gradients. In: Scholes, R. & Archer van Garderen, E., (eds.), Sustainability of Southern African Ecosystems Under Global Change: Science for Management and Policy Interventions. Cham: Springer International Publishing, pp. 23–88.

Smit, N.J. & Davies, A.J, 2001. The life cycle of *Haemogregarina bigemina* (Adeleina: Haemogregarinidae) in South African hosts. *Folia Parasitologica*, 48(3): 169–177.

Smit, N.J. & Hadfield, K.A., 2015. Marine fish parasitology in South Africa: History of discovery and future direction. *African Zoology*, 50(2): 79–92.

Smit, N.J. & Sures, B., 2025. Introduction to aquatic parasitology: Ecological and environmental concepts and implications of marine and freshwater parasites. In: Smit, N.J. & Sures, B. (eds.), Aquatic Parasitology: Ecological and Environmental Concepts and Implications of Marine and Freshwater Parasites. Cham: Springer Nature Switzerland, pp. 3–8.

Smit, N.J., Bruce, N.L. & Hadfield, K.A., 2014. Global diversity of fish parasitic isopod crustaceans of the family Cymothoidae. *International Journal for Parasitology: Parasites and Wildlife*, 3: 188–197.

Snyder, S.D. & Tkach, V.V., 2001. Phylogenetic and biogeographical relationships among some Holarctic frog lung flukes (Digenea: Haematoloechidae). *Journal of Parasitology*, 87(6): 1433–1440.

Song, Y., Wang, G.T., Yao, W.J., Gao, Q. & Nie, P., 2008. Phylogeny of freshwater parasitic copepods in the Ergasilidae (Copepoda: Poecilostomatoida) based on 18S and 28S rDNA sequences. *Parasitology Research*, 102: 299–306.

Sures, B., Díaz-Morales, D.M., Yong, R.Q., Erasmus, A. & Schwelm, J., 2025. Biology and life cycle of helminths. In: Smit, N.J. & Sures, B. (eds.), Aquatic Parasitology: Ecological and Environmental Concepts and Implications of Marine and Freshwater Parasites. Cham: Springer, pp. 89–123.

Suzuki, N., Murakami, K., Takeyama, H. & Chow, S., 2006. Molecular attempt to identify prey organisms of lobster phyllosoma larvae. *Fisheries Science*, 72(2): 342–349.

Svitin, R., Truter, M., Kudlai, O., Smit, N.J. & Du Preez, L., 2019. Novel information on the morphology, phylogeny and distribution of camallanid nematodes from marine and freshwater hosts in South Africa, including the description of *Camallanus sodwanaensis* n. sp. International Journal for Parasitology: *Parasites and Wildlife*, 10: 263–273.

Timi, J.T. & Poulin, R., 2020. Why ignoring parasites in fish ecology is a mistake. *International Journal for Parasitology*, 50(10–11): 755–761.

Timi, J.T. & Sardella, N.H., 2002. A new species of *Dichelyne* (Nematoda: Cucullanidae) parasitizing *Acanthistius brasilianus* (Pisces: Serranidae) from Argentinean waters. *Journal of Parasitology*, 88(3): 573–576.

Tkach, V.V., Vasileva, G.P. & Genov, T., 2003. Description of *Vaucherilepis trichophorus* sp. nov., gen. nov. (Cyclophyllidea, Hymenolepididae) from water shrews and gammarid crustaceans in Bulgaria and Ukraine. *Acta Parasitologica*, 48(2).

Truter, M., Yong, R.Y., Smit, W., Chakona, A., Luus-Powell, W.J. & Smit, N.J., 2025. Trematode diversity in southern Africa: metacercariae of the Clinostomidae and Cryptogonimidae in intermediate freshwater fish hosts. *Journal of Helminthology*, 99: e75.

Ulman, A., Harris, H.E., Doumpas, N., Deniz Akbora, H., Al Mabruk, S.A.A., Azzurro, E., Bariche, M., Çiçek, B.A., Deidun, A., Demirel, N. & Fogg, A.Q., 2021. Low pufferfish and lionfish predation in their native and invaded ranges suggests human control mechanisms may be necessary to control their Mediterranean abundances. *Frontiers in Marine Science*, 8: 670413.

Umehara, A., Kawakami, Y., Matsui, T., Araki, J. & Uchida, A., 2006. Molecular identification of *Anisakis simplex* sensu stricto and *Anisakis pegreffii* (Nematoda: Anisakidae) from fish and cetacean in Japanese waters. *Parasitology International*, 55(4): 267–271.

Van Der Spuy, L., Narciso, R.B., Hadfield, K.A., Wepener, V. & Smit, N.J., 2025. Exploring South Africa's hidden marine parasite diversity: Two new marine *Ergasilus* species (Copepoda: Cyclopoida: Ergasilidae) from the evileye blaasop, *Amblyrhynchotes honckenii* (Bloch). *Parasitology*, 152(1): 30–50.

Van Der Spuy, L., Smit, N.J. & Schaeffner, B.C., 2020. Four new species of *Acanthobothrium* van Beneden, 1849 (Cestoda: Onchoproteocephalidea) from the spotted skate, *Raja straeleni* Poll, off the Western Cape, South Africa. *Folia Parasitologica*, 67: 036.

Van Der Spuy, L., Smit, N.J. & Schaeffner, B.C., 2022. Threatened, host-specific affiliates of a red-listed host: Three new species of *Acanthobothrium* van Beneden, 1849 (Cestoda: Onchoproteocephalidea) from the endangered white skate, *Rostroraja alba* (Lacépède). *International Journal for Parasitology*, 17: 114–126.

Van Der Spuy, L., Smit, N.J., Naidoo, K. & Schaeffner, B.C., 2023. A new species of *Phoreiobothrium* Linton, 1889 (Cestoda: Onchoproteocephalidea) from the spinner shark, C*archarhinus brevipinna* (Valenciennes) off the coast of KwaZulu-Natal, South Africa. *Systematic Parasitology*, 100: 149–158.

van Steenkiste, N., Locke, S.A., Castelin, M., Marcogliese, D.J. & Abbott, C.L., 2015. New primers for DNA barcoding of digeneans and cestodes (Platyhelminthes). *Molecular Ecology Resources*, 15(4): 945–952.

Vaughan, D.B. & Chisholm, L.A., 2009. Three *Dendromonocotyle* species (Monogenea: Monocotylidae) reported from captive rays, including *D. lotteri* sp. n. from *Himantura gerrardi* (Elasmobranchii: Dasyatidae) in the public aquarium at the Atlantis resort, Dubai. *Folia Parasitologica*, 56: 99–106.

Vaughan, D.B. & Chisholm, L.A., 2010a. A new species of *Neoheterocotyle* Hargis, 1955 (Monogenea: Monocotylidae) from the gills of *Rhinobatos annulatus* Müller & Henle (Rhinobatidae) off the southern tip of Africa. *Systematic Parasitology*, 77: 205–213.

Vaughan, D.B. & Chisholm, L.A., 2010b. *Heterocotyle tokoloshei* sp. nov. (Monogenea: Monocotylidae) from the gills of *Dasyatis brevicaudata* (Dasyatidae) kept in captivity at Two Oceans Aquarium, Cape Town, South Africa: Description and notes on treatment. *Acta Parasitologica*, 55: 108–114.

Vaughan, D.B. & Chisholm, L.A., 2011. Amendment of *Pseudoleptobothrium* Young, 1967 (Monogenea, Microbothriidae) with the description of *Pseudoleptobothrium christisoni* sp. nov. from the dermal denticles of *Rhinobatos annulatus* (Rhinobatidae) off the southern tip of Africa. *Acta Parasitologica*, 56: 280–289.

Vaughan, D.B. & Christison, K.W., 2010. A new species of *Myxinidocotyle* (Monogenea: Acanthocotylidae: Myxinidocotylinae) from captive sixgill hagfish, *Eptatretus hexatrema* (Chordata: Myxinidae), with amendment of the subfamily diagnosis. *Zootaxa*, 2650: 47–56.

Vaughan, D.B., Chisholm, L.A. & Christison, K.W., 2008. Overview of South African *Dendromonocotyle* (Monogenea: Monocotylidae), with descriptions of two new species from stingrays (Dasyatidae) kept in public aquaria. *Zootaxa*, 1826: 26–44.

Vaughan, D.B., Christison, K.W., Hanson, H. & Shinn, A.P., 2010. *Gyrodactylus eyipayipi* sp. n. (Monogenea: Gyrodactylidae) from *Syngnathus acus* L. (Syngnathidae) from South Africa. *Folia Parasitologica*, 57: 11–15.

Vermaak, A., Kudlai, O., Yong, R.Q. & Smit, N.J., 2023b. Novel insights into the genetics, morphology, distribution and hosts of the global fish parasitic digenean *Proctoeces maculatus* (Looss, 1901) (Digenea: Fellodistomidae). *Parasitology*, 150(13): 1242–1253.

Vermaak, A., Smit, N.J. & Kudlai, O., 2023a. Molecular characterisation of three species of Coitocaecum (Digenea: Opecoelidae) infecting *Clinus superciliosus* (Clinidae) in South Africa, with description of *Coitocaecum brayi* sp. n. *Folia Parasitologica*, 70: 1–10.

Wee, N.Q., Cribb, T.H., Bray, R.A. & Cutmore, S.C., 2017. Two known and one new species of Proctoeces from Australian teleosts: Variable host-specificity for closely related species identified through multi-locus molecular data. *Parasitology International*, 66(2): 16–26.

Wood, C.L., Lafferty, K.D. & Micheli, F., 2010. Fishing out marine parasites? Impacts of fishing on rates of parasitism in the ocean. *Ecology Letters*, 13(6): 761–775.

Wood, C.L., Micheli, F., Fernández, M., Gelcich, S., Castilla, J.C. & Carvajal, J., 2013. Marine protected areas facilitate parasite populations among four fished host species of central Chile. *Journal of Animal Ecology*, 82(6): 1276–1287.

WoRMS, 2025. World Register of Marine Species. Available at: https://www.marinespecies.org/aphia.php?p=taxdetails&id=108432. (Date of access: 8 May 2025).

Yeld, M.E., 2009. Parasite assemblages of three endemic catshark species from the west and south coasts of South Africa. PhD thesis, University of Cape Town.

Yong, R.Q.Y., Bray, R.A., Schwelm, J., Louvard, C., Malherbe, W. & Smit, N.J., 2025. Lepocreadioidea (Digenea: Trematoda) of southern Africa, including a new genus and species of Lepidapedidae infecting the galjoen, *Dichistius capensis* (Cuvier) (Centrarchiformes: Dichistiidae) from off Namibia. *Parasitology International*, 109: e103110.

Yong, R.Q.Y., Martin, S.B. & Smit, N.J., 2023. A new species of *Siphoderina* Manter, 1934 (Digenea: Cryptogonimidae) infecting the Dory Snapper *Lutjanus fulviflamma* (Teleostei: Lutjanidae) from the east coast of South Africa. *Systematic Parasitology*, 100(6): 673–686.

Zhao, C.H., Chen, H.X., Wayland, M.T., Yang, R.J., Gu, X.H. & Li, L., 2025. Extreme phenotypic variation confounds acanthocephalan systematics: A case study of *Longicollum pagrosomi* and *Pomphorhynchus zhoushanensis* (Acanthocephala: Echinorhynchida). *Zoologica Scripta,* (in press).

4

The use of fish parasitic isopods as element accumulation indicators in marine pollution monitoring

Adapted from Marine Pollution Bulletin (2023) 194: 115385
https://doi.org/10.1016/j.marpolbul.2023.115385

4.1 Introduction

Marine ecosystems are continuously threatened by several anthropogenic pressures, such as pollutants, which influence the integrity of these systems and endanger marine biodiversity (Pinsino *et al.*, 2008; Webb and Mindel, 2015; Mahmoud *et al.*, 2019). Traditionally, pollution monitoring programs in marine environments have focused on the use of free-living bioindicator species, such as bivalves, to assess element exposure in the marine environment over spatial and temporal scales (Farrington *et al.*, 2016; Wepener and Degger, 2020). However, recent research has shown the value of the use of affiliate species and their fish hosts as sentinels for chemical pollution (Sures *et al.*, 2017). Parasites are highly sensitive to environmental change and respond either directly or indirectly to different degrees of pollution (Chine *et al.*, 2021; Sures *et al.*, 2023). Advances in environmental parasitology have demonstrated the advantages of using hosts and their parasites as sentinel systems for pollution monitoring over free-living species, such as mussels (Sures *et al.*, 2017; Chine *et al.*, 2021; Sures *et al.*, 2023). However, previous studies on host-parasite systems were primarily focused on freshwater environments and biased towards the use of endoparasitic helminths, such as acanthocephalans, cestodes, nematodes or digeneans (Sures, 2004; Vidal-Martínez *et al.*, 2010; Nachev and Sures, 2016; Erasmus *et al.*, 2020), while fewer studies focused on the use of ectoparasites, particularly in marine environments (e.g., Pérez-del-Olmo *et al.*, 2019).

In comparison to their endoparasitic counterparts, ectoparasites are exposed to both the external environment as well as the environment created by their fish hosts, which makes them potentially more susceptible and sensitive to environmental changes caused by pollution and/or other water quality parameters (Biswal and Chatterjee, 2020). They were shown to possess a

higher bioaccumulation capacity than their fish hosts, for instance, lead in monogeneans (Gao and Nie, 2000), and mercury in the cymothoid parasite, *Riggia paranensis* Szidat, 1948 (Lins *et al.*, 2008) and various other elements in parasitic isopods (Pérez-del-Olmo *et al.*, 2019). This indicates that similar to endoparasites, ectoparasites are able to bioconcentrate these elements, producing quantifiable results, which are normally only present in very low or undetectable concentrations in the environment (Gilbert and Avenant-Oldewage, 2017). The use of ectoparasites, such as isopods, could greatly facilitate our understanding of the biological availability of pollutants in the environment, ecological interactions and food web information, with a direct link to climate change (Longo *et al.*, 2013; van Gestel *et al.*, 2018; Sures *et al.*, 2023). Isopods represent a quarter (25%) of all ectoparasites known to infest fish globally (Öktener and Sezgin, 2000; Tansel and Fatih, 2012; Mahmoud *et al.*, 2019). They play crucial roles in marine ecosystems by providing food for larger species and helping to break down organic matter (van Gestel *et al.*, 2018). Results from ecotoxicological studies of terrestrial isopods over the last three decades highlight the great capability of these organisms to accumulate element contaminants (Drobne, 1997; van Gestel, 2012), making them suitable bioindicators for bioaccumulation monitoring programs. Further advantages of their use as bioaccumulation indicators in marine systems are the high host specificity, easy identification, well-defined physiologies, known life cycles and high occurrence in nature (Longo *et al.*, 2013).

The present study aims to determine the potential use of the parasitic isopod, *Cin. tetrodontis*, together with its fish host, *A. honckenii,* for analyses of metals and metalloids in marine environments. Specifically, we tested the hypothesis that external crustacean parasites, particularly *Cin. tetrodontis*, of *A. honckenii* accumulate significantly higher levels of elements than their host (Hypothesis 2, Chapter 1). To address this, we determined and compared the accumulation of elements in fish hosts (both infected and uninfected), as well as male and female parasites from a near-pristine and contaminated harbour locality. Elemental accumulation is also compared between male and female isopods from both localities. This marks the first study to conduct element analyses of parasitic isopods off the coast of Africa and first-implementing this host-ectoparasite system as an additional model for marine biomonitoring.

4.2 Materials and methods

4.2.1 Sampling and locality selection

As stated in Chapter 2, the Breede River Estuary is classified as one of the top twenty near-pristine estuaries in the Western Cape Province of South Africa (Breede River Estuarine Management Plan, 2016). It could therefore be assumed that this locality would not show high element concentrations, but rather reflect background geogenic concentrations. Nevertheless, potential threats that may still alter the quality and integrity of this estuary could be induced by

various urban developments and agricultural activities along the river, as well as vessel source pollution (Erasmus *et al.*, 2004; Breede River Estuarine Management Plan, 2016), such as those caused by recreational vessels launching from WS. Mossel Bay, on the other hand, being adjacent to the harbour, introduces many additional anthropogenic sources of pollution to the marine environment due to vessel pollution, vessel repairs, variable non-point discharges of elements, and coastal oceanographic changes in upwelling events (Wepener and Degger, 2020). Hence, it is expected to find high levels of element concentrations attributed to anthropogenic sources within this locality. *Amblyrhynchote honckenii* is the only known host of the ectoparasitic isopod, *Cin. tetrodontis*, which commonly infests the buccal cavity of fish (Hadfield *et al.*, 2010). Furthermore, this parasite is a protandric hermaphrodite, with commonly one male and one female present in the hosts' buccal cavity, consequently providing a valuable opportunity to determine element accumulation for four tissues per fish (i.e., liver, muscle, female parasite, and male parasite).

Fish hosts were collected from the relevant localities and humanely killed following the ethical and procedural protocols detailed in Chapter 2. The mouth of the fish was screened for isopods, and any isopods found were identified following Hadfield *et al.* (2010). All specimens of *Cin. tetrodontis* were removed, and the life cycle stage (i.e., juvenile or adult) and sex (i.e., male or female) were determined, frozen and stored at -20°C in pre-cleaned acid-washed polypropylene tubes. Axial muscle and liver tissue samples of the fish hosts were collected, frozen and stored at -20°C in pre-cleaned acid-washed polypropylene tubes.

4.2.2 Sample preparation

All samples were thawed and freeze-dried (FreeZone® 6, Labconco) for a duration of 96 h. Dried samples were homogenised using a mortar and pestle and accurately weighed to four decimals (±100 mg of muscle and liver tissue, as well as ±80 mg parasite tissue) and acid digested in 30 mL TFM® vessels with 4 mL HNO_3 (sub-boiled from 65%; p.a. quality, Merck) using a Mars 6 microwave digestion system (CEM Corporation, Kamp-Lintfort) for multi-element analysis. To avoid cross-contamination, the mortar and pestle were thoroughly cleaned using 5% HNO_3 before the next sample was homogenised. Digests were transferred to 5 mL volumetric flasks, brought to volume with ultrapure MilliQ water, transferred to pre-cleaned polypropylene tubes and stored at room temperature until analyses.

4.2.3 Analyses

According to the survey on elements in mussels by Wepener and Degger (2020), arsenic (As), cadmium (Cd), copper (Cu), manganese (Mn), nickel (Ni), lead (Pb), selenium (Se), and zinc (Zn) are generally present in all major harbours in South Africa. Accordingly, a multi-element

analysis was performed for these elements, using a quadrupole inductively coupled plasma-mass spectrometry (ICP-MS) (PerkinElmer, Elan 6000) equipped with an auto-sampler system (PerkinElmer, AS-90). The analysis was performed with the following operational specifications: 1000 W plasma power, 14 L/min gas flow, 0.95 L/min nebuliser gas flow and 1 mL/min sample flow rate. Yttrium (Y) and thulium (Tm) (Certipur®, Merck) were used as internal standards for quality measurements at a concentration of 10 µg/L. These elements were quantified by using the following mass lines: 75As, 114Cd, 63Cu, 55Mn, 60Ni, 208Pb, 82Se, and 66Zn. The ICP-MS was calibrated by using a series of 11 dilutions of multi-element standard solutions. Element concentrations were calculated for each sample by use of corresponding regression lines with a correlation factor of ≥0.999. The detection limits were calculated as three times the standard deviation of the blank measurements per digestion batch (Table 4.1).

Table 4.1: Percentage recovery (%) of two different certified reference materials (DOLT5 and SRM15666b), as well as the limit of detection (LOD) (ng/g dry weight) in different tissue samples. Detection limits for the fish and parasite samples were determined as three times the standard deviation of the blank measurements, considering a mean sample mass of 115 mg (muscle), 92 mg (liver), and 78 mg (parasites), respectively.

Metal	% Recovery		LOD (ng/g dry weight)		
	DOLT5	SRM15666b	Muscle	Liver	Parasite
As	93	92	0.25	0.15	0.64
Cd	87	88	0.015	0.014	0.020
Cu	109	105	0.75	0.44	0.70
Mn	106	104	0.37	0.20	0.28
Ni	109	106	2.02	15.2	4.13
Pb	118	93	0.98	0.19	1.53
Se	81	108	0.63	1.15	0.37
Zn	93	81	21.0	7.77	52.3

4.2.4 Quality control

Quality control of the element analysis was performed using applicable standard reference materials for all the elements. Reference materials, DOLT5 (Dogfish liver certified reference material for trace metals and other constituents, National Research Council, Canada) and SRM15666b (Oyster Tissue certified reference material, National Institute of Standards and Technology, USA) were used to validate the analytical procedure of biotic samples (Table 4.1). Internal procedural standards were analysed after every 20 samples for quality control and assurance.

4.2.5 Statistical analyses

For statistical data analysis, the data were tested for normality using the Shapiro-Wilk normality test. Since all data met the normal distribution assumption, a two-way ANOVA was performed, followed by Tukey's multiple comparison test using GraphPad Prism v7. Significance was regarded as $p<0.05$. Results of two-way ANOVA statistical analysis of variance comparing metal concentrations in species (parasite and fish host) from two localities (WS and MB) are presented in tabular form (Tables 4.2 and 4.3). Results of Tukey's multiple comparison tests, indicating significant differences ($p<0.05$) in element concentrations in species (parasite and fish host) from two localities (WS and MB), are illustrated in tabular form (Table 4.4).

4.3 Results

The concentrations of As, Cd, Cu, Mn, Ni, Pb, Se, and Zn were determined in muscle and liver tissues of both infected and uninfected fish, as well as in male and female parasites from WS and MB, on the South African temperate south coast. Female specimens of *A. honckenii* sampled from WS 180 ± 7 mm (175–185 mm) were much larger than males 150 ± 9 mm (140–165 mm). No juvenile fish were recorded from this locality (Supplementary data, Table S4.1). The adult *A. honckenii* from MB were significantly smaller than those sampled from WS (110 ± 7 mm). No female fish were recorded from this locality; however, two juvenile fish were recorded measuring 105 ± 7 mm (100–110 mm) in total length (Supplementary data, Table S4.2). There was a significant difference in the prevalence of infection by *Cin. tetrodontis* in *A. honckenii* between localities since only 40% of the fish were infested with *Cin. tetrodontis* at WS versus 90% of fish at MB. Since the isopod used in this study is a protandric parasitic species, both male and female sexes were present. Twelve adult specimens of *Cin. tetrodontis*, six males (64 ± 16 mg; range 47–95 mg) and six females (121 ± 17 mg; range 101–171 mg) were collected from six specimens of *A. honckenii* from WS (Supplementary data, Table S4.1). From MB, 18 adult specimens of *Cin. tetrodontis*, nine males, weighing 39 ± 4 mg (32–43 mg), and nine females weighing 125 ± 28 mg (80–189 mg), were collected from nine specimens of *A. honckenii* (Supplementary data, Table S4.2). Interestingly, all specimens of *Cin. tetrodontis* were collected from male *A. honckenii*, while none of the female fish were infested.

The concentrations of As, Cu, Mn, Ni, Pb and Zn in *Cin. tetrodontis* differed significantly ($p<0.05$) between the two localities, where MB's isopods had higher concentrations of Ni, Pb and Zn (Table 4.2). Significant differences in *Cin. tetrodontis* between localities are seen in the concentrations of Cu and Ni. Female *Cin. tetrodontis* from WS had higher concentrations of Cu than those from MB (Table 4.2). Male *Cin. tetrodontis* from MB had significantly ($p<0.05$) higher concentrations of Ni than those from WS (Table 4.2). Selenium concentrations in infected fish

muscle tissue differed significantly ($p<0.05$) between localities, with higher concentrations observed in fish collected from WS compared to those from MB (Table 4.2).

The instances of significant differences between the biological samples (parasites, uninfected and infected fish muscle and liver tissues) at a locality were far more than the differences between localities. The only significant interactions of elements in samples and localities were for Cu, Mn and Ni (Table 4.3).

Table 4.3: Two-way ANOVA analysis of variance table comparing element concentrations in species (*Cinusa tetrodontis* Schioedte & Meinert, 1884, infested *Amblyrhynchote honckenii* (Bloch), and uninfested *A. honckenii*) from two localities (Witsand and Mossel Bay) along the South African coastline.

Metal	Species (df = 5)	Sites (df = 1)	Interaction (df = 5)
As	*F*=32.22; p<0.0001	*F*=0.067; p=0.8	*F*=1.183; p=0.3267
Cd	*F*=34.76; p<0.0001	*F*=3.071; p=0.0842	*F*=2.335; p=0.0512
Cu	*F*=68.42; p<0.0001	*F*=3.520; p=0.0649	*F*=3.361; p=0.0090
Mn	*F*=46.67; p<0.0001	*F*=1.749; p=0.1905	*F*=5.523; p=0.0003
Ni	*F*=499.7; p<0.0001	*F*=4.469; p=0.0382	*F*=2.386; p=0.0470
Pb	*F*=4.399; p=0.0016	*F*=1.381; p=0.2440	*F*=1.033; p=0.4056
Se	*F*=173.2; p<0.0001	*F*=0.1952; p=0.6601	*F*=0.4499; p=0.8120
Zn	*F*=45.27; p<0.0001	*F*=8.058; p=0.0060	*F*=1.673; p=0.1529

The significant differences in element concentrations between species (*Cin. tetrodontis*, infected *A. honckenii*, and uninfected *A. honckenii*) from the two localities are summarised in Table 4.4. Apart from Cd, element concentrations were generally higher in male isopods compared to females. At WS significant differences ($p<0.05$) were found in concentrations of Mn, Ni and Se, while at MB, Pb, Mn, Ni, and Se were higher in male than female isopods (Table 4.4). The parasitic isopod accumulated significantly higher concentrations of elements when compared to its fish host (Table 4.2). Male isopods had significantly higher concentrations of As, Cu, Mn, Ni, Se and Zn than those of their fish hosts at both localities. At MB, males had significantly higher concentrations of As, Cu, Mn, Ni, Pb, Se and Zn compared to their fish hosts (Tables 4.2 and 4.4). Besides Pb, female *Cin. tetrodontis* showed the same trend when compared to their host, *A. honckenii* (Tables 4.2 and 4.4). In general, infected fish had lower element concentrations compared to uninfected fish. Only Cd and Mn levels in the liver tissues of uninfected fish at MB were significantly lower than the levels in the liver of infected fish (Table 4.4).

Table 4.2: Element concentrations (mean ± standard deviation) of *Cinusa tetrodontis* Schioedte & Meinert, 1884, infested *Amblyrhynchote honckenii* (Bloch) and uninfested *A. honckenii* from two localities (Witsand and Mossel Bay) along the South African coastline. Significant differences between the two localities are indicated with an asterisk (*). Significant differences between the parasites and host tissues at WS and MB, respectively, are presented in Table 4. Significance was taken as ($p<0.05$). Abbreviations: **DW** – dry weight.

Metal	Locality	Male *Cinusa tetrodontis* (µg/g DW)	Female *Cinusa tetrodontis* (µg/g DW)	Infected fish Muscle (µg/g DW)	Uninfected fish muscle (µg/g DW)	Infected fish Liver (µg/g DW)	Uninfected fish Liver (µg/g DW)
As	WS	40.40 ± 15.70	31.21 ± 8.88	6.42 ± 5.94	9.31 ± 11.27	4.93 ± 1.66	5.74 ± 4.23
	MB	33.70 ± 10.70	27.62 ± 7.35	8.38 ± 2.45	5.96	8.47 ± 6.17	17.81
Cd	WS	0.11 ± 0.05	0.11 ± 0.09	0.01 ± 0.001	0.01 ± 0.001	2.11 ± 1.36	2.16 ± 0.96
	MB	0.09 ± 0.04	0.06 ± 0.03	0.01 ± 0.001	0.01	1.94 ± 1.12	4.41
Cu	WS	81.57 ± 387.96	69.97 ± 12.44*	0.79 ± 0.16	0.78 ± 0.14	2.88 ± 1.55	3.55 ± 2.07
	MB	54.60 ± 18.30	45.34 ± 11.57*	0.90 ± 0.15	0.87	4.11 ± 1.64	8.62
Mn	WS	6.20 ± 2.10	3.36 ± 0.92	0.27 ± 0.04	0.27 ± 0.05	1.81 ± 0.52	1.67 ± 1.08
	MB	4.60 ± 1.20	2.57 ± 0.50	0.50 ± 0.24	0.33	2.99 ± 1.14	4.79
Ni	WS	8.44 ± 0.70*	3.44 ±0.75	0.12 ± 0.03	0.11 ± 0.02	0.31 ± 0.04	0.33 ± 0.15
	MB	9.77 ± 0.99*	3.81 ± 1.12	0.19 ± 0.11	0.18	0.29 ± 0.12	0.68
Pb	WS	1.11 ± 0.74	0.47 ± 0.18	0.07 ± 0.13	0.03 ± 0.01	0.06 ± 0.03	0.07 ± 0.07
	MB	3.02 ± 3.61	1.13 ± 1.44	0.06 ± 0.05	0.04	0.16 ± 0.12	0.25
Se	WS	20.34 ± 1.54	13.33 ± 4.88	1.18 ± 0.19*	1.19 ± 0.37	2.18 ± 0.31	2.57 ± 1.10
	MB	18.84 ± 3.12	12.33 ± 3.01	0.86 ± 0.09*	0.76	2.29 ± 0.66	4.07
Zn	WS	248.61 ± 82.22	205.44 ± 114.77	13.87 ± 1.54	14.14 ± 3.80	43.77 ± 9.53	69.44 ± 53.93
	MB	368.41 ± 110.33	284.44 ± 83.44	15.36 ± 3.44	15.69	71.66 ± 30.99	174.72

Table 4.4: Matrix indicating significant differences ($p<0.05$) in element concentrations in species (*Cinusa tetrodontis* Schioedte & Meinert, 1884, infested *Amblyrhynchote honckenii* (Bloch), and uninfested *A. honckenii*) from two localities (Witsand and Mossel Bay) along the South African coastline. Cells above the diagonal lines represent the elements that are statistically different between conditions at MB, while elements below the diagonal lines represent those conditions that differed significantly at WS. Abbreviations: ♂ – male; ♀ – female; **M** – muscle; **L** – liver.

	MB					
	Cinusa (♂)	**Cinusa (♀)**	**Infected fish (M)**	**Infected fish (L)**	**Uninfected fish (M)**	**Uninfected fish (L)**
Cinusa (♂)		Mn, Ni, Pb, Se	As, Cu, Mn, Ni, Pb, Se, Zn	As, Cd, Cu, Mn, Ni, Pb, Se, Zn	As, Cu, Mn, Ni, Se, Zn	Cd, Cu, Ni, Se
Cinusa (♀)	Mn, Ni, Se		As, Cu, Mn, Ni, Se, Zn	As, Cd, Cu, Ni, Se, Zn	Cu, Ni, Se, Zn	Cd, Ni, Se
Infected fish (M)	As, Cu, Mn, Ni, Se, Zn	As, Cu, Mn, Ni, Se, Zn		Cd, Mn		Cd, Mn
Infected fish (L)	As, Cd, Cu, Mn, Ni, Se, Zn	As, Cd, Cu, Ni, Se, Zn	Cd			Cd
Uninfected fish (M)	As, Cu, Mn, Ni, Se, Zn	As, Cu, Mn, Ni, Se, Zn		Cd, Mn		Cd, Mn
Uninfected fish (L)	As, Cd, Cu, Mn, Ni, Se, Zn	As, Cd, Cu, Mn, Ni, Se, Zn	Cd		Cd, Mn	
	WS					

4.4 Discussion

The present paper assessed the possible role of marine ectoparasitic isopods and their fish hosts as model bioindicators, complementary to traditional mussel indicators for marine pollution monitoring. To be considered an effective bioindicator, these isopods need to fulfil the criteria commonly accepted for established sentinel species. Accordingly, ectoparasitic isopods need to have high bioaccumulation capabilities, be resistant to pollutants with long pollutant half-lives once accumulated, and be prevalent, as well as widespread (van Gestel *et al.*, 2018).

The present study assessed element accumulation within the parasitic isopod, *Cin. tetrodontis*, together with its fish host, *A. honckenii*. The bioaccumulation potential of both male and female isopod parasites, as well as infected and uninfected fish from both a relatively unaffected locality (WS) and an element-contaminated harbour locality (MB), were compared. The parasitic isopod accumulated significantly higher concentrations of elements, except Cd, compared to its fish host. This is likely because these ectoparasites are exposed to both the external environment, as well as accumulating elements from feeding on their fish hosts, making them more susceptible and sensitive to environmental changes caused by pollution and/or other water quality parameters (Biswal and Chatterjee, 2020). The uptake and accumulation of elements, in general, are dependent on environmental and biological factors across different exposure routes (i.e., uptake from exposure to the external environment, dermal uptake or food uptake) (Somero *et al.*, 1977; Cani and Atli, 2003; Van Gestel *et al.*, 2018). Therefore, the degree of element exposure of these isopods is much higher than what is experienced by their fish host. However, unlike their hosts, these parasites have the ability to bioconcentrate these elements producing quantifiable results, which are normally only present in very low, or seemingly undetectable concentrations in the environment (Sures *et al.*, 2017). This is supported by the present study since concentrations between localities in the muscle or liver tissues of *A. honckenii* alone did not show any significant differences. Cadmium was the only element that accumulated in much lower concentrations in the isopod, compared to its fish host. According to the study by Vijver *et al.* (2006), this is most likely due to the isopod's high capability of sequestering elements, which is strongly related to the storage capacity of elements, such as Cd and Zn, within the hepatopancreas of isopods. Crustaceans also have the ability to store potential toxic elements in their exoskeleton and can reduce their body burdens by increasing the number of moults (O'Callaghan and Sullivan, 2020). It is, therefore, likely that *Cin. tetrodontis* has a high tolerance to element exposure, especially potentially toxic elements.

The significant differences between localities were related to concentrations of both essential and non-essential elements. According to Bosch *et al.* (2015), not all element contaminants are hazardous, since elements such as Cu, Fe, Se and Zn are essential in their

specific functions in body metabolism. Conversely, elements such as Cd, Cr, Hg, Ni and Pb are related to sources of pollution and considered non-essential and toxic to both fish and the environment in exceeding concentrations (Bosch *et al.*, 2015). In the present study, concentrations of Cu, Mn, Ni, Pb and Zn in *Cin. tetrodontis* differed significantly between the two localities, where MB's isopods had higher concentrations of Ni, Pb and Zn. Furthermore, the most significant differences in *Cin. tetrodontis* between localities were seen in the concentrations of Cu and Ni, where female isopods, from WS, had a higher concentration of Cu (essential) than those from MB. On the other hand, male isopods from MB had a higher concentration of Ni (non-essential) compared to those from WS. Hence, based on the data, it is clear that MB contains more toxic non-essential element concentrations than WS, containing more or higher essential element concentrations. Interestingly, WS had slightly higher Cd concentrations compared to MB. This was unexpected since the Breede River Estuary at WS has no known sources of element contamination and is regarded as a pristine, unaffected locality (Breede River Estuarine Management Plan, 2016). Similarly, Erasmus *et al.* (2021) found elevated element levels in klipfish, *Clinus superciliosus* (Linnaeus), from unimpacted localities along the same coastline. These authors attributed this to long-term exposure to elements derived from natural geogenic weathering introduced by freshwater runoff and frequent upwelling events along the South African coast. The levels of elements in the brown mussel, *Perna perna*, from localities along the South African south coast also support these findings (Degger *et al.*, 2011; Wepener and Degger, 2020).

By comparing element concentrations between male and female *Cin. tetrodontis*, element concentrations were generally higher in male isopods than in females. Interestingly, except with Cu, female *Cin. tetrodontis* showed significant relationships towards an increase in elements in host liver tissue samples, whereas male *Cin. tetrodontis* showed significant relationships towards an increase in elements in host muscle tissue. The reason for this is unclear; however, it could be explained by their food source because even though both male and female isopods attach in the host's buccal cavity, the male feeds predominantly on host tissue, while the female feeds on host blood (Smit *et al.,* unpublished data). This relationship between element concentrations and female isopods that feed on blood was also corroborated by Erasmus *et al.* (2020). These potential relationships between the host and or the external environment as metal sources in the parasitic isopods, should be explored further by analysing metals in host blood and the tissues of the buccal cavity.

4.5 Conclusion

The results of this study confirm our hypothesis (Hypothesis 2, Chapter1) that the parasitic isopod *Cin. tetrodontis* accumulates significantly higher concentrations of elements than its fish host, demonstrating its suitability as an effective accumulation bioindicator. Additionally, as a

group, ectoparasitic isopods possess a well-defined physiology, which accounts for increased tolerance or even resistance towards non-essential hazardous elements. Given the knowledge of their life cycles, attachment localities and food source information as described by Smit *et al.* (2014), ectoparasitic isopods provide an easier way to understand environmental changes and relative host behaviour and ecological interactions (Longo *et al.*, 2013; van Gestel *et al.*, 2018; Honda *et al.*, 2021). The present study highlights a future direction within environmental parasitology and emphasises the importance and utility of this particular ectoparasite-host model system, bioaccumulating higher element concentrations than their hosts, thereby acting as an effective early warning model.

References:

Acosta, A.A. & Smit, N.J., 2021. A first for Southern Africa: description of a new *Heterobothrium* (Monogenea: Diclidophoridae) parasitizing the evil eye pufferfish *Amblyrhynchotes honckenii* (Tetraodontiformes: Tetraodontidae). *Parasitology Research*, 120: 819–830.

Biswal, D. & Chatterjee, S., 2020. Fish parasites as biological indicators: a systematic review. *Biosciences Biotechnology Research Communications*, 13(4): 1743–1755.

Bosch, A.C., O'Neill, O., Sigge, G.O., Kerwath, S.E. & Hoffman, L.C., 2015. Heavy metals in marine fish meat and consumer health: a review. *Journal of the Science of Food and Agriculture*, 96: 32–48.

Breede River Estuarine Management Plan, 2016. Western Cape Estuary Management Framework and Implementation Strategy. SSI Environmental, 1st edition. Royal Haskoning D.H.V. (revised 2011, 2nd Edition, 2016).

Cani, M. & Atli, G., 2003. The relationships between heavy metal (Cd, Cr, Cu, Fe, Pb, Zn) levels and the size of six Mediterranean fish species. *Environmental Pollution*, 121: 129–136.

Chine, J.H., Nachev, M., Sures, B. & Gargouri, L., 2021. Trace element assessment in *Neoechinorhynchus agilis* (Rudolphi, 1918) (Acanthocephala: Neoechinorhynchidae) and its fish hosts, *Mugil cephalus* (Linnaeus, 1758) and *Chelon ramada* (Risso, 1827) from Ichkeul Lagoon, Tunisia. *Journal of Helminthology*, 95(e61): 1–7.

Degger, N., Wepener, V., Richardson, B.J. & Wu, R.S.S., 2011. Application of artificial mussels (AMs) under South African marine conditions: a validation study. *Marine Pollution Bulletin*, 63(5–12): 108–118.

Drobne, D., 1997. Terrestrial isopods—a good choice for toxicity testing of pollutants in the terrestrial environment. *Environmental Toxicology and Chemistry*, 16: 1159–1164.

Erasmus, A., Smit, N.J., Zimmermann, S., Nachev, M., Sures, B. & Wepener, V., 2021. Metal and metalloid concentrations in the southern African endemic inter- and infratidal super klipfish, *Clinus superciliosus*, from the west and south coasts of South Africa. *Marine Pollution Bulletin*, 172: 112852.

Erasmus, C.P., Rossouw, G. & Baird, D., 2004. The concentration of ten heavy metals in the tissues of shark species *Squalus megalops* and *Mustelus* (Chondrichthyes) occurring along the south eastern coast of South Africa. In: *Population*, English edition. University of Port Elizabeth.

Erasmus, J.H., Wepener, V., Nachev, M., Zimmermann, S., Malherbe, W., Sures, B. & Smit, N.J., 2020. The role of fish helminth parasites in monitoring metal pollution in aquatic ecosystems: a case study in the world's most productive platinum mining region. *Parasitology Research*, 119: 2783–2798.

Farrington, J.W., Tripp, B.W., Tanabe, S., Subramanian, A., Sericano, J.L., Wade, T.L. & Knap, A.H., 2016. Edward D. Goldberg's proposal of "the Mussel Watch": reflections after 40 years. *Marine Pollution Bulletin*, 110: 501–510.

Froese, R. & Pauly, D., 2023. *FishBase*. Available at: www.fishbase.org/search.php. (Date of access: 8 May 2025).

Gao, Q. & Nie, P., 2000. Lead content in the monogenean *Ancryocephalus mogurndae* and in different organs of its host, the mandarin fish, *Siniperca chuatsi*. *China Environmental Science*, 20: 233–236.

Gilbert, B.M. & Avenant-Oldewage, A., 2017. Parasites and pollution: the effectiveness of tiny organisms in assessing the quality of aquatic ecosystems, with a focus on Africa. *Environmental Science and Pollution Research*, 24: 18742–18769.

Hadfield, K.A., Bruce, N.L. & Smit, N.J., 2010. Redescription of the monotypic genus *Cinusa* Schioedte and Meinert, 1884 (Isopoda, Cymothoidae), a buccal-cavity isopod from South Africa. *Zootaxa*, 2437: 51–68.

Honda, M., Qiu, X., Lydia Undap, S., Kimura, T., Hori, T., Shimasaki, Y. & Oshima, Y., 2021. Contamination of heavy metals, polychlorinated dibenzo-p-dioxins/furans and dioxin-like polychlorinated biphenyls in wharf roach *Ligia* spp. in Japanese intertidal and supratidal zones. *Applied Sciences*, 11: 1856.

Lins, D.C., Meirelles, M.E., Malm, O. & Lima, N.R.W., 2008. Mercury concentration in the freshwater bonefish *Cyphocharax gilbert* (Curimatidae) and its parasite the crustacean *Riggia paranensis* (Cymothoidae). *Neotropical Ichthyology*, 6(2): 283–288.

Longo, G., Trovato, M., Mazzei, V., Ferrante, M. & Conti, G.O., 2013. *Ligia italica* (Isopoda, Oniscidea) as bioindicator of mercury pollution of marine rocky coasts. *PLoS ONE*, 8: e58548.

Mahmoud, N.E., Fahmy, M.M., Abuowarda, M.M., Zaki, M.M., Ismael, E. & Ismail, E.M., 2019. Influence of water quality parameters on the prevalence of *Livoneca redmanii* (Isopoda: Cymothoidae) infestation of Mediterranean Sea fishes, Egypt. *International Journal of Veterinary Science*, 8(3): 174–181.

Nachev, M. & Sures, B., 2016. Environmental parasitology: parasites as accumulation bioindicators in the marine environment. *Journal of Sea Research*, 113: 45–50.

O'Callaghan, I.O. & Sullivan, T., 2020. Shedding the load: moulting as a cause of variability in whole-body metal concentrations. *Journal of Crustacean Biology*, 40: 725–733.

Öktener, A. & Sezgin, M., 2000. *Mothocya epimerica* Costa, 1851 (Flabellifera: Cymothoidae), an isopod parasite in the branchial cavities of the Black Sea silverfish, *Atherina boyeri* Risso, 1810 (Perciformes, Atherinidae). *Turkish Journal of Marine Science*, 6(1): 23–29.

Pérez-del-Olmo, A., Nachev, M., Zimmermann, S., Fernández, M. & Sures, B., 2019. Medium-term dynamics of element concentrations in a sparid fish and its isopod parasite after the Prestige oil-spill: shifting baselines? *Science of the Total Environment*, 686: 648–656.

Pinsino, A., Della Torre, C., Sammarini, V., Bonaventura, R., Amato, E. & Matranga, V., 2008. Sea urchin coelomocytes as a novel cellular biosensor of environmental stress: a field study in the Tremiti Island Marine Protected Area, Southern Adriatic Sea, Italy. *Cell Biology and Toxicology*, 24: 541–552.

Smit, N.J., Bruce, N. & Hadfield, K.A., 2014. Global diversity of fish parasitic isopod crustaceans of the family Cymothoidae. *International Journal for Parasitology: Parasites and Wildlife*, 3: 188–197.

Somero, G.N., Chow, T.J., Yancey, P.H. & Snyder, C.B., 1977. Lead accumulation rates in tissues of the estuarine teleost fish, *Gillichthys mirabilis*: salinity and temperature effects. *Archives of Environmental Contamination and Toxicology*, 6: 337–348.

Sures, B., 2004. Environmental parasitology: relevancy of parasites in monitoring environmental pollution. *Trends in Parasitology*, 20: 170–177.

Sures, B., Nachev, M., Selbach, C. & Marcogliese, D.J., 2017. Parasite responses to pollution: what we know and where we go 'Environmental parasitology'. *Parasites & Vectors*, 10: 65.

Sures, B., Nachev, M., Schwelm, J., Grabner, D. & Selbach, C., 2023. Environmental parasitology: stressor effects on aquatic parasites. *Trends in Parasitology*, 39: 461–474.

Tansel, T. & Fatih, P., 2012. Ectoparasitic sea lice, *Caligus minimus* (Otto 1821, Copepoda: Caligidae) on brawn wrasse, *Labrus merula* L., in Izmir Bay, Aegean Sea. *Journal of Animal Science*, 11(38): 208–211.

van Gestel, C.A.M., 2012. Soil ecotoxicology: state of the art and future directions. *Zookeys*, 176: 275–296.

van Gestel, C.A.M., Loureiro, S. & Zidar, P., 2018. Terrestrial isopods as model organisms in soil ecotoxicology: a review. In: Hornung, E., Taiti, S. & Szlavecz, K. (Eds.), *Isopods in a Changing World*. *Zookeys*, 801: 127–162.

Vidal-Martínez, V.M., Pech, D., Sures, B., Purucker, S.T. & Poulin, R., 2010. Can parasites really reveal environmental impact? *Trends in Parasitology*, 26: 44–51.

Vijver, M.G., Vink, J.P.M., Jager, T., van Straalen, N.M., Wolterbeek, H.T. & van Gestel, C.A.M., 2006. Kinetics of Zn and Cd accumulation in the isopod *Porcellio scaber* exposed to contaminated soil and/or food. *Soil Biology and Biochemistry*, 38: 1554–1563.

Webb, T.J. & Mindel, B.L., 2015. Global patterns of extinction risk in marine and non-marine systems. *Current Biology*, 25: 506–511.

Wepener, V. & Degger, N., 2020. Monitoring of metals in South African harbours using resident brown mussels (*Perna perna*) as indicator organisms. *African Zoology*, 55(4): 267–277.

5

Persistent organic pollutants in South African coastal ecosystems: analysing the evileye blaasop *Amblyrhynchote honckenii* (Bloch) for PCB and OCP accumulation

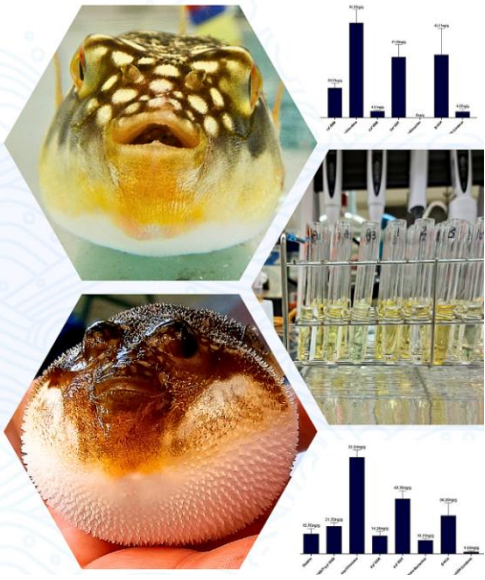

Adapted from Regional Studies in Marine Science (2025) 89: 104368
https://doi.org/10.1016/j.rsma.2025.104368

5.1 Introduction

Coastal marine environments are globally threatened by the presence of POPs, particularly OCPs and PCBs (Gakuba *et al*., 2019). These contaminants, widely used in agriculture and industry, are characterised by their long-lasting presence in the environment and their ability to bioaccumulate in aquatic organisms (Gakuba *et al*., 2019; Ramírez-Ayala *et al*., 2021). OCPs were primarily introduced for pest and disease control starting in the 1940s, while PCBs were used as coolants and lubricants in electrical equipment until their ban in the late 1970s (Serdar *et al*., 2014). Both groups of pollutants pose serious ecological risks, including disruptions to marine life and food webs (Serdar *et al*., 2014; Thompson *et al*., 2017). The persistence of these compounds poses ongoing risks to marine ecosystems, remaining detectable long after their initial application and raising concerns about their long-term effects on biota and human health, due to their biomagnification through the food chain (Jones and de Voogt, 1999; Li and Macdonald, 2005; Girones *et al*., 2020; D'Agostino *et al*., 2020).

Efforts to manage POPs have been initiated through international agreements such as the Stockholm Convention, which aims to eliminate or restrict these pollutants globally (Stockholm Convention, 2001; Gakuba *et al*., 2019). However, challenges persist due to existing stockpiles of POPs and ongoing releases from contaminated localities (Ramírez-Ayala *et al*., 2021). Currently, South Africa is the largest importer of pesticides in Africa, with an estimated value of $3.4 million between 2008 and 2017 (Tolera, 2021), resulting in the ongoing introduction of pesticides into rivers and ultimately the marine environment through various contamination pathways (Vogt *et al*., 2019; Wepener and Degger, 2019; Erasmus *et al*., 2020). For example, POPs such as DDT, banned in most other parts of the world, continue to be used for vector control

in malaria-endemic regions of South Africa (Burke *et al*., 2017; Thompson *et al*., 2017; Olisah *et al*., 2021). Studies have shown that these land-based sources of POPs resulted in the contamination of intertidal (Erasmus *et al*., 2020) and coral reef (Porter *et al*., 2018) ecosystems off the east coast of South Africa. Understanding the distribution and concentration of POPs along the South African coastline is critical for evaluating potential impacts on biodiversity and ecosystem health. The implications extend beyond ecological health to human health concerns for communities reliant on coastal resources (Ramírez-Ayala *et al*., 2021). Consumption of contaminated seafood can result in harmful substance bioaccumulation in humans, leading to adverse health outcomes (Ramírez-Ayala *et al*., 2021). Therefore, comprehending the dynamics of POP accumulation in marine species is vital for assessing risks to both ecological integrity and public health (D'Agostino *et al*., 2020).

Most marine pollution monitoring studies have relied on traditional sessile bioindicator species such as mussels (Wepener and Degger, 2012; Farrington *et al*., 2016). In South Africa, the focus has primarily been on the monitoring of metals in mussels (Wepener and Degger, 2020) but the need for assessing other classes of pollutants (Wepener and Degger, 2019) and using other species such as marine fish (Gakuba *et al*., 2019; Olisah *et al*., 2021) along the South African coastline has been identified. Although South African pufferfish are not commercially significant and are classified as “least concern” by the IUCN (Froese and Pauly, 2023), their use as an indicator of contamination offers advantages over mussels. Unlike mussels, which filter-feed from large volumes of water with low enzymatic activity for metabolising OCPs (León *et al*., 2013), pufferfish exhibit diverse metabolic pathways that provide insights into how various contaminants affect marine fish rather than sessile bivalves (Yuqi *et al*., 2014). Furthermore, their scavenger feeding habits expose them to different sources of contaminants (Sazima, 2024). Pufferfish liver has a high lipid content (Wang *et al*., 2019), which is crucial for the accumulation of POPs (Phillips and Rainbow, 2013) and for this reason, pufferfish have been used as indicator organisms of metal exposure in the Mediterranean Sea (Kosker *et al*., 2019; Doğdu *et al*., 2021) and the South African coastline (Van Der Spuy *et al*., 2023). Furthermore, biochemical and histological biomarkers in pufferfish were used as indicators of marine health in MPAs of Brazil (Marinsek *et al*., 2024) and coastal lagoons of the Yucatan (Pech *et al*., 2009).

A pufferfish species occurring in South Africa, the evileye blaasop, *A. honckenii*, has the potential to serve as a model for studying pollutants due to its wide distribution, ecological significance, and sensitivity to environmental changes, as evidenced by its accumulation of metals (Van Der Spuy *et al*., 2023). This species is also one of the most common marine and brackish fish associated with reefs, with a broad Indo-West Pacific distribution from South Africa to China and the Marshall Islands in Micronesia (Froese and Pauly, 2023). This study aimed to

provide insights into OCP and PCB accumulation in marine fish, using the evileye blaasop as an indicator organism, along the nearshore South African coastline. Specifically, we tested the hypothesis that levels of POPs in *A. honckenii* are significantly lower in MPAs than in non-protected localities (Hypothesis 3, Chapter 1). The study further aimed to compare OCP and PCB exposure concentrations between MPAs and non-MPA localities to determine whether MPAs provide a protective effect against contaminant accumulation.

5.2 Materials and methods

5.2.1 Sampling and locality selection

To explore the bioaccumulation of lipophilic pollutants, particularly OCPs and PCBs, in *A. honckenii,* specimens were collected as described in Chapter 2 from six distinct localities along the South African coast. These localities included those described in Chapter 2, as well as one additional non-MPA locality, St Francis Bay (FB)(Figure 5.1). St Francis Bay (-34.183333; 24.851667) combines recreational activities with residential development and a commercial fishing fleet harbour (Baird and Pereyra-Lago, 1992), highlighting the effects of mixed-use environments on contaminant levels.

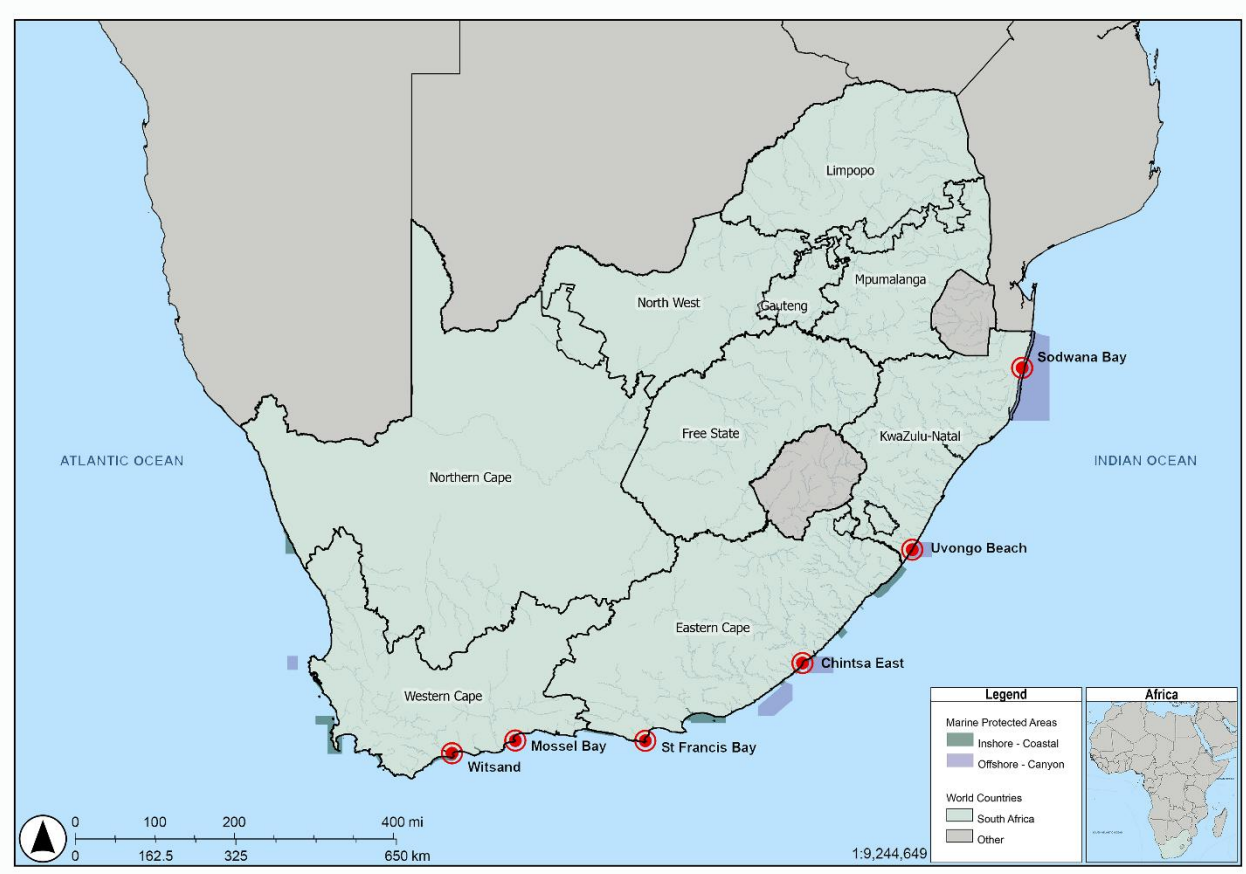

Figure 5.1: Map indicating the sampling localities (red circles) of specimens of *Amblyrhynchote honckenii* (Bloch). Map generated by Linda de Klerk on ArcGIS Online.

5.2.2 Sample preparation

Muscle and liver tissue were removed using pre-cleaned dissection equipment, placed in pre-cleaned aluminium foil, transferred to polypropylene Falcon tubes, and frozen at -20°C pending analyses. In the laboratory, samples were first thawed and weighed to determine their wet weight. They were then placed in a -80°C freezer for 24 h before being transferred to a freeze dryer (FreeZone 6, Labconco) for approximately 96 h. Following freeze-drying, the samples were reweighed to obtain their dry weight and subsequently homogenised using a mortar and pestle. Approximately 0.5 g of each sample was placed into 15 mL Falcon tubes. Two samples of approximately 0.2 g of rat liver were prepared for every 30 samples for recovery and quality control (QC). Similarly, two blank samples were prepared for every 30 samples using 500 µL of ultra-pure MilliQ water (MQ).

All tubes, except for the MQ, were spiked with OCP (Dr. Ehrenstorfer) and PCB (Dr. Ehrenstorfer) standard surrogates and internal standards before being vortexed. Internal standards were selected not for their structural similarity to the target analytes, but for their chemical stability, consistent recovery, and lack of interference with target compound detection. The use of these internal standards corrected for potential variations in extraction efficiency, injection volume, and instrumental response across all samples. The concentrations and spike volumes of these standards are detailed in Supplementary Tables 5.1 and 5.2. The OCP and PCB surrogates used are listed in Supplementary Table 5.3. Following this, 500 µL of 0.1% formic acid (99%, Fujifilm Wako) in acetonitrile (99.9%, Fujifilm Wako) was added to the biological and QC samples, which were then mixed thoroughly and vortexed for 1 min. After allowing the samples to stand for 1–2 h post-spiking, an additional 5 mL of 0.1% formic acid in acetonitrile was added to each falcon tube, while only the blanks and MQ samples received an additional 500 µL of sodium acetate (Fujifilm Wako) to facilitate the separation of water from the solvent. The samples were vortexed for 1 min and then ultrasonicated for 5 min before being shaken mechanically at maximum speed for 10 min. Following this, the samples were centrifuged at 10,000 rpm for 5 min at 5°C. To remove the lipids from the samples, the supernatant was decanted into activated EMR-Lipid tubes (Agilent Bond Elut), which had been pre-activated by adding 5 mL of MQ and shaking vigorously. For the blanks and MQ samples, only 5 mL of supernatant was transferred to the EMR-Lipid tubes. All samples were shaken vigorously and vortexed again before being placed in a mechanical shaker at maximum speed for another 10 min, followed by a second centrifugation at 10,000 rpm for five minutes at 5°C. The entire supernatant from each sample was then decanted into pre-prepared EMR-Polish tubes, which contained 1.4 g of $MgSO_4$ (Fujifilm Wako) and 0.6 g of NaCl (Kanto Chemical Co., Inc.). The samples were vortexed upright for one minute before undergoing final centrifugation at 10,000 rpm for 5 min at 5°C. Finally, a volume of 1 mL from the uppermost supernatant was pipetted into

the corresponding GC vial for analysis. The acetonitrile extract was not evaporated and was injected directly into the GC–MS.

5.2.3 Analyses

The OCPs and PCBs were analysed in muscle and liver tissue of the Evileye blaasop using a GC-20230 Plus (Shimadzu) coupled with a GCMS-TQ8050NX triple quadrupole mass spectrometer (Shimadzu). Chromatographic separation was performed using a Rxi-5Sil MS capillary column (30 m x 0.25 mm i.d., 0.25 µm df, Restek, Bellefonte, PA, USA).

For OCP analysis, the operating condition was splitless injection mode with an injection volume of 1 µL at an injector temperature of 250°C. Helium (≥99.999%) was used as the carrier gas with a linear velocity in flow control mode, 100.1 Kpa pressure, 30 mL/min total flow rate, 1.69 mL/min column flow, 47.2 cm/s linear velocity, 5 mL/min purge flow. The oven temperature program started at 50°C (held for 1 min), increased to 200°C at 30 °C/min, and finally ramped to 260°C at 5 °C/min, where it was held for 3 min. The total program duration was 20 min. The mass spectrometer system was operated in the electron ionisation (EI) mode at 70 eV. The ion source and interface temperatures were 230 and 250°C, respectively. The regression line was determined using the internal standard method, where the ratio of each analyte signal is taken to the internal standard signal and plotted against the analyte concentrations in the calibration solutions to obtain a regression line with a correlation factor of (R^2=0.99) before analysing the samples.

For PCB analysis, the operating condition was splitless injection mode with an injection volume of 1 µL at an injector temperature of 270°C. Helium (≥99.999%) was used as the carrier gas with a linear velocity in flow control mode, 41.1 KPa pressure, 30.0 mL/min total flow rate, 0.75 mL/min column flow, 31.8 cm/s linear velocity, 5 mL/min purge flow. The oven temperature program started at 75°C (held for 2 min), increased to 180°C at 15 °C/min, and finally ramped to 300°C at 4 °C/min, where it was held for 6 min. The total program duration was 45 min. The mass spectrometer system was operated in the electron ionisation (EI) mode at 70 eV. The ion source and interface temperatures were 230 and 290°C, respectively. The regression line was determined using the internal standard method, where the ratio of each analyte signal is taken to the internal standard signal and plotted against the analyte concentrations in the calibration solutions to obtain a regression line with a correlation factor of (R^2=0.98) before analysing the samples.

5.2.4 Quality control

Procedures used for the analysis of selected OCPs and PCBs were monitored with appropriate quality control and assurance measures. Procedural blanks were used in all the extraction, clean-up and analysis steps along with sample preparation and analysis to determine if there was any possible input from external sources during analysis. There were no detectable levels of target contaminants in blank samples. Target analyte recoveries were performed by spiking freeze-dried rat liver as reference material with separate OCP and PCB standards before extraction. The concentration of the analytes was determined using the internal standard method. The concentration of the spiked reference samples was divided by the known concentration of the spike in the sample and multiplied by 100 to obtain the percentage recoveries (Saadati *et al*., 2013). The limit of detection (LOD) was calculated as 3 times the signal-to-noise ratio using the standard deviation of 3 calibration intercepts divided by the slope, whereas the limit of quantification (LOQ) was 10 times this ratio (Saadati *et al*., 2013). The recovery rate (%), limit of detection (LOD) and limit of quantification (LOQ) of all the different OCP and PCB compounds of interest that were detected are shown in Table 5.1. The reference material in freeze-dried rat liver tissues was analysed, yielding recovery percentages of 103–148% for OCPs and 82–119% for PCBs (Table 5.1).

Table 5.1: The limit of detection (LOD), limit of quantification (LOQ) and recovery rates (%)(mean ± standard deviation) of all the different organochlorine pesticide (OCP) and polychlorinated biphenyl (PCB) compounds detected in the liver tissues of *Amblyrhynchote honckenii* (Bloch).

OCPs				PCBs			
Compounds	**LOD (ng/g)**	**LOQ (ng/g)**	**Recovery (%)**	**Compounds**	**LOD (ng/g)**	**LOQ (ng/g)**	**Recovery (%)**
Dieldrin	0.48	1.46	106 ± 18	**PCB #31**	2.55	7.74	119 ± 15.62
***o,p'*-DDD**	0.41	1.25	148 ± 5	**PCB #44**	2.39	7.25	108 ± 10.77
***o,p'*-DDT/ *p,p'*-DDD**	0.71	2.14	107 ± 10	**PCB #52**	2.76	8.35	107 ± 11.10
Oxychlordane	0.64	1.95	104 ± 14	**PCB #66**	1.57	4.77	94 ± 6.91
***p,p'*-DDE**	0.50	1.50	102 ± 9	**PCB #87**	0.38	1.15	91 ± 3.44
***p,p'*-DDT**	1.56	4.73	113 ± 10	**PCB #101**	0.83	2.50	98 ± 3.88
trans-Nonachlor	0.72	2.19	100 ± 14	**PCB #110**	0.27	0.81	104 ± 4.36
β-HCH	1.24	3.75	122 ± 14	**PCB #138**	0.71	2.16	92 ± 8.06
γ-HCH (Lindane)	0.47	1.42	103 ± 7	**PCB #141**	0.51	1.56	90 ± 7.96
				PCB #151	1.19	3.61	107 ± 4.95
				PCB #153	0.63	1.91	94 ± 4.13
				PCB #170	0.33	1.01	85 ± 9.20
				PCB #180	0.45	1.35	82 ± 1.17
				PCB #183	0.45	1.36	84 ± 8.87
				PCB #187	0.29	0.87	84 ± 7.93
				PCB #206	0.22	0.66	100 ± 4.54

5.2.5 Statistical analyses

Data were tested for normality using the Shapiro-Wilk normality test. Significant differences in OCP and PCB concentrations in *A. honckenii* tissues between the six localities were determined using a one-way ANOVA followed by Dunn's multiple comparisons test (GraphPad Prism v9.0.0). Significance was regarded as $p<0.05$. To allow for statistical analyses, all sample values below the LOD were substituted with LOD/2 (Kushner, 1976; Labuschagne *et al*., 2020).

5.3 Results

The overall recovery rates, typically within the acceptable range of 75% to 125% (Table 5.1), confirm the accuracy of the method and ability to minimise analyte losses during sample preparation and analysis (Saadati *et al*., 2013). The detection limits across both chemical groups demonstrate the method's capability to accurately identify contamination at trace levels, ensuring the reliability of reported concentrations. There were no detectable levels of target contaminants in fish muscle samples, while nine OCPs and 16 PCBs were detected in fish livers across the six localities (Supplementary Tables 5.4 and 5.5).

The distribution of OCPs across the six localities indicates significant spatial variation in exposure and subsequent contamination (Figure 5.2). Total OCP concentrations (∑OCP) were highest in WS (372 ± 161 ng/g) and lowest in SB (177 ± 131 ng/g) (Figure 5.2), suggesting greater contamination in the localities on the south west coast. Notably, oxychlordane concentrations were significantly higher when compared to the other localities (Figures 5.2–5.3), peaking in MB (296 ± 73 ng/g) and being lowest in SB (64 ± 28 ng/g). The concentrations of p,p'-DDT found in FB, UB, and SB were similar (Figures 5.2–5.3). Significant variation ($p<0.05$) was also observed for p,p'-DDE (Figure 5.2), with fish from FB having the highest concentrations (72 ± 36 ng/g) and SB having the lowest (5 ± 3 ng/g). Interestingly, β-HCH showed an increasing trend (albeit non-significant) (Figure 5.2) from WS (25 ± 21 ng/g) on the southwest to SB (43 ± 57 ng/g) in the northeast (Supplementary Table 5.4). Dieldrin and trans-nonachlor were detected exclusively in UB, whereas o,p'-DDD was only found in FB fish (Supplementary Table 5.4). Statistical analysis confirmed significant spatial differences in contamination levels. The ANOVA results indicate that o,p'-DDT/p,p'-DDD ($F=12.55$; $p<0.0001$), oxychlordane ($F=26.77$; $p<0.0001$), γ-HCH ($F=5.05$; $p=0.0013$), and p,p'-DDE ($F=15.84$; $p<0.0001$) exhibited significant variation across localities.

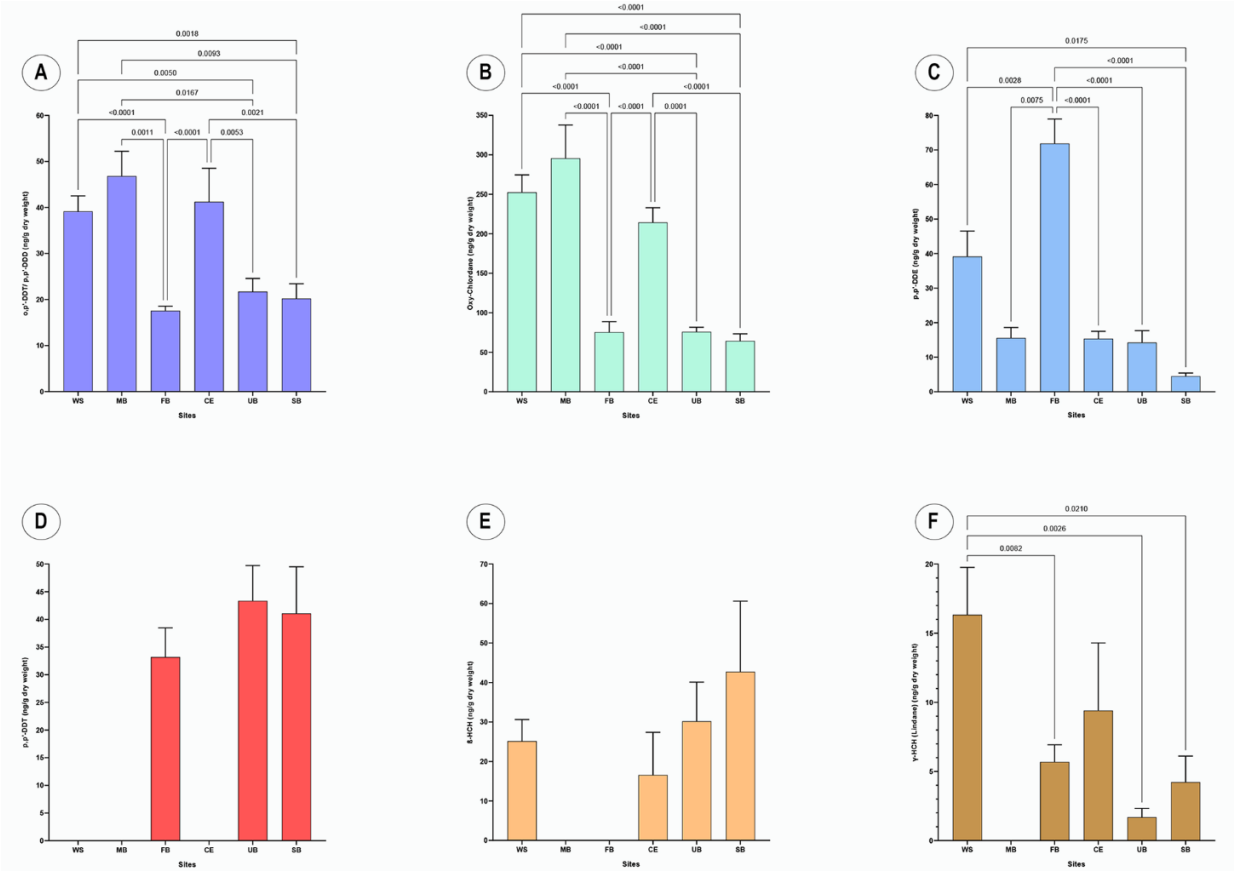

Figure 5.2: Organochlorine pesticide (OCP) concentrations (mean ± standard deviation) in fish liver tissues of *Amblyrhynchote honckenii* (Bloch) from six localities (Witsand, Mossel Bay, St Francis Bay, Chintsa East, Uvongo Beach, and Sodwana Bay) along the South African coastline. Significant differences between the six localities are indicated by the p-value. All concentrations are expressed as ng/g dry weight. Significance was taken as $p<0.05$. Abbreviations: **ND** – not detected; **WS** – Witsand; **MB** – Mossel Bay; **FS** – St Francis Bay; **CE** – Chintsa East; **UB** – Uvongo Beach; **SB** – Sodwana Bay. Concentrations that were only observed in one locality are listed in the supplementary material.

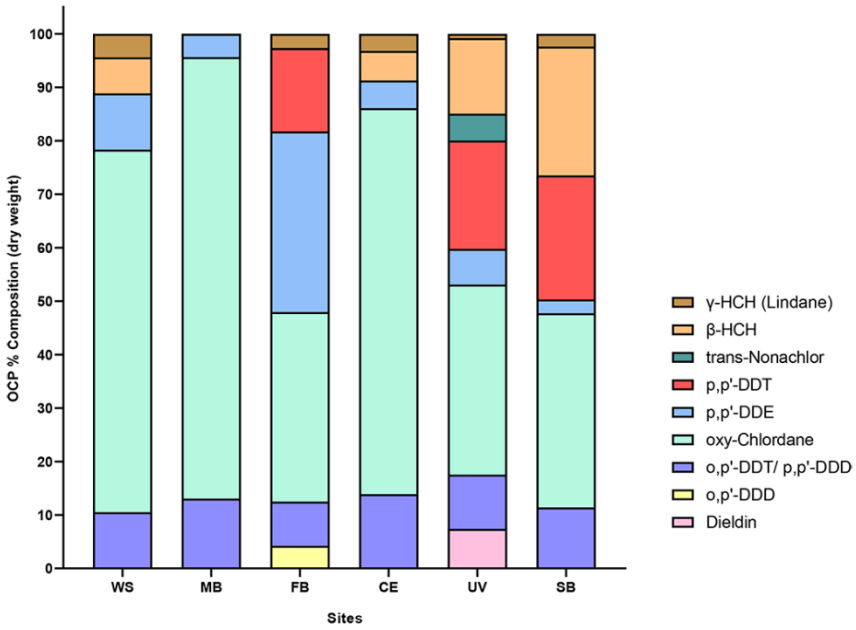

Figure 5.3: Percentage organochlorine pesticide composition in fish liver tissues of *Amblyrhynchote honckenii* (Bloch) from six localities (Witsand, Mossel Bay, St Francis Bay, Chintsa East, Uvongo Beach, and Sodwana Bay) along the South African coastline. Abbreviations: **WS** – Witsand; **MB** – Mossel Bay; **FS** – St Francis Bay; **CE** – Chintsa East; **UB** – Uvongo Beach; **SB** – Sodwana Bay.

PCB contamination exhibited a striking pattern, with FB fish having a significantly higher total PCB concentration (∑PCB = 929 ± 999 ng/g) compared to those from all other localities, where concentrations remained below 22 ng/g (Supplementary Table 5.5). The relatively high standard deviation in ∑PCB concentration at the FB locality (929 ± 999 ng/g) reflects both the detection of a wider range of PCB congeners at this location and the influence of LOD/2 substitution for non-detects. In contrast, the other localities exhibited fewer detectable congeners, with most PCB values below detection limits, leading to lower calculated means and standard deviations. PCB #153 was the most widespread congener, detected in fish from all localities except SB, and showed significantly higher concentrations in FB (235 ± 222 ng/g) (Figures 5.4–5.5). Among the PCBs, PCB #153 showed a significant difference ($F=9.474$; $p<0.0001$), reinforcing the pattern of elevated levels in FB. The statistical confirmation of these differences strengthens the argument for targeted investigations into contamination sources in this region. Several PCB congeners, such as PCB #180 ($F=8.96$; $p<0.0001$) and PCB #187 ($F=6.9$); $p<0.0001$), were also significantly elevated in FB fish compared to those from UB (Figure 5.4). In contrast, PCBs were below detection in SB fish, indicating a lower impact from such contaminants in this region (Figure 5.5). This suggests that north-eastern coastal localities have either remained unaffected by historical PCB contamination or benefit from oceanographic conditions that reduce contaminant accumulation.

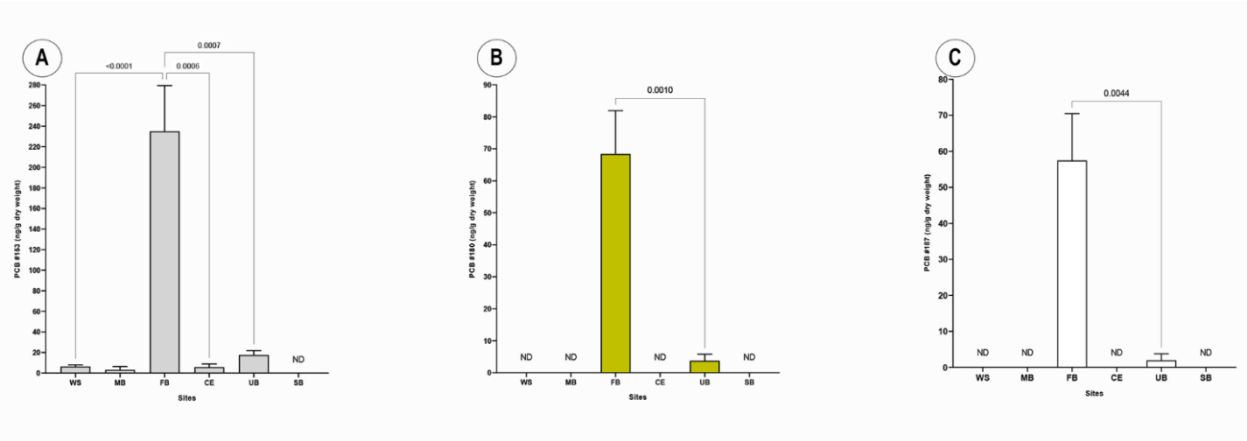

Figure 5.4: Polychlorinated biphenyl (PCB) concentrations (mean ± standard deviation) in fish liver tissues of *Amblyrhynchote honckenii* from six localities (Witsand, Mossel Bay, St Francis Bay, Chintsa East, Uvongo Beach, and Sodwana Bay) along the South African coastline. Significant differences between the six localities are indicated with the p-value. All concentrations are expressed as ng/g dry weight. Significance was taken as $p<0.05$. Abbreviations: **ND** – not detected; **WS** – Witsand; **MB** – Mossel Bay; **FS** – St Francis Bay; **CE** – Chintsa East; **UB** – Uvongo Beach; **SB** – Sodwana Bay.

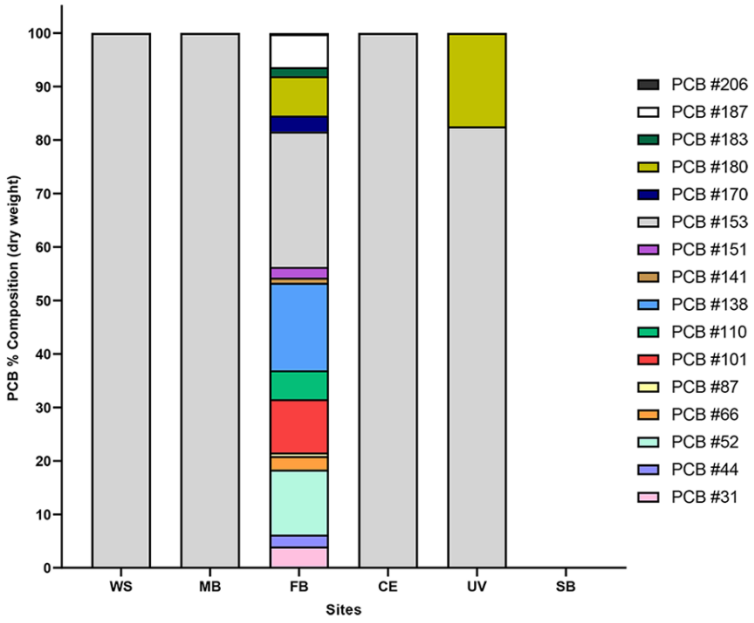

Figure 5.5: Percentage polychlorinated biphenyl congener composition in fish liver tissues of *Amblyrhynchote honckenii* (Bloch) from six localities (Witsand, Mossel Bay, St Francis Bay, Chintsa East, Uvongo Beach, and Sodwana Bay) along the South African coastline. Abbreviations: **WS** – Witsand; **MB** – Mossel Bay; **FS** – St Francis Bay; **CE** – Chintsa East; **UB** – Uvongo Beach; **SB** – Sodwana Bay.

5.4 Discussion

The results of this study provide valuable insights into the spatial distribution, persistence, and potential ecological risks associated with pesticide contamination across various sampling localities along the South African coastline. The detection of two global priority contaminants, OCPs and PCBs, highlights the widespread and complex nature of OCP contamination. Compounds such as o,p'-DDT/p,p'-DDD, oxychlordane, p,p'-DDE, and PCB #153 showed significant spatial variation, indicating point sources of contamination. Conversely, the relatively uniform distribution of p,p'-DDT and β-HCH suggests widespread historical contamination rather than locality-specific contamination events. The uniform presence of these compounds further suggests their mobility and persistence in the marine environment, potentially transported via water currents or bioaccumulated across broader regions.

POPs, such as OCPs and PCBs, have been extensively studied along the South African coastline, with previous research highlighting long-term trends and potential sources. Ryan *et al*. (2012) reported a decreasing trend between 1884 and 2008 in legacy OCPs in beached plastic pellets. However, they also found that PCB concentrations have not shown the same decline, likely due to their continued leaching from historical sources and industrial activities. This is consistent with the present findings, where OCP contamination showed variability across localities, while PCB contamination was particularly pronounced in FB, pointing to potential ongoing industrial inputs. These findings are consistent with global research indicating that despite regulatory restrictions, pesticide residues persist due to their long half-lives, continued use, and secondary contamination sources (Ali *et al*., 2021). The selected bioindicator species, *A. honckenii*, revealed distinct contamination trends indicative of both historical and ongoing contamination. The distribution of these POPs provides insights into the interplay between anthropogenic activities, oceanographic transport mechanisms, and the potential role that MPAs play in reducing contaminant exposure in the nearshore environment.

Total OCP concentrations varied significantly across locations, with WS exhibiting the highest concentrations and SB the lowest, suggesting an increasing east to west gradient along the coast of South Africa. This pattern is likely driven by regional differences in land use, historical pesticide application, and hydrodynamic conditions affecting sediment deposition and resuspension (Berrojalbiz *et al*., 2011; Cao *et al*., 2022; Liu *et al*., 2024). This spatial trend aligns with studies by Degger *et al*. (2011), that found that OCP levels in *Perna perna* (brown mussels) were highest in areas with strong agricultural runoff, particularly in regions of the Western Cape Province, supporting the hypothesis that historical pesticide application continues to influence coastal contamination through runoff and sediment resuspension. The elevated concentrations observed on the southwestern coast are consistent with agricultural runoff from the Western

Cape, a region historically associated with pesticide use, mirroring contamination patterns observed in metal pollution studies (Wepener and Degger, 2020). Similarly, Firth *et al*. (2019) monitored organic pollutants in *Choromytilus meridionalis* Krauss (black mussels) along the South African coastline and found that contaminants such as DDT metabolites and PCBs are highly persistent in marine environments, accumulating in bioindicator species. This aligns with the present study, where high concentrations of p,p'-DDE in FB further support the persistence of DDT residues in marine sediments and biota despite regulatory bans. Furthermore, Erasmus *et al*. (2020) reported that South African coastal localities continue to receive inputs of DDT from malaria vector control programs, which aligns with the detection of parent p,p'-DDT. The presence of p,p'-DDT in SB and UB likely results from WHO-approved malaria vector control programs in northeastern South Africa (WHO, 2011; Thompson *et al*., 2017), whereas in FB, it raises concerns about illegal agricultural use.

Hydrodynamic conditions also play a crucial role in the spatial distribution of OCPs, as coastal currents and sediment transport influence contaminant dispersion and accumulation (Berrojalbiz *et al*., 2011; Cao *et al*., 2022; Liu *et al*., 2024). The strong Agulhas Current activity in the north and east likely facilitates contaminant dispersion (Liu *et al*., 2024), while the slower-moving Agulhas counter-current in the southwest contributes to contaminant accumulation. This could also explain the higher OCP concentrations observed in the southwestern coastal localities. The detection of oxychlordane in MB suggests localised degradation of legacy chlordane, consistent with findings that older OCPs undergo gradual transformation in marine environments (Degger *et al*., 2011; Firth *et al*., 2019). The persistence of these pollutants can be attributed to factors such as microbial activity, temperature, and sediment characteristics, which influence degradation rates (Aislabie *et al*., 1997; Yu *et al*., 2011). Additionally, the accumulation of various POPs, including PCBs and other halogenated compounds, has been well-documented in estuaries along the South African coastline and offshore (Kampire *et al*., 2016; Ryan *et al*., 2012; Wu *et al*., 2019). These studies highlight the long-term stability of such compounds in coastal ecosystems, reinforcing the urgent need for continued monitoring and stricter enforcement of pesticide regulations in South Africa to mitigate their lasting environmental impact.

The β-HCH concentrations exhibited a decreasing trend from the northeast (SB) to the southwest (WS), suggesting that its presence is linked to historical and possibly ongoing use in northern regions rather than long-range atmospheric transport. Previous studies have indicated that β-HCH remains more prevalent in the northern parts of South Africa, likely due to past agricultural applications and industrial sources (Kampire *et al*., 2016; Wu *et al*., 2019). This spatial distribution aligns with the hypothesis that OCPs are transported from their primary regions of use rather than through atmospheric mechanisms, as prevailing wind patterns predominantly move

south-westward. Limited detections of dieldrin and trans-nonachlor in UB suggest historical termiticide use near urban settlements (Colt *et al*., 2006), while the detection of o,p'-DDD only in FB implies localised reductive dechlorination processes in sediment under low-oxygen conditions (Venkatesan *et al*., 1999). The restricted spatial occurrence of these compounds further supports the role of locality-specific contamination sources and retention mechanisms in shaping pollutant distributions along the South African coastline.

The presence of PCBs in the study area is of particular concern due to their high persistence, bioaccumulation potential, and toxic effects (Girones *et al*., 2020; Barhoumi *et al*., 2023). PCBs exhibited spatial variability along the South African coastline, with the highest concentrations observed at FB. This pattern aligns with findings from previous studies, which have identified the Gqeberha (previously known as Port Elizabeth) region as a hotspot for PCB contamination due to historical and industrial sources (Kampire *et al*., 2016; Porter *et al*., 2018; Wu *et al*., 2019). Detailed insights into PCB congener profiles reveal PCB #153 as the predominant congener, attributed to its remarkable chemical stability and resistance to metabolic degradation (Kampire *et al*., 2016; Marinsek *et al*., 2024). The present study's detection of elevated PCB levels near FB supports observations by Wu *et al*. (2019), who found that *Loligo reynaudii* d'Orbigny (chokka squid) accumulated higher PCB concentrations in this region, likely influenced by proximity to the fishing fleets of the large-scale squid fisheries and regional contamination inputs from the metropolitan region of Gqeberha. Further supporting this, Degger *et al*. (2011) demonstrated that semi-permeable membrane devices (SPMDs) deployed along the South African coast efficiently accumulated dioxin-like PCBs, whereas mussels showed limited bioaccumulation due to their metabolic capacity to degrade these toxic congeners. This suggests that while PCBs are present in the water column, their bioavailability to certain marine organisms may vary depending on species-specific metabolism. The presence of PCBs in the FB region is likely attributed to historical use in e.g. harbour activities, electrical transformers, industrial activities, and continued remobilisation from contaminated sediments, as discussed in Kampire *et al*. (2016). This highlights the necessity for long-term monitoring efforts in this area, particularly given the potential for PCB bioaccumulation in commercially important marine species such as squid and mussels. That this species of pufferfish accumulate PCBs further supports its use as a valuable bioindicator species, complementing existing monitoring efforts and enhancing our understanding of PCB distribution along the South African coastline. The findings of these studies reinforce concerns regarding the persistence of PCBs in South African coastal waters and their potential risks to marine ecosystems. In contrast, the absence of detectable PCBs in SB suggests a reduced industrial footprint, potentially influenced by oceanographic dilution or conservation measures within the MPA.

The observed spatial variability in OCP and PCB levels reflects multiple environmental and anthropogenic factors. Agricultural runoff remains a key contributor to OCP contamination, particularly in WS and MB, paralleling patterns observed in heavy metal contamination studies (Erasmus *et al*., 2020). Industrial activity and urbanisation appear to be dominant contributors to PCB contamination, especially in FB. The high standard deviation in PCB concentrations at this locality suggests localised contamination hotspots or sediment resuspension during seasonal oceanographic shifts (Liu *et al*., 2024). Moreover, the wide range of PCB congeners detected at FB compared to other localities further contributes to the variability, suggesting either diverse contamination sources or differential retention of congeners in sediments or biota. Similarly, the Benguela Current on the west coast and the Agulhas Current on the east and south coasts could facilitate the redistribution of contaminants, influencing bioaccumulation patterns in marine organisms (Liu *et al*., 2024). Firth *et al*. (2019) demonstrated that hydrodynamic conditions significantly impact pollutant accumulation in mussels, with stronger currents in the east dispersing contaminants, while slower currents in the west lead to their accumulation. These findings further support our results showing lower OCP and PCB concentrations in SB compared to southwestern localities such as WS and FB.

The ecological implications of pesticide residues are significant, particularly for aquatic ecosystems and associated biota. Chronic exposure to DDT and its metabolites has been linked to endocrine disruption in fish and wildlife, raising concerns about bioaccumulation in local food webs (Bouwman *et al*., 2008; Serdar *et al*., 2014; van den Berg *et al*., 2017; Bennett *et al*., 2021). Similarly, PCBs pose severe risks to marine ecosystems, with established links to reproductive impairments, immune suppression, and developmental defects in aquatic species (Serdar *et al*., 2014; van den Berg *et al*., 2017; Bennett *et al*., 2021). This study was not able to conclusively demonstrate that localities in MPAs would be able to protect resident nearshore fish species from OCP and PCB exposure. Reduced PCB concentrations in SB (MPA) likely reflect the absence of industrial and urban exposure routes. *Amblyrhynchote honckenii's* non-migratory behaviour (reflecting a localised habitat) indicates locality-specific exposure and demonstrates that MPAs remain vulnerable to POPs transported via long-range atmospheric and ocean current pathways. While this study did not specifically investigate the biology of *A. honckenii*, nor fine-scale environmental heterogeneity, these factors could contribute to individual variability in contaminant accumulation and warrant further investigation. Future studies incorporating these variables may help clarify sources of variability and improve the interpretation of bioaccumulation patterns. The widespread detection of OCPs across all localities, including MPAs, demonstrates the diffuse sources and persistent nature of contaminants through various transport mechanisms (Boersma *et al*., 1999). This aligns with evidence that POPs persist and migrate globally, challenging the isolation of even well-managed MPAs from transboundary contamination (Erasmus *et al*., 2020).

Elevated OCP and PCB levels in non-MPA localities, particularly FB and MB, emphasise the need for stricter contamination management strategies. Implementing buffer zones and catchment-level management could help mitigate pollutant inputs from surrounding land-use activities (Boersma *et al*., 1999).

5.5 Conclusion

This study highlights the ongoing risks posed by OCPs and PCBs in South African coastal ecosystems despite international regulatory measures. The spatial variability in contamination levels suggests contributions from both localised and long-range transport mechanisms, emphasising the need for a multifaceted approach to contamination management. The evileye blaasop, *A. honckenii*, used here as a bioindicator, demonstrated locality-specific contamination patterns, reflecting both historical and current pollutant exposures and underlining its value in monitoring marine ecosystem health and pollutant bioaccumulation. While MPAs showed some reduction in PCB concentrations compared to non-protected sites, the differences were not consistent across all compounds, and thus our hypothesis (Hypothesis 3, Chapter 1) that POP levels in *A. honckenii* would be significantly lower in MPAs than in non-protected localities was only partially supported. These findings indicate that although MPAs can help mitigate certain industrial pollutants, broader regulatory enforcement and pollution mitigation strategies beyond protected areas are essential. Future research should focus on identifying specific contamination sources, assessing long-term bioaccumulation trends, and evaluating the ecological and human health implications of these contaminants. Overall, this study highlights the complexity of POPs contamination, influenced by historical and ongoing usage, environmental transport mechanisms, and degradation dynamics. The significant spatial variability observed in pesticide residues highlights the need for locality-specific risk assessments and targeted remediation efforts. Proactive measures, including reducing pesticide inputs, enhancing environmental monitoring, and ensuring regulatory compliance, are essential to minimising the long-term ecological impact of pesticide contamination.

References

Aislabie, J.M., Richards, N.K. & Boul, H.L., 1997. Microbial degradation of DDT and its residues—a review. *New Zealand, Journal of Agricultural Research*, 40(2): 269–282.

Ali, S., Ullah, M.I., Sajjad, A., Shakeel, Q. & Hussain, A., 2021. Environmental and health effects of pesticide residues. *Sustainable Agriculture Reviews 48: Pesticide Occurrence, Analysis and Remediation vol. 2 Analysis*, pp. 311–336.

Baird, D. & Pereyra-Lago, R., 1992. Nutrient status and water quality assessment of the Marina Glades canal system, Kromme Estuary, St. Francis Bay. *Water SA*, 18(1): 37–42.

Barhoumi, B., Metian, M., Zaghden, H., Derouiche, A., Ameur, W.B., Hassine, S.B., Oberhaensli, F., Mora, J., Mourgkogiannis, N., Al-Rawabdeh, A.M. & Chouba, L., 2023. Microplastic-sorbed persistent organic pollutants in coastal Mediterranean Sea areas of Tunisia. *Environmental Science: Processes & Impacts*, 25(8): 1347–1364.

Bennett, K.A., Robinson, K.J., Armstrong, H.C., Moss, S.E., Scholl, G., Tranganida, A., Eppe, G., Thomé, J.P., Debier, C. & Hall, A.J., 2021. Predicting consequences of POP-induced disruption of blubber glucose uptake, mass gain rate and thyroid hormone levels for weaning mass in grey seal pups. *Environment International*, 152: 106506.

Berrojalbiz, N., Dachs, J., Ojeda, M.J., Valle, M.C., Castro-Jiménez, J., Wollgast, J., Ghiani, M., Hanke, G. & Zaldivar, J.M., 2011. Biogeochemical and physical controls on concentrations of polycyclic aromatic hydrocarbons in water and plankton of the Mediterranean and Black Seas. *Global Biogeochemical Cycles*, 25(4): 1–14.

Binning, K. & Baird, D., 2001. Survey of heavy metals in the sediments of the Swartkops River Estuary, Port Elizabeth South Africa. *Water SA*, 27(4): 461–466.

Boersma, P.D. & Parrish, J.K., 1999. Limiting abuse: MPAs, a limited solution. *Ecological Economics*, 31(2): 287–304.

Bouwman, H., Polder, A., Venter, B. & Skaare, J.U., 2008. Organochlorine contaminants in cormorant, darter, egret, and ibis eggs from South Africa. *Chemosphere*, 71(2): 227–241.

Breede River Estuarine Management Plan, 2016. Western Cape Estuary Management Framework and Implementation Strategy. SSI Environmental, 1st edition. Royal Haskoning D.H.V. (revised 2011, 2nd Edition, 2016).

Burke, A., Dandalo, L., Munhenga, G., Dahan-Moss, Y., Mbokazi, F., Ngxongo, S., Coetzee, M., Koekemoer, L. & Brooke, B., 2017. A new malaria vector mosquito in South Africa. *Scientific Reports*, 7(1): 43779.

Cao, X., Huo, S., Zhang, H., Zhao, X., Guo, W., He, Z., Ma, C., Zheng, J. & Song, S., 2022. Polycyclic aromatic hydrocarbons in China: will decoupling of their emissions and socioeconomic growth emerge? *Earth's Future*, 10(1): e2021EF002360.

Colt, J.S., Davis, S., Severson, R.K., Lynch, C.F., Cozen, W., Camann, D., Engels, E.A., Blair, A. & Hartge, P., 2006. Residential insecticide use and risk of non-Hodgkin's lymphoma. *Cancer Epidemiology Biomarkers & Prevention*, 15(2): 251–257.

D'Agostino, F., Bellante, A., Quinci, E., Gherardi, S., Placenti, F., Sabatino, N., Buffa, G., Avellone, G., Di Stefano, V. & Del Core, M., 2020. Persistent and emerging organic pollutants in the marine coastal environment of the Gulf of Milazzo (Southern Italy): human health risk assessment. *Frontiers in Environmental Science*, 8: 117.

Degger, N., Wepener, V., Richardson, B.J. & Wu, R.S.S., 2011. Application of artificial mussels (AMs) under South African marine conditions: A validation study. *Marine Pollution Bulletin*, 63(5–12): 108–118.

Doğdu, S.A., Çiftçi, N., Ayas, D. & Turan, C., 2021. Potential usage of pufferfish dentin as a metal accumulation indicator. *Journal of Water Chemistry and Technology*, 43: 269–275.

Erasmus, A., Ikenaka, Y., Nakayama, S.M., Ishizuka, M., Smit, N.J. & Wepener, V., 2020. Trophic transfer of pollutants within two intertidal rocky shore ecosystems in different biogeographic regions of South Africa. *Marine Pollution Bulletin*, 157: 111309.

Erasmus, C.P., Rossouw, G. & Baird, D., 2004. The concentration of ten heavy metals in the tissues of shark species *Squalus megalops* and *Mustelus* (Chondrichthyes) occurring along the south eastern coast of South Africa. In: *Population*, English edition. University of Port Elizabeth.

Farrington, J.W., Tripp, B.W., Tanabe, S., Subramanian, A., Sericano, J.L., Wade, T.L. & Knap, A.H., 2016. Edward D. Goldberg's proposal of "the Mussel Watch": reflections after 40 years. *Marine Pollution Bulletin*, 110(1): 501–510.

Firth, D.C., Auerswald, L., Strydom, P.E. & Hoffman, L.C., 2023. The status of marine mussel pollution research in South Africa (2012–2022). *Foods*, 12(21): 3983.

Firth, D.C., O'Neill, B., Salie, K. & Hoffman, L.C., 2019. Monitoring of organic pollutants in *Choromytilus meridionalis* and *Mytilus galloprovincialis* from aquaculture facilities in Saldanha Bay, South Africa. *Marine Pollution Bulletin*, 149: 110637.

Froese, R. & Pauly, D., 2023. *FishBase*. Available at: www.fishbase.org/search.php. (Date of access: 8 May 2025).

Gakuba, E., Moodley, B., Ndungu, P. & Birungi, G., 2019. Evaluation of persistent OCPs and PCBs in Umgeni River bank soil, KwaZulu-Natal, South Africa. *Water SA*, 45(4): 592–607.

Girones, L., Oliva, A.L., Marcovecchio, J.E. & Arias, A.H., 2020. Spatial distribution and ecological risk assessment of residual OCPs in South American marine environments. *Current Environmental Health Reports*, 7: 147–160.

Jones, K.C. & De Voogt, P., 1999. Persistent organic pollutants (POPs): state of the science. *Environmental Pollution*, 100(1–3): 209–221.

Kampire, E., Rubidge, G., Adams, J.B. & Human, L., 2016. Congener profiles of PCBs and the effect on marine mussels at an outfall site, Port Elizabeth, South Africa. *Water SA*, 42(3): 496–504.

Kosker, A.R., Ozogul, F., Ayas, D., Durmus, M. & Ucar, Y., 2019. Elemental composition of pufferfish species from Northeastern Mediterranean Sea. *Environmental Monitoring and Assessment*, 191: 1–15.

Kushner, E.J., 1976. On determining the statistical parameters for pollution concentration from a truncated data set. *Atmospheric Environment (1967)*, 10(11): 975–979.

Labuschagne, M., Wepener, V., Nachev, M., Zimmermann, S., Sures, B. & Smit, N.J., 2019. The application of artificial mussels in conjunction with transplanted bivalves to assess elemental exposure in a platinum mining area. *Water*, 12(1): 32.

León, V.M., Moreno-González, R., González, E., Martínez, F. & García, V., 2013. Interspecific comparison of polycyclic aromatic hydrocarbons and persistent organochlorines bioaccumulation in bivalves from a Mediterranean coastal lagoon. *Science of the Total Environment*, 463: 975–987.

Li, Y.F. & Macdonald, R.W., 2005. Sources and pathways of selected OCPs to the Arctic and the effect of pathway divergence on HCH trends in biota: a review. *Science of the Total Environment*, 342(1–3): 87–106.

Liu, H., Hu, J., Tan, Y., Zheng, Z., Liu, M., Lohmann, R., Vojta, S., Katz, S., Liu, Y., Li, Z. & Fang, Z., 2024. Identification of key anthropogenic and land use factors and ecological risk assessment of dissolved polycyclic aromatic hydrocarbons (PAHs) and OCPs in an urbanized estuary in China. *Marine Pollution Bulletin*, 207: 116876.

Marinsek, G.P., Ribeiro, C.C., Gusso-Choueri, P.K., Choueri, R.B., de Souza Abessa, D.M. & de Britto Mari, R., 2024. Multiple biomarkers in pufferfish as a proxy of environmental health in Brazilian MPAs. *Science of the Total Environment*, 914: 169742.

Olisah, C., Adams, J.B. & Rubidge, G., 2021. The state of persistent organic pollutants in South African estuaries: A review of environmental exposure and sources. *Ecotoxicology and Environmental Safety*, 219: 112316.

Pech, D., Vidal-Martínez, V.M., Aguirre-Macedo, M.L., Gold-Bouchot, G., Herrera-Silveira, J., Zapata-Pérez, O. & Marcogliese, D.J., 2009. The checkered puffer (*Spheroides testudineus*) and its helminths as bioindicators of chemical pollution in Yucatan coastal lagoons. *Science of the Total Environment*, 407(7): 2315–2324.

Phillips, D.J. & Rainbow, P.S., 1994. *Biomonitoring of Trace Aquatic Contaminants (Vol. 37).* Springer Science & Business Media.

Porter, S.N., Humphries, M.S., Buah-Kwofie, A. & Schleyer, M.H., 2018. Accumulation of OCPs in reef organisms from marginal coral reefs in South Africa and links with coastal groundwater. *Marine Pollution Bulletin*, 137: 295–305.

Ramírez-Ayala, E., Arguello-Pérez, M.A., Tintos-Gómez, A., Hernández-Anguiano, J.H., Pérez-Rodríguez, R.Y., Ilizaliturri-Hernández, C.A., Núñez-Nogueira, G. & Sepúlveda-Quiroz, C.A., 2021. Persistent organic pollutants (POPs) in fish from two coastal lagoons of the central Mexican Pacific. *Latin American Journal of Aquatic Research*, 49(4): 663–670.

Ryan, P.G., Bouwman, H., Moloney, C.L., Yuyama, M. & Takada, H., 2012. Long-term decreases in persistent organic pollutants in South African coastal waters detected from beached polyethylene pellets. *Marine Pollution Bulletin*, 64(12): 2756–2760.

Saadati, N., Abdullah, M.P., Zakaria, Z., Sany, S.B.T., Rezayi, M. & Hassonizadeh, H., 2013. Limit of detection and limit of quantification development procedures for OCPs analysis in water and sediment matrices. *Chemistry Central Journal*, 7: 1–10.

Sazima, I., 2024. A pufferfish that scavenges on aquatic and terrestrial invertebrate and vertebrate carcasses. *Ichthyological Research*, pp. 1–5. DOI:10.1007/s10228-024-00982-0.

Serdar, B., LeBlanc, W.G., Norris, J.M. & Dickinson, L.M., 2014. Potential effects of PCBs and selected OCPs on immune cells and blood biochemistry measures: a cross-sectional assessment of the NHANES 2003-2004 data. *Environmental Health*, 13: 1–12.

Stockholm Convention on Persistent Organic Pollutants, Convention Text, 2001. United Nations Environment Programme, Geneva. http://www.pops.int/documents/convtext/convtext_en.pdf.

Thompson, L.A., Darwish, W.S., Ikenaka, Y., Nakayama, S.M., Mizukawa, H. & Ishizuka, M., 2017. Organochlorine pesticide contamination of foods in Africa: incidence and public health significance. *Journal of Veterinary Medical Science*, 79(4): 751–764.

Tolera, S.T., 2021. Adverse effect of pesticide on top ten importers of African countries: systematic review. *EC Pharmacology and Toxicology*, 9: 61–79.

UNESCO, 1999. *World Communication and Information 1999–2000 Report.* Published by United Nations Educational, Scientific and Cultural Organization.

Van den Berg, H., Manuweera, G. & Konradsen, F., 2017. Global trends in the production and use of DDT for control of malaria and other vector-borne diseases. *Malaria Journal*, 16: 1–8.

Van Der Spuy, L., Erasmus, J.H., Nachev, M., Schaeffner, B.C., Sures, B., Wepener, V. & Smit, N.J., 2023. The use of fish parasitic isopods as element accumulation indicators in marine pollution monitoring. *Marine Pollution Bulletin*, 194: 115385.

Venkatesan, M.I., De Leon, R.P., Van Geen, A. & Luoma, S.N., 1999. Chlorinated hydrocarbon pesticides and PCBs in sediment cores from San Francisco Bay. *Marine Chemistry*, 64(1–2): 85–97.

Vogt, T., Pieters, R., Giesy, J. & Newman, B.K., 2019. Biological toxicity estimates show involvement of a wider range of toxic compounds in sediments from Durban, South Africa than indicated from instrumental analyses. *Marine Pollution Bulletin*, 138: 49–57.

Wang, T., Wei, X., Chen, T., Wang, W., Xia, X., Miao, J. & Yin, S., 2019. Studies of the mechanism of fatty liver formation in *Takifugu fasciatus* following copper exposure. *Ecotoxicology and Environmental Safety*, 181: 353–361.

Wepener, V. & Degger, N., 2012. Status of marine pollution research in South Africa (1960–present). *Marine Pollution Bulletin*, 64(7): 1508–1512.

Wepener, V. & Degger, N., 2019. South Africa. In: Sheppard, C. (2nd eds), *World Seas: An Environmental Evaluation, Volume II: The Indian Ocean to the Pacific.* London: Elsevier, pp. 101–119.

Wepener, V.W. & Degger, N.D., 2020. Monitoring metals in South African harbours between 2008 and 2009, using resident mussels as indicator organisms. *African Zoology*, 55(4): 267–277.

WHO, 2011. *The Use of DDT in Malaria Vector Control: WHO Position Statement on DDT*. Available at: http://whqlibdoc.who.int/hq/2011/WHO_HTM_GMP_2011_eng.pdf. (Date of access: 8 May 2025).

Wu, J., Kauhanen, P.G., Hunt, J.A., Senn, D.B., Hale, T. & McKee, L.J., 2019. Optimal selection and placement of green infrastructure in urban watersheds for PCB control. *Journal of Sustainable Water in the Built Environment*, 5(2): 04018019.

Yu, H.Y., Bao, L.J., Liang, Y. & Zeng, E.Y., 2011. Field validation of anaerobic degradation pathways for dichlorodiphenyltrichloroethane (DDT) and 13 metabolites in marine sediment cores from China. *Environmental Science & Technology*, 45(12): 5245–5252.

Yuqi, L., Liya, W. & Ningping, T., 2014. Analysis and evaluation of nutritional composition of farmed male pufferfish (*Takifugu obscurus*). In *SHS Web of Conferences* (Vol. 6, p. 03010). EDP Sciences.

6

Metazoan parasite diversity of the evileye blaasop *Amblyrhynchote honckenii* (Bloch): factors influencing parasite community composition.

6.1 Introduction

Parasites, though frequently overlooked, are critical components of marine ecosystems. They serve as both indicators of ecological health and important regulators of marine food web structure and function (Marcogliese, 2005). The diversity and composition of parasite communities in marine environments are shaped by a dynamic interplay of host biology and a wide range of environmental conditions, including anthropogenic stressors (Marcogliese, 2016; Sures *et al*., 2023). Along South Africa's diverse coastline, spatial scales in temperature and anthropogenic stressors lead to pronounced variation in these communities (Erasmus *et al*., 2022), making it essential to consider such gradients to understand regional patterns and their broader ecological significance.

Marine parasite communities are particularly sensitive to a variety of environmental stressors, including organic pollutants, metals, temperature fluctuations, and habitat alteration resulting from fisheries and coastal development (Lafferty and Kuris, 1999; Grabner *et al*., 2023; Sures *et al*., 2023). Chronic exposure to organic contaminants such as OCPs and PCBs can disrupt host immune responses (Serdar *et al*., 2014; Thompson *et al*., 2017), modify susceptibility to infection, and sometimes impact the free-living, larval, or developmental stages of parasite lifecycles (Molbert, 2020; Grabner *et al*., 2023). However, these impacts are not uniform; for example, parasites with complex heteroxenous life cycles that require multiple host species and transmission steps, tend to be more vulnerable to habitat fragmentation and biodiversity loss, as they depend on the health and presence of several hosts and intact food webs (Lafferty, 2012; Marcogliese, 2023). In contrast, directly transmitted parasites or those with simple, monoxenous

life cycles may dominate stressed environments, reflecting the simplification or degradation of ecological interactions (Cable *et al*., 2017; Poulin *et al*., 2024).

Temperature stands out as a key abiotic driver of both host and parasite physiology, influencing rates of parasite development, reproduction, and transmission success (Poulin *et al*., 2024). The South African coastline is marked by a striking gradient from the cooler, temperate waters of the Agulhas Bank to the warmer, subtropical and tropical waters of the Natal Ecoregion (Spalding *et al*., 2007). These temperature gradients not only delineate marked changes in host assemblages but also shape parasite communities, with some species favouring the higher temperatures of the Natal region and others restricted to the cooler waters of the Agulhas Bank (Nunkoo, 2019; Mackintosh, 2019; Pfingst *et al*., 2021). This biogeographic transition affects both the composition and richness of parasite taxa, as well as the dynamics of host-parasite interactions, with higher temperatures generally promoting faster parasite development (Cable *et al*., 2017; Poulin *et al*., 2024). In addition, regional differences in oceanographic features, such as current regimes, nutrient upwelling, and productivity, further shape the food web structure and pollution exposure, thereby indirectly influencing parasite assemblages (Marcogliese, 2002).

The establishment of MPAs along the coast is a growing strategy for conserving marine biodiversity and fostering ecosystem resilience (Davies, 2021), and these interventions carry distinct implications for parasite communities (Wood *et al*., 2013). By restricting extractive activities and safeguarding habitat complexity, MPAs help sustain or restore robust host assemblages and the trophic interactions upon which many complex parasites depend (Wood *et al*., 2013). In this way, parasite diversity can actually increase inside MPAs, highlighting the importance of intact food webs and niche diversity (Wood *et al*., 2013; Wood *et al*., 2018). Furthermore, parasites, especially those with complex, multi-host life cycles, are useful indicators of ecosystem health and restoration success within protected areas (Marcogliese, 2023). However, MPAs can also have unintended consequences. In certain cases, MPAs cannot always buffer against pollutants delivered by ocean currents from outside their boundaries, a factor that may continue to stress both host and parasite populations (Boersma and Parrish, 1999; Carr *et al*., 2017).

Understanding the interconnected impacts of environmental stressors, temperature gradients, and management interventions such as MPAs is therefore crucial for effective conservation in coastal South Africa. By integrating parasitological data with biogeographic, ecological, and conservation contexts, we are better positioned to interpret spatial and temporal patterns across the Agulhas Bank and Natal Ecoregions. Monitoring parasite communities offers valuable insight into ecosystem structure, function, and resilience. Such knowledge is critical for

informing future expansions of MPAs, targeting pollution mitigation, and incorporating parasite data into biodiversity assessments, ultimately supporting more robust and holistic ecosystem management strategies.

This chapter aims to examine how parasite diversity and community structure in the evileye blaasop, *A. honckenii*, vary along the South African coast. The focus is on understanding the spatial patterns that emerge due to differences in regional climate and habitat, gradients of environmental contamination, and the presence or absence of MPAs. By using a combination of parasitological, ecological, and contamination data from localities with different protection status and environmental conditions, this chapter seeks to reveal the primary factors shaping parasite assemblages in this ecologically significant host species. It is hypothesised that parasite diversity will follow distinct spatial patterns, with the highest richness and complexity occurring in subtropical regions, particularly within the Natal ecoregion, and a gradual decline toward temperate and cold-temperate regions such as the Agulhas Bank (Hypothesis 4, Chapter 1). These patterns are anticipated to reflect underlying biogeographic and climatic gradients. Furthermore, it is expected that elevated levels of organic pollutants, as indicated by OCP and PCB burdens in *A. honkenii*, will be associated with reduced parasite richness and evenness and with communities dominated by directly transmitted or opportunistic taxa (Hypothesis 5, Chapter 1). In contrast, more pristine and ecologically intact localities, especially those within or near-MPAs, are predicted to support richer and more complex parasite communities, including heteroxenous species dependent on intact food web structures (Hypothesis 5, Chapter 1). Consequently, MPAs, through their higher ecological integrity and habitat quality, are expected to support more diverse and evenly structured parasite assemblages compared to unprotected areas. These findings will help clarify how biogeography, contaminant exposure, and conservation measures interact to shape parasite biodiversity along the South African coastline.

6.2 Materials and methods

6.2.1 Sampling

Site selection and fish sampling followed protocols already described in Chapter 2, while parasite collection and identification are described in Chapter 3 and tissue sampling and pesticide analyses are described in Chapter 5. Table 6.1 summarises the regional considerations associated with each locality sampled according to Chapter 2.

Table 6.1: Summary of environmental and host characteristics of sampling surveys.

Locality	Coordinates	Ecoregion	Protection status	No. fish (n)
Witsand (WS)	-34.40° S, 20.84° E	Agulhas bank	Near-MPA	15
Mossel Bay (MB)	-34.18° S, 22.15° E	Agulhas bank	Non-MPA	10
Chintsa East (CE)	-32.84° S, 28.12° E	Natal	Near-MPA	10
Uvongo Beach (UB)	-30.84° S, 30.40° E	Natal	Non-MPA	10
Sodwana Bay (SB)	-27.54° S, 32.68° E	Natal	MPA	10

6.2.2 Statistical analyses

To characterise parasite population and community structure in *A. honckenii*, various ecological descriptors were applied following standardised protocols outlined by Bush *et al*. (1997). This included prevalence, mean intensity, and mean abundance. These measures were previously calculated and presented in Chapter 3.

Parasite assemblages were analysed at two hierarchical levels: the infra-community level, representing all parasite taxa found within an individual host, and the component community level, which encompassed all parasite taxa recorded in the host population at a specific locality and time point. Diversity metrics for infra-communities were calculated using PRIMER v7 and included species richness (mean number of parasite taxa per fish), total abundance (mean number of individual parasites per fish), and Brillouin's diversity index (Bush *et al*, 1997; Poulin, 2015). At the component community level, overall diversity was assessed using Pielou's evenness index (J′), Shannon-Wiener index (H′), and Simpson's index, which together provided insight into both taxon richness and dominance patterns across localities (Poulin, 2015). All data were tested for normality using the Shapiro-Wilk test in GraphPad Prism v9.0.0. For data that were normally distributed, a one-way ANOVA was conducted, followed by Tukey's multiple comparison test to detect statistically significant differences among localities. Where data did not conform to normality assumptions, the Kruskal-Wallis test was applied, followed by Dunn's post-hoc test. Statistical significance was accepted at a threshold of $p<0.05$. Diversity indices were calculated per locality, while grouped comparisons based on protection status (i.e., MPA, near-MPA, and non-MPA).

To evaluate spatial patterns in parasite community composition and identify key environmental and biological drivers, multivariate statistical analyses were conducted. Explanatory environmental variables considered were OCP and PCB concentrations in liver tissue of *A. honkenii* (Chapter 5), as well as host condition factor (CF) and hepatosomatic index (HSI). Bray-Curtis similarity coefficients were calculated from log-transformed abundance data to assess both infra-community and component community similarities among localities.

To determine which parasite taxa contributed most to within- and between-site similarities, a SIMPER (Similarity Percentage) analysis was conducted using Bray-Curtis resemblance matrices with a 90% cut-off for low-contribution species. Differences in parasite assemblages between localities were statistically tested using an ANOSIM (Analysis of Similarities), also based on Bray-Curtis similarity matrices. For visual representation of community structure, a non-metric multidimensional scaling (nMDS) ordination was performed and rotated via Principal Components Analysis (PCA) in Canoco v5.12. Additionally, a redundancy analysis (RDA) was conducted in Canoco v5.12 to determine how much variation in parasite taxon composition could be explained by the explanatory variables. The RDA included interactive forward selection and Monte Carlo permutation tests to identify the most influential variables, accounting for up to 90% of the explained variation. Prior to analysis, all abundance and environmental data were log-transformed, then centred and standardised.

Finally, a species accumulation curve was constructed using iNEXTOnline (Chao *et al*., 2016) to assess the relationship between sampling effort and observed parasite richness. The curve was generated both per protection status (near-MPA, non-MPA and MPA localities) and for the entire sampled population, with 95% confidence intervals applied to estimate sampling completeness and richness asymptotes. All statistical analyses were conducted using a significance threshold of $p<0.05$.

6.3 Results

6.3.1 Parasite diversity

A total of 22 metazoan parasite taxa, representing four phyla and eight classes, were identified from *A. honckenii* collected at the five coastal localities across South Africa. These included acanthocephalans (n=2), isopods (n=1), copepods (n=3), nematodes (n=5), cestodes (n=4), monopisthocotyleans (n=1), polyopisthocotyleans (n=1) and trematodes (n=5) (see Chapter 3, Table 3.3).

6.3.2 Infra-community composition

Infra-community descriptors (Figure 6.1) show significant spatial variation in parasite community metrics across the five sampling localities. Parasite species richness (Figure 6.1A) was highest in WS and CE (near-MPA), with lower values in MB and UB (non-MPA). Sodwana Bay (MPA) exhibited more median species richness. Parasite abundance (Figure 6.1B) followed a reversed pattern, being significantly higher in MB compared to all other localities, followed by UB. The lowest parasite abundances were at WS and CE, while SB again showed a median parasite abundance between that of the near-MPA and non-MPA localities. Brillouin's diversity index (Figure 6.1D), which integrates both richness and abundance, was significantly higher in

WS and CE, significantly lower in MB and UB and intermediate in SB. Component community-level indices also varied significantly. Pielou's evenness (Figure 6.1C) was more uniform across localities with similar protection status (near-MPA, non-MPA and MPA). Witsand and CE localities have significantly higher values closer to 1, suggesting a more even distribution of individuals among parasite taxa at those localities. Mossel Bay and UB localities had significantly lower values, while the MPA locality, SB, again was in the middle. Shannon-Wiener diversity (Figure 6.1E) and Simpsons diversity (Figure 6.1F) was significantly higher at near-MPA localities than the MPA and non-MPA localities. Diversity was highest at CE, followed by WS and SB, while MB and UB had the lowest diversity.

Table 6.2: Grouped parasite diversity indices for localities with the same protection statuses (near-MPA, non-MPA and MPA). Diversity is given as the mean followed by the standard deviation.

Diversity index	Near-MPA	Non-MPA	MPA
Species richness	4.12 ± 1.54	2.75 ± 0.85	2.50 ± 1.35
Abundance	14.68 ± 7.56	147.90 ± 122.61	56.90 ± 66.14
Pielou's evenness	0.79 ± 0.17	0.25 ± 0.23	0.54 ± 0.31
Brilouin's diversity	0.78 ± 0.28	0.19 ± 0.17	0.38 ± 0.27
Shannon-Wiener diversity	1.05 ± 0.37	0.23 ± 0.22	0.43 ± 0.36
Simpson's diversity	0.61 ± 0.19	0.12 ± 0.15	0.31 ± 0.26

The proportional abundance of parasite taxa varied noticeably across the three protection status locations, with near-MPA localities exhibiting the broadest diversity of taxa. Parasites such as *E. arenalbus* (100%), *A. simplex* (100%), *Nybelinia* sp. (100%), *O. amplicoelus* (100%), and *Raphidascaris* sp. (100%) were found exclusively in near-MPA fish (Figure 6.2). Additionally, taxa like *Cal. tetrodontis* (45.5%), *Cin. tetrodontis* (47.1%), and Zoogonidae gen. sp. (26.6%) also occurred in moderate abundances in near-MPA areas. Other species, including *E. chintensis*, *D. szidati*, and *K. pronosoma* appeared in both near-MPA and non-MPA localities, though with greater representation in the former. Near-MPAs thus harboured a wide range of both monoxenous and heteroxenous parasites. The dominance of heteroxenous parasites characterised non-MPA localities, particularly the trematodes Bucephalidae gen. sp. (98.4%) and *Rhipidocotyle* sp. (96.9%), which together formed the majority of infections at these localities.

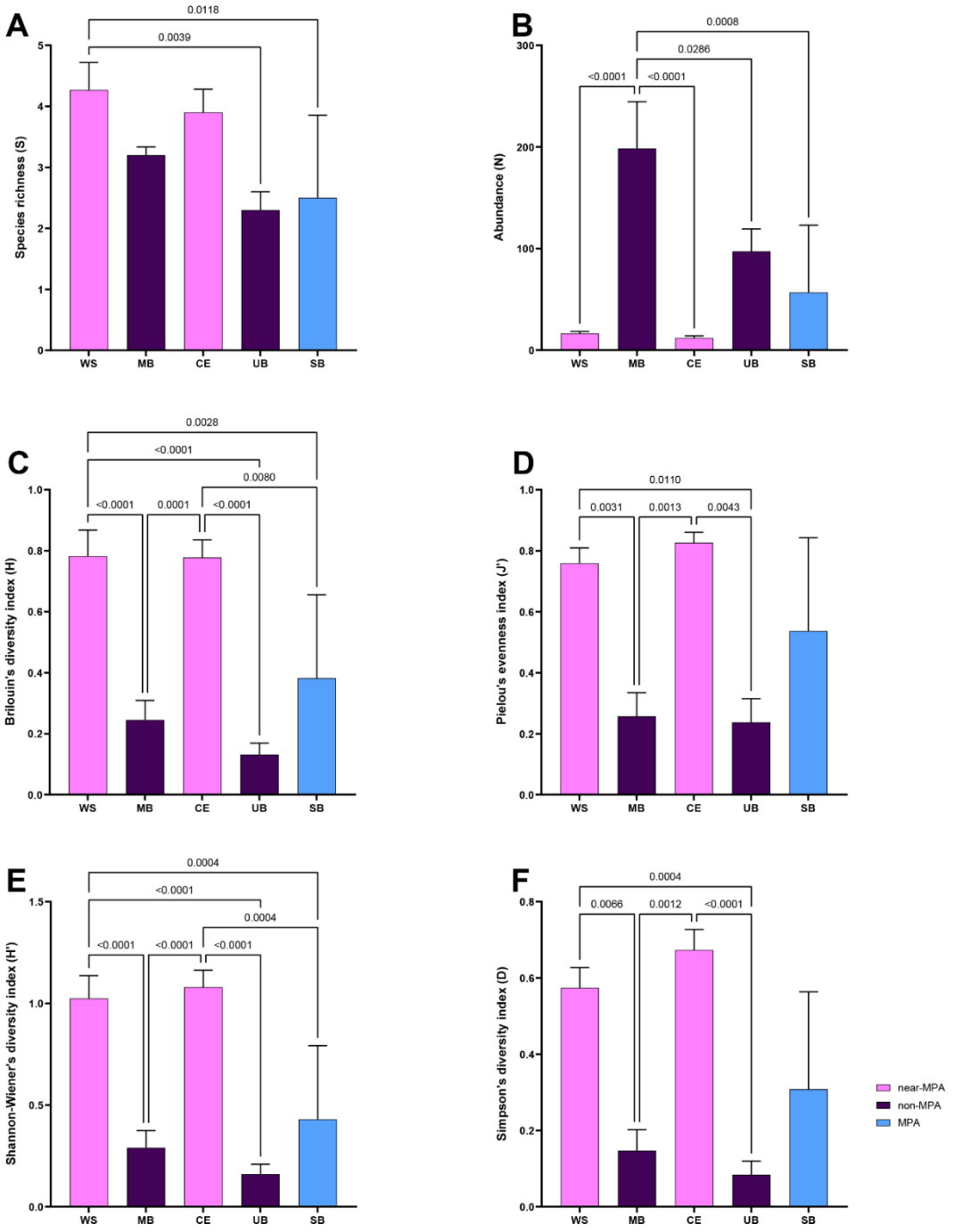

Figure 6.1: Parasite infra-community of *Amblyrhynchote honckenii* (Bloch) sampled along the South African coastline. **A** – Species richness; **B** – Abundance; **C** – Pielou's evenness index; **D** – Brillouin's diversity index; **E** – Shannon-Wiener index; **F** – Simpson's diversity index. Significant differences (p-values) between locations are presented on the bars. Abbreviations: **WS** – Witsand; **MB** – Mossel Bay; **CE** – Chintsa East; **UB** – Uvongo Beach; **SB** – Sodwana Bay.

Udonella australis, *Acanthobothrium* sp., and *Dichelyne* sp. were also exclusive (100%) to non-MPA fish. Copepod taxa such as *Cal. tetrodontis* (54.6%) and *Cin. tetrodontis* (52.9%) were proportionally more abundant in non-MPAs compared to near-MPAs. Some taxa shared between localities, such as *H. victorwepeneri* and *K. pronosoma*, had a higher representation in

non-MPA fish. In contrast, the parasite community in MPA fish was compositionally restricted and dominated by a few taxa. *Scyphophyllidium* sp. accounted for the majority of infections (95.7%), followed by *Zoogonidae* gen. sp. (72.9%). *Rhadinorhynchus gerberi* (100%), Physalopteridae gen. sp. (100%), and *Helicometrina* sp. (100%) were exclusive to SB. Bucephalidae gen. sp. was present but in low proportion (1.5%). Most other taxa were absent from the MPA fish.

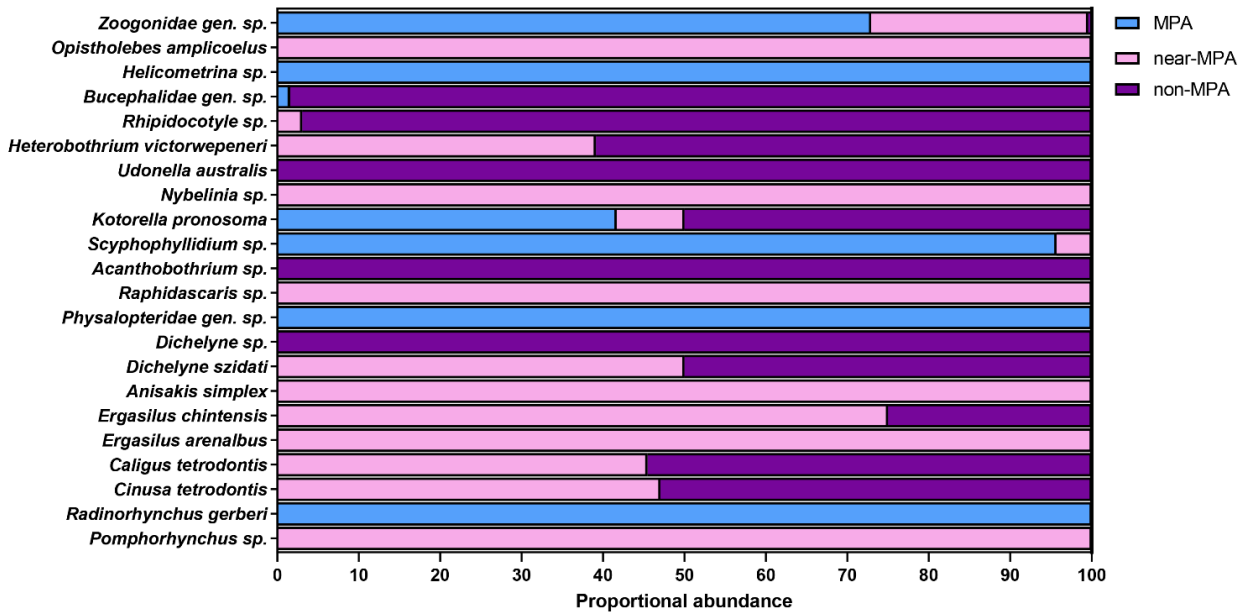

Figure 6.2: Proportional abundance of parasite taxa infecting *Amblyrhynchote honckenii* (Bloch) in near-MPA, non-MPA and MPA localities, along the South African coastline.

6.3.3 Component community composition

Based on the SIMPER analysis, parasite community composition within and between the five sampled localities showed clear patterns of within-site similarity and between-site dissimilarity, driven by a small number of key parasite taxa (Table 6.3). At MB, the within-group similarity was the highest at 81.59%, with the parasite Bucephalidae gen. sp. contributing the most to this similarity (65.61%), followed by *Cal. tetrodontis* (19.37%) and *Cin. tetrodontis* (15.02%). Similarly, UB had a relatively high within-group similarity of 61.64%, primarily structured by *Rhipidocotyle* sp. (85.24%) and *H. victorwepeneri* (13.79%). Chintsa East showed a moderate average similarity of 51.28%, dominated by Zoogonidae gen. sp. (60.67%) and *O. amplicoelus* (25.95%). WS had a slightly lower similarity of 46.52%, with *E. arenalbus* (47.69%), *Cal. tetrodontis* (20.82%), and *Cin. tetrodontis* (10.58%) as main contributors. SB had the lowest within-group similarity at 40.21%, primarily structured by Bucephalidae gen. sp. (52.44%) and *Scyphophyllidium* sp. (37.87%).

Table 6.3: Similarity results from the SIMPER analysis showing the mean similarity for each locality, as well as the mean abundance (MA), mean similarity ± SD, contribution (%) and cumulative contribution (%) for the most abundant taxa per locality.

Taxa per locality	MA	Mean similarity	Contribution (%)	Cumulative (%)
Witsand			**Mean similarity = 46.52%**	
E. arenalbus	1.82	22.18 ± 1.33	47.69	47.69
Cal. tetrodontis	0.85	9.68 ± 0.86	20.82	68.51
Cin. tetrodontis	0.59	4.92 ± 0.59	10.58	79.09
Rhipidocotyle sp.	0.59	3.74 ± 0.59	8.04	87.13
Nybelinia sp.	0.37	1.75 ± 0.32	3.77	90.90
Mossel Bay			**Mean similarity = 81.59%**	
Bucephalidae gen. sp.	4.77	53.53 ± 4.56	65.61	65.61
Cal. tetrodontis	1.43	15.81 ± 3.98	19.37	84.98
Cin. tetrodontis	0.99	12.25 ± 1.86	15.02	91.56
Chintsa East			**Mean similarity = 51.28%**	
Zoogonidae gen. sp.	1.77	31.11 ± 3.53	60.67	60.67
O. amplicoelus	0.79	13.31 ± 1.79	25.95	86.62
Rhipidocotyle sp.	0.51	2.53 ± 0.35	4.94	91.56
Uvongo Beach			**Mean similarity = 61.64%**	
Rhipidocotyle sp.	2.49	52.55 ± 3.02	85.24	85.24
H. victorwepeneri	0.70	8.50 ± 0.88	13.79	99.03
Sodwana Bay			**Mean similarity = 40.21%**	
Bucephalidae gen. sp.	1.32	21.08 ± 1.23	52.44	52.44
Scyphophyllidium sp.	2.24	15.23 ± 0.77	37.87	90.30

Between-location dissimilarities were also substantial (Table 6.4). For example, the highest dissimilarity was observed between MB and UB (100%), driven by Bucephalidae gen. sp. and *Rhipidocotyle* sp., which were each abundant at only one of the two localities. Comparatively, dissimilarity between WS and CE was 87.77%, mainly due to differences in the abundance of *E. arenalbus* and Zoogonidae gen. sp. Other prominent taxa driving dissimilarity across pairs included *Cal. tetrodontis*, *Scyphophyllidium* sp., *Cin. tetrodontis* and *O. amplicoelus*, depending on locality pairing.

Table 6.4: Results from the SIMPER analysis, indicating the average dissimilarity between localities. Abbreviations: **WS** – Witsand; **MB** – Mossel Bay; **CE** – Chintsa East; **UB** – Uvongo Beach; **SB** – Sodwana Bay.

	WS	MB	CE	UB	SB
WS					
MB	79.51				
CE	87.77	94.17			
UB	86.10	100.00	83.90		
SB	96.29	77.41	94.12	99.42	

The ANOSIM results confirmed statistically significant differences in parasite community composition across the five sampling localities (Table 6.5). The overall global R-value was 0.8369, indicating strong separation between groups. Pairwise comparisons between localities showed very high R-values, all close to or exceeding 0.89, with most reaching or surpassing 0.90, supporting a clear structuring of parasite assemblages by locality. Similar to the SIMPER analysis, the strongest dissimilarity was observed between MB and CE or MB and UB (both with an R = 1). Further, SB and CE (R = 0.96) showed the strongest dissimilarity, followed closely by SB and UB (R = 0.93), and SB and MB (R = 0.92). All comparisons showed R values above 0.75, suggesting that each region hosts a significantly distinct parasite community with minimal overlap.

Table 6.5: Results from the ANOSIM analysis indicating the R-statistic matrix for each locality. Abbreviations: **WS** – Witsand; **MB** – Mossel Bay; **CE** – Chintsa East; **UB** – Uvongo Beach; **SB** – Sodwana Bay.

	WS	MB	CE	UB	SB
WS					
MB	0.84				
CE	0.90	1			
UB	0.89	1	0.90		
SB	0.93	0.79	0.92	0.96	

The nMDS ordination had a stress value of 0.11, indicating that the two-dimensional configuration reliably represents the underlying Bray-Curtis dissimilarities, with minimal distortion. Clear spatial structuring of parasite communities was observed across the five sampling localities, with most separation occurring along the first two axes (Figure 6.3). Axis 1, which accounted for the largest proportion of the variation (63.64%), primarily captured dissimilarities between UB, MB, and CE, as well as SB. A looser clustering was observed between WS and CE near the centre of the plot, with WS extending toward the negative end of Axis 2. This placement reflects its unique community structure dominated by *E. arenalbus* and *Nybelinia* sp. In contrast, SB was positioned at the far positive end of Axis 1, characterised by a distinct assemblage dominated by

Scyphophyllidium sp. and *R. gerberi*, and marked by the absence of many parasite taxa present at other localities. Axis 2, which explained an additional 22.90% of the variation, further distinguished UB from CE, and MB from SB. Mossel Bay formed a tightly packed cluster, whereas the other localities showed more diffuse spatial arrangements. Uvongo Beach was loosely clustered but positioned closer to WS and CE, reflecting moderate overlap in community structure and influenced by taxa such as *Rhipidocotyle sp.* and *H. victorwepeneri*. In contrast, MB was distinctly separated and positioned between SB and WS, with no overlap. The convergence of CE and WS in the central region of the ordination suggests intermediate community similarity between these localities.

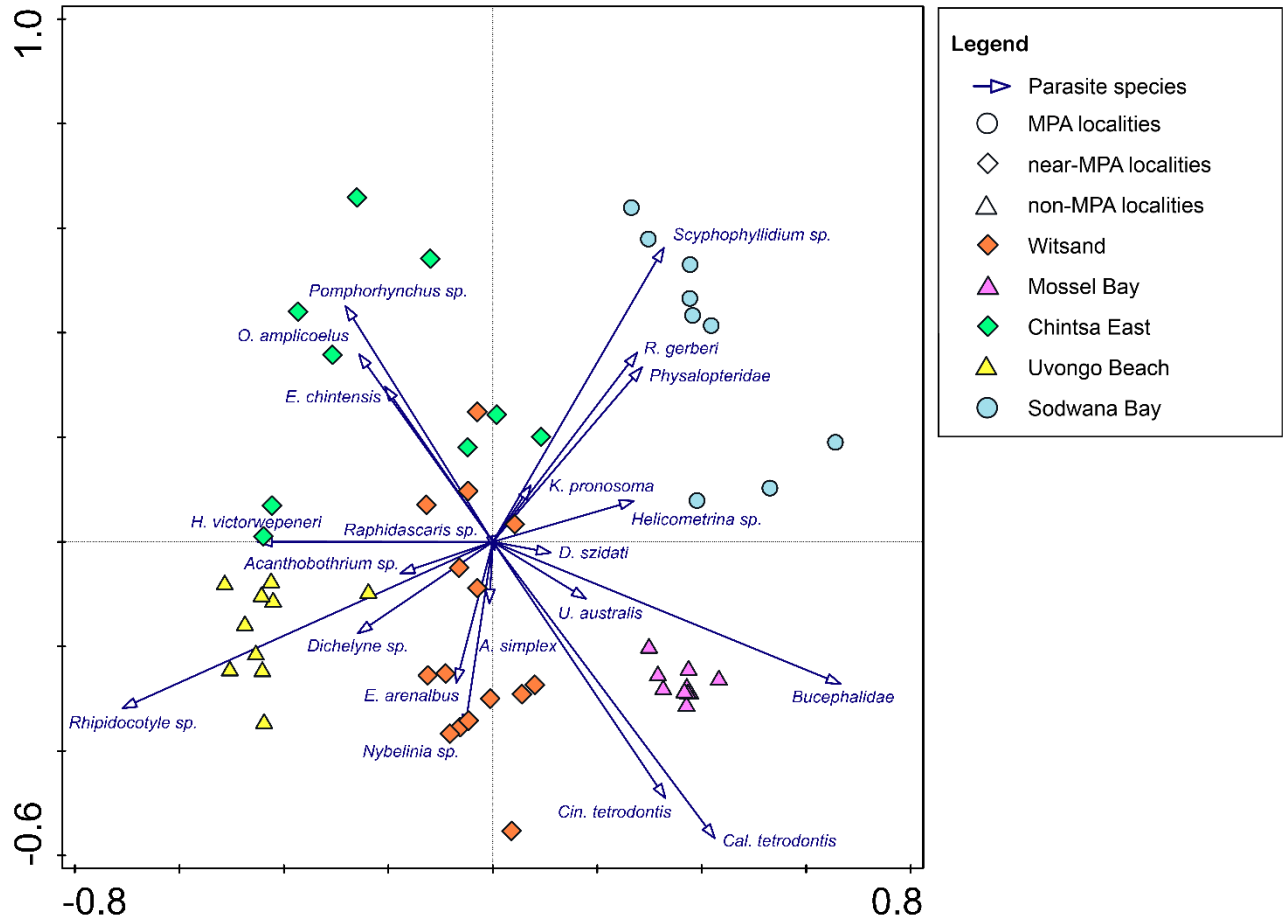

Figure 6.3: Ordination plot (nMDS) based on parasite infra-community diversity and abundance in *Amblyrhynchote honckenii* (Bloch) sampled along the coastline of South Africa. The two axes display 86.5% of the total variation with a stress value of 0.11.

6.3.4 Factors contributing to community composition

The distance-based redundancy analysis (db-RDA) (Figure 6.4) revealed that the explanatory variables collectively accounted for 45.3% of the total variation in parasite community composition, with an adjusted explained variation of 29.3%. Axis 1 explained 21.89% of the total variation and 48.34% of the fitted variation, while Axis 2 contributed an additional 11.94% to the

total and 26.35% to the fitted variation, resulting in a cumulative explained variation of 33.83% and 74.69% by the first two axes. The first two axes also exhibited strong pseudo-canonical correlations (Axis 1 = 0.8887, Axis 2 = 0.8673), indicating a high level of association between the ordination axes and the explanatory variables. Forward selection identified trans-Nonachlor as the most influential variable, explaining 14.2% of the variation (pseudo-F = 8.6, p = 0.002), followed by p,p′-DDE (7.9%, pseudo-F = 5.1, p = 0.002), and HSI (6.3%, pseudo-F = 4.4, p = 0.002). The legacy pesticides p,p′-DDT and ratio's of o,p′-DDT / p,p′-DDD were also retained as significant contributors, explaining 4.7% (p = 0.004) and 3.2% (p = 0.014) of the variation, respectively. Other variables, including fish condition factor (CF), various PCBs, and other organochlorine pesticides, were not significant contributors to parasite community structures (p > 0.05). The combined effect of the selected variables captured over 90% of the fitted variation by the fourth axis, with consistently high pseudo-canonical correlations for the supplementary variables (Axis 1 = 0.9585, Axis 2 = 0.9639, Axis 3 = 0.9765, Axis 4 = 0.9588), indicating strong explanatory power of the retained factors on parasite community patterns.

In the RDA ordination plot, a noticeable separation was observed in the spatial distribution of the localities. Witsand and CE exhibited increased convergence, indicating a greater similarity in community structure compared to previous analyses (Figure 6.4). This overlap extended to include a subset of individuals from MB, forming a broader, central cluster. This grouping was characterised predominantly by monoxenous parasites, particularly isopods and copepods, including *Cin. tetrodontis* and *Cal. tetrodontis*. Despite this overlap, WS was influenced by higher abundances of *E. arenalbus* and *Nybelinia sp.*, both monoxenous taxa. Chintsa East and WS were further associated with the presence of heteroxenous digeneans, including *O. amplicoelus*, and larval nematodes such as *Raphidascaris sp.*, reflecting a mixed assemblage of direct and indirect life cycle parasites. Mossel Bay remained partially distinct, loosely aligned with SB; however, the community structure at SB appeared to be more similar to CE and MB. Notably, SB did not display a strong association with any pesticide but was more loosely aligned with host-related metrics such as CF, although this variable was not statistically significant in the forward selection. Uvongo Beach community structures were different compared to other localities, dominated by heteroxenous taxa, particularly *Acanthobothrium* sp., *Rhipidocotyle* sp., and one monoxenous taxon, *H. victorwepeneri*. These assemblages were closely associated with elevated concentrations of trans-Nonachlor, Dieldrin, and PCB #180. In contrast, DDT strongly fit in the central region of the ordination space, positioned between UB and MB, indicating a broader influence across these localities, while its metabolites, particularly p,p'-DDE, contributed towards the ordination closer ordination to CE and WS. Overall, the ordination reflects a gradient in parasite community composition driven by both parasite life-history strategies and environmental contamination profiles, particularly organochlorine pesticide exposure.

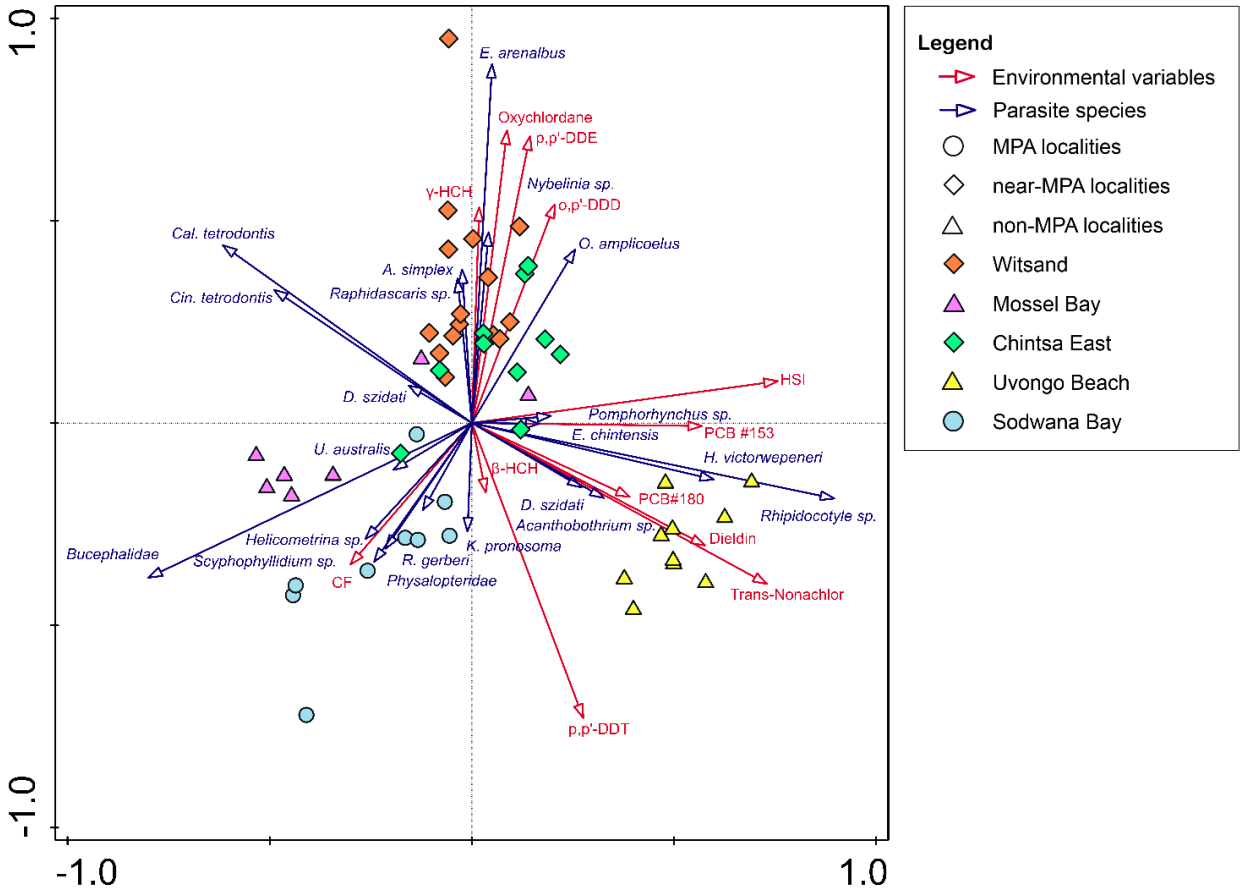

Figure 6.4: RDA tri-plot illustrating associations between the parasite infra-community taxa abundance of *Amblyrhynchote honckenii* (Bloch), explained by explanatory variables. The two axes display 45.3% of the total variation.

6.3.5 Estimated parasite diversity

Figure 6.5 presents the species accumulation curve for metazoan parasites detected in *A. honckenii* across all sampled localities. The X-axis represents the cumulative number of host individuals examined, while the Y-axis indicates the cumulative number of parasite taxa recorded. The accumulation curve shows a steady and pronounced increase in parasite species with increasing sampling effort. Importantly, the curve does not reach a plateau, even at the maximum number of hosts sampled. Moreover, the wide confidence intervals at higher sampling efforts further reflect continued uncertainty regarding the true parasite richness, reinforcing the interpretation that rare or low-prevalence taxa remain undetected. Pooled data from all localities further support this, as the overall accumulation curve rises consistently without levelling off. The trend observed in Figure 6.5 demonstrates that the estimated parasite diversity in *A. honckenii* is high but remains underestimated given the sampling effort applied in this study.

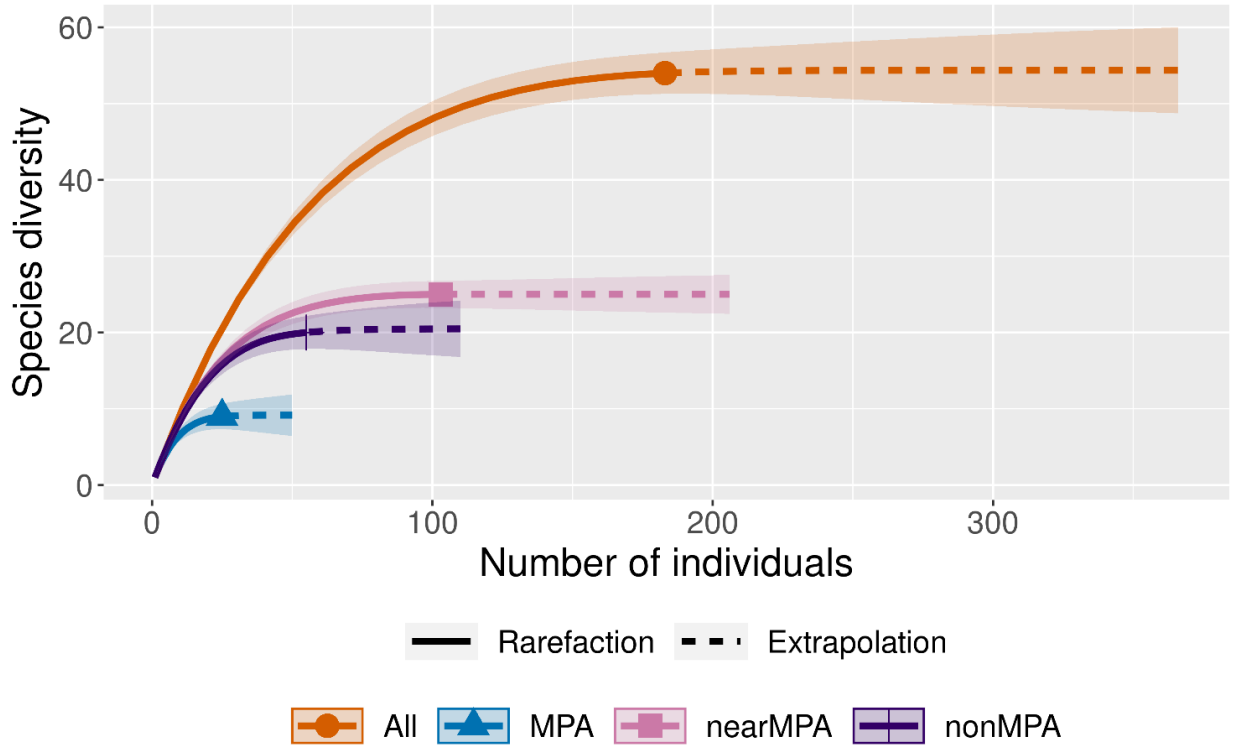

Figure 6.5: Species accumulation curve estimating the diversity of parasites as a function of sampling effort for each locality, as well as for the whole population of parasites of *Amblyrhynchote honckenii* (Bloch).

6.4 Discussion

This study provides the first comprehensive analysis of the metazoan parasite communities of the evileye blaasop, *A. honckenii*, across five coastal localities on the South African coastline, extending from the temperate Agulhas Bank to the tropical Natal ecoregion. Parasite communities were strongly structured by the interaction of biogeographic gradients, contaminant exposure and the degree of marine protection. In total, 22 taxa of metazoan parasites were identified across WS, MB, CE, UB and SB, including both monoxenous parasites with direct life cycles and heteroxenous parasites. It is well documented that *A. honckenii* is a widespread Indo-Pacific host, occurring from South Africa to as far north as China (Froese and Pauly, 2024), and these data further confirm that it is also a sensitive integrator of local ecosystem processes. Pufferfish are generally avoided by predators due to their tetrodotoxin (Lorentz *et al*., 2016) and can therefore act as long-lived and site-associated hosts that integrate parasite transmission pathways. Their parasite communities thus reflect the ecological complexity of local food webs and host availability, even though the fish themselves are not a major food resource for other vertebrates.

The results revealed a strong spatial structuring of parasite communities between localities. The near-MPA localities of WS and CE displayed the richest and most even assemblages, with high values for Shannon-Wiener, Brillouin and Simpson indices, with Pielou's evenness closest to 1. These assemblages comprised a wide range of taxa, including heteroxenous parasites such as *A. simplex*, *Nybelinia* sp., *Raphidascaris* sp., *O. amplicoelus* and *E. arenalbus*, alongside monoxenous species, such as *H. victorwepneneri*, *Cal. tetrodontis* and *Cin. tetrodontis*. These patterns indicate that the near-MPA localities maintain ecological conditions that allow the persistence of parasites with complex life cycles that rely on multiple intermediate hosts, which is a well-recognised signal of habitat integrity and connectivity (Wood *et al*., 2010; Cable *et al*., 2017). Similar results have been reported for *Diplodus capensis* (Smith) in the Agulhas Bank, where Vermaak (2024) recorded 30 metazoan parasite species, with the richest communities in MPA or near-MPA localities. Erasmus *et al*. (2022) found that parasite diversity and evenness in *Clinus superciliosus* (Linnaeus) were maximised in moderately protected areas with low levels of contamination. These parallels demonstrate that a pattern of high diversity in lightly impacted habitats is consistent across multiple host species in southern Africa.

In contrast, parasite assemblages at the non-MPA localities of MB and UB were simplified, characterised by high parasite abundance but low diversity, and dominated by a narrow set of resilient taxa, especially bucephalid and *Rhipidocotyle* metacercariae encysted in cardiac tissues. The collapse of community structure into dominance by a few opportunistic species is a classic indicator of degraded environments and is consistent with the high contaminant loads and poor host condition recorded at these localities (Marcogliese, 2005; Vidal-Martínez *et al*., 2019). The replacement of heteroxenous taxa by monoxenous taxa, such as *H. victorwepeneri*, mirrors findings in other marine and estuarine systems, where pollutant exposure produced communities dominated by larval trematodes, monopisthocotyleans and polyonopisthocotyleans (Lafferty and Kuris, 1999; Grabner *et al*., 2023), and it is consistent with the ecological filtering processes described by Sures (2008) and Timi and Poulin (2020). The single fully protected MPA locality, SB, exhibited intermediate parasite richness and a restricted assemblage dominated by *Scyphophyllidium* sp. and zoogonid digeneans. Although this locality is in an MPA, its limited diversity suggests that protection alone does not guarantee a return to a complex, heteroxenous-dominated parasite community if stressors from outside the protected area (such as contaminant inflow or reduced densities of intermediate hosts) are still present. This outcome parallels studies of Mediterranean MPAs where protection was insufficient to offset large-scale pollutant input and host depletion (Guidetti and Sala, 2007).

Community-level analyses confirmed these spatial distinctions. SIMPER analysis revealed high within-locality similarity in MB (81.59%) and UB, driven by dominance of a single species, while near-MPA localities exhibited more moderate similarity values and a richer mix of taxa. SB had the lowest similarity value (40.21%), reflecting its lower richness and compositional skew. ANOSIM tests produced a global R of 0.8369, demonstrating strong separation between localities, with pairwise comparisons between MB and CE and between MB and UB both yielding R-values of 1.0, indicating completely distinct, non-overlapping communities. These analyses clearly demonstrated that the patterns observed were not random but strongly structured by environmental gradients. Environmental drivers underpinning these differences were revealed by distance-based redundancy analysis. The pollutants trans-Nonachlor, p,p′-DDE and p,p′-DDT explained a significant portion of the variance in parasite composition, with trans-Nonachlor alone accounting for 14.2% of the explained variation. Pollutant exposure acts both directly, by damaging free-living stages and suppressing host immune systems, and indirectly, by reducing the abundance of intermediate hosts, leading to the loss of heteroxenous species (Sures, 2008; Blanar *et al*., 2009; Grabner *et al*., 2023). Uvongo Beach, with the highest of these pollutant loads, showed simplified communities dominated by monoxenous and metacercaria parasites. These patterns are congruent with the study by Wood *et al*. (2023) documenting a century-scale decline in complex life cycle taxa associated with global warming and human pressures. In contrast, WS and CE, which had lower contaminant burdens and healthier fish condition (higher HSI values), supported diverse communities of heteroxenous and monoxenous taxa.

The composition of parasite assemblages in *A. honckenii* thus closely mirrored that of other coastal fish hosts studied along South Africa's southern and eastern coasts. In *D. capensis*, Vermaak (2024) found that heteroxenous parasites, particularly trematodes and larval cestodes, dominated communities in near-MPA areas, while non-MPA localities had simplified assemblages dominated by bucephalid larvae. Similarly, Erasmus *et al*. (2022) reported that *C. superciliosus* populations in near-MPA localities supported rich parasite assemblages including multiple larval stages of cestodes, nematodes and acanthocephalans, while heavily impacted localities hosted only a few generalist taxa. These results highlight that parasite communities across different fish hosts respond similarly to gradients of disturbance and protection.

One striking outcome of the present study was that the highest parasite richness and evenness were not found at the warm tropical locality of SB, contrary to the expectation of the latitudinal diversity gradient (Poulin, 2010). Instead, the richest assemblages occurred in transitional near-MPA localities such as CE, where environmental quality was higher and contamination levels lower. This pattern mirrors that observed in *D. capensis* and *C. superciliosus* and suggests that, at a regional scale, habitat quality, host population structure and connectivity

are stronger determinants of parasite diversity than temperature alone (Costello *et al*., 2015; Poulin and Morand, 2000; Poulin, 2010). Such findings emphasise that local-scale factors can override broad climatic gradients in shaping parasite communities. Furthermore, the species accumulation curve for *A. honckenii* continued to rise without reaching an asymptote, indicating that a substantial proportion of its parasite fauna remains undiscovered. This is not surprising given that marine parasitology has historically concentrated on a few southern and eastern localities in South Africa, leaving the northern regions relatively understudied (Nunkoo, 2019). It is likely that expanded sampling across seasons, host size classes, and especially across the tropical and subtropical parts of *A. honckenii*'s range, will reveal even greater parasite diversity, including cryptic species. The lack of additional sampling in the host's northeastern distribution could also explain the lower diversity reported in the Natal ecoregion, such as SB.

6.5 Conclusion

The data affirm the utility of parasites as integrative indicators of habitat quality and anthropogenic impact. Parasite communities reflect both present and historical ecological processes, providing insights complementary to those derived from contaminant bioaccumulation. The observed sensitivity of parasite assemblages to chemical exposure, host condition, and food web structure underlines their value in biodiversity monitoring and marine management. While MPAs can enhance parasite richness and stability, their effectiveness is constrained without broader ecological connectivity and pollution control. The central coast near-MPA localities, particularly WS and CE, emerged as contemporary biodiversity hotspots for parasitic fauna, providing a model for the conditions under which complex, and ecologically integrated parasite communities can persist. This pattern suggests that the protective benefits of MPAs may extend into adjacent non-protected areas. Similar “spillover” effects have been documented in fish communities, where biomass and abundance in waters just outside MPAs increase over time as marine life from the reserve spills over into fished areas (Francheschini *et al*., 2024). These results underscore the need to incorporate parasite diversity into ecosystem health assessments and advocate for long-term, cross-ecoregion monitoring of parasite communities in South African marine fish.

In conclusion, this study set out to test two key hypotheses: (i) that parasite diversity in *A. honckenii* would display clear spatial patterns, with richness and complexity peaking in subtropical regions, particularly the Natal ecoregion, and declining toward temperate and cold-temperate regions such as the Agulhas Bank (Hypothesis 4, Chapter 1); and (ii) that elevated contaminant burdens in hosts would be associated with reduced richness and evenness, resulting in communities dominated by directly transmitted or opportunistic taxa, whereas more pristine or

near-MPA localities would support richer, more complex parasite assemblages (Hypothesis 5, Chapter 1).

The results show that these hypotheses were only partially supported. Although spatial trends were evident, the predicted peak diversity at the tropical Natal locality (SB) was not observed. Instead, the highest richness and complexity occurred at WS and CE, localities located near-MPAs, characterised by lower contaminant loads and healthier host populations. These findings suggest that while biogeographic gradients influence parasite communities, local factors such as habitat quality and pollution can override these large-scale patterns. As predicted, parasite assemblages in contaminated localities such as MB and UB were simplified and dominated by directly transmitted taxa, whereas near-MPA areas supported more diverse communities with numerous heteroxenous species. The expectation that MPAs enhance diversity was supported in part, although the limited diversity of SB suggests that protection alone does not guarantee restoration. The findings demonstrate that parasite assemblages are shaped by the interplay of temperature, pollution and management, and confirm their value as bioindicators of ecosystem integrity.

References:

Blanar, C.A., Munkittrick, K.R., Houlahan, J., MacLatchy, D.L. & Marcogliese, D.J., 2009. Pollution and parasitism in aquatic animals: a meta-analysis of effect size. *Aquatic Toxicology*, 93(1): 18–28.

Boersma, P.D. & Parrish, J.K., 1999. Limiting abuse: marine protected areas, a limited solution. *Ecological Economics*, 31(2): 287–304.

Bush, A.O., Lafferty, K.D., Lotz, J.M. & Shostak, A.W., 1997. Parasitology meets ecology on its own terms: Margolis et al. revisited. *Journal of Parasitology*, 83: 575–583.

Cable, J., Barber, I., Boag, B., Ellison, A.R., Morgan, E.R., Murray, K., Pascoe, E.L., Sait, S.M., Wilson, A.J. & Booth, M., 2017. Global change, parasite transmission and disease control: lessons from ecology. *Philosophical Transactions of the Royal Society B: Biological Sciences*, 372(1719): 20160088.

Carr, M.H., Robinson, S.P., Wahle, C., Davis, G., Kroll, S., Murray, S., Schumacker, E.J. & Williams, M., 2017. The central importance of ecological spatial connectivity to effective coastal marine protected areas and to meeting the challenges of climate change in the marine environment. *Aquatic Conservation: Marine and Freshwater Ecosystems*, 27: 6–29.

Chao, A., Ma, K.H. & Hsieh, T.C., 2016. iNEXT (iNterpolation and EXTrapolation) Online. Program and User's Guide. Available at: http://chao.stat.nthu.edu.tw/wordpress/software_download/. (Date accessed: 12 June 2025).

Costello, M.J., Wilson, S. & Houlding, B., 2012. Predicting total global species richness using rates of species description and estimates of taxonomic effort. *Systematic Biology*, 61(5): 871.

Davies, C.E., 2021. Invertebrate health in marine protected areas (MPAs). *Journal of Invertebrate Pathology*, 186: 107524.

Erasmus, A., Wepener, V., Hadfield, K.A., Sures, B. & Smit, N.J., 2022. Metazoan parasite diversity of the endemic South African intertidal klipfish, *Clinus superciliosus*: factors influencing parasite community composition. *Parasitology International*, 90: 102611.

Franceschini, S., Lynham, J. & Madin, E.M., 2024. A global test of MPA spillover benefits to recreational fisheries. *Science Advances*, 10(29): eado9783.

Froese, R. & Pauly, D., 2025. FishBase. Available at: www.fishbase.org/search.php. (Date accessed: 8 May 2025).

Grabner, D., Rothe, L.E. & Sures, B., 2023. Parasites and pollutants: effects of multiple stressors on aquatic organisms. *Environmental Toxicology and Chemistry*, 42(9): 1946–1959.

Guidetti, P. & Sala, E., 2007. Community-wide effects of marine reserves in the Mediterranean Sea. *Marine Ecology Progress Series*, 335: 43–56.

Lafferty, K.D. & Kuris, A.M., 1999. How environmental stress affects the impacts of parasites. *Limnology and Oceanography*, 44(3part2): 925–931.

Lafferty, K.D., 2012. Biodiversity loss decreases parasite diversity: theory and patterns. *Philosophical Transactions of the Royal Society B: Biological Sciences*, 367(1604): 2814–2827.

Lorentz, M.N., Stokes, A.N., Rößler, D.C., & Lötters, S., 2016. Tetrodotoxin. *Current biology*, 26(19): 870–872.

Mackintosh, A.L., 2019. Parasite communities associated with the Cape gurnard (*Chelidonichththys capensis*) and the lesser gurnard (*C. queketti*) from South Africa. PhD Thesis, University of Cape Town

Marcogliese, D.J., 2002. Food webs and the transmission of parasites to marine fish. *Parasitology*, 124(7): 83–99.

Marcogliese, D.J., 2005. Parasites of the superorganism: are they indicators of ecosystem health? *International Journal for Parasitology*, 35(7): 705–716.

Marcogliese, D.J., 2016. The distribution and abundance of parasites in aquatic ecosystems in a changing climate: more than just temperature. *Integrative and Comparative Biology*, 56(4): 611–619.

Marcogliese, D.J., 2023. Major drivers of biodiversity loss and their impacts on helminth parasite populations and communities. *Journal of Helminthology*, 97: e34.

Molbert, N., 2020. Host-parasites transfer of micropollutants and eco-physiological consequences on a freshwater fish: case study of chub-acanthocephalan model. PhD Thesis, Sorbonne Université.

Nunkoo, M.A.I., 2019. Studies on the diversity and distribution of marine ichthyoparasites in southern Africa. PhD Thesis, University of Cape Town.

Pfingstl, T., Baumann, J., Neethling, J.A., Bardel-Kahr, I. & Hugo-Coetzee, E.A., 2021. Distribution patterns of intertidal oribatid mites (*Acari, Oribatida*) from South African shores and their relationship to temperature. *African Journal of Marine Science*, 43(2): 215–225.

Poulin, R. & Morand, S., 2000. The diversity of parasites. *The Quarterly Review of Biology*, 75(3): 277–293.

Poulin, R., 2010. Latitudinal gradients in parasite diversity: bridging the gap between temperate and tropical areas. *Neotropical Helminthology*, 4(2): 169–177.

Poulin, R., 2015. *Quantifying parasite diversity. In: Parasite diversity and diversification: evolutionary ecology meets phylogenetics.* Cambridge University Press, pp. 9–26.

Poulin, R., Salloum, P.M. & Bennett, J., 2024. Evolution of parasites in the Anthropocene: new pressures, new adaptive directions. *Biological Reviews*, 99(6): 2234–2252.

Serdar, B., LeBlanc, W.G., Norris, J.M. & Dickinson, L.M., 2014. Potential effects of polychlorinated biphenyls (PCBs) and selected organochlorine pesticides (OCPs) on immune cells and blood biochemistry measures: a cross-sectional assessment of the NHANES 2003-2004 data. *Environmental Health*, 13: 1–12.

Spalding, M.D., Fox, H.E., Allen, G.R., Davidson, N., Ferdaña, Z.A., Finlayson, M., Halpern, B.S., Jorge, M.A., Lombana, A., Lourie, S.A., Martin, K.D., McManus, E., Molnar, J., Recchia, C.A. & Robertson, J., 2007. Marine ecoregions of the world: A bioregionalization of coastal and shelf areas. *BioScience*, 57(7): 573–583.

Sures, B., 2008. Environmental parasitology. Interactions between parasites and pollutants in the aquatic environment. *Parasite*, 15(3): 434–438.

Sures, B., Nachev, M., Schwelm, J., Grabner, D. & Selbach, C., 2023. Environmental parasitology: stressor effects on aquatic parasites. *Trends in Parasitology*, 39(6): 461–474.

Thompson, L.A., Darwish, W.S., Ikenaka, Y., Nakayama, S.M., Mizukawa, H. & Ishizuka, M., 2017. Organochlorine pesticide contamination of foods in Africa: incidence and public health significance. *Journal of Veterinary Medical Science*, 79(4): 751–764.

Timi, J.T. & Poulin, R., 2020. Why ignoring parasites in fish ecology is a mistake. International *Journal for Parasitology*, 50(10–11): 755–761.

Vermaak, A., 2024. Metazoan parasite diversity of *Diplodus capensis* from South Africa and the role of marine protected areas in their conservation. PhD Thesis, North-West University.

Vidal-Martínez, V.M., Velázquez-Abunader, I., Centeno-Chalé, O.A., May-Tec, A.L., Soler-Jiménez, L.C., Pech, D., Mariño-Tapia, I., Enriquez, C., Zapata-Pérez, O., Herrera-Silveira, J. & Hernández-Mena, D.I., 2019. Metazoan parasite infracommunities of the dusky flounder (Syacium papillosum) as bioindicators of environmental conditions in the continental shelf of the Yucatan Peninsula, Mexico. *Parasites & Vectors*, 12(1): 277.

Wood, C.L., Lafferty, K.D. & Micheli, F., 2010. Fishing out marine parasites? Impacts of fishing on rates of parasitism in the ocean. *Ecology Letters*, 13(6): 761–775.

Wood, C.L., Micheli, F., Fernández, M., Gelcich, S., Castilla, J.C. & Carvajal, J., 2013. Marine protected areas facilitate parasite populations among four fished host species of central Chile. *Journal of Animal Ecology*, 82(6): 1276–1287.

Wood, C.L., Welicky, R.L., Preisser, W.C., Leslie, K.L., Mastick, N., Greene, C., Maslenikov, K.P., Tornabene, L., Kinsella, J.M. & Essington, T.E., 2023. A reconstruction of parasite burden reveals one century of climate-associated parasite decline. *Proceedings of the National Academy of Sciences*, 120(3): e2211903120.

Wood, C.L., Zgliczynski, B.J., Haupt, A.J., Guerra, A.S., Micheli, F. & Sandin, S.A., 2018. Human impacts decouple a fundamental ecological relationship. The positive association between host diversity and parasite diversity. *Global Change Biology*, 24(8): 3666–3679.

7 Evaluating the combined effect of *Cinusa tetrodontis* Schioedte & Meinert, 1884, infestation and copper exposure on the accumulation and metallothionein expression in the evileye blaasop, *Amblyrhynchote honckenii* (Bloch)

7.1 Introduction

Marine ecosystems are increasingly impacted by a range of anthropogenic stressors, among which heavy metals are of particular concern due to their persistence, bioavailability, and toxicity (Nachev and Sures, 2016). Copper is a prevalent and essential trace element that plays crucial roles in enzymatic activity and cellular metabolism in fish (Malhotra *et al*., 2020). However, Cu's beneficial properties are negated by its potential toxicity when present in elevated concentrations, often due to anthropogenic inputs such as antifouling paints used on ships and marine infrastructure, mining runoff, industrial effluents, and agricultural activities (Malhotra *et al*., 2020; Lu *et al*., 2022; Cui *et al*., 2024).

Coastal and estuarine areas are particularly susceptible to Cu pollution, given their proximity to concentrated human activities and their ability to retain metals in sediments and organisms (Nachev and Sures, 2016; Li *et al*., 2022). Even at sublethal levels, Cu exposure can induce oxidative stress and disrupt ion regulation in marine fish (Malhotra *et al*., 2020; Wang *et al*., 2024). The gills, which are the primary site for waterborne metal uptake, are particularly susceptible, often exhibiting structural damage such as epithelial lifting, lamellar fusion, and necrosis following exposure (Malhotra *et al*., 2020; Martínez-Durazo *et al*., 2023). The liver and kidneys, which are critical organs for detoxification and excretion, may also be impaired, compromising immune function, metabolic efficiency, and ultimately increasing mortality risk, thereby threatening fish populations and ecosystem stability (Malhotra *et al*., 2020; Wang *et al*., 2024). The bioavailability and severity of Cu toxicity are influenced by environmental parameters, including pH, salinity, water hardness, and the concentration of dissolved organic carbon (DOC) (Nachev and Sures, 2016; Cui *et al*., 2024). For instance, lower pH and salinity conditions tend

to increase Cu toxicity by elevating the availability of free cupric ions (Cu^{2+}). In contrast, higher DOC and water hardness can mitigate toxicity by binding Cu and reducing its bioavailability (Cui *et al*., 2024). These variables are known to fluctuate considerably in coastal estuarine ecosystems, further complicating the assessment of Cu's ecological impact and highlighting the need for context-specific environmental monitoring (Cui *et al*., 2024).

A key physiological response to Cu exposure in fish is the synthesis of metallothionein (MTs), which are low-molecular-weight, cysteine-rich proteins that bind to metal ions, thus mitigating their toxicity and facilitating homeostasis and detoxification of trace elements (Amiard *et al*., 2006; Le *et al*., 2016; Singh and Sharma, 2024). Metallothionein levels are commonly used as a biomarker in ecotoxicological studies, with elevated expression reflecting increased metal exposure and physiological stress (Amiard *et al*., 2006; Le *et al*., 2016). However, MT responses are known to vary depending on factors such as exposure duration, metal concentration, speciation, and co-occurring stressors, reflecting the complexity of detoxification pathways (Amiard *et al*., 2006; Malhotra *et al*., 2020). In some cases, prolonged or high-level Cu exposure can suppress MT expression, indicating a breakdown of detoxification capacity (Malhotra *et al*., 2020). Parasitism introduces an additional layer of complexity to these interactions. Several studies have shown that intestinal helminths such as acanthocephalans and cestodes are capable of accumulating trace metals, including lead and cadmium, at concentrations far exceeding those found in host tissues (Sures, 2003). This bioaccumulation capacity effectively reduces the bioavailable fraction of metals in the host, potentially lessening the physiological burden (Nachev and Sures, 2016; Sures *et al*., 2025). For example, parasitised fish have been shown to exhibit lower concentrations of certain metals in their tissues compared to non-parasitised individuals (Nachev and Sures, 2016).

While much of this research has focused on freshwater environments and endoparasites, marine ectoparasites, particularly isopods, remain relatively underexplored (Sures, 2004; Vidal-Martínez *et al*., 2010; Nachev and Sures, 2016; Erasmus *et al*., 2020; van der Spuy *et al*., 2023; Sures *et al*., 2025). A recent study by van der Spuy *et al*. (2023), detailed in Chapter 4 of this thesis, demonstrated that the cymothoid isopod *Cin. tetrodontis*, which infests the buccal cavity of the evileye blaasop, *A. honckenii*, accumulates significantly higher levels of Cu than its host. Given its direct contact with both host tissue and ambient seawater, and its blood-feeding behaviour, *Cin. tetrodontis* has the potential to serve as both a bioindicator of environmental metal contamination and a potential modulator of host metal burdens (van der Spuy *et al*., 2023). Other studies on element exposure and the interaction between hosts and parasites showed that infected hosts may benefit from reduced internal Cu levels due to sequestration by the parasite, potentially resulting in altered physiological responses such as MT expression (Sures and

Radszuweit, 2007; Sures *et al*., 2017). Alternatively, parasitism may increase the levels of stress responses if the host faces additional immune or metabolic challenges (Gismondi *et al*., 2012; Sures *et al*., 2017). For example, the acanthocephalan *Pomphorhynchus laevis* (Zoega in Müller, 1776) Porta, 1908 has been shown to accumulate lead 2,000-fold the levels found in fish muscle (Sures *et al*., 2017), while the nematode *Raphidascaris acus* (Bloch, 1779) Railliet & Henry, 1915 has been associated with lower selenium accumulation and reduced oxidative stress in infected rainbow trout (Hursky and Pietrock, 2015; Sures *et al*., 2017). However, these effects are dependent on different internal and external factors, particularly the parasite species, host physiology, metal type, and exposure conditions (Sures, 2006; Marcogliese and Pietrock, 2011; Sures *et al*., 2017).

Ectoparasitic isopods in marine systems have received limited attention in studies on contaminant dynamics (Pérez-del-Olmo *et al*., 2019; van der Spuy *et al*., 2023). Furthermore, in chapter 4, only the environmental results suggestive of modulation were highlighted. Understanding how parasitic infections or infestations interact with chemical pollutants in marine organisms is essential in evaluating ecosystem health and pollutant impacts (Sures *et al*., 2017; Sures *et al*., 2025). Although environmental Cu exposure is a well-known stressor in aquatic systems, the role of ectoparasitic isopods in modulating its accumulation and associated physiological responses in marine fish has remained poorly understood (Sures *et al*., 2017; Sures *et al*., 2025). The potential for *Cin. tetrodontis* to influence Cu accumulation and MT responses in *A. honckenii* has not yet been explored under controlled experimental conditions. This study aims to fill that gap by assessing Cu accumulation and MT expression in infected and uninfected *A. honckenii* following a 24-hour sublethal Cu exposure in a controlled laboratory setting. The short-term exposure design enables the detection of early physiological responses and avoids confounding effects related to chronic stress or long-term adaptation (Mahotra *et al*., 2020). The laboratory exposures were further compared to the Cu concentrations in field-sampled *A. honckenii* and *Cin. tetrodontis* (see Chapter 4). Based on the known capacity of parasites to accumulate metals and influence host physiology, this study tests several key hypotheses (Hypotheses 6–9, Chapter 1). First, it is hypothesised that infestation by *Cin. tetrodontis* reduces Cu accumulation in host tissues by acting as a biological sink, thereby modulating host exposure. Second, the presence of the parasite is expected to alter the host's detoxification response, particularly metallothionein (MT) expression, which lessens the need for biomarker activation. Third, it is hypothesised that *Cin. tetrodontis* itself actively responds to Cu exposure, with sex-specific variation in MT induction, reflecting physiological differences between males and females. Lastly, the study proposes that short-term laboratory exposures can reproduce Cu accumulation and biomarker trends observed in environmental conditions, validating the use of controlled experiments in assessing complex host–parasite–pollutant interactions.

The significance of this research lies in its contribution to our understanding of how ectoparasites may influence trace metal dynamics in marine fish. By elucidating whether *Cin. tetrodontis* modulates Cu accumulation and alters biomarker responses such as MT induction, this study provides new insight into the role of parasites in ecotoxicological processes. Moreover, these findings have practical implications for biomonitoring and environmental assessment (Sures *et al*., 2017). Incorporating host-parasite interactions into pollution monitoring frameworks can enhance sensitivity to contaminant exposure and improve ecological risk assessments in marine ecosystems increasingly impacted by anthropogenic stressors.

7.2 Materials and Methods

7.2.1 Fish source, husbandry and acclimation

Twenty evileye blaasop, *A. honckenii*, were obtained from the Two Oceans Aquarium, Cape Town, with 10 specimens naturally infested with the parasitic isopod, *Cin. tetrodontis,* and 10 uninfested controls. All procedures involving the fish were approved by the Two Oceans Aquarium Animal Ethics Committee (TOAAEC; approval number: TOA-RES003-21) and the AnimCare Animal Research Ethics Committee of the North-West University (FNASREC; NWU-00565-19-A5). Upon arrival, fish were housed at the National Aquatic Bioassay Facility (NABF) of the North-West University under environmental and welfare conditions aligned with the aquarium's care guidelines and current best practices for marine species research.

Fish were housed for a period of 22 months in two separate 500 L circular tanks filled with artificial seawater, one for infested fish specimens and the other for uninfested fish specimens. Infestation status was determined through screening under mild anaesthesia that involved using clove oil at 0.05 mL per 500 mL of water, administering only 75% of the full dose for no more than 20 s (Fernandes *et al*., 2016). Fish were visually examined for the presence of *Cin. tetrodontis* and allowed to recover in aerated tanks. Infested and uninfested fish were separated into distinct groups following screening and were observed for any adverse responses to anaesthesia or handling. All fish adapted well during this period, with no mortality or signs of disease reported. The housing tanks were equipped with a sandy substrate to accommodate the natural burrowing behaviour of the fish species and included PVC pipes as shelter to reduce stress and promote natural behaviours (Figure 7.1). The tanks were completely grey, allowing fewer visual disturbances and minimising stress and physical trauma. Water quality was consistently maintained within optimal ranges for marine fish, with the temperature controlled between 18–19°C, salinity maintained at 33–34 ppt, pH between 8.0–8.2, and ammonia levels kept below 0.1 mg/L. These parameters were monitored daily using automated meters.

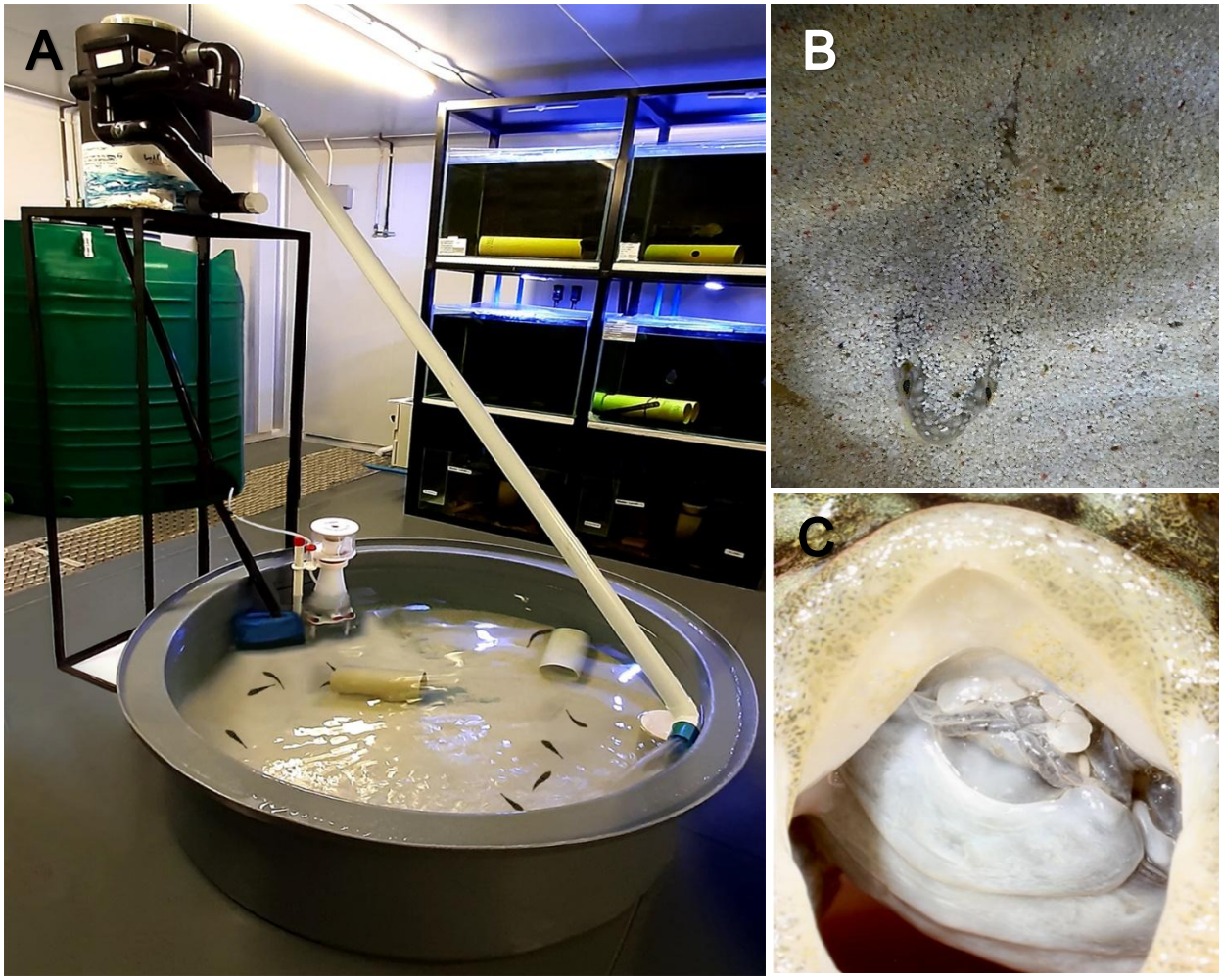

Figure 7.1: Photograph of the housing tanks in the NABF facility at the North-West Univ ersity, along with some close-up photos of the evileye blaasop, *Amblyrhynchote honckenii* (Bloch). **A** – housing tank; **B** – *A. honckenii* hiding under the sand (uninfested); **C** – *Cinusa tetrodontis*. Photographs **A–C** by Linda de Klerk.

Fish were fed five times per week (Monday to Friday) with a varied diet of commercial pellets and a customised gel-based formula consisting of seafood, vitamin and mineral supplements, spirulina, garlic, calcium, and fish oil. Both infested and uninfested fish received the same type and quantity of food throughout the study. The gel food was finely blended to avoid choking or respiratory obstruction, following species-specific feeding precautions. Feeding responses were observed daily to monitor health and appetite. The aquarium system also included skimmer cups designed to remove dissolved proteins and organic waste from the water, helping to maintain optimal water quality. Skimmer cups were cleaned every second day, with 30–50% water changes conducted every two to three weeks, depending on the rate of waste accumulation, with regular siphoning of the sandy substrate to remove uneaten food and debris. Weekly salinity and temperature checks and daily health assessments were completed, which included evaluation of abrasions, fin condition, feeding response, body integrity, and behaviour.

Monthly video and photo health reports were submitted to the Two Oceans Aquarium to ensure compliance with ethical standards. Infested fish were observed to be more active and responsive to feeding, while uninfested fish tended to remain buried except during feeding. This careful acclimation and husbandry ensured that all fish specimens were in optimal condition prior to the commencement of exposure experiments, following the standards set by the Two Oceans Aquarium.

7.2.2 Exposure design and experimental procedures

The exposure protocol followed OECD guidelines for fish toxicity testing (OECD, 2019), with modifications to accommodate marine species and ethical welfare considerations. All fish originated from the same source population and had undergone long-term acclimation to laboratory conditions, ensuring uniformity in age, health, and consistent environmental history. Before exposure, fish were visually screened for general health and absence of disease.

Twenty individual 8 L polycarbonate (ZebTEC) tanks were filled with artificial seawater and left to stabilise for 24 h before transferring the fish to the tanks. Tanks were randomly distributed in the test area and visually shielded to minimise external disturbance. Artificial seawater was prepared by dissolving commercial marine salts (Vibrant Sea, Seachem) in reverse osmosis water, and each tank was aerated to achieve full oxygen saturation. Individual fish were transferred into a static, aerated 8 L ZebTEC tank to prevent social stress and allowed to acclimate to the new tank for 24 h prior to exposure. Water quality was carefully maintained, with the temperature set between 20–22°C, salinity between 30–34 ppt, pH at 8.0–8.2, and dissolved oxygen above 80% air saturation, with a 12–16 h photoperiod. Fish were divided into four test groups (n=5 fish specimens per group) (Figure 7.2): control, uninfested; control, infested; Cu-exposed, uninfested; Cu-exposed, infested.

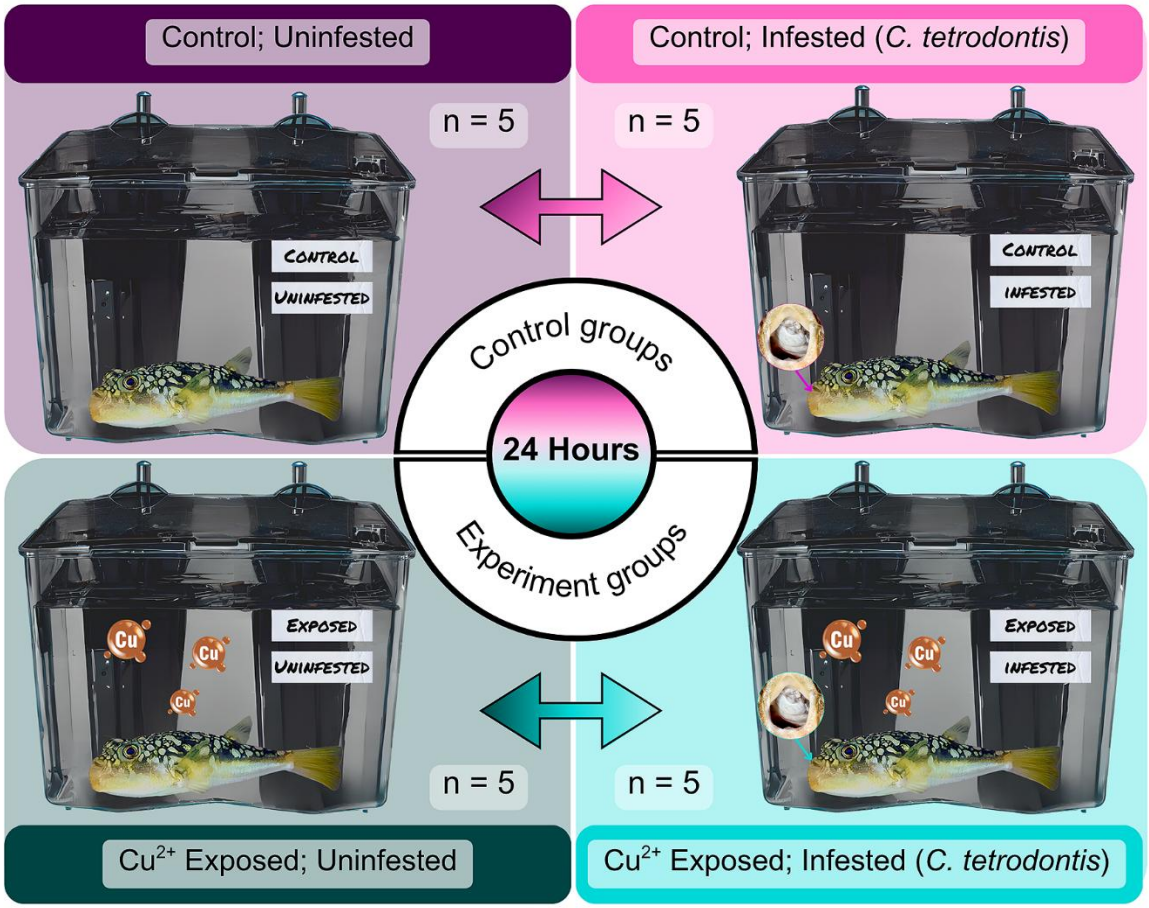

Figure 7.2: Experimental design for four test exposure groups of *Amblyrhynchote honckenii* (Bloch) specimens during a 24-hour exposure to a hazard concentration of copper (Cu) affecting 20% of the population (HC20). A – Control fish, without parasites, n=5; B – Control fish, infested with *Cinusa tetrodontis* Schioedte & Meinert, 1884, n=5; C – Cu exposed fish, without parasites, n=5; D – Cu exposed fish, infested with *Cinusa tetrodontis* Schioedte & Meinert, 1884, n=5. Diagram by Linda de Klerk.

The Cu exposure solution was prepared using Cu (II) chloride ($CuCl_2$) with the test concentration calculated to represent the hazardous concentration for 20% of species (HC20) based on the species sensitivity distribution (Fantke *et al*., 2018). The final exposure concentration was 486 µg/L Cu, prepared by adding 3.88 mL of a 1000 mg/L Cu standard stock solution to each 8 L tank and mixed thoroughly. Control tanks received no Cu addition. Fish were exposed for a duration of 24 h. No feeding occurred during the 24 h exposure period to prevent confounding effects from food and waste. Throughout the exposure period, fish were monitored for signs of behavioural change, discomfort, or mortality. Additionally, water parameters, including dissolved oxygen, temperature, and pH were also monitored for the duration of the exposure. Copper concentrations in exposure tanks were monitored throughout the exposure period by collecting water samples from each tank before and after exposure. The dosed nominal Cu concentrations were analytically confirmed at the start of the exposure as recommended by

OECD guidelines (OECD, 2019), ensuring the accuracy and reproducibility of dosing (see Figure 7.3). No mortalities, visible abnormalities, or behavioural changes were observed throughout the exposure.

Following exposure, fish were humanely killed using percussive stunning followed by pithing, following the approved SOP for aquatic ectotherms (NWU-00267-17-A5). Fish length (cm) was measured and weighed (g) to calculate the condition factor (K). Following dissection, fish livers and gonads were weighed to calculate the hepatosomatic index (HSI) and gonadosomatic index (GSI) (see Figure 7.4). Parasites were carefully removed from the buccal cavity of infested fish and confirmed as *Cin. tetrodontis* based on morphology (Hadfield *et al*., 2010). The sex (male or female) and life stage (juvenile or adult) of each parasite were recorded. Parasites and fish tissues, including gills, liver, muscle, stomach, and gall bladder, were collected, frozen, and stored at -80°C in pre-cleaned acid-washed polypropylene tubes for Cu accumulation analysis. Additionally, sub-samples of liver, muscle, and parasite tissue were collected for MT analysis.

7.2.3 Analytical procedures

For Cu analysis, frozen samples were thawed, weighed to determine wet weight (g) and freeze-dried (FreeZone 6, Labconco) for approximately 96 h. Dried samples were reweighed to determine dry weight (g) and homogenised using a mortar and pestle. Approximately 0.2 g of fish tissue and 0.08 g of parasite tissue were acid-digested in Teflon vessels, using 7.5 mL of 65% HNO_3 (sub-boiled p.a. quality, Merck) and 2.5 mL of 37% HCl (supra-pure, Merck), or 750 µL 65% HNO_3 and 250 µL 37% HCl for parasite samples, using an Ethos Easy MAXII-44 microwave digestion system. After digestion, each vessel was emptied, rinsed, and brought to a volume of 50 mL (fish tissue) or 10 mL (parasite tissue) with 1% HNO_3, transferred to acid-washed tubes, and kept in the dark at room temperature until analysis (Degger *et al*., 2011; Labuschagne *et al*., 2021). All digested samples were diluted 1:10 in 1% HNO_3 and analysed using graphite furnace atomic absorption spectrometry (GF-AAS, PerkinElmer Analyst 600 with Zeeman-effect background correction) (Erasmus *et al*., 2020). For each sample, 600 µL was pipetted into AAS vials, and 20 µL was automatically injected into the graphite furnace. Samples were analysed in triplicate, with mean peak area values used for final calculations. Copper concentrations were calculated from the regression line with a correlation factor of ≥0.999. Three blank samples per digestion run were prepared and analysed alongside quality standards analysed after every 20 samples. Furthermore, analytical accuracy was verified using the DOLT-5 reference material (dogfish liver certified reference material for trace metals and other constituents, National Research Council, Canada), with Cu recoveries calculated between 87% and 112%. Limits of detection (LOD) and quantification (LOQ) were calculated as 3 and 10 times the signal-to-noise ratio using the standard deviation of the calibration intercept divided by the slope (Saadati *et al*.,

2013), respectively, and adjusted for the average sample weights of 184 mg for fish tissue and 55 mg for parasite tissue (Table 7.1).

For MT analyses, tissues stored at -80°C were placed on ice and allowed to thaw to approximately 0°C. Approximately 0.2–0.3 g of fish liver and muscle tissue, as well as parasite tissue samples, were homogenised using a VELP OV5 homogeniser (VELP Scientifica, Italy) in a 0.25 M sucrose solution in a 1:4 tissue: volume ratio. Homogenates were centrifuged at 20,000 g for 20 min at 4°C. Three 300 µL aliquots of supernatant were prepared for MT analysis using a modified silver saturation method (Scheuhammer and Cherian, 1986; Frank *et al*., 2008). Each aliquot was mixed with 500 µL of a 20 mg/L $AgNO_3$ solution and incubated at room temperature for 20 min to displace bound Cu with a lower affinity for MTs than Ag, saturating the MT binding sites with Ag. To remove excess Ag ions, 100 µL of red blood cell hemolysate (10% haematocrit, Sigma-Aldrich, Germany) was added. Samples were then subjected to three cycles of heating in a water bath at 100°C and centrifuged at 1,200 g for 10 min to precipitate the Ag-bound haemoglobin, leaving heat-stable MT proteins in suspension, and to remove the denatured proteins. The final supernatant was centrifuged at 16,000 g for 15 min before determining the silver concentration, which is considered proportional to the amount of MT. Silver content was analysed using graphite furnace atomic absorption spectrometry (GF-AAS, PerkinElmer), following the method of Erasmus *et al*. (2020) as described for Cu. Samples were also analysed in triplicate, with mean peak area values used for final calculations. Final MT concentrations were calculated from the regression line with a correlation factor of ≥0.989. Limits of detection (LOD) and quantification (LOQ) were calculated as 3 and 10 times the signal-to-noise ratio using the standard deviation of the calibration intercept divided by the slope (Saadati *et al*., 2013) and adjusted for the average sample weight of 271 mg (Table 7.1).

7.2.4 Statistical analysis

Statistical analyses were conducted using GraphPad Prism v10. Data were tested for normality using the Shapiro-Wilk normality test. As all data met the normal distribution assumption, a one-way ANOVA and a two-way ANOVA were performed, followed by Tukey's multiple comparison test. Significance was set at $p<0.05$. Results of the one-way ANOVA and Tukey's multiple comparison tests, indicating significant differences ($p<0.05$) comparing Cu and MT concentrations in parasite and fish host species from control and exposed groups, are presented in figures, with significant differences indicated (Figures 7.5–7.6). Results of the two-way ANOVA statistical analysis of variance comparing metal concentrations in species (parasite and fish host) from two treatment groups (control and exposure) are presented in tabular form (Table 7.2).

7.3 Results

The controlled Cu exposure experiment revealed clear patterns in both Cu accumulation and MT induction across tissues and between infested and uninfested *A. honckenii*.

Table 7.1 presents the analytical performance metrics for Cu and MT quantification across parasite and fish tissues. The percentage recovery of Cu from the DOLT-5 certified reference material was 96.05 ± 9.42 %, confirming the accuracy and reliability of the digestion and quantification protocol used in this study. Limits of detection and LOQ were calculated based on signal-to-noise ratios and adjusted for tissue mass. For fish tissue, the LOD and LOQ were 0.02 µg/g and 0.40 µg/g dry weight, respectively, while for parasite tissue, slightly higher values were reported (0.90 µg/g LOD and 2.72 µg/g LOQ). Metallothioneins were quantified with equal LOD (0.30 µg/g) and LOQ (0.90 µg/g) values for both parasite and fish tissue. Overall, the values reported confirm that the study employed sensitive and robust analytical methods, capable of detecting both background levels and treatment-induced changes in trace metal accumulation and biomarker responses in both host and parasite tissues.

Table 7.1: Percentage recovery (%) of DOLT-5 certified reference material, as well as the limit of detection (LOD) (µg/g dry weight) and limit of quantification (LOQ) (µg/g dry weight) in different tissue samples.

Analyte	Recovery (%)	LOD (µg/g dry weight)		LOQ (µg/g dry weight)	
		Parasite	Fish tissue	Parasite	Fish tissue
Cu	96.05	0.90	0.02	2.72	0.40
MTs	-	0.30	0.30	0.90	0.90

The results from the water analyses (Figure 7.3; Supplementary Table 7.1) confirmed that exposure tanks reached the dosed nominal sublethal Cu concentration of approximately 486 µg/L, with values ranging from 407.50 ± 71.59 µg/L to 417.73 ± 70.87 µg/L. The Cu levels in the control tanks remained lower (8.79–12.46 µg/L), ensuring the integrity of the experimental design.

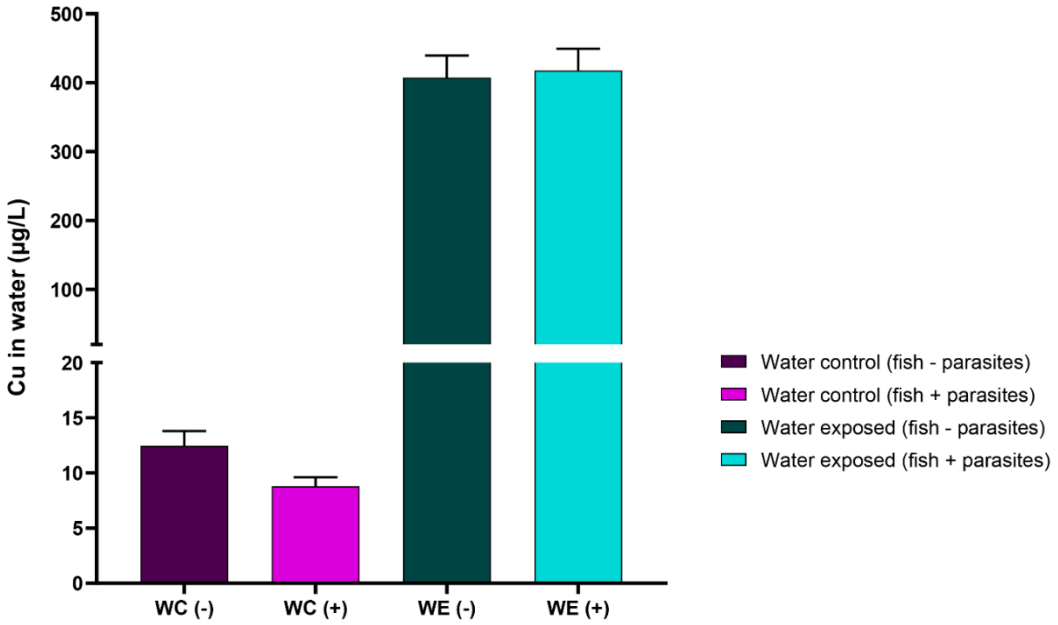

Figure 7.3: Copper concentrations measured in control and exposure tanks at the start of the exposure period. Graph values represent means ± standard deviation (n=5 per treatment). All abbreviations are defined in the graph legends.

Morphometric indices (Figure 7.4) did not show any significant changes over the short exposure duration. The K was slightly lower in exposed fish than in control fish (Figure 7.4A), and slightly higher in environmental fish than in laboratory fish (Figure 7.4B). Additionally, infested laboratory fish had slightly higher K values than uninfested fish, mirroring the same trend seen in field-sampled environmental fish (see Chapter 4). In contrast, the HSI was slightly higher in exposed fish (Figure 7.4B), particularly in uninfested rather than infested fish (Figure 7.4B). The HSI results show the same trend as seen in environmental fish. The GSI remained relatively stable across the treatment groups (Figure 7.4C). Environmental fish did, however, show uninfested fish with significantly higher GSI values than infested fish (Figure 7.4C).

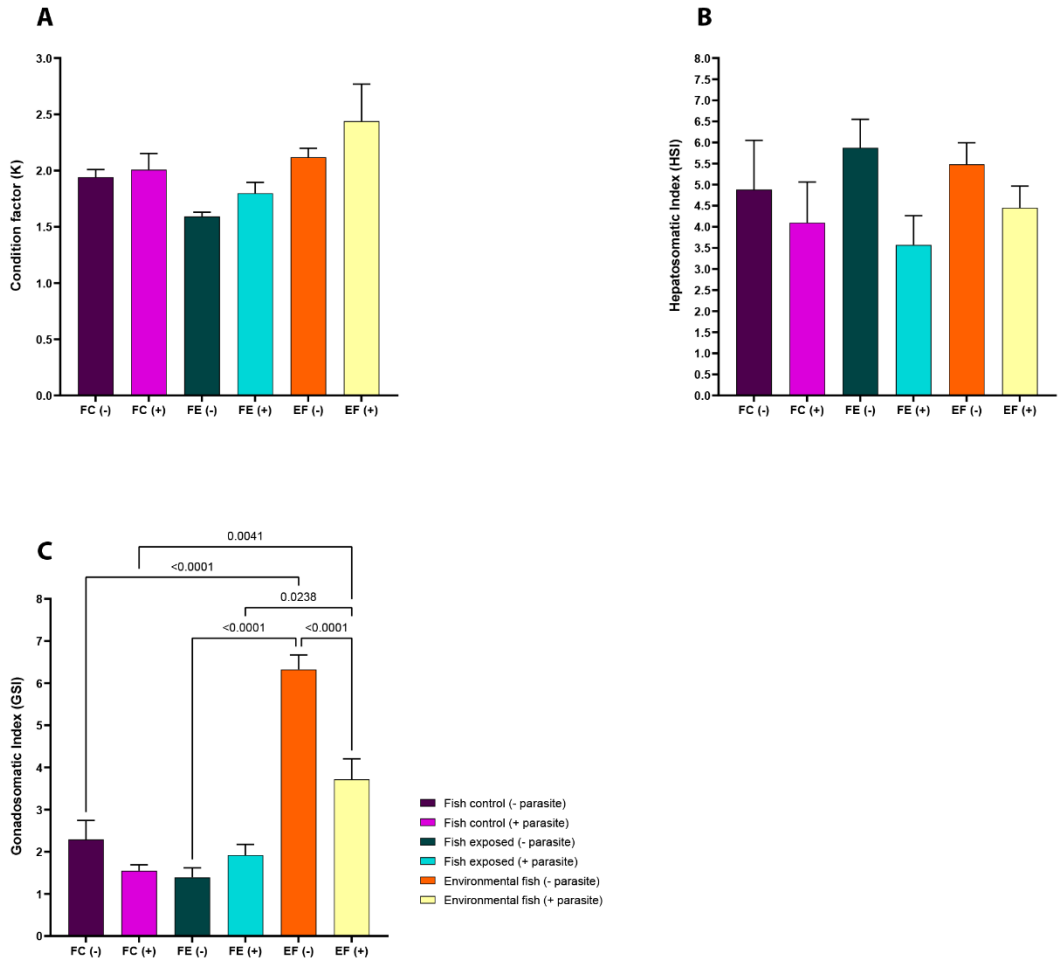

Figure 7.4: Condition factor (K), hepatosomatic index (HSI), and gonadosomatic index (GSI) of *Amblyrhynchote honckenii* (Bloch) across different treatment groups. **A** – Condition factor (K) for infested and uninfested control fish, exposed fish, and environmental fish; **B** – Hepatosomatic index (HSI) for infested and uninfested control fish, exposed fish, and environmental fish; **C** – Gonadosomatic index (GSI) for infested and uninfested control fish, exposed fish, and environmental fish. "Environmental fish" refers to specimens described in Chapter 4. All abbreviations are defined in the graph legends.

Cu accumulation patterns across host and parasite tissues (Figure 7.5; Supplementary Table 7.2) aligned with trends observed in environmental samples, but were higher, most probably due to the elevated exposure concentration. For example, Cu levels in *Cin. tetrodontis* females reached 286 µg/g dry weight compared to 55.19 µg/g in environmental samples; in *Cin. tetrodontis* males, 762 µg/g versus 65.37 µg/g. In host tissues, Cu concentrations were also elevated: uninfested liver tissue showed 8 µg/g versus 4 µg/g; infested liver tissue, 17 µg/g versus 4 µg/g; infested muscle tissue, 3 µg/g versus 0.8 µg/g; and uninfested muscle tissue, 3 µg/g versus 0.9 µg/g. In both control and exposed groups, *Cin. tetrodontis* accumulated significantly more Cu ($p<0.05$) than any host tissue (Figure 7.5A). Male isopods consistently had higher Cu

concentrations than females, reaching up to 762 ± 249 µg/g dry weight in the Cu exposure group, which was significantly higher ($p<0.05$) compared to 286 ± 40 µg/g in females (Figure 7.5A). These values were also significantly higher than those observed in isopods from wild-caught fish, reaffirming their strong capacity to bioaccumulate metals under elevated metal exposure conditions.

The liver tissue had the highest Cu concentrations in exposed individuals, with uninfested fish accumulating 16.6 ± 5.9 µg/g compared to 7.6 ± 1.8 µg/g in infested fish (Figure 7.5D). This pattern was consistent across other tissues, with gills and stomachs of uninfested fish also exhibiting higher Cu levels than those of infested individuals (Figure 7.5B–C). Muscle tissue consistently had the lowest Cu concentrations across all groups (Figure 7.4E). Importantly, infested fish displayed significantly lower ($p<0.05$) hepatic Cu concentrations than uninfested fish following Cu exposure, a trend that strongly reflected observations in environmental fish reported in Chapter 4. Furthermore, Cu concentrations increased significantly ($p<0.05$) in all exposed fish tissues relative to their respective controls. In uninfested fish, this increase was especially prominent in the gill, liver, and muscle tissues (Figure 7.5B, D, E), while in infested fish, the liver, stomach, and muscle tissues also demonstrated significant Cu accumulation following exposure. Overall, Cu accumulated most prominently in the liver and gills, in line with their roles in metal uptake and detoxification. The trend of lower accumulation in parasitised fish and higher concentrations in *Cin. tetrodontis* strongly parallels the patterns observed under natural environmental conditions, but with much higher concentrations following experimental exposure.

In response to Cu exposure, MT concentrations increased significantly ($p<0.05$) in the liver of uninfested and infested fish, with liver MT concentrations in uninfested fish increasing from 21 ± 3.3 µg/g in controls to 32 ± 2.3 µg/g, compared to infested fish increasing from 17± 3.6 µg/g to 23 ± 3.8 µg/g (Figure 7.6 B; Supplementary table 7.2). The MT concentrations in the muscle of uninfested fish increased from 26 ± 4.52µg/g to 32 ± 2.7 µg/g compared to more stable concentrations in infested fish, ranging between 24.6 ± 5.9 µg/g to 25.2 ± 3.5 µg/g (Figure 7.6 C). Notably, the MT concentrations in *Cin. tetrodontis* also increased following the exposure of the hosts to Cu, particularly the males displaying significantly ($p<0.05$) higher levels than exposed females and control males (Figure 7.6A).

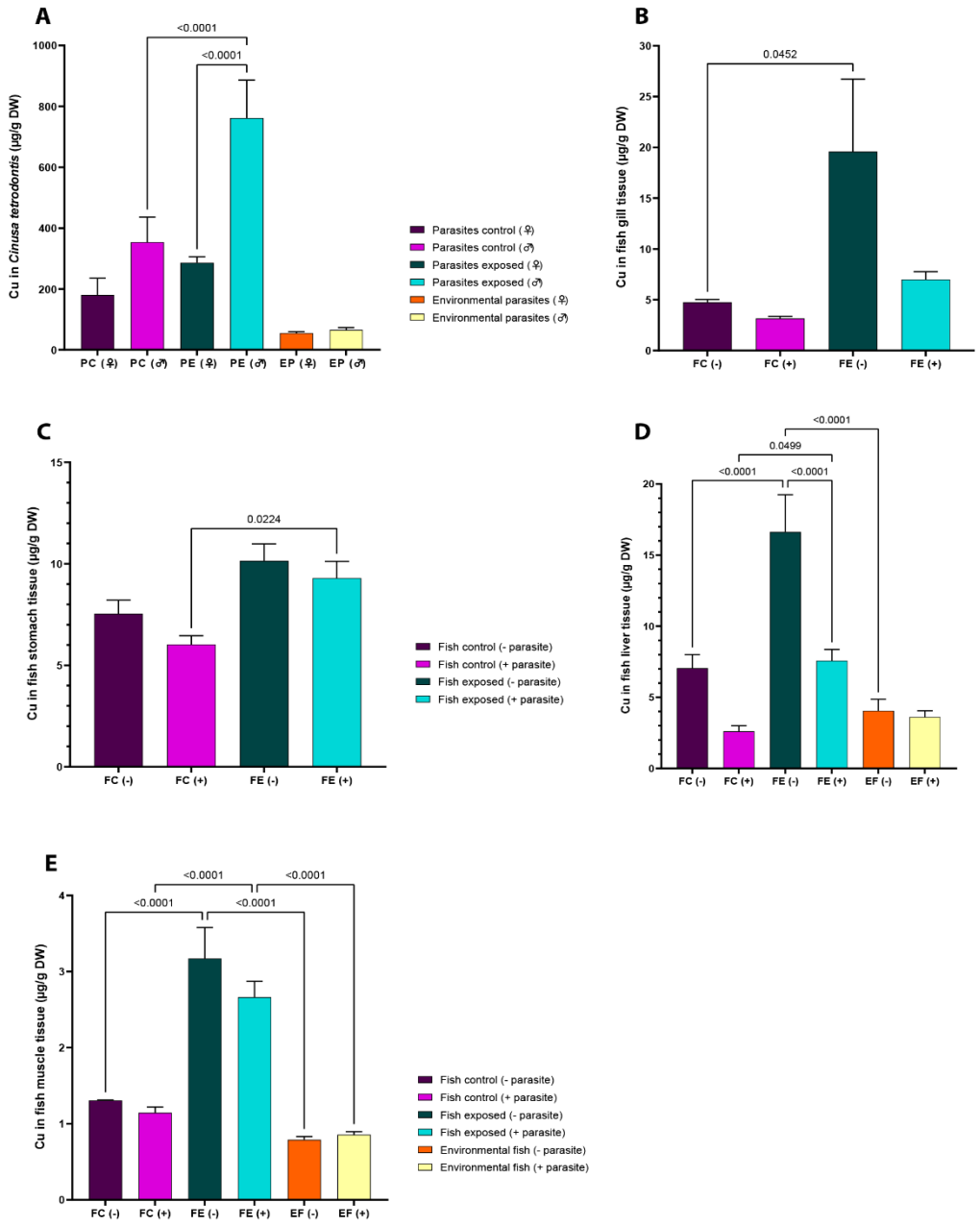

Figure 7.5: Copper (accumulation in *Cinusa tetrodontis* Schioedte & Meinert, 1884, and *Amblyrhynchote honckenii* (Bloch) across different treatment groups. **A** – *C. tetrodontis* collected from control fish, exposed fish, and environmental fish; **B** – Gill tissue of *A. honckenii* from infested and uninfested control fish and exposed fish; **C** – Stomach tissue of *A. honckenii* from infested and uninfested control fish and exposed fish; **D** – Liver tissue of *A. honckenii* from infested and uninfested control fish, exposed fish, and environmental fish; **E** – Muscle tissue of *A. honckenii* from infested and uninfested control fish, exposed fish, and environmental fish. "Environmental fish" refers to fish described in Chapter 4. All abbreviations are defined in the graph legends.

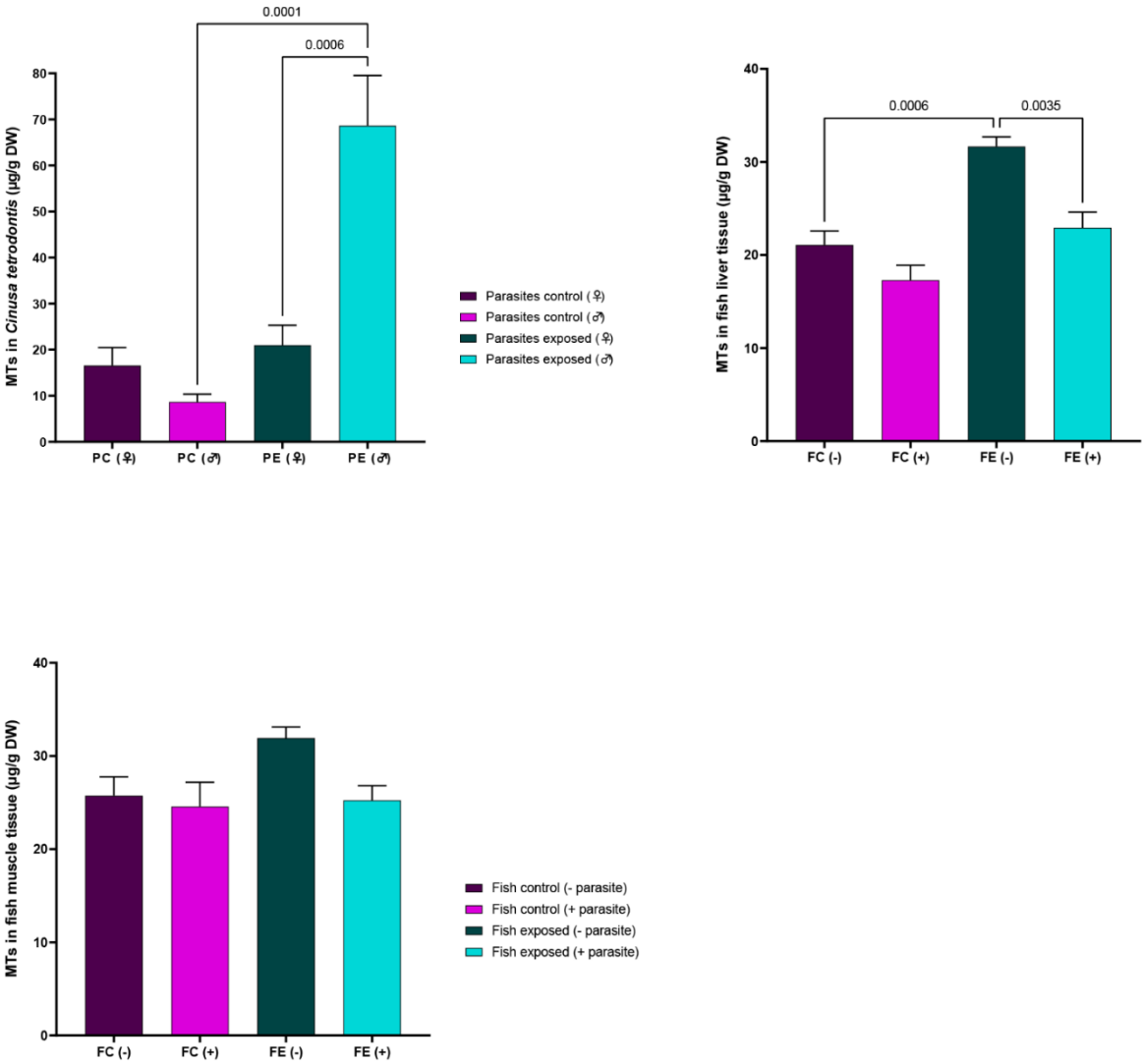

Figure 7.6: Metallothionein accumulation in *Cinusa tetrodontis* Schioedte & Meinert, 1884, and *Amblyrhynchote honckenii* (Bloch) across different treatment groups. **A** – *C. tetrodontis* collected from control fish and exposed fish; **B** – Liver tissue of *A. honckenii* from infested and uninfested control fish and exposed fish; **E** – Muscle tissue of *A. honckenii* from infested and uninfested control fish and exposed fish. All abbreviations are defined in the graph legends.

The two-way ANOVA (Table 7.4) confirmed that both species (i.e., parasite versus host tissue type) and treatment (control versus exposure) significantly affected Cu and MT concentrations ($p < 0.0001$), with notable interaction effects. This highlights the complexity of parasite-host-metal dynamics and suggests that both biotic (infestation) and abiotic (metal exposure) variables need to be considered in ecotoxicological assessments.

Table 7.2: Two-way ANOVA analysis of variance table comparing copper (Cu) and metallothionein (MTs) concentrations across species (*Cinusa tetrodontis* Schioedte & Meinert, 1884, infested and uninfested *Amblyrhynchote honckenii* (Bloch) liver and muscle tissue, and treatment groups (control and 24-hour Cu exposure).

	Species (df = 5)	Treatment (df = 1)	Interaction (df = 5)
Cu	F = 61.77; p < 0.0001	F = 15.52; p = 0.0003	F = 7.798; p < 0.0001
MTs	F = 8.046; p < 0.0001	F = 68.95; p < 0.0001	F = 19.79; p < 0.0001

7.4 Discussion

This study provides novel insights into the intricate interactions between parasitism and Cu exposure in a marine teleost host. Under controlled sublethal exposure conditions, infestation by the cymothoid isopod *Cin. tetrodontis* was shown to significantly alter Cu accumulation patterns and detoxification responses in *A. honckenii*. These findings advance the growing field of environmental parasitology and emphasise the importance of incorporating parasitic infections into interpretations of biomarker responses and pollutant bioaccumulation in aquatic organisms (Sures *et al*., 2017; Grabner *et al*., 2023).

Following Cu exposure, uptake was demonstrated, with uninfested *A. honckenii* showing the highest Cu concentrations in the gill and liver tissues. In fish, Cu uptake occurs primarily through the gills and is transported to the liver for detoxification, storage, or excretion (Wang *et al*., 2024). This pathway was evident in uninfested *A. honckenii*, with the liver and gill tissues displaying the highest Cu concentrations, reflecting their roles in metal uptake and biotransformation. These tissues are key to detoxification and metal homeostasis and typically show early signs of contaminant-induced physiological stress (Singh and Sharma, 2024). Fish infested with *Cin. tetrodontis* exhibited reduced Cu accumulation in host tissues, particularly in the liver. This suggests that parasitism by the isopod alters the host's internal metal burden, either through direct sequestration of Cu by the parasite or indirectly by modifying host physiology, such as ion regulation across the gill epithelium (Sures, 2003; Nachev and Sures, 2016; Sures and Nachev, 2022). Given that *Cin. tetrodontis* is a large parasite (female ~20 x 12 mm; male ~17 x 13 mm) and resides within the buccal cavity (Hadfield *et al*., 2010), it may physically inhibit metal uptake or induce changes in gill function, such as reduced ventilation rates or altered morphology, ultimately limiting Cu absorption (Sures and Nachev, 2022). Similar patterns have been observed in freshwater fish parasitised by internal parasites, like acanthocephalans or cestodes, that exhibited consistently lower tissue concentrations of metals like cadmium and lead (Sures and Siddall, 1999; Sures and Radszuweit, 2007). The present study, therefore, extends this ecotoxicological interaction to a marine ectoparasite-host system.

Consistent with previous field observations (Chapter 4), *Cin. tetrodontis* demonstrated a pronounced ability to bioaccumulate Cu, often exceeding the concentrations recorded in host tissues. In exposed male parasites, tissue concentrations exceeded 760 µg/g dry weight, several magnitudes higher than host levels, reflecting similar patterns observed in intestinal parasites such as acanthocephalans (Sures, 2003; Nachev and Sures, 2016). Additionally, male isopods accumulated more Cu than females, mirroring a sexually dimorphic trend reported in other ectoparasites and aquatic invertebrates, potentially linked to differences in size, surface area, metabolic rate, or feeding frequency (Vidal-Martínez *et al*., 2010). For instance, in the parasitic crustacean *Argulus japonicus* Thiele, 1900, males show higher Cu sequestration in their sclerotised carapace compared to females, as evidenced by more intense Phen-Green fluorescence in male thoracic regions (Gilbert and Avenant-Oldewage, 2018). Similarly, male marine amphipods, *Allorchestes compressa* Dana, 1852, not only accumulate more Cu but also exhibit greater Cu tolerance, linked to elevated metallothionein and glutathione-S-transferase levels, relative to females (Dong *et al*., 2020). These findings support similar trends observed in other ectoparasitic isopods such as *Ceratothoa oestroides* (Risso, 1827), suggesting that cymothoid isopods may serve as important modulating agents in marine pollution scenarios (Pérez-del Olmo *et al*., 2019). Although Cu concentration differences between infested and uninfested hosts were not always statistically significant, with significance only observed in liver tissues, the consistent trend of reduced accumulation in infested fish supports the role of the parasite as a biological metal sink. Sures *et al*. (2025) caution that such reductions may reflect passive metal competition rather than evolved adaptive strategies, where the isopod parasite, as a high-capacity sink, might indirectly limit metal uptake by the host.

The host's physiological response to Cu exposure was further evaluated through increased production of MTs. Metallothioneins are key proteins involved in binding metals and protecting cells from oxidative stress (Amiard *et al*., 2006; Singh and Sharma, 2024). The increase in hepatic MT concentrations in uninfested *A. honckenii*, indicates an active detoxification response. However, parasitised fish exhibited a reduced response with only a slight increase, in comparison to control fish, in liver MT concentrations under the same conditions. This suggests that lower tissue Cu burdens in parasitised fish reduce the need for MT induction. This finding is also consistent with earlier research demonstrating suppressed biomarker responses in parasitised hosts. Sures and Radszuweit (2007) found that the acanthocephalan *P. laevis* infecting the chub, *Squalius cephalus* (Linnaeus), exhibited lower hepatic MT levels following cadmium exposure. Similarly, Frank *et al*. (2013) observed reduced palladium-induced biomarker responses in the freshwater amphipod *Gammarus fossarum* Koch, 1836 infected with acanthocephalan parasites, reinforcing the concept that parasites can potentially buffer the host against toxicant-induced stress. Moreover, MT levels were also lower in parasitised control fish

than in uninfested controls, implying a chronic reduction in detoxification potential due to parasite presence. These results clearly show that while both infested and uninfested groups responded to Cu, the presence of *Cin. tetrodontis* was associated with a reduction of MTs in both control and Cu-exposed fish.

Interestingly, MT induction in male *C. tetrodontis* was significantly higher following Cu exposure, whereas females showed a significantly reduced response under the same conditions. While MT induction has been extensively studied in fish, comparatively little is known about this process in crustacean ectoparasites. Vidal-Martínez *et al.* (2010) demonstrated MT upregulation in helminths, and this study provides some of the first evidence for similar responses in cymothoid isopods. Outside of parasitic systems, free-living isopods such as the common woodlouse *Porcellio scaber* Latreille, 1804, have been extensively studied for their metal detoxification strategies. In this species, exposure to Cu and zinc leads to upregulation of MT-like proteins and compartmentalisation of metals primarily within the hepatopancreas (Prosi and Dallinger, 1988; Žnidaršič *et al*., 2005). Similarly, the woodlouse *Oniscus asellus* Linnaeus, 1758, stores large quantities of Cu, zinc, cadmium, and lead in lysosomal vesicles within the hepatopancreas and upregulates stress proteins when exposed to mixed metal stress (Köhler and Eckwert, 1997). While MT responses have been less frequently documented in parasitic crustaceans, there is emerging evidence suggesting similar capabilities. For instance, studies on parasitic copepods, such as *Lepeophtheirus salmonis* (Krøyer, 1837), have shown upregulation of metal-binding proteins following pollutant exposure (Lauritano *et al*., 2012). Similar detoxification responses have also been documented in free-living copepods and isopods. For example, the copepod *Tigriopus japonicus* Mori, 1938, upregulates antioxidant enzymes such as superoxide dismutase (SOD) and displays metal-responsive transcriptional changes when exposed to Cu and other pollutants (Kim *et al*., 2011). Likewise, *Gladioferens pectinatus* (Brady, 1899) shows broad-scale transcriptomic responses to Cu, including altered expression of stress and detoxification pathways across multiple generations (Barrick *et al*., 2022). In this context, the response of *C. tetrodontis* provides some of the first clear evidence of MT induction in parasitic cymothoids. Importantly, unlike helminths and cestodes, which lack free-living relatives, cymothoids are closely related to these well-studied free-living taxa, enabling ecotoxicological comparisons across parasitic and non-parasitic lifestyles. Importantly, this comparison highlights a unique advantage in studying cymothoids: unlike internal helminths or cestodes, they have ecologically and phylogenetically comparable free-living counterparts, allowing for more nuanced interpretations of metal handling in parasitic versus non-parasitic lifestyles.

Given that both sexes were parasitising the same host and thus exposed to the same environmental Cu concentrations, this sexually dimorphic pattern likely reflects intrinsic

physiological differences between the sexes. One plausible explanation lies in the role of Cu as an essential micronutrient in crustaceans, particularly in female reproductive physiology. Cu is required for processes such as vitellogenesis and oocyte development (Ahearn *et al*., 2004; Rainbow, 2002), and females may therefore possess more robust regulatory mechanisms for maintaining internal Cu homeostasis. These mechanisms may involve tightly controlled Cu uptake, binding, and excretion pathways that buffer internal concentrations and minimise the need for acute MT synthesis. In contrast, males, lacking these homeostatic demands, may accumulate Cu more rapidly, triggering a protective upregulation of MTs in response to the sudden metal influx. This is supported by the observation that male isopods not only accumulated more Cu but also showed significantly elevated MT levels within just 24 h, a remarkably rapid detoxification response. The speed and magnitude of this response suggest that MT induction in males acts as an immediate buffering mechanism against acute Cu toxicity. However, it remains unclear whether this response is sustainable over longer periods. Prolonged exposure may eventually overwhelm the MT capacity in males, potentially leading to toxic effects such as oxidative damage, protein denaturation, or impaired physiological function. Conversely, female isopods may initially avoid MT induction due to effective baseline Cu regulation, but chronic or high-dose exposures could eventually saturate these pathways, triggering delayed MT upregulation. This potential divergence in short-term vs. long-term detoxification strategies between the sexes warrants further investigation and could have important implications for parasite survival, reproductive success, and metal cycling dynamics within host-parasite systems. What makes this even more intriguing is the protandrous hermaphroditism seen in cymothoid isopods: individuals mature first as males, and some later transition into females (Aneesh and Kappalli, 2020). This life-history pattern has been documented in a variety of cymothoids, including *Mothocya renardi* (Bleeker, 1857) and *Ichthyoxenus fushanensis* Tsai & Dai, 1999 (Tsai *et al*., 1999) and *C. tetrodontis* (Hadfield *et al*., 2010). Consequently, every current female was once a male and may have experienced the same chronic MT response during that phase. The lingering physiological effects of early-life MT induction, or how transitioning females ‘reprogram’ their Cu regulation, are entirely unknown but could influence reproductive capacity or longevity. Exploring whether MT profiles persist post-transition, or if MT expression resets during sex change offers rich avenues for future research.

Additionally, fish morphometric indices were also assessed as complementary indicators of fish health. These indices are widely used as indicators of nutritional status, overall health, energy reserves, and reproductive investment of fish (Marshall *et al*., 2004; Choi *et al*., 2004; Cade *et al*., 2008; Wuenschel *et al*., 2019). The slightly reduced K-values in Cu-exposed fish compared to control groups suggest a mild energetic cost associated with metal exposure. Interestingly, both in the laboratory and environmental samples, parasitised fish exhibited slightly

higher K values than uninfested fish, possibly due to compensatory feeding induced by infestation. It is also possible that differences in parasite attachment sites or host size classes could subtly influence mass-to-length ratios over short periods. The HSI increased in exposed uninfested fish, likely due to hepatic hypertrophy associated with detoxification (Wang *et al*., 2024). However, parasitised fish exhibited slightly reduced HSI under Cu exposure, suggesting lowered hepatic activity or metal uptake, which aligns with the hypothesis of parasitism-induced modulation of liver detoxification (Sures, 2003; Sures and Nachev, 2022). The GSI values remained stable across treatments but were lower in parasitised fish in environmental samples, suggesting that chronic parasitism may impair reproductive investment in natural settings. Such effects have been observed in multiple host-parasite systems, where long-term parasitic burdens have been linked to reduced gonadal development and altered endocrine regulation (Marcogliese and Pietrock, 2011). Though morphometric responses were not statistically significant over the short duration of exposure, the subtle trends detected in K, HSI, and GSI highlight the value of combining biochemical biomarkers with organism-level indicators. These indices provide a useful supplementary framework for interpreting physiological trade-offs under pollutant exposure and biological stress, particularly when integrated with data from longer-term environmental monitoring.

7.5. Conclusion

The results of this study support the proposed hypotheses (Hypotheses 6–9, Chapter 1), that *Cin. tetrodontis* functions as a biological metal sink, modulates host detoxification responses, and exhibits sex-specific physiological reactions to Cu exposure under controlled laboratory conditions. The results highlight the dual ecological role of *Cin. tetrodontis* as both a biological accumulator of metals and a modulator of host physiology. Its presence consistently reduced host tissue Cu burdens and altered biomarker patterns, particularly MT expression, while simultaneously upregulating its own detoxification pathways. However, rather than directly suppressing host detoxification, the parasite likely modulates the host's need to initiate MT-based responses by acting as an initial sink for Cu, thereby buffering the host from full toxicant exposure. In this way, *Cin. tetrodontis* may effectively absorb the ‘first wave’ of metal influx, reducing the physiological burden on the host and delaying or diminishing the induction of host detoxification pathways. These findings align with the ecological framework proposed by Smit and Sures (2025), in which parasites are recognised as integral components of contaminant cycling and biological response in aquatic ecosystems. It is important to recognise, however, that the relationship between parasitism, metal accumulation, and host stress responses is highly context-dependent. While parasite-mediated sequestration of metals can reduce tissue metal concentrations and associated biomarker responses, parasitism itself imposes energetic and immunological costs on the host (Marcogliese and Pietrock, 2011; Birk *et al*., 2020). Under certain conditions, co-exposure

to parasites and pollutants may result in additive or synergistic stress effects. Although this study did not reveal such effects during its short-term 24 h exposure duration and moderate infestation levels, longer-term studies are needed to assess cumulative impacts on growth, immunity, reproduction, and survival (Malhotra *et al*., 2020; Sures *et al*., 2017). Future research should therefore prioritise multi-stressor laboratory investigations incorporating chronic exposure periods, variable parasite intensities, and environmentally relevant fluctuations such as temperature or salinity. Chronic exposures, varying environmental conditions, and different parasite species or loads may yield more complex outcomes than those observed here. Integrating parasite-based metrics into environmental risk assessment offers a more ecologically realistic view of contaminant effects. Furthermore, the observed modulation of MT expression highlights the need for careful interpretation of biomarker data in parasitised organisms, as failure to account for parasitic influence may lead to underestimations of environmental contamination (Grabner *et al*., 2023; Sures and Nachev, 2022). Ultimately, this study contributes to a broader understanding of host-parasite-pollutant interactions in marine environments and emphasises the importance of laboratory exposures and integrating parasitology into aquatic ecotoxicology. Parasites like *Cin. tetrodontis* not only influence metal dynamics but also affect host physiology in subtle, yet ecologically meaningful ways, making them indispensable components of marine ecosystem health assessments.

References

Ahearn, G.A., Mandal, P.K. & Mandal, A., 2004. Mechanisms of heavy-metal sequestration and detoxification in crustaceans: a review. *Journal of Comparative Physiology B*, 174: 439–452.

Amiard, J.C., Amiard-Triquet, C., Barka, S., Pellerin, J. & Rainbow, P.S., 2006. Metallothioneins in aquatic invertebrates: their role in metal detoxification and their use as biomarkers. *Aquatic Toxicology*, 76(2): 160–202.

Aneesh, P.T. & Kappalli, S., 2020. Protandrous hermaphroditic reproductive system in the adult phases of *Mothocya renardi* (Bleeker, 1857) (Cymothoidae: Isopoda: Crustacea) – light and electron microscopy study. *Zoological Studies*, 59: e61.

Barrick, A., Laroche, O., Boundy, M., Pearman, J.K., Wiles, T., Butler, J., Pochon, X., Smith, K.F. & Tremblay, L.A., 2022. First transcriptome of the copepod *Gladioferens pectinatus* subjected to chronic contaminant exposures. *Aquatic Toxicology*, 243: 106069.

Birk, S., Chapman, D., Carvalho, L., Spears, B.M., Andersen, H.E., Argillier, C., Auer, S., Baattrup-Pedersen, A., Banin, L., Beklioğlu, M. & Bondar-Kunze, E., 2020. Impacts of multiple stressors on freshwater biota across spatial scales and ecosystems. *Nature Ecology & Evolution*, 4(8): 1060–1068.

Cade, B.S., Terrell, J.W. & Porath, M.T., 2008. Estimating fish body condition with quantile regression. *North American Journal of Fisheries Management*, 28(2): 349–359.

Choi, J.S., Frank, K.T., Leggett, W.C. & Drinkwater, K., 2004. Transition to an alternate state in a continental shelf ecosystem. *Canadian Journal of Fisheries and Aquatic Sciences*, 61(4): 505–510.

Cui, L., Li, X., Luo, Y., Gao, X., Chen, L., Lv, X., Peng, J., Zhang, H. & Lei, K., 2024. Comprehensive effects of salinity, dissolved organic carbon and Cu on mortality, osmotic regulation and bioaccumulation of Cu in *Oryzias melastigma*. *Science of The Total Environment*, 927: 172289.

Degger, N., Wepener, V., Richardson, B.J. & Wu, R.S.S., 2011. Application of artificial mussels (AMs) under South African marine conditions: a validation study. *Marine Pollution Bulletin*, 63(5–12): 108–118.

Dong, D.T., Miranda, A.F., Carve, M., Shen, H., Trestrail, C., Dinh, K.V. & Nugegoda, D., 2020. Population- and sex-specific sensitivity of the marine amphipod *Allorchestes compressa* to metal exposure. *Ecotoxicology and Environmental Safety*, 206: 111130.

Erasmus, J.H., Wepener, V., Nachev, M., Zimmermann, S., Malherbe, W., Sures, B. & Smit, N.J., 2020. The role of fish helminth parasites in monitoring metal pollution in aquatic ecosystems: a case study in the world's most productive platinum mining region. *Parasitology Research*, 119(9): 2783–2798.

Fantke, P., Aurisano, N., Bare, J., Backhaus, T., Bulle, C., Chapman, P.M., De Zwart, D., Dwyer, R., Ernstoff, A., Golsteijn, L. & Holmquist, H., 2018. Toward harmonizing ecotoxicity characterization in life cycle impact assessment. *Environmental Toxicology and Chemistry*, 37(12): 2955–2971.

Fernandes, I.M., Bastos, Y.F., Barreto, D.S., Lourenço, L.S. & Penha, J.M., 2016. The efficacy of clove oil as an anaesthetic and in euthanasia procedure for small-sized tropical fishes. *Brazilian Journal of Biology*, 77(3): 444–450.

Frank, S.N., Godehardt, S., Nachev, M., Trubiroha, A., Kloas, W. & Sures, B., 2013. Influence of the cestode *Ligula intestinalis* and the acanthocephalan *Polymorphus minutus* on levels of heat shock proteins (HSP70) and metallothioneins in their fish and crustacean intermediate hosts. *Environmental Pollution*, 180: 173–179.

Frank, S.N., Singer, C. & Sures, B., 2008. Metallothionein (MT) response after chronic palladium exposure in the zebra mussel, *Dreissena polymorpha*. *Environmental Research*, 108(3): 309–314.

Gilbert, B.M. & Avenant-Oldewage, A., 2018. Trace element biomineralisation in the carapace in male and female *Argulus japonicus*. *PLoS ONE*, 13(6): e0197804.

Gismondi, E., Rigaud, T., Beisel, J.N. & Cossu-Leguille, C., 2012. Microsporidia parasites disrupt the responses to cadmium exposure in a gammarid. *Environmental Pollution*, 160: 17–23.

Grabner, D., Rothe, L.E. & Sures, B., 2023. Parasites and pollutants: effects of multiple stressors on aquatic organisms. *Environmental Toxicology and Chemistry*, 42(9): 1946–1959.

Hadfield, K.A., Bruce, N.L. & Smit, N.J., 2010. Redescription of the monotypic genus *Cinusa* Schioedte and Meinert, 1884 (Isopoda, Cymothoidae), a buccal-cavity isopod from South Africa. *Zootaxa*, 2437(1): 51–68.

Hursky, O. & Pietrock, M., 2015. Intestinal nematodes affect selenium bioaccumulation, oxidative stress biomarkers, and health parameters in juvenile rainbow trout (*Oncorhynchus mykiss*). *Environmental Science & Technology*, 49(4): 2469–2476.

Kim, B.M., Rhee, J.S., Park, G.S., Lee, J., Lee, Y.M. & Lee, J.S., 2011. Cu/Zn- and Mn-superoxide dismutase (SOD) from the copepod *Tigriopus japonicus*: molecular cloning and expression in response to environmental pollutants. *Chemosphere*, 84(10): 1467–1475.

Kohler, H.R. & Eckwert, H., 1997. The induction of stress proteins (HSP) in *Oniscus asellus* (Isopoda) as a molecular marker of multiple heavy metal exposure. II: Joint toxicity and transfer to field situations. *Ecotoxicology*, 6: 263–274.

Labuschagne, M., Zimmermann, S., Smit, N.J., Erasmus, J.H., Nachev, M., Sures, B. & Wepener, V., 2021. Laboratory and field studies on the use of artificial mussels as a

monitoring tool of platinum exposure in the freshwater environment. *Environmental Sciences Europe*, 33: 1–15.

Lauritano, C., Procaccini, G. & Ianora, A., 2012. Gene expression patterns and stress response in marine copepods. *Marine Environmental Research*, 76: 22–31.

Le, T.Y., Zimmermann, S. & Sures, B., 2016. How does the metallothionein induction in bivalves meet the criteria for biomarkers of metal exposure? *Environmental Pollution*, 212: 257–268.

Li, C., Wang, H., Liao, X., Xiao, R., Liu, K., Bai, J., Li, B. & He, Q., 2022. Heavy metal pollution in coastal wetlands: A systematic review of studies globally over the past three decades. *Journal of Hazardous Materials*, 424: 127312.

Lu, Y., Wang, P., Wang, C., Zhang, M., Cao, X., Chen, C., Wang, C., Xiu, C., Du, D., Cui, H. & Li, X., 2022. Multiple pollutants stress the coastal ecosystem with climate and anthropogenic drivers. *Journal of Hazardous Materials*, 424: 127570.

Malhotra, N., Ger, T.R., Uapipatanakul, B., Huang, J.C., Chen, K.H.C. & Hsiao, C.D., 2020. Review of Cu and Cu nanoparticle toxicity in fish. *Nanomaterials*, 10(6): 1126.

Marcogliese, D.J. & Pietrock, M., 2011. Combined effects of parasites and contaminants on animal health: parasites do matter. *Trends in Parasitology*, 27(3): 123–130.

Marshall, C.T., Needle, C.L., Yaragina, N.A., Ajiad, A.M. & Gusev, E., 2004. Deriving condition indices from standard fisheries databases and evaluating their sensitivity to variation in stored energy reserves. *Canadian Journal of Fisheries and Aquatic Sciences*, 61(10): 1900–1917.

Martínez-Durazo, Á., Rivera-Domínguez, M., García-Gasca, S.A., Betancourt-Lozano, M., Cruz-Acevedo, E. & Jara-Marini, M.E., 2023. Assessing metal(loid)s concentrations and biomarkers in tilapia (*Oreochromis niloticus*) and largemouth bass (*Micropterus salmoides*) of three ecosystems of the Yaqui River basin, Mexico. *Ecotoxicology*, 32(2): 166–187.

Nachev, M. & Sures, B., 2016. Environmental parasitology: parasites as accumulation bioindicators in the marine environment. *Journal of Sea Research*, 113: 45–50.

OECD, 2019. *Test No. 203: Fish, Acute Toxicity Test*. OECD Guidelines for the Testing of Chemicals, Section 2. Paris: OECD Publishing. Available at: https://www.oecd-ilibrary.org/environment/test-no-203-fish-acute-toxicity-test_9789264069961-en. (Date accessed: 25 June 2023).

Pérez-del-Olmo, A., Nachev, M., Zimmermann, S., Fernández, M. & Sures, B., 2019. Medium-term dynamics of element concentrations in a sparid fish and its isopod parasite after the Prestige oil-spill: shifting baselines? *Science of the Total Environment*, 686: 648–656.

Prosi, F. & Dallinger, R., 1988. Heavy metals in the terrestrial isopod *Porcellio scaber* Latreille. I. Histochemical and ultrastructural characterization of metal-containing lysosomes. *Cell Biology and Toxicology*, 4: 81–96.

Rainbow, P.S., 2002. Trace metal concentrations in aquatic invertebrates: why and so what? *Environmental Pollution*, 120(3): 497–507.

Saadati, N., Abdullah, M.P., Zakaria, Z., Sany, S.B.T., Rezayi, M. & Hassonizadeh, H., 2013. Limit of detection and limit of quantification development procedures for organochlorine pesticides analysis in water and sediment matrices. *Chemistry Central Journal*, 7: 1.

Scheuhammer, A.M. & Cherian, M.G., 1986. Quantification of metallothioneins by a silver-saturation method. *Toxicology and Applied Pharmacology*, 82(3): 417–425.

Singh, G. & Sharma, S., 2024. Heavy metal contamination in fish: sources, mechanisms and consequences. *Aquatic Sciences*, 86(4): 107.

Smit, N.J. & Sures, B. (eds.), 2025. *Aquatic Parasitology: Ecological and Environmental Concepts and Implications of Marine and Freshwater Parasites*. Cham: Springer Nature.

Sures, B. & Nachev, M., 2022. Effects of multiple stressors in fish: how parasites and contaminants interact. *Parasitology*, 149(14): 1822–1828.

Sures, B. & Radszuweit, H., 2007. Pollution-induced heat shock protein expression in the amphipod *Gammarus roeseli* is affected by larvae of *Polymorphus minutus* (Acanthocephala). *Journal of Helminthology*, 81(2): 191–197.

Sures, B. & Siddall, R., 1999. *Pomphorhynchus laevis*: the intestinal acanthocephalan as a lead sink for its fish host, chub (*Leuciscus cephalus*). *Experimental Parasitology*, 93(2): 66–72.

Sures, B., 2003. Accumulation of heavy metals by intestinal helminths in fish: an overview and perspective. *Parasitology*, 126(S7): S53–S60.

Sures, B., 2004. Fish acanthocephalans of the genus *Pomphorhynchus* sp. as globally applicable bioindicators for metal pollution in the aquatic environment? *Wiener Klinische Wochenschrift*, 116: 611–619.

Sures, B., 2006. How parasitism and pollution affect the physiological homeostasis of aquatic hosts. *Journal of Helminthology*, 80(2): 151–157.

Sures, B., Nachev, M., Grabner, D., Wepener, V. & Zimmermann, S., 2025. Environmental parasitology: interactions between parasites and pollutants. In: N.J. Smit & B. Sures, eds. *Aquatic Parasitology: Ecological and Environmental Concepts and Implications of Marine and Freshwater Parasites*. Cham: Springer, pp. 509–534.

Sures, B., Nachev, M., Selbach, C. & Marcogliese, D.J., 2017. Parasite responses to pollution: what we know and where we go in ‘Environmental parasitology’. *Parasites & Vectors*, 10(1): 1–19.

Van Der Spuy, L., Erasmus, J.H., Nachev, M., Schaeffner, B.C., Sures, B., Wepener, V. & Smit, N.J., 2023. The use of fish parasitic isopods as element accumulation indicators in marine pollution monitoring. *Marine Pollution Bulletin*, 194: 115385.

Vidal-Martínez, V.M., Pech, D., Sures, B., Purucker, S.T. & Poulin, R., 2010. Can parasites really reveal environmental impact? *Trends in Parasitology*, 26(1): 44–51.

Wang, L., Wang, H., Gao, C., Wang, C., Yan, Y. & Zhou, F., 2024. Dietary Cu for fish: homeostasis, nutritional functions, toxicity, and affecting factors. *Aquaculture*, 740875.

Wuenschel, M.J., McElroy, W.D., Oliveira, K. & McBride, R.S., 2019. Measuring fish condition: an evaluation of new and old metrics for three species with contrasting life histories. *Canadian Journal of Fisheries and Aquatic Sciences*, 76(6): 886–903.

Žnidarŝiĉ, N., Tuŝek-Žnidariĉ, M., Falnoga, I., Ŝĉanĉar, J. & Ŝtrus, J., 2005. Metallothionein-like proteins and zinc-Cu interaction in the hindgut of *Porcellio scaber* (Crustacea: Isopoda) exposed to zinc. *Biological Trace Element Research*, 106: 253–264.

8 General discussion and conclusions

8.1 General discussion

The findings of this study reinforce key concepts in environmental parasitology, particularly the value of parasites as bioindicators of marine pollution and ecosystem health. Each chapter of this study presents various interrelated findings. First, a rich diversity of metazoan parasites was documented in *A. honckenii*, including several new species and records (Chapter 3). Second, the parasitic isopod *Cin. tetrodontis* was shown to accumulate trace elements at significantly higher concentrations than host tissues, indicating its value as a bioindicator for element pollution (Chapter 4). Third, significant levels of OCPs and PCBs were detected in *A. honckenii* across multiple coastal localities, with notable hotspots of contamination (Chapter 5). Fourth, parasite community structure shifts along environmental gradients, where factors such as contaminant load and biogeographic region, as well as conservation status (MPA, near-MPA and non-MPA), were identified as key drivers of parasite community composition (Chapter 6). Lastly, controlled laboratory exposures demonstrated that parasite infection by *Cin. tetrodontis* can markedly alter metal uptake and detoxification responses in the fish host (Chapter 7).

8.1.1 Rich parasite diversity

Across all sampled fish, nearly 3900 individual parasites were recorded, spanning eight major groups: acanthocephalans, cestodes, copepods, isopods, monopisthocotyleans, polyonopisthocotyleans, nematodes and trematodes. This diversity greatly exceeds prior records for *A. honckenii* (Bray, 1986; Smit and Davies, 2001; Hadfield *et al*., 2010; Lisitsyna *et al*., 2019; Hayes *et al*., 2021; Acosta and Smit, 2021; Van Der Spuy *et al*., 2025), confirming that its parasite fauna had been underestimated. Furthermore, the discovery of previously undescribed species (e.g., two new species of *Ergasilus*) and new host or geographic records for several of the

documented parasite taxa further demonstrates how little was known about *A. honckenii* prior to this research.

This high parasite diversity reflects the species' broad habitat range and omnivorous benthic diet, which exposes it to multiple pathways for parasite transmission. *Amblyrhynchote honckenii* inhabits various habitats, from estuaries and intertidal pools to deeper coastal reefs (Smith and Heemstra, 2012; Froese and Pauly, 2025), and feeds on diverse prey, including crustaceans and molluscs, each potentially serving as an intermediate host of unique parasites. Its relative size (~30 cm) (Smith and Heemstra, 2012) further supports infection by a wide range of parasite species (Marcogliese, 2023). The parasite community thus mirrors South Africa's complex coastal food webs and highlights parasites as indicators of biodiversity and ecological interactions (Marcogliese, 2023). Characterising these parasites provides insights into the ecological role of this non-commercial host and establishes a foundation for understanding marine parasite biodiversity in the region.

When compared to well-studied commercial pufferfishes, such as the Japanese tiger puffer *T. rubripes*, which hosts at least 18 parasite species (Ogawa and Inouye 1997), the 22 parasite species recorded in *A. honckenii* from limited sampling size are striking. New parasite species continue to be described in Japanese puffers, exemplified by five new species of *Heterobothrium* described as recently as 2022 (Ogawa and Itoh, 2022). The parasite fauna of *T. rubripes* is thus extremely well-characterised in terms of taxonomy, life cycles, and pathogenic effects, largely because of aquaculture-driven concern and research investment. This has not only improved fish health management in aquaculture but also provided a model system for host-parasite ecology and coevolution studies in Japan (Ogawa and Inouye 1997). This comparison challenges the notion that only commercially important fish warrant extensive parasite surveys and shows that non-commercial species like *A. honckenii* can host equally diverse parasite communities. These findings support the hypothesis that South Africa's marine fishes, rich in diversity and endemism, harbour many undescribed parasites (Smit and Hadfield, 2015). Baseline parasitological surveys of diverse fish hosts are urgently needed. Without them, a substantial portion of marine biodiversity remains hidden. Building parasite inventories for African fishes, following the Japanese model, will greatly enhance scientific understanding and resource management in southern African marine ecosystems.

8.1.2 *Cinusa tetrodontis* as bioindicators

This research further demonstrated that the marine parasitic isopod *Cin. tetrodontis* and its fish host *A. honckenii* can serve as a sensitive bioindicator combination for trace element pollution. *Cinusa tetrodontis* accumulated significantly higher levels of elements like As, Cu, Mn,

Ni, Pb, Se, and Zn in its tissues compared to the host's liver and muscle across both pristine and polluted environments (Van Der Spuy *et al*., 2023). This finding extends previous knowledge that certain endoparasites bioconcentrate heavy metals (Sures, 2004; Vidal-Martínez *et al*., 2010; Nachev and Sures, 2016; Erasmus *et al*., 2020), by demonstrating that ectoparasitic isopods also sequester bioavailable elements from the marine environment. The accumulation of elements within the parasite's tissues indicates biological uptake rather than mere surface adsorption, confirming the parasite as a living accumulation indicator of marine pollution (Sures *et al*., 2017; Sures *et al*., 2025).

Furthermore, *Cin. tetrodontis* reflected site-specific differences in pollution exposure, with higher Ni and Cu burdens found in parasites from an industrialised harbour compared to those from a near-pristine estuary, mirroring local contaminant profiles (Van Der Spuy *et al*., 2023). In contrast, *A. honckenii* exhibited less consistent spatial differences, possibly due to physiological regulation or parasite sequestration of elements. For most elements, except Cd, parasite concentrations exceeded those in the fish liver (Van Der Spuy *et al*., 2023), emphasising the parasite's role as a natural concentrator that amplifies trace contamination signals that may be undetectable in host tissues or water samples alone (Gilbert and Avenant-Oldewage, 2017; Sures *et al*., 2017; Pérez-del-Olmo *et al*., 2019). This bioaccumulation provides an integrated, time-averaged measure of pollutant bioavailability, essential for marine pollution monitoring.

This host-parasite system also offers insight into host-pollutant interactions. Although *A. honckenii* accumulated elements in its organs, parasite presence appeared to influence this accumulation. Previous studies have shown that parasites, acting as sinks, reduce host element burdens (Sures *et al*., 2017; Sures *et al*., 2025). Significant correlations between element concentrations in parasites and host livers suggest a coupled dynamic in polluted environments, where fish with more contaminated livers also harboured parasites with higher element loads. While evidence for a protective effect of parasites on host metal levels was complex and subtle, these findings highlight the importance of considering parasite infection status in biomonitoring studies (Sures *et al*., 2017; Sures *et al*., 2025).

From a bioindicator perspective, the *A. honckenii*-*Cin. tetrodontis* combination presents practical advantages as a sentinel system. *Amblyrhynchote honckenii* is an endemic, non-commercial fish species (Froese and Pauly, 2025), reducing confounding effects from fisheries or translocation. The parasite, residing in the fish's buccal cavity over a long term (Hadfield *et al*., 2010), is continuously exposed to host pollutant conditions, thereby providing a time-integrated record of contaminant exposure. This approach addresses a gap in marine pollution monitoring, where free-living bioindicators and water sampling often miss biologically sequestered pollutants

or only detect surface adsorption (Sures *et al*., 2017; Erasmus *et al*., 2022). Including parasite indicators ensures that measured pollutants have entered the trophic network (Sures *et al*., 2017). This work advances environmental parasitology by demonstrating the utility of a marine ectoparasite as a trace element bioindicator, broadening the predominantly freshwater and endoparasite-focused literature (Sures *et al*., 2017; 2025). It represents a significant step in applying parasite-based indicators to complex coastal marine environments, where such approaches remain underutilised. Overall, the findings support the hypothesis that *Cin. tetrodontis* effectively indicates trace metal pollution, and the *A. honckenii*-parasite system enhances marine pollution biomonitoring, forming a foundation for future exploration of host-parasite-pollutant dynamics and global comparisons.

8.1.3 *Amblyrhynchote honckenii* as bioindicator

Building on the parasite-related bioindicator findings, the focus expanded to examine the accumulation of organic pollutants, specifically OCPs and PCBs, in *A. honckenii* across multiple coastal localities with varying protection statuses. Although parasites were not directly analysed for these organic pollutants, the study emphasises that both parasites and their hosts reflect environmental contaminant burdens. This investigation considers how MPAs might mitigate pollutant accumulation, linking ecosystem integrity to lower pollution levels and higher biodiversity. Measuring chemical residues in a sentinel fish provides ecological context for understanding parasite responses and highlights multiple stressors affecting marine health.

Consistent with global findings, banned OCPs and PCBs persist in marine food webs, even within MPAs (Ramírez-Ayala *et al*., 2021; de Klerk *et al*., 2025). By comparing six localities from near-pristine to impacted environments, the study showed that fish from high-impacted localities near urban runoff or harbours had elevated POPs, whereas fish from well-managed MPAs, such as SB, showed lower concentrations. However, MPAs do not fully prevent pollution to reach the organisms living there, as oceanographic transport and atmospheric deposition can introduce contaminants into reserve waters (Boersma *et al*., 1999; De Klerk *et al*., 2025). For instance, Firth *et al*. (2019) documented local urban pollutants affecting protected reefs, paralleling observations of detectable OCP and PCB levels in fish from near-MPA areas. Although fewer studies have used fish parasites as indicators of organic pollutants, emerging evidence indicates that acanthocephalans and cestodes can also accumulate POPs at higher levels than their hosts (Molbert *et al*., 2020), which could extend to the *A. honckenii-Cin. tetrodontis* combination.

Using *A. honckenii* as a bioindicator species for organic pollutants potentially offers more practical advantages. As a non-commercial, reef-associated fish (Froese and Pauly, 2025), *A.*

honckenii remains in local reef habitats and is not subject to fishing pressure. This means its contaminant load reflects local pollution exposure without confounding factors like fisheries-driven population changes or long-distance migrations (Wood and Lafferty, 2015). Unlike sessile mussel bioindicators that measure water quality at fixed points (Wepener and Degger, 2020), this mobile species integrates exposure across reef habitats through multiple pathways, including sediment and prey. Sampling inside and outside MPAs enables assessment of whether protection reduces contaminant burdens in marine biota, informing conservation policy. Evidence suggests that MPAs like SB support fish populations with lower POP concentrations, supporting the role of MPAs in preserving both biodiversity and environmental quality (de Klerk *et al*., 2025). However, moderate pollutant levels detected near but outside MPAs, such as CE, highlight the influences of land-based runoff and regional pollution. This indicates that MPAs are necessary, but not sufficient alone for pollution mitigation (Boersma *et al*., 1999; de Klerk *et al*., 2025). Integrated coastal management must combine MPAs with broader pollution controls, including upstream agricultural practices and harbour emission regulations, to safeguard biodiversity and ecosystem health effectively.

Conceptually, this integrated approach links chemical pollutant monitoring with ecological context, reinforcing the value of studying host-parasite systems along contamination gradients rather than in isolation. The contaminant data provide a foundation for interpreting parasite community responses.

8.1.4 Ecological parasitology

The identification of parasites and their hosts as bioindicators of contaminant burdens provides a foundation for understanding how parasite community structure varies along environmental gradients, including climate, pollution, and protection status and provides critical insights into parasites as effect indicators of ecosystem condition. Consistent with foundational concepts in aquatic parasitology, changes in parasite diversity and composition mirror differences in habitat quality and anthropogenic stress. Localities with lower pollution and MPAs support richer, more balanced parasite assemblages dominated by complex, multi-host taxa such as cestodes or trematodes, which reflect intact food webs and ecological connectivity (Lafferty and Kuris, 1999; Grabner *et al*., 2023). In contrast, heavily polluted or degraded localities harbour simplified communities dominated by opportunistic, direct-cycle parasites, indicating loss of parasite life cycle complexity due to anthropogenic stress (Erasmus *et al*., 2022; Grabner *et al*., 2023; Vermaak, 2024). This pattern aligns with global studies that disturbance reduces parasite biodiversity, particularly specialists, while protection fosters richness (Marcogliese, 2023). Moreover, conservation status and local water quality often outweigh latitudinal influences on parasite diversity, as well-managed temperate MPAs can host unexpected diversity hotspots

(Marcogliese, 2023). The species accumulation data for *A. honckenii* further support the need for more comprehensive parasite biodiversity surveys in understudied regions (Nunkoo, 2019).

Using *A. honckenii* and its parasites as integrated bioindicators offers distinct advantages owing to the fish's resident, non-commercial status and broad parasite fauna. Its distribution across temperate to subtropical ecoregions and minimal fishing pressure allows confident environmental comparisons (Smith and Heemstra, 2012; Froese and Pauly, 2025). The coupled host-parasite system integrates chemical and biological signals of environmental stress. Contaminant burdens in fish tissues reflect chemical exposure, while parasite community composition reveals the ensuing effect to the biological integrity (Sures *et al*., 2017; Erasmus *et al*., 2022). This approach captures biodiversity facets often missed by monitoring programs focused solely on commercially important species, supporting recent recommendations to incorporate parasite data in marine conservation and monitoring (Wood *et al*., 2010; 2013; 2018). Importantly, parasite surveys in such hosts can provide early warnings of ecosystem degradation before fish populations or chemical parameters exhibit change.

This research substantiates parasite community metrics, such as richness, evenness, and diversity, as effective indicators of host biological integrity disturbances and the success of protection efforts, linking parasitology and conservation science (Wood *et al*., 2018; Marcogliese, 2023). MPAs promote parasite diversity by sustaining host populations and intact food webs, but their efficacy depends on adequate size, enforcement, and complementary pollution control to counter external contaminant influx (Boersma, 1999). Given parasites' long-lived life cycles, they can integrate environmental changes over time, enhancing long-term monitoring and management, especially in multi-stressor regions like South Africa (Smit and Hadfield, 2015). The identification of parasite diversity hotspots near MPAs, such as WS and CE, provides key information for conservation prioritisation and management practices. Integrating parasitological, environmental, and biogeographic data reinforces the paradigm that biodiversity promotes further biodiversity; monitoring parasite communities offers a more complete assessment of ecosystem health than free-living species alone (Marcogliese, 2023). These findings confirm that parasite communities in *A. honckenii* are sensitive and reliable indicators of environmental quality and anthropogenic impact. This reinforces the value of parasite-based indices within marine ecosystem assessment and furthers the necessity for their routine inclusion in biodiversity monitoring, conservation planning, and pollution mitigation efforts.

8.1.5 Experimental insight into host-parasite-pollutant interactions

The experimental investigation on the influence of parasite infection on pollutant bioaccumulation and physiological responses in *A. honckenii* provides critical insights into host-

parasite-pollutant interactions, which is a core focus of environmental parasitology (Sures *et al*., 2017; Grabner *et al*., 2023; Sures *et al*., 2025). Exposing both parasitised and uninfected fish to acute Cu concentrations revealed that fish infested with the ectoparasitic isopod, *Cin. tetrodontis* accumulated significantly less Cu in tissues. This suggests that the parasite, by residing in the buccal cavity, either sequesters Cu itself or alters host uptake pathways, effectively reducing the host's metal burden, thereby providing direct experimental evidence of parasites acting as pollutant sinks (Sures *et al*., 2025). Additionally, the presence of the parasite influenced the host's detoxification mechanisms, as demonstrated by modified MT induction levels, indicating complex interactions between infection status and contaminant exposure. These findings highlight the broader concept that parasites modulate the toxicological pathways of pollutants, which can alter ecotoxicological biomarker responses and may confound standard toxicity assessments that typically neglect symbiotic status (Sures *et al*., 2017; Grabner *et al*., 2023; Sures *et al*., 2025).

This experimental evidence complements and advances recent literature documenting the multifaceted roles of parasites in ecotoxicology, where infections can either exacerbate contaminant toxicity or initiate unexpected tolerance (Sures *et al*., 2025). The study also highlights the significance of incorporating naturally infected, non-commercial host-parasite models in pollution research, addressing a critical gap where laboratory toxicology often excludes parasitism (Sures *et al*., 2017). By demonstrating that parasites accumulate elements and thereby alter host tissue contaminant levels, this work suggests that monitoring both host and parasite tissues yields a more complete understanding of pollutant distribution and ecological risk.

These results emphasise the need to integrate biotic interactions such as parasitism into risk assessments and biomonitoring protocols (Sures *et al*., 2025). Practically, parasite infection status must be considered when interpreting biomarker data to avoid under- or over-estimation of pollutant effects (Sures and Nachev, 2022; Grabner *et al*., 2023). Parasite contaminant burdens and biomarkers may serve as complementary indicators of environmental contamination alongside traditional host indicators. Establishing a marine host-ectoparasite experimental model using *A. honckenii* and *Cin. tetrodontis* demonstrates the feasibility of studying complex pollutant interactions in ecologically relevant organisms beyond standard parasite-free laboratory species. This approach opens avenues for future research exploring host-parasite models following exposure to various pollutants (e.g., microplastics, hydrocarbons) and expands the toolkit for environmental parasitology and ecotoxicology integration. Furthermore, Chapter 7 provides mechanistic confirmation that parasite infections shape host pollutant accumulation patterns and biomarker responses, a critical acknowledgement for marine environmental health assessments. These findings reinforce the notion that parasite-pollutant interactions are complex but essential

to incorporate within ecosystem-level monitoring and management strategies aimed at accurately evaluating pollution impacts (Sures and Nachev, 2022; Grabner *et al*., 2023).

8.2 Knowledge gaps and future recommendations

Despite advances in marine parasitology, critical gaps remain in understanding host-parasite interactions and their ecological roles. Marine ecosystems are increasingly threatened by multiple stressors, including pollution, habitat degradation, and climate change, necessitating robust tools for environmental health assessment. Parasites, as integral components of biodiversity and ecosystem function, offer valuable insights into ecological integrity and anthropogenic impacts. Building on the insights gained from evaluating *A. honckenii* and its diverse parasite communities as sensitive bioindicators of marine ecosystem health, several targeted recommendations emerge to advance both fundamental research and applied environmental monitoring. These proposals aim to strengthen our understanding of host-parasite interactions, refine bioindicator frameworks, and support more effective management of South Africa's marine environments in the face of ongoing ecological change.

1. **Expand parasite biodiversity surveys using *A. honckenii*:**
   Continue targeted parasitological surveys of *A. honckenii* across broader spatial and temporal gradients along the South African coast and its wider distribution. This will uncover further undescribed and regionally rare parasite taxa, refine host-parasite association records, and establish comprehensive baselines for monitoring changes in marine biodiversity.

2. **Integrate parasite metrics in routine marine health monitoring:**
   Embed parasite richness, community structure, and infection parameters into ongoing marine environmental assessment programs, especially within and around MPAs. Regular monitoring using *A. honckenii* and its parasite fauna can provide early warning signals of ecosystem degradation and track the effectiveness of conservation measures.

3. **Advance host-parasite-pollutant research:**
   Undertake experimental studies with longer exposure durations to manipulate both contaminant levels and parasite infection, particularly with *Cin. tetrodontis*, to clarify the mechanistic pathways by which parasites influence bioaccumulation, biomarker response, and host resilience. Comparative laboratory and fieldwork will improve the understanding and support of biomonitoring protocols that account for infection status.

In addition, this experimental framework can also be used to test the effects of other priority elements and pollutants as well.

4. **Employ molecular and integrative detection methods:**
   Combine classical morphology with molecular tools (e.g., eDNA, whole genome sequencing, and stable isotope analysis) in parasite detection and characterisation. Applying these to *A. honckenii* and its now known parasite communities will resolve cryptic diversity, clarify life cycles, and strengthen food web and biomarker analyses.

5. **Assess parasite responses to multiple stressors:**
   Investigate how parasite communities in *A. honckenii* respond to combined pressures from pollution, habitat change, fishing effort, and climate variability. This should include examining shifts in community composition, functional traits, and infection dynamics under realistic environmental scenarios.

6. **Strengthen comparative studies across protected and impacted localities:**
   Continue sampling *A. honckenii* and parasites from both MPAs and adjacent non-protected or intermediate localities, to better understand the effects of protection status, local habitat factors, and pollutant gradients on parasite biodiversity and bioindicator potential.

7. **Evaluate parasites as pollutant accumulators, not as remediation tools:** Emerging evidence suggests that acanthocephalans and cestodes can accumulate POPs and trace elements at levels higher than their hosts. Future work should assess this for *Cin. tetrodontis* in *A. honckenii*. However, while such findings highlight their potential as sensitive bioassays for locality-specific pollutant risks, their use should remain restricted to understanding contaminant pathways and improving biomonitoring.

8. **Develop a South African host-parasite laboratory model:**
   South Africa could benefit from establishing a controlled laboratory model using *A. honckenii* and its parasites, parallel to the established *Takifugu* pufferfish systems in Japan. Such a model would enable experimental work on parasite-pollutant interactions, parasite life cycles, and physiological effects under controlled conditions, thereby bridging field observations and mechanistic research.

9. **Initiate long-term, evolutionary, and adaptive monitoring:**

Begin longitudinal studies to monitor evolutionary shifts in both host and parasite populations related to environmental change. Tracking adaptive responses in *A. honckenii's* parasite system over time under changing pollution and climate regimes will improve predictive power for future management.

10. Promote interdisciplinary collaboration:

Foster partnerships among parasitologists, ecotoxicologists, conservation biologists, and resource managers. Such collaboration is vital for translating *A. honckenii*-parasite system research into effective ecosystem health management and policy interventions.

By addressing these recommendations, research on *A. honckenii* and its parasites can continue to shape environmental parasitology and reinforce the value of non-commercial host-parasite systems as foundational bioindicators for marine health in a changing world.

8.3 Conclusions

This study tested several key hypotheses concerning the parasite communities of *A. honckenii* and their interactions with environmental contaminants (Chapter 1):

1. *Amblyrhynchote honckenii* hosts a greater diversity of metazoan parasites than currently documented, including undescribed or regionally rare taxa, reflecting potentially host-specific associations (Chapter 3).
2. External crustacean parasites, particularly *Cin. tetrodontis*, of *A. honckenii* accumulate significantly higher levels of elements than their host (Chapter 4).
3. Levels of POPs in *A. honckenii* are significantly lower in MPAs than in non-protected localities (Chapter 5).
4. Parasite diversity displays spatial trends, with richness and complexity expected to peak in subtropical regions, particularly the Natal ecoregion, and decline toward temperate and colder zones like the Agulhas Bank (Chapter 6).
5. Elevated organic pollutants in hosts correlate with reduced parasite richness and dominance of directly transmitted or opportunistic taxa, while pristine and ecologically intact localities, especially within or near-MPAs, are expected to support rich, complex parasite communities (Chapter 6).
6. Infestation by the ectoparasite *Cin. tetrodontis* reduces copper (Cu) accumulation in host tissues by acting as a biological sink (Chapter 7).
7. The presence of *Cin. tetrodontis* alters host detoxification, particularly metallothionein (MT) expression, reducing biomarker activation needs (Chapter 7).

8. *Cinusa tetrodontis* itself actively responds to Cu exposure, exhibiting sex-specific MT induction patterns linked to physiological differences (Chapter 7).
9. Short-term laboratory exposures can reproduce Cu accumulation and biomarker trends observed in environmental conditions, validating controlled experiments for host-parasite-pollutant interaction studies (Chapter 7).

The findings of the study comprehensively support these hypotheses with nuances in spatial diversity patterns. *A. honckenii* harbours a richly diverse metazoan parasite assemblage, including previously undocumented taxa, underscoring the host's sentinel value. The study supports that external parasites bioaccumulate elements at significantly higher levels than their host tissues, validating their role as pollutant sinks. POP burdens in *A. honckenii* are lower within MPAs relative to impacted areas, affirming conservation effectiveness in reducing chemical stressors. While spatial trends in parasite diversity generally reflect expected latitudinal gradients, the highest parasite richness occurred not directly within the SB MPA but rather in a near-MPA intermediate locality (CE). This pattern reflects the complexity of local environmental conditions and conservation management, illustrating that protection status alone does not entirely dictate parasite diversity. Similarly, parasite communities in highly contaminated localities showed expected reductions in richness and evenness, dominated by opportunistic, direct-cycle taxa. Yet, the responses were influenced by a combination of pollution levels, habitat quality, and host ecology. Experimental exposures with the ectoparasite *Cin. tetrodontis* substantiated its role as a biological sink, reducing Cu accumulation in host tissues and modulating MT induction in infected fish. Furthermore, *Cin. tetrodontis* exhibited sex-specific MT responses under Cu exposure, indicating physiological differences between males and females. Laboratory trials successfully reproduced environmentally observed contaminant and biomarker patterns, validating controlled experiments as effective tools for elucidating host-parasite-pollutant dynamics.

The study advocates integrating parasite community and pollutant bioaccumulation data to enhance biodiversity monitoring, conservation planning, and environmental risk assessments. By elucidating complex host-parasite interactions, this work deepens our understanding of marine ecosystem functionality and provides a scientifically grounded framework to inform adaptive management strategies in the face of accelerating environmental change. The comprehensive examination of parasite communities of *A. honckenii* within marine ecosystems reveals their indispensable role as integral components of biodiversity and ecosystem functionality. Parasites not only reflect the complexity of host populations and food web interactions but also serve as sensitive indicators of environmental change, anthropogenic impacts, and habitat quality. The spatial and temporal patterns observed along the South African coastline, particularly between the Agulhas Bank and Natal ecoregions, underscore the influence of biogeographic gradients,

environmental contaminants, and conservation measures such as MPAs on parasite diversity and community structure. These findings highlight that parasite assemblages are shaped by a multifaceted interplay of abiotic factors such as temperature and pollution, biotic factors including host size, condition, and behaviour, and anthropogenic pressures that alter habitat integrity and host availability. Collectively, this research positions the *A. honckenii*-parasite system as a robust, integrative bioindicator for assessing marine environmental health. It effectively captures information on chemical contamination, ecological connectivity, and anthropogenic impacts across spatial gradients.

References:

Acosta, A.A. & Smit, N.J., 2021. A first for Southern Africa: Description of a new *Heterobothrium* (Monogenea: Diclidophoridae) parasitizing the evileye pufferfish *Amblyrhynchotes honckenii* (Tetraodontiformes: Tetraodontidae). *Parasitology Research*, 120(3): 819–830.

Boersma, P.D., Parrish, J.K., 1999. Limiting abuse: marine protected areas, a limited solution. *Ecological Economics*, 31(2): 287–304.

Bray, R.A., 1986. Some helminth parasites of marine fishes of South Africa: Families Enenteridae, Opistholebetidae and Pleorchiidae (Digenea). *Journal of Natural History*, 20(2): 471–488.

de Klerk, L., Smit, N.J., Yohannes, Y.B., Ikenaka, Y., Nimako, C., Nakayama, S.M.M., Ishizuka, M. & Wepener, V., 2025. Persistent organic pollutants in South African coastal ecosystems: analysing the evileye blaasop Amblyrhynchote honckenii (Bloch, 1785) for PCB and OCP accumulation. *Regional Studies in Marine Science*, 104368.

Erasmus, A., Wepener, V., Hadfield, K.A., Sures, B. & Smit, N.J., 2022. Metazoan parasite diversity of the endemic South African intertidal klipfish, *Clinus superciliosus*: factors influencing parasite community composition. *Parasitology International*, 90: 102611.

Erasmus, J.H., Wepener, V., Nachev, M., Zimmermann, S., Malherbe, W., Sures, B., Smit, N.J., 2020. The role of fish helminth parasites in monitoring metal pollution in aquatic ecosystems: a case study in the world's most productive platinum mining region. *Parasitology Research*, 119: 2783–2798.

Firth, D.C., O'Neill, B., Salie, K., Hoffman, L.C., 2019. Monitoring of organic pollutants in *Choromytilus meridionalis* and *Mytilus galloprovincialis* from aquaculture facilities in Saldanha Bay, South Africa. *Marine Pollution Bulletin*, 149:110637.

Froese, R. & Pauly, D., 2025. FishBase. Available at: www.fishbase.org/search.php. (date of access: 08 May 2025).

Gilbert, B.M., Avenant-Oldewage, A., 2017. Parasites and pollution: the effectiveness of tiny organisms in assessing the quality of aquatic ecosystems, with a focus on Africa. *Environmental Science and Pollution Research*, 24: 18742–18769.

Grabner, D., Rothe, L.E. & Sures, B., 2023. Parasites and pollutants: effects of multiple stressors on aquatic organisms. *Environmental Toxicology and Chemistry*, 42(9): 1946–1959.

Hadfield, K.A., Bruce, N.L. & Smit, N.J., 2010. Redescription of the monotypic genus *Cinusa* Schioedte and Meinert, 1884 (Isopoda, Cymothoidae), a buccal-cavity isopod from South Africa. *Zootaxa*, 2437(1): 51–68.

Hayes, P.M., Christison, K.W., Vaughan, D.B., Smit, N.J. & Boxshall, G.A., 2021. Sea lice (Copepoda: Caligidae) from South Africa, with descriptions of two new species of *Caligus*. *Systematic Parasitology*, 98(4): 369–397.

Lafferty, K.D. & Kuris, A.M., 1999. How environmental stress affects the impacts of parasites. *Limnology and Oceanography*, 44(3 part 2): 925–931.

Lee, Y.M., Kim, K.S., Jacobs Jr, D.R. & Lee, D.H., 2017. Persistent organic pollutants in adipose tissue should be considered in obesity research. *Obesity Reviews*, 18(2): 129–139.

Lisitsyna, O.I., Kudlai, O., Cribb, T.H. & Smit, N.J., 2019. Three new species of acanthocephalans (Palaeacanthocephala) from marine fishes collected off the East coast of South Africa. *Folia Parasitologica*, 66: 1–20.

Marcogliese, D.J., 2023. Major drivers of biodiversity loss and their impacts on helminth parasite populations and communities. *Journal of Helminthology*, 97:e34.

Molbert, N., Alliot, F., Leroux-Coyau, M., Médoc, V., Biard, C., Meylan, S., Jacquin, L., Santos, R. & Goutte, A., 2020. Potential benefits of acanthocephalan parasites for chub hosts in polluted environments. *Environmental Science & Technology*, 54(9): 5540–5549.

Nachev, M., Sures, B., 2016. Environmental parasitology: parasites as accumulation bioindicators in the marine environment. *Journal of Sea Research*, 113: 45–50.

Nunkoo, M.A.I., 2019. Studies on the diversity and distribution of marine ichthyoparasites in southern Africa. PhD Thesis, University of Cape Town.

Ogawa, K. & Inouye, K., 1997. *Heterobothrium* infection of cultured tiger puffer, *Takifugu rubripes* (Teleostei: Tetraodontidae)—a field study. *Fish Pathology*, 32: 15–20.

Ogawa, K. & Itoh, N., 2022. Five new and two known species of *Heterobothrium* (Monogenea: Diclidophoridae) infecting puffers of the genus *Takifugu* from Japanese waters. *Systematic Parasitology*, 99(3): 317–340.

Pérez-del-Olmo, A., Nachev, M., Zimmermann, S., Fernández, M., Sures, B., 2019. Medium-term dynamics of element concentrations in a sparid fish and its isopod parasite after the Prestige oil-spill: shifting baselines? *Science of the Total Environment*, 686: 648–656.

Ramírez-Ayala, E., Arguello-Pérez, M.A., Tintos-Gómez, A., Hernández-Anguiano, J.H., Pérez-Rodríguez, R.Y., Ilizaliturri-Hernández, C.A., Núñez-Nogueira, G., Sepúlveda-Quiroz, C.A., 2021. Persistent organic pollutants (POPs) in fish from two coastal lagoons of the central Mexican Pacific. *Latin American Journal of Aquatic Research*, 49(4): 663–670.

Smit, N.J. & Davies, A.J, 2001. The life cycle of *Haemogregarina bigemina* (Adeleina: Haemogregarinidae) in South African hosts. *Folia Parasitologica*, 48(3): 169–177.

Smit, N.J. & Hadfield, K.A., 2015. Marine fish parasitology in South Africa: History of discovery and future direction. *African Zoology*, 50(2): 79–92.

Smith, M.M. & Heemstra, P.C., 2012. Smith's Sea Fishes. Heidelburg, Germany: Springer Science & Business Media, pp. 1191.

Sures, B. & Nachev, M., 2022. Effects of multiple stressors in fish: how parasites and contaminants interact. *Parasitology*, 149(14): 1822–1828.

Sures, B., 2004. Fish acanthocephalans of the genus *Pomphorhynchus* sp. as globally applicable bioindicators for metal pollution in the aquatic environment? *Wiener Klinische Wochenschrift*, 116: 611–619.

Sures, B., Nachev, M., Grabner, D., Wepener, V. & Zimmermann, S., 2025. Environmental Parasitology: Interactions Between Parasites and Pollutants. In: N.J. Smit & B. Sures, eds. *Aquatic Parasitology: Ecological and Environmental Concepts and Implications of Marine and Freshwater Parasites*. Cham: Springer, pp.509–534.

Sures, B., Nachev, M., Selbach, C. & Marcogliese, D.J., 2017. Parasite responses to pollution: what we know and where we go in 'Environmental Parasitology'. *Parasites & Vectors*, 10(1): 1–19.

Van Der Spuy, L., Erasmus, J.H., Nachev, M., Schaeffner, B.C., Sures, B., Wepener, V. & Smit, N.J., 2023. The use of fish parasitic isopods as element accumulation indicators in marine pollution monitoring. *Marine Pollution Bulletin*, 194: 115385.

Van Der Spuy, L., Narciso, R.B., Hadfield, K.A., Wepener, V. & Smit, N.J., 2025. Exploring South Africa's hidden marine parasite diversity: Two new marine *Ergasilus* species (Copepoda: Cyclopoida: Ergasilidae) from the evileye blaasop, *Amblyrhynchotes honckenii* (Bloch). *Parasitology*, 152(1): 30–50.

Vermaak, A., 2024. Metazoan parasite diversity of *Diplodus capensis* from South Africa and the role of marine protected areas in their conservation. PhD Thesis, North-West University.

Vidal-Martínez, V.M., Pech, D., Sures, B., Purucker, S.T., Poulin, R., 2010. Can parasites really reveal environmental impact? *Trends in Parasitology*, 26: 44–51.

Wood, C.L. & Lafferty, K.D., 2015. How have fisheries affected parasite communities? *Parasitology*, 142(1): 134–144.

Wood, C.L., Lafferty, K.D. & Micheli, F., 2010. Fishing out marine parasites? Impacts of fishing on rates of parasitism in the ocean. *Ecology Letters*, 13(6):761–775.

Wood, C.L., Micheli, F., Fernández, M., Gelcich, S., Castilla, J.C. & Carvajal, J., 2013. Marine protected areas facilitate parasite populations among four fished host species of central Chile. *Journal of Animal Ecology*, 82(6): 1276–1287.

Wood, C.L., Zgliczynski, B.J., Haupt, A.J., Guerra, A.S., Micheli, F. & Sandin, S.A., 2018. Human impacts decouple a fundamental ecological relationship-The positive association between host diversity and parasite diversity. *Global Change Biology*, 24(8): 3666–3679.

Supplementary Material:

Supplementary Table S3.1: List of GenBank sequences included in the phylogenetic analyses. Outgroups are marked in grey shade. **Taxon from the Barcode of Life Database (BOLD).

Taxon	Host	Locality	Accession numbers			Reference
			18S	28S	COI	
Acanthocephala: Pomphorhynchidae						
Gymnorhadinorhynchus decapteri	*Decapterus punctatus*	Brazil	KJ590125	-	-	Braicovich *et al*., 2014
Pomphorhynchus bulbocoli	Unknown	Unknown	AF001841	-	-	Near *et al*., 1998
Pomphorhynchus kashmirensis	Freshwater fish	India	MZ381411	-	-	Amin *et al*., 2022
Pomphorhynchus laevis	Unknown	France	AY423346	-	-	Perrot-Minoot, 2004
Pomphorhynchus pagrosomi	*Pagrus major*	Japan	LC195887	-	-	Unpublished
Pomphorhynchus tereticollis	Unknown	France	AY423347	-	-	Perrot-Minoot, 2004
Acanthocephalus nanus	*Cynops pyrrhogaster*	Japan	LC100043	-	-	Nakao, 2016
Acanthocephala: Rhadinorhynchidae						
Rhadinorhynchus biformis	*Pelates sexlineatus*	Australia	-	-	MN692682	Huston *et al*., 2020
Rhadinorhynchus carangis	*Trachinotus coppingeri*	Australia	-	-	MN692684	Huston *et al*., 2020
Rhadinorhynchus dorsoventrospinosus	*Decapterus kurroides*	Vietnam	-	-	MN267179	Chaudhary *et al*., 2020
Rhadinorhynchus gerberi	*Trachinotus botla*	South Africa	-	-	MN104897	Lisitsyna *et al*., 2019
Rhadinorhynchus hiansi	*Sarda orientalis*	Vietnam	-	-	MN203136	Amin *et al*., 2020
Rhadinorhynchus johnstoni	*Auxis thazard*	Australia	-	-	MN692680	Huston *et al*., 2020
Rhadinorhynchus laterospinosus	*Auxis rochei*	Vietnam	-	-	MK572743	Amin *et al* ., 2020
Rhadinorhynchus pristis	*Nyctiphanes couchii*	Spain	-	-	JQ061132	Gregori *et al*. 2013
Rhadinorhynchus seriolae	*Thunnus orientalis*	Japan	-	-	LC777825	Kita *et al*., 2024
Rhadinorhynchus trachinoti	*Trachinotus rhodopus*	Mexico	-	-	PQ541022	Grano-Maldonado *et al*., 2025
Acanthocephalus anguillae	*Anguilla anguilla*	Germany	-	-	MN416027	Amin *et al*., 2019
Arthropoda: Caligidae						
Caligus asymmetricus	Unknown	Malaysia	-	-	PQ468448	Unpublished
Caligus belones	*Salmo salar; Salmo trutta*	Norway	-	-	AY861368	Øines and Heuch, 2005
Caligus bonito	Unknown	India	-	-	MH651760	Unpublished

Taxon	Host	Locality	Accession numbers			Reference
			18S	28S	COI	
Caligus callyodoni	Unknown	India	-	-	PQ687497	Unpublished
Caligus centrodonti	*Salmo salar; Salmo trutta*	Norway	-	-	AY861370	Øines and Heuch, 2005
Caligus cheilodactyli	*Sebastes oculatus*	Chile	-	-	KU317605	Gonzales *et al*., 2016
Caligus clemensi	*Dicentrarchus labrax*	Egypt	-	-	PP549199	Abdelsalam *et al*., 2024
Caligus confuses	Unknown	India	-	-	MZ983788	Nikhila *et al*., 2019
Caligus cordyla	Unknown	India	-	-	OP425697	Unpublished
Caligus curtus	*Chondracanthus merluccii*	North Sea	-	-	KT209233	Raupach *et al*., 2015
Caligus cybii	Unknown	Malaysia	-	-	PQ461336	Unpublished
Caligus dakari	*Argyrosomus japonicus*	South Africa	-	-	MW911362	Hayes *et al*., 2021
Caligus diaphanus	*Triglid fishes*	Norway	-	-	EF065616	Øines and Schram, 2008
Caligus elongatus	Unknown	Norway	-	-	AY386273	Unpublished
Caligus epidemicus	Unknown	India	-	-	OP957023	Unpublished
Caligus fugu	Unknown	Korea	-	-	KR049056	Unpublished
Caligus furcisetifer	*Carcharias taurus*	South Africa	-	-	MW911361	Hayes *et al*., 2021
Caligus gurnardi	*Salmo salar; Salmo trutta*	Norway	-	-	AY861369	Øines and Heuch, 2005
Caligus hamruri	Unknown	India	-	-	MW971507	Unpublished
Caligus hirsutus	Unknown	India	-	-	PQ638939	Unpublished
Caligus hoplognathi	Unknown	Korea	-	-	KR049058	Unpublished
Caligus infestans	*Scomberomorus commerson*	Malaysia	-	-	PQ469596	Unpublished
Caligus kanagurta	Unknown	India	-	-	ON023681	Nikhila *et al*., 2019
Caligus lacustris	*Oncorhynchus mykiss*	Russia	-	-	MT920720	Parshukov *et al*., 2021
Caligus lalandei	*Seriola lalandi*	South Africa	-	-	MW911365	Hayes *et al*., 2021
Caligus lobodes	Unknown	India	-	-	PQ687496	Unpublished
Caligus longirostris	*Salmonids*	Australia	-	-	HQ667343	Nowak *et al*., 2011
Caligus minimus	*Dicentrarchus labrax*	Turkey	-	-	PQ166292	Yanar *et al*., 2025
Caligus neunonnae	*Latris lineata*	Tamania	-	-	EF452642	Andrews *et al*., 2009
Caligus pelamydis	*Salmo salar; Salmo trutta*	Norway	-	-	AY861367	Øines and Heuch, 2005
Caligus priacanthid	Unknown	India	-	-	MH651759	Unpublished

Taxon	Host	Locality	Accession numbers			Reference
			18S	28S	COI	
Caligus punctatus	Unknown	Korea	-	-	KR049057	Unpublished
Caligus quadratus	Unknown	Korea	-	-	EF065619	Unpublished
Caligus rogercresseyi	*Salmo salar*	Chile	-	-	MT795966	Gonzales *et al*., 2016
Caligus rotundigenitalis	Unknown	India	-	-	MH651757	Unpublished
Caligus sclerotinosus	Unknown	Japan	-	-	LC835012	Unpublished
Caligus stromatei	Unknown	India	-	-	MH651758	Unpublished
Caligus tetrodontis	*Amblyrhynchote honckenii*	South Africa	-		MW911366	Hayes *et al*., 2021
Caligus warlandi	*Thunnus maccoyii*	Australia	-	-	EF452644	Nowak *et al*., 2011
Lepeophtheirus pectoralis	*Salmo salar; Salmo trutta*	Norway	-	-	AY861364	Øines and Heuch, 2005
Arthropoda: Ergasilidae						
Acusicola margulisae	*Amphilophus citrinellus*	Nicaragua	MN852694 MN852695	MN852849 MN852850	MN854868 MN854869	Santacruz *et al*., 2022
Dermoergasilus madagascarensis	*Paretroplupolyactis*	Madagascar	PP115568 -	PP115569 -	PP117931 PP117932	Míč *et al*., 2024
Ergasilus anchoratus	*Pseudobagrus fulvidraco*	China	DQ107564	DQ107528	-	Song *et al*., 2008
***Ergasilus auritus*	*Gasterosteus aculeatus*	Canada	-	-	ECTCR091-14	BOLD
Ergasilus briani	*Misgurnus anguillicaudatus*	China	DQ107572	DQ107532	-	Song *et al*., 2008
Ergasilus caparti	*Neolamprologus brichardi*	Burundi	OQ407469	OQ407474	-	Míč *et al*., 2023
Ergasilus hypomesi	*Acanthogobius hasta*	China	DQ107573	DQ107539	-	Song *et al*., 2008
***Ergasilus lizae*	*Fundulus diaphanus*	Canada	-	-	ECTCR024-14	BOLD
Ergasilus macrodactylus	*Gnathochromis permaxillaris*	Burundi	OQ407465	OQ407470	-	Míč *et al*., 2023
Ergasilus megacheir	*Simochromis diagramma*	Burundi	OQ407466	OQ407471	-	Míč *et al*., 2023
Ergasilus mirabilis	*Clarias gariepinus*	South Africa Zambia	OR449753 OR449754	OR449755 OR449756	OR448769 OR448770	Fikiye *et al*., 2023
Ergasilus parasarsi	*Simochromis diagramma*	Burundi	OQ407467	OQ407473	-	Míč *et al*., 2023
Ergasilus parvus	*Spathodus erythrodon*	Burundi	OQ407468	OQ407472	-	Míč *et al*., 2023
Ergasilus parasiluri	*Tachysurus fulvidraco*	China	DQ107567	DQ107536	-	Song *et al*., 2008
Ergasilus peregrinus	*Siniperca chuatsi*	China	DQ107577	DQ107531	-	Song *et al*., 2008

Taxon	Host	Locality	Accession numbers			Reference
			18S	28S	COI	
Ergasilus scalaris	*Tachysurus dumerili*	China	DQ107565	DQ107538	-	Song *et al*., 2008
Ergasilus sieboldi	*Perca fluviatilis*; *Sparus aurata*	Czech Republic	MW810238	MW810242	-	Kvach *et al*., 2021
Ergasilus tumidus	*Acanthorhodeus taenianalis*	China	DQ107569 DQ107570	DQ107533 DQ107534	- -	Song *et al*., 2008
Ergasilus wilsoni	Free-living	South Korea	KR048765	KR048843	KR049036	Baek *et al*., 2016
Ergasilus yaluzangbus	*Gymnocypris stewartii*	China	DQ107578	DQ107540	-	Song *et al*., 2008
Neoergasilus japonicus	*Lepomis gibbosus* *Scardinius erythrophthalmus*	Czech Republic USA	MH167970 MW810236 - -	MH167968 MW810240 - -	- - MZ964935 MZ964938	Ondračková *et al*., 2019 Kvach *et al*., 2021 Vasquez *et al*., 2021
Paraergasilus brevidigitus	*Cyprinus carpio*	China	DQ107576	DQ107530	-	Song *et al*., 2008
Paraergasilus longidigitus	*Abramis brama*; *Perca fluviatilis*; *Scardinius erythrophthalmu*	Czech Republic	MW810239	MW810243	-	Kvach *et al*., 2021
Paraergasilus medius	*Ctenopharyngodon idellus*	China	DQ107574	DQ107529	-	Song *et al*., 2008
Sinergasilus major	*Ctenopharyngodon Idella* *Silurus glanis*	China Hungary	DQ107558 -	- MZ047815	- -	Song *et al*., 2008 Dos Santos *et al*., 2021
Sinergasilus polycolpus	*Hypophthalmichthys molitrix*	China	DQ107563	DQ107525	-	Song *et al*., 2008
Sinergasilus undulatus	*Cyprinus carpio*	China	DQ107561 -	DQ107526 -	- MW080644	Song *et al*., 2008 Hua *et al*., 2021
Paracyclopina nana	Free-living	Korea	- FJ214952	- FJ214952	EU877959 -	Ki *et al*., 2009 Ki *et al*., 2011
Nematoda: Anisakidae						
Anisakis pegreffii	*Scomber australasicus*	Taiwan	-	MF422214	-	Chen *et al*., 2015
Anisakis simplex	*Mirounga angustirostris*	California	-	AY821754	-	Nadeler *et al*., 2005
Anisakis typica	*Selar crumenophthalmus*	Indonesia	-	MZ350222	-	Syarifah *et al*., 2023
Anisakis ziphidarum	*Mesoplodon hotaula*	Philipines	-	KF214798	-	Quiazon *et al*., 2021
Contracaecum osculatum	*Gadus morhua*	Baltic sea	-	KM273050	-	Mehrdana *et al*., 2014
Nematoda: Cucullanidae						
Cucullanus bourdini	*Caesio xanthonota*	Taiwan	-	KX910701	-	Xu *et al*., 2017
Cucullanus grandistomis	*Oxydoras niger*	Brazil	-	KX752093	-	Pereira and Luque, 2017

Taxon	Host	Locality	Accession numbers			Reference
			18S	28S	COI	
Cucullanus opithoporus	*Cichla pinima*	Brazil	-	KX752095	-	Pereira and Luque, 2017
Cucullanus pinai pinai	*Pimelodus fur*	Brazil	-	OP942396	-	Ailan-Choke *et al*., 2023
Cucullanus pulcherrimus	*Micropogonias furnieri*	Brazil	-	MF187076	-	Unpublished
Dichelyne mexicanus	*Ictalurus balsanus*	Mexico	-	MG182630	-	Mejia-Madrid, 2018
Dichelyne pleuronectidis	*Pleuronichthys cornutus*	China	-	KF470872	-	Li *et al*., 2014
Dichelyne szidati	*Acanthistius patachonicus*	Argentina	-	MK131262	-	Bagnato *et al*., 2022
Truttaedacnitis truttae	*Oncorhynchus mykiss*	*Colorado*	-	KY857891	-	Mejia-Madrid, 2018
Rhabditis terricola	*Free living*	Turkey	-	KP027185	-	Azizolu *et al*., 2016
Nematoda: Raphidascaridae						
Raphidascaris acus	*Neogobius fluviatilis*	Lithuania	-	PQ570400	-	Kudlai *et al*., 2024
Raphidascaris andersoni	Gymnogeophagus balzanii	Brazil	-	MK141032	-	Malta *et al*., 2020
Raphidascaris gigi	*Hypomesus nipponensis*	Japan	-	AB558480	-	Abe, 2011
Raphidascaris lanfrediae	*Geophagus proximus*	Brazil	-	KX859078	-	Pereira and Luque, 2017
Raphidascaris longispicula	*Uroconger lepturus*	China	-	MF094288	-	Li *et al*., 2018
Raphidascaris lophii	*Lophius litulon*	China	-	MH211582	-	Zhang *et al*., 2018
Raphidascaris mahnerti	*Loricariichthys labialis*	Brazil	-	MK766746	-	Malta *et al*., 2020
Raphidascaris trichiuri	*Chiloscyllium plagiosum*	Taiwan	-	FJ009682	-	Damin and Heqing, 2001
Contracaecum rudolphii	*Pelecanus occidentalis*	Florida	-	MN557379	-	D'Amelio *et al*., 2012
Cestoda: Onchobothriidae						
Acanthobothrium brevissime	*Dasyatis say*	Florida	-	EU170364	-	Holland *et al*., 2009
Acanthobothrium cleofanus	*Hypanus longus*	Mexico	-	MZ081426	-	Unpublished
Acanthobothrium cornoatum	*Scyliorhinus stellaris*	Meditterranean	-	MZ243218	-	Santoro et al., 2021
Acanthobothrium coronatum	*Scyliorhinus stellaris*	Italy	-	MZ243216	-	Santoro *et al*., 2021
Acanthobothrium filicolle	*Zearaja nasuta*	New Zealand	-	MH913266	-	Bennett *et al*., 2019
Acanthobothrium golsteini	Unknown	USA	-	PQ580682	-	Unpublished
Acanthobothrium hypermekkolpos	*Rhynchobatus laevis*	Australia	-	HQ917930	-	Fyler and Caira, 2011
Acanthobothrium jeanneae	*Rhynchobatus laevis*	Australia	-	HQ917928	-	Fyler and Caira, 2011
Acanthobothrium katherineae	*Squaliolus aliae*	Taiwan	-	MT395344	-	Gallagher and Caira, 2020
Acanthobothrium margieae	*Orectolobus maculatus*	Australia	-	MH729998	-	Cutmore *et al*., 2018

Taxon	Host	Locality	Accession numbers			Reference
			18S	28S	COI	
Acanthobothrium masnihae	*Himantura sp*	Australia	-	FJ843604	-	Fyler *et al*., 2009
Acanthobothrium mattaylori	*Rhynchobatus laevis*	Australia	-	HQ917927	-	Fyler and Caira, 2011
Acanthobothrium oceanharvestae	*Himantura sp.*	Australia	-	FJ843594	-	Fyler *et al*., 2009
Acanthobothrium parviuncinatum	*Urobatis maculatus*	Mexico	-	EF095264	-	Waeschenbach *et al*., 2017
Acanthobothrium popi	*Himantura sp.*	Australia	-	FJ843600	-	Fyler *et al*., 2009
Acanthobothrium robostum	*Unknown*	USA	-	PQ580683	-	Unpublished
Acanthobothrium rodmani	*Himantura sp.*	Australia	-	FJ843596	-	Fyler *et al*., 2009
Acanthobothrium romanowi	*Himantura sp.*	Australia	-	FJ843598	-	Fyler *et al*., 2009
Acanthobothrium santarosaliense	*Heterodontus mexicanus*	Mexico	-	KF685751	-	Caira *et al*., 2014
Acanthobothrium sp.	*Dasyatis say*	Mexico	-	FJ843592	-	Jensen and Bullard, 2010
Acanthobothrium wedli	*Zearaja nasuta*	New Zealand	-	MH913270	-	Benett *et al*., 2019
Acanthobothrium zimmeri	*Himantura sp.*	Australia	-	FJ843602	-	Fyler *et al*., 2009
Potamotrygonocestus cf. fitzgeraldae	*Potamotrygon castexi*	Mexico	-	KF685773	-	Caira *et al*., 2014
Cestoda: Phyllobothriidae						
Scyphophyllidium arnoldi	*Negaprion acutidens*	Australia	-	MN686528	-	Ruhnke *et al*., 2020
Scyphophyllidium bai	*Mustelus mustelus*	Senegal	-	KC505625	-	Ruhnke and Workman, 2013
Scyphophyllidium bullardi	*Carcharhinus acronotus*	Mexixo	-	MN686531	-	Ruhnke *et al*., 2020
Scyphophyllidium campbelli	*Rhizoprionodon terraenovae*	Florida	-	MN686538	-	Ruhnke *et al*., 2020
Scyphophyllidium christopheri	*Carcharhinus sorrah*	Australia	-	MG008931	-	Cutmore *et al*., 2017
Scyphophyllidium deburonae	*Carcharhinus isodon*	Sout Carolina	-	MN686546	-	Ruhnke *et al*., 2020
Scyphophyllidium exiguum	*Alopias vulpinus*	New York	-	MN686548	-	Ruhnke *et al*., 2020
Scyphophyllidium giganteum	*Galeorhinus galeus*	New Zealand	-	KF685901	-	Caira *et al*., 2014
Scyphophyllidium harti	*Carcharhinus leucas*	Australia	-	MG008939	-	Cutmore *et al*., 2017
Scyphophyllidium janineae	*Hemipristis elongata*	Australia	-	MN686550	-	Ruhnke *et al*., 2020
Scyphophyllidium kirstenae	*Hemigaleus microstoma*	Borneo	-	KC505626	-	Ruhnke and Workman, 2013
Scyphophyllidium latipi	*Scoliodon macrorhynchos*	Borneo	-	KF685900	-	Caira *et al*., 2014
Scyphophyllidium mattisi	*Carcharhinus limbatus*	Mexico	-	MN686552	-	Ruhnke *et al*., 2020
Scyphophyllidium orectobiobi	*Orectolobus maculatus*	Australia	-	MG008940	-	Cutmore *et al*., 2017

Taxon	Host	Locality	Accession numbers			Reference
			18S	28S	COI	
Scyphophyllidium paulum	*Galeocerdo cuvier*	New York	-	MN686556	-	Ruhnke *et al*., 2020
Scyphophyllidium prionacis	*Prionace glauca*	New York	-	MN686557	-	Ruhnke *et al*., 2020
Scyphophyllidium randyi	*Chiloscyllium hasseltii*	Borneo	-	KF685767	-	Caira *et al*., 2014
Scyphophyllidium sinclairtaylori	*Carcharhinus amboinensis*	Australia	-	MG008934	-	Cutmore *et al*., 2017
Scyphophyllidium taylori	*Hemigaleus australiensis*	Australia	-	HQ680632	-	Cutmore *et al*., 2017
Scyphophyllidium timvickiorum	*Pseudocarcharias kamoharai*	Ecuador	-	MN706182	-	Caira *et al*., 2020
Scyphophyllidium tyleri	*Chiloscyllium punctatum*	Borneo	-	KF685890	-	Caira *et al*., 2014
Allexandercestus gibsoni	*Carcharhinus leucas*	Australia	-	MG008925	-	Cutmore *et al*., 2017
Cestoda: Tentaculariidae						
Heteronybelinia estigmena	*Coryphaena hippurus*	Indonesia	-	FJ572931	-	Palm *et al*., 2009
Heteronybelinia yamagutii	*Promethichthys prometheus*	Australia	-	FJ572932	-	Palm *et al*., 2009
Hetronybelinia estigmena	*Carcharhinus limbatus*	Malaysia	-	DQ642789	-	Olsen *et al*., 201
Kotorella pronosoma	*Dasyatis say*	USA	-	DQ642788	-	Olsen *et al*., 2010
Myxonybelinia lepturi	*Gempylus serpens*	Indonesia	-	FJ572933	-	Palm *et al*., 2009
Nybelinia aequidentata	*Rhinoptera neglecta*	Malaysia	-	DQ642790	-	Olsen *et al*., 2010
Nybelinia africana	*Lamiopsis temminckii*	Malaysia	-	DQ642786	-	Olsen *et al*., 2010
Nybelinia indica	*Heteropriacanthus cruentatus*	Hawai	-	FJ572930	-	Palm *et al*., 2009
Nybelinia queenslandensis	*Carcharinus melanopterus*	Australia	-	AF286975	-	Olsen *et al*., 2001
Nybelinia sphyrnae	*Sphyrna lewini*	Malaysia	-	DQ642791	-	Olsen *et al*., 2010
Nybelinia surmenicola	Unknown	Japan	-	FJ572929	-	Palm *et al*., 2009
Tentacularia coryphaenae	*Katsuwonus pelamys*	Australia	-	EF095269	-	Palm *et al*., 2007
Sphyriocephlus viridis	*Dalatias licha*	Indonesia	-	FJ572940	-	Palm *et al*., 2009
Monopisthocotylea: Udonelidae						
Udonella australis	*Caligus rogercresseyi ex Eleginops maclovinus*	Chile	FJ946832	-	-	Freeman and Ogawa, 2010
Udonella brasiliensis	*Caligus sp. on Genidens barbus*	Brazil	MW763077 MW763065	-	-	Soares *et al*., 2021

Taxon	Host	Locality	Accession numbers			Reference
			18S	28S	COI	
Udonella caligorum	*Caligus sp. ex Gadus morhua*	Japan	AJ228796 FJ946831	-	-	Littlewood *et al*., 1999; Freeman and Ogawa, 2010
Udonella fugu	*Pseudocaligus fugu ex Takifugu spp.*	Japan	FJ946830	-	-	Freeman and Ogawa, 2010
Udonella myliobatid	*Caligid copepod ex Myliobatis australis*	Australia	FJ946833	-	-	Freeman and Ogawa, 2010
Gyrodactylus salmonis	*rainbow trout*	Mexico	JN230350	-	-	Rubio-Godoy *et al*., 2012
Polyonopisthocotylea: Diclidophoridae						
Heterobothrium gotoi	*Takifugu porphyreus*	Japan	-	-	LC658933	Ogawa and Itoh, 2022
Heterobothrium matsubarai	*Takifugu stictonotus*	Japan	-	-	LC658936	Ogawa and Itoh, 2022
Heterobothrium okamotoi	*Takifugu rubripes*	Japan	-	-	LC658930	Ogawa and Itoh, 2022
Heterobothrium praeorchis	*Takifugu pardalis*	Japan	-	-	LC658931	Ogawa and Itoh, 2022
Heterobothrium tetrodontis	*Takifugu pardalis*	Japan	-	-	LC658932	Ogawa and Itoh, 2022
Heterobothrium victorwepeneri	*Amblyrhynchote honckenii*	South Africa	-	-	MW115855	Acosta and Smit, 2021
Neoheterobothrium paralichthyi	*Paralichthys patagonicus*	Argentinia	-	-	LC658938	Ogawa and Itoh, 2022
Trematoda: Bucephalidae						
Aenigmatrema grandiovum	*Sphyraena obtusata*	Australia	-	MT809145	-	Corner *et al*., 2020
Aenigmatrema inopinatum	*Sphyraena obtusata*	Australia	-	MT809144	-	Corner *et al*., 2020
Aenigmatrema undecimtentaculum	*Sphyraena obtusata*	Australia	-	MT809143	-	Corner *et al*., 2020
Bucephalus cynoscion	*Bairdiella chrysoura*	USA	-	KT273397	-	Nolan *et al*., 2015
Bucephalus gorgon	*Seriola dumerili*	USA	-	KT273400	-	Nolan *et al*., 2015
Bucephalus margaritae	*Caranx crysos*	USA	-	KT273395	-	Nolan *et al*., 2015
Bucephalus polymorphus	*Dreissena polymorpha*	Belarus	-	AY289247	-	Stunz *et al*., 2004
Bucephalus skrjabani	Unknown	Asia	-	OM615429	-	Atopkin *et al*., 2022
Dollfustrema durum	*Gymnothorax javanicus*	USA	-	KT213572	-	Nolan *et al*., 2015
Heterobucephalopsis yongi	*Gymnothorax eurostus*	Australia	-	MH754949	-	Cutmore *et al*., 2018
Paurorhynchus hiodontis	*Hiodon alosoides*	USA	-	KT273401	-	Nolan *et al*., 2015
Prosorhynchoides apogonis	*Cheilodipterus macrodon*	USA	-	KT213576	-	Nolan *et al*., 2015
Prosorhynchoides brayi	*Epinephelus coioides*	Australia	-	MH754950	-	Cutmore *et al*., 2018
Prosorhynchoides caecorum	*Sciaenops ocellatus*	USA	-	KT273392	-	Nolan *et al*., 2015

Taxon	Host	Locality	Accession numbers			Reference
			18S	28S	COI	
Prosorhynchoides cutmorei	*Tylosurus gavialoides*	Australia	-	MG953232	-	Hammond *et al*., 2018
Prosorhynchoides galaktionovi	*Tylosurus crocodilus*	Australia	-	MN310395	-	Hammond *et al*., 2018
Prosorhynchoides karvei	Unknown	Asia	-	OM615433	-	Atopkin *et al*., 2022
Prosorhynchoides kohnae	*Tylosurus crocodilus*	Australia	-	MN310397	-	Hammond *et al*., 2018
Prosorhynchoides longoviferus	*Sphyraena barracuda*	USA	-	KT273387	-	Nolan *et al*., 2015
Prosorhynchoides megacirrus	*Sciaenops ocellatus*	USA	-	KT273391	-	Nolan *et al*., 2015
Prosorhynchoides moretonensis	*Tylosurus gavialoides*	Australia	-	MG953230	-	Hamond *et al*., 2018
Prosorhynchoides ovatus	*Lobotes surinamensis*	USA	-	KT273399	-	Nolan *et al*., 2015
Prosorhynchoides paralichthydis	*Paralichthys lethostigma*	USA	-	KT273398	-	Nolan *et al*., 2015
Prosorhynchoides Scomberomorus	*Scomberomorus cavalla*	USA	-	KT273389	-	Nolan *et al*., 2015
Rhipidocotyle angusticolle	*Euthynnus alletteratus*	USA	-	KT273383	-	Nolan *et al*., 2015
Rhipidocotyle campanula	*Anodonta anatina*	Lithuania	-	KF184355	-	Petkeviviute *et al*., 2014
Rhipidocotyle fennica	*Anodonta anatina*	Lithuania	-	KF184363	-	Petkeviviute *et al*., 2014
Rhipidocotyle galeata	*Eutrigla gurnardus*	United Kingdom	-	AY222225	-	Olsen *et al*., 2003
Rhipidocotyle husi	Unknown	Asia	-	OM615425	-	Atopkin *et al*., 2022
Rhipidocotyle lepisostei	*Lepisosteus oculatus*	USA	-	KT273390	-	Nolan *et al*., 2015
Rhipidocotyle santanaensis	*Acestrothynchus pantaneiro*	Argentina	-	OQ244080	-	Montes *et al*., 2023
Rhipidocotyle transversalis	*Strongylura marina*	USA	-	KT273394	-	Nolan *et al*., 2015
Rhipidocotyle tridecapapillata	*Micropterus salmoides*	USA	-	KT273384	-	Nolan *et al*., 2015
Coitocaecum capense	*Clinus superciliosus*	South Africa	-	OR129144	-	Vermaak *et al*., 2023
Trematoda: Helicometrinae						
Helicometra antarcticae	Unknown	Russia	-	OK644193	-	Unpublished
Helicometra boseli	*Sargocentron spiniferum*	New Caledonia	-	KU320600	-	Bray *et al*., 2016
Helicometra fasciata	*Epinephelus fasciatus*	New Caledonia	-	KU320597	-	Bray *et al*., 2016
Helicometra manteri	*Prionotus alatus*	Florida	-	KJ701238	-	Andres *et al*., 2014
Helicometrina nemia	*Syacium papillosum*	Mexico	-	MK908868	-	Vidal-Martínez *et al*., 2019

Taxon	Host	Locality	Accession numbers			Reference
			18S	28S	COI	
Coitocaecum capense	*Clinus superciliosus*	South Africa	-	OR129144	-	Vermaak *et al*., 2023
Trematoda: Opistholebetinae						
Gaevskajatrema perezi	Unknown	France	-	AF184255		Tkach *et al*., 2001
Heterolebes maculosus	*Diodon hystrix*	Australia	-	MH933878	-	Martin *et al*. (2018a)
Maculifer diodontis	*Diodon hystrix*	Australia	-	MH933879	-	Martin *et al*. (2018a)
Macvicaria bartolii	*Diplodus annularis*	Tunisia	-	KR149465	-	Antar *et al*. (2015); Rima *et al*. (2017)
Macvicaria crassigula	*Calamus bajonado*	Mexico	-	KJ701237	-	Andres *et al*. (2014)
Macvicaria dubia	*Oblada melanura*	Tunisia	-	KR149470	-	Antar *et al*. (2015)
Macvicaria gibsoni	*Diplodus vulgaris*	Algeria	-	MF166845	-	Rima *et al*. (2017)
Macvicaria maamouriae	*Lithognathus mormyrus*	Tunisia	-	KR149468	-	Antar *et al*. (2015)
Macvicaria mormyri	*Sparus aurata;* Unknown	France	-	AF184256	-	Tkach *et al*. (2001); Rima *et al*. (2017)
Macvicaria obovata	*Cyclope neritea*	Spain	-	JQ694147	-	Born-Torrijos *et al*. (2012)
Magnaosimum brooksae	*Tripodichthys angustifrons*	Australia	-	MG813907	-	Martin *et al.* (2018b)
Opistholebes amplicoelus	*Lagocephalus lunaris; Tetractenos hamiltoni*	Australia	-	MH933875	MH933883; MH933884; MH933885; MH933886; MH933887; MH933888	Martin *et al*. (2018a)
Paralellolebes virilis	*Meuschenia hippocrepis*	Australia	-	MH933880	-	Martin *et al*. (2018a)
Peracreadium idoneum	*Anarhichas lupus*	UK	-	AY222209	-	Olsen *et al*. (2003)
Propycnadenoides philippinensis	*Gymnocranius grandoculis*	Australia	-	KU320604	-	Bray *et al*. (2016)
Pseudoheterolebes diodontis	*Diodon liturosus; Diodon hysterix*	Australia	-	MH933876	-	Martin *et al*. (2018a)
Pseudoheterolebes stellaglobulus	*Dicotylichthys punctulatus*	Australia	-	MH933877	-	Martin *et al*. (2018a)
Pseudopycnadena fischtali	*Diplodus vulgaris*	Algeria	-	MF166851	-	Rima *et al*. (2017)
Neolebouria georgiensis	*Parachaenichthys charcoti*	Ukraine	-	ON123036	-	Faltýnková *et al*. (2022)
Trematoda: Zoogoninae						
Brevicreadium sp.	*Forsterygion capito*	New Zealand	-	PV521839	-	Viriyautsahakul *et al*., 2025

Taxon	Host	Locality	Accession numbers			Reference
			18S	28S	COI	
		United Kingdom				
Diphterostomum brusinae	*Cerastoderma edule*	Portugal	-	MN263044	-	Gilardoni *et al*., 2020
Pseudozoogonoides subaequiporus	*Anarhichas lupus*	Russia	-	OP956068	-	Kremnev *et al*., 2023
Pseudozoogonoides ugui	Pseudaspius hakonensis	Russia	-	PP317550	-	Atopkin *et al*., 2024
Zoogonidae sp	*Anentome helena*	Thailand	-	MZ825155 MZ825156	-	Chomchoei *et al*., 2022
Zoogonoides viviparus	*Callionymus lyra* *Nuculana pernula*	United Kingdom; Russia	-	AY222271 OP956062	-	Olsen *et al*., 2003; Kremnev *et al*., 2023
Zoogonus rubellus	*Diplodus sargus*	Geneva	-	AJ241804	-	Jousson *et al*., 1999
Coitocaecum capense	*Clinus superciliosus*	South Africa	-	OR129144	-	Vermaak *et al*., 2023

Supplementary Table S4.1: Biometric information (sex, size, weight) on host specimens of *Amblyrhynchote honckenii* (Bloch), including presence or absence of *Cinusa tetrodontis* Schjödte et Meinert, 1884 and their relevant information (sex, weight), collected from Witsand, South Africa. Abbreviations: (+) – parasite present; (-) – parasite absent.

Collection code	Sex	Length (mm)	Weight (g)	Locality	Presence of *Cinusa tetrodontis*	Sex	Weight (mg)
WSAH21-01	F	185	140	Breede River Estuary, Witsand	-	-	-
WSAH21-02	M	165	100	Breede River Estuary, Witsand	+	M F	95 106
WSAH21-03	M	145	70	Breede River Estuary, Witsand	-	-	-
WSAH21-04	M	160	80	Breede River Estuary, Witsand	-	-	-
WSAH21-05	M	140	60	Breede River Estuary, Witsand	+	M F	47 101
WSAH21-06	M	160	80	Breede River Estuary, Witsand	-	-	-
WSAH21-07	F	175	110	Breede River Estuary, Witsand	-	-	-
WSAH21-08	M	140	50	Breede River Estuary, Witsand	-	-	-
WSAH21-09	M	145	60	Breede River Estuary, Witsand	+	M F	54 106
WSAH21-10	M	150	80	Breede River Estuary, Witsand	-	-	-
WSAH21-11	M	145	60	Breede River Estuary, Witsand	+	M F	59 171
WSAH21-12	M	160	100	Breede River Estuary, Witsand	-	-	-
WSAH21-13	M	140	60	Breede River Estuary, Witsand	+	M F	66 135
WSAH21-14	M	150	70	Breede River Estuary, Witsand	+	M F	63 102
WSAH21-15	M	150	80	Breede River Estuary, Witsand	-	-	-

Supplementary Table S4.2: Biometric information (sex, size, weight) on host specimens of *Amblyrhynchote honckenii* (Bloch), including presence or absence of *Cinusa tetrodontis* Schjödte et Meinert, 1884 and their relevant information (sex, weight), collected from Mossel Bay, South Africa. Abbreviations: (+) – parasite present; (-) – parasite absent.

Collection code	Sex	Length (mm)	Weight (g)	Locality	Presence of *Cinusa tetrodontis*	Sex	Weight (mg)
MBAH22-01	M	125	40	Mosselbay	+	M F	38 103
MBAH22-02	J	100	18	Mosselbay	+	M F	43 106
MBAH22-03	M	105	30	Mosselbay	+	M F	43 80
MBAH22-04	M	110	40	Mosselbay	+	M F	35 103
MBAH22-05	M	110	30	Mosselbay	+	M F	40 110
MBAH22-06	M	105	20	Mosselbay	+	M F	32 94
MBAH22-07	M	110	30	Mosselbay	+	M F	39 127
MBAH22-08	M	105	20	Mosselbay	+	M F	36 208
MBAH22-09	M	110	30	Mosselbay	+	M F	40 189
MBAH22-10	J	105	20	Mosselbay	-	-	-

Supplementary Table S5.1: Concentrations of the standard surrogates and internal standards in µg/L. Abbreviations: **STD** – standard compounds; **IS** – internal standard compounds.

Chemicals	OCP	TMX	PCB #77	PCB #209	PCB STD	PCB IS
Stock concentration	1000	1000	1000	1000	1000	1000
Final concentration	5	10	10	10	50	5

Supplementary Table S5.2: The volume of the standard surrogates and internal standards in µL used to spike the blanks, distilled water, quality control and biological samples. Abbreviations: **DW** – distilled water; **QC** – quality control; **STD** – standard compounds; **IS** – internal standard compounds.

Sample	Weight	Volume spiked µL					
		OCP	TMX	PCB #77	PCB# 209	PCB STD	PCB IS
Blank	500 µL	-	50	50	50	-	25
DW	500 µL	25	50	50	50	50	25
QC	0.2g	25	50	50	50	50	25
Samples	0.3-0.5g	-	50	50	50	-	25

Supplementary Table S5.3: Organochlorine pesticide (OCP) and polychlorinated biphenyl (PCB) standards used.

OCP Standards				PCB Standards			
OCP Mix		OCP Internal standards		PCB 981 Mix		PCB Internal standards	
Analytes	Purity (%)	Analytes	Purity (%)	Analytes	Purity (%)	Analytes	Purity (%)
Aldrin	98	PCB 77 (3,3′,4,4′-Tetrachlorobiphenyl)	99	PCB #1 (2-chlorobiphenyl)	99	PCB #77 (3,3′,4,4′-Tetrachlorobiphenyl-C13)	99
cis-Chlordane (Alpha)	99	PCB 209 (2,2′,3,3′,4,4′,5,5′,6,6′-Decachlorobiphenyl)	99	PCB #5 (1,3-dichlorobiphenyl)	99	PCB #118 (2,3',4,4',5-Pentachlorobiphenyl-C13)	99
cis-Heptachlor Epoxide	99			PCB #18 (2,2',5-trichlorobiphenyl)	99	PCB #126 (3,3',4,4',5-Pentachlorobiphenyl-C13)	99
cis-Nonachlor	99			PCB #31 (2,4',5-trichlorobiphenyl)	99	PCB #156 (2,3,3',4,4',5-Hexachlorobiphenyl-C13)	99
Dieldrin	98			PCB #44 (2,2',3,5'-tetrachlorobiphenyl)	99	PCB #169 (2,3',4,4',5',6-Hexachlorobiphenyl-C13)	99
Endrin	99			PCB #52 (2,2',5,5'-tetrachlorobiphenyl)	99		
Heptachlor	99			PCB #66 (2,3',4,4'-tetrachlorobiphenyl)	99		
Hexachlorobenzene	99			PCB #87 (2,2',3,4,5'-pentachlorobiphenyl)	99		
o,p′-DDD (2,4'-DDD): 1-Chloro-2-[2,2-dichloro-1-(4-chlorophenyl)ethyl]benzene	99			PCB #101 (2,2',3,5,5'-pentachlorobiphenyl)	99		
o,p′-DDE (2,4'-DDE): 1,1-Dichloro-2,2-bis(p-chlorophenyl)ethylene	99			PCB #110 (2,3,3',4',5-pentachlorobiphenyl)	99		
o,p′-DDT (2,4'-DDT): 1,1-Dichloro-2,2-bis(p-chlorophenyl)ethane (same as 4,4'-DDT)	99			PCB #138 (2,2',3,4,4',5'-hexachlorobiphenyl)	99		
Oxychlordane	99			PCB #141 (2,2',3,4,5,5'-hexachlorobiphenyl)	99		
p,p′-DDD (4,4'-DDD) 4,4'-Dichlorodiphenyldichloroethane:	99			PCB #151 (2,2',3,5,5',6-hexachlorobiphenyl)	99		

OCP Standards				PCB Standards			
OCP Mix		OCP Internal standards		PCB 981 Mix		PCB Internal standards	
Analytes	Purity (%)	Analytes	Purity (%)	Analytes	Purity (%)	Analytes	Purity (%)
p,p'-DDE (4,4'-DDE): 4,4'-Dichlorodiphenyldichloroethylene	99			PCB #153 (2,2',4,4',5,5'-hexachlorobiphenyl)	99		
p,p'-DDT (4,4'-DDT): 1,1,1-Trichloro-2,2-bis(p-chlorophenyl)ethane	99			PCB #170 (2,2',3,3',4,4',5-heptachlorobiphenyl)	99		
trans-Chlordane (Gamma)	99			PCB #180 (2,2',3,4,4',5,5'-heptachlorobiphenyl)	99		
trans-Heptachlor Epoxide	99			PCB #183 (2,2',3,4,4'5',6-heptachlorobiphenyl)	99		
trans-Nonachlor	99			PCB #187 (2,2',3,4',5,5',6-heptachlorobiphenyl)	99		
α-HCH: Alpha-hexachlorocyclohexane	98			PCB #206 (2,2',3,3',4,4',5,5',6-nonachlorobiphenyl)	99		
β-HCH: Beta-hexachlorocyclohexane	99						
γ-HCH: (Lindane): Gamma-Hexachlorocyclohexane	99						

Comments on the recovery rates for OCPs and PCBs

Nine OCPs and 16 PCBs were detected in fish livers across the six sites (Table 5.1). There were no detectable levels of target contaminants in fish muscle samples. Table 5.1 presents the analytical sensitivity of the methods used to detect and quantify organochlorine pesticides (OCPs) and polychlorinated biphenyls (PCBs) in liver tissues of *A. honckenii*. The limit of detection (LOD) and limit of quantification (LOQ) vary between compounds, indicating differential sensitivity in analytical measurements (Saadati *et al*., 2013). Among OCPs, p,p'-DDT exhibited the highest LOQ (4.73 ng/g), suggesting a higher threshold for reliable quantification compared to other OCPs, such as γ-HCH (1.42 ng/g) (Table 1). Recovery rates for most OCPs exceeded 100%, with o,p'-DDD showing the highest recovery (148.37%) (Table 5.1), which may suggest matrix effects or analytical overestimations (Saadati *et al*., 2013). The variation in recovery rates, particularly those exceeding 100%, indicates possible interferences or matrix complexities affecting analyte extraction and detection efficiency (Saadati *et al*., 2013). Similarly, among PCBs, PCB #31 had the highest LOQ (7.74 ng/g), and PCB #206 had the lowest (0.66 ng/g) (Table 5.1). Recovery rates were consistently high, ranging between 82% and 148%, which indicates the reliability of the extraction and quantification processes (Table 5.1). Recovery rates for PCBs were slightly lower than for OCPs, with PCB #180 having the lowest recovery (82.24%), indicating potential losses during extraction and analysis (Table 5.1). The relatively lower recovery rates for certain PCBs may suggest minor extraction inefficiencies, compound volatility, or potential degradation during sample preparation (Saadati *et al*., 2013).

Supplementary Table S5.4: Organochlorine pesticide (OCP) concentrations (mean ± standard deviation) in fish liver tissues of *Amblyrhynchote honckenii* (Bloch) from six localities (Witsand, Mossel Bay, St Francis Bay, Chintsa East, Uvongo Beach, and Sodwana Bay) along the South African coastline. Significant differences between the six sites are indicated with an asterisk (*). All concentrations are provided in ng/g. Significance was taken as $p<0.05$. Abbreviations: **ND** – not detected.

Compounds	Localities					
	Witsand	**Mossel Bay**	**St Francis Bay**	**Chintsa East**	**Uvongo Beach**	**Sodwana Bay**
∑ OCP	372 ± 161	358 ± 88	213 ± 143	297 ± 131	214 ± 109	177 ± 131
Dieldrin	ND	ND	ND	ND	16 ± 13	ND
***o,p'*-DDD**	ND	ND	9 ± 4	ND	ND	ND
***o,p'*-DDT/ *p,p'*-DDD**	39 ± 13*	47 ± 9*	18 ± 5*	41 ± 22*	22 ± 9*	20 ± 10*
Oxy-Chlordane	252 ± 86*	296 ± 73*	76 ± 66*	214 ± 56*	76 ± 18*	64 ± 28*
***p,p'*-DDE**	39 ± 28*	16 ± 5*	72 ± 36*	15 ± 6*	14 ± 11*	5 ± 3*
***p,p'*-DDT**	ND	ND	33 ± 26	ND	43 ± 20	41 ± 27
trans-Nonachlor	ND	ND	ND	ND	11 ± 4	ND
β-HCH	25 ± 21	ND	ND	17 ± 33	30 ± 31	43 ± 57
γ-HCH (Lindane)	16 ± 13*	ND	6 ± 6*	9 ± 15	2 ± 2*	4 ± 6*

Supplementary Table S5.5: Polychlorinated biphenyl (PCB) concentrations (mean ± standard deviation) in fish liver tissues of *Amblyrhynchote honckenii* (Bloch) from six localities (Witsand, Mossel Bay, St Francis Bay, Chintsa East, Uvongo Beach, and Sodwana Bay) along the South African coastline. Significant differences between the six sites are indicated with an asterisk (*). All concentrations are provided in ng/g. Significance was taken as $p<0.05$. Abbreviations: **ND** – not detected.

Compounds	Localities					
	Witsand	Mossel Bay	St Francis Bay	Chintsa East	Uvongo Beach	Sodwana Bay
∑ PCB	6 ± 5	3 ± 5	929 ± 999	6 ± 9	21 ± 20	ND
PCB #31	ND	ND	37 ± 24	ND	ND	ND
PCB #44	ND	ND	21 ± 36	ND	ND	ND
PCB #52	ND	ND	113 ± 130	ND	ND	ND
PCB #66	ND	ND	23 ± 26	ND	ND	ND
PCB #87	ND	ND	6 ± 15	ND	ND	ND
PCB #101	ND	ND	93 ± 98	ND	ND	ND
PCB #110	ND	ND	50 ± 65	ND	ND	ND
PCB #138	ND	ND	152 ± 151	ND	ND	ND
PCB #141	ND	ND	9 ± 18	ND	ND	ND
PCB #151	ND	ND	19 ± 23	ND	ND	ND
PCB #153	6 ± 5*	3 ± 5*	235 ± 222*	6 ± 9*	18 ± 14*	ND
PCB #170	ND	ND	28 ± 33	ND	ND	ND
PCB #180	ND	ND	68 ± 68*	ND	4 ± 6*	ND
PCB #183	ND	ND	16 ± 22	ND	ND	ND
PCB #187	ND	ND	58 ± 65*	ND	2 ± 5*	ND
PCB #206	ND	ND	2 ± 5	ND	ND	ND

Supplementary Table S7.1: Copper (Cu) concentrations measured in control and exposure tanks at the start of the exposure period. Values represent means ± standard deviation (n = 5 per treatment). Abbreviations: (+) – parasite present; (-) – parasite absent.

		Water (-)	Water (+)
Cu	Control	12.46 ± 2.99	8.79 ± 1.85
	Exposure	407.50 ± 71.59	417.73 ± 70.87

Supplementary Table S7.2: Copper (Cu) and metallothionein (MT) accumulation in *Cinusa tetrodontis* Schioedte and Meinert, 1884, and *Amblyrhynchote honckenii* (Bloch) across different treatment groups: female and male *C. tetrodontis*; gill tissue of *A. honckenii* from infested and uninfested fish; stomach tissue of *A. honckenii* from infested and uninfested fish; liver tissue of *A. honckenii* from infested and uninfested fish, muscle tissue of *A. honckenii* from infested and uninfested fish. Values are presented as means ± standard deviation. Abbreviations: ♂ – male; ♀ – female; (+) – parasite present; (-) – parasite absent.

		Cinusa (♀)	Cinusa (♂)	Gill (-)	Gill (+)	Stomach (-)	Stomach (+)	Liver (-)	Liver (+)	Muscle (-)	Muscle (+)
Cu	Control	180.06 ± 109.96	254.00 ± 164.36	4.75 ± 0.62	3.16 ± 0.46	7.54 ± 1.49	6.03 ± 0.96	7.05 ± 2.13	2.61 ± 0.87	1.31 ± 0.02	1.14 ± 0.17
	Exposure	286.04 ± 39.46	761.63 ± 248.94	19.58 ± 15.99	7.00 ± 1.71	10.15 ± 1.86	9.30 ± 1.83	16.62 ± 5.87	7.58 ± 1.76	3.17 ± 0.91	2.66 ± 0.46
	Environmental	55.19 ± 16.94	65.37 ± 29.89	-	-	-	-	4.06 ± 2.53	3.62 ± 1.67	0.79 ± 0.13	0.86 ± 0.15
MTs	Control	16.57 ± 8.71	8.66 ± 2.94	-	-	-	-	21.08 ± 3.33	17.30 ± 3.56	25.74 ± 4.52	24.57 ± 5.85
	Exposure	21.00 ± 8.64	68.65 ± 18.87	-	-	-	-	31.65 ± 2.32	22.93 ± 3.75	31.92 ± 2.65	25.24 ± 3.51

References:

Abdelsalam, M., Attia, M.M., Marzouk, M.S., Korany, R.M., Elgendy, M.Y., Soliman, A.W., Prince, A. & Hamada, A.H., 2024. Investigating dynamics, etiology, pathology, and therapeutic interventions of *Caligus clemensi* and *Vibrio alginolyticus* co-infection in farmed marine fish. *Scientific Reports*, 14(1): 20704.

Abe, N., 2011. Molecular and morphological identification of helminthes found in Japanese smelt, *Hypomesus transpacificus nipponensis*, with notes on new host records of *Eustrongylides ignotus* and *Raphidascaris gigi*. *Acta Parasitologica*, 56(2): 227–231.

Ailan-Choke, L.G., Davies, D., Malta, L.S., Couto, J.V., Tavares, L.E.R., Luque, J.L. & Pereira, F.B., 2023. *Cucullanus pinnai pinnai* and *C. pinnai pterodorasi* (Nematoda Cucullanidae): what does the integrative taxonomy tell us about these species and subspecies classification?. *Parasitology Research*, 122(2): 557–569.

Amin, O.M. & Sharifdini, M., 2022. Molecular analysis of *Pomphorhynchus kashmirensis* based on 18S rDNA and ITS-rDNA. *International Journal of Zoology and Animal Biology*, 5(2): 1–8.

Amin, O.M., Heckmann, R.A., Dallarés, S., Constenla, M. & Van Ha, N., 2020. Morphological and molecular description of *Rhadinorhynchus hiansi* Soota & Bhattacharya, 1981 (Acanthocephala: Rhadinorhynchidae) from marine fish off the Pacific coast of Vietnam. *Journal of Parasitology*, 106(1): 56–70.

Amin, O.M., Heckmann, R.A., Fišer, Ž., Zakšek, V., Herlyn, H. & Kostanjšek, R., 2019. Description of *Acanthocephalus anguillae balkanicus* subsp. n. (Acanthocephala: Echinorhynchidae) from *Proteus anguinus* Laurenti (Amphibia: Proteidae) and the cave ecomorph of *Asellus aquaticus* (Crustacea: Asellidae) in Slovenia. *Folia Parasitologica*, 66.

Andres, M.J., Ray, C.L., Pulis, E.E., Curran, S.S. & Overstreet, R.M., 2014. Molecular characterization of two opecoelid trematodes from fishes in the Gulf of Mexico, with a description of a new species of *Helicometra*. *Acta Parasitologica*, 59(3): 405–412.

Andrews, M., Bott, N., Battaglene, S. & Nowak, B., 2009. A new species of copepod (Siphonostomatoida: Caligidae) parasitic on the striped trumpeter, *Latris lineata* (Forster), from Tasmania. *Zootaxa*, 1971(1): 59–68.

Antar, R., Georgieva, S., Gargouri, L. & Kostadinova, A., 2015. Molecular evidence for the existence of species complexes within *Macvicaria* Gibson & Bray, 1982 (Digenea: Opecoelidae) in the western Mediterranean, with descriptions of two new species. *Systematic Parasitology*, 91: 211–229.

Atopkin, D.M., Ivashko, Y.I., Izrailskaia, A.V., Tatonova, Y.V. & Besprozvannykh, V.V., 2024. Morphological and molecular data on *Pseudozoogonoides ugui* Shimazu, 1974 (Digenea: Microphalloidea: Zoogonidae) ex *Pseudaspius hakonensis* (Günther, 1877) and taxonomic problems in Zoogoninae genera. *Journal of Helminthology*, 98: e36.

Atopkin, D.M., Shedko, M.B., Rozhkovan, K.V., Nguyen, H.V. & Besprozvannykh, V.V., 2022. *Rhipidocotyle husi* n. sp. and three known species of Bucephalidae Poche, 1907 from the East Asian Region: morphological and molecular data. *Parasitology*, 149: 774–785.

Azizoğlu, U., Karaborklu, S., Ayvaz, A. & Yilmaz, S., 2016. Phylogenetic relationships of insect-associated free-living rhabditid nematodes from eastern Mediterranean region of Turkey. *Applied Ecology and Environmental Research*, 14(3).

Baek, S.Y., Jang, K.H., Choi, E.H., Ryu, S.H., Kim, S.K., Lee, J.H., Lim, Y.J., Lee, J., Jun, J., Kwak, M., Lee, Y.S., Hwang, J.S., Venmathi-Maran, B.A., Chang, C.Y., Kim, I.H. & Hwang, U.W., 2016. DNA barcoding of metazoan zooplankton copepods from South Korea. *PLoS ONE*, 11: e0157307.

Bagnato, E., Gilardoni, C. & Cremonte, F., 2022. Relevamiento parasitológico del mero patagónico *Acanthistius patachonicus* (Perciformes: Serranidae) en los arrecifes patagónicos. *Revista Argentina de Parasitología*, 11(1): 21–31.

Bennet, J., Jorge, F., Poulin, R. & Randhawa, H., 2019. Revealing trophic transmission pathways of marine tapeworms. *Parasitology Research*, 118(1): 1–10.

Born Torrijos, A., Kostadinova, A., Raga, J.A. & Holzer, A.S., 2012. Molecular and morphological identification of larval opecoelids (Digenea: Opecoelidae) parasitising prosobranch snails in a Western Mediterranean lagoon. *Parasitology International*, 61(3): 450–460.

Braicovich, P.E., Lanfranchi, A.L., Farber, M.D., Marvaldi, A., Luque, J.L. & Timi, J.T., 2014. Genetic and morphological evidence reveals the existence of a new family, genus and species of Echinorhynchida (Acanthocephala).

Bray, R.A., Cribb, T.H., Littlewood, D.T.J. & Waeschenbach, A., 2016. The molecular phylogeny of the digenean family Opecoelidae Ozaki, 1925 and the value of morphological characters, with the erection of a new subfamily. *Folia Parasitologica*, 63: 1.

Caira, J.N., Jensen, K., Hayes, C. & Ruhnke, T.R., 2020. Insights from new cestodes of the crocodile shark, *Pseudocarcharias kamoharai* (Lamniformes: Pseudocarchariidae), prompt expansion of *Scyphyophyllidum* and formal synonymization of seven phyllobothriidean genera – at last!. *Journal of Helminthology*, 94: e132.

Caira, J.N., Jensen, K., Waeschenbach, A., Olson, P.D. & Littlewood, D.T.J., 2014. Orders out of chaos – molecular phylogenetics reveals the complexity of shark and stingray tapeworm relationships. *International Journal for Parasitology*, 44(1): 55–73.

Chaudhary, A., Amin, O.M., Heckmann, R. & Singh, H.S., 2020. The molecular profile of *Rhadinorhynchus dorsoventrospinosus* Amin, Heckmann & Ha, 2011 (Acanthocephala: Rhadinorhynchidae) from Vietnam. *Journal of Parasitology*, 106(3): 418–427.

Chen, H.Y. & Shih, H.H., 2015. Occurrence and prevalence of fish-borne *Anisakis* larvae in the spotted mackerel *Scomber australasicus* from Taiwanese waters. *Acta Tropica*, 145: 61–67.

Chomchoei, N., Backeljau, T., Segers, B., Wongsawad, C., Butboonchoo, P. & Nantarat, N., 2022. Morphological and molecular characterization of larval trematodes infecting the assassin snail genus *Anentome* in Thailand. *Journal of Helminthology*, 96: e52.

Corner, R.D., Cribb, T.H. & Cutmore, S.C., 2020. A new genus of Bucephalidae Poche, 1907 (Trematoda: Digenea) for three new species infecting the yellowtail pike, *Sphyraena obtusata* Cuvier (Sphyraenidae), from Moreton Bay, Queensland, Australia. *Systematic Parasitology*, 97: 455–476.

Curran, S.S., Calhoun, D.M., Tkach, V.V., Warren, M.B. & Bullard, S.A., 2022. A new species of *Prosorhynchoides* Dollfus, 1929 (Digenea: Bucephalidae) infecting chain pickerel, *Esox niger* Lesueur, 1818 (Perciformes: Esocidae), from the Pascagoula River, Mississippi, USA, with phylogenetic analysis and nucleotide-based elucidation of a three-host life cycle. *Comparative Parasitology*, 89: 82–101.

Cutmore, S.C., Bennett, M.B., Miller, T.L. & Cribb, T.H., 2017. Patterns of specificity and diversity in species of *Paraorygmatobothrium* Ruhnke, 1994 (Cestoda: Phyllobothriidae) in Moreton Bay, Queensland, Australia, with the description of four new species. *Systematic Parasitology*, 94(9): 941–970.

Cutmore, S.C., Cribb, T.H., Bennett, M. & Beveridge, I., 2018. Tetraphyllidean and onchoproteocephalidean cestodes of elasmobranchs from Moreton Bay, Australia: description of two new species and new records for seven described species. *Systematic Parasitology*, 95: 807–827.

Cutmore, S.C., Nolan, M.J. & Cribb, T.H., 2018. Heterobucephalopsine and prosorhynchine trematodes (Digenea: Bucephalidae) from teleost fishes of Moreton Bay, Queensland, Australia, with the description of two new species. *Systematic Parasitology*, 95: 783–806.

D'Amelio, S., Cavallero, S., Dronen, N.O., Barros, N.B. & Paggi, L., 2012. Two new species of *Contracaecum* Railliet & Henry, 1912 (Nematoda: Anisakidae), *C. fagerholmi* n. sp. and *C. rudolphii F* from the brown pelican *Pelecanus occidentalis* in the northern Gulf of Mexico. *Systematic Parasitology*, 81(1): 1–16.

Damin, L. & Heqing, H., 2001. *Heliconema minnanensis* n. sp. (Physalopteroidae: Physalopteridae) and *Raphidascaris trichiuri* (Yin & Zhang) n. comb. (Ascaridoidea: Anisakidae) in marine fishes. *Journal of Parasitology*, 87(5): 1090–1094.

Dos Santos, Q.M., Avenant-Oldewage, A., Piasecki, W., Molnár, K., Sellyei, B. & Szekely, C., 2021. An alien parasite affects local fauna: confirmation of *Sinergasilus major* (Copepoda: Ergasilidae) switching hosts and infecting native *Silurus glanis* (Actinopterygii: Siluridae) in Hungary. *International Journal for Parasitology: Parasites and Wildlife*, 15: 127–131.

Dumbo, J., Dos Santos, Q. & Avenant-Oldewage, A., 2024. Morphological and molecular characterisation of two new species of *Rhipidocotyle* (Digenea: Bucephalidae Poche,

1907) from *Sphyraena putnamae* Jordan & Seale in Mozambique. *Journal of Helminthology*, 98: e56.

Faltýnková, A., Kudlai, O., Salganskiy, O.O., Korol, E.M. & Kuzmina, T.A., 2022. Trematodes from Antarctic teleost fishes off Argentine Islands, West Antarctica: molecular and morphological data. *Systematic Parasitology*, 99(4): 491–523.

Fikiye, P.P., Smit, N.J., Van As, L.L., Truter, M. & Hadfield, K.A., 2023. Integrative morphological and genetic characterisation of the fish parasitic copepod *Ergasilus mirabilis* Oldewage & van As, 1987: insights into host specificity and distribution in Southern Africa. *Diversity*, 15: 965.

Freeman, M.A. & Ogawa, K., 2010. Variation in the small subunit ribosomal DNA confirms that *Udonella* (Monogenea: Udonellidae) is a species-rich group. *International Journal for Parasitology*, 40(2): 255–264.

Fyler, C.A. & Caira, J.N., 2011. Phylogenetic status of four new species of *Acanthobothrium* (Cestoda: Tetraphyllidea) parasitic on the wedgefish *Rhynchobatus laevis* (Elasmobranchii: Rhynchobatidae): implications for interpreting host associations. *Invertebrate Systematics*, 24(5): 419–433.

Fyler, C.A., Caira, J.N. & Jensen, K., 2009. Five new species of *Acanthobothrium* (Cestoda: Tetraphyllidea) from an unusual species of *Himantura* (Rajiformes: Dasyatidae) from northern Australia. *Folia Parasitologica*, 56(2): 107–128.

Gallagher, K.A. & Caira, J.N., 2020. A new species of *Acanthobothrium* (Cestoda: Onchoproteocephalidea) from the smalleye pygmy shark, *Squaliolus aliae* (Chondrichthyes: Squaliformes: Dalatiidae), from Taiwan. *Journal of Parasitology*, 106(6): 818–827.

Gilardoni, C., Etchegoin, J., Cribb, T., Pina, S., Rodrigues, P., Diez, M.E. & Cremonte, F., 2020. Cryptic speciation of the zoogonid digenean *Diphterostomum flavum* n. sp. demonstrated by morphological and molecular data. *Parasite*, 27: 44.

González, M.T., Castro, R., Muñoz, G. & López, Z., 2016. Sea lice (Siphonostomatoida: Caligidae) diversity on littoral fishes from the south-eastern Pacific coast determined from morphology and molecular analysis, with description of a new species (*Lepeophtheirus confusum*). *Parasitology International*, 65(6): 685–695.

Grano-Maldonado, M.I., Sereno-Uribe, A.L., Payán, J.C.H., de León, G.P.P. & García-Varela, M., 2025. Linking adults and cystacanths of a new species of *Rhadinorhynchus* Lühe, 1911 (Acanthocephala: Rhadinorhynchidae) from the Pacific coast of Mexico by using morphological and molecular data. *Systematic Parasitology*, 102(1): 10.

Gregori, M., Aznar, F.J., Abollo, E., Roura, A., González, A.F. & Pascual, S., 2013. *Nyctiphanes couchii* as intermediate host for *Rhadinorhynchus* sp. (Acanthocephala,

Echinorhynchidae) from NW Iberian Peninsula waters. *Diseases of Aquatic Organisms*, 105(1): 9–20.

Hammond, M.D., Cribb, T.H. & Bott, N.J., 2018. Three new species of *Prosorhynchoides* (Digenea: Bucephalidae) from *Tylosurus gavialoides* (Belonidae) in Moreton Bay, Queensland, Australia. *Parasitology International*, 67: 454–464.

Holland, N.D., Campbell, T.G., Garey, J.R., Holland, L.Z. & Wilson, N.G., 2009. The Florida amphioxus (Cephalochordata) hosts larvae of the tapeworm *Acanthobothrium brevissime*: natural history, anatomy and taxonomic identification of the parasite. *Acta Zoologica*, 90: 75–86.

Hua, C.J., Su, M.Y., Sun, Z.W., Lu, Y.H. & Feng, J.M., 2021. Complete mitochondrial genome of the copepod *Sinergasilus undulatus* (Copepoda: Poecilostomatoida). *Mitochondrial DNA B Resources*, 6: 1226–1228.

Huston, D.C., Cribb, T.H. & Smales, L.R., 2020. Molecular characterisation of acanthocephalans from Australian marine teleosts: proposal of a new family, synonymy of another and transfer of taxa between orders. *Systematic Parasitology*, 97(1): 1–23.

Jensen, K. & Bullard, S.A., 2010. Characterization of a diversity of tetraphyllidean and rhinebothriidean cestode larval types, with comments on host associations and life-cycles. *International Journal for Parasitology*, 40: 889–910.

Jousson, O., Bartoli, P. & Pawlowski, J., 1999. Molecular identification of developmental stages in Opecoelidae (Digenea). *International Journal for Parasitology*, 29(11): 1853–1858.

Ki, J.-S., Park, H.G. & Lee, J.-S., 2009. The complete mitochondrial genome of the cyclopoid copepod *Paracyclopina nana*: a highly divergent genome with novel gene order and atypical gene numbers. *Gene*, 435: 13–22.

Ki, J.-S.H., Park, G. & Lee, J.S., 2011. Extensive analysis of nuclear cistron rDNA sequence of *Paracyclopina nana* (Cyclopoida: Cyclopettidae). *Hydrobiologia*, 666: 3–9.

Kita, Y., Nitta, M. & Kajihara, H., 2024. Morphological and molecular characteristics of two species of the genus *Rhadinorhynchus* (Palaeacanthocephala: Echinorhynchida) from the western Pacific. *Species Diversity*, 29(1): 171–178.

Kremnev, G., Gonchar, A., Uryadova, A., Krapivin, V., Skobkina, O., Gubler, A. & Krupenko, D., 2023. No tail no fail: life cycles of the Zoogonidae (Digenea). *Diversity*, 15(1): 121.

Kudlai, O., Rakauskas, V., Baker, N.J., Pantoja, C., Lisitsyna, O. & Binkienė, R., 2024. Helminth parasites of invasive freshwater fish in Lithuania. *Animals: an Open Access Journal from MDPI*, 14(22): 3293.

Kvach, Y., Tkachenko, M.Y., Seifertová, M. & Ondračková, M., 2021. Insights into the diversity, distribution and phylogeny of three ergasilid copepods (Hexanauplia: Ergasilidae) in lentic water bodies of the Morava River basin, Czech Republic. *Limnologica*, 91: 125922.

Li, L., Du, L.Q., Xu, Z., Guo, Y.N., Wang, S.X. & Zhang, L.P., 2014. Morphological variability and molecular characterisation of *Dichelyne (Cucullanellus) pleuronectidis* (Yamaguti, 1935) (Ascaridida: Cucullanidae) from the flatfish *Pleuronichthys cornutus* (Temminck & Schlegel) (Pleuronectiformes: Pleuronectidae) in the East China Sea. *Systematic Parasitology*, 87(1): 87–98.

Li, L., Lü, L., Nadler, S.A., Gibson, D.I., Zhang, L.P., Chen, H.X., Zhao, W.T. & Guo, Y.N., 2018. Molecular phylogeny and dating reveal a terrestrial origin in the early Carboniferous for ascaridoid nematodes. *Systematic Biology*, 67(5): 888–900.

Littlewood, D.T.J., Rohde, K. & Clough, K.A., 1999. The interrelationships of all major groups of Platyhelminthes: phylogenetic evidence from morphology and molecules. *Biological Journal of the Linnean Society*, 66(1): 75–114.

Malsawmtluangi, C. & Lalramliana, 2023. A new species of *Prosorhynchoides* Dollfus, 1929 (Digenea: Bucephalidae) from *Xenentodon cancila* Hamilton, 1822 in Mizoram, Northeast India. *Parasitology International*, 92: 102690.

Malta, L.S., Paiva, F., Elisei, C., Tavares, L.E.R. & Pereira, F.B., 2020. A new species of *Raphidascaris* (Nematoda: Raphidascarididae) infecting the fish *Gymnogeophagus balzanii* (Cichlidae) from the Pantanal wetlands, Brazil and a taxonomic update of the subgenera of *Raphidascaris* based on molecular phylogeny and morphology. *Journal of Helminthology*, 94: e24.

Martin, S.B., Crouch, K., Cutmore, S.C. & Cribb, T.H., 2018b. Expansion of the concept of the Opistholebetinae Fukui, 1929 (Digenea: Opecoelidae Ozaki, 1925), with *Magnaosimum brooksae* ng, n. sp. from *Tripodichthys angustifrons* (Hollard) (Tetraodontiformes: Triacanthidae) in Moreton Bay, Australia. *Systematic Parasitology*, 95(2): 121–132.

Martin, S.B., Ribu, D., Cutmore, S.C. & Cribb, T.H., 2018a. Opistholobetines (Digenea: Opecoelidae) in Australian tetraodontiform fishes. *Systematic Parasitology*, 95(8): 743–781.

Mehrdana, F., Bahlool, Q.Z., Skov, J., Marana, M.H., Sindberg, D., Mundeling, M., Overgaard, B.C., Korbut, R., Strøm, S.B., Kania, P.W. & Buchmann, K., 2014. Occurrence of zoonotic nematodes *Pseudoterranova decipiens*, *Contracaecum osculatum* and *Anisakis simplex* in cod (*Gadus morhua*) from the Baltic Sea. *Veterinary Parasitology*, 205(3–4): 581–587.

Mejia-Madrid, H.H., 2018. A molecular phylogeny of the *Rhigonematomorpha* De Ley & Blaxter, 2002 as inferred from SSU and LSU rDNA sequences. *Nematology*, 20(6): 547–565.

Míč, R., Řehulková, E., Šimková, A., Razanabolana, J.R. & Seifertová, M., 2024. New species of *Dermoergasilus* Ho & Do, 1982 (Copepoda: Cyclopoida: Ergasilidae) parasitizing endemic cichlid *Paretroplus polyactis* (Bleeker) in Madagascar. *Parasitology*, 151: 319–336.

Montes, M.M., Vercellini, C., Ostoich, N., Shimabukuro, M.I., Cavallo, G., Reig Cardarella, G. & Martorelli, S., 2023. Phylogenetic position of the South American freshwater *Rhipidocotyle*

santaensis (Digenea: Bucephalidae) based on partial 28S rDNA. *Parasitology Research*, 122: 1765–1774.

Nadler, S.A., D'Amelio, S., Dailey, M.D., Paggi, L., Siu, S. & Sakanari, J.A., 2005. Molecular phylogenetics and diagnosis of *Anisakis*, *Pseudoterranova*, and *Contracaecum* from northern Pacific marine mammals. *Journal of Parasitology*, 91(6): 1413–1429.

Nakao, M., 2016. *Pseudoacanthocephalus toshimai* sp. nov. (Palaeacanthocephala: Echinorhynchidae), a common acanthocephalan of anuran and urodelan amphibians in Hokkaido, Japan, with a finding of its intermediate host. *Parasitology International*, 65(4): 323–332.

Near, T.J., Garey, J.R. & Nadler, S.A., 1998. Phylogenetic relationships of the Acanthocephala inferred from 18S ribosomal DNA sequences. *Molecular Phylogenetics and Evolution*, 10(3): 287–298.

Nikhila, R.M.V., Drisya, O.K., Rijin, K., Mumthaz, T.M.V., Helna, A.K., Ivanenko, V.N. & Sudha, K., 2019. Copepod crustaceans parasitizing marine fish of the Kerala coast, India. *Arthropoda Selecta*, 28(4): 529–544.

Nolan, M.J., Miller, T.L., Cutmore, S.C., Cantacessi, C. & Cribb, T.H., 2015. *Dollfustrema durum* n. sp. and *Heterobucephalopsis perardua* n. sp. (Digenea: Bucephalidae) from the giant moray eel, *Gymnothorax javanicus* (Bleeker) (Anguilliformes: Muraenidae), and proposal of the Heterobucephalopsinae n. subfam. *Parasitology International*, 64: 559–570.

Nowak, B.F., Hayward, C.J., Gonzalez, L., Bott, N.J. & Lester, R.J.G., 2011. Sea lice infections of salmonids farmed in Australia. *Aquaculture*, 320(3–4): 171–177.

Ogawa, K. & Itoh, N., 2022. Five new and two known species of *Heterobothrium* (Monogenea: Diclidophoridae) infecting puffers of the genus *Takifugu* from Japanese waters. *Systematic Parasitology*, 99(3): 317–340.

Øines, Ø. & Heuch, P.A., 2005. Identification of sea louse species of the genus *Caligus* using mtDNA. *Journal of the Marine Biological Association of the United Kingdom*, 85(1): 73–79.

Øines, Ø. & Schram, T., 2008. Intra- or inter-specific difference in genotypes of *Caligus elongatus* Nordmann, 1832?. *Acta Parasitologica*, 53(1): 93–105.

Olson, P.D., Caira, J.N., Jensen, K., Overstreet, R.M., Palm, H.W. & Beveridge, I., 2010. Evolution of the trypanorhynch tapeworms: parasite phylogeny supports independent lineages of sharks and rays. *International Journal for Parasitology*, 40(2): 223–242.

Olson, P.D., Cribb, T.H., Tkach, V.V., Bray, R.A. & Littlewood, D.T.J., 2003. Phylogeny and classification of the Digenea (Platyhelminthes: Trematoda). *International Journal for Parasitology*, 33(7): 733–755.

Olson, P.D., Littlewood, D.T.J., Bray, R.A. & Mariaux, J., 2001. Interrelationships and evolution of the tapeworms (Platyhelminthes: Cestoda). *Molecular Phylogenetics and Evolution*, 19(3): 443–467.

Ondračková, M., Fojtu, J., Seifertová, M., Kvach, Y. & Jurajda, P., 2019. Non-native parasitic copepod *Neoergasilus japonicus* (Harada, 1930) utilizes non-native fish host *Lepomis gibbosus* (L.) in the floodplain of the river Dyje (Danube basin). *Parasitology Research*, 118: 57–62.

Palm, H.W., Waeschenbach, A. & Littlewood, D.T.J., 2007. Genetic diversity in the trypanorhynch cestode *Tentacularia coryphaenae* Bosc, 1797: evidence for a cosmopolitan distribution and low host specificity in the teleost intermediate host. *Parasitology Research*, 101(1): 153–159.

Palm, H.W., Waeschenbach, A., Olson, P.D. & Littlewood, D.T.J., 2009. Molecular phylogeny and evolution of the Trypanorhyncha (Platyhelminthes: Cestoda). *Molecular Phylogenetics and Evolution*, 52(2): 351–367.

Parshukov, A., Vlasenko, P., Simonov, E., Ieshko, E., Burdukovskaya, T., Anikieva, L., Kashinskaya, E., Andree, K.B. & Solovyev, M., 2021. Parasitic copepods *Caligus lacustris* (Copepoda: Caligidae) on the rainbow trout *Oncorhynchus mykiss* in cage aquaculture: morphology, population demography, and first insights into phylogenetic relationships. *Parasitology Research*, 120(7): 2455–2467.

Pereira, F.B. & Luque, J.L., 2017. Morphological and molecular characterization of cucullanid nematodes including *Cucullanus opisthoporus* n. sp. in freshwater fish from the Brazilian Amazon. *Journal of Helminthology*, 91(6): 739–751.

Perrot-Minnot, M.J., 2004. Larval morphology, genetic divergence, and contrasting levels of host manipulation between forms of *Pomphorhynchus laevis* (Acanthocephala). *International Journal for Parasitology*, 34(1): 45–54.

Petkevičiūtė, R., Stunžėnas, V. & Stanevičiūtė, G., 2014. Differentiation of European freshwater bucephalids (Digenea: Bucephalidae) based on karyotypes and DNA sequences. *Systematic Parasitology*, 87: 199–212.

Quiazon, K.M.A., Santos, M.D., Blatchley, D.D., Aguila, R.D. & Yoshinaga, T., 2021. Molecular and morphological identifications of *Anisakis* Dujardin, 1845 (Nematoda: Anisakidae) from a rare Deraniyagala's beaked whale (*Mesoplodon hotaula* Deraniyagala, 1963) and Blainville's beaked whale (*Mesoplodon densirostris* Blainville, 1817) stranded off southern Philippines. *Philippine Journal of Science*, 150: 823–835.

Raupach, M.J., Barco, A., Steinke, D., Beermann, J., Laakmann, S., Mohrbeck, I., Neumann, H., Kihara, T.C., Pointner, K., Radulovici, A. & Segelken-Voigt, A., 2015. The application of DNA barcodes for the identification of marine crustaceans from the North Sea and adjacent regions. *PLoS ONE*, 10(9): e0139421.

Rima, M., Marzoug, D., Pérez-del-Olmo, A., Kostadinova, A., Bouderbala, M. & Georgieva, S., 2017. New molecular and morphological data for opecoelid digeneans in two Mediterranean sparid fishes with descriptions of *Macvicaria gibsoni* n. sp. and *M. crassigula* (Linton, 1910) (sensu stricto). *Systematic Parasitology*, 94: 739–763.

Rubio-Godoy, M., Paladini, G., Freeman, M.A., Garcia-Vasquez, A. & Shinn, A.P., 2012. Morphological and molecular characterisation of *Gyrodactylus salmonis* (Platyhelminthes, Monogenea) isolates collected in Mexico from rainbow trout (*Oncorhynchus mykiss* Walbaum). *Veterinary Parasitology*, 186(3–4): 289–300.

Ruhnke, T.R. & Workman, R.E., 2013. Two new species and a new phyllobothriid cestode genus from sharks of the genus *Negaprion* Whitley (Carcharhiniformes). *Systematic Parasitology*, 85(1): 37–48.

Ruhnke, T.R., Daniel, V. & Jensen, K., 2020. Four new species of *Paraorygmatobothrium* (Eucestoda: Phyllobothriidea) from sharks of the Gulf of Mexico and the Atlantic Ocean, with comments on their host specificity. *Journal of Parasitology*, 106(1): 133–156.

Santacruz, A., Morales-Serna, F.N., Leal-Cardín, M., Barluenga, M. & Pérez-Ponce de León, G., 2020. *Acusicola margulisae* n. sp. (Copepoda: Ergasilidae) from freshwater fishes in a Nicaraguan crater lake based on morphological and molecular evidence. *Systematic Parasitology*, 97: 165–177.

Santoro, M., Iaccarino, D. & Bellisario, B., 2020. Host biological factors and geographic locality influence predictors of parasite communities in sympatric sparid fishes of the southern Italian coast. *Scientific Reports*, 10: 13283.

Soares, G.B., Domingues, M.V. & Adriano, E.A., 2021. Morphological and molecular characterization of *Udonella brasiliensis* n. sp. (Monogenoidea), an epibiont on *Caligus* sp. parasite of Ariidae from the southeastern coast of Brazil. *Parasitology International*, 83: 102371.

Song, Y., Wang, G.T., Yao, W.J., Gao, Q. & Nie, P., 2008. Phylogeny of freshwater parasitic copepods in the Ergasilidae (Copepoda: Poecilostomatoida) based on 18S and 28S rDNA sequences. *Parasitology Research*, 102: 299–306.

Stunž, V., Cryan, J.R. & Molloy, D.P., 2004. Comparison of rDNA sequences from colchicine treated and untreated sporocysts of *Phyllodistomum folium* and *Bucephalus polymorphus* (Digenea). *Parasitology International*, 53: 223–228.

Syarifah, R.F., Murwantoko, M. & Setyobudi, E., 2023. Prevalence and intensity of larvae of the genus *Anisakis* sensu lato (Nematoda, Anisakidae) in bigeye scad, *Selar crumenophthalmus* (Bloch, 1793), from the Indian Ocean off Java, Indonesia. *Asian Fisheries Science*, 36(4).

Tkach, V.V., Pawlowski, J., Mariaux, J. & Swiderski, Z., 2001. Molecular phylogeny of the suborder Plagiorchiata and its position in the system of Digenea. In: *Interrelationships of the Platyhelminthes*. CRC Press, pp. 186–193.

Vasquez, A.A., Bonnici, B.L., Kashian, D.R., Trejo-Martinez, J., Miller, C.J. & Ram, J.L., 2023. The biodiversity of freshwater crustaceans revealed by taxonomy and mitochondrial DNA barcodes. *Physiology Faculty Research Publications*, 3. Available at: https://digitalcommons.wayne.edu/physio_frp/3 (Date accessed: 1 April 2023).

Vidal-Martínez, V.M., Velázquez-Abunader, I., Centeno-Chalé, O.A., May-Tec, A.L., Soler-Jiménez, L.C., Pech, D., Mariño-Tapia, I., Enriquez, C., Zapata-Pérez, O., Herrera-Silveira, J. & Hernández-Mena, D.I., 2019. Metazoan parasite infracommunities of the dusky flounder (*Syacium papillosum*) as bioindicators of environmental conditions in the continental shelf of the Yucatan Peninsula, Mexico. *Parasites & Vectors*, 12(1): 277.

Viriyautsahakul, S., Poulin, R., Johnson, S.L. & Bennett, J., 2025. Unravelling hidden battles: Genetic insights into parasite diversity and competition in mottled triplefin (*Forsterygion capito*). *Parasitology Research*, 124(6): 62.

Waeschenbach, A., Webster, B.L.W., Bray, R.A. & Littlewood, D.T.J., 2007. Added resolution among ordinal level relationships of tapeworms (Platyhelminthes: Cestoda) with complete small and large subunit nuclear ribosomal RNA genes. *Molecular Phylogenetics and Evolution*, 45(1): 311–325.

Xu, Z., Chen, H.X., Ju, H.D. & Li, L., 2017. Morphological and molecular characterization of *Cucullanus bourdini* Petter et Le Bel, 1992 (Ascaridida: Cucullanidae) from the yellowback fusilier *Caesio xanthonota* Bleeker (Perciformes: Caesionidae). *Acta Parasitologica*, 62(1): 199–206.

Yanar, A., Kamanli, S.A., Sönmez, S., Hamdi, İ., Özak, A.A. & Boxshall, G.A., 2025. *Caligus minimus* Otto, 1821 (Copepoda: Caligidae): A commercially important but poorly described parasite of cultured European sea bass, *Dicentrarchus labrax* (Linnaeus, 1758). *Parasitology International*, 104: 102964.

Zhang, K., Xu, Z., Chen, H.X., Guo, N. & Li, L., 2018. Anisakid and raphidascaridid nematodes (Ascaridoidea) infection in the important marine food-fish *Lophius litulon* (Jordan) (Lophiiformes: Lophiidae). *International Journal of Food Microbiology*, 284: 105–111.

Appendix A:

Marine Pollution Bulletin 194 (2023) 115385

Contents lists available at ScienceDirect

Marine Pollution Bulletin

journal homepage: www.elsevier.com/locate/marpolbul

Baseline

The use of fish parasitic isopods as element accumulation indicators in marine pollution monitoring

L. Van Der Spuy [a,*], J.H. Erasmus [a], M. Nachev [b], B.C. Schaeffner [a,c], B. Sures [a,b,d], V. Wepener [a], N.J. Smit [a]

[a] Water Research Group, Unit for Environmental Sciences and Management, North-West University, 11 Hoffman Street, Potchefstroom 2520, South Africa
[b] Department of Aquatic Ecology and Centre for Water and Environmental Research, University of Duisburg-Essen, Universitätsstrasse 5, 45141 Essen, Germany
[c] Institute for Experimental Pathology at Keldur, University of Iceland, Keldnavegur 3, 112 Reykjavík, Iceland
[d] Research Center One Health Ruhr, Research Alliance Ruhr, University of Duisburg-Essen, Universitätsstrasse 5, 45141 Essen, Germany

ARTICLE INFO

Keywords:
Environmental parasitology
Marine fish parasite
Ectoparasite
Marine pollution monitoring

ABSTRACT

Marine ecosystems are continuously under threat due to pollutants, which endanger marine biodiversity. The present study determines the potential use of the parasitic isopod, *Cinusa tetrodontis* Schjödte et Meinert, 1884, together with its fish host, *Amblyrhynchotes honckenii* (Bloch) for marine bioaccumulation monitoring. The concentrations of As, Cd, Cu, Mn, Ni, Pb, Se, and Zn were determined in muscle and liver tissues of infested and uninfested fish, and male and female parasites on the South African temperate south coast. The concentrations of Cu and Ni in *C. tetrodontis* differed significantly between two sampling sites, a near-pristine (Breede River Estuary, Witsand) and a more polluted site (harbour area in Mossel Bay). Mossel Bay isopods had higher concentrations of Ni, while Witsand isopods had higher concentrations of Cu. In contrast to fish hosts, parasitic isopods accumulated significantly higher levels of all elements except Cd. Most significant relationships between elements accumulated by *C. tetrodontis* and an increase of elements in fish tissues were seen in liver, rather than muscle tissue samples. Specimens of *C. tetrodontis* can be defined as good bioindicators for elements such as As, Cu, Mn, Ni, Pb, Se, and Zn, as they possess high bioaccumulation capabilities. This study addresses one of several future directions needed within environmental parasitology and highlights the importance of studying and utilising this host-ectoparasite model system.

Marine ecosystems are continuously threatened by several anthropogenic pressures, such as pollutants, which influence the integrity of these systems and endanger marine biodiversity (Pinsino et al., 2008; Webb and Mindel, 2015; Mahmoud et al., 2019). Traditionally, pollution monitoring programs in marine environments have focused on the use of free-living bioindicator species, such as bivalves, to assess element exposure in the marine environment over spatial and temporal scales (Farrington et al., 2016; Wepener and Degger, 2020). However, recent research has shown the value of the use of affiliate species and their fish hosts as sentinels for chemical pollution (Sures et al., 2017). Parasites are highly sensitive to environmental change and respond either directly or indirectly to different degrees of pollution (Chine et al., 2021; Sures et al., 2023). Advances in environmental parasitology have demonstrated the advantages of using hosts and their parasites as sentinel systems for pollution monitoring over free-living species, such as mussels (Sures et al., 2017; Chine et al., 2021; Sures et al., 2023). However, previous studies on host-parasite systems were primarily focused on freshwater environments and biased towards the use of endoparasitic helminths, such as acanthocephalans, cestodes, nematodes or digeneans (Sures, 2004; Vidal-Martínez et al., 2010; Nachev and Sures, 2016; Erasmus et al., 2020), while fewer studies focused on the use of ectoparasites, particularly in marine environments (e.g., Pérez-del-Olmo et al., 2019).

In comparison to their endoparasitic counterparts, ectoparasites are exposed to both the external environment, as well as the environment created by their fish hosts, which makes them potentially more susceptible and sensitive to environmental changes caused by pollution and/or other water quality parameters (Biswal and Chatterjee, 2020). They were shown to possess a higher bioaccumulation capacity than their fish hosts, for instance, Pb in monogeneans (Gao and Nie, 2000),

* Corresponding author.
E-mail addresses: 27014452@mynwu.ac.za (L. Van Der Spuy), hannes.erasmus@nwu.ac.za (J.H. Erasmus), milen.nachev@uni-due.de (M. Nachev), bjoern@hi.is (B.C. Schaeffner), bernd.sures@uni-due.de (B. Sures), victor.wepener@nwu.ac.za (V. Wepener), nico.smit@nwu.ac.za (N.J. Smit).

https://doi.org/10.1016/j.marpolbul.2023.115385
Received 9 June 2023; Received in revised form 2 August 2023; Accepted 4 August 2023
Available online 12 August 2023
0025-326X/© 2023 Published by Elsevier Ltd.

Appendix A

and Hg in the cymothoid parasite, *Riggia paranensis* Szidat, 1948 (Quoy et Gaimard) (Lins et al., 2008) and various other elements in parasitic isopods (Pérez-del-Olmo et al., 2019). This indicates that similar to endoparasites, ectoparasites are able to bioconcentrate these elements, producing quantifiable results, which are normally only present in very low, or undetectable concentrations in the environment (Gilbert and Avenant-Oldewage, 2017). The use of ectoparasites, such as isopods, could greatly facilitate our understanding of the biological availability of pollutants in the environment, ecological interactions and food web information, with a direct link to climate change (Longo et al., 2013; van Gestel et al., 2018; Sures et al., 2023). Isopods represent a quarter (25%) of all ectoparasites known to infest fish globally (Öktener and Sezgin, 2000; Tansel and Fatih, 2012; Mahmoud et al., 2019). They play crucial roles in marine ecosystems by providing food for larger species and helping to break down organic matter (van Gestel et al., 2018). Results from ecotoxicological studies of terrestrial isopods over the last three decades highlight the great capability of these organisms to accumulate element contaminants (Drobne, 1997; van Gestel, 2012), making them suitable bioindicators for bioaccumulation monitoring programs. Further advantages of their use as bioaccumulation indicators in marine systems are the high host specificity, easy identification, well-defined physiologies, known life cycles and high occurrence in nature (Longo et al., 2013).

The present study aims to determine the potential use of the parasitic isopod, *Cinusa tetrodontis* Schjödte et Meinert, 1884, together with its fish host, *Amblyrhynchotes honckenii* (Bloch) for analyses of metals and metalloids in marine environments. We determine and compare the accumulation of elements in fish hosts (both infected and uninfected), as well as male and female parasites from a near-pristine and contaminated harbour site. Elemental accumulation is also compared between male and female isopods from both sites. This marks the first study to conduct element analyses of parasitic isopods off the coast of Africa and first-implementing this host-ectoparasite system as an additional model for marine biomonitoring.

The study focussed on the warm temperate South Coast and fish were sampled from the Breede River Estuary at Witsand, and in Mossel Bay adjacent to the harbour (Fig. 1). The Breede River Estuary is classified as one of the top twenty near-pristine estuaries in the Western Cape Province of South Africa (Breede River Estuarine Management Plan, 2016). It could therefore be assumed that this site would not show high element concentrations, but rather reflect background geogenic concentrations. Nevertheless, potential threats that may still alter the quality and integrity of this estuary could be induced by various urban developments and agricultural activities along the river, as well as vessel source pollution (Erasmus et al., 2004; Breede River Estuarine Management Plan, 2016), such as those caused by recreational vessels launching from Witsand. Mossel Bay, on the other hand, being adjacent to the harbour, introduces many additional anthropogenic sources of pollution to the marine environment due to vessel pollution, vessel repairs, variable non-point discharges of elements, and coastal oceanographic changes in upwelling events (Wepener and Degger, 2020). Hence, it is expected to find high levels of element concentrations attributed to anthropogenic sources within this site.

The evil-eye blaasop, *A. honckenii* is a fairly understudied fish species (Acosta and Smit, 2021) although it is one of the most common marine and brackish fish species, associated with reefs with a wide Indo-West

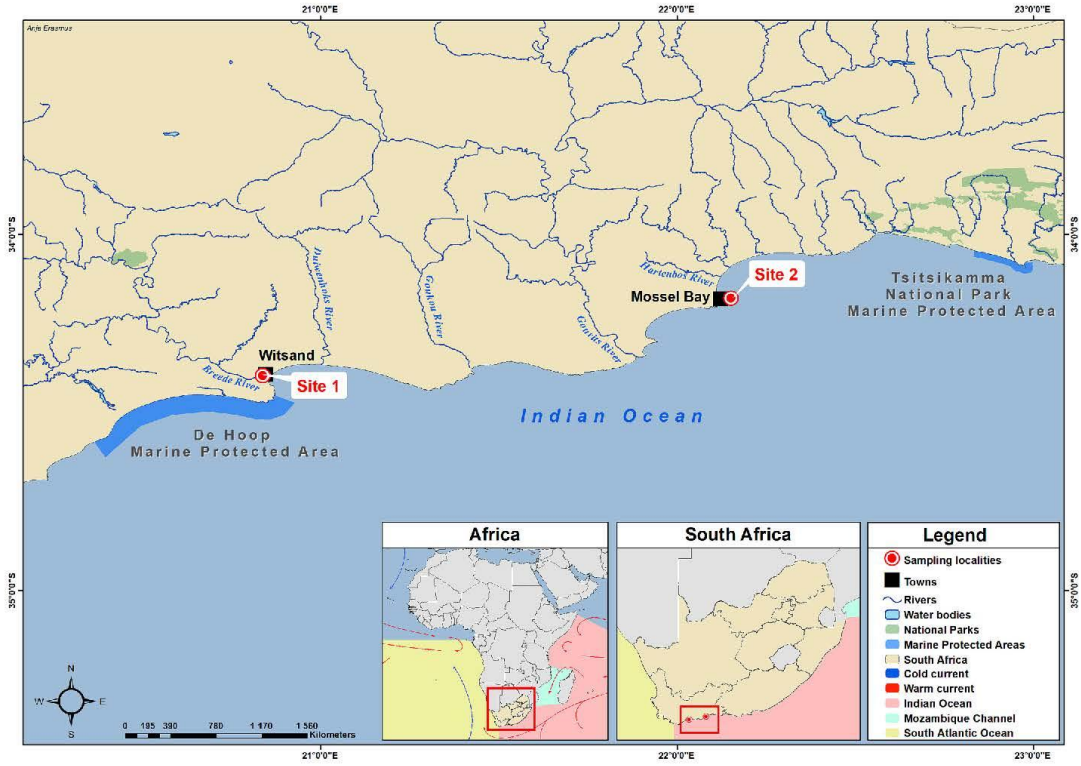

Fig. 1. Map indicating the sampling localities of specimens of *Amblyrhynchotes honckenii* (Bloch).

Appendix A

Pacific distribution from South Africa to China, and the Marshall Islands in Micronesia (Froese and Pauly, 2023). It is not a commercially important fish species and is currently listed as "least concern" in the IUCN database (Froese and Pauly, 2023). *Amblyrhynchotes honckenii* is the only known host of the ectoparasitic isopod, *C. tetrodontis*, which commonly infests the buccal cavity of fish (Hadfield et al., 2010). Furthermore, this parasite is a protandric hermaphrodite, with commonly one male and one female present in the hosts' buccal cavity, consequently providing a valuable opportunity to determine element accumulation for four tissues per fish (i.e., liver, muscle, female parasite, and male parasite).

Using rod and reel, 15 specimens of *A. honckenii*, 13 males and two females, were collected from Witsand (−34.397323; 20.837474) in November 2021 and 10 specimens, eight males and two juveniles, from Mossel Bay (−34.179656; 22.152093) in February/March 2022 (Fig. 1). Following capture, fish were transported in aerated water containers from the collection site to the nearby field station for dissection.

The fish were identified, photographed, weighed, measured, and killed using percussive stunning followed by pithing (Ethics Committee approved standard operation procedure NWU-00267-17-A5). The mouth of the fish was screened for isopods and any isopods found were identified following Hadfield et al. (2010). All specimens of *C. tetrodontis* were removed, and the life cycle stage (i.e., juvenile or adult) and sex (i.e., male or female) were determined, frozen and stored at −20°C in pre-cleaned acid-washed polypropylene tubes. Axial muscle and liver tissue samples of the fish hosts were collected, frozen and stored at −20°C in pre-cleaned acid-washed polypropylene tubes.

All samples were thawed and freeze-dried (FreeZone® 6, Labconco) for a duration of 96 h. Dried samples were homogenised using a mortar and pestle and accurately weighed to four decimals (±100 mg of muscle and liver tissue, as well as ±80 mg parasite tissue) and acid digested in 30 ml TFM® vessels with 4 ml HNO_3 (sub-boiled from 65%; p.a. quality, Merck) using a Mars 6 microwave digestion system (CEM Corporation, Kamp-Lintfort) for multi-element analysis. To avoid cross-contamination, the mortar and pestle were thoroughly cleaned using 5% HNO_3 before the next sample was homogenised. Digests were transferred to 5 ml volumetric flasks, brought to volume with ultrapure MilliQ water, transferred to pre-cleaned polypropylene tubes and stored at room temperature until analyses. According to the survey on elements in mussels by Wepener and Degger (2020), As, Cd, Cu, Mn, Ni, Pb, Se, and Zn are generally present in all major harbours in South Africa. Accordingly, a multi-element analysis was performed for these elements, using a quadrupole inductively coupled plasma-mass spectrometry (ICP-MS) (PerkinElmer, Elan 6000) equipped with an auto-sampler system (PerkinElmer, AS-90). The analysis was performed with the following operational specifications: 1000 W plasma power, 14 l/min gas flow, 0.95 l/min nebulizer gas flow and 1 ml/min sample flow rate. Yttrium and Tm (Certipur®, Merck) were used as internal standards for quality measurements at a concentration of 10 μg/l. These elements were quantified by using the following mass lines: ^{75}As, ^{114}Cd, ^{63}Cu, ^{55}Mn, ^{60}Ni, ^{208}Pb, ^{82}Se, and ^{66}Zn. The ICP-MS was calibrated by using a series of 11 dilutions of multi-element standard solutions. Element concentrations were calculated for each sample by use of corresponding regression lines with a correlation factor of ≥0.999. The detection limits were calculated as three times the standard deviation of the blank measurements per digestion batch (Table 1). Quality control of the element analysis was performed using applicable standard reference materials for all the elements. Reference materials, DOLT5 (Dogfish liver certified reference material for trace metals and other constituents, National Research Council, Canada) and SRM15666b (Oyster Tissue certified reference material, National Institute of Standards and Technology, USA) were used to validate the analytical procedure of biotic samples (Table 1). Internal procedural standards were analysed after every 20 samples for quality control and assurance.

For statistical data analysis, the data were tested for normality using the Shapiro-Wilk normality test. Since all data met the normal distribution assumption, a two-way ANOVA was performed followed by Tukey's multiple comparison test using GraphPad Prism v7. Significance was regarded as $p < 0.05$. Results of two-way ANOVA statistical analysis of variance comparing metal concentrations in species (parasite and fish host) from two localities (Witsand and Mossel Bay) are presented in tabular form (Tables 2 and 3). Results of Tukey's multiple comparison tests, indicating significant differences ($p < 0.05$) in element concentrations in species (parasite and fish host) from two localities (Witsand and Mossel Bay), are illustrated in tabular form (Table 4).

Table 1
Percentage recovery (%) of two different certified reference materials (DOLT5 and SRM15666b), as well as the limit of detection (LOD) (ng/g dry weight) in different tissue samples. Detection limits for the fish and parasite samples were determined as three times the standard deviation of the blank measurements considering a mean sample mass of 115 mg (muscle), 92 mg (liver), and 78 mg (parasites), respectively.

Element	% recovery		LOD (ng/g dry weight)		
	DOLT5	SRM15666b	Muscle	Liver	Parasite
As	93	92	0.25	0.15	0.64
Cd	87	88	0.015	0.014	0.020
Cu	109	105	0.75	0.44	0.70
Mn	106	104	0.37	0.20	0.28
Ni	109	106	2.02	15.2	4.13
Pb	118	93	0.98	0.19	1.53
Se	81	108	0.63	1.15	0.37
Zn	93	81	21.0	7.77	52.3

Ethical approval for this project was received from the Faculty of Natural and Agricultural Sciences' Ethics Committee (FNASREC) of the North-West University with ethics number NWU-00565-19-A5. Permits for the collection of *A. honckenii* for research were issued by the South African Department of Agriculture, Forestry and Fisheries (permit no. RES2022-44).

The concentrations of As, Cd, Cu, Mn, Ni, Pb, Se, and Zn were determined in muscle and liver tissues of both infected and uninfected fish, as well as in male and female parasites from Witsand and Mossel Bay, on the South African temperate south coast. Female specimens of *A. honckenii* sampled from Witsand 180 ± 7 mm (175–185 mm) were much larger than males 150 ± 9 mm (140–165 mm). No juvenile fish were recorded from this site (Supplementary data, Table S1). The adult *A. honckenii* from Mossel Bay were significantly smaller than those sampled from Witsand (110 ± 7 mm). No female fish were recorded from this site, however, two juvenile fish were recorded measuring 105 ± 7 mm (100–110 mm) in total length (Supplementary data, Table S2).

There was a significant difference in the prevalence of infection by *C. tetrodontis* in *A. honckenii* between sites since only 40% of fish were infested with *C. tetrodontis* at Witsand versus 90% of fish at Mossel Bay. Since the isopod used in this study is a protandric parasitic species, both male and female sexes were present. Twelve adult specimens of *C. tetrodontis*, six males (64 ± 16 mg; range 47–95 mg) and six females (121 ± 17 mg; range 101–171 mg) were collected from six specimens of *A. honckenii* from Witsand (Supplementary data, Table S1). From Mossel Bay, 18 adult specimens of *C. tetrodontis*, nine males, weighing 39 ± 4 mg (32–43 mg), and nine females weighing 125 ± 28 mg (80–189 mg), were collected from nine specimens of *A. honckenii* (Supplementary data, Table S2). Interestingly, all specimens of *C. tetrodontis* were collected from male *A. honckenii*, while none of the female fish were infested.

The concentrations of As, Cu, Mn, Ni, Pb and Zn in *C. tetrodontis* differed significantly ($p < 0.05$) between the two sites, where Mossel Bay's isopods had higher concentrations of Ni, Pb and Zn (Table 2). Significant differences in *C. tetrodontis* between sites are seen in the concentrations of Cu and Ni. Female *C. tetrodontis* from Witsand had higher concentrations of Cu than those from Mossel Bay (Table 2). Male *C. tetrodontis* from Mossel Bay had significantly ($p < 0.05$) higher concentrations of Ni than those from Witsand (Table 2). Selenium

Appendix A

Table 2
Element concentrations (mean ± standard deviation) of *Cinusa tetrodontis* Schjödte et Meinert, 1884, infested *Amblyrhynchotes honckenii* (Bloch) and uninfested *A. honckenii* from two localities (Witsand and Mossel Bay) along the South African coastline. Significant differences between the two sites are indicated with an asterisk (*). Significant differences between the parasites and host tissues at Witsand and Mossel Bay, respectively are presented in Table 4. Significance was taken as $p < 0.05$.

Element	Locality	Male *Cinusa tetrodontis* (μg/g DW)	Female *Cinusa tetrodontis* (μg/g DW)	Infected fish Muscle (μg/g DW)	Uninfected fish Muscle (μg/g DW)	Infected fish Liver (μg/g DW)	Uninfected fish Liver (μg/g DW)
As	Witsand	40.40 ± 15.70	31.21 ± 8.88	6.42 ± 5.94	9.31 ± 11.27	4.93 ± 1.66	5.74 ± 4.23
	Mossel Bay	33.70 ± 10.70	27.62 ± 7.35	8.38 ± 2.45	5.96	8.47 ± 6.17	17.81
Cd	Witsand	0.11 ± 0.05	0.11 ± 0.09	0.01 ± 0.001	0.01 ± 0.001	2.11 ± 1.36	2.16 ± 0.96
	Mossel Bay	0.09 ± 0.04	0.06 ± 0.03	0.01 ± 0.001	0.01	1.94 ± 1.12	4.41
Cu	Witsand	81.57 ± 387.96	69.97 ± 12.44*	0.79 ± 0.16	0.78 ± 0.14	2.88 ± 1.55	3.55 ± 2.07
	Mossel Bay	54.60 ± 18.30	45.34 ± 11.57*	0.90 ± 0.15	0.87	4.11 ± 1.64	8.62
Mn	Witsand	6.20 ± 2.10	3.36 ± 0.92	0.27 ± 0.04	0.27 ± 0.05	1.81 ± 0.52	1.67 ± 1.08
	Mossel Bay	4.60 ± 1.20	2.57 ± 0.50	0.50 ± 0.24	0.33	2.99 ± 1.14	4.79
Ni	Witsand	8.44 ± 0.70*	3.44 ± 0.75	0.12 ± 0.03	0.11 ± 0.02	0.31 ± 0.04	0.33 ± 0.15
	Mossel Bay	9.77 ± 0.99*	3.81 ± 1.12	0.19 ± 0.11	0.18	0.29 ± 0.12	0.68
Pb	Witsand	1.11 ± 0.74	0.47 ± 0.18	0.07 ± 0.13	0.03 ± 0.01	0.06 ± 0.03	0.07 ± 0.07
	Mossel Bay	3.02 ± 3.61	1.13 ± 1.44	0.06 ± 0.05	0.04	0.16 ± 0.12	0.25
Se	Witsand	20.34 ± 1.54	13.33 ± 4.88	1.18 ± 0.19*	1.19 ± 0.37	2.18 ± 0.31	2.57 ± 1.10
	Mossel Bay	18.84 ± 3.12	12.33 ± 3.01	0.86 ± 0.09*	0.76	2.29 ± 0.66	4.07
Zn	Witsand	248.61 ± 82.22	205.44 ± 114.77	13.87 ± 1.54	14.14 ± 3.80	43.77 ± 9.53	69.44 ± 53.93
	Mossel Bay	368.41 ± 110.33	284.44 ± 83.44	15.36 ± 3.44	15.69	71.66 ± 30.99	174.72

Table 3
Two-way ANOVA analysis of variance table comparing element concentrations in species (*Cinusa tetrodontis* Schjödte et Meinert, 1884, infested *Amblyrhynchotes honckenii* (Bloch), and uninfested *A. honckenii*) from two localities (Witsand and Mossel Bay) along the South African coastline.

Element	Species (df = 5)	Sites (df = 1)	Interaction (df = 5)
As	$F = 32.22$; $p < 0.0001$	$F = 0.067$; $p = 0.8$	$F = 1.183$; $p = 0.3267$
Cd	$F = 34.76$; $p < 0.0001$	$F = 3.071$; $p = 0.0842$	$F = 2.335$; $p = 0.0512$
Cu	$F = 68.42$; $p < 0.0001$	$F = 3.520$; $p = 0.0649$	$F = 3.361$; $p = 0.0090$
Mn	$F = 46.67$; $p < 0.0001$	$F = 1.749$; $p = 0.1905$	$F = 5.523$; $p = 0.0003$
Ni	$F = 499.7$; $p < 0.0001$	$F = 4.469$; $p = 0.0382$	$F = 2.386$; $p = 0.0470$
Pb	$F = 4.399$; $p = 0.0016$	$F = 1.381$; $p = 0.2440$	$F = 1.033$; $p = 0.4056$
Se	$F = 173.2$; $p < 0.0001$	$F = 0.1952$; $p = 0.6601$	$F = 0.4499$; $p = 0.8120$
Zn	$F = 45.27$; $p < 0.0001$	$F = 8.058$; $p = 0.0060$	$F = 1.673$; $p = 0.1529$

concentrations in infected fish muscle tissue differed significantly ($p < 0.05$) between sites, with higher concentrations observed in fish collected from Witsand compared to those from Mossel Bay (Table 2). The instances of significant differences between the biological samples (parasites, uninfected and infected fish muscle and liver tissues) at a site were far more than the differences between sites. The only significant interactions of elements in samples and sites were for Cu, Mn and Ni (Table 3).

The significant differences in element concentrations between species (*C. tetrodontis*, infected *A. honckenii*, and uninfected *A. honckenii*) from the two localities are summarised in Table 4. Apart from Cd, element concentrations were generally higher in male isopods compared to females. At Witsand significant differences ($p < 0.05$) were found in concentrations of Mn, Ni and Se, while at Mossel Bay Pb, Mn, Ni and Se were higher in male than female isopods (Table 4). The parasitic isopod accumulated significantly higher concentrations of elements when compared to its fish host (Table 2). Male isopods had significantly higher concentrations of As, Cu, Mn, Ni, Se and Zn than that of their fish hosts at both localities. At Mossel Bay, males had significantly higher concentrations of As, Cu, Mn, Ni, Pb, Se and Zn compared to their fish hosts (Tables 2 and 4). Besides Pb, female *C. tetrodontis* showed the same trend when compared to their host, *A. honckenii* (Tables 2 and 4). In general, infected fish had lower element concentrations compared to uninfected fish. Only Cd and Mn levels in the liver tissues of uninfected fish at

Table 4
Matrix indicating significant differences ($p < 0.05$) in element concentrations in species (*Cinusa tetrodontis* Schjödte et Meinert, 1884, infested *Amblyrhynchotes honckenii* (Bloch), and uninfested *A. honckenii*) from two localities (Witsand and Mossel Bay) along the South African coastline. Cells above the diagonal lines represent the elements that are statistically different between conditions at Mossel Bay, while elements below the diagonal lines represent those conditions that differed significantly at Witsand.

	Mossel Bay					
	Cinusa (♂)	Cinusa (♀)	Infected fish (M)	Infected fish (L)	Uninfected fish (M)	Uninfected fish (L)
Cinusa (♂)		Mn, Ni, Pb, Se	As, Cu, Mn, Ni, Pb, Se, Zn	As, Cd, Cu, Mn, Ni, Pb, Se, Zn	As, Cu, Mn, Ni, Se, Zn	Cd, Cu, Ni, Se
Cinusa (♀)	Mn, Ni, Se		As, Cu, Mn, Ni, Se, Zn	As, Cd, Cu, Ni, Se, Zn	Cu, Ni, Se, Zn	Cd, Ni, Se
Infected fish (M)	As, Cu, Mn, Ni, Se, Zn	As, Cu, Mn, Ni, Se, Zn		Cd, Mn		Cd, Mn
Infected fish (L)	As, Cd, Cu, Mn, Ni, Se, Zn	As, Cd, Cu, Ni, Se, Zn	Cd			Cd
Uninfected fish (M)	As, Cu, Mn, Ni, Se, Zn	As, Cu, Mn, Ni, Se, Zn		Cd, Mn		Cd, Mn
Uninfected fish (L)	As, Cd, Cu, Mn, Ni, Se, Zn	As, Cd, Cu, Mn, Ni, Se, Zn	Cd		Cd, Mn	
	Witsand					

Abbreviations: (♂) Male; (♀) Female; (M) Muscle; (L) Liver.

Appendix A

Mossel Bay were significantly lower than the levels in the liver of infected fish (Table 4).

The present paper assessed the possible role of marine ectoparasitic isopods and their fish hosts as model bioindicators, complementary to traditional mussel indicators for marine pollution monitoring. To be considered an effective bioindicator, these isopods need to fulfil the criteria commonly accepted for established sentinel species. Accordingly, ectoparasitic isopods need to have high bioaccumulation capabilities, be resistant to pollutants with long pollutant half-lives once accumulated, and be prevalent, as well as widespread (van Gestel et al., 2018).

The present study assessed element accumulation within the parasitic isopod, *C. tetrodontis*, together with its fish host, *A. honckenii*. The bioaccumulation potential of both male and female isopod parasites, as well as infected and uninfected fish from both a relatively unaffected site (Witsand) and an element-contaminated harbour site (Mossel Bay), were compared. The parasitic isopod accumulated significantly higher concentrations of elements, except Cd, compared to its fish host. This is likely because these ectoparasites are exposed to both the external environment, as well as accumulating elements from feeding on their fish hosts, making them more susceptible and sensitive to environmental changes caused by pollution and/or other water quality parameters (Biswal and Chatterjee, 2020). The uptake and accumulation of elements, in general, are dependent on environmental and biological factors across different exposure routes (i.e., uptake from exposure to the external environment, dermal uptake or food uptake) (Somero et al., 1977; Cani and Atli, 2003; Van Gestel et al., 2018). Therefore, the degree of element exposure of these isopods is much higher than what is experienced by their fish host. However, unlike their hosts, these parasites have the ability to bioconcentrate these elements producing quantifiable results, which are normally only present in very low, or seemingly undetectable concentrations in the environment (Sures et al., 2017). This is supported by the present study since concentrations between sites in the muscle or liver tissues of *A. honckenii* alone did not show any significant differences. Cadmium was the only element that accumulated in much lower concentrations in the isopod, compared to its fish host. According to the study by Vijver et al. (2006), this is most likely due to the isopod's high capability of sequestering elements, which is strongly related to the storage capacity of elements, such as Cd and Zn, within the hepatopancreas of isopods. Crustaceans also have the ability to store potential toxic elements in their exoskeleton and can reduce their body burdens by increasing the number of moults (O'Callaghan and Sullivan, 2020) It is, therefore, likely that *C. tetrodontis* has a high tolerance to element exposure, especially potentially toxic elements.

The significant differences between sites were related to concentrations of both essential and non-essential elements. According to Bosch et al. (2015), not all element contaminants are hazardous, since elements such as Cu, Fe, Se and Zn are essential in their specific functions in body metabolism. Conversely, elements such as Cd, Cr, Hg, Ni and Pb are related to sources of pollution and considered non-essential and toxic to both fish and the environment in exceeding concentrations (Bosch et al., 2015). In the present study, concentrations of Cu, Mn, Ni, Pb and Zn in *C. tetrodontis* differed significantly between the two sites, where Mossel Bay's isopods had higher concentrations of Ni, Pb and Zn. Furthermore, the most significant differences in *C. tetrodontis* between sites were seen in the concentrations of Cu and Ni, where female isopods, from Witsand, had a higher concentration of Cu (essential) than those from Mossel Bay. On the other hand, male isopods from Mossel Bay had a higher concentration of Ni (non-essential) compared to those from Witsand. Hence, based on the data it is clear that Mossel Bay contains more toxic non-essential element concentrations, than that of Witsand, containing more or higher essential element concentrations. Interestingly, Witsand had slightly higher Cd concentrations compared to Mossel Bay. This was unexpected since the Breede River Estuary at Witsand has no known sources of element contamination and is regarded as a pristine unaffected site (Breede River Estuarine Management Plan, 2016). Similarly, Erasmus et al. (2021) found elevated element levels in klipfish, *Clinus superciliosus*, from unimpacted sites along the same coastline. These authors attributed this to long-term exposure to elements derived from natural geogenic weathering introduced by freshwater runoff and frequent upwelling events along the South African coast. The levels of elements in the Brown mussel, *Perna perna*, from sites along the South African south coast also support these findings (Degger et al., 2011; Wepener and Degger, 2020).

By comparing element concentrations between male and female *C. tetrodontis*, element concentrations were generally higher in male isopods than in females. Interestingly, except with Cu, female *C. tetrodontis* showed significant relationships towards an increase in elements in host liver tissue samples, whereas male *C. tetrodontis* showed significant relationships towards an increase in elements in host muscle tissue. The reason for this is unclear, however, it could be explained by their food source because even though both male and female isopods attach in the host's buccal cavity, the male feeds predominantly on host tissue, while the female feeds on host blood (Smit et al. unpublished data). This relationship between element concentrations and female isopods that feeds on blood was also corroborated by Erasmus et al. (2020). These potential relationships between the host and or the external environment as metal sources in the parasitic isopods should be explored further by analysing metals in host blood and the tissues of the buccal cavity,

The results of this study demonstrate the suitability of *C. tetrodontis* as a good accumulation bioindicator, due to its high bioaccumulation capability. Additionally, as a group, ectoparasitic isopods possess a well-defined physiology, which accounts for increased tolerance or even resistance towards non-essential hazardous elements. Given the knowledge of their life cycles, attachment sites and food source information as described by Smit et al. (2014), ectoparasitic isopods provide an easier way to understand environmental changes and relative host behaviour and ecological interactions (Longo et al., 2013; van Gestel et al., 2018; Honda et al., 2021). The present study highlights a future direction within environmental parasitology and emphasises the importance and utility of this particular ectoparasite-host model system, bioaccumulating higher element concentrations than their hosts, thereby acting as an effective early warning model.

CRediT authorship contribution statement

L. Van Der Spuy: Methodology, Investigation, Formal analysis, Funding acquisition, Writing – original draft. **J.H. Erasmus:** Methodology, Investigation, Formal analysis, Writing – review & editing. **M. Nachev:** Writing – review & editing. **B.C. Schaeffner:** Writing – review & editing. **B. Sures:** Writing – review & editing. **V. Wepener:** Conceptualization, Data curation, Funding acquisition, Writing – review & editing. **N.J. Smit:** Conceptualization, Data curation, Funding acquisition, Writing – review & editing.

Declaration of competing interest

The authors declare that they have no known competing financial interests or personal relationships that could have appeared to influence the work reported in this paper.

Data availability

Data will be made available on request.

Acknowledgements

We would like to thank the Unit for Environmental Sciences and Management, North-West University (NWU) and Research Center One Health Ruhr, University of Duisburg-Essen for the use of field equipment

Appendix A

and laboratory facilities. We thank Anja Erasmus from NWU-WRG, for the creation of the study area map. Additional thanks go to our colleagues Francois Retief, Reese Alberts, Anja Erasmus, Marliese Truter, Anja Vermaak, and Coret van Wyk, from the NWU who assisted with the collection of samples. This is contribution No. 790 from the NWU-Water Research Group.

This work is based on the research and researchers supported by the National Research Foundation (NRF) of South Africa (grant 132805; L. van der Spuy). Opinions, findings, conclusions, and recommendations expressed in this publication are that of the authors, and the NRF and NWU accept no liability whatsoever in this regard.

Appendix A. Supplementary data

Supplementary data to this article can be found online at https://doi.org/10.1016/j.marpolbul.2023.115385.

References

Acosta, A.A., Smit, N.J., 2021. A first for Southern Africa: description of a new *Heterobothrium* (Monogenea: Diclidophoridae) parasitizing the evil eye pufferfish *Amblyrhynchotes honckenii* (Tetraodontiformes: Tetraodontidae). Parasitol. Res. 120, 819–830. https://doi.org/10.1007/s00436-020-06960-5.

Biswal, D., Chatterjee, S., 2020. Fish parasites as biological indicators: a systematic review. Biosci. Biotechnol. Res. Commun. 13 (4), 1743–1755. https://doi.org/10.21786/bbrc/13.4/16.

Bosch, A.C., O'Neill, O., Sigge, G.O., Kerwath, S.E., Hoffman, L.C., 2015. Heavy metals in marine fish meat and consumer health: a review. J. Sci. Food Agric. 96, 32–48. https://doi.org/10.1002/jsfa.7360.

Breede River Estuarine Management Plan, 2016. Western Cape Estuary Management Framework and Implementation Strategy. SSI Environmental, 1st edition. Royal Haskoning D.H.V. (revised 2011, 2nd Edition, 2016).

Cani, M., Atli, G., 2003. The relationships between heavy metal (Cd, Cr, Cu, Fe, Pb, Zn) levels and the size of six Mediterranean fish species. Environ. Pollut. 121, 129–136.

Chine, J.H., Nachev, M., Sures, B., Gargouri, L., 2021. Trace element assessment in *Neoechinorhynchus agilis* (Rudolphi, 1918) (Acanthocephala: Neoechinorhynchidae) and its fish hosts, *Mugil cephalus* (Linnaeus, 1758) and *Chelon ramada* (Risso, 1827) from Ichkeul Lagoon, Tunisia. J. Helminthol. 95 (e61), 1–7. https://doi.org/10.1017/S0022149X21000572.

Degger, N., Wepener, V., Richardson, B.J., Wu, R.S.S., 2011. Application of artificial mussels (AMs) under South African marine conditions: a validation study. Mar. Pollut. Bull. 63 (5–12), 108–118. https://doi.org/10.1016/j.marpolbul.2011.04.040.

Drobne, D., 1997. Terrestrial isopods—a good choice for toxicity testing of pollutants in the terrestrial environment. Environ. Toxicol. Chem. 16, 1159–1164. https://doi.org/10.1897/1551-5028(1997)016<1159:TIAGCF>2.3.CO;2.

Erasmus, A., Smit, N.J., Zimmermann, S., Nachev, M., Sures, B., Wepener, V., 2021. Metal and metalloid concentrations in the southern African endemic inter- and infratidal super klipfish, *Clinus superciliosus*, from the west and south coasts of South Africa. Mar. Pollut. Bull. 172, 112852 https://doi.org/10.1016/j.marpolbul.2021.112852.

Erasmus, C.P., Rossouw, G., Baird, D., 2004. The concentration of ten heavy metals in the tissues of shark species Squalus megalops and *Mustelus* (Chondrichthyes) occurring along the south eastern coast of South Africa. In: Population, English edition. University of Port Elizabeth.

Erasmus, J.H., Wepener, V., Nachev, M., Zimmermann, S., Malherbe, W., Sures, B., Smit, N.J., 2020. The role of fish helminth parasites in monitoring metal pollution in aquatic ecosystems: a case study in the world's most productive platinum mining region. Parasitol. Res. 119, 2783–2798. https://doi.org/10.1007/s00436-020-06813-1.

Farrington, J.W., Tripp, B.W., Tanabe, S., Subramanian, A., Sericano, J.L., Wade, T.L., Knap, A.H., 2016. Edward D. Goldberg's proposal of "the Mussel Watch": reflections after 40 years. Mar. Pollut. Bull. 110, 501–510. https://doi.org/10.1016/j.marpolbul.2016.05.074.

Froese, R., Pauly, D., 2023. FishBase, World Wide Web electronic publication. www.fishbase.org/search.php.

Gao, Q., Nie, P., 2000. Lead content in the monogenean *Ancryocephalus mogurndae* and in different organs of its host, the mandarin fish, *Siniperca chuatsi*. China Environ. Sci. 20, 233–236.

Gilbert, B.M., Avenant-Oldewage, A., 2017. Parasites and pollution: the effectiveness of tiny organisms in assessing the quality of aquatic ecosystems, with a focus on Africa. Environ. Sci. Pollut. Res. 24, 18742–18769. https://doi.org/10.1007/s11356-017-9481-8.

Hadfield, K.A., Bruce, N.L., Smit, N.J., 2010. Redescription of the monotypic genus *Cirusa* Schioedte and Meinert, 1884 (Isopoda, Cymothoidae), a buccal-cavity isopod from South Africa. Zootaxa. 2437, 51–68. https://doi.org/10.5281/zenodo.194854.

Honda, M., Qiu, X., Lydia Undap, S., Kimura, T., Hori, T., Shimasaki, Y., Oshima, Y., 2021. Contamination of heavy metals, polychlorinated dibenzo-p-dioxins/furans and dioxin-like polychlorinated biphenyls in wharf roach *Ligia* spp. in Japanese intertidal and supratidal zones. Appl. Sci. 11, 1856. https://doi.org/10.3390/app11041856.

Lins, D.C., Meirelles, M.E., Malm, O., Lima, N.R.W., 2008. Mercury concentration in the freshwater bonefish *Cyphocharax gilbert* (Curimatidae) and its parasite the crustacean *Riggia paranensis* (Cymothoidae). Neotrop. Ichthyol. 6 (2), 283–288. https://doi.org/10.1590/S1679-62252008000200017.

Longo, G., Trovato, M., Mazzei, V., Ferrante, M., Conti, G.O., 2013. *Ligia italica* (Isopoda, Oniscidea) as bioindicator of mercury pollution of marine rocky coasts. PLoS ONE 8, e58548. https://doi.org/10.1371/journal.pone.0058548.

Mahmoud, N.E., Fahmy, M.M., Abuowarda, M.M., Zaki, M.M., Ismael, E., Ismail, E.M., 2019. Influence of water quality parameters on the prevalence of *Livoneca redmanii* (Isopoda: Cymothoidae) infestation of Mediterranean Sea fishes, Egypt. Int. J. Vet. Sci. 8 (3), 174–181. https://doi.org/10.21608/jesp.2019.68309.

Nachev, M., Sures, B., 2016. Environmental parasitology: parasites as accumulation bioindicators in the marine environment. J. Sea Res. 113, 45–50. https://doi.org/10.1016/j.seares.2015.06.005.

O'Callaghan, I.O., Sullivan, T., 2020. Shedding the load: moulting as a cause of variability in whole-body metal concentrations. J. Crustac. Biol. 40, 725–733. https://doi.org/10.1093/jcbiol/ruaa077.

Öktener, A., Sezgin, M., 2000. *Mothocya epimerica* Costa, 1851 (Flabellifera: Cymothoidae), an isopod parasite in the branchial cavities of the Black Sea Silverfish, *Atherina boyeri* Risso, 1810 (Perciformes, Atherinidae). Turk. J. Mar. Sci. 6 (1), 23–29. https://doi.org/10.3354/dao054243.

Pérez-del-Olmo, A., Nachev, M., Zimmermann, S., Fernández, M., Sures, B., 2019. Medium-term dynamics of element concentrations in a sparid fish and its isopod parasite after the Prestige oil-spill: shifting baselines? Sci. Total Environ. 686, 648–656. https://doi.org/10.1016/j.scitotenv.2019.05.455.

Pinsino, A., Della Torre, C., Sammarini, V., Bonaventura, R., Amato, E., Matranga, V., 2008. Sea urchin coelomocytes as a novel cellular biosensor of environmental stress: a field study in the Tremiti Island Marine Protected Area, Southern Adriatic Sea, Italy. Cell Biol. Toxicol. 24, 541–552. https://doi.org/10.1007/s10565-008-9055-0.

Smit, N.J., Bruce, N., Hadfield, K.A., 2014. Global diversity of fish parasitic isopod crustaceans of the family Cymothoidae. Int. J. Parasitol. Parasites Wildl. 3, 188–197. https://doi.org/10.1016/j.ijppaw.2014.03.004.

Somero, G.N., Chow, T.J., Yancey, P.H., Snyder, C.B., 1977. Lead accumulation rates in tissues of the estuarine teleost fish, *Gillichthys mirabilis*: salinity and temperature effects. Arch. Environ. Contam. Toxicol. 6, 337–348. https://doi.org/10.1007/BF02097774.

Sures, B., 2004. Environmental parasitology: relevancy of parasites in monitoring environmental pollution. Trends Parasitol. 20, 170–177. https://doi.org/10.1016/j.pt.2004.01.014.

Sures, B., Nachev, M., Selbach, C., Marcogliese, D.J., 2017. Parasite responses to pollution: what we know and where we go 'Environmental parasitology'. Parasit. Vectors 10, 65. https://doi.org/10.1186/s13071-017-2001-3.

Sures, B., Nachev, M., Schwelm, J., Grabner, D., Selbach, C., 2023. Environmental parasitology: stressor effects on aquatic parasites. Trends Parasitol. 39, 461–474. https://doi.org/10.1016/j.pt.2023.03.005.

Tansel, T., Fatih, P., 2012. Ectoparasitic sea lice, *Caligus minimus* (Otto 1821, Copepoda: Caligidae) on Brawn wrasse, *Labrus merula* L., in Izmit Bay, Aegean Sea. J. Anim. Sci. 11 (38), 208–2011. https://doi.org/10.4081/ijas.2012.e38.

van Gestel, C.A.M., 2012. Soil ecotoxicology: state of the art and future directions. Zookeys 176, 275–296. https://doi.org/10.3897/zookeys.176.2275.

van Gestel, C.A.M., Loureiro, S., Zidar, P., 2018. Terrestrial isopods as model organisms in soil ecotoxicology: a review. In: Hornung, E., Taiti, S., Szlavecz, K. (Eds.), Isopods in a Changing World, Zookeys, vol. 801, pp. 127–162. https://doi.org/10.3897/zookeys.801.21970.

Vidal-Martínez, V.M., Pech, D., Sures, B., Purucker, S.T., Poulin, R., 2010. Can parasites really reveal environmental impact? Trends Parasitol. 26, 44–51. https://doi.org/10.1017/S0022149X16000432.

Vijver, M.G., Vink, J.P.M., Jager, T., van Straalen, N.M., Wolterbeek, H.T., van Gestel, C. A.M., 2006. Kinetics of Zn and Cd accumulation in the isopod *Porcellio scaber* exposed to contaminated soil and/or food. Soil Biol. Biochem. 38, 1554–1563. https://doi.org/10.1016/j. soilbio.2005.11.006.

Webb, T.J., Mindel, B.L., 2015. Global patterns of extinction risk in marine and non-marine systems. Curr. Biol. 25, 506–511. https://doi.org/10.1016/j.cub.2014.12.023.

Wepener, V., Degger, N., 2020. Monitoring of metals in South African harbours using resident brown mussels (*Perna perna*) as indicator organisms. Afr. Zool. 55 (4), 267–277. https://doi.org/10.1080/15627020.2020.1799720.

Appendix B:

Parasitology

cambridge.org/par

Research Article

Cite this article: van der Spuy L, Narciso RB, Hadfield KA, Wepener V, Smit NJ (2025). Exploring South Africa's hidden marine parasite diversity: two new marine *Ergasilus* species (Copepoda: Cyclopoida: Ergasilidae) from the Evileye blaasop, *Amblyrhynchote honckenii* (Bloch). *Parasitology* **152**, 30–50. https://doi.org/10.1017/S0031182024001550

Received: 23 August 2024
Revised: 26 October 2024
Accepted: 14 November 2024
First published online: 21 November 2024

Keywords:
28S rDNA; COI mtDNA; Crustacea; marine fish parasite; molecular; phylogenetics; tetraodontid pufferfishes

Corresponding author:
Nico J. Smit;
Email: nico.smit@nwu.ac.za

© The Author(s), 2024. Published by Cambridge University Press. This is an Open Access article, distributed under the terms of the Creative Commons Attribution-NonCommercial-NoDerivatives licence (http://creativecommons.org/licenses/by-nc-nd/4.0), which permits non-commercial re-use, distribution, and reproduction in any medium, provided that no alterations are made and the original article is properly cited. The written permission of Cambridge University Press must be obtained prior to any commercial use and/or adaptation of the article.

Exploring South Africa's hidden marine parasite diversity: two new marine *Ergasilus* species (Copepoda: Cyclopoida: Ergasilidae) from the Evileye blaasop, *Amblyrhynchote honckenii* (Bloch)

Linda van der Spuy[1], Rodrigo B. Narciso[1,2], Kerry A. Hadfield[1], Victor Wepener[1] and Nico J. Smit[1]

[1]Water Research Group, Unit for Environmental Sciences and Management, North-West University, Potchefstroom, South Africa and [2]Section of Parasitology, Institute of Biosciences, São Paulo State University (UNESP), Botucatu, São Paulo, Brazil

Abstract

Marine parasites remain understudied in South Africa with little information available on their diversity and the effects these parasites may have on their hosts. This is especially true for parasitic copepods within the family Ergasilidae. Among the 4 genera known in Africa, *Ergasilus* Nordmann, 1832 is the most speciose with 19 reported species. However, this represents only 12% (19/163) of the global diversity. Furthermore, only 5 known African species are reported from marine environments, and only 1 is reported from the South African coastline. Given the rich biodiversity along this coastline, a high marine parasite diversity could be expected from these shores. As a case study, the Evileye blaasop, *Amblyrhynchote honckenii* (Bloch), a marine and brackish fish species, was screened for parasites along the South African coastline. This resulted in the discovery of 2 species of *Ergasilus* new to science (*Ergasilus arenalbus* n. sp. and *Ergasilus chintensis* n. sp.), which makes them the second and third ergasilid species reported for tetraodontid pufferfishes worldwide. Although genetically distinct, the 2 newly described species clustered in the same subclade within the Ergasilidae based on 18S rDNA, 28S rDNA and COI mtDNA phylogenies. The newly described species differ morphologically from each other, and their respective congeners based on the size and armature of the antenna; body segmentation; and general ornamentation throughout the entire body. The addition of these 2 new species from a single host species indicates that South Africa's marine fishes contain most probably a hidden parasitic copepod diversity that is worth exploring.

Introduction

Exploring diversity within marine ecosystems has become increasingly important in recent years, revealing a previously unnoticed level of species richness and genetic variation. This is particularly true for parasitic copepods within the family Ergasilidae Burmeister, 1835 (Boxshall and Defaye, 2008). Among the various genera in this family, *Ergasilus* Nordmann, 1832, stands out as one of the most speciose and widely distributed (Oldewage and van As, 1988; Oldewage and Avenant-Oldewage, 1993; Fikiye *et al.*, 2023; Míč *et al.*, 2023). However, the extent of this diversity remains largely unexplored in Africa (Killian and Avenant-Oldewage, 2013; Fikiye *et al.*, 2023; Míč *et al.*, 2023), with merely 19 reported species, 12% (19/163), of the global diversity (Fikiye *et al.*, 2023; WoRMS, 2024).

The lack of comprehensive studies in Africa limits our understanding of *Ergasilus* diversity, where unique environmental conditions and host communities may foster an even higher diversity of distinct *Ergasilus* species. While some investigations have provided insights into *Ergasilus* species in African freshwater systems (Oldewage and van As, 1988; Fikiye *et al.*, 2023), marine or brackish environments in this region remain largely unexplored, hosting only 5 known species and a single species from the South African coastline (Fikiye *et al.*, 2023; WoRMS, 2024). Additionally, the limited knowledge regarding their diversity and the lack of genetic data, compared to those of other well-studied organisms, hinder comprehensive genomic analyses, creating further challenges in gaining deeper insights into their phylogeny and biology (Fikiye *et al.*, 2023; Míč *et al.*, 2023).

The discovery of new *Ergasilus* species, especially in unexplored regions would aid in filling these crucial gaps and understanding these parasites' biogeography and evolution (Boxshall and Halsey, 2004; Song *et al.*, 2008; Míč *et al.*, 2023). Furthermore, marine regions across the Atlantic and Indian oceans represent hotspots for parasitic diversity due to their wide range of marine habitats (Everett *et al.*, 2015; Miller *et al.*, 2018). Hence, given the rich diversity of *Ergasilus* species described from the southern Atlantic and Indian Ocean regions (see Table 1), South Africa could provide an ideal setting to study marine *Ergasilus* species and

Appendix B

Table 1. Updated information for all marine species of *Ergasilus* Nordmann, 1832 described within the South Atlantic and Indian oceans, with information on host species, host families, distribution and available GenBank data

Species	Host family	Host species	Distribution	Ocean	18S	28S	COI	References
***E. arenalbus* n. sp. present study**	**Tetraodontidae**	**TH: *Amblyrhynchote honckenii* (Bloch)**	**TLOC: Witsand, Breede River Estuary, South Africa**	**South Atlantic**	✓	✓	✓	**Present study**
E. atafonensis Amado and Rocha, 1996	Mugilidae	**TH:** *Mugil curema* Valenciennes, 1836 *M. liza* Valenciennes, 1836; *M. rubrioculus* Harrison *et al.*, 2007; *M. trichodon* Poey, 1875	**TLOC:** Rio de Janeiro, Brazil Sergipe, Brazil; Rio Grande do Sul, Brazil; São Paulo, Brazil; Santos, Brazil; Maranhão, Brazil; Bahia, Brazil	South Atlantic	–	–	–	(Amado and Rocha, 1996)
E. bahiensis Amado and Rocha, 1996	Mugilidae Ariidae	**TH:** *Mugil curema* Valenciennes, 1836 *Sciades herzbergii* (Bloch, 1794)	**TLOC:** Bahia, Brazil Caeté estuary, Brazil; Ajuruteua beach, Brazil	South Atlantic	–	–	–	(Amado and Rocha, 1996; Dos Santos *et al.*, 2021)
E. caraguatatubensis Amado and Rocha, 1996	Mugilidae	**TH:** *Mugil curema* Valenciennes, 1836 *M. liza* Valenciennes, 1836; *M. rubrioculus* Harrison *et al.*, 2007	**TLOC:** Caraguatatuba, Brazil São Paulo, Brazil; Cananeia, Brazil; Rio de Janeiro, Brazil; Maranhão, Brazil	South Atlantic	–	–	–	(Amado and Rocha, 1996)
***E. chintensis* n. sp. present study**	**Tetraodontidae**	**TH: *Amblyrhynchote honckenii* (Bloch)**	**TLOC: Chintsa East, South Africa**	**Indian**	✓	✓	✓	**Present study**
E. cyanopictus Carvalho, 1962	Mugilidae	**TH:** *Mugil cephalus* Linnaeus, 1758	**TLOC:** Rio Nóbrega, Brazil	South Atlantic	–	–	–	(Carvalho, 1962)
E. felichthys (Pearse, 1947) **Syn:** *E. elongatus* Thomsen, 1949	Polyodontidae Ariidae	**TH:** *Bagre marinus* (Mitchill, 1815) *Ariopsis felis* (Linnaeus, 1766); *Genidens barbus* (Lacepède, 1803); *Polyodon spathula* (Walbaum, 1792)	**TLOC**: Beaufort, USA Uruguay; Mobile Bay, USA; St. Louis Bay, USA; Tallapoosa River, USA; Colyell Bay, USA	North Atlantic South Atlantic Gulf of Mexico	–	–	–	(Pearse, 1947; Thomsen, 1949; Johnson and Rogers, 1972)
E. foresti Boxshall *et al.*, 2002	-	Free-living (Plankton nets)	**TLOC:** Piau River estuary, Brazil; Grande do Sul, Brazil	South Atlantic	–	–	–	Boxshall *et al.* (2002)
E. ilani Oldewage and van As, 1988	Mugilidae	**TH:** *Mugil cephalus* Linnaeus, 1758	**TLOC:** Sodwana estuary, Sodwana Bay, KZN, SA	Indian	–	–	–	(Oldewage and van As, 1988)
E. lizae Krøyer, 1863 **Syn:** *E. nanus* Beneden, 1870	Mugilidae Anguillidae Bagridae Cochleae Cyprinodontidae Fundulidae Oxudercidae Sparidae	**TH:** *Mugil liza* Valenciennes, 1836 *Anguilla anguilla* (Linnaeus, 1758); *Acanthopagrus butcheri* (Munro, 1949); *A. australis* (Günther, 1859); *A. berda* (Fabricius, 1775); *Chelon auratus* (Risso, 1810); *C. ramada* (Risso, 1827); *C. saliens* (Risso, 1810); *Coptodon zillii* (Gervais, 1848); *Fundulus similis* (Baird and Girard, 1853); *F. heteroclitus* (Linnaeus, 1766); *Floridichthys carpio* (Günther, 1866); *M. cephalus* Linnaeus, 1758; *M. trichodon*, Poey, 1875; *Mystus gulio* (Hamilton, 1822); *Pseudapocryptes elongatus* (Cuvier, 1816); *Sarotherodon galilaeus* (Linnaeus, 1758); *Trachystoma petardi* (Castelnau, 1875);	**TLOC:** New Orleans, USA Louisiana, USA; Brisbane River, Australia; Texas coast, USA; Georgia coast, USA; Israel; Rio Aconcagua, Chile; La Parguera, Puerto Rico; Melbourne, Australia; Lakes Entrance, Australia; Port Lincoln, Australia; Coffs Harbour, Australia; Gladstone, Australia; Port Canning, India	North Atlantic Pacific Caribbean Mediterranean Gulf of Mexico Indian	–	–	✓	(Beneden, 1870; Bymes, 1986; Kabata, 1992)
E. myctarothes Wilson, 1913	Sphyrnidae	**TH:** *Sphyrna zygaena* (Linnaeus, 1758)	**TLOC:** Indian Ocean islands	Indian	–	–	–	(Wilson, 1913)
E. pakistanicus Jafri, 1995	Mastacembelidae	**TH:** *Mastacembelus armatus* (Lacepède, 1800)	**TLOC:** Sindh, Pakistan	Indian	–	–	–	(Jafri, 1995)
			TLOC: Veli Lake, India	Indian	–	–	–	Ho *et al.* (1992)
E. parvitergum Ho *et al.*, 1992	Cichlidae Carangidae	**TH:** *Etroplus suratensis* (Bloch, 1790); *Carangoides malabaricus* (Bloch and Schneider, 1801)						
E. polynemi Redkar *et al.*, 1952	Polynemidae	**TH:** *Eleutheronema tetradactylum* (Shaw, 1804)	**TLOC:** Maharashtra, Mumbai, India	Indian	–	–	–	Redkar *et al.* (1952)
E. rostralis Ho *et al.*, 1992	Mugilidae	**TH:** *Planiliza parsia* (Hamilton, 1822) *Osteomugil cunnesius* (Valenciennes, 1836); *P. tade* (Fabricius, 1775); *P. abu* (Heckel, 1843); *P. macrolepis* (Smith, 1846);	**TLOC:** Madras, India Mangalore, Pakistan; Veli Lake, India; Neendakara, India; Shatt Al-Arab River, India	Indian	–	–	–	Ho *et al.* (1992); El-Rashidy and Boxshall (2002)
E. uniseriatus Ho *et al.*, 1992	Gobiidae Belonidae	**TH:** *Glossogobius giuris* (Hamilton, 1822) *Xenentodon cancila* (Hamilton, 1822)	**TLOC:** Veli Lake, India Karuvanoor River, India	Indian	–	–	–	Ho *et al.* (1992)
E. vembanadensis Thomas, 1993	Siluridae	**TH:** *Wallago attu* (Bloch and Schneider, 1801)	**TLOC:** Vembanad Lake, India	Indian	–	–	–	(Thomas, 1993)
E. xenomelanirisi Carvalho, 1955	Atherinopsidae	**TH:** *Atherinella brasiliensis* (Quoy and Gaimard, 1825)	**TLOC:** Cananéia, Brazil	South Atlantic	–	–	–	(Carvalho, 1955)
E. youngi Tavares and Luque, 2005	Ariidae	**TH:** *Aspistor luniscutis* (Valenciennes, 1840) *Sciades herzbergii* (Bloch, 1794)	**TLOC:** Angra dos Reis, Brazil Caeté estuary, Brazil	South Atlantic	–	–	–	(Tavares and Luque, 2005; Dos Santos *et al.*, 2021)

Information from the present study is represented in bold.
Syn, synonym; TH, type host; TLOC, type locality.

Appendix B

their host associations, possibly yielding a hidden marine parasite diversity within these shores. Understanding the distribution and diversity of *Ergasilus* species across South Africa can provide valuable insights into evolutionary patterns, connectivity between populations and the impact of environmental factors on parasite distribution (Boxshall and Halsey, 2004). Additionally, such comparisons can aid in identifying potential host-switching events and the emergence of novel host–parasite associations (Boxshall and Halsey, 2004; Fikiye *et al.*, 2023; Míč *et al.*, 2023).

This study aimed to start filling this gap by investigating the presence, diversity and molecular characteristics of *Ergasilus* copepods associated with the Evileye blaasop, *Amblyrhynchote honckenii* (Bloch), along the South African coastline. Combining morphological examination and molecular analyses based on partial ribosomal RNA (rRNA) gene regions (18S and 28S), and 1 mitochondrial DNA gene region (COI), 2 new marine *Ergasilus* species were found and described. Revealing and documenting these new species enhances our understanding of the marine parasite diversity within this region, revealing new host–parasite interactions and evolutionary links.

Materials and methods

Sampling

As part of a larger study on the biodiversity of marine fish parasites in southern Africa, 25 *A. honckenii* specimens were collected from 2 coastal localities. Using rod and reel, 15 specimens of *A. honckenii* (13 males and 2 females) were collected from the Breede River Estuary, Witsand (−34.397323; 20.837474) in November 2021 and 10 specimens (1 male, 8 females and 1 juvenile) from the intertidal rocky shore at Chintsa East (−32.836538; 28.116997) in July 2022 (Fig. 1). Following capture, the fish were transported in aerated water containers to a nearby field station for dissection. The specimens were then identified, photographed, weighed, measured and humanely killed using percussive stunning followed by pithing (ethics committee approved standard operation procedure NWU-00267-17-A5). Ethical approval for this project was received from the AnimCare Ethics Committee of the North-West University with ethics number NWU-00565-19-A5. Permits for collecting *A. honckenii* were issued by Cape Nature, Western Cape Province and the South African Department of Agriculture, Forestry and Fisheries (permit no. CN44-87-18289 and RES2022-44, respectively).

Fish were identified using Smith Sea Fishes (Smith and Heemstra, 2012), with fish nomenclature following FishBase (Froese and Pauly, 2024) and Eschmeyer's Catalog of Fishes (Fricke *et al.*, 2024). Host authorities are not included in the text or references.

Morphological analyses

Fish gills were removed and screened for parasites using a Zeiss Stemi 305 compact stereomicroscope (Zeiss, Oberkochen, Germany). Copepod specimens were removed from the gills and preserved in 80% ethanol for morphology and 96% for molecular analysis. Twelve selected specimens underwent morphological observations after being cleared in lactic acid, dissected and temporarily mounted onto slides with glycerine. Photomicrographs of various body structures were captured using a Nikon Y-TV55 video camera mounted on a Nikon ECLIPSE Ni microscope (Nikon, Tokyo, Japan). Image analysis

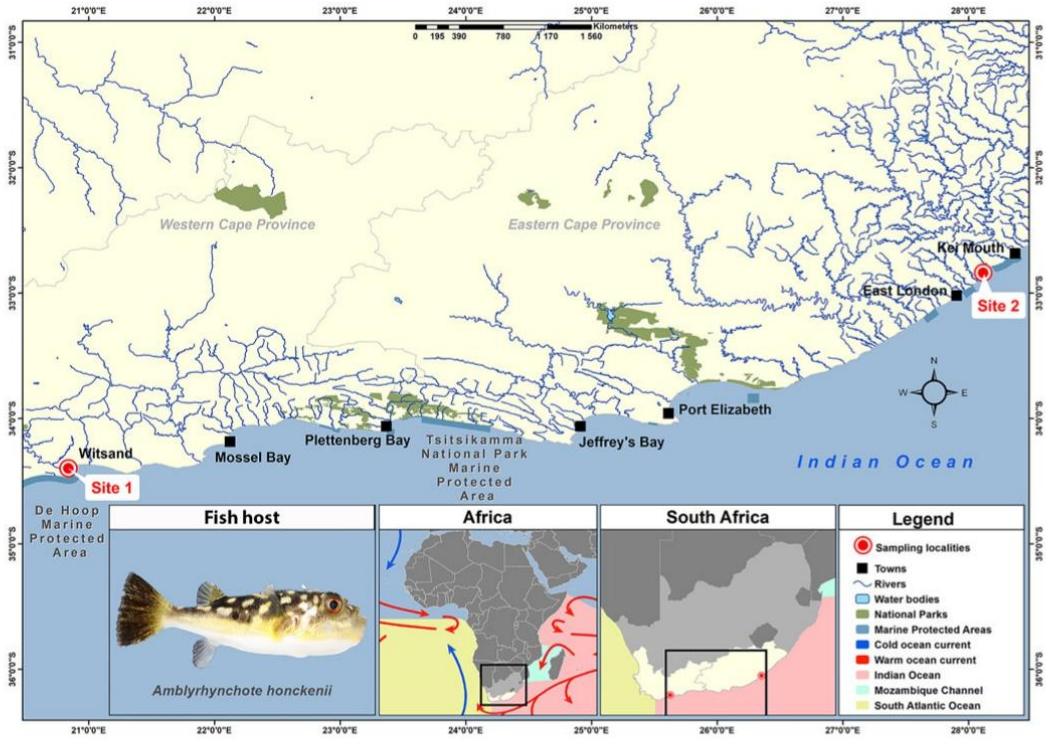

Figure 1. Map indicating the sampling localities of specimens of *Amblyrhynchote honckenii* (Bloch).

software, Image-Pro Express (Nikon), facilitated obtaining all necessary measurements for descriptive analyses. All measurements and terminology for describing body somites and cephalic appendages follow Boxshall and Montú's (1997) guidelines. Measurements are provided in text descriptions and tabular form, with text descriptions including average measurements followed by the range and number of specimens in parentheses. Table 2 presents metrical data as the mean, followed by the standard deviation and the number of specimens examined. Measurements are in micrometres unless otherwise specified. Pencil drawings of specimens and dissected appendages were created using a drawing tube attached to a Nikon ECLIPSE Ni microscope (Nikon). Final digital illustrations were made with Adobe Photoshop version 23.0.1 software using a Wacom Intuos Pro tablet (Wacom, Saitama, Japan).

Furthermore, 6 adult specimens collected from the Breede River Estuary, Witsand, were used for scanning electron microscopy (SEM). SEM could not be performed on specimens from Chintsa East due to the limited availability of specimens. Each specimen selected for SEM observation was cleaned by lightly brushing the surface. Cleaned specimens were dehydrated, placed in hexamethyldisilisane (HMDS), mounted onto carbon tape, placed on aluminium stubs and sputter-coated with carbon (Emscope TB500, Quorum Technologies, Puslinch, ON, USA), followed by 20–30 nm gold/palladium (Eiko IB2 ion coater, Eiko, Japan). Specimens were examined with a FEI Nova NanoSEM 450 scanning electron microscope (FEI, Hillsboro, OR, USA). Images were taken of various characteristic body structures to aid in the morphological description and for comparisons among species.

Molecular analyses

Genomic DNA extraction was conducted using egg strings from 2 copepod specimens from the Breede River Estuary, Witsand, and 1 copepod specimen from Chintsa East. Extraction followed the Macherey-Nagel NucleoSpin® Tissue extraction kit protocol (GmbH and Co. KG, Sandton, South Africa), with an adapted 4 h pre-lysis period and adding 50% more buffer BE. Partial gene amplification targeted 3 gene regions: 2 rRNA gene regions (18S and 28S) and 1 mitochondrial DNA gene region (cytochrome c oxidase I or COI), using primers (18SF, 18SR; 28SF, 28SR) prepared by Song *et al.* (2008) for 18S and 28S, and universal mitochondrial primers (LCO1490 and HCO2198) (Folmer *et al.*, 1994) for COI (Table 3). Amplification reactions were conducted in 25 µL volumes, made up of 12.5 µL of DreamTaq PCR Master Mix (Thermo Fischer Scientific, Waltham, MA, USA), 1.25 µL of 10 µM of each primer, 3 µL of DNA product and 7 µL of double distilled water. Thermocycling conditions followed adapted protocols established by Folmer *et al.* (1994) and Song *et al.* (2008). The PCR thermocycling profile followed adapted conditions: 94°C for 5 min, followed by 40 amplification cycles of 95°C for 30 s, 47°C for 30 s and 72°C for 1 min with a final extension at 72°C for 7 min. Positive PCR products were verified *via* 1% agarose gel electrophoresis and then sent for purification and sequencing in both forward and reverse directions to Inqaba Biotechnical Industries (Pty) Ltd. (Pretoria, South Africa).

Sequences were assembled, aligned, edited and trimmed using Geneious Prime version 2023.1.2 (Biomatters, Auckland, New Zealand). Additionally, the nucleotide Basic Local Alignment Search Tool (BLAST) was used to select *Paracyclopina nana* Smirnov, 1935 (Cyclopettidae Martínez Arbizu, 2000), as the outgroup of the study (Table 4). Considering the limited availability of COI sequences, unpublished sequences of *Ergasilus* species, sourced from the Barcode of Life Database (BOLD), were also included in the COI alignment (Table 4). Alignments for the novel sequences were generated and trimmed using default parameters of MAFFT version 7.4.9 (Katoh *et al.*, 2002; Katoh and Standley, 2013). Genetic divergences among aligned specimens were calculated within Geneious Prime version 2023.1.2, presenting percentage similarities and differences in base numbers.

Table 2. Metrical information of the new species of *Ergasilus* Nordmann, 1832

Character	*Ergasilus arenalbus* n. sp.	*Ergasilus chintensis* n. sp.
Body (L)	1182 ± 137; 12	1035 ± 47; 2
Body (W)	408 ± 49; 12	424 ± 17; 2
Cephalothorax (L)	626 ± 93; 12	608 ± 5; 2
Cephalothorax (W)	397 ± 53; 12	417 ± 6; 2
Cephalosome (L)	336 ± 43; 12	Fused
Cephalosome (W)	387 ± 38; 12	Fused
First pedigerous somite (L)	176 ± 27; 12	Fused
First pedigerous somite (W)	358 ± 42; 12	Fused
Second pedigerous somite (L)	107 ± 24; 12	138 ± 6; 2
Second pedigerous somite (W)	274 ± 31; 12	292 ± 7; 2
Third pedigerous somite (L)	105 ± 18; 12	106 ± 10; 2
Third pedigerous somite (W)	212 ± 37; 12	224 ± 10; 2
Fourth pedigerous somite (L)	61 ± 9; 12	40 ± 3; 2
Fourth pedigerous somite (W)	140 ± 11; 12	112 ± 3; 2
Fifth pedigerous somite (L)	31 ± 6; 12	14 ± 6; 2
Fifth pedigerous somite (W)	80 ± 12; 12	83 ± 16; 2
Genital double somite (L)	135 ± 8; 12	113 ± 4; 2
Genital double somite (W)	109 ± 8; 12	88 ± 3; 2
First abdomen (L)	43 ± 6; 12	28 ± 6; 2
First abdomen (W)	73 ± 8; 12	53 ± 3; 2
Second abdomen (L)	31 ± 6; 12	23 ± 4; 2
Second abdomen (W)	63 ± 3; 12	50 ± 1; 2
Third abdomen (L)	28 ± 4; 12	21 ± 6; 2
Third abdomen (W)	63 ± 2; 12	46 ± 1; 2
Caudal rami (L)	30 ± 2; 12	25 ± 2; 2
Caudal rami (W)	24 ± 1; 12	18 ± 1; 2
Seta I (L)	92 ± 5; 12	61 ± 2; 2
Seta II (L)	77 ± 7; 12	55 ± 2; 2
Seta III (L)	28 ± 5; 12	24 ± 4; 2
Seta IV (L)	282 ± 24; 12	183 ± 3; 2
Antennule (L)	121 ± 8; 12	98 ± 1; 2
Coxobasis (L)	174 ± 23; 12	102 ± 3; 2
Coxobasis (W)	95 ± 10; 12	65 ± 4; 2
First endopodal segment (L)	339 ± 25; 12	184 ± 2; 2
Second endopodal segment (L)	196 ± 15; 12	108 ± 3; 2
Third endopodal segment (L)	28 ± 4; 12	13 ± 2; 2
Claw (L)	161 ± 13; 12	86 ± 3; 2
Eggs (L)	1269 ± 257; 12	1101 ± 4; 2
Eggs (W)	256 ± 42; 12	193 ± 3; 2

L, length; W, width.
Information is presented as the mean, followed by the standard deviation and the number of specimens examined.
All measurements are in micrometres.

Table 3. List of primers used for DNA amplification of parasitic copepods with sequences and references, used to amplify partial 18S, 28S and COI genes in this study

Gene regions	Primers	Sequences	Sources
18S	18SF	5′-AAG GTG TGM CCT ATC AAC T-3′	Song *et al.* (2008)
	18SR	5′-TTA CTT CCT CTA AAC GCT C-3′	
28S	28SF	5′-ACA ACT GTG ATG CCC TTA G-3′	Song *et al.* (2008)
	28SR	5′-TGG TCC GTG TTT CAA GAC G-3′	
COI	LCO1490 (F)	5′-GGTCAACAAATCATAAAGATATTGG-3′	Folmer *et al.* (1994)
	HCO2198 (R)	5′-TAAACTTCAGGGTGACCAAAAAATCA-3′	

The optimal nucleotide substitution model for each dataset was estimated using the Akaike Information Criterion (AIC) in jModelTest 2.1.4 (Posada, 2008; Darriba *et al.*, 2012). The general time-reversible model with invariant sites and gamma-distributed rate variation (GTR + I + G) was recommended for all datasets (18S, 28S and COI). Phylogenetic analyses were performed using Maximum Likelihood (ML) and Bayesian Inference (BI) methods with this suggested model. BI analyses were conducted on the CIPRES Science Gateway version 3.3 (Miller *et al.*, 2010) using MrBayes version 3.2.7a (Ronquist *et al.*, 2012), with 2 independent Markov Chain Monte Carlo (MCMC) runs of 4 chains for 10 million generations, sampling every 1000 generations, and a burn-in of the first 25 000 generations. ML analyses were performed using PhyML version 3.0 (Guindon *et al.*, 2010) on the ATGC bioinformatics platform, with model parameters estimated and 1000 bootstrap repetitions for nodal support. The resulting phylogenetic trees from BI and ML analyses were visualized using TreeViewer version 2.2.0 (Bianchini and Sánchez-Baracaldo, 2024).

Results

Two distinct gill-associated parasitic species, morphologically and molecularly differentiated, were obtained from subsets of 10–15 *A. honckenii* specimens, ranging from 95 to 185 mm in length and weighing 30 to 140 g. Both morphotypes were classified as *Ergasilus* (Ergasilidae) based on specific characteristics, such as body typically cyclopiform with clear segmentation, biramous legs IV with 2-segmented exopods and 3-segmented endopods, 6-segmented antennules, antennas featuring a single claw and the absence of maxillipeds in females, following descriptions by Boxshall and Montú (1997) and Boxshall and Halsey (2004). Notably, only 1 morphotype was found and described from each location, highlighting the uniqueness of both morphotypes in their respective collection sites.

Taxonomy

***Ergasilus arenalbus* n. sp.**: *Figures 2–5*

ZooBank LSID: urn:lsid:zoobank.org:act:4B5580B2-C5BA-4B8E-99C3-14E9BBF32D3D

Type host: *Amblyrhynchote honckenii* (Bloch) (Tetraodontiformes: Tetraodontidae).

Type locality: Breede River Estuary, Witsand (−34.397323; 20.837474), Western Cape Province, South Africa.

Site on host: Gill filaments.

Prevalence of infection: 67% (10 of 15 pufferfish).

Type material: 151 *Ergasilus* specimens (adult females) were collected. Only adult females were examined: 6 were used for SEM; 2 for dissection; 12 for morphology; and 2 egg strings were used for DNA extraction. The hologenophores (NMB P 1044–NMB P 1045), holotype (NMB P 1042) and 11 paratypes (NMB P 1043) were deposited in the parasitological collections of the National Museum, Bloemfontein, South Africa; the remaining specimens are in the possession of the Water Research Group, North-West University, Potchefstroom, South Africa.

Representative DNA sequences: GenBank accession numbers and numbers of bases (bp) are given as follows: 18S: 1333 and 1344 bp long sequences of 2 specimens, accession numbers: PQ451954 and PQ451956; 28S: 668 and 664 bp long sequences of 2 specimens, accession numbers: PQ451957 and PQ451958; and COI: 701 bp long sequence of 1 specimen, accession number: PQ439339.

Etymology: The species name '*arenalbus*' is derived from 'arena albus' meaning white sand (English) or wit sand (Afrikaans) in Latin. This refers to 'Witsand' the name of the type locality of this species.

Description

Adult female description (based on 12 specimens). Body length (measured from the anterior margin of cephalosome to posterior margin of caudal rami) 1182 (959–1370; $n = 12$). Body comprises prosome, urosome and caudal rami. Prosome 5-segmented, composed of cephalosome and 4 free pedigerous somites. Cephalothorax composed of cephalosome and first pedigerous somite; cephalosome separated dorsally from previous somite by flexible cuticle (Figs 2A and 5A). Cephalosome slightly shorter than wide, 336 (272–414; $n = 12$) long by 387 (316–460; $n = 12$) wide, oval to trapezoidal, with antennules and antenna visible in dorsal view. Cephalic ornamentation comprising of anterior circular eyespot and inverted T-shaped mark of thickened chitin situated medially on dorsal side (Fig. 2A and B). Paired sensory pores and papillae observed anterior to eyespot with numerous sensory papillae and pores scattered over dorsal surface of cephalosome. Rostrum well-developed, with truncated posterior margin. All pedigerous somites wider than long and progressively smaller. Paired sensory papillae observed mid-dorsally on segments 2–5. First pedigerous somite 176 (129–218; $n = 12$) long by 358 (297–428; $n = 12$) wide; second pedigerous somite 107 (82–154; $n = 12$) long by 274 (241–334; $n = 12$) wide; third pedigerous somite 105 (78–138; $n = 12$) long by 212 (163–268; $n = 12$) wide; fourth pedigerous somite 61 (44–82; $n = 12$) long by 140 (127–169; $n = 12$) wide.

Urosome comprising reduced fifth pedigerous somite, genital double somite and 3 free abdominal somites (Fig. 3A). Reduced fifth pedigerous somite 31 (20–39; $n = 12$) long by 80 (72–114; $n = 12$) wide. Genital double-somite longer than wide, 135 (120–152; $n = 12$) long by 109 (100–130; $n = 12$) wide (Fig. 3A), bearing a pair of multiseriate egg sacs dorsally (Figs 2A and 4A), measuring 1269 (989–1662; $n = 12$) long by 256 (222–340; $n = 12$) wide (Figs 2A and 4A). Abdomen 3-segmented; first abdominal somite widest, 43 (36–56; $n = 12$) long by 73 (64–92; $n = 12$) wide; second abdominal somite shorter, 31 (23–40; $n =$

Appendix B

Table 4. List of GenBank and Barcode of Life Database (BOLD) Ergasilidae sequences included in the phylogenetic analyses

Taxon	Host	Locality	GenBank accession numbers			References
			18S	28S	COI	
Acusicola margulisae	*Amphilophus citrinellus*; *Parachromis managuensis*; *Oreochromis* sp.; *Poecilia exicana*	Nicaragua	MN852694 MN 852695	MN852849 MN852850	MN854868 MN854869	Santacruz *et al.* (2020)
Dermoergasilus madagascarensis	*Paretroplus*; *polyactis*	Madagascar	PP115568 –	PP115569 –	PP117931 PP117932	Míč *et al.* (2024)
Ergasilus anchoratus	*Pseudobagrus fulvidraco*	China	DQ107564	DQ107528	–	Song *et al.* (2008)
***Ergasilus arenalbus* n. sp.**	***Amblyrhynchote honckenii***	**South Africa**	**PQ451954 PQ451956**	**PQ451957 PQ451958**	**PQ439339 –**	**Present study**
**Ergasilus auritus*	*Gasterosteus aculeatus*	Canada	–	–	ECTCR091-14	BOLD
Ergasilus briani	*Misgurnus anguillicaudatus*	China	DQ107572	DQ107532	–	Song *et al.* (2008)
Ergasilus caparti	*Neolamprologus brichardi*	Burundi	OQ407469	OQ407474	–	Míč *et al.* (2023)
***Ergasilus chintensis* n. sp.**	***Amblyrhynchote honckenii***	**South Africa**	**PQ451955**	**PQ451959**	**PQ439340**	**Present study**
Ergasilus hypomesi	*Acanthogobius hasta*	China	DQ107573	DQ107539	–	Song *et al.* (2008)
**Ergasilus lizae*	*Fundulus diaphanus*	Canada	–	–	ECTCR024-14	BOLD
Ergasilus macrodactylus	*Gnathochromis permaxillaris*	Burundi	OQ407465	OQ407470	–	Míč *et al.* (2023)
Ergasilus megacheir	*Simochromis diagramma*	Burundi	OQ407466	OQ407471	–	Míč *et al.* (2023)
Ergasilus mirabilis	*Clarias gariepinus*	South Africa Zambia	OR449753 OR449754	OR449755 OR449756	OR448769 OR448770	Fikiye *et al.* (2023)
Ergasilus parasarsi	*Simochromis diagramma*	Burundi	OQ407467	OQ407473	–	Míč *et al.* (2023)
Ergasilus parvus	*Spathodus erythrodon*	Burundi	OQ407468	OQ407472	–	Míč *et al.* (2023)
Ergasilus parasiluri	*Tachysurus fulvidraco*	China	DQ107567	DQ107536	–	Song *et al.* (2008)
Ergasilus peregrinus	*Siniperca chuatsi*	China	DQ107577	DQ107531	–	Song *et al.* (2008)
Ergasilus scalaris	*Tachysurus dumerili*	China	DQ107565	DQ107538	–	Song *et al.* (2008)
Ergasilus sieboldi	*Perca fluviatilis*; *Sparus aurata*	Czech Republic	MW810238	MW810242	–	Kvach *et al.* (2021)
Ergasilus tumidus	*Acanthorhodeus taenianalis*	China	DQ107569 DQ107570	DQ107533 DQ107534	– –	Song *et al.* (2008)
Ergasilus wilsoni	Free-living	South Korea	KR048765	KR048843	KR049036	Baek *et al.* (2016)
Ergasilus yaluzangbus	*Gymnocypris stewartii*	China	DQ107578	DQ107540	–	Song *et al.* (2008)
Neoergasilus japonicus	*Lepomis gibbosus* *Scardinius erythrophthalmus*	Czech Republic USA	MH167970 MW810236 – –	MH167968 MW810240 – –	– – MZ964935 MZ964938	Ondračková *et al.* (2019), Kvach *et al.* (2021), Vasquez *et al.* (2023)
Paraergasilus brevidigitus	*Cyprinus carpio*	China	DQ107576	DQ107530	–	Song *et al.* (2008)
Paraergasilus longidigitus	*Abramis brama*; *Perca fluviatilis*; *Scardinius erythrophthalmu*	Czech Republic	MW810239	MW810243	–	Kvach *et al.* (2021)
Paraergasilus medius	*Ctenopharyngodon idellus*	China	DQ107574	DQ107529	–	Song *et al.* (2008)
Sinergasilus major	*Ctenopharyngodon Idella* *Silurus glanis*	China Hungary	DQ107558 –	– MZ047815	– –	Song *et al.* (2008) Dos Santos *et al.* (2021)
Sinergasilus polycolpus	*Hypophthalmichthys molitrix*	China	DQ107563	DQ107525	–	Song *et al.* (2008)
Sinergasilus undulatus	*Cyprinus carpio*	China	DQ107561 –	DQ107526 –	– MW080644	Song *et al.* (2008) Hua *et al.* (2021)
**Thersitina gastorostei*	*Gasterosteus aculeatus*	Canada	–	–	ECTCR063-14	BOLD
Paracyclopina nana	Free-living	Korea	– FJ214952	– FJ214952	EU877959 –	Ki *et al.* (2009) Ki *et al.* (2011)

The taxa in bold fonts are sequences generated from the present study. *Paracyclopina nana* (in the grey shade) was used as the outgroup.
**Taxon from the Barcode of Life Database (BOLD).

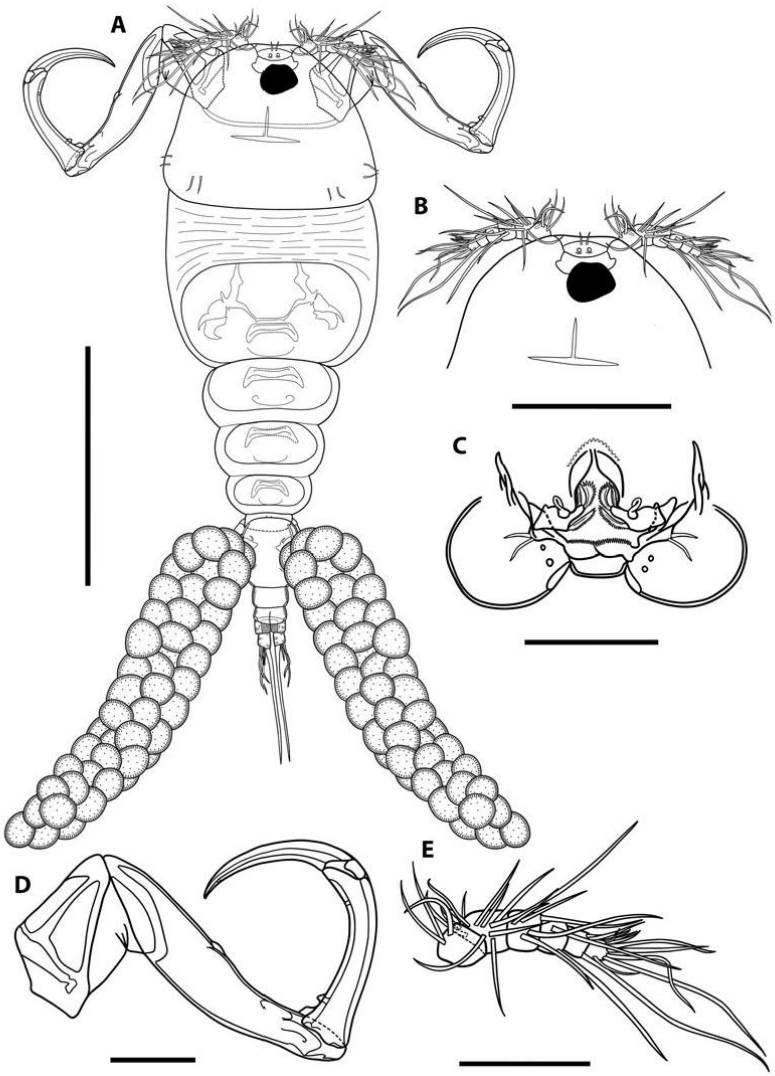

Figure 2. Illustrations of adult female of *Ergasilus arenalbus* n. sp: (A) entire specimen, dorsal view; (B) detail of cephalosome, dorsal view; (C) mouth, mandible, maxillule and maxilla; (D) antenna; (E) antennule. Scale bars: A – 500 µm; B – 250 µm; C–E – 100 µm.

12) long by 63 (55–67; $n = 12$) wide; third somite (= anal somite) incised dorsoventrally (= anal opening or anus) forming attachment for caudal rami, 28 (22–32; $n = 12$) long by 63 (59–68; $n = 12$) wide, ornamented with pair of pores on dorsal side; each pore located laterally to anal opening and carrying bristle (Figs 3A, 4E, 5C). All abdominal somites with posterior row of ventral spinules (Figs 4E and 5C).

Caudal rami slightly elongated, 30 (26–33; $n = 12$) long by 24 (22–28; $n = 12$) wide, with 4 setae (Fig. 3A). Innermost seta (IV) longest 282 (226–308; $n = 12$), followed by shortest seta (III) 28 (20–39; $n = 12$) and 2 longer setae (II and I) 77 (60–87; $n = 12$) and 92 (83–99; $n = 12$), respectively (Fig. 3A).

Antennule 6-segmented, armed with long and short setae (Fig. 2E). Setal formula from proximal to distal segments given as 3–12–6–2–3–8 (total 34). Antenna 4-segmented (Figs 2D and 4B) comprising coxobasis, 174 (110–196; $n = 12$) long by 95 (73–114; $n = 12$) wide; and 3-segmented endopod; armed with curved terminal claw (Figs 2D and 4B). First endopod segment longest 339 (288–366; $n = 12$), followed by second endopod segment 196 (152–215; $n = 12$) and small third endopod segment 28 (24–40; $n = 12$). Prominent spine observed on anterior second endopod segment (Figs 2D, 4B, 5D). Terminal claw pointed and smooth 161 (127–186; $n = 12$), with fossa on concave margin.

Mouth positioned ventrally on cephalosome. Labrum with internal teeth; teeth arranged in an arch. Mandible armed with 3 blades (anterior, medial and posterior blades); anterior blade thinner and shorter than others, ornamented along anterior margin; medial and posterior blades, both with teeth on opposite

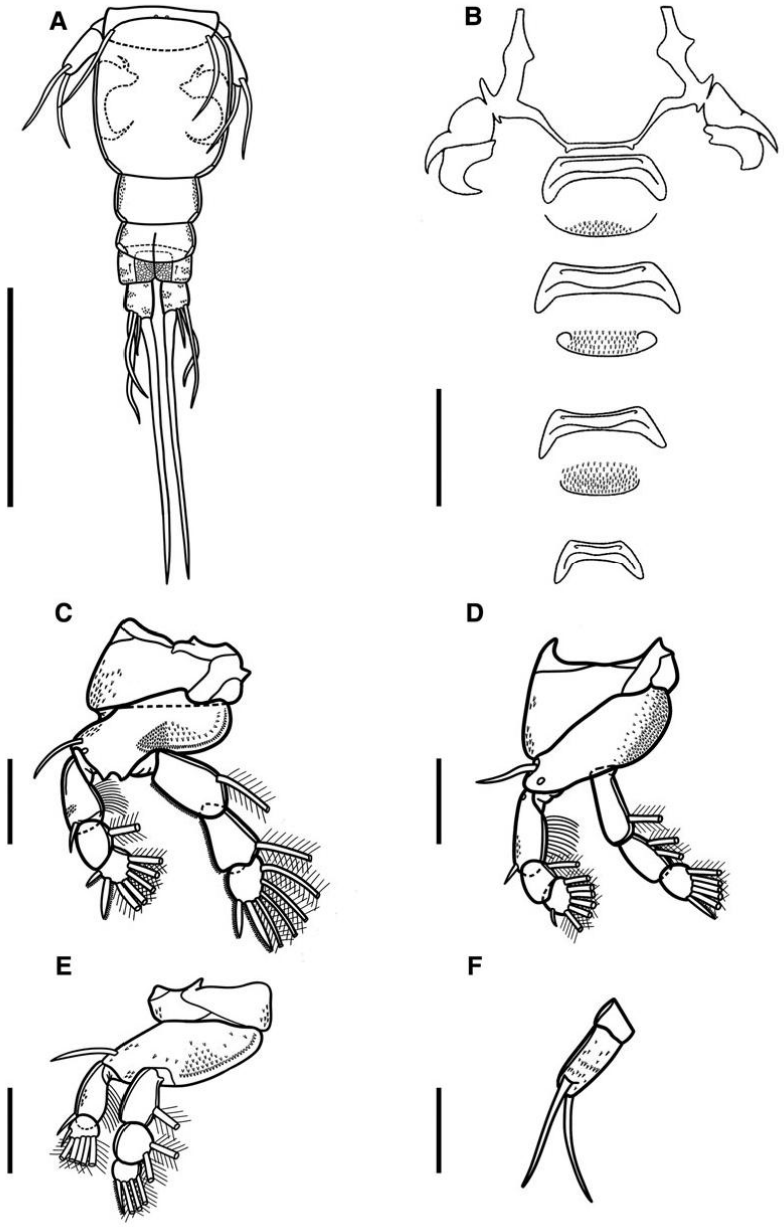

Figure 3. Illustrations of adult female of *Ergasilus arenalbus* n. sp: (A) urosome, dorsal view; (B) intercoxal sclerites and interpodal plates; (C) leg 1; (D) leg 2 and leg 3; (E) leg 4; (F) leg 5. Scale bars: A – 200 µm; B – 100 µm; C–F – 50 µm.

margin. Maxillule armed with 2 unequal setae; innermost seta shortest; ornamented with 1 pore and multiple spinules; pore lacking bristle (Fig. 2C). Maxilla 2-segmented, comprising syncoxa (= first segment) and basis (= second segment); syncoxa broad, with 2 distal pores; basis ornamented with multiple spinules on posterior margin. Labium broad, unornamented; midregion produced posteriorly, with truncated posterior margin.

Swimming legs I to IV; each comprising coxa, basis and 2 segmented rami (i.e. exopod, endopod). Rami of all legs 3-segmented, except 2-segmented exopod of leg IV. Segments distinct, typical with similar basic morphology as in other species of *Ergasilus*. Armature on rami as Roman and Arabic numerals indicating spines and plumose setae, respectively, in Table 5.

Leg I (Fig. 3C). Coxa ornamented with spinules on outer margin. Basis armed with bare outer seta, ornamented with spinules on both sides; posterior margin protrudes posteriorly forming 1 spinous process; spines located between rami (Figs 3C and 4C). Exopod 3-segmented; first endopodal segment with distal spine,

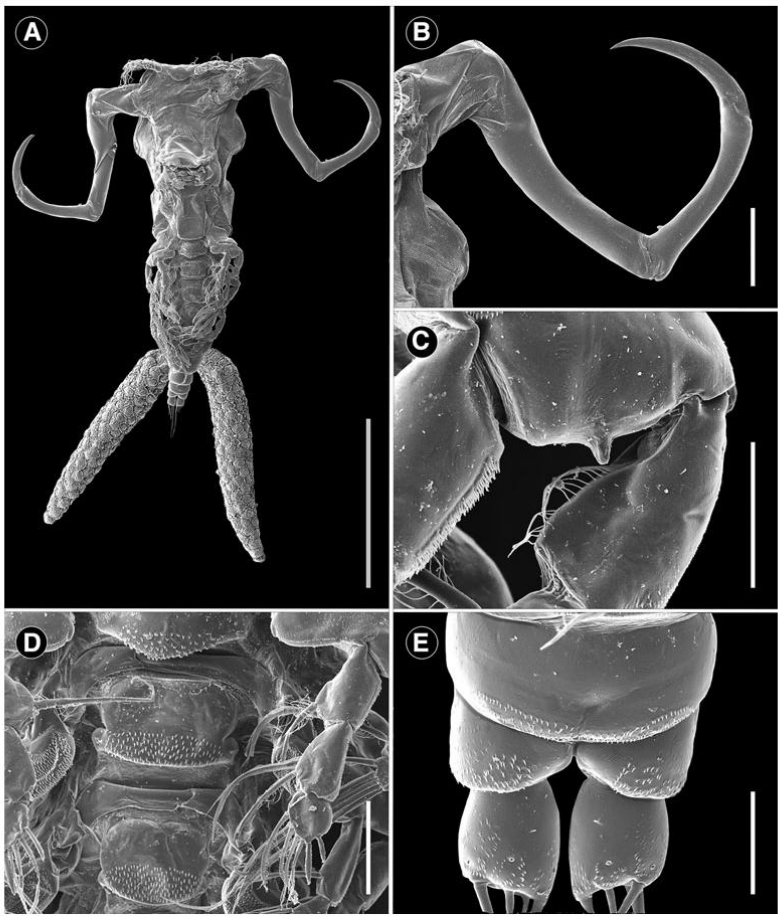

Figure 4. Scanning electron microscope photomicrographs of adult female *Ergasilus arenalbus* n. sp. showing features from the ventral and dorsal view: (A) entire specimen; (B) antenna; (C) base of first leg; (D) ventral view of interpodal plates; (E)– dorsal view of ornamentation on caudal rami. Scale bars: A – 500 µm; B – 100 µm; C–E – 25 µm.

ornamented with patch of spinules on outer margin; spinules located just above distal spine; and bristles along outer margin; second exopodal segment with 1 plumose seta, unornamented; third exopodal segment armed with 2 serrated spines (inner and outer spine); inner spine about 2.0 times longer than outer spine; and 5 plumose setae. Endopod 3-segmented; all segments with spinules along inner margin; first and second endopodal segment, each with 1 plumose seta on inner margin; third endopodal segment armed with 2 serrated spines (inner and outer spine); inner spine about 2.0 times longer than outer spine; and 4 plumose setae.

Leg II (Fig. 3D). Coxa ornamented with spinules on outer margin. Basis armed with bare outer seta, ornamented with spinules on both sides. Exopod 3-segmented; first exopodal segment with distal spine, ornamented with patch of spinules on outer margin; spinules located just above distal spine; and bristles along inner margin; second exopodal segment armed with 1 plumose seta; third exopodal segment with simple spine (or non-serrated) and 6 plumose setae. Endopod 3-segmented; first and second endopodal segments with 1 and 2 plumose setae, respectively; third endopodal segment with serrated spine and 4 plumose setae. Leg III with the same armament and ornamentation described for leg II.

Leg IV (Fig. 3E). Coxa ornamented with spinules on both sides. Basis armed with bare outer seta, with spinules scattered across surface. Exopod 2-segmented; first exopodal segment armed with distal spine, ornamented with spinules and bristles on outer and inner margin, respectively; second exopodal segment with 1 spine and 5 plumose setae. Endopod 3-segmented, all segments lacking ornaments on both margins; first and second endopodal segment with 1 and 2 plumose setae, respectively; third endopodal segment with 1 serrated spine and 3 plumose setae.

Leg V (Fig. 3F) with single ramus. Ramus 2-segmented; proximal segment rectangular, without any armaments or ornaments; distal segment about 3.0 times longer than previous segment, with spinules scattered across surface, armed with 2 bare setae.

Intercoxal sclerites and interpodal plates of all legs, present (Figs 2A, 3B, 4D). Intercoxal sclerites unornamented, with both ends directed posteriorly. Interpodal plates present; first to third plate with spinules; fourth plate absent (Figs 2A and 3B).

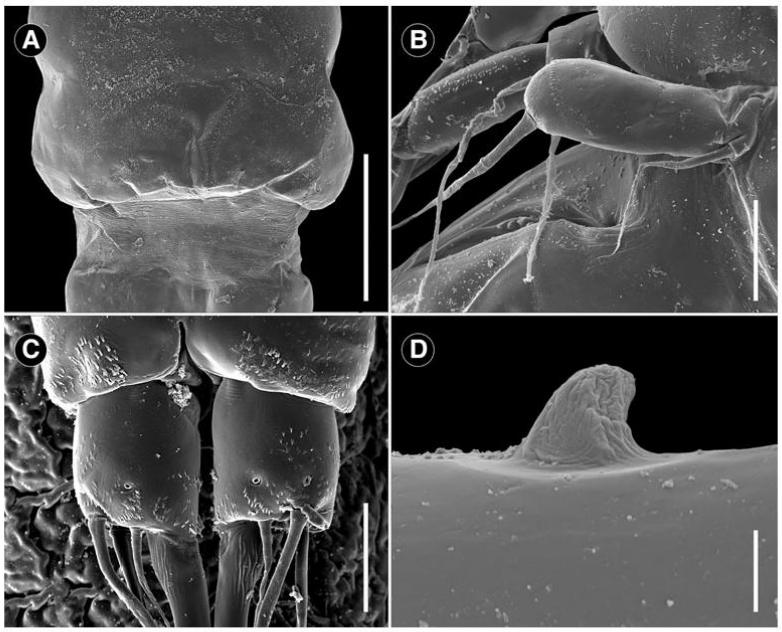

Figure 5. Scanning electron microscope photomicrographs of adult female *Ergasilus arenalbus* n. sp showing features from the ventral and dorsal view: (A) detail of the cuticular membrane of cephalothorax; (B) leg 5; (C) ventral view of detail of the caudal rami; (D) detail of the spine of the third antennal segment. Scale bars: A – 150 µm; B – 25 µm; C – 20 µm; D – 5 µm.

Table 5. Spine–setae formula on swimming legs of *Ergasilus arenalbus* n. sp.

	Coxa	Basis	Exopod	Endopod
Leg I	0-0	0-1	I-0; 0-1; II-5	0-1; 0-1; II-4
Leg II	0-0	0-1	I-0; 0-1; I-6	0-1; 0-2; I-4
Leg III	0-0	0-1	I-0; 0-1; I-6	0-1; 0-2; I-4
Leg IV	0-0	0-1	I-0; I-5	0-1; 0-2; I-3

Number of spines in Roman numerals, number of setae in Arabic numerals.

Remarks

The detailed morphological description of *E. arenalbus* n. sp. sheds light on its distinctiveness among the recognized species of *Ergasilus* worldwide. With 163 valid species known, comparisons were only made with other marine *Ergasilus* species from the southern Atlantic and Indian Ocean regions. Among the 17 marine species from these regions (Table 1), *E. arenalbus* n. sp. stands out in several key morphological aspects, notably in size; armature of the antenna; the segmentation in the body (free *vs* fused prosome somites); and general ornamentation throughout the entire body. Firstly, its larger body size, with a length averaging 1182 µm, sets it apart from species such as *E. atafonensis* Amado and Rocha, 1996, *E. bahiensis* Amado and Rocha, 1996, *E. caraguatatubensis* Amado and Rocha, 1996, *E. ilani* Oldewage and van As, 1988, *E. myctarothes* Wilson, 1913, *E. parvitergum* Ho *et al.*, 1992, *E. rostralis* Ho *et al.*, 1992 and *E. uniseriatus* Ho *et al.*, 1992 which typically have a smaller total length, below 1054 µm. Conversely, *E. felichthys* (Pearse, 1947) and *E. youngi* Tavares and Luque, 2005 present larger body sizes, approximately 1400 µm, emphasizing the distinctive size range of the newly described species. The segmentation of the body, particularly the free *vs* fused prosome somites, is another distinguishing factor. For instance, *E. arenalbus* n. sp. shows variations in abdominal somite dimensions, contrasting with the more uniform structures seen in species like *E. atafonensis*. This variability extends to cephalosome characteristics, with *E. caraguatatubensis* exhibiting an inflated shape absent in *E. arenalbus* n. sp. The spine-setae formulae on the swimming legs of *E. arenalbus* n. sp. further differentiate it, particularly when compared to all other marine congeners, except for *E. lizae* Krøyer, 1863. *Ergasilus atafonensis*, *E. bahiensis*, *E. myctarothes*, *E. parvitergum* and *E. xenomelanirisi* Carvalho, 1955, have a spine on the outer margin of the second exopodite of leg I, which is absent in the new species. In addition, *E. ilani* lacks a certain number of armaments that are common on the legs of the species in the group, for example, spines and setae on the first segments of the exopod and endopod, respectively. In *E. caraguatatubensis*, *E. felichthys*, *E. foresti* Boxshall *et al.*, 2002, *E. ilani*, *E. parvitergum* and *E. youngi*, leg V is extremely reduced and is represented by 1 or 2 setae. While the setae formula of the antennule is also a clear distinguishing factor, species like *E. ilani*, *E. rostralis* and *E. uniseriatus* were further excluded due to their antennules being described as only 5-segmented, unlike the 6-segmented antennules observed in the other *Ergasilus* species. Although *E. arenalbus* n. sp. morphologically resembles *E. lizae* in many aspects, it differs notably in the armature of the antenna, with *E. arenalbus* n. sp. exhibiting a single spine on the anterior second endopod segment, unlike *E. lizae*. Additionally, a distinctive feature of the new species is the spine projections on the posterior margin of the basis of the first leg, a characteristic absent in all other species examined. This comprehensive morphological analysis of *E. arenalbus* n. sp. provides a clear understanding of its unique features within the *Ergasilus* genus, emphasizing size, body segmentation, appendage armature and ornamentation as crucial factors in species differentiation.

Appendix B

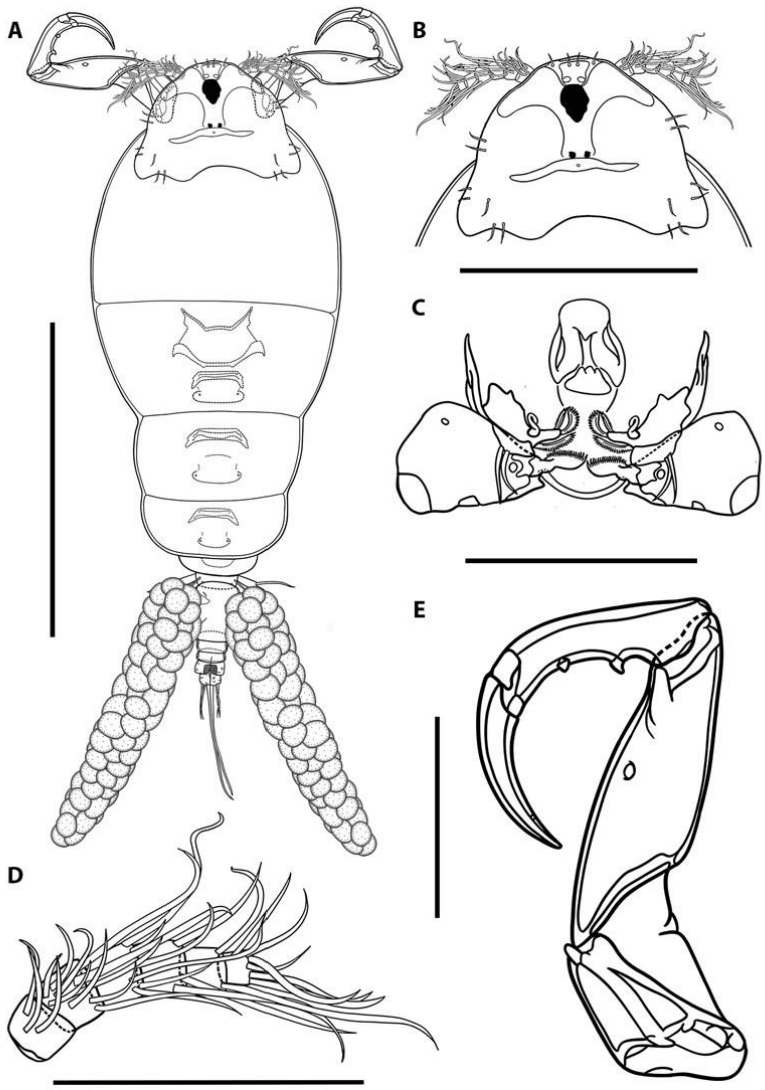

Figure 6. Illustrations of adult female of *Ergasilus chintensis* n. sp: (A) entire specimen, dorsal view; (B) detail of the cephalosome, dorsal view; (C) mouth, mandible, maxillule and maxilla; (D) antennule; (E) antenna. Scale bars: A – 500 µm; B – 250 µm; C–E – 100 µm.

Ergasilus chintensis n. sp.: Figures 6–7

ZooBank LSID: urn:lsid:zoobank.org:act:E51F54EC-9CF7-47DA-B4B7-61DEC73B430F.

Type host: *Amblyrhynchote honckenii* (Bloch) (Tetraodontiformes: Tetraodontidae).

Type locality: Chintsa East (−32.836538; 28.116997), Eastern Cape Province, South Africa.

Site on host: Gill filaments.

Prevalence of infection: 20% (2 of 10 pufferfish observed).

Type material: 2 ergasilids (adult females) were collected. Only adult females were examined: 2 were used for morphology, and 1 egg string was used for DNA extraction. The hologenophore (NMB P 1047) and holotype (NMB P 1046) were deposited in the parasitological collections of the National Museum, Bloemfontein, South Africa.

Representative DNA sequences: GenBank accession numbers and numbers of bases (bp) are given as follows: 18S: 1353 bp long sequence of 1 specimen, accession number: PQ451955; 28S: 668 bp long sequence of 1 specimen, accession number: PQ451959; and COI: 692 bp long sequence of 1 specimen, accession number: PQ439340.

Etymology: The species name '*chintensis*' is derived from Chintsa, representing the type locality of the species.

Description

Adult female description (based on 2 specimens). Body length (measured from the anterior margin of cephalosome to the posterior margin of caudal rami) 1035 (1002–1068; $n = 2$). Body

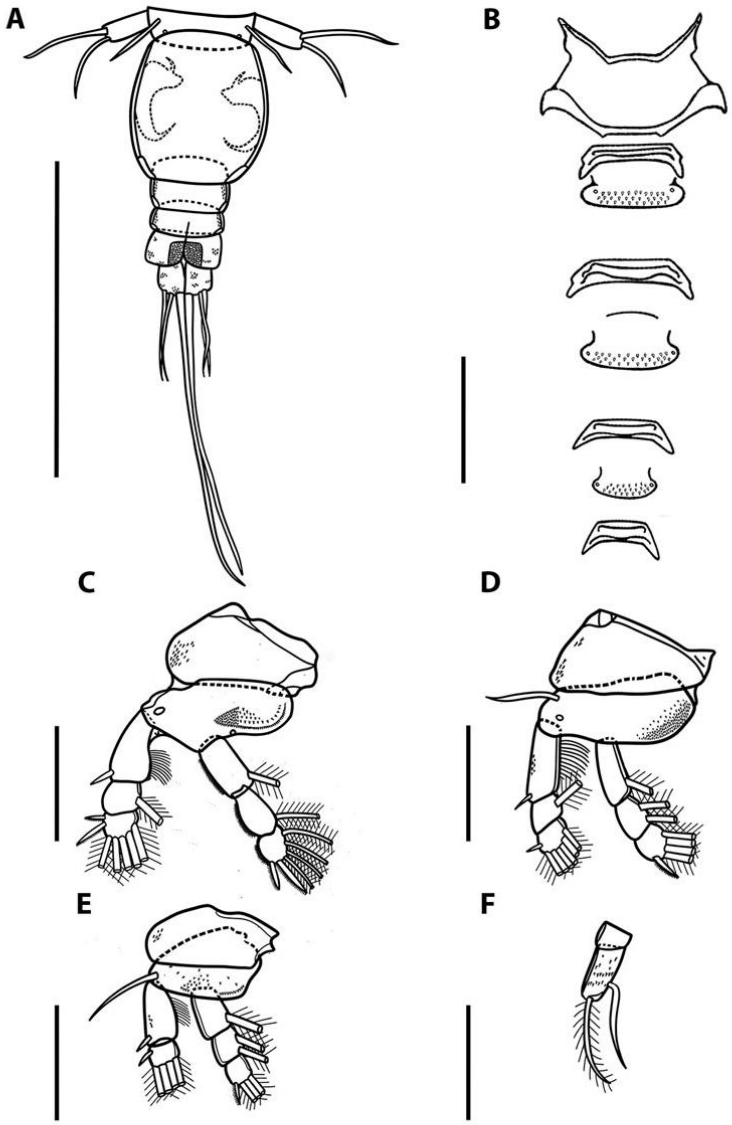

Figure 7. Illustrations of adult female of *Ergasilus chintensis* n. sp: (A) urosome, dorsal view; (B) intercoxal sclerites and interpodal plates; (C) leg 1; (D) leg 2 and leg 3; (E) leg 4; (F) leg 5. Scale bars: A – 200 μm; B – 100 μm; C–F – 50 μm.

comprises prosome, urosome and caudal rami. Prosome composed of cephalosome, fused somites (first to third pedigerous somites) and fourth free somite (Fig. 6A). Cephalosome slightly shorter than wide, oval to trapezoidal, with antennules and antenna visible in dorsal view. Cephalic ornamentation comprising of anterior circular eyespot and an inverted T-structure of thickened chitin situated medially on dorsal side (Fig. 6A and B). Paired sensory pores and papillae observed anterior to eyespot with numerous sensory papillae and pores scattered over the dorsal surface of cephalosome. Rostrum well-developed, with truncated posterior margin. All pedigerous somites wider than long and progressively smaller. Second pedigerous somite 104 (98–110; $n = 2$) long by 292 (287–297; $n = 2$) wide; third pedigerous somite 106 (99–113; $n = 2$) long by 224 (217–231; $n = 2$) wide; fourth pedigerous somite 40 (38–42; $n = 2$) long by 112 (110–114; $n = 2$) wide.

Urosome comprising reduced fifth pedigerous somite, non-pedigerous barrel-shaped genital double somite, and 3 free abdominal somites (Fig. 7A). Reduced fifth pedigerous somite 14 (10–18; $n = 2$) long by 83 (72–94; $n = 2$) wide. Genital double-somite longer, 113 (110–115; $n = 2$), than wide, 88 (86–90; $n = 2$) (Fig. 7A), bearing a pair of multiseriate egg sacs dorsally, measuring 1098 (1101–1095; $n = 2$) long by 190 (192–188; $n = 2$) wide (Fig. 6A). Abdomen 3-segmented, first abdominal somite widest,

Appendix B

Table 6. Spine–setae formula on swimming legs of *Ergasilus chintensis* n. sp.

	Coxa	Basis	Exopod	Endopod
Leg I	0-0	0-0	I-0; 0-1; II-5	0-1; 0-1; II-4
Leg II	0-0	0-1	I-0; 0-1; I-6	0-1; 0-2; I-4
Leg III	0-0	0-1	I-0; 0-1; I-6	0-1; 0-2; I-4
Leg IV	0-0	0-1	I-0; I-4	0-1; 0-2; I-3

Number of spines in Roman numerals, number of setae in Arabic numerals.

28 (24–32; $n = 2$) long by 53 (51–55; $n = 2$) wide, second abdominal somite shorter, 23 (20–25; $n = 2$) long by 50 (49–51; $n = 2$) wide; third somite (= anal somite) incised dorsoventrally (= anal opening or anus) forming attachment for caudal rami, 21 (17–25; $n = 2$) long by 46 (45–47; $n = 2$) wide (Fig. 7A). All abdominal somites with posterior row of ventral spinules.

Caudal rami slightly elongated, 23 (22–25; $n = 2$) long by 18 (17–18; $n = 2$) wide, with 4 setae (Fig. 7A). Innermost seta (IV) longest 184 (182–186; $n = 2$), followed by shortest seta (III) 24 (23–24; $n = 2$) and 2 longer setae (II and I) 55 (54–56; $n = 2$) and 59 (57–60; $n = 2$), respectively (Fig. 7A). Two sensory pores on posterior ventral margins on each ramus.

Antennule 6-segmented, armed with long and short setae (Fig. 6D). Setal formula from proximal to distal segments given as 3–10–6–3–2–6 (total 30). Antenna 4-segmented, comprising of coxobasis, 99 (97–101; $n = 2$) long by 61 (58–65; $n = 2$) wide; and 3-segmented endopod, armed with curved terminal claw (Fig. 6E). First endopod segment longest 182 (181–184; $n = 2$), followed by second endopod segment 110 (108–112; $n = 2$), and small third endopod segment 14 (13–15; $n = 2$). Two spines observed on second endopod segment. Terminal claw pointed and smooth 83 (81–85; $n = 2$), with fossa on inner margin (Fig. 6E).

Mouth positioned ventrally on cephalosome. Mandible armed with 3 blades (anterior, medial and posterior blades); anterior blade thinner and shorter than others, ornamented along anterior margin; medial and posterior blades, both with teeth on opposite margin (Fig. 6C). Maxillule armed with 2 bare setae. Maxilla 2-segmented, comprising syncoxa (= first segment) and basis (= second segment); syncoxa broad with large maxillary pore; basis distally ornamented with numerous teeth on convex margin. Labium broad, unornamented; mid-region produced posteriorly, with rounded posterior margin.

Swimming legs I to IV; each comprising coxa, basis and 2 segmented rami (i.e. exopod, endopod). Rami of all legs 3-segmented, except 2-segmented exopod of leg IV. Segments distinct, typical with similar basic morphology as in other species of *Ergasilus*. Armature on rami as follows (Roman and Arabic numerals indicating spines and plumose setae, respectively) in Table 6.

Leg I (Fig. 7C). Coxa ornamented with spinules on outer margin. Basis lacking outer setae, ornamented with spinules on inner margin. Exopod 3-segmented; first segment with small outer spine; second segment with 1 inner plumose seta, lacking spine; third segment with small spine on outer corner, longer apical spine; both spines with serrated margins; and 5 plumose setae. Endopod 3-segmented; first and second segment each with 1 plumose seta; third segment with 4 plumose setae and 2 distal serrated spines.

Leg II (Fig. 7D). Coxa ornamented with spinules on outer margin. Basis with outer seta and pore, ornamented with multiple spinules on inner margin. Exopod 3-segmented; first segment with small outer spine; second segment with 1 plumose seta, lacking spine; third segment with small spine on outer corner and 6 plumose setae. Endopod 3-segmented; first segment with 1 plumose seta; second segment with 2 plumose setae; third segment with 4 plumose setae and 1 distal serrated spine (Fig. 7D). Leg III (Fig. 7D) with same ornamentation and armament described for leg 2.

Leg IV (Fig. 7E). Coxa ornamented with spinules on outer margin. Basis with outer seta, ornamented with multiple spinules on inner margin. Exopod 2-segmented; first segment with small outer spine; second segment with small spine on outer corner and 4 plumose setae. Endopod 3-segmented; first segment with 1 plumose seta; second segment with 2 plumose setae; third segment with 3 plumose setae and 1 distal serrated spine.

Leg V (Fig. 7F) with single ramus. Ramus 2-segmented: proximal segment rectangular, without any armaments or ornaments; distal segment about 2.5 times longer than previous segment, with spinules scattered across surface, bearing 2 setae (lateral and inner setae); lateral seta plumose.

Intercoxal sclerites of all legs, present (Figs 6A and 7B); each sclerite with both ends directed posteriorly. Interpodal plates of leg I to III ornamented with spinules; fourth plate absent (Fig. 7B).

Remarks

The detailed description of *E. chintensis* n. sp. highlights its unique characteristics among *Ergasilus* species worldwide, especially compared to marine congeners from these geographic regions. Notably, similar to *E. arenalbus* n. sp., its body size averaging 1035 µm sets it apart from both larger species like *E. felichthys* and *E. youngi*, ranging around 1400 µm, and also from species with smaller sizes below 1054 µm, such as *E. atafonensis*, *E. bahiensis*, *E. caraguatatubensis*, *E. ilani*, *E. myctarothes*, *E. parvitergum*, *E. rostralis* and *E. uniseriatus*. Similarities emerge due to their shared size range when comparing the 2 newly described South African species; however, subtle proportional variations in body segments and appendages are key to their differentiation upon closer examination. Additionally, *E. chintensis* n. sp. displays a more intricate armature on its antenna segments than *E. arenalbus* n. sp., where the second endopod segment in this species shows 2 developed spines rather than just 1 as present in *E. arenalbus* n. sp. The most striking feature of *E. chintensis* n. sp. is its body segmentation, characterized by a fused 2-segmented prosome. This completely contrasts with the free prosome somites observed not only in *E. arenalbus* n. sp. but also concerning all the other compared marine ergasilid species. *Ergasilus caraguatatubensis* also exhibits a fused prosome structure, although, to a lesser degree than *E. chintensis* n. sp. The antennule setae formula also contributes to this distinction, with *E. chintensis* n. sp. differing from *E. ilani*, *E. rostralis* and *E. uniseriatus* in antennule segmentation (6- *vs* 5-segmented). These distinguishing features collectively characterize *E. chintensis* n. sp. within the *Ergasilus* genus, highlighting body segmentation, appendage armature and ornamentation as key characteristics for species differentiation.

Molecular characterization and phylogenetic position of African marine Ergasilus *species*

The molecular analyses revealed distinct genetic profiles for the newly described *Ergasilus* species. This study successfully generated a total of 8 sequences. For *E. arenalbus* n. sp., 5 sequences were produced: 2 18S, 2 28S and 1 COI sequence. For *E. chintensis* n. sp., 3 sequences were obtained: 1 18S, 1 28S and 1 COI sequence. Nucleotide comparisons of the 2 new species against the partial 18S rDNA, 28S rDNA and COI mtDNA gene sequences of the genus *Ergasilus* were performed, as detailed in Tables 7–9, respectively. Both ML and BI analyses were conducted on the partial 18S rDNA, 28S rDNA and COI gene alignments, producing phylogenetic trees with congruent topologies. Thus,

Appendix B

Table 7. Nucleotide comparison of the partial 18S rDNA sequences of the genus *Ergasilus* Nordman, 1832, based on 1354 bp-long alignment.

Number of bases/residues which are not identical																			
	E. arenalbus	*E. chintensis*	*E. caparti*	*E. parvus*	*E. macrodactylus*	*E. megacheir*	*E. parasarsi*	*E. sieboldi*	*E. mirabilis*	*E. hypomesi*	*E. tumidus*	*E. briani*	*E. anchoratus*	*E. yaluzangbus*	*E. wilsoni*	*E. parasiluri*	*E. peregrinus*	*E. scalaris*	*P. nana*
E. arenalbus		0	14	14	14	15	15	15	15	19	23	23	25	26	26	27	31	33	99
E. chintensis	100		14	14	14	15	15	16	17	20	24	24	26	30	27	29	32	35	103
E. caparti	98.60	98.60		0	0	1	1	14	3	12	19	19	14	16	18	24	27	19	76
E. parvus	98.60	98.60	100		0	1	1	14	3	12	19	19	14	16	18	24	27	19	76
E. macrodactylus	98.60	98.60	100	100		1	1	14	3	12	19	19	14	16	18	24	27	19	76
E. megacheir	98.50	98.50	99.90	99.90	99.90		0	13	4	13	20	20	15	15	19	25	28	20	76
E. parasarsi	98.50	98.50	99.90	99.90	99.90	100		13	4	13	20	20	15	15	19	25	28	20	76
E. sieboldi	98.87	98.82	98.59	98.59	98.59	98.69	98.69		13	19	21	21	24	23	24	28	33	32	100
E. mirabilis	98.87	98.74	99.70	99.70	99.70	99.60	99.60	99.04		20	22	22	24	23	25	29	36	32	102
E. hypomesi	98.57	98.52	98.80	98.80	98.80	98.69	98.69	98.59	98.52		14	14	24	34	30	20	31	35	104
E. tumidus	98.27	98.23	98.09	98.09	98.09	97.99	97.99	98.45	98.37	98.96		4	31	36	30	20	36	41	106
E. briani	98.27	98.23	98.09	98.09	98.09	97.99	97.99	98.45	98.37	98.96	99.70		31	36	30	20	37	41	106
E. anchoratus	98.12	98.08	98.59	98.59	98.59	98.49	98.49	98.22	98.22	98.22	97.71	97.71		37	37	34	39	28	105
E. yaluzangbus	98.05	97.78	98.39	98.39	98.39	98.49	98.49	98.30	98.30	97.49	97.34	97.34	97.26		33	39	39	45	103
E. wilsoni	98.05	98.00	98.19	98.19	98.19	98.09	98.09	98.22	98.15	97.78	97.78	97.78	97.26	97.56		38	42	49	108
E. parasiluri	97.98	97.86	97.59	97.59	97.59	97.49	97.49	97.93	97.86	98.52	98.52	98.52	97.49	97.12	97.19		42	44	110
E. peregrinus	97.67	97.63	97.29	97.29	97.29	97.19	97.19	97.56	97.34	97.71	97.34	97.26	97.11	97.12	96.89	96.89		50	107
E. scalaris	97.52	97.41	98.09	98.09	98.09	97.99	97.99	97.63	97.63	97.41	96.97	96.97	97.93	96.67	96.37	96.75	96.3		116
P. nana	92.58	92.39	92.38	92.38	92.38	92.38	92.38	92.61	92.47	92.32	92.17	92.17	92.25	92.39	92.02	91.88	92.1	91.4	
Percentage of basis/residues which are identical																			

Table 8. Nucleotide comparison of the partial 28S rDNA sequences of genus *Ergasilus* Nordman, 1832, based on 682 bp-long alignment

Number of bases/residues which are not identical																			
	E. arenalbus	*E. chintensis*	*E. wilsoni*	*E. hypomesi*	*E. peregrinus*	*E. sieboldi*	*E. briani*	*E. tumidus*	*E. scalaris*	*E. parasiluri*	*E. caparti*	*E. megacheir*	*E. macrodactylus*	*E. anchoratus*	*E. parvus*	*E. mirabiis*	*E. parasarsi*	*E. yaluzangbus*	*P. nana*
E. arenalbus		6	37	37	38	48	50	54	55	55	61	62	63	66	68	69	70	71	176
E. chintensis	99.10		36	38	40	46	47	50	54	54	61	62	63	66	68	65	72	72	176
E. wilsoni	94.46	94.61		38	40	42	37	40	42	44	66	66	67	66	70	69	73	70	171
E. hypomesi	94.47	94.32	94.32		40	36	32	35	34	32	55	62	59	67	63	61	60	64	169
E. peregrinus	94.31	94.01	94.01	94.02		44	42	45	46	44	56	57	56	66	59	60	64	64	168
E. sieboldi	92.55	92.86	93.48	94.41	93.17		40	41	43	43	65	72	70	72	74	62	75	66	168
E. briani	92.53	92.97	94.47	95.22	93.72	93.8		19	22	18	65	67	64	77	68	64	69	75	169
E. tumidus	91.93	92.53	94.02	94.78	93.27	93.64	97.16		29	25	67	70	66	80	70	65	72	72	168
E. scalaris	91.77	91.92	93.71	94.92	93.11	93.32	96.71	95.67		8	71	74	71	79	73	76	72	70	173
E. parasiluri	91.77	91.92	93.41	95.22	93.41	93.32	97.31	96.26	98.80		70	73	70	80	70	70	69	72	167
E. caparti	90.67	90.67	89.91	91.59	91.44	89.83	90.08	89.77	89.14	89.30		14	13	78	17	32	18	73	180
E. megacheir	90.52	90.52	89.91	90.52	91.28	88.73	89.77	89.31	88.69	88.84	97.86		9	81	13	41	19	73	180
E. macrodactylus	90.37	90.37	89.76	90.98	91.44	89.05	90.23	89.92	89.14	89.30	98.01	98.62		81	6	43	15	71	177
E. anchoratus	90.13	90.13	90.13	90.00	90.13	88.82	88.51	88.06	88.19	88.04	88.07	87.61	87.61		85	84	85	95	180
E. parvus	89.60	89.60	89.30	90.37	90.98	88.42	89.62	89.31	88.84	89.30	97.40	98.01	99.08	87.00		45	15	74	180
E. mirabilis	89.69	90.28	89.69	90.88	91.03	90.37	90.45	90.30	88.64	89.54	95.10	93.72	93.42	87.44	93.11		44	81	176
E. parasarsi	89.30	88.99	88.84	90.83	90.21	88.26	89.47	89.01	88.99	89.45	97.24	97.09	97.70	87.00	97.70	93.26		70	177
E. yaluzangbus	89.47	89.32	89.61	90.50	90.50	89.81	88.89	89.33	89.61	89.32	88.91	88.91	89.21	85.93	88.75	87.96	89.36		174
P. nana	74.00	74.00	74.74	75.07	75.18	74.27	75.07	75.22	74.45	75.33	72.85	72.85	73.30	73.45	72.85	74.04	73.30	74.37	
Percentage of basis/ residues which are identical																			

Table 9. Nucleotide comparison of the mtDNA COI gene sequences of genus *Ergasilus* Nordman, 1832, based on 700 bp-long alignment.

Number of bases/residues which are not identical							
	E. arenalbus	*E. chintensis*	*E. wilsoni*	*E. auritus*	*E. lizae*	*E. mirabilis*	*P. nana*
E. arenalbus		43	111	119	128	139	177
E. chintensis	93.78		114	123	134	137	179
E. wilsoni	80.93	80.41		111	114	122	146
E. auritus	81.91	81.31	80.93		133	141	177
E. lizae	80.55	79.64	80.41	79.79		130	181
E. mirabilis	79.94	80.17	79.04	78.57	80.24		184
P. nana	74.46	74.36	74.91	73.10	72.49	73.45	
Percentage of basis/residues which are identical							

only the ML tree of the 28S and COI gene regions are presented (Figs 8 and 9, respectively).

The 18S phylogenetic analyses yielded a final alignment consisting of 1354 bases. The 18S sequences exhibited no interspecific variability (0 bp difference) since no differences were found among the 18S rDNA sequences of *E. arenalbus* n. sp. and *E. chintensis* n. sp. (Table 7). The analysis revealed *E. scalaris* Markevich, 1940, as the most genetically distant species from *E. arenalbus* n. sp. (33 bp/2.48%) and *E. chintensis* n. sp. (35 bp/2.59%) (Table 7). The lowest interspecific differences (1.13–1.18%) were observed between the new species and *E. sieboldi* von Nordmann, 1832 (Table 7).

The 28S phylogenetic analysis produced a final alignment of 682 bases. These 28S sequences displayed minor interspecific variability (6 bp) among the 28S rDNA sequences of *E. arenalbus* n. sp. and *E. chintensis* n. sp. (Table 8). The analysis showed *E. parasarsi* Míč *et al.*, 2023, and *E. yaluzangbus* Kuang and Qian, 1985, as the most genetically distant species from *E. arenalbus* n. sp. (71 bp/10.70%) and *E. chintensis* n. sp. (72 bp/10.68%), respectively (Table 8). The smallest interspecific differences (5.39–5.60%) were noted between the new species and *E. wilsoni* Markevich, 1933 (Table 8). ML and BI analyses using rDNA alignment that included partial 28S sequences of Ergasilidae produced trees with consistent topologies and similar nodal support values.

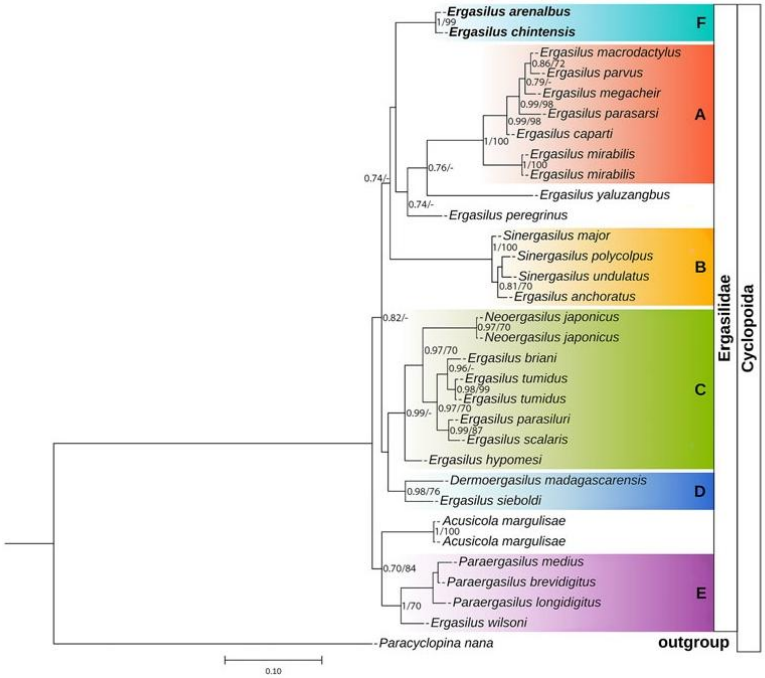

Figure 8. Phylogenetic tree of Ergasilidae copepods based on partial 28S rRNA gene alignments. Newly generated sequences for *Ergasilus arenalbus* n. sp. and *Ergasilus chintensis* n. sp. are provided in bold. Nodal support presented above or below branches for Bayesian Inference (>0.7) and Maximum Likelihood (>70%) analyses (BI/ML). Dashes indicate values below 0.7 and 70%, respectively. *Paracyclopina nana* Smirnov, 1935, was used as the outgroup.

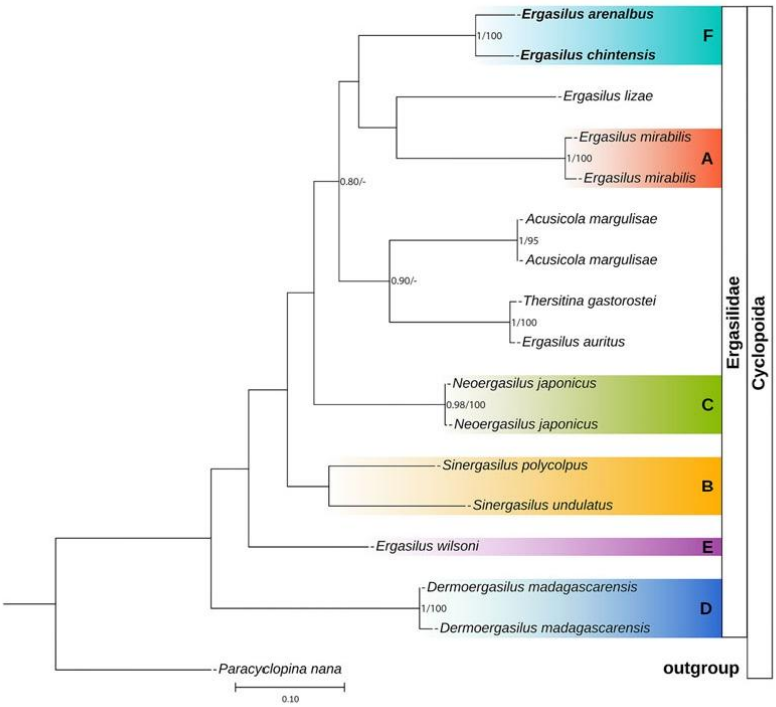

Figure 9. Phylogenetic tree of Ergasilidae copepods based on partial COI mtDNA gene alignments. Newly generated sequences for *Ergasilus arenalbus* n. sp. and *Ergasilus chintensis* n. sp. are provided in bold. Nodal support presented above or below branches for Bayesian Inference (>0.7) and Maximum Likelihood (>70%) analyses (BI/ML). Dashes indicate values below 0.7 and 70%, respectively. *Paracyclopina nana* Smirnov, 1935, was used as the outgroup.

Consistent with previous phylogenetic studies on ergasilids (Song *et al*., 2008; Santacruz *et al*., 2020; Fikiye *et al*., 2023; Míč *et al*., 2023, 2024), the analyses identified 5 well-supported polyphyletic *Ergasilus* groups (Fig. 8): (A) the African freshwater *Ergasilus* species, (B) the *Sinergasilus* Yin, 1949, species and the *E. anchoratus* Markevich, 1946, group, (C) the Asian *Ergasilus* species and the *Neoergasilus japonicus* (Harada, 1930) group, (D) the recently described *Dermoergasilus madagascarensis* Míč *et al.* , 2024, and *E. sieboldi* group and (E) the *Paraergasilus* Markevich, 1937, species and the *E. wilsoni* group (Fig. 8). Despite forming a distinct subclade (F), the newly described species still clustered within the larger clade that includes subclade (A) comprising African freshwater species, along with non-African species like *E. yaluzangbus* and *E. peregrinus* Heller, 1865 (Fig. 8).

COI sequences were aligned using invertebrate mitochondrial translation, resulting in an alignment length of 700 bases. The sequences included GenBank and BOLD sequences submitted from Canada (Table 4). These results displayed substantial interspecific variability (43 bp) among the COI sequences of *E. arenalbus* n. sp. and *E. chintensis* n. sp. and more than 110 bases from all other *Ergasilus* congeners (Table 9). The analysis showed *E. mirabilis* Oldewage and van As, 1987, and *E. lizae* as the most genetically distant species from *E. arenalbus* n. sp. (139 bp/20.06%) and *E. chintensis* n. sp. (134 bp/20.36%), respectively (Table 9). The smallest interspecific differences (19.07–19.59%) were noted between the new species and *E. wilsoni* (Table 9). Similar to the 28S tree topology, the novel sequences of *E. arenalbus* n. sp. and *E. chintensis* n. sp. formed the same subclade (F), within the larger clade that includes subclade (A) comprising African freshwater species, *E. mirabilis*, and the morphologically similar marine species *E. lizae*, which is also found within the Indian Ocean (Fig. 9).

Based on these analyses, this study proposes the existence of a sixth clade (F) consisting of African marine *Ergasilus* species (Figs 8 and 9). However, this proposition remains speculative as their precise phylogenetic placement within Ergasilidae remains unresolved due to low support values and limited molecular data, concerning marine ergasilids.

Discussion

The discovery of 2 new *Ergasilus* species, *E. arenalbus* n. sp. and *E. chintensis* n. sp., from the Evileye blaasop, *A. honckenii*, significantly enhances our understanding of marine parasite diversity in South Africa. These findings highlight the underexplored nature of marine parasites in this region, particularly within the genus *Ergasilus*, known for its rich diversity in global freshwater and marine environments (Boxshall and Defaye, 2008; Fikiye *et al*., 2023; Míč *et al*., 2023). To date, only a limited number of *Ergasilus* species have been reported from African marine environments, with only 5 documented, including just 1 from South Africa (Fikiye *et al*., 2023; WoRMS, 2024). Moreover, despite *Ergasilus* being found in a wide range of fish host families (see Table 1), only a single species, *E. colomesus* Thatcher and Boeger, 1983, has been described from the family Tetraodontidae Bonaparte, 1832 (Thatcher and Boeger, 1983) in the Amazon River, Brazil.

The addition of *E. arenalbus* n. sp. and *E. chintensis* n. sp. not only introduces new host records but also suggests a higher hidden diversity of *Ergasilus* within South Africa's coastal region and the Tetraodontidae family. This hints at a potentially broader copepod diversity and novel host–parasite relationships yet to be explored, aligning with global trends revealing extensive species diversity in under-studied marine ecosystems (Boxshall and Defaye, 2008). The presence of these new species along the South African coastline highlights the region's rich marine biodiversity and emphasizes the importance of investigating lesser-known areas and hosts for hidden parasite diversity.

Taxonomically, detailed morphological examinations of these species, focusing on size, body segmentation, appendage armature and ornamentation, provide crucial insights into their distinctiveness from known congeners. Integrating traditional morphological taxonomy with molecular techniques has been instrumental in characterizing these new *Ergasilus* species. Molecular analyses alongside morphological assessments confirm the uniqueness of these species with greater accuracy (Míč *et al.*, 2024; Walter and Boxshall, 2024). This integration is valuable as morphological characters alone often yield conflicting results in distinguishing new species and understanding their placement within Ergasilidae lineages (Míč *et al.*, 2024; Walter and Boxshall, 2024).

The nomenclatural history of ergasilids emphasizes the significant challenge of formulating generic diagnoses that effectively distinguish species. This complexity is evidenced by the synonymization of 33 *Ergasilus* species either with other previously described *Ergasilus* species or with species from different genera within the Ergasilidae family (Walter and Boxshall, 2024). Moreover, genera such as *Acusicola* Cressey, in Cressey and Collette, 1970, *Dermoergasilus* Ho and Do, 1982, *Neoergasilus* Yin, 1956, *Paraergasilus* and *Sinergasilus*, have consistently been confirmed as monophyletic (Song *et al.*, 2008; Santacruz *et al.*, 2020; Kvach *et al.*, 2021; Míč *et al.*, 2023, 2024). However, these genera render *Ergasilus* polyphyletic, with certain species, like *E. anchoratus*, *E. sieboldi* and *E. wilsoni*, showing closer relationships to *Sinergasilus*, *Dermoergasilus* and *Paraergasilus*, respectively (Figs 8 and 9).

Phylogenetics pose significant challenges that hinder comprehensive genomic analyses of *Ergasilus* species, creating obstacles in gaining deeper insights into their biology. The limited knowledge regarding their diversity and the lack of genetic data, compared to those of other well-studied organisms, are major contributing factors. Previous studies (Song *et al.*, 2008; Santacruz *et al.*, 2020; Kvach *et al.*, 2021; Míč *et al.*, 2023, 2024) have attempted to overcome these challenges through molecular characterization using rRNA genes, particularly the 18S and 28S rDNA regions. However, the effectiveness of these markers in species-level differentiation has been variable (Míč *et al.*, 2023, 2024). The 18S rDNA region of the present study has shown minimal or even zero variation (0–2.59%) in some cases, making it unsuitable for distinguishing between closely related species. This is consistent with findings from earlier studies, which reported that the 18S rRNA gene is highly conserved and not suitable for identification at lower taxonomic levels (Taniguchi *et al.*, 2004; Huys *et al.*, 2006; Tang *et al.*, 2012; Marrone *et al.*, 2013). This lack of variation reinforces the limitations of the 18S rDNA marker for species-level differentiation within this genus.

In contrast, the 28S rDNA analyses have proven more effective in distinguishing between species (Song *et al.*, 2008; Santacruz *et al.*, 2020; Kvach *et al.*, 2021; Míč *et al.*, 2023, 2024). The present study supports these findings to an extent, revealing higher, albeit minor interspecific divergence (6 bp between *E. arenalbus* n. sp. and *E. chintensis* n. sp.). The analysis also identified other *Ergasilus* species as genetically distant from the newly described taxa, highlighting the potential of 28S rDNA in elucidating phylogenetic relationships within the family Ergasilidae. However, despite its relative effectiveness, the genetic variation observed in the 28S rDNA is still limited, with little variation (0.90–10.70%), compared to other markers, raising questions about its adequacy for reliable species identification.

The COI gene, a widely used barcode for species-level differentiation (Tang *et al.*, 2012; Baek *et al.*, 2016; Mayor *et al.*, 2017; Míč *et al.*, 2023, 2024), demonstrated high resolution at the species level for the *Ergasilus* species described in this study and indicated significant interspecific variability. The COI analyses revealed substantial differences (43 bp) among the COI sequences of *E. arenalbus* n. sp. and *E. chintensis* n. sp., as well as notable variation from other *Ergasilus* congeners. This suggests that the COI gene may be a more suitable marker for species-level differentiation in this group. However, it is important to note that the limited availability of only 4 other *Ergasilus* COI sequences (see Fig. 9 and Table 9) means that drawing definitive conclusions from these results is premature. While COI shows promise for more precise species identification, further research is needed to expand the dataset and validate its effectiveness across a broader range of *Ergasilus* species. Moving forward, prioritizing the COI gene in future studies may provide a clearer understanding of the diversity and evolutionary relationships within the family Ergasilidae.

The phylogenetic relationships of ergasilid copepods remain largely unclear, with only 11% (31 out of 277) of the known species with any molecular data available (Míč *et al.*, 2023, 2024; Walter and Boxshall, 2024). Limited studies have examined the genetic characteristics of African *Ergasilus* species (Fikiye *et al.*, 2023, Míč *et al.*, 2023), and no genetic studies exist for the characterization of marine species. Notably, the present study provides the first marine sequences for this genus. The only available brackish sequences are for *Ergasilus wilsoni* and *Ergasilus sieboldi* (Walter and Boxshall, 2024), both of which are primarily associated with freshwater environments rather than being strictly marine or brackish. *Ergasilus wilsoni* and *E. sieboldi* can inhabit fresh or brackish waters, while recognized as typical freshwater species found in the Palearctic region, particularly in rivers and lakes (Kvach *et al.*, 2021), distinguishing them from the newly discovered *Ergasilus* species, as close relationships among ergasilids may be influenced by the geographical origin of the species or the endemism of their hosts (Míč *et al.*, 2023). This means that parasite distribution is closely linked to the geographic distribution of their hosts (Morand and Guégan, 2000), suggesting potential coevolution between parasites and hosts. The discovery of 2 genetically similar species from the same host species suggests that the 2 newly identified *Ergasilus* species associated with pufferfish along the South African coast reflect coevolutionary patterns and host-specific endemism. These findings are consistent with conclusions drawn from previous phylogenetic studies (Song *et al.*, 2008; Santacruz *et al.*, 2020; Kvach *et al.*, 2021; Oliveira *et al.*, 2021). Therefore, the geographic separation between *E. sieboldi* and *E. wilsoni* from the newly discovered species further highlights the critical need for more comprehensive genetic data on marine *Ergasilus* species to enhance our understanding of their diversity, evolutionary relationships and distribution patterns.

Conclusion

The discovery and descriptions of *E. arenalbus* n. sp. and *E. chintensis* n. sp. in association with the Evileye blaasop represent a significant advance in our understanding of marine parasite diversity in South Africa. These results highlight the rich marine ecosystems of the region and emphasize the importance of investigating

under-explored areas to uncover the hidden biodiversity. Furthermore, the new *Ergasilus* sequences and phylogenetic analyses presented in this study provide the first insight into the phylogenetic relationships of marine *Ergasilus* species within the South Atlantic and Indian Ocean regions. Alongside the studies by Míč *et al.* (2023, 2024) and Fikiye *et al.* (2023), this research also offers a further understanding of the African clade lineage, making the molecular data presented here the first to elucidate the phylogenetic relationships of this genus in African and marine systems. Our phylogenetic analysis suggests that African marine ergasilids form a distinct monophyletic lineage separate from freshwater species, proposing the recognition of a sixth clade (F) for African marine *Ergasilus* species (Figs 8 and 9). Nonetheless, due to low support values and the scarcity of molecular data for marine ergasilids, their exact phylogenetic placement within the family Ergasilidae remains unresolved. Further studies that integrate both morphological and molecular data are essential to elucidate these relationships.

Data available statement. Sequence data are available on the NCBIGenBank database. All other necessary data are included in the article.

Acknowledgements. We would like to thank the Unit for Environmental Sciences and Management, North-West University (NWU) for the use of field equipment and laboratory facilities. We thank Anja Erasmus from NWU-WRG, for the creation of the study area map. Additional thanks go to our colleagues Francois Retief, Reese Alberts, Anja Erasmus, Marliese Truter, Anja Vermaak and Coret van Wyk, from the NWU who assisted with the collection of samples. This is contribution No. 920 from the NWU-Water Research Group.

Author contributions. L. van der Spuy: methodology, investigation, funding acquisition, writing – original draft. R. B. Narciso: methodology, investigation, drawing, writing – review and editing. K. A. Hadfield: methodology, funding acquisition, writing – review and editing. V. Wepener: conceptualization, data curation, funding acquisition, writing – review and editing. N. J. Smit: conceptualization, data curation, funding acquisition, writing – review and editing.

Financial support. This work is based on the research supported by the National Research Foundation (NRF) of South Africa (grant 132805; L. van der Spuy; grant 150623; N. J. Smit). Opinions, findings, conclusions and recommendations expressed in this publication are those of the authors, and the NRF accept no liability whatsoever in this regard. The authors acknowledge The Nippon Foundation-Nekton Ocean Census Programme (https://oceancensus.org/) for supporting the description of these species. These are Ocean Census Species Numbers 49–50.

Competing interests. The authors declare that they have no known competing financial interests or personal relationships that could have appeared to influence the work reported in this paper.

References

Amado MAPM and Rocha CEF (1996) Three new species of parasitic copepods of the genus *Ergasilus* (Poecilostomatoida, Ergasilidae) collected from the branchial filaments of the mugilid fishes in Brazil. *Nauplius, Rio Grande* **3**, 33–48.

Baek SY, Jang KH, Choi EH, Ryu SH, Kim SK, Lee JH, Lim YJ, Lee J, Jun J, Kwak M, Lee YS, Hwang JS, Maran BAV, Chang CY, Kim IH and Hwang UW (2016) DNA barcoding of metazoan zooplankton copepods from South Korea. *PLoS ONE* **11**, e157307. doi: 10.1371/journal.pone.0157307.

Barcode of Life Database, BOLD SYSTEMS. Available at http://www.boldsystems.org/index.php/TaxBrowser_TaxonPage?taxid=598126 (accessed 7 June 2023).

Beneden E (1870) Recherches sur la composition et la signification de l'oeuf, basées sur l'étude de son mode de formation et des premiers phénomènes embryonnaires (Mammifères, Oiseaux, Crustacés, Vers). *Mémoires Couronnes et Mémoires des Savants Étrangers de l'Académie Royale des Sciences de Belgique* **34**, 1–283.

Bianchini G and Sánchez-Baracaldo P (2024) Treeviewer: flexible, modular software to visualise and manipulate phylogenetic trees. *Ecology and Evolution* **14**, e10873. doi: 10.1002/ece3.10873.

Boxshall GA and Defaye D (2008) Global diversity of copepods (Crustacea: Copepoda) in freshwater. *Hydrobiologia* **595**, 195–207. doi: 10.1007/s10750-007-9014-4.

Boxshall GA and Halsey SH (2004) *An Introduction to Copepod Diversity*. London: The Ray Society.

Boxshall GA and Montú MA (1997) Copepods parasitic on Brazilian coastal fishes: a handbook. *Nauplius* **5**, 1–225.

Boxshall GA, Araujo HMP and Montu M (2002) A new species of *Ergasilus* Nordmann, 1832 (Copepoda, Ergasilidae) from Brazil. *Crustaceana Leiden* **75**, 269–276.

Byrnes TB (1986) Some ergasilids (Copepoda) parasitic on four species of Australian bream, *Acanthopagrus* spp. *Australian Journal of Marine and Freshwater Research* **37**, 81–93. doi: 10.1071/MF9860081.

Carvalho J (1955) *Ergasilus xenomelanirisi* n. sp. parasito de Peixe-Rei: *Xenomelaniris brasiliensis* (Quoy & Gaimard) (Copepoda - Cyclopoida - Pisces - Mugiloidei). *Boletim do Instituto Oceanográfico* **6**, 215–226.

Carvalho J (1962) *Ergasilus* cyanopictus sp. nov, parasito da Tainha – *Mugil cephalus* (L.). *Archivos do Museu Nacional do Rio de Janeiro* **52**, 31–36.

Darriba D, Taboada GL, Doallo R and Posada D (2012) Jmodeltest 2: more models, new heuristics and parallel computing. *Nature Methods* **9**, 772. doi: 10.1038/nmeth.2109.

Dos Santos QM, Avenant-Oldewage A, Piasecki W, Molnar K, Sellyei B and Szekely C (2021) An alien parasite affects local fauna: confirmation of *Sinergasilus major* (Copepoda: Ergasilidae) switching hosts and infecting native *Silurus glanis* (Actinopterygii: Siluridae) in Hungary. *International Journal for Parasitology: Parasites and Wildlife* **15**, 127–131. doi: 10.1016/j.ijppaw.2021.04.011.

El-Rashidy HH and Boxshall GA (2002) New species and new records of *Ergasilus* Nordmann (Copepoda: Ergasilidae) from the gills of grey mullet (Mugilidae). *Systematic Parasitology* **51**, 37–58.

Everett B, Groeneveld J, Fennessy S, Porter S, Munga C, Dias N, Filipe O, Zacarias L, Igulu M, Kuguru B, Kimani E, Rabarison G and Razafindrakoto H (2015) Demersal trawl surveys show ecological gradients in Southwest Indian Ocean slope fauna. *Western Indian Ocean Journal of Marine Science* **14**, 73–92.

Fikiye PP, Smit NJ, Van As LL, Truter M and Hadfield KA (2023) Integrative morphological and genetic characterisation of the fish parasitic copepod *Ergasilus mirabilis* Oldewage & van As, 1987: insights into host specificity and distribution in Southern Africa. *Diversity* **15**, 965. doi: 10.3390/d15090965.

Folmer O, Black M, Hoeh W, Lutz R and Vrijenhoek R (1994) DNA primers for amplification of mitochondrial cytochrome c oxidase subunit I from diverse metazoan invertebrates. *Molecular Marine Biology and Biotechnology* **3**, 294–299, PMID: 7881515.

Fricke R, Eschmeyer WN and Van der Laan R (eds) (2024) Eschmeyer's catalog of fishes: genera, species, references. Available at http://researcharchive.calacademy.org/research/ichthyology/catalog/fishcatmain.asp (accessed 20 July 2024).

Froese R and Pauly D (eds) (2024) FishBase. World Wide Web electronic publication. Available at www.fishbase.org (accessed 20 July 2024).

Guindon S, Dufayard JF, Lefort V, Anisimova M, Hordijk W and Gascuel O (2010) New algorithms and methods to estimate maximum-likelihood phylogenies: assessing the performance of PhyML 3.0. *Systematic Biology* **59**, 307–321. doi: 10.1093/sysbio/syq010.

Ho JS, Jayarajan P and Radhakrishnan S (1992) Copepods of the family Ergasilidae (Poecilostomatoida) parasitic on coastal fishes of Kerala, India. *Journal of Natural History* **26**, 1227–1241. doi: 10.1080/00222939200770691.

Hua CJ, Su MY, Sun ZW, Lu YH and Feng JM (2021) Complete mitochondrial genome of the copepod *Sinergasilus undulatus* (Copepoda: Poecilostomatoida). *Mitochondrial DNA B Resources* **6**, 1226–1228. doi: 10.1080/23802359.2020.1870890.

Huys R, Llewellyn-Hughes J, Olson PD and Nagasawa K (2006) Small subunit rDNA and Bayesian inference reveal *Pectenophilus ornatus* (Copepoda incertae sedis) as highly transformed Mytilicolidae, and support assignment of Chondracanthidae and Xarifiidae to Lichomolgoidea (Cyclopoida). *Biological Journal of the Linnean Society* **87**, 403–425. doi: 10.1111/j.1095-8312.2005.00579.

Jafri SIH (1995) A new copepod parasite, *Ergasilus pakistanicus*, new species (Poecilostomatoida: Ergasilidae) from a freshwater fish in Sindh, Pakistan. *Pakistan Journal of Zoology* **27**, 153–156.

Appendix B

Johnson SK and Rogers WA (1972) *Ergasilus clupeidarum* sp. n. (Copepoda: Cyclopoida) from clupeid fishes of the southeastern U.S. with a synopsis of the North American *Ergasilus* species with a two-jointed first endopod. *Journal of Parasitology* **58**, 385–392.

Kabata Z (1992) Copepoda parasitic on Australian fishes, XV. Family Ergasilidae (Poecilostomatoida). *Journal of Natural History* **26**, 47–66.

Katoh K and Standley M (2013) MAFFT multiple sequence alignment software version 7: improvements in performance and usability. *Molecular Biology and Evolution* **30**, 772–780. doi: 10.1093/molbev/mst010.

Katoh K, Misawa K, Kuma KI and Miyata T (2002) MAFFT: a novel method for rapid multiple sequence alignment based on fast Fourier transform. *Nucleic Acids Research* **30**, 3059–3066. doi: 10.1093/nar/gkf436.

Ki J-S, Park HG and Lee J-S (2009) The complete mitochondrial genome of the cyclopoid copepod *Paracyclopina nana*: a highly divergent genome with novel gene order and atypical gene numbers. *Gene* **435**, 13–22. doi: 10.1016/j.gene.2009.01.005.

Ki JSH, Park G and Lee JS (2011) Extensive analysis of nuclear cistron rDNA sequence of *Paracyclopina nana* (Cyclopoida: Cyclopettidae). *Hydrobiologia* **666**, 3–9. doi: 10.1007/s10750-010-0563-6.

Killian E and Avenant-Oldewage A (2013) Infestation and pathological alterations by *Ergasilus sarsi* (Copepoda) on the Tanganyika killifish from Africa. *Journal of Aquatic Animal Health* **25**, 237–242. doi: 10.1080/08997659.2013.812874.

Kvach Y, Tkachenko MY, Seifertová M and Ondračková M (2021) Insights into the diversity, distribution and phylogeny of three ergasilid copepods (Hexanauplia: Ergasilidae) in lentic water bodies of the Morava River basin, Czech Republic. *Limnologica* **91**, 125922. doi: 10.1016/j.limno.2021.125922.

Marrone F, Lo Brutto S, Hundsdoerfer AK and Arculeo M (2013) Overlooked cryptic endemism in copepods: systematics and natural history of the calanoid subgenus *Occidodiaptomus* Borutzky 1991 (Copepoda, Calanoida. Diaptomidae). *Molecular Phylogenetics and Evolution* **66**, 190–202. doi: 10.1016/j.ympev.2012.09.016.

Mayor TY, Galimova YA, Sheveleva NG, Sukhanova LV and Kirilchik SV (2017) Molecular phylogenetic analysis of *Diacyclops* and *Acanthocyclops* (Copepoda: Cyclopoida) from Lake Baikal based on COI gene. *Russian Journal of Genetics* **53**, 252–258. doi: 10.1134/S1022795417020041.

Míč R, Řehulková E and Seifertová M (2023) Species of *Ergasilus* von Nordmann, 1832 (Copepoda: Ergasilidae) from cichlid fishes in Lake Tanganyika. *Parasitology* **150**, 579–598. doi: 10.1017/S0031182023000239.

Míč R, Řehulková E, Šimková A, Razanabolana JR and Seifertová M (2024) New species of *Dermoergasilus* Ho & Do, 1982 (Copepoda: Cyclopoida: Ergasilidae) parasitizing endemic cichlid *Paretroplus polyactis* (Bleeker) in Madagascar. *Parasitology* **151**, 319–336. doi: 10.1017/S0031182024000088.

Miller M, Pfeiffer WT and Schwartz T (2010) Creating the CIPRES science gateway for inference of large phylogenetic trees. *Proceedings of the Gateway Computing Environments Workshop* **14**, 1–8. doi: 10.1109/GCE.2010.5676129.

Miller EC, Hayashi KT, Song D and Wiens JJ (2018) Explaining the ocean's richest biodiversity hotspot and global patterns of fish diversity. *Proceedings of the Royal Society B: Biological Sciences* **285**, 20181314. doi: 10.1098/rspb.2018.1314.

Morand S and Guégan J-F (2000) Patterns of endemism in host-parasite associations: lessons from epidemiological models and comparative tests. *Belgian Journal of Entomology* **2**, 135–147.

Oldewage WH and Avenant-Oldewage A (1993) Checklist of the parasitic Copepoda (Crustacea) of African fishes. *Koninklijk Museum voor Midden-Afrika – Zoology Documents* **23**, 2–28.

Oldewage WH and van As JG (1988) A key for the identification of African piscine parasitic Ergasilidae (Copepoda:Poecilostomatoida). *South African Journal of Zoology* **23**, 42–46. doi: 10.1080/02541858.1988.11448075.

Oliveira MSB, Corrêa LL, Adriano EA and Tavares-Dias M (2021) Integrative taxonomy of a new species of *Therodamas* (Ergasilidae) infecting the Amazonian freshwater fish *Leporinus fasciatus* (Anostomidae). *Parasitology Research* **120**, 3137–3147. doi: 10.1007/s00436-021-07256-y.

Ondračková M, Fojtu J, Seifertová M, Kvach Y and Jurajda P (2019) Non-native parasitic copepod *Neoergasilus japonicus* (Harada, 1930) utilizes non-native fish host *Lepomis gibbosus* (L.) in the floodplain of the river Dyje (Danube basin). *Parasitology Research* **118**, 57–62. doi: 10.1007/s00436-018-6114-1.

Pearse AS (1947) Parasitic copepods from Beaufort, North Carolina. *Journal of the Elisha Mitchell Scientific Society* **63**, 1–16.

Posada D (2008) Jmodeltest: phylogenetic model averaging. *Molecular Biology and Evolution* **25**, 1253–1256. doi: 10.1093/molbev/msn083.

Redkar MV, Rangnekar PG and Murti NN (1952) *Ergasilus polynemi* sp. nov. (Copepoda) parasitic on the fish *Polynemus tetradactylus* Shaw. *Journal of the Zoological Society of India* **3**, 223–227.

Ronquist F, Teslenko M, van der Mark P, Ayres DL, Darling A, Höhna S, Larget B, Liu L, Suchard MA and Huelsenbeck JP (2012) Mrbayes 3.2: efficient Bayesian phylogenetic inference and model choice across a large model space. *Systematic Biology* **61**, 539–542. doi: 10.1093/sysbio/sys029.

Santacruz A, Morales-Serna FN, Leal-Cardín M, Barluenga M and Pérez-Ponce de León G (2020) *Acusicola margulisae* n. sp. (Copepoda: Ergasilidae) from freshwater fishes in a Nicaraguan crater lake based on morphological and molecular evidence. *Systematic Parasitology* **97**, 165–177. doi: 10.1007/s11230-020-09906-8.

Smith MM and Heemstra PC (2012) *Smith's Sea Fishes.* Heidelburg, Germany: Springer Science & Business Media, 1191 pp.

Song Y, Wang GT, Yao WJ, Gao Q and Nie P (2008) Phylogeny of freshwater parasitic copepods in the Ergasilidae (Copepoda: Poecilostomatoida) based on 18S and 28S rDNA sequences. *Parasitology Research* **102**, 299–306. doi: 10.1007/s00436-007-0764-8.

Tang CQ, Leasi F, Obertegger U, Kieneke A, Barraclough TG and Fontaneto D (2012) The widely used small subunit 18S rDNA molecule greatly underestimates true diversity in biodiversity surveys of the meiofauna. *Proceedings of the National Academy of Sciences* **109**, 16208–16212. doi: 10.1073/pnas.1209160109.

Taniguchi M, Kanehisa T, Sawabe T, Christen R and Ikeda T (2004) Molecular phylogeny of *Neocalanus* copepods in the subarctic Pacific Ocean, with notes on non-geographical genetic variations for *Neocalanus cristatus*. *Journal of Plankton Research* **26**, 1249–1255. doi: 10.1093/plankt/fbh115.

Tavares LER and Luque JL (2005) *Ergasilus youngi* sp. nov. (Copepoda: Poecilostomatoida: Ergasilidae) parasitic on *Aspistor luniscutis* (Actinopterygii: Ariidae) from off the State of Rio de Janeiro, Brazil. *Acta Parasitologica* **50**, 150–155.

Thatcher VE and Boeger WA (1983) The parasitic crustaceans of fishes from the Brazilian Amazon. 4. *Ergasilus colomesus* n. sp. (Copepoda: Cyclopoida) from an ornamental fish, *Colomesus asellus* (Tetraodontidae) and aspects of its pathogenicity. *Transactions of the American Microscopical Society* **102**, 371–379.

Thomas S (1993) A new species of the genus *Ergasilus* Nordmann, 1832 (Copepoda: Poecilostomatoida) from Kerala. *Journal of the Bombay Natural History Society* **90**, 451–454.

Thomsen R (1949) Copépodos parásitos de los peces marinos del Uruguay. *Comunicaciones Zoologicas del Museo de Historia Natural de Montevideo* **3**, 1–41.

Vasquez AA, Bonnici BL, Kashian, R, Trejo-Martinez J, Miller CJ and Ram JL (2023) The biodiversity of freshwater crustaceans revealed by taxonomy and mitochondrial DNA barcodes; Physiology Faculty Research Publications: Wayne State University: Detroit, MI, USA, 2021; Volume 3, Available at https://digitalcommons.wayne.edu/physio_frp/3 (accessed 1 April 2023).

Walter TC and Boxshall G (2024) World of copepods database. *Ergasilus* Nordmann, 1832. Accessed through: World Register of Marine Species. Available at https://www.marinespecies.org/aphia.php?p=taxdetails&id=128641 (accessed 15 May 2024).

Wilson CB (1913) Crustacean parasites of West Indian fishes and land crabs, with description of new genera and species. *Proceedings of the United States National Museum* **44**, 189–277.

WoRMS Editorial Board (2024) World Register of Marine Species. Available at https://www.marinespecies.org at VLIZ. doi: 10.14284/170 (accessed 15 May 2024).

Appendix C:

Regional Studies in Marine Science 89 (2025) 104368

Contents lists available at ScienceDirect

Regional Studies in Marine Science

journal homepage: www.elsevier.com/locate/rsma

Persistent organic pollutants in South African coastal ecosystems: Analysing the evileye blaasop *Amblyrhynchote honckenii* (Bloch, 1785) for PCB and OCP accumulation

L. de Klerk [a,1], N.J. Smit [a,*,2], Y.B. Yohannes [b,3], Y. Ikenaka [a,b,c,d,4], C. Nimako [b,c,5], S.M.M. Nakayama [b,6], M. Ishizuka [b,7], V. Wepener [a,8]

[a] Water Research Group, Unit for Environmental Sciences and Management, North-West University, 11 Hoffman Street, Potchefstroom 2520, South Africa
[b] Laboratory of Toxicology, Department of Environmental Veterinary Sciences, Graduate School of Veterinary Medicine, Hokkaido University, Kita 18, Nishi 9, Kita-ku, Sapporo 060-0818, Japan
[c] One Health Research Center, Hokkaido University, Kita 18, Nishi 9, Kita-ku, Sapporo 060-0818, Japan
[d] Translational Research Unit, Veterinary Teaching Hospital, Faculty of Veterinary Medicine, Hokkaido University, Kita 18, Nishi 9, Kita-ku, Sapporo 060-0818, Japan

ARTICLE INFO

Keywords:
Pollution monitoring
Polychlorinated biphenyls
Organochlorine pesticides
Marine Protected Areas
Life below water

ABSTRACT

South Africa's coastal regions are increasingly affected by pollutants from industrial and agricultural runoff, sewage discharge, stormwater drainage, and effluents from informal settlements. Persistent organic pollutants (POPs) have significant ecological impacts among these stressors. The study focused on assessing two global priority contaminants, polychlorinated biphenyls (PCBs) and organochlorine pesticides (OCPs), in muscle and liver tissue of the evileye blaasop, *Amblyrhynchote honckenii (Bloch, 1785)*, a common pufferfish along the South African coast. Six sites inside, near and outside marine protected areas (MPAs) were assessed. Liver samples from non-MPA sites exhibited higher levels of POPs compared to MPA or near-MPA sites. Nine OCPs were detected in fish liver tissue at each site, with oxy-chlordane particularly prevalent in Witsand, Mossel Bay, and Chintsa East. Among PCBs, 16 congeners were identified in fish liver tissue, with the most detected exclusively at St Francis Bay. Sodwana Bay was the only site where no PCBs were detected. Furthermore, hexachlorobiphenyl (PCB 153) was detected at all other sites, with fish from St Francis Bay exhibiting the highest concentrations of all 16 congeners. This study highlighted the persistent nature of PCBs and OCPs in South African coastal ecosystems. The differences in contamination levels at the sites highlight the need for targeted environmental management strategies to mitigate the impact of industrial, agricultural, and urban activities, thereby safeguarding the long-term sustainability of these vital coastal ecosystems.

1. Introduction

Coastal marine environments are globally threatened by the presence of persistent organic pollutants (POPs), particularly organochlorine pesticides (OCPs) and polychlorinated biphenyls (PCBs) (Gakuba et al., 2019). These contaminants, widely used in agriculture

* Corresponding author.
E-mail addresses: 27014452@mynwu.ac.za (L. de Klerk), nico.smit@nwu.ac.za (N.J. Smit), ybyared@gmail.com (Y.B. Yohannes), y_ikenaka@vetmed.hokudai.ac.jp (Y. Ikenaka), conimako@gmail.com (C. Nimako), shouta-nakayama@vetmed.hokudai.ac.jp (S.M.M. Nakayama), ishizum@vetmed.hokudai.ac.jp (M. Ishizuka), victor.wepener@nwu.ac.za (V. Wepener).
[1] 0000-0003-4492-6588
[2] 0000-0001-7950-193X
[3] 0000-0002-7629-6173
[4] 0000-0002-6633-6637
[5] 0000-0002-9115-805
[6] 0000-0003-1635-2898
[7] 0000-0001-5486-5745
[8] 0000-0002-9374-7191

https://doi.org/10.1016/j.rsma.2025.104368
Received 1 May 2025; Received in revised form 21 July 2025; Accepted 22 July 2025
Available online 23 July 2025
2352-4855/© 2025 The Author(s). Published by Elsevier B.V. This is an open access article under the CC BY-NC-ND license (http://creativecommons.org/licenses/by-nc-nd/4.0/).

Appendix C

and industry, are characterised by their long-lasting presence in the environment and their ability to bioaccumulate in aquatic organisms (Gakuba et al., 2019; Ramírez-Ayala et al., 2021). OCPs were primarily introduced for pest and disease control starting in the 1940s, while PCBs were used as coolants and lubricants in electrical equipment until their ban in the late 1970s (Serdar et al., 2014). Both groups of pollutants pose serious ecological risks, including disruptions to marine life and food webs (Serdar et al., 2014; Thompson et al., 2017). The persistence of these compounds poses ongoing risks to marine ecosystems, remaining detectable long after their initial application and raising concerns about their long-term effects on biota and human health, due to their biomagnification through the food chain (Jones, De Voogt., 1999; Li and Macdonald, 2005; Girones et al., 2020; D'Agostino et al., 2020).

Efforts to manage POPs have been initiated through international agreements such as the Stockholm Convention that aims to eliminate or restrict these pollutants globally (tockholm Convention on persistent organic pollutants, convention text., 2001; Gakuba et al., 2019). However, challenges persist due to existing stockpiles of POPs and ongoing releases from contaminated sites (Ramírez-Ayala et al., 2021). Currently, South Africa is the largest importer of pesticides in Africa, with an estimated value of $3.4 million between 2008 and 2017 (Tolera, 2021), resulting in the ongoing introduction of pesticides into rivers and ultimately the marine environment through various contamination pathways (Vogt et al., 2019; Wepener and Degger, 2019; Erasmus et al., 2020). For example, persistent organic pollutants such as DDT, banned in most other parts of the world, continue to be used for vector control in malaria-endemic regions of South Africa (Burke et al., 2017; Thompson et al., 2017; Olisah et al., 2021). Studies have shown that these land-based sources of POPs resulted in the contamination of intertidal (Erasmus et al., 2020) and coral reef (Porter et al., 2018) ecosystems off the east coast of South Africa. Understanding the distribution and concentration of POPs along the South African coastline is critical for evaluating potential impacts on biodiversity and ecosystem health. The implications extend beyond ecological health to human health concerns for communities reliant on coastal resources (Ramírez-Ayala et al., 2021). Consumption of contaminated seafood can result in harmful substance bioaccumulation in humans, leading to adverse health outcomes (Ramírez-Ayala et al., 2021). Therefore, comprehending the dynamics of POP accumulation in marine species is vital for assessing risks to both ecological integrity and public health (D'Agostino et al., 2020).

Most marine pollution monitoring studies have relied on traditional sessile bioindicator species such as mussels (Wepener and Degger, 2012; Farrington et al., 2016). In South Africa, the focus has primarily been on the monitoring of metals in mussels (Wepener and Degger, 2020) but the need for assessing other classes of pollutants (Wepener and Degger, 2019) and using other species such as marine fish (Gakuba et al., 2019; Olisah et al., 2021) along the South African coastline has been identified. Although South African pufferfish are not commercially significant and are classified as "least concern" by the IUCN (Froese and Pauly, 2023), their use as an indicator of contamination offers advantages over mussels. Unlike mussels, which filter-feed from large volumes of water with low enzymatic activity for metabolising OCPs (León et al., 2013), pufferfish exhibit diverse metabolic pathways that provide insights into how various contaminants affect marine fish rather than sessile bivalves (Yuqi et al., 2014). Furthermore, their scavenger feeding habits expose them to different sources of contaminants (Sazima, 2024). Pufferfish liver has a high lipid content (Wang et al., 2019), which is crucial for the accumulation of POPs (Phillips, Rainbow., 1994) and for this reason, pufferfish have been used as indicator organisms of metal exposure in the Mediterranean Sea (Kosker et al., 2019; Doğdu et al., 2021) and the South African coastline (Van Der Spuy et al., 2023). Furthermore, biochemical and histological biomarkers in pufferfish were used as indicators of marine health in marine protected areas (MPAs) of Brazil (Marinsek et al., 2024) and coastal lagoons of the Yucatan (Pech et al., 2009).

A pufferfish species occurring in South Africa, the evileye blaasop, *Amblyrhynchote honckenii (Bloch, 1785)*, has the potential to serve as a model for studying pollutants due to its wide distribution, ecological significance, and sensitivity to environmental changes, as evidenced by its accumulation of metals (Van Der Spuy et al., 2023). This species is also one of the most common marine and brackish fish associated with reefs, with a broad Indo-West Pacific distribution from South Africa to China and the Marshall Islands in Micronesia (Froese and Pauly, 2023). This study aimed to provide insights into OCP and PCB accumulation in marine fish, using the evileye blaasop as an indicator organism, along the nearshore South African coastline. The study further aimed to compare OCP and PCB exposure concentrations between MPAs and non-MPA sites to determine whether MPAs provide a protective effect against contaminant accumulation.

2. Materials and methods

2.1. Sampling and site selection

To explore the bioaccumulation of lipophilic pollutants, particularly OCPs and PCBs, in *A. honckenii,* 10–25 specimens were collected using rod and reel at six distinct sites along the South African coast. The sites were selected to represent inside, near and outside MPAs (Fig. 1). Witsand (WS) (-34.397323; 20.837474) is situated at the Breede River Estuary, which is known for its near-pristine status but faces threats from urban development and agricultural runoff (Erasmus et al., 2004; Breede River Estuarine Management Plan, 2016). Mossel Bay (MB) (-34.179656; 22.152093), adjacent to a small commercial harbour, is impacted by significant anthropogenic contamination sources, such as vessel emissions (Wepener and Degger, 2020). St Francis Bay (FB) (-34.183333; 24.851667) combines recreational activities with residential development and a commercial fishing fleet harbour (Baird and Pereyra-Lago, 1992), highlighting the effects of mixed-use environments on contaminant levels. Chintsa East (CE) (-32.836538; 28.116997) may experience contamination from agricultural runoff and tourism (Binning and Baird, 2001), making it vital to understand land-use impacts on marine ecosystems. Uvongo (UV) (-30.836667; 30.395556) faces potential pollutant loads from urbanisation and tourism (Firth et al., 2023), emphasising local economic influences on marine health. Sodwana Bay (SB) (-27.539760; 32.680600) is in an MPA (UNESCO, 1999) and serves as a critical site for evaluating the effectiveness of protected areas in mitigating pollution despite external influences.

Following capture, fish were transported in aerated water containers to a nearby field station, where they were identified, photographed, weighed, measured, and humanely killed. Muscle and liver tissue were removed using pre-cleaned dissection equipment, placed in pre-cleaned aluminium foil, transferred to polypropylene Falcon tubes, and frozen at −20 °C pending analyses. Ethical approval for this project was received from the AnimCare Research Ethics Committee of North-West University (NWU-00565–19-A5). Permits for the collection of *A. honckenii* for research were issued by the South African Department of Agriculture, Forestry and Fisheries (permit nos. RES2022–44 and RES2022–86) and Cape Nature (permit no. CN44–8718289).

2.2. Sample preparation

In the laboratory, samples were first thawed and weighed to determine their wet weight. They were then placed in a −80 °C freezer for 24 h before being transferred to a freeze dryer (FreeZone 6, Labconco) for approximately 96 h. Following freeze-drying, the samples were reweighed to obtain their dry weight and subsequently homogenised using a mortar and pestle. Approximately 0.5 g of each sample was placed into 15 mL Falcon tubes. Two samples of approximately 0.2 g of rat liver were prepared for every 30 samples for recovery and quality control (QC). Similarly, two blank samples were prepared for every 30 samples using 500 µL of ultra-pure MilliQ water (MQ).

All tubes, except for the MQ, were spiked with OCP (Dr.

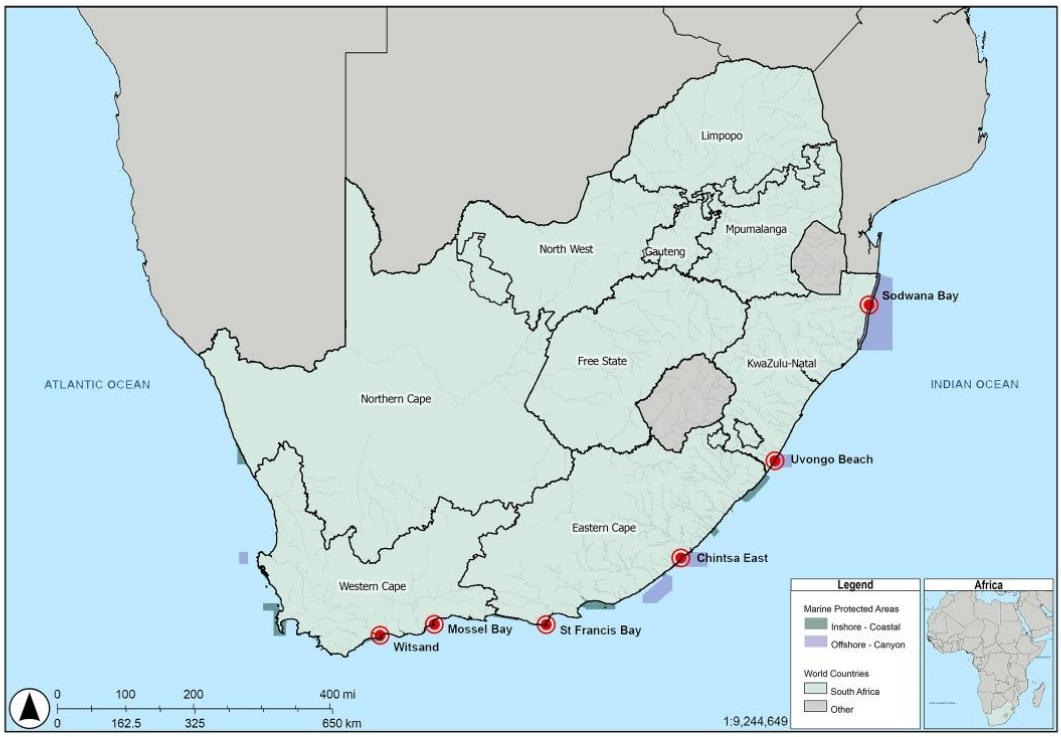

Fig. 1. Map indicating the sampling localities of specimens of *Amblyrhynchote honckenii*.

Ehrenstorfer) and PCB (Dr. Ehrenstorfer) standard surrogates and internal standards before being vortexed. Internal standards were selected not for their structural similarity to the target analytes, but for their chemical stability, consistent recovery, and lack of interference with target compound detection. The use of these internal standards corrected for potential variations in extraction efficiency, injection volume, and instrumental response across all samples. The concentrations and spike volumes of these standards are detailed in Supplementary Tables 1 and 2. The OCP and PCB surrogates used are listed in Supplementary Table 3. Following this, 500 µL of 0.1 % formic acid (99 %, Fujifilm Wako) in acetonitrile (99.9 %, Fujifilm Wako) was added to the biological and QC samples, which were then mixed thoroughly and vortexed for 1 min. After allowing the samples to stand for 1–2 h post-spiking, an additional 5 mL of 0.1 % formic acid in acetonitrile was added to each falcon tube, while only the blanks and MQ samples received an additional 500 µL of sodium acetate (Fujifilm Wako) to facilitate the separation of water from the solvent. The samples were vortexed for 1 min and then ultrasonicated for 5 min before being shaken mechanically at maximum speed for 10 min. Following this, the samples were centrifuged at 10,000 rpm for 5 min at 5°C. To remove the lipids from the samples, the supernatant was decanted into activated EMR-Lipid tubes (Agilent Bond Elut), which had been pre-activated by adding 5 mL of MQ and shaking vigorously. For the blanks and MQ samples, only 5 mL of supernatant was transferred to the EMR-Lipid tubes. All samples were shaken vigorously and vortexed again before being placed in a mechanical shaker at maximum speed for another 10 min, followed by a second centrifugation at 10,000 rpm for five minutes at 5 °C. The entire supernatant from each sample was then decanted into pre-prepared EMR-Polish tubes, which contained 1.4 g of $MgSO_4$ (Fujifilm Wako) and 0.6 g of NaCl (Kanto Chemical Co., Inc.). The samples were vortexed upright for one minute before undergoing final centrifugation at 10,000 rpm for 5 min at 5 °C. Finally, a volume of 1 mL from the uppermost supernatant was pipetted into the corresponding GC vial for analysis. The acetonitrile extract was not evaporated and was injected directly into the GC–MS.

2.3. Analyses

The OCPs and PCBs were analysed in muscle and liver tissue of the Evileye blaasop using a GC-20230 Plus (Shimadzu) coupled with a GCMS-TQ8050NX triple quadrupole mass spectrometer (Shimadzu). Chromatographic separation was performed using a Rxi-5Sil MS capillary column (30 m x 0.25 mm i.d., 0.25 µm df, Restek, Bellefonte, PA, USA).

For OCP analysis, the operating condition was splitless injection mode with an injection volume of 1 µL at an injector temperature of 250 °C. Helium (≥99.999 %) was used as the carrier gas with a linear velocity in flow control mode, 100.1 Kpa pressure, 30 mL/min total flow rate, 1.69 mL/min column flow, 47.2 cm/s linear velocity, 5 mL/min purge flow. The oven temperature program started at 50°C (held for 1 min), increased to 200 °C at 30 °C/min, and finally ramped to 260°C at 5 °C/min, where it was held for 3 min. The total program duration was 20 min. The mass spectrometer system was operated in the electron ionisation (EI) mode at 70 eV. The ion source and interface temperatures were 230 and 250°C, respectively. The regression line was determined using the internal standard method, where the ratio of each analyte signal is taken to the internal standard signal and plotted against the analyte concentrations in the calibration solutions to obtain a regression

Appendix C

line with a correlation factor of (R^2=0.99) before analysing the samples.

For PCB analysis, the operating condition was splitless injection mode with an injection volume of 1 µL at an injector temperature of 270 °C. Helium (≥99.999 %) was used as the carrier gas with a linear velocity in flow control mode, 41.1 KPa pressure, 30.0 mL/min total flow rate, 0.75 mL/min column flow, 31.8 cm/s linear velocity, 5 mL/min purge flow. The oven temperature program started at 75°C (held for 2 min), increased to 180°C at 15 °C/min, and finally ramped to 300°C at 4 °C/min, where it was held for 6 min. The total program duration was 45 min. The mass spectrometer system was operated in the electron ionisation (EI) mode at 70 eV. The ion source and interface temperatures were 230 and 290°C, respectively. The regression line was determined using the internal standard method, where the ratio of each analyte signal is taken to the internal standard signal and plotted against the analyte concentrations in the calibration solutions to obtain a regression line with a correlation factor of (R^2=0.98) before analysing the samples.

2.4. Quality control

Procedures used for the analysis of selected OCPs and PCBs were monitored with appropriate quality control and assurance measures. Procedural blanks were used in all the extraction, clean-up and analysis steps along with sample preparation and analysis to determine if there was any possible input from external sources during analysis. There were no detectable levels of target contaminants in blank samples. Target analyte recoveries were performed by spiking freeze-dried rat liver as reference material with separate OCP and PCB standards before extraction. The concentration of the analytes was determined using the internal standard method. The concentration of the spiked reference samples was divided by the known concentration of the spike in the sample and multiplied by 100 to obtain the percentage recoveries (Saadati et al., 2013). The limit of detection (LOD) was calculated as 3 times the signal-to-noise ratio using the standard deviation of 3 calibration intercepts divided by the slope, whereas the limit of quantification (LOQ) was 10 times this ratio (Saadati et al., 2013). The recovery rate (%), limit of detection (LOD) and limit of quantification (LOQ) of all the different OCP and PCB compounds of interest that were detected are shown in Table 1. The reference material in freeze-dried rat liver tissues was analysed, yielding recovery percentages of 103–148 % for OCPs and 82–119 % for PCBs (Table 1).

2.5. Statistical analyses

Data were tested for normality using the Shapiro-Wilk normality test. Significant differences in OCP and PCB concentrations in *A. honckenii* tissues between the six sites were determined using a one-way ANOVA followed by Dunn's multiple comparisons test (GraphPad Prism v9.0.0). Significance was regarded as $p < 0.05$. To allow for statistical analyses, all sample values below the LOD were substituted with LOD/2 (Kushner, 1976; Labuschagne et al., 2019).

3. Results

The overall recovery rates, typically within the acceptable range of 75–125 % (Table 1), confirm the accuracy of the method and ability to minimise analyte losses during sample preparation and analysis (Saadati et al., 2013). The detection limits across both chemical groups demonstrate the method's capability to accurately identify contamination at trace levels, ensuring the reliability of reported concentrations. There were no detectable levels of target contaminants in fish muscle samples, while nine OCPs and 16 PCBs were detected in fish livers across the six sites (Supplementary Tables 4 and 5).

The distribution of OCPs across the six sites indicates significant spatial variation in exposure and subsequent contamination (Fig. 2). Total OCP concentrations (∑OCP) were highest in Witsand (372 ± 161 ng/g) and lowest in Sodwana Bay (177 ± 131 ng/g) (Fig. 2), suggesting greater contamination in the sites on the south west coast. Notably, oxychlordane concentrations were significantly higher when compared to the other sites (Figs. 2–3), peaking in Mossel Bay (296 ± 73 ng/g) and being lowest in Sodwana Bay (64 ± 28 ng/g). The concentrations of p,p'-DDT found in St Francis Bay, Uvongo, and Sodwana Bay were similar (Figs. 2–3). Significant variation ($p < 0.05$) was also observed for p,p'-DDE (Fig. 2), with fish from St Francis Bay having the highest concentrations (72 ± 36 ng/g) and Sodwana Bay having the lowest (5 ± 3 ng/g). Interestingly, β-HCH showed an increasing trend (albeit non-significant) (Fig. 2) from Witsand (25 ± 21 ng/g) on the southwest to Sodwana Bay (43 ± 57 ng/g) in the northeast (Supplementary Table 4). Dieldrin and trans-nonachlor were detected exclusively in Uvongo, whereas o,p'-DDD was only found in St Francis Bay fish (Supplementary Table 4). Statistical analysis confirmed significant spatial differences in contamination levels. The ANOVA results indicate that o,p'-DDT/p,p'-DDD ($F=12.55$; $p < 0.0001$), oxychlordane ($F=26.77$; $p < 0.0001$), γ-HCH ($F=5.05$; $p = 0.0013$), and p,p'-DDE ($F=15.84$; $p < 0.0001$) exhibited significant variation across sites.

PCB contamination exhibited a striking pattern, with St Francis Bay fish having a significantly higher total PCB concentrations (∑PCB = 929 ± 999 ng/g) compared to those from all other sites, where concentrations remained below 22 ng/g (Supplementary Table 5). The relatively high standard deviation in ∑PCB concentration at the St Francis Bay site (929 ± 999 ng/g) reflects both the detection of a wider

Table 1
The limit of detection (LOD), limit of quantification (LOQ) and recovery rates (%) of all the different organochlorine pesticide (OCP) and polychlorinated biphenyl (PCB) compounds detected in the liver tissues of *Amblyrhynchote honckenii*.

OCPs				PCBs			
Compounds	**LOD (ng/g)**	**LOQ (ng/g)**	**Recovery (%)**	**Compounds**	**LOD (ng/g)**	**LOQ (ng/g)**	**Recovery (%)**
Dieldrin	0.48	1.46	106 ± 18	**PCB #31**	2.55	7.74	119 ± 15.62
***o,p'*-DDD**	0.41	1.25	148 ± 5	**PCB #44**	2.39	7.25	108 ± 10.77
***o,p'*-DDT/ *p,p'*-DDD**	0.71	2.14	107 ± 10	**PCB #52**	2.76	8.35	107 ± 11.10
Oxychlordane	0.64	1.95	104 ± 14	**PCB #66**	1.57	4.77	94 ± 6.91
***p,p'*-DDE**	0.50	1.50	102 ± 9	**PCB #87**	0.38	1.15	91 ± 3.44
***p,p'*-DDT**	1.56	4.73	113 ± 10	**PCB #101**	0.83	2.50	98 ± 3.88
trans-Nonachlor	0.72	2.19	100 ± 14	**PCB #110**	0.27	0.81	104 ± 4.36
β-HCH	1.24	3.75	122 ± 14	**PCB #138**	0.71	2.16	92 ± 8.06
γ-HCH (Lindane)	0.47	1.42	103 ± 7	**PCB #141**	0.51	1.56	90 ± 7.96
				PCB #151	1.19	3.61	107 ± 4.95
				PCB #153	0.63	1.91	94 ± 4.13
				PCB #170	0.33	1.01	85 ± 9.20
				PCB #180	0.45	1.35	82 ± 1.17
				PCB #183	0.45	1.36	84 ± 8.87
				PCB #187	0.29	0.87	84 ± 7.93
				PCB #206	0.22	0.66	100 ± 4.54

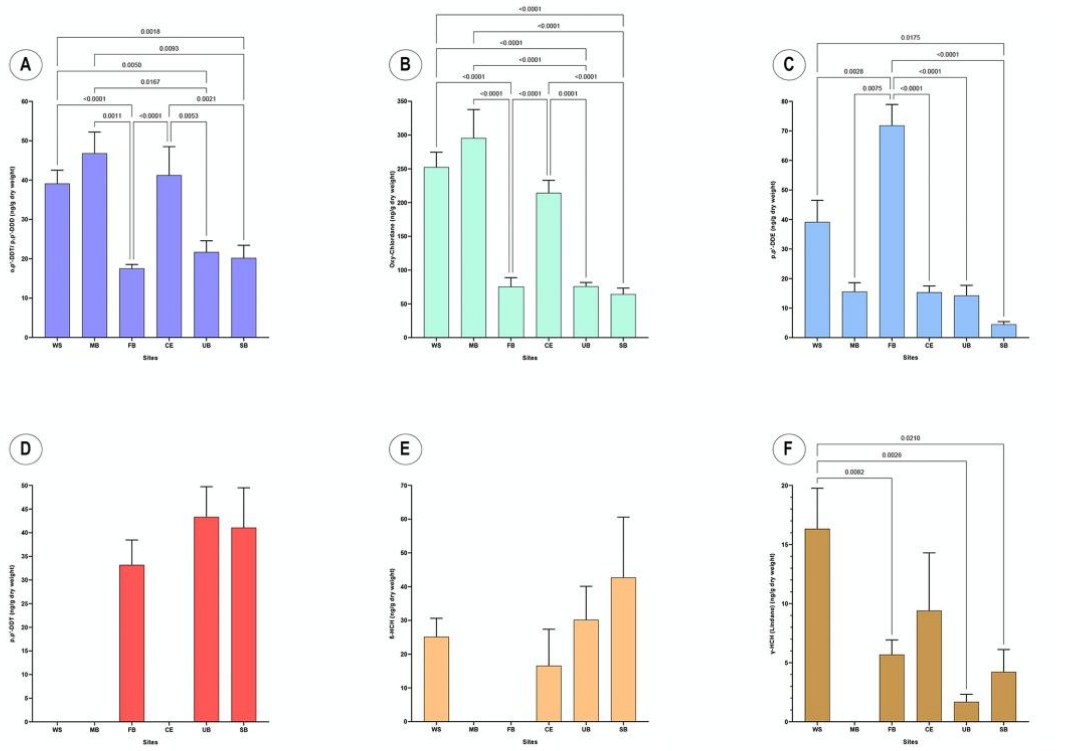

Fig. 2. Organochlorine pesticide (OCP) concentrations (mean ± standard deviation) in fish liver tissues of *Amblyrhynchote honckenii* from six localities (Witsand, Mossel Bay, St Francis Bay, Chintsa East, Uvongo Beach, and Sodwana Bay) along the South African coastline. Significant differences between the six sites are indicated with the p-value. All concentrations are expressed as ng/g dry weight. Significance was taken as $p < 0.05$.Abbreviations: ND – not detected. Concentrations that were only observed in one site are listed in the supplementary material.

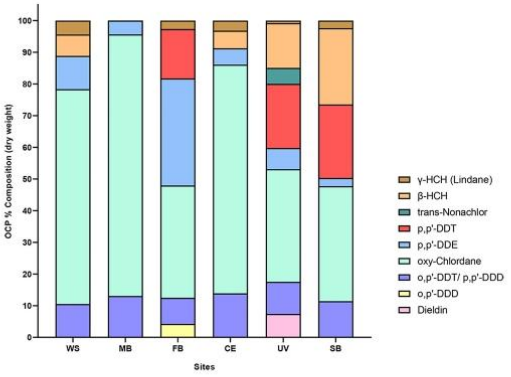

Fig. 3. Percentage organochlorine pesticide composition in fish liver tissues of *Amblyrhynchote honckenii* from six localities (Witsand, Mossel Bay, St Francis Bay, Chintsa East, Uvongo Beach, and Sodwana Bay) along the South African coastline.

range of PCB congeners at this location and the influence of LOD/2 substitution for non-detects. In contrast, the other sites exhibited fewer detectable congeners, with most PCB values below detection limits, leading to lower calculated means and standard deviations. PCB #153 was the most widespread congener, detected in fish from all sites except Sodwana Bay, and showed significantly higher concentrations in St Francis Bay (235 ± 222 ng/g) (Figs. 4–5). Among the PCBs, PCB #153 showed a significant difference ($F=9.474$; $p < 0.0001$), reinforcing the pattern of elevated levels in St Francis Bay. The statistical confirmation of these differences strengthens the argument for targeted investigations into contamination sources in this region. Several PCB congeners, such as PCB #180 ($F=8.96$; $p < 0.0001$) and PCB #187 ($F=6.9$); $p < 0.0001$), were also significantly elevated in St Francis Bay fish compared to those from Uvongo (Fig. 4). In contrast, PCBs were below detection in Sodwana Bay fish, indicating a lower impact from such contaminants in this region (Fig. 5). This suggests that north-eastern coastal sites have either remained unaffected by historical PCB contamination or benefit from oceanographic conditions that reduce contaminant accumulation.

4. Discussion

The results of this study provide valuable insights into the spatial distribution, persistence, and potential ecological risks associated with pesticide contamination across various sampling sites along the South African coastline. The detection of two global priority contaminants,

Appendix C

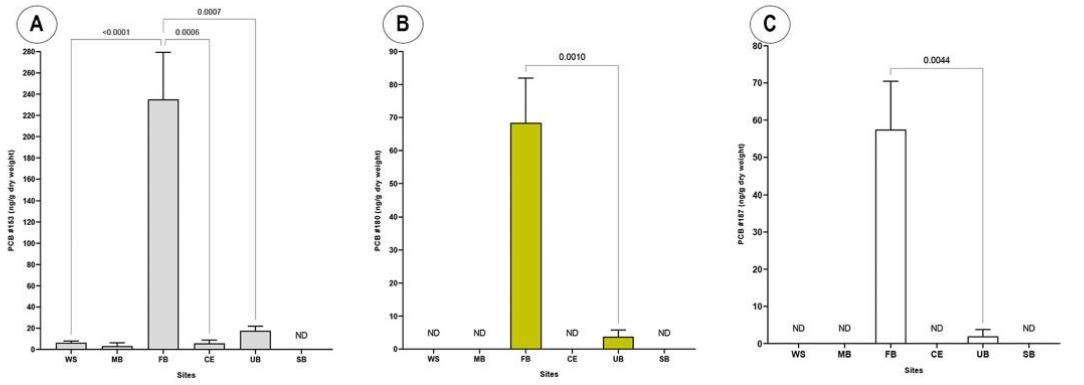

Fig. 4. Polychlorinated biphenyl (PCB) concentrations (mean ± standard deviation) in fish liver tissues of *Amblyrhynchote honckenii* from six localities (Witsand, Mossel Bay, St Francis Bay, Chintsa East, Uvongo Beach, and Sodwana Bay) along the South African coastline. Significant differences between the six sites are indicated with the p-value. All concentrations are expressed as ng/g dry weight. Significance was taken as $p < 0.05$. Abbreviations: ND – not detected.

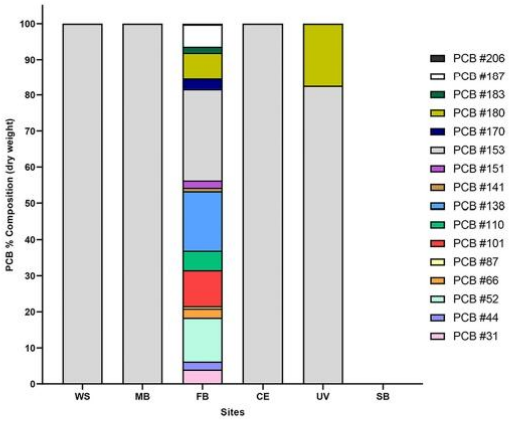

Fig. 5. Percentage polychlorinated biphenyl congener composition in fish liver tissues of *Amblyrhynchote honckenii* from six localities (Witsand, Mossel Bay, St Francis Bay, Chintsa East, Uvongo Beach, and Sodwana Bay) along the South African coastline.

OCPs and PCBs, highlights the widespread and complex nature of OCP contamination. Compounds such as o,p′-DDT/p,p′-DDD, oxychlordane, p,p′-DDE, and PCB #153 showed significant spatial variation, indicating point sources of contamination. Conversely, the relatively uniform distribution of p,p′-DDT and β-HCH suggests widespread historical contamination rather than site-specific contamination events. The uniform presence of these compounds further suggests their mobility and persistence in the marine environment, potentially transported via water currents or bioaccumulated across broader regions.

Persistent organic pollutants, such as OCPs and PCBs, have been extensively studied along the South African coastline, with previous research highlighting long-term trends and potential sources. Ryan et al. (2012) reported a decreasing trend between 1884 and 2008 in legacy OCPs in beached plastic pellets. However, they also found that PCB concentrations have not shown the same decline, likely due to their continued leaching from historical sources and industrial activities. This is consistent with the present findings, where OCP contamination showed variability across sites, while PCB contamination was particularly pronounced in St Francis Bay, pointing to potential ongoing industrial inputs. These findings are consistent with global research indicating that despite regulatory restrictions, pesticide residues persist due to their long half-lives, continued use, and secondary contamination sources (Ali et al., 2021). The selected bioindicator species, *A. honckenii*, revealed distinct contamination trends indicative of both historical and ongoing contamination. The distribution of these POPs provides insights into the interplay between anthropogenic activities, oceanographic transport mechanisms, and the potential role that MPAs play in reducing contaminant exposure in the nearshore environment.

Total OCP concentrations varied significantly across locations, with Witsand exhibiting the highest concentrations and Sodwana Bay the lowest, suggesting an increasing east to west gradient along the coast of South Africa. This pattern is likely driven by regional differences in land use, historical pesticide application, and hydrodynamic conditions affecting sediment deposition and resuspension (Berrojalbiz et al., 2011; Cao et al., 2022; Liu et al., 2024). This spatial trend aligns with studies by Degger et al. (2011), that found that OCP levels in *Perna perna* (brown mussels) were highest in areas with strong agricultural runoff, particularly in regions of the Western Cape Province, supporting the hypothesis that historical pesticide application continues to influence coastal contamination through runoff and sediment resuspension. The elevated concentrations observed on the southwestern coast are consistent with agricultural runoff from the Western Cape, a region historically associated with pesticide use, mirroring contamination patterns observed in metal pollution studies (Wepener and Degger, 2020). Similarly, Firth et al. (2019) monitored organic pollutants in *Choromytilus meridionalis* (black mussels) along the South African coastline and found that contaminants such as DDT metabolites and PCBs are highly persistent in marine environments, accumulating in bioindicator species. This aligns with the present study, where high concentrations of p,p′-DDE in St Francis Bay further support the persistence of DDT residues in marine sediments and biota despite regulatory bans. Furthermore, Erasmus et al. (2020) reported that South African coastal sites continue to receive inputs of DDT from malaria vector control programs, which aligns with the detection of parent p,p′-DDT. The presence of p,p′-DDT in Sodwana Bay and Uvongo likely results from WHO-approved malaria vector control programs in northeastern South Africa (WHO, 2011; Thompson et al., 2017), whereas in St Francis Bay, it raises concerns about illegal agricultural use.

Hydrodynamic conditions also play a crucial role in the spatial distribution of OCPs, as coastal currents and sediment transport influence contaminant dispersion and accumulation (Berrojalbiz et al., 2011; Cao

Appendix C

et al., 2022; Liu et al., 2024). The strong Agulhas Current activity in the north and east likely facilitates contaminant dispersion (Liu et al., 2024), while the slower-moving Agulhas counter-current in the southwest contributes to contaminant accumulation. This could also explain the higher OCP concentrations observed in the southwestern coastal sites. The detection of oxychlordane in Mossel Bay suggests localised degradation of legacy chlordane, consistent with findings that older OCPs undergo gradual transformation in marine environments (Degger et al., 2011; Firth et al., 2019). The persistence of these pollutants can be attributed to factors such as microbial activity, temperature, and sediment characteristics, which influence degradation rates (Aislabie et al., 1997; Yu et al., 2011). Additionally, the accumulation of various POPs, including PCBs and other halogenated compounds, has been well-documented in estuaries along the South African coastline and off-shore (Kampire et al., 2016; Ryan et al., 2012; Wu et al., 2019). These studies highlight the long-term stability of such compounds in coastal ecosystems, reinforcing the urgent need for continued monitoring and stricter enforcement of pesticide regulations in South Africa to mitigate their lasting environmental impact.

The β-HCH concentrations exhibited a decreasing trend from the northeast (Sodwana Bay) to the southwest (Witsand), suggesting that its presence is linked to historical and possibly ongoing use in northern regions rather than long-range atmospheric transport. Previous studies have indicated that β-HCH remains more prevalent in the northern parts of South Africa, likely due to past agricultural applications and industrial sources (Kampire et al., 2016; Wu et al., 2019). This spatial distribution aligns with the hypothesis that OCPs are transported from their primary regions of use rather than through atmospheric mechanisms, as prevailing wind patterns predominantly move south-westward. Limited detections of dieldrin and trans-nonachlor in Uvongo suggest historical termiticide use near urban settlements (Colt et al., 2006), while the detection of o,p′-DDD only in St Francis Bay implies localised reductive dechlorination processes in sediment under low-oxygen conditions (Venkatesan et al., 1999). The restricted spatial occurrence of these compounds further supports the role of site-specific contamination sources and retention mechanisms in shaping pollutant distributions along the South African coastline.

The presence of PCBs in the study area is of particular concern due to their high persistence, bioaccumulation potential, and toxic effects (Girones et al., 2020; Barhoumi et al., 2023). Polychlorinated biphenyls exhibited spatial variability along the South African coastline, with the highest concentrations observed at St Francis Bay. This pattern aligns with findings from previous studies, which have identified the Gqeberha (previously known as Port Elizabeth) region as a hotspot for PCB contamination due to historical and industrial sources (Kampire et al., 2016; Porter et al., 2018; Wu et al., 2019). Detailed insights into PCB congener profiles reveal PCB #153 as the predominant congener, attributed to its remarkable chemical stability and resistance to metabolic degradation (Kampire et al., 2016; Marinsek et al., 2024). The present study's detection of elevated PCB levels near St Francis Bay supports observations by Wu et al. (2019), who found that *Loligo reynaudii* (chokka squid) accumulated higher PCB concentrations in this region, likely influenced by proximity to the fishing fleets of the large-scale squid fisheries and regional contamination inputs from the metropolitan region of Gqeberha. Further supporting this, Degger et al. (2011) demonstrated that semi-permeable membrane devices (SPMDs) deployed along the South African coast efficiently accumulated dioxin-like PCBs, whereas mussels showed limited bioaccumulation due to their metabolic capacity to degrade these toxic congeners. This suggests that while PCBs are present in the water column, their bioavailability to certain marine organisms may vary depending on species-specific metabolism. The presence of PCBs in the St Francis Bay region is likely attributed to historical use in e.g. harbour activities, electrical transformers, industrial activities, and continued remobilisation from contaminated sediments, as discussed in Kampire et al. (2016). This highlights the necessity for long-term monitoring efforts in this area, particularly given the potential for PCB bioaccumulation in commercially important marine species such as squid and mussels. That this species of pufferfish accumulate PCBs further supports its use as a valuable bioindicator species, complementing existing monitoring efforts and enhancing our understanding of PCB distribution along the South African coastline. The findings of these studies reinforce concerns regarding the persistence of PCBs in South African coastal waters and their potential risks to marine ecosystems. In contrast, the absence of detectable PCBs in Sodwana Bay suggests a reduced industrial footprint, potentially influenced by oceanographic dilution or conservation measures within the MPA.

The observed spatial variability in OCP and PCB levels reflects multiple environmental and anthropogenic factors. Agricultural runoff remains a key contributor to OCP contamination, particularly in Witsand and Mossel Bay, paralleling patterns observed in heavy metal contamination studies (Erasmus et al., 2020). Industrial activity and urbanisation appear to be dominant contributors to PCB contamination, especially in St Francis Bay. The high standard deviation in PCB concentrations at this site suggests localised contamination hotspots or sediment resuspension during seasonal oceanographic shifts (Liu et al., 2024). Moreover, the wide range of PCB congeners detected at St Francis Bay compared to other sites further contributes to the variability, suggesting either diverse contamination sources or differential retention of congeners in sediments or biota. Similarly, the Benguela Current on the west coast and the Agulhas Current on the east and south coasts could facilitate the redistribution of contaminants, influencing bioaccumulation patterns in marine organisms (Liu et al., 2024). Firth et al. (2019) demonstrated that hydrodynamic conditions significantly impact pollutant accumulation in mussels, with stronger currents in the east dispersing contaminants, while slower currents in the west lead to their accumulation. These findings further support our results showing lower OCP and PCB concentrations in Sodwana Bay compared to southwestern sites such as Witsand and St Francis Bay.

The ecological implications of pesticide residues are significant, particularly for aquatic ecosystems and associated biota. Chronic exposure to DDT and its metabolites has been linked to endocrine disruption in fish and wildlife, raising concerns about bioaccumulation in local food webs (Bouwman et al., 2008; Serdar et al., 2014; Van den Berg et al., 2017; Bennett et al., 2021). Similarly, PCBs pose severe risks to marine ecosystems, with established links to reproductive impairments, immune suppression, and developmental defects in aquatic species (Serdar et al., 2014; Van den Berg et al., 2017; Bennett et al., 2021). This study was not able to conclusively demonstrate that sites in MPAs would be able to protect resident nearshore fish species from OCP and PCB exposure. Reduced PCB concentrations in Sodwana Bay (MPA) likely reflect the absence of industrial and urban exposure routes. *Amblyrhynchote honckenii's* non-migratory behaviour (reflecting a localised habitat) indicates site-specific exposure and demonstrates that MPAs remain vulnerable to POPs transported via long-range atmospheric and ocean current pathways. While this study did not specifically investigate the biology of *A. honckenii*, nor fine-scale environmental heterogeneity, these factors could contribute to individual variability in contaminant accumulation and warrant further investigation. Future studies incorporating these variables may help clarify sources of variability and improve the interpretation of bioaccumulation patterns. The widespread detection of OCPs across all sites, including MPAs, demonstrates the diffuse sources and persistent nature of contaminants through various transport mechanisms (Boersma, Parrish., 1999). This aligns with evidence that POPs persist and migrate globally, challenging the isolation of even well-managed MPAs from transboundary contamination (Erasmus et al., 2020). Elevated OCP and PCB levels in non-MPA sites, particularly St Francis Bay and Mossel Bay, emphasise the need for stricter contamination management strategies. Implementing buffer zones and catchment-level management could help mitigate pollutant inputs from surrounding land-use activities (Boersma, Parrish., 1999).

Appendix C

5. Conclusion

This study highlights the ongoing risks posed by OCPs and PCBs in South African coastal ecosystems despite international regulatory measures. The spatial variability in contamination levels suggests contributions from both localised and long-range transport mechanisms, emphasising the need for a multifaceted approach to contamination management. The evileye blaasop, *A. honckenii*, used here as a bioindicator, demonstrated site-specific contamination patterns, reflecting both historical and current pollutant exposures and underlining its value in monitoring marine ecosystem health and pollutant bioaccumulation. While MPAs could be effective in reducing industrial pollutants such as PCBs, broader regulatory enforcement and pollution mitigation strategies beyond protected areas are essential. Future research should focus on identifying specific contamination sources, assessing long-term bioaccumulation trends, and evaluating the ecological and human health implications of these contaminants. Overall, this study highlights the complexity of POPs contamination, influenced by historical and ongoing usage, environmental transport mechanisms, and degradation dynamics. The significant spatial variability observed in pesticide residues highlights the need for site-specific risk assessments and targeted remediation efforts. Proactive measures, including reducing pesticide inputs, enhancing environmental monitoring, and ensuring regulatory compliance, are essential to minimising the long-term ecological impact of pesticide contamination.

CRediT authorship contribution statement

L. de Klerk: Methodology, Investigation, Formal analysis, Writing – original draft, Writing - review & editing. **N.J. Smit:** Conceptualisation, Data curation, Writing – review & editing, Supervision. **Y.B. Yohannes:** Methodology, Investigation, Formal analysis, Validating, Writing – review & editing. **Y. Ikenaka:** Resources, Writing – review & editing. **C. Nimako:** Methodology, Writing—review & editing. **S.M.M. Nakayama**: Resources, Validating. M. Ishizuka: Funding acquisition, Resources, Writing – review & editing. **V. Wepener:** Conceptualisation, Data curation, Funding acquisition, Writing – review & editing, Supervision.

Author agreement

All authors have seen and approved the final version of the manuscript being submitted. We warrant that the article is the authors' original work, hasn't received prior publication and isn't under consideration for publication elsewhere.

Declaration of Competing Interest

The authors declare that they have no known competing financial interests or personal relationships that could have appeared to influence the work reported in this paper.

Acknowledgements

We would like to thank the Unit for Environmental Sciences and Management, North-West University (NWU) for the use of field equipment and laboratory facilities. The Laboratory of Toxicology, Department of Environmental Veterinary Sciences, University of Hokkaido, is thanked for the analyses of organic compounds. Additional thanks go to our colleagues Francois Retief, Reese Alberts, Anja Erasmus, Marliese Truter, Anja Vermaak, Coret van Wyk, Hannes Erasmus, Chandra le Roux, and Angela Minnie from the NWU, who assisted with the collection of samples. The research was supported through funding from the Africa–Japan Collaborative Research (AJ-CORE) Programme jointly funded by the Japan Science and Technology Agency – JST (Grant Number: PJ36210002, PI: Mayumi Ishizuka) and the NRF (Grant number: 132805, PI: Victor Wepener). Linda van der Spuy was supported by the NRF of South Africa (Grant Number: 132805). Opinions, findings, conclusions, and recommendations expressed in this publication are that of the authors, and the NRF and NWU accept no liability whatsoever in this regard. This is contribution No. 953 from the NWU-Water Research Group.

Appendix A. Supporting information

Supplementary data associated with this article can be found in the online version at doi:10.1016/j.rsma.2025.104368.

Data availability

Data will be made available on request.

References

Aislabie, J.M., Richards, N.K., Boul, H.L., 1997. Microbial degradation of DDT and its residues—a review. N. Z. J. Agric. Res. 40 (2), 269–282. https://doi.org/10.1080/00288233.1997.9513247.

Ali, S., Ullah, M.I., Sajjad, A., Shakeel, Q., Hussain, A., 2021. Environmental and health effects of pesticide residues. Sustainable agriculture reviews 48: pesticide occurrence. Anal. Remediat. Vol. 2 Anal. 311–336. https://doi.org/10.1007/978-3-030-54719-6_8.

Baird, D., Pereyra-Lago, R., 1992. Nutrient status and water quality assessment of the Marina Glades canal system, Kromme Estuary. St. Fr. Bay. Water SA 18 (1), 37–42.

Barhoumi, B., Metian, M., Zaghden, H., Derouiche, A., Ameur, W.B., Hassine, S.B., Oberhaensli, F., Mora, J., Mourgkogiannis, N., Al-Rawabdeh, A.M., Chouba, L., 2023. Microplastic-sorbed persistent organic pollutants in coastal Mediterranean Sea areas of Tunisia. Environmental Science Processes Impacts 25 (8), 1347–1364. https://doi.org/10.1039/d3em00169e.

Bennett, K.A., Robinson, K.J., Armstrong, H.C., Moss, S.E., Scholl, G., Tranganida, A., Eppe, G., Thomé, J.P., Debier, C., Hall, A.J., 2021. Predicting consequences of POP-induced disruption of blubber glucose uptake, mass gain rate and thyroid hormone levels for weaning mass in grey seal pups. Environ. Int. 152, 106506. https://doi.org/10.1016/j.envint.2021.106506.

Berrojalbiz, N., Dachs, J., Ojeda, M.J., Valle, M.C., Castro-Jiménez, J., Wollgast, J., Ghiani, M., Hanke, G., Zaldivar, J.M., 2011. Biogeochemical and physical controls on concentrations of polycyclic aromatic hydrocarbons in water and plankton of the Mediterranean and Black Seas. Glob. Biogeochem. Cycles 25 (4), 1–14. https://doi.org/10.1029/2010GB003775, 2.

Binning, K., Baird, D., 2001. Survey of heavy metals in the sediments of the Swartkops River Estuary, Port Elizabeth South Africa. Water SA 27 (4), 461–466.

Boersma, P.D., Parrish, J.K., 1999. Limiting abuse: marine protected areas, a limited solution. Ecol. Econ. 31 (2), 287–304. https://doi.org/10.1016/S0921-8009(99)00085-3.

Bouwman, H., Polder, A., Venter, B., Skaare, J.U., 2008. Organochlorine contaminants in cormorant, darter, egret, and ibis eggs from South Africa. Chemosphere 71 (2), 227–241. https://doi.org/10.1016/j.chemosphere.2007.09.057.

Breede River Estuarine Management Plan, 2016. Western Cape Estuary Management Framework and Implementation Strategy. SSI Environmental, 1st edition. Royal Haskoning D.H.V. (revised 2011, 2nd Edition, 2016).

Burke, A., Dandalo, L., Munhenga, G., Dahan-Moss, Y., Mbokazi, F., Ngxongo, S., Coetzee, M., Koekemoer, L., Brooke, B., 2017. A new malaria vector mosquito in South Africa. Sci. Rep. 7 (1), 43779. https://doi.org/10.1038/srep43779.

Cao, X., Huo, S., Zhang, H., Zhao, X., Guo, W., He, Z., Ma, C., Zheng, J., Song, S., 2022. Polycyclic aromatic hydrocarbons in China: will decoupling of their emissions and socioeconomic growth emerge. e2021EF002360 Earth'S. Future 10 (1). https://doi.org/10.1029/2021EF002360.

Colt, J.S., Davis, S., Severson, R.K., Lynch, C.F., Cozen, W., Camann, D., Engels, E.A., Blair, A., Hartge, P., 2006. Residential insecticide use and risk of non-Hodgkin's lymphoma. Cancer Epidemiol. Biomark. Prev. 15 (2), 251–257. https://doi.org/10.1158/1055-9965.EPI-05-0556.

D'Agostino, F., Bellante, A., Quinci, E., Gherardi, S., Placenti, F., Sabatino, N., Buffa, G., Avellone, G., Di Stefano, V., Del Core, M., 2020. Persistent and emerging organic pollutants in the marine coastal environment of the Gulf of Milazzo (Southern Italy): human health risk assessment. Front. Environ. Sci. 8, 117. https://doi.org/10.3389/fenvs.2020.00117.

Degger, N., Wepener, V., Richardson, B.J., Wu, R.S.S., 2011. Application of artificial mussels (AMs) under South African marine conditions: a validation study. Mar. Pollut. Bull. 63 (5-12), 108–118. https://doi.org/10.1016/j.marpolbul.2011.04.040.

Doğdu, S.A., Çiftçi, N., Ayas, D., Turan, C., 2021. Potential usage of pufferfish dentin as a metal accumulation indicator. J. Water Chem. Technol. 43, 269–275. https://doi.org/10.3103/S1063455X21030061.

Erasmus, A., Ikenaka, Y., Nakayama, S.M., Ishizuka, M., Smit, N.J., Wepener, V., 2020. Trophic transfer of pollutants within two intertidal rocky shore ecosystems in different biogeographic regions of South Africa. Mar. Pollut. Bull. 157, 111309. https://doi.org/10.1016/j.marpolbul.2020.111309.

Erasmus, C.P., Rossouw, G., Baird, D., 2004. The concentration of ten heavy metals in the tissues of shark species Squalus megalops and Mustelus (Chondrichthyes) occurring

Appendix C

along the south eastern coast of South Africa. In: Population, English edition. University of Port Elizabeth.
Farrington, J.W., Tripp, B.W., Tanabe, S., Subramanian, A., Sericano, J.L., Wade, T.L., Knap, A.H., 2016. Edward D. Goldberg's proposal of "the mussel watch": reflections after 40 years. Mar. Pollut. Bull. 110 (1), 501–510. https://doi.org/10.1016/j.marpolbul.2016.05.074.
Firth, D.C., Auerswald, L., Strydom, P.E., Hoffman, L.C., 2023. The status of marine mussel pollution research in South Africa (2012–2022. Foods 12 (21), 3983. https://doi.org/10.3390/foods12213983.
Firth, D.C., O'Neill, B., Salie, K., Hoffman, L.C., 2019. Monitoring of organic pollutants in *Choromytilus meridionalis* and *Mytilus galloprovincialis* from aquaculture facilities in Saldanha Bay, South Africa. Mar. Pollut. Bull. 149, 110637. https://doi.org/10.1016/j.marpolbul.2019.110637.
Froese, R., Pauly, D., 2023. FishBase, World Wide Web electronic publication. ⟨www.fishbase.org/search.php⟩.
Gakuba, E., Moodley, B., Ndungu, P., Birungi, G., 2019. Evaluation of persistent organochlorine pesticides and polychlorinated biphenyls in Umgeni River bank soil, KwaZulu-Natal, South Africa. Water SA 45 (4), 592–607. https://doi.org/10.17159/wsa/2019.v45.i4.7540.
Girones, L., Oliva, A.L., Marcovecchio, J.E., Arias, A.H., 2020. Spatial distribution and ecological risk assessment of residual organochlorine pesticides (OCPs) in South American marine environments. Curr. Environ. Health Rep. 7, 147–160. https://doi.org/10.1007/s40572-020-00272-7.
Jones, K.C., De Voogt, P., 1999. Persistent organic pollutants (POPs): state of the science. Environ. Pollut. 100 (1-3), 209–221. https://doi.org/10.1016/S0269-7491(99)00098-6.
Kampire, E., Rubidge, G., Adams, J.B., Human, L., 2016. Congener profiles of polychlorinated biphenyls and the effect on marine mussels at an outfall site, Port Elizabeth, South Africa. Water SA 42 (3), 496–504. https://doi.org/10.4314/wsa.v42i3.16.
Kosker, A.R., Ozogul, F., Ayas, D., Durmus, M., Ucar, Y., 2019. Elemental composition of pufferfish species from Northeastern Mediterranean Sea. Environ. Monit. Assess. 191, 1–15.
Kushner, E.J., 1976. On determining the statistical parameters for pollution concentration from a truncated data set. Atmos. Environ. (1967) 10 (11), 975–979. https://doi.org/10.1016/0004-6981(76)90205-5.
Labuschagne, M., Wepener, V., Nachev, M., Zimmermann, S., Sures, B., Smit, N.J., 2019. The application of artificial mussels in conjunction with transplanted bivalves to assess elemental exposure in a platinum mining area. Water 12 (1), 32. https://doi.org/10.3390/w12010032.
León, V.M., Moreno-González, R., González, E., Martínez, F., García, V., Campillo, J.A., 2013. Interspecific comparison of polycyclic aromatic hydrocarbons and persistent organochlorines bioaccumulation in bivalves from a Mediterranean coastal lagoon. Sci. Total Environ. 463, 975–987. https://doi.org/10.1016/j.scitotenv.2013.06.075.
Li, Y.F., Macdonald, R.W., 2005. Sources and pathways of selected organochlorine pesticides to the Arctic and the effect of pathway divergence on HCH trends in biota: a review. Sci. Total Environ. 342 (1-3), 87–106. https://doi.org/10.1016/j.scitotenv.2004.12.027.
Liu, H., Hu, J., Tan, Y., Zheng, Z., Liu, M., Lohmann, R., Vojta, S., Katz, S., Liu, Y., Li, Z., Fang, Z., 2024. Identification of key anthropogenic and land use factors and ecological risk assessment of dissolved polycyclic aromatic hydrocarbons (PAHs) and organochlorine pesticides (OCPs) in an urbanized estuary in China. Mar. Pollut. Bull. 207, 116876. https://doi.org/10.1016/j.marpolbul.2024.116876.
Marinsek, G.P., Ribeiro, C.C., Gusso-Choueri, P.K., Choueri, R.B., de Souza Abessa, D.M., de Britto Mari, R., 2024. Multiple biomarkers in pufferfish as a proxy of environmental health in Brazilian marine protected areas. Sci. Total Environ. 914, 169742. https://doi.org/10.1016/j.scitotenv.2023.169742.
Olisah, C., Adams, J.B., Rubidge, G., 2021. The state of persistent organic pollutants in South African estuaries: a review of environmental exposure and sources. Ecotoxicol. Environ. Saf. 219, 112316. https://doi.org/10.1016/j.ecoenv.2021.112316.
Pech, D., Vidal-Martínez, V.M., Aguirre-Macedo, M.L., Gold-Bouchot, G., Herrera-Silveira, J., Zapata-Pérez, O., Marcogliese, D.J., 2009. The checkered puffer (*Spheroides testudineus*) and its helminths as bioindicators of chemical pollution in Yucatan coastal lagoons. Sci. Total Environ. 407 (7), 2315–2324. https://doi.org/10.1016/j.scitotenv.2008.11.054.
Phillips, D.J., Rainbow, P.S., 1994. Biomonitoring of Trace Aquatic Contaminants. Springer Science & Business Media vol. 37.
Porter, S.N., Humphries, M.S., Buah-Kwofie, A., Schleyer, M.H., 2018. Accumulation of organochlorine pesticides in reef organisms from marginal coral reefs in South Africa and links with coastal groundwater. Mar. Pollut. Bull. 137, 295–305. https://doi.org/10.1016/j.marpolbul.2018.10.028.
Ramírez-Ayala, E., Arguello-Pérez, M.A., Tintos-Gómez, A., Hernández-Anguiano, J.H., Pérez-Rodríguez, R.Y., Ilizaliturri-Hernández, C.A., Núñez-Nogueira, G., Sepúlveda-Quiroz, C.A., 2021. Persistent organic pollutants (POPs) in fish from two coastal lagoons of the central Mexican Pacific. Lat. Am. J. Aquat. Res. 49 (4), 663–670. https://doi.org/10.3856/vol49-issue4-fulltext-2639.
Ryan, P.G., Bouwman, H., Moloney, C.L., Yuyama, M., Takada, H., 2012. Long-term decreases in persistent organic pollutants in South African coastal waters detected from beached polyethylene pellets. Mar. Pollut. Bull. 64 (12), 2756–2760. https://doi.org/10.1016/j.marpolbul.2012.09.013.
Saadati, N., Abdullah, M.P., Zakaria, Z., Sany, S.B.T., Rezayi, M., Hassonizadeh, H., 2013. Limit of detection and limit of quantification development procedures for organochlorine pesticides analysis in water and sediment matrices. Chem. Central J. 7, 1–10.
Sazima, I., 2024. A pufferfish that scavenges on aquatic and terrestrial invertebrate and vertebrate carcasses. Ichthyol. Res. 1–5. https://doi.org/10.1007/s10228-024-00982-0.
Serdar, B., LeBlanc, W.G., Norris, J.M., Dickinson, L.M., 2014. Potential effects of polychlorinated biphenyls (PCBs) and selected organochlorine pesticides (OCPs) on immune cells and blood biochemistry measures: a cross-sectional assessment of the NHANES 2003-2004 data. Environ. Health 13, 1–12. https://doi.org/10.1186/1476-069X-13-114.
Stockholm Convention on persistent organic pollutants, convention text, 2001. United Nations Environment Programme, Geneva. ⟨http://www.pops.int/documents/convtext/convtext en.pdf.⟩.
Thompson, L.A., Darwish, W.S., Ikenaka, Y., Nakayama, S.M., Mizukawa, H., Ishizuka, M., 2017. Organochlorine pesticide contamination of foods in Africa: incidence and public health significance. J. Vet. Med. Sci. 79 (4), 751–764. https://doi.org/10.1292/jvms.16-0214.
Tolera, S.T., 2021. Adverse effect of pesticide on top ten importers of African countries: systematic review. EC. Pharmacol. Toxicol. 9, 61–79.
UNESCO, 1999. World Communication and Information 1999–2000 Report Published by United Nations Educational. Scientific and Cultural Organization. UNESCO.
Van den Berg, H., Manuweera, G., Konradsen, F., 2017. Global trends in the production and use of DDT for control of malaria and other vector-borne diseases. Malar. J. 16, 1–8. https://doi.org/10.1186/s12936-017-2050-2.
Van Der Spuy, L., Erasmus, J.H., Nachev, M., Schaeffner, B.C., Sures, B., Wepener, V., Smit, N.J., 2023. The use of fish parasitic isopods as element accumulation indicators in marine pollution monitoring. Mar. Pollut. Bull. 194, 115385. https://doi.org/10.1016/j.marpolbul.2023.115385.
Venkatesan, M.I., De Leon, R.P., Van Geen, A., Luoma, S.N., 1999. Chlorinated hydrocarbon pesticides and polychlorinated biphenyls in sediment cores from San Francisco Bay. Mar. Chem. 64 (1-2), 85–97. https://doi.org/10.1016/S0304-4203(98)90086-X.
Vogt, T., Pieters, R., Giesy, J., Newman, B.K., 2019. Biological toxicity estimates show involvement of a wider range of toxic compounds in sediments from Durban, South Africa than indicated from instrumental analyses. Mar. Pollut. Bull. 138, 49–57. https://doi.org/10.1016/j.marpolbul.2018.11.019.
Wang, T., Wei, X., Chen, T., Wang, W., Xia, X., Miao, J., Yin, S., 2019. Studies of the mechanism of fatty liver formation in *Takifugu fasciatus* following copper exposure. Ecotoxicol. Environ. Saf. 181, 353–361. https://doi.org/10.1016/j.ecoenv.2019.06.013.
Wepener, V., Degger, N., 2012. Status of marine pollution research in South Africa (1960–present. Mar. Pollut. Bull. 64 (7), 1508–1512. https://doi.org/10.1016/j.marpolbul.2012.05.037.
Wepener, V., Degger, N., 2019. South Africa. In: Sheppard, C. (Ed.), World Seas: An environmental evaluation, Volume 11: the Indian Ocean to the Pacific, second ed. Elsevier, London, pp. 101–119.
Wepener, V.W., Degger, N.D., 2020. Monitoring metals in South African harbours between 2008 and 2009, using resident mussels as indicator organisms. Afr. Zool. 55 (4), 267–277. https://doi.org/10.1080/15627020.2020.1799720.
WHO, 2011. The use of DDT in malaria vector control: WHO position statement on DDT. Available at: ⟨http://whqlibdoc.who.int/hq/2011/WHO_HTM_GMP_2011_eng.pdf⟩.
Wu, J., Kauhanen, P.G., Hunt, J.A., Senn, D.B., Hale, T., McKee, L.J., 2019. Optimal selection and placement of green infrastructure in urban watersheds for PCB control. J. Sustain. Water Built Environ. 5 (2), 04018019. https://doi.org/10.1061/JSWBAY.0000876.
Yu, H.Y., Bao, L.J., Liang, Y., Zeng, E.Y., 2011. Field validation of anaerobic degradation pathways for dichlorodiphenyltrichloroethane (DDT) and 13 metabolites in marine sediment cores from China. Environ. Sci. Technol. 45 (12), 5245–5252. https://doi.org/10.1021/es2006397.
Yuqi, L., Liya, W., Ningping, T., 2014. Analysis and evaluation of nutritional composition of farmed male pufferfish (Takifugu obscurus). In SHS Web of Conferences (Vol. 6, p. 03010). EDP Sciences. DOI:10.1051/shsconf/20140603010.

Appendix D:

Taxonomic reassessment of the opistholebetine opecoelid *Pseudoheterolebes cotylophorus* (Ozaki, 1935) Yamaguti, 1959, in South Africa.

Linda de Klerk[1], Russell Q-Y. Yong [1], Kerry A. Hadfield[1], and Nico J. Smit[1]

[1] Water Research Group, Unit for Environmental Sciences and Management, North-West University, 11 Hoffman Street, Potchefstroom 2520, South Africa.

Abstract

The taxonomic status of *Pseudoheterolebes cotylophorus* (Ozaki, 1935) Yamaguti, 1959 (Opecoelidae: subfam. Opistholebetinae) has been a subject of taxonomic confusion since its initial description by Ozaki in 1935 as *Opistholebes cotylophorus* Ozaki, 1935. The species' current recognised classification dates back to Yamaguti's reclassification of *O. cotylophorus* as *Pseudoheterolebes cotylophorus*; however, doubts persist regarding this classification and the validity of this species. The species was reported by Bray in 1986 from off the coast of South Africa, infecting the evileye blaasop *Amblyrhynchote honckenii* (Bloch) (Tetraodontidae). Recent parasitological assessments of South African marine fishes have resulted in the recollection of this taxon from the same host species, allowing for a reassessment of its status. Morphological and molecular phylogenetic analyses, incorporating ITS2 and 28S rDNA, as well as COI and *nad*1 mtDNA sequence data, confirmed that the South African *P. cotylophorus* is conspecific with *Opistholebes amplicoelus* Nicoll, 1915, resolving decades of uncertainty and demonstrating the critical role of molecular techniques in identifying marine parasites.

Keywords: Taxonomic uncertainties, Morphology, Molecular characterisation, Taxonomic clarification, Biodiversity

Introduction

Opistholebetine trematodes of the family Opecoelidae represent a morphologically diverse yet taxonomically complex group of marine parasites. Despite their global distribution, their true diversity remains substantially underestimated, particularly in regions such as South Africa. To date, only two of the 114 (approximately 2 %) valid opistholebetine species have been reported from the South African coastline (WoRMS 2025), pointing to a significant gap in our understanding of their taxonomy, biogeography, and ecological roles within local marine ecosystems. This underrepresentation likely stems from limited historical sampling efforts and persistent difficulties in resolving taxonomic uncertainties (Cribb *et al*. 2025).

Among this limited representation, *Pseudoheterolebes cotylophorus* (Ozaki, 1935) Yamaguti, 1959 has been subject to taxonomic confusion, with a complex history dating back to its initial description (Martin *et al*. 2018a). Following its original description as *Opistholebes cotylophorus* Ozaki, 1935 from the diodontid fish *Diodon holocanthus* Linnaeus, in Japan (Ozaki 1935), this species has undergone multiple

reassignments and misidentifications, contributing to its ambiguous status (Yamaguti 1959; Manter and Prichard 1962; Martin *et al*. 2018a). Yamaguti (1959) proposed the genus *Pseudoheterolebes* Yamaguti, 1959 nec Gupta, 1968, based on the presence of distinctive tegument folds surrounding the ventral sucker, and designated *O. cotylophorus* as the type species of the genus, as *Pseudoheterolebes cotylophorus*. This reassignment was contested by Manter and Pritchard (1962), who prioritised internal morphological features, particularly gonad arrangement, as more reliable taxonomic traits for taxonomic classification, and returned the species to *Opistholebes* Nicoll, 1915. In 1986, Bray reported *O. cotylophorus* from the evileye blaasop, *Amblyrhynchote honckenii* (Bloch) (Tetraodontidae), from Algoa Bay, off the coast of South Africa. Later, Martin *et al*. (2018a) resurrected the genus *Pseudoheterolebes* to accommodate *O. cotylophorus* (now *P. cotylophorus*) along with four other species. However, they noted that Bray's material appeared to be more consistent with species of *Opistholebes*, and suggested that it represents *Opistholebes amplicoelus* Nicoll, 1915, *O. microovus* Ku and Shen, 1965 or potentially a new species (Martin *et al*. 2018a). The identity of this South African tetraodontid-infecting opistholebetine hence remains unresolved.

These ongoing taxonomic challenges highlight the difficulty of distinguishing between closely related opistholebetine species and the limitations of traditional morphology-based taxonomy in this group (Martin *et al*. 2018b). These uncertainties impact our understanding of host specificity, parasite distribution, and evolutionary patterns in marine ecosystems (Cribb *et al*. 2025). Molecular systematics, using ribosomal (ITS2, 28S rDNA) and mitochondrial (COI, *nad*1 mtDNA) markers, has become a key tool in resolving these ambiguities and clarifying species identities and evolutionary relationships (Bray *et al*. 2016; Fayton and Andres 2016; Martin *et al*. 2018b). These methods are particularly effective in addressing the challenges posed by ambiguous or convergent morphological traits (Martin *et al*. 2018b). Given these challenges, the present study aimed to reassess the identity of *P. cotylophorus sensu* Bray (1986) from *A. honckenii* off the south coast of South Africa. Information on species of *Opistholebes* and *Pseudoheterolebes*, including host records, geographical distribution, and available GenBank data, was compiled for comparison of the genera (see Table 1). By refining generic classifications and integrating morphological and molecular approaches, this study will advance knowledge of Opistholebetinae systematics, highlighting the importance of combining traditional morphological methods with modern molecular tools to address species diversity and improve species identification within marine parasitic taxa.

Appendix D

Table 1 Updated information for species of *Opistholebes* Nicoll, 1915 and *Pseudoheterolebes* Yamaguti, 1959 nec Gupta, 1968, with information on host species, host families, distribution, and available GenBank data. Abbreviations: **Syn** – synonym; **TH** – type host; **TLOC** – type locality

Species	Host family	Host species	Distribution	ITS2	28S	COI	References
Genus *Opistholebes* Nicoll, 1915							
O. amplicoelus Nicoll, 1915 **Syns:** *Heterolebes buckleyi* (Gupta, 1968) Cribb, 2005; *H. dongshanensis* Liu, 1999; *O. buckleyi* Gupta, 1968; *O. dongshanensis* Liu, 1999; *O. indicus* Gupta, 1968; *O. tetraodontis* Gupta, 1968	Tetraodontidae	**TH:** *Lagocephalus lunaris* (Bloch and Schneider) *Dichotomyctere nigroviridis* (Marion de Procé); *Arothron manilensis* (Marion de Procé); *Tetractenos hamiltoni* (Richardson)	**TLOC:** Cleveland Bay, Australia China; India; Moreton Bay, Australia; Green Island, Australia; Fisherman's Island, Australia; Bramble Bay, Australia; Peel Island, Australia	✓	✓	✓	Nicoll, 1915; Krishna and Sreeramulu, 1993; Olson *et al*., 2003; Martin *et al*., 2018a
O. microovus Ku & Shen, 1965	Tetraodontidae	**TH:** *Takifugu niphobles* (Jordan and Snyder)	**TLOC:** Taiwan, China	-	-	-	Ku and Shen, 1965 Martin *et al*., 2018a
Genus *Pseudoheterolebes* Yamaguti, 1959 nec Gupta, 1968							
P. adcotylophorus (Manter, 1947) Martin, Ribu, Cutmore & Cribb, 2018 **Syn:** *O. adcotylophorus* Manter, 1947	Diodontidae	**TH:** *Diodon holocanthus* Linnaeus	**TLOC:** Dry Tortugas, Florida, U.S.A.	-	-	-	Manter, 1947; Martin *et al*., 2018a
P. corazonae Martin, Ribu, Cutmore & Cribb, 2018	Diodontidae	**TH:** *Diodon nicthemerus* Cuvier	**TLOC:** Stanley, Tasmania	-	-	-	Martin *et al*., 2018a
P. cotylophorus (Ozaki, 1935) Yamaguti, 1959 **Syn:** *O. cotylophorus* Ozaki, 1935	Diodontidae Tetraodontidae	**TH:** *Diodon holocanthus* Linnaeus *Chilomycterus reticulatus* (Linnaeus); *Takifugu niphobles* (Jordan and Snyder); *Amblyrhynchote honckenii* (Bloch)	**TLOC:** Japan Shirahama, Japan; Algoa Bay, South Africa	-	-	-	Ozaki, 1935; Ozaki, 1937; Yamaguti, 1959; Bray, 1986;
P. diodontis (Cable, 1956) Martin, Ribu, Cutmore & Cribb, 2018 **Syn:** *O. diodontis* Cable, 1956	Diodontidae	**TH:** *Diodon hystrix* Linnaeus *D. liturosus* Shaw	**TLOC:** Puerto Rico Curacao; Jamaica; Hawaii; Arabian Sea off Karachi, Pakistan; Heron Island, southern Great Barrier Reef, Queensland; Lizard Island, northern Great Barrier Reef.	✓	✓	✓	Cable, 1956; Martin *et al*., 2018a
P. stellaglobulus Martin, Ribu, Cutmore & Cribb, 2018	Diodontidae	**TH:** *Dicotylichthys punctulatus* Kaup	**TLOC:** Green Island, Moreton Bay, southeast Queensland, Australia. Mud Island, Wellington Point; Dunwich, North Stradbroke Island.	✓	✓	✓	Martin *et al*., 2018a

Materials and methods

Collection of specimens

A total of seventy-four specimens of *A. honckenii* were collected using rod and reel from seven coastal locations along the South African coastline, arranged from west to east in Table 2. The table lists each sampling location with corresponding geographic coordinates, the number of individual fish collected, sampling periods, and the approximate distance of each site relative to the Swartkops River Estuary, Algoa Bay, which serves as a geographic reference point as the original location where *P. cotylophorus* was first reported by Bray in 1986 (see Table 1–2; Fig. 1). Following capture, the fish were transported in aerated containers to a nearby field station for dissection. Each specimen was identified, photographed, weighed, measured, and humanely killed by percussive stunning followed by spinal severance and pithing, according to the standard operating procedure approved by the North-West University Ethics Committee (NWU-00267-17-A5). Fish nomenclature follows FishBase (Froese and Pauly 2025). Ethical approval for this project was received from the AnimCare Research Ethics Committee of North-West University (NWU-00565-19-A5). Permits for the collection of *A. honckenii* for research were issued by the South African Department of Agriculture, Forestry and Fisheries (permit nos.: RES2020-29; RES2022-44; RES2022-86; and RES2025-16) and Cape Nature (permit no. CN44-87-18289).

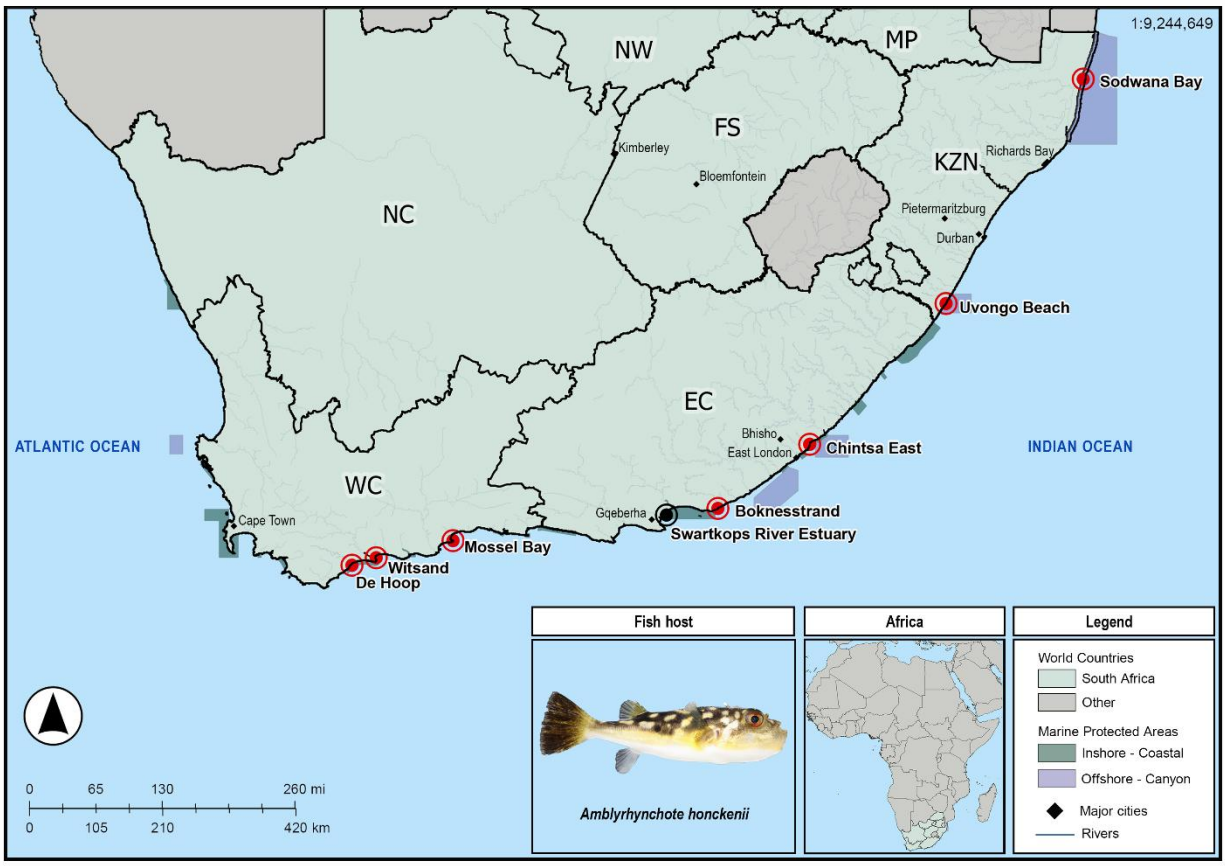

Fig. 1 Map indicating the sampling localities (red circles) of specimens of *Amblyrhynchote honckenii* (Bloch). The black circle indicate the original sampling locality (Swartkops River Estuary, Algoa Bay) of *A. honckenii* by Bray, 1986.

Appendix D

Table 2 Summary of *Amblyrhynchote honckenii* (Bloch) specimen collections along the South African coastline. The table details each sampling location with geographic coordinates, the number of fish collected, the prevalence of infection, the sampling periods, and the approximate distance of each location relative to the Swartkops River Estuary, Algoa Bay, which serves as the geographic reference point of the original collection locality of *Pseudoheterolebes cotylophorus* (Ozaki, 1935) Yamaguti, 1959

Location	GPS coordinates	No. of fish (infected)	No. of *Opistholebes amplicoelus* specimens per fish	Distance relative to the Swartkops River estuary, Algoa Bay	Sampling period
De Hoop Nature Reserve, Western Cape	-34.48° S, 20.51° E	1 (1)	8	475 km west	Nov 2021
Breede River estuary at Witsand, Western Cape	-34.40° S, 20.84° E	15 (6)	3–12	445 km west	Nov 2021
Mossel Bay, Western Cape	-34.18° S, 22.15° E	10 (0)	-	323 km west	Mar 2022
Boknesstrand, Eastern Cape	-33.73° S, 26.58° E	2 (2)	2–6	90 km east	Apr 2025
Chintsa East, Eastern Cape	-32.84° S, 28.12° E	18 (4)	1–13	230 km east	Oct 2020; Jul 2022
Uvongo Beach, KwaZulu-Natal	-30.84° S, 30.40° E	10 (0)	-	560 km east	Dec 2022
Sodwana Bay, iSimangaliso National Park, KwaZulu-Natal	-27.54° S, 32.68° E	10 (0)	-	974 km northeast	Sept 2022

Morphological analyses

After euthanasia, the internal organs of each fish were carefully removed and examined for parasites using a Zeiss Stemi 305 compact stereomicroscope (Zeiss, Oberkochen, Germany). Digenean trematodes were carefully removed with fine needles, fixed in hot saline, and preserved in 80% ethanol for further analysis. Six specimens were selected for detailed morphological examination. These specimens were rehydrated, stained with Mayer's haematoxylin, destained with 1% hydrochloric acid, neutralised in 1% ammonia, dehydrated in a graded ethanol series, cleared in methyl salicylate and permanently mounted on slides using Canada balsam. Observations were made using a Nikon Y-TV55 camera mounted on a Nikon ECLIPSE Ni light microscope (Nikon, Tokyo, Japan). Measurements and photographs for each species were captured using Image-Pro Express software (Nikon, Japan). Morphological characterisation of the specimens, including measurements of internal organs and body structures, followed Martin *et al*. (2018a). Measurements are presented in tabular form (Table 3), with each value shown as a range, followed by the mean in parentheses. All measurements are in micrometres (µm), unless otherwise stated. Detailed drawings were created using a drawing tube attached to the microscope and digitised with Adobe Photoshop v. 23.0.1.

Voucher specimens and type series were deposited in the British Museum of Natural History, London, United Kingdom (BMNH), the Parasite Collection at the National Museum (NMB) in Bloemfontein, South Africa, and the Iziko South African Museum (SAM) in Cape Town, South Africa.

Molecular analyses

Genomic DNA was extracted from a total of 11 specimens, including five syngenophores *sensu* Pleijel *et al*. (2008) collected across four locations: De Hoop Nature Reserve (n=3), the Breede River Estuary at Witsand (n=3), Boknesstrand (n=2), and Chintsa East (n=3). Extractions were performed using the PCRBiosystems Rapid DNA Extraction Kit, following the manufacturer's instructions with slight modifications. Specifically, 10 µL of lysis buffer and 5 µL of proteinase K-containing buffer were used, and the final extracted DNA was diluted to a volume of 300 µL. Subsequent gene amplification targeted the ITS2 and partial 28S regions of ribosomal DNA (rDNA) and the COI and *nad*1 regions of mitochondrial DNA (mtDNA) (primers and thermocycling profiles used for amplification are listed in Table 4). Successful PCR amplifications were confirmed by electrophoresis on 1% agarose gels. Verified products were then submitted to Inqaba Biotechnical Industries (Pty) Ltd. in Pretoria, South Africa, for purification and sequencing.

Sequences were assembled, aligned, edited and trimmed using Geneious Prime version 2024.0.7 (Biomatters, Auckland, New Zealand). Additionally, the nucleotide Basic Local Alignment Search Tool (BLAST) was used to support identification of sequence affiliations and outgroup selections (Table 5). ITS2 rDNA, partial 28S rDNA, and COI mtDNA sequences were used to confirm the species-level identity of the sequenced specimens, as no comparable sequences were available for the *nad*1 mtDNA region.

The COI mtDNA sequences, in combination with the *nad*1 mtDNA sequences, were used to construct haplotype networks and assess population-level trends for the South African specimens. Partial

28S rDNA sequences were aligned with those of Opistholebetinae species for which sequence data were available on GenBank. *Neolebouria georgiensis* Gibson, 1976, was used as the outgroup taxon for the 28S rDNA phylogenetic analyses. Alignments were constructed, generated and trimmed using default parameters of MAFFT version 7.490 (Katoh *et al*. 2002; Katoh and Stanley 2013) on the Geneious Prime platform v 2024.0.7 (Kearse *et al*. 2012). The COI mtDNA dataset was translated and inspected in Mesquite v 3.03 (Maddison and Maddison 2017) for stop codons per Huston *et al*. (2021), tested for non-stationarity caused by base composition bias using the χ^2 test function on PAUP* (Swofford 2002) and for substitution saturation using Xia's test function on DAMBE 7 (Xia 2018). No base composition bias was detected on any codon positions (P = 1.00 for all codon positions), nor any substitution saturation (I_{ss} = 0.0318; $I_{ss.c}$ = 0.7099). Genetic differences across all sequenced specimens and DNA regions were calculated on the Geneious Prime platform, with results shown as percentage similarities and number of base-pair differences (Tables 6–9).

The optimal nucleotide substitution model for each dataset was estimated using the Akaike Information Criterion (AIC) in jModelTest 2.1.4 (Posada 2008; Darriba *et al*. 2012). The general time-reversible model with invariant sites and gamma-distributed rate variation (GTR+I+G) was recommended for the 28S rRNA and COI analyses. Phylogenetic analyses were performed using Maximum Likelihood (ML) and Bayesian Inference (BI) methods with this suggested model. BI analyses were conducted on Geneious Prime version 2024.0.7, the CIPRES Science Gateway version 3.3 (Miller *et al*. 2010) using MrBayes version 3.2.7a (Ronquist *et al*. 2012), with 2 independent Markov Chain Monte Carlo (MCMC) runs of 4 chains for 10 million generations, sampling every 1000 generations, and a burn-in of the first 25000 generations. ML analyses were performed using PhyML version 3.0 (Guindon *et al*. 2010) on the ATGC bioinformatics platform, with model parameters estimated and 1000 bootstrap repetitions for nodal support. The resulting phylogenetic trees from BI and ML analyses were visualised using TreeViewer version 2.2.0 (Bianchini and Sánchez-Baracaldo 2024).

For the haplotype network analyses, two alignments were constructed: one using COI mtDNA sequences for the South African taxa and *Opistholebes amplicoelus* from Moreton Bay, Australia; the other a concatenated alignment of COI and *nad*1 mtDNA sequences from the South African specimens. As *nad*1 mtDNA sequence data for *O. amplicoelus* from Australia were not available, the analyses were performed separately. Alignments were generated using the MUSCLE algorithm in MEGA 7 (Kumar *et al*. 2016), with UPGMA clustering applied during iterations 1 and 2. Haplotypes were identified and assigned using DnaSP v6.12 (Rozas *et al*. 2017), and haplotype networks were constructed and visualised using the Median-Joining Network function in PopART v1.7 (Leigh and Bryant 2015).

Results

Specimens of opistholebetine trematodes from *A. honckenii* were recovered from four localities: De Hoop Nature Reserve, the Breede River Estuary at Witsand, Boknesstrand, and Chintsa East. Assessments of fish from off Mossel Bay, Uvongo Beach and Sodwana Bay did not yield any specimens of opistholebetine trematodes. Morphological measurements of the newly collected specimens are presented in Table 3 along with published metrical data for all valid species of *Opistholebes* and

Pseudoheterolebes. A combination of morphometric and molecular phylogenetic comparisons confirmed the identity of these specimens as *Opistholebes amplicoelus*.

Taxonomic summary

***Opistholebes amplicoelus* Nicoll, 1915 (Fig. 2)**

Synonyms: *Heterolebes buckleyi* (Gupta, 1968) Cribb, 2005; *H. dongshanensis* Liu, 1999; *O. buckleyi* Gupta, 1968; *O. dongshanensis* Liu, 1999; *O. indicus* Gupta, 1968; *O. tetraodontis* Gupta, 1968.

Type-host: *Lagocephalus lunaris* (Bloch & Schneider) (Tetraodontiformes: Tetraodontidae).

Type-locality: Cleveland Bay, Australia.

Other records: Ex *L. lunaris* from China by Liu (1999); *L. lunaris* from off Visakhapatnam, India by Krishna and Sreeramulu (1993) (as *O. tetraodontis* Gupta, 1968); *L. lunaris* from Moreton Bay, off North Stradbroke Island, Australia by Martin *et al*. (2018a); *Dichotomyctere nigroviridis* (Marion de Procé) from off Madras and Mumbai, India by Gupta (1968) (as *O. indicus* Gupta, 1968 and *O. tetraodontis*); *Tetractenos hamiltoni* (Richardson) from off North Stradbroke Island, Australia by Olson *et al*. (2003) and Martin *et al*. (2018a); *Arothron manilensis* (Marion de Procé) from off Peel Island, Moreton Bay, Australia by Martin *et al*. (2018a); *A. honckenii* from Algoa Bay, South Africa by Bray (1986).

New localities: De Hoop Nature Reserve, Western Cape, South Africa (-34.48°S, 20.51°E); Breede River Estuary, Witsand, Western Cape, South Africa (-34.40°S, 20.84°E); Boknesstrand, Eastern Cape, South Africa (-33.73°S, 26.58°E); Chintsa East, Eastern Cape, South Africa (-32.84°S, 28.12°E).

New material: Voucher specimens ex *A. honckenii* collected from De Hoop Nature Reserve (XX–XX, including one syngenophore XX); Breede River Estuary, Witsand (XX–XX, including two syngenophores XX and XX); Boknesstrand (XX–XX, including two syngenophores XX and XX), Chintsa East (XX–XX, including two syngenophores XX and XX).

Site in host: Intestine.

Representative DNA sequences: ITS2 rDNA: Five identical replicates of 428 bp (one from De Hoop Nature Reserve, and two each from Chintsa East and Boknesstrand), one submitted to GenBank (XX); 28S rDNA: Three identical replicates of 1,250–1,268 bp (one from De Hoop Nature Reserve, and two from Chintsa East), one submitted to GenBank (XX); COI mtDNA: eleven sequences of 475–790 bp comprising three genotypes (three each from De Hoop Nature Reserve, Witsand, and Chintsa East, and two from Boknesstrand), three submitted to GenBank (XX); *nad*1 mtDNA: ten sequences of 474 bp comprising two genotypes (three each from De Hoop Nature Reserve, Witsand, and Chintsa East, and one from Boknesstrand), two submitted to GenBank (XX).

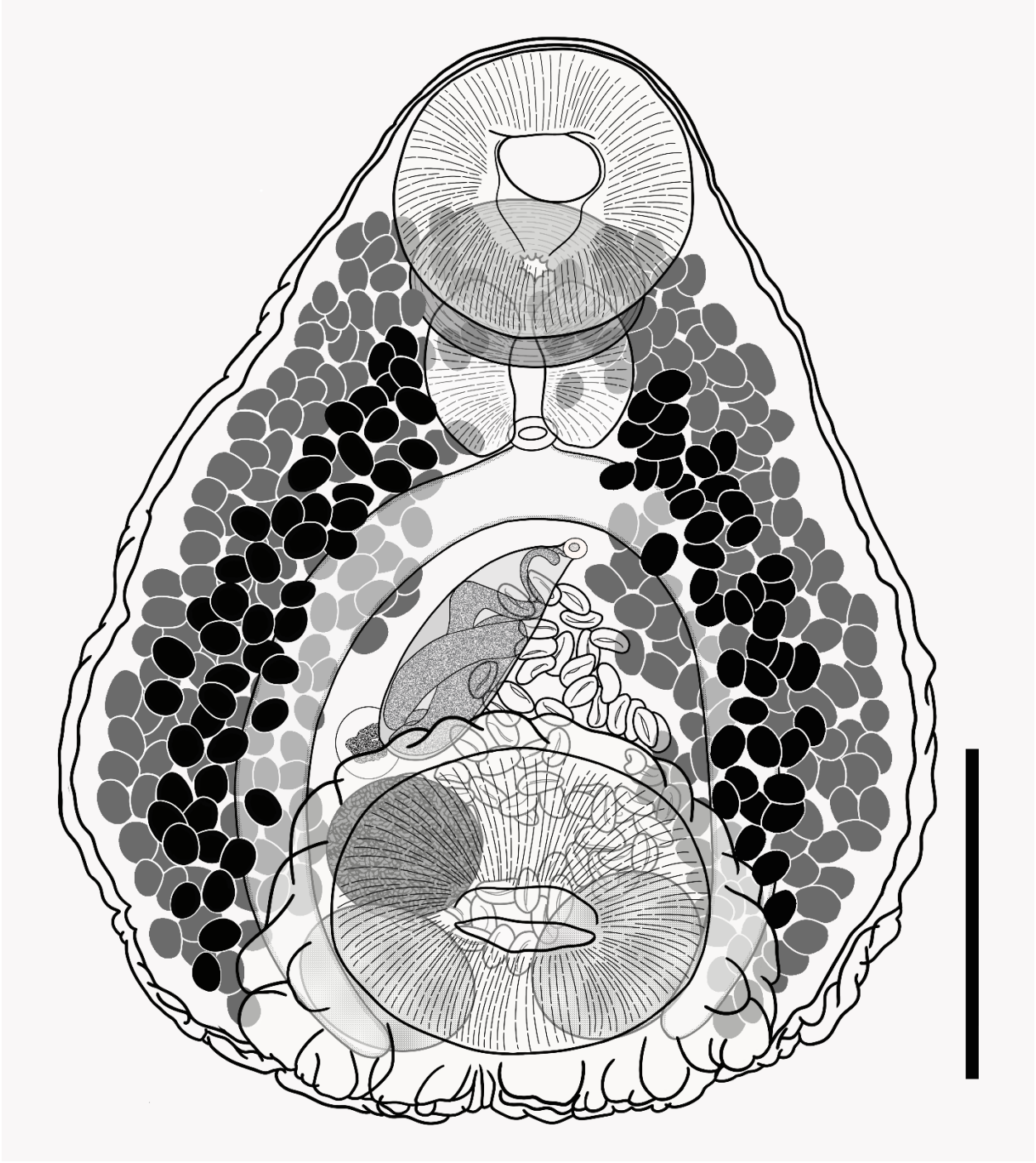

Fig. 2 Illustration of an adult voucher specimen (NMB XX) of *Opistholebes amplicoelus* from the evileye blaasop, *Amblyrhynchote honckenii* (Bloch), from Chintsa East, South Africa. Scale bar: 500µm

Appendix D

Table 3 Morphometric information for *Opistholebes amplicoelus* Nicoll, 1915 from this study and from literature, and *Pseudoheterolebes cotylophorus* (Ozaki, 1935) and *Opistholebes microovus* Ku & Shen, 1965 from literature. Entries marked with "*" (in reference) represent original descriptions. Information is presented as the range, followed by the mean. All measurements are in micrometres. Abbreviations: **L**, length; **W**, width; **B**, body; **FB**, forebody; **OS**, oral sucker; **VS**, ventral sucker; **Ph**, pharynx; **RT**, right testis; **LT**, left testis; **Ov**, ovary; **CS**, cirrus-sac; **GP**, genital pore

Species	***O. amplicoelus***	*O. amplicoelus*	*O. amplicoelus*	*O. amplicoelus* (as *P. cotylophorus*)	*O. amplicoelus*	*O. amplicoelus* (as *O. buckleyi)*	*O. amplicoelus* (as *O. indicus*)	*O. amplicoelus* (as *O. tetraodontis*)	*O. amplicoelus* (as *Heterolebes dongshanensis*)	*P. cotylophorus*	*P. cotylophorus*	*P. cotylophorus*	*O. microovus*
Reference	**Present study**	Nicoll (1915) *	Martin *et al.* (2018a)	Bray (1986)	Zhukov (1977)	Gupta (1968)	Gupta (1968)	Gupta (1968)	Liu (1999)	Ozaki (1935) *	Ozaki (1937)	Yamaguti (1959)	Ku & Shen (1965)
Host family	**Tetraodontidae**	Tetraodontidae	Tetraodontidae	Tetraodontidae	Tetraodontidae	Tetraodontidae	Tetraodontidae	Tetraodontidae	Tetraodontidae	Diodontidae	Diodontidae	Diodontidae	Tetraodontidae
Location	**South Africa**	Moreton Bay, Australia	Moreton Bay, Australia	Algoa Bay, South Africa	Madras, India	Mumbai, India	Madras, India	Mumbai, India	Dongshan, China	Japan	Okinawa Island, Yakushima & Hiroshima, Japan	Hawaii	Weihai, China
BL	**954–1,679 (1,349)**	2,000	612–1,393 (1,036)	1220	930	735–975	1,210–1,950	890–937	960–1,600 (1,340)	2,900–3,800	800–3,800	2,100–2,800	1,620–2,739
BW	**716–1,330 (1,021)**	1,300	406–1,096 (761)	780	720	555–875	630–1,270	574–688	690–1,130 (884)	2,300–3,600	600–2,300	2,300–2,800	1,136–1,837
BL/ BW	**1.06–1.52 (1.31)**	-	1.08–1.74 (1.37)	1.56	-	-	-	-	-	1.06–1.26	-	-	1.43–1.49
FBL	**689–1,219 (948)**	-	444–994 (764)	-	-	-	-	-	-	-	-	-	-
FBL/BL (%)	**58–78 (69)**	-	67–79 (74)	-	-	-	-	-	-	-	-	-	-
OSL	**248–482 (349)**	-	165–285 (220)	300	200	116 –120	75–215	118–130	184–240 (210)	-	-	200–300	317–434
OSW	**223–474 (344)**	280	163–561 (233)	300	140	125–140	150–315	135–156	176–272 (227)	-	-	300–420	418–501
OSW/L	**0.78–1.22 (0.99)**	-	0.89–2.07 (1.05)	1	-	-	-	-	-	-	-	-	1.15–1.32
VSL	**231–458 (341)**	-	154–321 (238)	280	170	180–185	180–375	153–162	192–280 (224)	-	-	500–680	198–578
VSW	**313–564 (441)**	340	229–408 (290)	400	220	187–190	135–285	197–220	216–316 (261)	-	600–800	560–730	578–957
VSW/ L	**1.09–1.53 (1.31)**	-	1.01–1.53 (1.23)	1.43	-	-	-	-	-	1.5	-	-	1.66–2.92
VSL/OSL	**0.91–1.06 (0.98)**	-	0.81–1.26 (1.08)	0.93	-	-	-	-	-	-	-	-	0.62–1.33
VSW/OSW	**1.16–1.42 (1.30)**	-	0.65–1.48 (1.28)	1.33	-	1.5	-	-	-	-	-	-	1.38–1.91
PhL	**168–302 (230)**	170	95–241 (155)	160	110	135–150	75–180	77–91	104–160 (129)	-	-	170–220	334–434
PhW	**177–315 (234)**	220	119–208 (155)	200	120	135–165	90–225	128–160	136–176 (158)	-	-	260–380	418–501
PhW/L	**0.87–1.13 (1.02)**	-	0.75–1.47 (1.02)	1.25	-	-	-	-	-	-	-	-	1.15–1.25
OSL/PhL	**1.28–1.80 (1.52)**	-	1.13–1.85 (1.44)	1.88	-	-	-	-	-	-	-	-	0.95–1
OSW/PhW	**1.17–1.79 (1.46)**	-	1.23–3.03 (1.5)	1.50	-	-	-	-	-	-	-	-	1
RTL	**170–286 (213)**	180	82–288 (154)	140	-	120–135	150–180	146–160	112–184 (152)	-	-	200–300	150–434
RTW	**162–204 (185)**	220	107–223 (157)	180–200	-	105–115	180–225	135–164	128–208 (174)	-	200–350	270–380	284–367
RTW/L	**0.71–0.96 (0.89)**	-	0.67–1.37 (1.05)	1.29–1.43	-	-	-	-	-	-	-	-	0.83–1.89
LTL	**164–274 (196)**	180	97–241 (152)	140	-	-	195–225	163–175	120–184 (150)	-	-	200–300	150–434
LTW	**139–187 (172)**	220	99–273 (157)	180–200	-	-	210–255	147–182	120–192 (165)	-	200–350	270–380	284–367

LTW/L	**0.68–0.87 (0.89)**	-	0.66–2.31 (1.06)	1.29–1.43	-	-	-	-	-	-	-	-	0.83–1.89
LTL/RTL	**0.89–1.01 (0.95)**	-	0.84–1.49 (1.01)	1	-	-	-	-	-	-	-	-	1
LTW/RTW	**0.85–1.13 (0.93)**	-	0.69–1.86 (1.01)	1	-	-	-	-	-	-	-	-	1
OvL	**108–260 (184)**	160	77–187 (120)	160	-	-	105–135	129–134	120–184 (153)	-	280–360	160–200	200–401
OvW	**122–326 (201)**	220	75–209 (138)	200	-	-	120–210	75–125	144–240 (192)	-	170–220	220–340	200–443
CSL	**200–442 (295)**	450	116–365 (235)	280	-	120–300	270–420	164–209	204–320 (258)	-	-	-	83
CSW	**66–141 (113)**	125	55–158 (108)	80	-	75–120	-	68–72	96–114 (108)	-	-	-	-
CSL/BL (%)	**19–28 (22)**	-	14–37 (23)	23	-	-	-	-	-	-	-	-	3–5
PreGP/BL (%)	**37–67 (51)**	-	37–67 (49)	-	-	-	-	-	-	-	-	-	-
GP-VS/BL (%)	**5–22 (19)**	-	19–59 (30)	-	-	-	-	-	-	-	-	-	-
Egg L**	**60–65 (63)**	65–70	51–67 (57)	73–80	58	60	60	49–61	58–68 (61)	62–64	70–77	78–86	44–59
Egg W **	**34–39 (38)**	30	27–40 (33)	35–42	29–33	30	45	21–33	31–38 (34)	40–42	47–52	46–62	22–36

** Egg measurements represent the average of multiple subsamples per specimen.

Table 4 List of primers used for DNA amplification and sequencing in this study

Gene Regions	Primers	Sequences	Sources	Thermocycling profile reference
*nad*1	NDJ11	5′-AGA TTC GTA AGG GGC CTA ATA-3′	Kostadinova *et al*. (2003)	Kostadinova *et al*. (2003)
	NDJ2a	5'-CTT CAG CCT CAG CAT AAT-3'	Kostadinova *et al*. (2003)	
ITS2	3S	5'-GGT ACC GGT GGA TCA CGT GGC TAG TG-3'	Morgan and Blair (1995)	Yong *et al*. (2016)
	ITS2.2	5'-CCT GGT TAG TTT CTT TTC CTC CGC-3'	Cribb *et al*. (1998)	
28S	LSU5	5'-TAG GTC GAC CCG CTG AAY TTA AGC A-3'	Littlewood (1994)	Yong *et al*. (2016)
	300F (sequencing only)	5'-CAA GTA CCG TGA GGG AAA GTT G-3'	Littlewood *et al*. (1999)	
	ECD2 (sequencing only)	5'-CCT TGG TCC GTG TTT CAA GAC GGG-3'	Littlewood *et al*. (1997)	
	1500R	5'-GCT ATC CTG AGG GAA ACT TCG-3'	Snyder and Tkach (2001)	
COI	Digcox1Fa	5′-ATG ATW TTY TTY TTY YTD ATG CC-3′	Wee *et al*. (2017)	Vermaak *et al*. (2023)
	Digcox1R	5′-TCN GGR TGH CCR AAR AAY CAA AA-3′	Wee *et al*. (2017)	
	DICE1F	5’-ATT AAC CCT CAC TAA ATT WCN TTR GAT CAT AAG-3’	Moszczynska *et al*. (2009)	Wee *et al*. (2017)
	DICE14R	5'-TAA TAC GAC TCA CTA TAC CHA CMR TAA ACA TAT GAT G-3'	Van Steenkiste *et al*. (2015)	

Appendix D

Table 5 List of GenBank Opistholebetinae sequences included in the phylogenetic analyses. The taxa in bold fonts are sequences generated from the present study. *Neolebouria georgiensis* Gibson, 1976 (in the grey shade) was used as the outgroup for the 28S rDNA alignment and phylogenetic analyses

Taxon	Host	Locality	Accession numbers				Sources
			ITS2	28S	COI	*nad*1	
Gaevskajatrema perezi	*Unidentified fish host*	France	AJ241800	AF184255	-	-	Tkach *et al*. (2001)
Heterolebes maculosus	*Diodon hystrix*	Australia	MH933871	MH933878	-	-	Martin *et al*. (2018a)
Maculifer diodontis	*Diodon hystrix*	Australia	MH933873	MH933879	-	-	Martin *et al*. (2018a)
Macvicaria bartolii	*Diplodus annularis*	Tunisia	KR149471	KR149465	-	-	Antar *et al*. (2015); Rima *et al*. (2017)
Macvicaria crassigula	*Calamus bajonado*	Mexico	MF166834	KJ701237	-	-	Andres *et al*. (2014)
Macvicaria dubia	*Oblada melanura*	Tunisia	KR149488	KR149470	-	-	Antar *et al*. (2015)
Macvicaria gibsoni	*Diplodus vulgaris*	Algeria	MF166830	MF166845	-	-	Rima *et al*. (2017)
Macvicaria maamouriae	*Lithognathus mormyrus*	Tunisia	KR149474	KR149468	-	-	Antar *et al*. (2015)
Macvicaria mormyri	*Sparus aurata;* Unidentified fish host	France	MF166839	AF184256	-	-	Tkach *et al*. (2001); Rima *et al*. (2017)
Macvicaria obovata	*Cyclope neritea*	Spain	JQ694145	JQ694147	-	-	Born-Torrijos *et al*. (2012)
Magnaosimum brooksae	*Tripodichthys angustifrons*	Australia	MG813905	MG813907	-	-	Martin *et al*. (2018b)
Opistholebes amplicoelus	*Lagocephalus lunaris; Tetractenos hamiltoni*	Australia	MH933868	MH933875	MH933883; MH933884; MH933885; MH933886; MH933887; MH933888	-	Martin *et al*. (2018a)
Opistholebes amplicoelus	***Amblyrhynchote honckenii***	**South Africa**	**XXX**	**XXX**	**XXX; XXX; XXX;**	**XXX; XXX**	**Present study**
Paralellolebes virilis	*Meuschenia hippocrepis*	Australia	MH933874	MH933880	-	-	Martin *et al*. (2018a)
Peracreadium idoneum	*Anarhichas lupus*	UK	-	AY222209	-	-	Olsen *et al*. (2003)
Propycnadenoides philippinensis	*Gymnocranius grandoculis*	Australia	-	KU320604	-	-	Bray *et al*. (2016)
Pseudoheterolebes diodontis	*Diodon liturosus; Diodon hysterix*	Australia	MH933869	MH933876	-	-	Martin *et al*. (2018a)
Pseudoheterolebes stellaglobulus	*Dicotylichthys punctulatus*	Australia	MH933870	MH933877	-	-	Martin *et al*. (2018a)
Pseudopycnadena fischtali	*Diplodus vulgaris*	Algeria	MF166841	MF166851	-	-	Rima *et al*. (2017)
Neolebouria georgiensis	*Parachaenichthys charcoti*	Ukraine	-	ON123036	-	-	Faltýnková *et al*. (2022)

Appendix D

Table 6 Nucleotide comparison of partial ITS2 rDNA sequences of Opistholebetinae, based on a 433 bp alignment.

	Number of bases/ residues which are not identical																		
	***O. amplicoelus* DH**	***O. amplicoelus* BS**	***O. amplicoelus* CE**	*O. amplicoelus*	*M. diodontis*	*P. virilis*	*P. diodontis*	*P. stellaglobulus*	*H. maculosus*	*G. perezi*	*M. mormyri*	*M. maamouriae*	*M. gibsoni*	*M. dubia*	*M. bartolii*	*M. crassigula*	*M. obovata*	*P. fischthali*	*M. brooksae*
***O. amplicoelus* DH**		0	0	0	12	13	13	15	17	17	18	20	20	21	21	21	22	24	42
***O. amplicoelus* BS**	100		0	0	12	13	13	15	17	17	18	20	20	21	21	21	22	24	42
***O. amplicoelus* CE**	100	100		0	12	13	13	15	17	17	18	20	20	21	21	21	22	24	42
O. amplicoelus	100	100	100		12	13	13	15	17	17	18	20	20	21	21	21	22	24	42
M. diodontis	97.21	97.21	97.21	97.21		10	10	11	14	15	17	21	20	22	20	21	23	22	38
P. virilis	96.97	96.97	96.97	96.97	97.67		11	12	10	10	14	19	16	20	15	14	21	18	38
P. diodontis	96.98	96.98	96.98	96.98	97.67	97.44		2	18	18	15	21	18	22	18	19	23	23	40
P. stellaglobulus	96.51	96.51	96.51	96.51	97.44	97.2	99.53		19	19	15	21	18	22	18	19	23	22	39
H. maculosus	96.03	96.03	96.03	96.03	96.74	97.66	95.8	95.57		17	20	24	20	25	22	22	26	24	40
G. perezi	96.04	96.04	96.04	96.04	96.5	97.66	95.8	95.57	96.03		12	17	14	17	13	14	19	15	36
M. mormyri	95.8	95.8	95.8	95.8	96.04	96.73	96.5	96.5	95.33	97.2		12	5	12	5	6	14	18	33
M. maamouriae	95.36	95.36	95.36	95.36	95.13	95.58	95.13	95.13	94.42	96.05	97.21		13	2	10	11	2	18	33
M. gibsoni	95.34	95.34	95.34	95.34	95.34	96.26	95.8	95.8	95.33	96.73	98.83	96.98		13	7	6	15	20	36
M. dubia	95.14	95.14	95.14	95.14	94.91	95.36	94.91	94.91	94.2	96.06	97.22	99.54	96.98		10	11	4	18	33
M. bartolii	95.12	95.12	95.12	95.12	95.35	96.5	95.81	95.81	94.87	96.97	98.83	97.67	98.37	97.68		3	12	18	32
M. crassigula	95.12	95.12	95.12	95.12	95.12	96.74	95.58	95.58	94.87	96.74	98.6	97.44	98.6	97.45	99.3		13	19	33
M. obovata	94.9	94.9	94.9	94.9	94.66	95.12	94.66	94.66	93.95	95.58	96.74	99.53	96.51	99.07	97.21	96.98		20	35
P. fischthali	94.43	94.43	94.43	94.43	94.9	95.81	94.66	94.9	94.42	96.51	95.81	95.81	95.35	95.82	95.81	95.58	95.35		29
M. brooksae	90.26	90.26	90.26	90.26	91.18	91.16	90.72	90.95	90.7	91.63	92.33	92.33	91.63	92.34	92.56	92.33	91.86	93.26	

Percentage of basis/ residues which are identical

Appendix D

Table 7 Nucleotide comparison of partial 28S rDNA sequences of Opistholebetinae, based on a 1,250 bp-long alignment.

Number of bases/ residues which are not identical

	***O. amplicoelus* DH**	***O. amplicoelus* CE**	*O. amplicoelus*	*M. diodontis*	*P. virilis*	*H. maculosus*	*P. diodontis*	*P. stellaglobulus*	*M. maamouriae*	*M. gibsoni*	*P. fischthali*	*M. obovata*	*M. dubia*	*M. bartolii*	*M. crassigula*	*M. mormyri*	*P. philippinensis*	*P. idoneum*	*G. perezi*	*M. brooksae*	*N. georgiensis*
***O. amplicoelus* DH**		0	0	14	15	17	17	17	21	24	26	26	27	27	31	34	34	38	41	50	108
***O. amplicoelus* CE**	0		0	14	15	17	17	17	21	24	26	26	27	27	31	34	34	38	41	50	108
O. amplicoelus	100	100		14	15	17	17	17	21	24	26	26	27	27	31	34	34	38	41	50	108
M. diodontis	98.94	98.94	98.94		14	22	11	11	34	33	31	38	37	36	39	42	36	38	45	46	109
P. virilis	98.78	98.78	98.78	98.94		23	16	16	31	28	24	35	32	31	34	37	33	31	38	39	109
H. maculosus	98.62	98.62	98.62	98.29	98.13		22	22	35	38	32	39	39	41	44	47	43	46	48	56	110
P. diodontis	98.62	98.62	98.62	99.19	98.70	98.21		0	35	32	28	37	37	35	38	41	33	35	42	45	112
P. stellaglobulus	98.62	98.62	98.62	99.19	98.70	98.21	100		35	32	28	37	37	35	38	41	33	35	42	45	112
M. maamouriae	98.22	98.22	98.21	97.19	97.36	97.02	97.02	97.02		20	32	3	17	21	22	25	29	37	37	50	108
M. gibsoni	97.96	97.96	97.96	97.28	97.62	96.77	97.28	97.27	98.30		22	21	18	11	7	11	30	29	32	41	105
P. fischthali	97.79	97.79	97.79	97.45	97.96	97.28	97.62	97.61	97.28	98.13		33	29	25	24	27	27	23	24	40	103
M. obovata	97.92	97.92	97.89	96.99	97.16	96.83	96.99	96.99	99.75	98.21	97.19		18	22	24	27	32	40	40	52	114
M. dubia	97.71	97.71	97.70	96.94	97.28	96.68	96.85	96.85	98.56	98.47	97.53	98.47		22	22	23	32	36	39	48	105
M. bartolii	97.71	97.71	97.70	97.02	97.36	96.51	97.02	97.02	98.22	99.06	97.87	98.13	98.13		7	12	30	32	29	44	104
M. crassigula	97.52	97.52	97.48	96.91	97.24	96.43	96.91	96.91	98.13	99.40	97.96	98.08	98.13	99.41		10	32	34	35	48	108
M. mormyri	97.25	97.25	97.24	96.67	96.99	96.18	96.67	96.66	97.88	99.06	97.70	97.81	98.05	98.98	99.19		32	35	39	47	110
P. philippinensis	97.28	97.28	97.24	97.16	97.32	96.51	97.32	97.31	97.54	97.45	97.70	97.44	97.29	97.46	97.44	97.41		25	31	46	116
P. idoneum	96.96	96.96	96.91	96.99	97.48	96.26	97.16	97.15	96.86	97.53	98.04	96.80	96.95	97.29	97.28	97.17	98.00		33	37	110
G. perezi	96.68	96.68	96.67	96.43	96.91	96.10	96.59	96.58	96.86	97.28	97.96	96.76	96.69	97.54	97.17	96.84	97.49	97.33		47	114
M. brooksae	96.00	96.00	95.94	96.30	96.83	95.45	96.34	96.34	95.76	96.51	96.60	95.84	95.93	96.27	96.16	96.19	96.32	97.04	96.19		106
N. georgiensis	91.00	91.00	90.94	90.90	90.86	90.77	90.60	90.59	90.83	91.06	91.23	90.50	91.09	91.17	91.00	90.79	90.34	90.84	90.47	91.17	

Percentage of basis/ residues which are identical

Appendix D

Table 8 Nucleotide comparison of *Opistholebes* Nicoll, 1915, mitochondrial COI (mtDNA) gene sequences, based on a 475 bp alignment.

	Number of bases/ residues which are not identical													
	***O. amplicoelus* DH**	***O. amplicoelus* WS**	***O. amplicoelus* BS**	***O. amplicoelus* CE**	***O. amplicoelus* DH**	***O. amplicoelus* CE**	***O. amplicoelus* WS**	***O. amplicoelus* BS**	*O. amplicoelus*	*O. amplicoelus*	*O. amplicoelus*	*O. amplicoelus*	*O. amplicoelus*	*O. amplicoelus*
***O. amplicoelus* DH**		0	0	0	1	1	2	2	69	71	71	71	72	72
***O. amplicoelus* WS**	100		0	0	1	1	2	2	69	71	71	71	72	72
***O. amplicoelus* BS**	100	100		0	1	1	2	2	69	71	71	71	72	72
***O. amplicoelus* CE**	100	100	100		1	1	2	2	69	71	71	71	72	72
***O. amplicoelus* DH**	99.79	99.79	99.79	99.79		2	3	1	68	70	70	70	71	71
***O. amplicoelus* CE**	99.79	99.79	99.79	99.79	99.58		1	3	68	70	70	70	71	71
***O. amplicoelus* WS**	99.58	99.58	99.58	99.58	99.37	99.79		4	69	71	71	71	72	72
***O. amplicoelus* BS**	99.58	99.58	99.58	99.58	99.79	99.37	99.16		69	71	71	71	72	72
O. amplicoelus	85.47	85.47	85.47	85.47	85.68	85.68	85.47	85.47		2	2	4	5	3
O. amplicoelus	85.05	85.05	85.05	85.05	85.26	85.26	85.05	85.05	99.58		0	2	3	1
O. amplicoelus	85.05	85.05	85.05	85.05	85.26	85.26	85.05	85.05	99.58	100		2	3	1
O. amplicoelus	85.05	85.05	85.05	85.05	85.26	85.26	85.05	85.05	99.16	99.58	99.58		3	1
O. amplicoelus	84.84	84.84	84.84	84.84	85.05	85.05	84.84	84.84	98.95	99.37	99.37	99.37		2
O. amplicoelus	84.84	84.84	84.84	84.84	85.05	85.05	84.84	84.84	99.37	99.79	99.79	99.79	99.58	

Percentage of basis/ residues which are identical

Appendix D

Table 9 Nucleotide comparison of *Opistholebes amplicoelus* Nicoll, 1915, nuclear *nad*1 (nDNA) gene sequences, based on a 474 bp alignment. Abbreviations: **DH** – De Hoop; **WS** – Witsand; **BS** – Boknesstrand; **CE** – Chintsa East

	Number of bases/ residues which are not identical					
	***O. amplicoelus* DH**	***O. amplicoelus* WS**	***O. amplicoelus* BS**	***O. amplicoelus* CE**	***O. amplicoelus* DH**	***O. amplicoelus* CE**
***O. amplicoelus* DH**		0	0	0	1	1
***O. amplicoelus* WS**	100		0	0	1	1
***O. amplicoelus* BS**	100	100		0	1	1
***O. amplicoelus* CE**	100	100	100		1	1
***O. amplicoelus* DH**	99.79	99.79	99.79	99.79		2
***O. amplicoelus* CE**	99.79	99.79	99.79	99.79	99.58	
	Percentage of basis/ residues which are identical					

Description

Based on six ventrally whole-mounted specimens, measurements in Table 3. Body robustly pyriform, with rounded to flat posterior. Tegument thick, smooth to wrinkled, with variably rugose frill posteriorly. Forebody approximately three-quarters of total body length. Oral sucker subterminal, spherical to subspherical. Ventral sucker subterminal from posterior extremity, subspherical to transversely-ellipsoidal, slightly larger than oral sucker, surrounded by tegumental folds which form posterior rugose "frill". Tegumental folds varying from almost non-existent in some specimens to somewhat extensive, but never completely enveloping ventral sucker. Pre-pharynx surrounded by prominent, muscular post-oral ring. Pharynx muscular, ellipsoidal, smaller than oral sucker. Oesophagus short. Intestinal bifurcation broad, in anterior third of body. Caeca broad with thick internal gastrodermis, slightly tapered posteriorly, extending to level of posterior margin of ventral sucker. Testes two, spherical to ovoid, approximately equal in size, margins not contiguous, situated dorsal to ventral sucker, spanning entire intercaecal space. Cirrus-sac elongated oval, medial. Seminal vesicle broad, tubular, looped, occupies majority of cirrus-sac, sharply constricted prior to *pars prostatica*. *Pars prostatica* short, meets genital atrium. Common genital atrium short, simple, immediately preceding common genital pore. Genital pore medial to just sinistral of midline, overlapping caeca in some specimens, entirely post-caecal in others. Ovary roughly spherical, margins smooth, slightly smaller than testes, dextro-submedial, antero-dorsal to and slightly overlapping dextral testis. Canalicular seminal receptacle prominent, smaller than and immediately anterior to ovary. Laurer's canal short, opens dorsal to ovarian complex. Oötype not observed; Mehlis' gland not prominent. Uterus convoluted, thin-walled, mostly pre-testicular in sinistral intercaecal region, slightly dorsally overlapping anterior margin of sinistral testis. Eggs oval, tanned, operculate. Vitelline follicles numerous, dense, relatively large, distributed from level of pharynx to posterior extremity, more extensive dorsally than ventrally; dorsal distribution fills most of body, somewhat but not entirely overlapping intercaecal space; ventral distribution partially overlapping caeca, not confluent. Pigment granules sparsely interspersed among vitelline follicles. Excretory vesicle difficult to observe, short, saccular, at most reaching to posterior margin of ovary. Excretory pore subterminal, dorsal to ventral sucker.

Morphological remarks

This study represents the first record of the opistholebetine trematode infecting *A. honckenii* off the coast of South Africa since Bray (1986) reported a single specimen from the Swartkops River estuary near Gqeberha. Morphological comparisons between the specimen described by Bray (1986) and those examined in the present study indicate that they belong to the same taxon. Martin *et al*. (2018a) previously suggested that the South African specimen identified by Bray (1986) may have closer affinities to species of *Opistholebes* rather than *Pseudoheterolebes*, noting its morphological similarity to *O. amplicoelus* and *O. microovus*, and proposing it might represent a distinct, undescribed species. However, the South African specimens can be distinguished from *O. microovus* by a combination of morphological features, including a narrower ventral sucker (<564 µm vs. 578–957 µm in width), a shorter pharynx (<302 µm vs. 334–434 µm in length), a thinner pharynx (<315 µm vs. 418–501 µm in width), narrower testes (<273 µm vs. 284–367 µm in width), and a longer cirrus-sac (>116 µm vs. 83 µm in length) (Table 3). Comparison of these features with both the original description of *O. amplicoelus* by Nicoll (1915) and the redescription by Martin *et al*. (2018a) supports the identification of the South African specimens as *O. amplicoelus* and suggests

that Bray's original classification of the specimen as *Pseudoheterolebes cotylophorus* was likely erroneous. Detailed morphological comparisons among the present specimens, Bray's (1986) specimen, and previously reported descriptions of both *O. amplicoelus* and *P. cotylophorus* (summarised in Table 3) reveal strong similarity to *O. amplicoelus* and clear distinctions from *P. cotylophorus*. The South African specimens conform to the generic characteristics of *Opistholebes* as outlined by Martin *et al*. (2018a), including a broad body (Fig. 2), with total length less than twice the width, and a ventral sucker positioned posteriorly, dorsally to the testes (Fig. 2), and measuring less than 1.5 times the width of the oral sucker (Table 3). These traits closely match those described by Nicoll (1915) and subsequent redescriptions (e.g., Manter and Pritchard 1962; Martin *et al*. 2018a), with only minor metrical variation (Table 3). Previous reports consistently note that gravid individuals of *O. amplicoelus* are smaller than those of *P. cotylophorus*, with Nicoll (1915) reporting a maximum size of 2,000 µm for *O. amplicoelus*, although the specimen was noted as flattened. In contrast, *P. cotylophorus* specimens are generally larger, ranging from 2,000–3,800 µm. Ozaki (1937a) reported specimens as small as 800 µm, though the maturity of these individuals was not specified. Although egg size has been considered a potential diagnostic character in opistholebetines, it does not reliably distinguish *O. amplicoelus* from *P. cotylophorus*. The egg sizes reported for *O. amplicoelus* from the type locality range from 51–70 × 27–40 µm (Nicoll 1915; Martin *et al*. 2018a), which is consistent with the present South African specimens (60–65 × 34–39 µm). However, Bray's specimen exhibited distinctly larger eggs (73–80 × 35–42 µm), overlapping with those reported for *P. cotylophorus* as 70–77 × 47–52 µm (Ozaki 1937a) and 78–85 × 46–62 µm (Yamaguti 1959). Notably, the original description of *P. cotylophorus* by Ozaki (1935) reported egg dimensions (62–64 × 40–42 µm) more typical of *O. amplicoelus*. These findings suggest that egg size is not a reliable taxonomic character for distinguishing between these two species. A key morphological feature of *Pseudoheterolebes*, including *P. cotylophorus*, is the presence of pronounced tegumental folds or "frills" surrounding the ventral sucker. This character was a primary justification for the establishment of the genus and the designation of *P. cotylophorus* as its type species (Yamaguti 1959). However, these prominent tegumental folds are absent in Bray's (1986) specimen and mostly absent in the South African specimens examined in the present study (Fig. 2). While some individuals exhibit slight frilling around the ventral sucker, none show the extensive development typical of *Pseudoheterolebes* species.

Molecular results

The ITS2 rDNA and partial 28S rDNA molecular phylogenetic analyses produced final alignments of 433 bp and 1,250 bp, respectively. The newly generated ITS2 and partial 28S rDNA sequences for South African specimens were identical across all specimens, exhibiting no intraspecific variation (i.e. 0 bp difference). In the ITS2 rDNA analyses, all South African sequence replicates (collected from De Hoop, Boknesstrand and Chintsa East) were identical to that of a sequence of *Opistholebes amplicoelus* from off North Stradbroke Island, Australia (ex *L. lunaris*) (Table 6). Similarly, in the partial 28S rDNA analysis, the newly generated South African specimens (collected from De Hoop and Chintsa) showed no differences (0 bp) to the sequence of *O. amplicoelus* from off North Stradbroke Island, Australia (ex *L. lunaris*) (Table 7). These validate the identity of the South African taxon as *O. amplicoelus*. Maximum likelihood (ML) and Bayesian inference (BI) analyses based on the rDNA alignment, which included partial 28S sequences of Opistholebetinae, yielded phylogenetic trees with congruent topologies and comparable nodal support (Fig.

3). These results align with previously reported phylogenetic patterns for Opistholebetinae (Martin *et al*. 2018a). The South African sequences formed a well-supported clade with *O. amplicoelus* (highlighted in green in Fig. 3), clearly separated from all *Pseudoheterolebes* species, which grouped into a distinct clade (highlighted in orange). The newly generated South African specimens showed clear genetic distinction from species of *Pseudoheterolebes*, exhibiting 17 bp differences in the 28S rDNA region when compared to those taxa (Table 7). The smallest interspecific differences (14 bp/ 1.06%) were observed between *O. amplicoelus* and *Maculifer diodontis* Martin, Ribu, Cutmore & Cribb, 2018. Conversely, *Magnaosimum brooksae* Martin, Crouch, Cutmore & Cribb, 2018, was the most genetically distant species from *O. amplicoelus*, with 50 bp differences (4%) in the 28S rDNA region (Table 7).

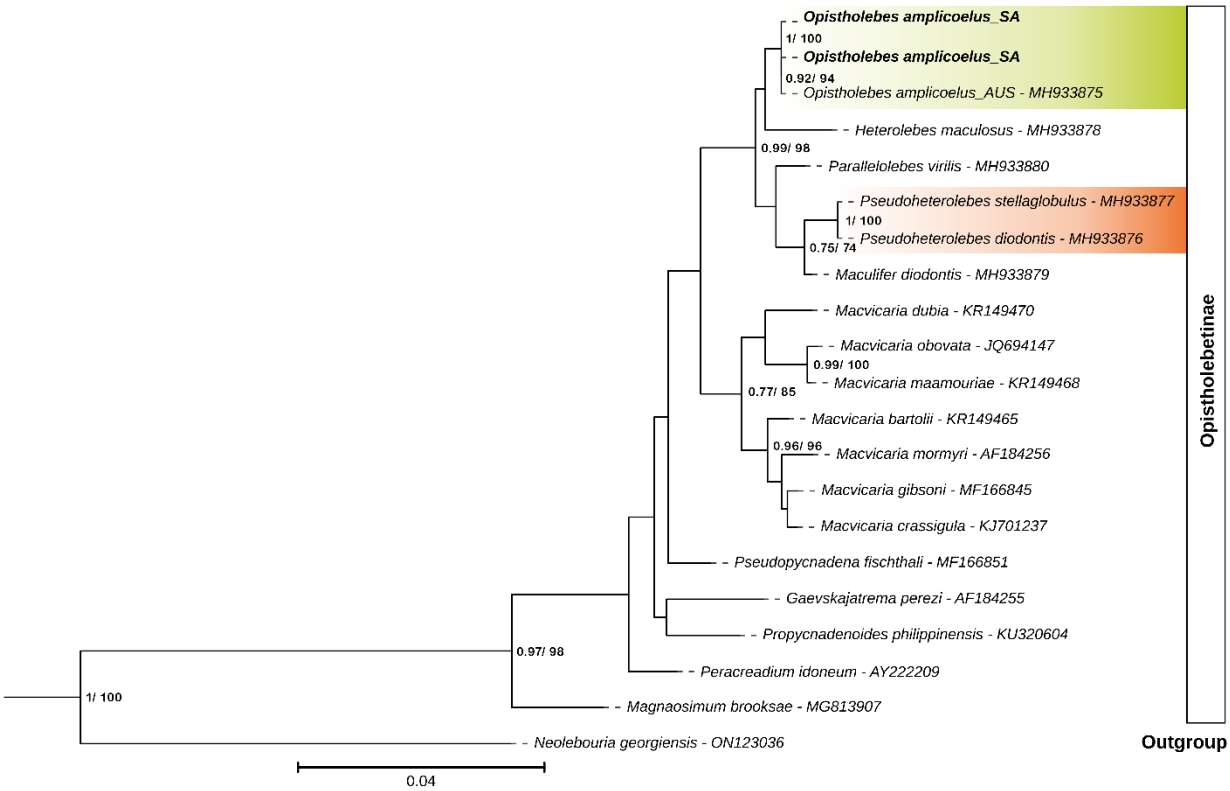

Fig. 3 Phylogenetic tree of the subfamily Opistholebetinae based on partial 28S rRNA gene alignments. Newly generated sequences for *Opistholebes amplicoelus* Nicoll, 1915, are provided in bold. Nodal support presented above or below branches for Bayesian Inference (>0.7) and Maximum Likelihood (>70%) analyses (BI/ML). Dashes indicate values below 0.70 and 70%, respectively. *Neolebouria georgiensis* Gibson, 1976, was used as the outgroup

Alignment of the COI mtDNA dataset, comprising *Opistholebes amplicoelus* specimens from South Africa and six replicates from Moreton Bay, Australia, yielded 475 bp for analysis. South African specimens exhibited 0–4 bp (0–0.42%) variation at the COI locus (Table 8), with three genotypes identified across all localities and seven of 11 replicates sharing an identical sequence (Fig. 4). The Australian replicates showed a comparable level of intraspecific variation (0–5 bp; 0–1.1%). However, the South African and Australian specimens differed by 69–72 bp (14.5–15.2%). Alignment of the *nad*1 mtDNA dataset yielded 474 bp for analysis. South African *O. amplicoelus* specimens showed minimal variation (0–2 bp; 0–0.42%)

across localities, with eight of 11 replicates being identical (Table 9). A concatenated dataset of the COI and *nad*1 loci produced a total alignment of 952 bp. This dataset, along with the COI mtDNA alignment alone, was used to construct haplotype networks to visualise population structure for *O. amplicoelus* (Fig. 5). The South African and Australian populations of *O. amplicoelus* were highly distinct, showing no shared haplotypes or evidence of population connectivity. Within each population, no geographic structuring was observed, and both loci indicated a lack of divergence among individuals from different sampling localities in South Africa.

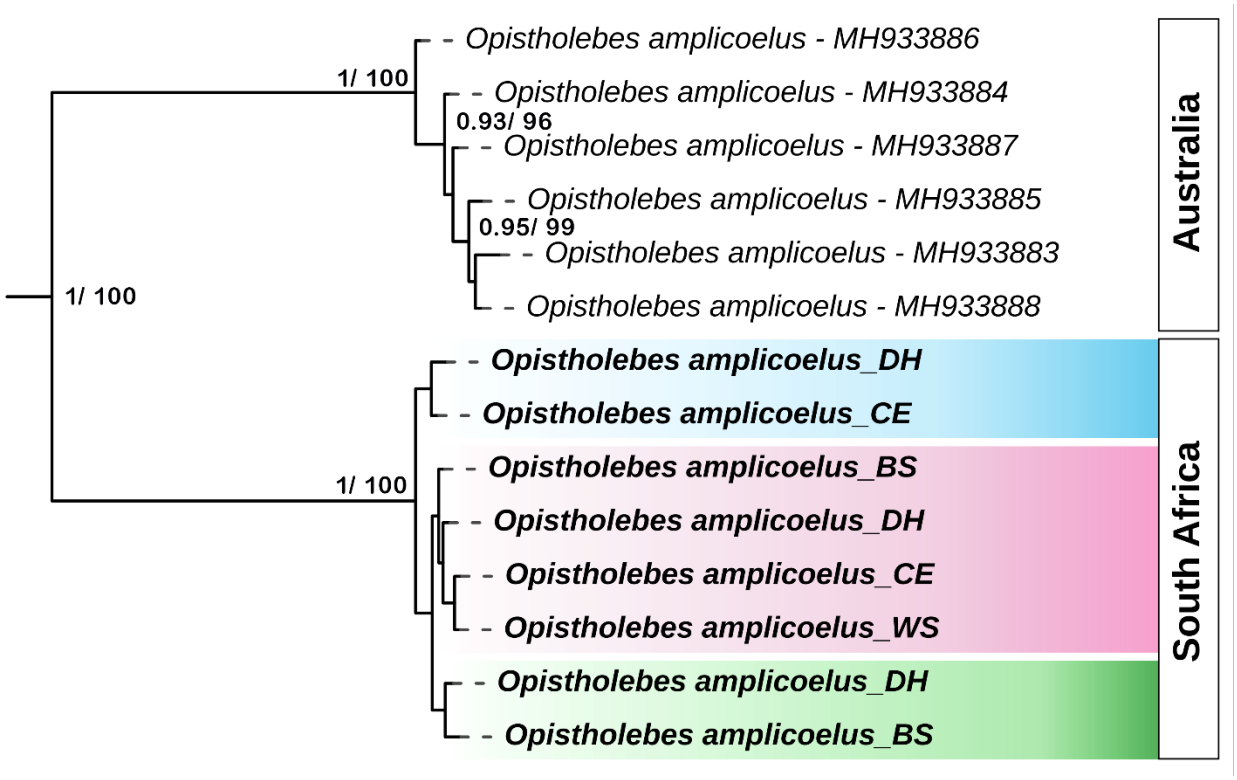

Fig. 4 Phylogenetic tree of *Opistholebes* Nicoll, 1915, trematodes based on partial COI mtDNA gene alignments. Newly generated sequences for *Opistholebes amplicoelus* Nicoll, 1915, are provided in bold. Nodal support presented above or below branches for Bayesian Inference (>0.7) and Maximum Likelihood (>70%) analyses (BI/ML). Dashes indicate values below 0.7 and 70%, respectively

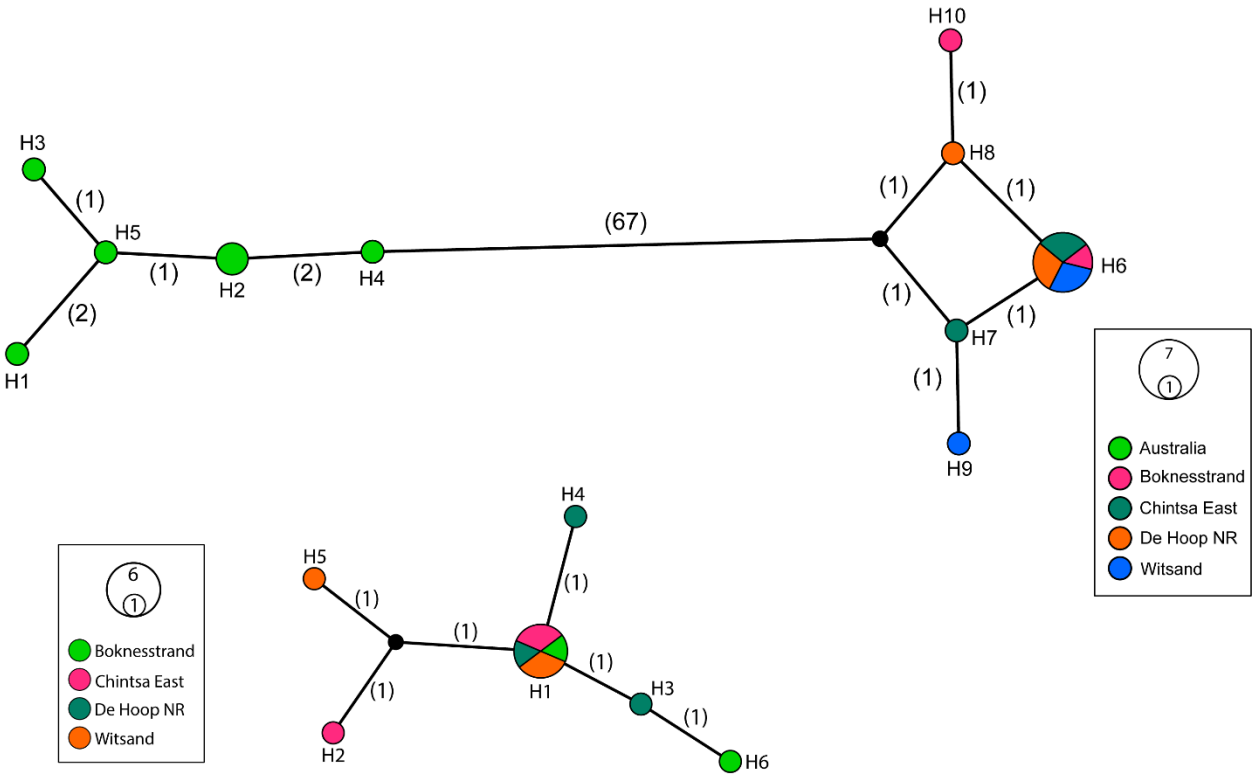

Fig. 5 Haplotype networks for *Opistholebes amplicoelus* Nicoll, 1915, based on mitochondrial DNA sequence data: **A** – Network based on COI mtDNA sequences from South African specimens and specimens from Moreton Bay, Australia; **B** – Network based on a concatenated alignment of COI and nad1 mtDNA sequences from South African specimens only

Discussion

This study resolves a longstanding taxonomic uncertainty regarding the identity of opistholebetine trematodes infecting *A. honckenii* off the South African coast. Through detailed morphological analyses, the newly collected specimens are shown to conform to *O. amplicoelus*, particularly in body proportions, sucker size, arrangement of reproductive organs, and the absence of pronounced tegumental folds around the ventral sucker. These features distinguish the specimens from *Pseudoheterolebes cotylophorus*. Molecular data further support this reassignment: sequences from the ITS2, 28S rDNA, and COI mtDNA regions were identical across all South African specimens and matched reference sequences of *O. amplicoelus*, exhibiting no intraspecific variation. Phylogenetic analyses based on ITS2 and partial 28S rDNA placed these specimens in a well-supported clade with *O. amplicoelus* from the type locality, distinct from *Pseudoheterolebes* species, which formed a separate lineage with greater sequence divergence.

Since its original description from Moreton Bay, Australia by Nicoll (1915), *O. amplicoelus* has rarely been reported and often misidentified, with several specimens later synonymised (e.g., Gupta 1968; Liu 1999). The redescription by Martin *et al*. (2018a) from the type locality, based on new material, and the sequences presented in their study, and this one, remain the only molecular data available for the species. Future analyses of specimens from India and China currently assigned to *O. amplicoelus* are needed.

Host specificity and distribution data further reinforce this taxonomic reassignment. *Pseudoheterolebes cotylophorus* was originally described from the diodontid *Diodon holocanthus* (Ozaki 1935) and has predominantly been reported from diodontid hosts (e.g., Ozaki 1937b; Manter and Pritchard 1962; Yamaguti 1970), with only two records from tetraodontids and a single uncorroborated record from a carangid, *Trachurus mediterraneus*, (Steindachner) (Caranginae) in the Black Sea (Nikolaeva and Kovaleva 1966). The latter record was made without comment in a broad, parasite-wide survey and, due to host identity and geographic mismatch, is regarded here as likely erroneous. Ozaki (1937a, b) listed the tetraodontid *Takifugu niphobles* (Jordan & Snyder) (Tetraodontidae) as a host of *P. cotylophorus* without comment, and Bray (1986) similarly made no note of host associations when assigning a South African specimen from *A. honckenii* to that species. In contrast, *O. amplicoelus* is reliably known from tetraodontiform hosts, reported from five genera: *Amblyrhynchotes*, *Arothron*, *Dichotomyctere*, *Lagocephalus*, and *Tetractenos*, making its occurrence in *A. honckenii* ecologically consistent.

Together, these morphological, molecular, and ecological data demonstrate that the trematodes previously identified as *P. cotylophorus* by Bray (1986) actually represent *O. amplicoelus*. This correction not only clarifies historical misidentifications but also highlights the value of integrated morphological and molecular approaches in resolving taxonomic ambiguities among marine parasites. Future work focusing on the type host and locality of *P. cotylophorus* in Japan is needed to refine the genus boundaries and confirm its phylogenetic placement.

It is noteworthy that specimens of *O. amplicoelus* from South Africa are genetically identical in the ITS2 and 28S rDNA regions to those from eastern Australia. Ribosomal markers, such as ITS2, are widely used to delineate cryptic species, especially in trematode taxa where morphological convergence can obscure true identity (Martin *et al*. 2018b; Bray *et al*. 2022). The absence of ribosomal sequence divergence across this broad Indo-West Pacific range suggests a single, widespread species, likely sustained by connectivity among host populations. Most known hosts of *O. amplicoelus* are tetraodontids with extensive ranges across the region (Froese and Pauly 2025), although host movement and population structure remain poorly studied in southern Africa. Sampling of other tetraodontiform fishes in this region may reveal further hosts, but such studies are currently lacking.

Despite broad geographic coverage in the current sampling, genetic variation among South African *O. amplicoelus* was minimal: no variation in ITS2 and 28S, only 1–2 bp differences in *nad*1 mtDNA, and 0–4 bp differences in COI mtDNA (Tables 6–9). Australian specimens showed similar low intraspecific variation, but COI mtDNA differed from South African sequences by 68–72 bp. This level of mitochondrial divergence, although high, is consistent with patterns observed in other widely distributed trematodes (e.g., *Emprostiotrema fusum* (Goto & Ozaki, 1929) Cianferoni & Ceccolini, 2021) (Huston *et al*. 2024), where ribosomal sequences remain conserved, but mitochondrial markers show greater geographic variability. In some instances, such patterns mask cryptic speciation (e.g., *Doorochen* spp. Bray, Cutmore & Cribb, 2022) (Bray *et al*. 2023), however, given the complete morphological congruence and lack of sequence data from intermediate regions, the most parsimonious conclusion is that Australian and South African *O. amplicoelus* represent a single, widespread species. Continued refinement of trematode systematics, especially regarding reconciliation of mitochondrial and nuclear markers, is ongoing (Cribb *et al*. 2025), and future

studies across the Indian Ocean and western Pacific may yield further insights into the extent of *O. amplicoelus*' range.

Mitochondrial haplotype analyses reveal no population structuring among South African *O. amplicoelus*. Three COI genotypes were detected: two occurred across a 700 km stretch from De Hoop Nature Reserve to Chintsa East, and the third was present in specimens from Witsand and Boknesstrand, separated by ~550 km. While movement and population genetics of several commercially important South African fishes have been well studied (e.g., *Dichistius capensis* (Cuvier)(Dichistiidae), *Lichia amia* (Linnaeus)(Carangidae), *Atractoscion aequidens* (Cuvier)(Sciaenidae)) (Attwood and Cowley 2010; Henriques *et al*. 2012, 2014), no such studies exist for *A. honckenii* or other tetraodontids in the region. Interestingly, no *O. amplicoelus* were found in *A. honckenii* sampled north of Chintsa East, at either Uvongo Beach (n = 10) or Sodwana Bay (n = 18) (Table 2). This absence may be explained by oceanographic factors. The southward-flowing Agulhas Current in eastern South Africa creates biogeographic separation from the cooler southern systems (Halo and Raj 2020), potentially limiting host or intermediate host dispersal. The identity of the intermediate host for *O. amplicoelus* remains unknown, further complicating biogeographic interpretation.

Reconciling parasite and host distributions in southern African marine systems remains an emerging field. Several recent studies hint at broad parasite homogeneity across wide distances. For instance, Vermaak *et al*. (in review) found *Macvicaria* sp. Gibson & Bray, 1982 (Opecoelidae) infecting *Diplodus capensis* (Smith) from De Hoop to Chintsa East, mirroring our findings. Similarly, Yong *et al*. (2025) reported genetically indistinguishable lepidapedids in *Dichistius capensis* and its second intermediate host, *Perna perna* (Linnaeus) (Mytilidae), from central Namibia to southwestern South Africa. Louvard *et al*. (in review) described a new *Bucephalidae* Poche, 1907, species spanning 2,700 km, from Langstrand, Namibia, to Uvongo Beach, South Africa. While these studies were not biogeographically focused and lacked comprehensive dual-host molecular data, they suggest low parasite population structuring along the southern African coast. Broader, finer-scale studies with robust sampling are needed to confirm these patterns and reveal the underlying mechanisms of connectivity and speciation in marine parasites, like *O. amplicoelus*. Taken together, these findings resolve a longstanding taxonomic uncertainty surrounding *Opistholebes amplicoelus* and highlight the value of integrative taxonomic approaches in uncovering cryptic parasite diversity and clarifying host–parasite biogeographic relationships across marine ecosystems.

Acknowledgements

We would like to thank the Unit for Environmental Sciences and Management, North-West University (NWU), for the use of field equipment and laboratory facilities. Additional thanks go to our colleagues Francois Retief, Reese Alberts, Hannes Erasmus, Anja Erasmus, Marliese Truter, Anja Vermaak, Angela Minie, Chandra le Roux, Wiets Neetling and Coret van Wyk, from the NWU, who assisted with the collection of samples. This is contribution No. XXX from the NWU-Water Research Group. RQY Yong acknowledges the support of a NWU Senior Postdoctoral Fellowship. This work is supported by the National Research Foundation (NRF) of South Africa (grant 132805; L. van der Spuy; grant 150623; N. J.

Smit). Opinions, findings, conclusions and recommendations expressed in this publication are those of the authors, and the NRF accept no liability whatsoever in this regard.

References

Andres MJ, Ray CL, Pulis EE, Curran SS, Overstreet RM (2014) Molecular characterization of two opecoelid trematodes from fishes in the Gulf of Mexico, with a description of a new species of *Helicometra*. *Acta Parasitol* 59:405–412. doi: 10.2478/s11686-014-0258-7

Antar R, Georgieva S, Gargouri L, Kostadinova A (2015) Molecular evidence for the existence of species complexes within *Macvicaria* Gibson & Bray, 1982 (Digenea: Opecoelidae) in the western Mediterranean, with descriptions of two new species. *Syst Parasitol* 91:211–229. doi: 10.1007/s11230-015-9577-9

Attwood CG, Cowley PD (2010) Alternate explanations of the dispersal pattern of galjoen *Dichistius capensis*. *Afr J Mar Sci* 27:141–156. doi: 10.2989/18142320509504074

Bianchini G, Sánchez-Baracaldo P (2024) Treeviewer: flexible, modular software to visualise and manipulate phylogenetic trees. *Ecol Evol* 14:e10873. doi: 10.1002/ece3.10873

Born-Torrijos A, Kostadinova A, Raga JA, Holzer AS (2012) Molecular and morphological identification of larval opecoelids (Digenea: Opecoelidae) parasitising prosobranch snails in a Western Mediterranean lagoon. *Parasitol Int* 61(3):450–460. doi:10.1016/j.parint.2012.03.002

Bray RA (1986) Some helminth parasites of marine fishes of South Africa: families Enenteridae, Opistholebetidae and Pleorchiidae (Digenea). *J Nat Hist* 20(2):471–488. doi: 10.1080/00222938600770371

Bray RA, Cribb TH, Littlewood DTJ, Waeschenbach A (2016) The phylogeny of the digenean family Opecoelidae Ozaki, 1925: molecular phylogenetic inference and the value of morphological characters. *Parasitol Int* 1:1–10. doi: 10.1079/9780851995878.0443

Bray RA, Cutmore SC, Cribb TH (2022) A paradigm for the recognition of cryptic trematode species in tropical Indo-west Pacific fishes: the problematic genus *Preptetos* (Trematoda: Lepocreadiidae). *Int J Parasitol* 52(2–3):169–203. doi: 10.1016/j.ijpara.2021.08.004

Cable RM (1956) *Opistholebes diodontis* n. sp., its development in the final host, the affinities of some amphistomatous trematodes from marine fishes and the allocreadioid problem. *Parasitology* 46(1–2):1–13. doi: 10.1017/S0031182000026305

Cribb TH, Adlard RD, Bray RA (1998) A DNA-based demonstration of a three-host life-cycle for the Bivesiculidae (Platyhelminthes: Digenea). *Int J Parasitol* 28(11):1791–1795. doi: 10.1016/S0020-7519(98)00127-1

Cribb TH, Barton D P, Blair D, Bott NJ, Bray RA, Corner RD, Cutmore SC, De Silva MLI, Duong B, Faltýnková A, Gonchar A (2025) Challenges in the recognition of trematode species: Consideration of hypotheses in an inexact science. *J Helminthol* 99:e54. doi: 10.1017/S0022149X25000367

Darriba D, Taboada GL, Doallo R, Posada D (2012) jModelTest 2: more models, new heuristics and parallel computing. *Nat Methods* 9:772. doi: 10.1038/nmeth.2109

Faltýnková A, Kudlai O, Salganskiy OO, Korol EM, Kuzmina TA (2022) Trematodes from Antarctic teleost fishes off Argentine Islands, West Antarctica: molecular and morphological data. *Syst Parasitol* 99(4):491–523. doi: 10.1007/s11230-022-10041-9

Fayton TJ, Andres MJ (2016) New species of *Plagioporus* Stafford, 1904 (Digenea: Opecoelidae) from California, with an amendment of the genus and a phylogeny of freshwater plagioporines of the Holarctic. *Syst Parasitol* 93:731–748. doi: 10.1007/s11230-016-9664-6

Froese R, Pauly D (eds) (2025) *FishBase*. World Wide Web electronic publication, www.fishbase.org (accessed 08 May 2025).

Guindon S, Dufayard JF, Lefort V, Anisimova M, Hordijk W, Gascuel O (2010) New algorithms and methods to estimate maximum-likelihood phylogenies: assessing the performance of PhyML 3.0. *Syst Biol* 59:307–321. doi: 10.1093/sysbio/syq010

Gupta AN (1968) On three new species of *Opistholebes* (Opistholebetidae Fukui, 1929) from the globe fish, *Tetraodon viridipunctatus* (Gunther) from India. *J Helminthol* 42:283–288. doi: 10.1017/S0022149X00017879

Halo I, Raj RP (2020) Comparative oceanographic eddy variability during climate change in the Agulhas Current and Somali Coastal Current Large Marine Ecosystems. *Environ Dev* 36:e100586. doi: 10.1016/j.envdev.2020.100586

Henriques R, Potts W, Sauer W, Shaw P (2012) Evidence of deep genetic divergence between populations of an important recreational fishery species, *Lichia amia* L. 1758, around southern Africa. *Afr J Mar Sci* 34:585–591. doi: 10.2989/1814232X.2012.749809

Henriques R, Potts WM, Santos CV, Sauer WH, Shaw PW (2014) Population connectivity and phylogeography of a coastal fish, *Atractoscion aequidens* (Sciaenidae), across the Benguela Current region: evidence of an ancient vicariant event. *PLoS ONE* 9:e87907. doi: 10.1371/journal.pone.0087907

Huston DC, Cutmore SC, Cribb TH, Sasal P, Smit NJ (2021) Gorgocephalidae (Digenea: Lepocreadioidea) in the Indo-West Pacific: new species, life-cycle data and perspectives on species delineation over geographic range. *Zool J Linnean Soc* 193:1416–1455. doi: 10.1093/zoolinnean/zlab002

Huston DC, Cutmore SC, Cribb TH, Sasal P (2024) Taxonomy and systematics of *Emprostiotrema* Cianferoni & Ceccolini, 2021 (Digenea: Emprostiotrematidae), parasites of rabbitfish (Siganidae) from the Indo-West Pacific marine region. *Parasitol* 1–15. doi: 10.1017/ S0031182024001252

Katoh K, Misawa K, Kuma KI, Miyata T (2002) MAFFT: a novel method for rapid multiple sequence alignment based on fast Fourier transform. *Nucleic Acids Res* 30:3059–3066. doi: 10.1093/nar/gkf436

Katoh K, Standley DM (2013) MAFFT multiple sequence alignment software version 7: improvements in performance and usability. *Mol Biol Evol* 30:772–780. doi: 10.1093/molbev/mst010

Kearse M, Moir R, Wilson A, Stones-Havas S, Cheung M, Sturrock S, Buxton S, Cooper A, Markowitz S, Duran C, Thierer T, Ashton B, Meintjes P, Drummond A (2012) Geneious Basic: an integrated and extendable desktop software platform for the organization and analysis of sequence data. *Bioinformatics* 28:1647–1649. doi: 10.1093/bioinformatics/bts199

Kostadinova A, Herniou EA, Barrett J, Littlewood DTJ (2003) Phylogenetic relationships of *Echinostoma* Rudolphi, 1809 (Digenea: Echinostomatidae) and related genera re-assessed via DNA and morphological analyses. *Syst Parasitol* 54:159–176. doi: 10.1023/A:1022681123340

Krishna PV, Sreeramulu K (1993) *Ophistholebes tetrodontis* (Trematoda: Digenea) a new record from Waltair Coast. *Uttar Pradesh J Zool* 13:89–90.

Ku CT, Shen JW (1965) Studies on some digenetic trematodes from marine fishes in China. *Acta Parasitol Sinica* 2:355–365.

Kumar S, Stecher G, Tamura K (2016) MEGA7: Molecular Evolutionary Genetics Analysis Version 7.0 for Bigger Datasets. *Mol Biol Evol* 33:1870–1874. doi: 10.1093/molbev/msw054

Leigh JW, Bryant D (2015) PopART: full-feature software for haplotype network construction. *Methods Ecol Evol* 6(9):1110–1116. doi: 10.1111/2041-210X.12410

Littlewood DTJ (1994) Molecular phylogenetics of cupped oysters based on partial 28S rRNA gene sequences. *Mol Phylogenet Evol* 3(3):221–229. doi: 10.1006/mpev.1994.1024

Littlewood DTJ, Rohde K, Clough KA (1997) Parasite speciation within or between host species?—Phylogenetic evidence from site-specific polystome monogeneans. *Int J Parasitol* 27(11):1289–1297. doi: 10.1016/S0020-7519(97)00086-6

Littlewood DTJ, Rohde K, Bray RA, Herniou EA (1999) Phylogeny of the Platyhelminthes and the evolution of parasitism. *Biol J Linn Soc* 68(1–2):257–287.

Liu SF (1999). Description of three new species of Opistholebetidae (Trematodes: Digenea). *Acta Zootaxonomica Sinica*, 24: 265–271 (In Chinese).

Maddison WP, Maddison DR (2017) *Mesquite: a modular system for evolutionary analysis*. Version 3.0. http://mesquiteproject.org

Manter HW (1947) The digenetic trematodes of marine fishes of Tortugas, Florida. *Am Midl Nat* 1:257–416.

Manter HW, Pritchard MH (1962) Studies on digenetic trematodes of Hawaiian fishes: Families Fellodistomatidae, Opistholebetidae and Gyliauchenidae. *Trans Am Micros Soc* 81(2):113–123.

Martin SB, Ribu D, Cutmore SC, Cribb TH (2018a). Opistholobetines (Digenea: Opecoelidae) in Australian tetraodontiform fishes. *Syst Parasitol* 95(8):743–781. doi: 10.1007/s11230-018-9826-9

Martin SB, Crouch K, Cutmore SC, Cribb TH (2018b) Expansion of the concept of the Opistholebetinae Fukui, 1929 (Digenea: Opecoelidae Ozaki, 1925), with *Magnaosimum brooksae* ng, n. sp. from *Tripodichthys angustifrons* (Hollard) (Tetraodontiformes: Triacanthidae) in Moreton Bay, Australia. *Syst Parasitol* 95(2):121–132. doi: 10.1007/s11230-018-9783-3

Miller M, Pfeiffer WT, Schwartz T (2010) Creating the CIPRES science gateway for inference of large phylogenetic trees. *Proc Gateway Comput Environ Workshop* 14:1–8. doi: 10.1109/GCE.2010.5676129

Morgan JAT, Blair D (1995) Nuclear rDNA ITS sequence variation in the trematode genus *Echinostoma*: an aid to establishing relationships within the 37-collar-spine group. *Parasitology* 111(5):609–615. doi: 10.1017/S003118200007709X

Moszczynska A, Locke SA, McLaughlin JD, Marcogliese DJ, Crease TJ (2009) Development of primers for the mitochondrial cytochrome c oxidase I gene in digenetic trematodes (Platyhelminthes) illustrates the challenge of barcoding parasitic helminths. *Mol Ecol Resour* 9:75–82. doi: 10.1111/j.1755-0998.2009.02634.x

Nicoll W (1915) The trematode parasites of north Queensland. III.: parasites of fishes. *Parasitology* 8(1):22–41.

Nikolaeva VM, Kovaleva AA (1966) Parasite fauna of *Trachurus* from the Mediterranean Basin. *Biologiya Morya*, Kiev. Helminth fauna of animals of the Southern Seas:67–79.

Olson PD, Cribb TH, Tkach VV, Bray RA, Littlewood DTJ (2003) Phylogeny and classification of the Digenea (Platyhelminthes: Trematoda). *Int J Parasitol* 33(7):733–755.

Ozaki Y (1935) Two new trematodes of the family Opistholebetidae Travassos. *Proceedings of the Imperial Academy*, 11(6): 244–246.

Ozaki Y (1937a) Studies on the trematode families Gyliauchenidae and Opistholebetidae, with special reference to the lymph system. I. Journal of Science of the Hiroshima University, 5: 125–165.

Ozaki Y (1937b) Studies on the trematode families Gyliauchenidae and Opistholebetidae, with special reference to the lymph system. II. Journal of Science of the Hiroshima University, 5: 167–244.

Pleijel F, Jondelius U, Norlinder E, Nygren A, Oxelman B, Schander C, Sundberg P, Thollesson M (2008) Phylogenies without roots? A plea for the use of vouchers in molecular phylogenetic studies. *Mol Phylogenet Evol* 48(1):369–371. doi: 10.1016/S0020-7519(03)00049-3

Posada D (2008) jModelTest: phylogenetic model averaging. *Mol Biol Evol* 25:1253–1256. doi: 10.1093/molbev/msn083

Rima M, Marzoug D, Pérez-del-Olmo A, Kostadinova A, Bouderbala M, Georgieva S (2017) New molecular and morphological data for opecoelid digeneans in two Mediterranean sparid fishes with descriptions of *Macvicaria gibsoni* n. sp. and *M. crassigula* (Linton, 1910) (sensu stricto). *Syst Parasitol* 94:739–763. doi: 10.1007/s11230-017-9736-2

Ronquist F, Teslenko M, van der Mark P, Ayres DL, Darling A, Höhna S, Larget B, Liu L, Suchard MA, Huelsenbeck JP (2012) MrBayes 3.2: efficient Bayesian phylogenetic inference and model choice across a large model space. *Syst Biol* 61:539–542. doi: 10.1093/sysbio/sys029

Rozas J, Ferrer-Mata A, Sánchez-DelBarrio JC, Guirao-Rico S, Librado P, Ramos-Onsins SE, Sánchez-Gracia A (2017) DnaSP 6: DNA Sequence Polymorphism Analysis of Large Datasets. *Mol Biol Evol* 34:3299–3302. doi: 10.1093/molbev/msx248

Snyder SD, Tkach VV (2001) Phylogenetic and biogeographical relationships among some holarctic frog lung flukes (Digenea: Haematoloechidae). *J Parasitol* 87(6):1433–1440. doi: 10.1645/0022-3395(2001)087[1433:PABRAS]2.0.CO;2

Swofford D (2002) *PAUP*. Phylogenetic Analysis Using Parsimony (*and other methods*). Version 4.0a169. Sinauer Associates, Sunderland, MA.

Tkach VV, Pawlowski J, Mariaux J, Swiderski Z (2001) Molecular phylogeny of the suborder Plagiorchiata and its position in the system of Digenea. In: *Interrelationships of the Platyhelminthes.* CRC Press, 186–193.

Van Steenkiste N, Locke SA, Castelin M, Marcogliese DJ, Abbott CL (2015) New primers for DNA barcoding of digeneans and cestodes (Platyhelminthes). *Mol Ecol Resour* 15(4):945–952. doi: 10.1111/1755-0998.12358

Vermaak A, Smit NJ, Kudlai O (2023) Molecular characterisation of three species of *Coitocaecum* (Digenea: Opecoelidae) infecting *Clinus superciliosus* (Clinidae) in South Africa, with description of *Coitocaecum brayi* sp. n. *Folia Parasitol* 70:1–10. doi: 10.14411/fp.2023.015

Wee NQ, Cribb TH, Bray RA, Cutmore SC (2017) Two known and one new species of *Proctoeces* from Australian teleosts: variable host-specificity for closely related species identified through multi-locus molecular data. *Parasitol Int* 66(2):16–26. doi: 10.1016/j.parint.2016.11.008

WoRMS (2025) *World Register of Marine Species*. Opecoelidae Ozaki, 1925. Available at: https://www.marinespecies.org/aphia.php?p=taxdetails&id=108432 on 2025-07-09 (accessed 08 May 2025)

Xia X (2018) DAMBE7: new and improved tools for data analysis in molecular biology and evolution. *Mol Biol Evol* 35:1550–1552. doi: 10.1093/molbev/msy073

Yamaguti S (1970) *Digenetic trematodes of Hawaiian fishes*.

Yamaguti S (1959) Studies on the helminth fauna of Japan, Part 54. Trematodes of fishes, XIII. *Publ Seto Mar Biol Lab* 7(2):241–262.

Yong RQ-Y, Bray RA, Schwelm J, Louvard C, Malherbe W, Smit NJ (2025) Lepocreadioidea (Digenea: Trematoda) of southern Africa, including a new genus and species of Lepidapedidae infecting the galjoen, *Dichistius capensis* (Cuvier) (Centrarchiformes: Dichistiidae) from off Namibia. *Parasitol Int* 109:e103110. doi: 10.1016/j.parint.2025.103110

Zhukov EV (1977) Contribution to the knowledge of trematodes of marine fishes of India. *Parazitologicheskii Sbornik* 27:51–79 (In Russian).